ANSYS Verification Manual

ANSYS Release 10.0

002184
August 2005

ANSYS, Inc. and ANSYS Europe, Ltd. are UL registered ISO 9001:2000 Companies.

ANSYS Verification Manual

ANSYS Release 10.0

ANSYS, Inc.
Southpointe
275 Technology Drive
Canonsburg, PA 15317
ansysinfo@ansys.com
http://www.ansys.com
(T) 724-746-3304
(F) 724-514-9494

Copyright and Trademark Information

© 2005 SAS IP, Inc. All rights reserved. Unauthorized use, distribution or duplication is prohibited.

ANSYS, ANSYS Workbench, CFX, AUTODYN, and any and all ANSYS, Inc. product and service names are registered trademarks or trademarks of ANSYS, Inc. or its subsidiaries located in the United States or other countries. ICEM CFD is a trademark licensed by ANSYS, Inc. All other trademarks or registered trademarks are the property of their respective owners.

Disclaimer Notice

THIS ANSYS SOFTWARE PRODUCT AND PROGRAM DOCUMENTATION INCLUDE TRADE SECRETS AND ARE CONFIDENTIAL AND PROPRIETARY PRODUCTS OF ANSYS, INC., ITS SUBSIDIARIES, OR LICENSORS. The software products and documentation are furnished by ANSYS, Inc., its subsidiaries, or affiliates under a software license agreement that contains provisions concerning non-disclosure, copying, length and nature of use, compliance with exporting laws, warranties, disclaimers, limitations of liability, and remedies, and other provisions. The software products and documentation may be used, disclosed, transferred, or copied only in accordance with the terms and conditions of that software license agreement.

ANSYS, Inc. and ANSYS Europe, Ltd. are UL registered ISO 9001:2000 Companies.

U.S. GOVERNMENT RIGHTS

For U.S. Government users, except as specifically granted by the ANSYS, Inc. software license agreement, the use, duplication, or disclosure by the United States Government is subject to restrictions stated in the ANSYS, Inc. software license agreement and FAR 12.212 (for non-DOD licenses).

Third-Party Software

See the online documentation in the product help files for the complete Legal Notice for ANSYS proprietary software and third-party software. The ANSYS third-party software information is also available via download from the Customer Portal on the ANSYS web page. If you are unable to access the third-party legal notices, please contact ANSYS, Inc.

Published in the U.S.A.

Table of Contents

I. Verification Test Case Descriptions

1. **Introduction** 1–1
1.1. Program Overview 1–1
1.2. Program Verification 1–2
1.3. Finding Test Cases of Interest 1–2
1.4. Accessing Test Case Inputs 1–3
1.5. ANSYS Verification Manual Versus Other Manuals 1–3
1.6. ANSYS Verification Manual Contents 1–3
1.7. Theoretical Solutions 1–3
1.8. Test Case Selection and Method of Solution 1–4
1.9. Numerical Comparisons 1–4
1.10. References 1–5
1.11. Test Case Format 1–5
1.12. Symbols and Nomenclature 1–5
1.13. Memory Requirements and Run Times 1–5
1.14. Abbreviation, Element, and Product Lists 1–6
1.14.1. Abbreviation and Symbol List 1–6
1.14.2. Units Abbreviation List 1–7
1.14.3. Index by Element Number 1–8
VM1 1–19
VM2 1–21
VM3 1–23
VM4 1–24
VM5 1–26
VM6 1–28
VM7 1–30
VM8 1–33
VM9 1–34
VM10 1–36
VM11 1–37
VM12 1–39
VM13 1–41
VM14 1–43
VM15 1–45
VM16 1–47
VM17 1–49
VM18 1–51
VM19 1–53
VM20 1–55
VM21 1–57
VM22 1–59
VM23 1–61
VM24 1–63
VM25 1–65
VM26 1–69
VM27 1–71
VM28 1–73
VM29 1–75
VM30 1–77

VM31 1–80
VM32 1–82
VM33 1–84
VM34 1–87
VM35 1–90
VM36 1–92
VM37 1–94
VM38 1–97
VM39 1–99
VM40 1–101
VM41 1–103
VM42 1–105
VM43 1–107
VM44 1–109
VM45 1–111
VM46 1–112
VM47 1–115
VM48 1–117
VM49 1–119
VM50 1–121
VM51 1–123
VM52 1–127
VM53 1–129
VM54 1–131
VM55 1–133
VM56 1–135
VM57 1–137
VM58 1–139
VM59 1–141
VM60 1–143
VM61 1–145
VM62 1–147
VM63 1–150
VM64 1–152
VM65 1–153
VM66 1–155
VM67 1–157
VM68 1–159
VM69 1–161
VM70 1–163
VM71 1–165
VM72 1–167
VM73 1–169
VM74 1–172
VM75 1–174
VM76 1–176
VM77 1–178
VM78 1–180
VM79 1–182
VM80 1–184
VM81 1–186
VM82 1–188

VM83 1–190
VM84 1–193
VM85 1–196
VM86 1–199
VM87 1–201
VM88 1–203
VM89 1–205
VM90 1–207
VM91 1–209
VM92 1–212
VM93 1–214
VM94 1–215
VM95 1–217
VM96 1–219
VM97 1–221
VM98 1–223
VM99 1–226
VM100 1–228
VM101 1–231
VM102 1–233
VM103 1–235
VM104 1–237
VM105 1–241
VM106 1–243
VM107 1–244
VM108 1–246
VM109 1–248
VM110 1–250
VM111 1–252
VM112 1–254
VM113 1–255
VM114 1–258
VM115 1–260
VM116 1–262
VM117 1–265
VM118 1–267
VM119 1–269
VM120 1–272
VM121 1–274
VM122 1–281
VM123 1–283
VM124 1–285
VM125 1–287
VM126 1–289
VM127 1–291
VM128 1–293
VM129 1–295
VM130 1–297
VM131 1–299
VM132 1–301
VM133 1–303
VM134 1–305

VM135 1–307
VM136 1–308
VM137 1–311
VM138 1–313
VM139 1–314
VM140 1–316
VM141 1–318
VM142 1–320
VM143 1–322
VM144 1–324
VM145 1–326
VM146 1–328
VM147 1–330
VM148 1–332
VM149 1–334
VM150 1–336
VM151 1–338
VM152 1–340
VM153 1–342
VM154 1–344
VM155 1–347
VM156 1–350
VM157 1–352
VM158 1–354
VM159 1–356
VM160 1–359
VM161 1–361
VM162 1–363
VM163 1–365
VM164 1–368
VM165 1–370
VM166 1–373
VM167 1–375
VM168 1–378
VM169 1–380
VM170 1–383
VM171 1–385
VM172 1–388
VM173 1–392
VM174 1–394
VM175 1–396
VM176 1–400
VM177 1–403
VM178 1–407
VM179 1–409
VM180 1–411
VM181 1–413
VM182 1–414
VM183 1–416
VM184 1–418
VM185 1–421
VM186 1–425

VM187 1–428
VM188 1–430
VM189 1–432
VM190 1–436
VM191 1–438
VM192 1–441
VM193 1–443
VM194 1–445
VM195 1–447
VM196 1–449
VM197 1–451
VM198 1–452
VM199 1–455
VM200 1–457
VM201 1–460
VM202 1–463
VM203 1–466
VM204 1–468
VM205 1–470
VM206 1–473
VM207 1–475
VM208 1–477
VM209 1–479
VM210 1–484
VM211 1–487
VM212 1–491
VM213 1–493
VM214 1–496
VM215 1–498
VM216 1–500
VM217 1–503
VM218 1–507
VM219 1–511
VM220 1–513
VM221 1–515
VM222 1–518
VM223 1–521
VM224 1–524
VM225 1–526
VM226 1–528
VM227 1–534
VM228 1–536
VM229 1–537
VM230 1–539
VM231 1–542
VM232 1–544
VM233 1–549
VM234 1–553
VM235 1–555
VM236 1–558
VM237 1–560
VM238 1–563

VM239 1–565
VM240 1–568
VM241 1–570
VM242 1–574
VM243 1–576
VM244 1–578
VM245 1–580
VM246 1–582

II. Benchmark Study Descriptions

2. **Overview** 2–1
2.1. Description of the Benchmark Studies 2–1
2.2. Benchmark Test Case Content and Nomenclature 2–2
2.3. Running the Benchmark Test Cases 2–3
2.4. Energy Norm 2–3
2.5. Benchmark Test Case Coverage Index 2–3
Benchmark C1 2–5
Benchmark C2 2–9
Benchmark C3 2–12
Benchmark C4 2–15
Benchmark C5 2–19
Benchmark C6 2–23
Benchmark C7 2–26
Benchmark C8 2–29
Benchmark D1 2–32
Benchmark D2 2–36
Benchmark D3 2–40

III. ANSYS LS-DYNA Study Descriptions

3. **ANSYS LS-DYNA Study Overview** 3–1
VME1 3–2
VME2 3–4
VME3 3–6
VME4 3–8
VME5 3–10
VME6 3–12

IV. NAFEMS Benchmarks

4. **NAFEMS Benchmarks Overview** 4–1
VMR027-3A 4–2
VMR027-3B 4–3
VMR027-4C 4–4
VMR027-5B 4–5
VMR027-6B 4–6
VMR027-10A 4–7
VMR027-10B 4–8
VMR027-10C 4–9
VMR027-12B 4–10
VMR027-12C 4–11
VMR049-CR1 4–12

VMR049-CR2 4–14
VMR049-CR3 4–15
VMR049-CR4 4–16
VMR049-CR5 4–17
VMR049-CR6 4–18
VMR049-PL1 4–19
VMR049-PL2 4–21
VMR049-PL3 4–23
VMR049-PL5 4–25
Index Index–1

List of Tables

2.1. Structural Solid Elements 2–3
2.2. Structural Shell Elements 2–4
2.3. Thermal Solid Elements 2–4
2.4. Analysis Type Coverage 2–4

Part I. Verification Test Case Descriptions

Chapter 1: Introduction

The ANSYS computer program is a large-scale multipurpose finite element program which may be used for solving several classes of engineering analyses. The analysis capabilities of ANSYS include the ability to solve static and dynamic structural analyses, steady-state and transient heat transfer problems, mode-frequency and buckling eigenvalue problems, static or time-varying magnetic analyses, and various types of field and coupled-field applications. The program contains many special features which allow nonlinearities or secondary effects to be included in the solution, such as plasticity, large strain, hyperelasticity, creep, swelling, large deflections, contact, stress stiffening, temperature dependency, material anisotropy, and radiation. As ANSYS has been developed, other special capabilities, such as substructuring, submodeling, random vibration, kinetostatics, kinetodynamics, free convection fluid analysis, acoustics, magnetics, piezoelectrics, coupled-field analysis and design optimization have been added to the program. These capabilities contribute further to making ANSYS a multipurpose analysis tool for varied engineering disciplines.

The ANSYS program has been in commercial use since 1970, and has been used extensively in the aerospace, automotive, construction, electronic, energy services, manufacturing, nuclear, plastics, oil, and steel industries. In addition, many consulting firms and hundreds of universities use ANSYS for analysis, research, and educational use. ANSYS is recognized worldwide as one of the most widely used and capable programs of its type.

The primary purpose of this manual is to demonstrate a wide range of ANSYS elements and capabilities in straightforward problems which have "classical" or readily-obtainable theoretical solutions. Furthermore, the close agreement of the ANSYS solutions to the theoretical results in this manual is intended to provide user confidence in the ANSYS solutions. An attempt has been made to include most element types and major solution capabilities of ANSYS in this set of test cases. These problems may then serve as the basis for additional validation and qualification of ANSYS capabilities by the user for specific applications that may be of interest.

The following *ANSYS Verification Manual* topics are available:

1.1. Program Overview
1.2. Program Verification
1.3. Finding Test Cases of Interest
1.4. Accessing Test Case Inputs
1.5. ANSYS Verification Manual Versus Other Manuals
1.6. ANSYS Verification Manual Contents
1.7. Theoretical Solutions
1.8. Test Case Selection and Method of Solution
1.9. Numerical Comparisons
1.10. References
1.11. Test Case Format
1.12. Symbols and Nomenclature
1.13. Memory Requirements and Run Times
1.14. Abbreviation, Element, and Product Lists

1.1. Program Overview

The ANSYS element library contains more than sixty elements for static and dynamic analyses, over twenty for heat transfer analyses, and includes numerous magnetic, field, and special purpose elements. This variety of elements allows the ANSYS program to analyze 2-D and 3-D frame structures, piping systems, 2-D plane and axisymmetric solids, 3-D solids, flat plates, axisymmetric and 3-D shells and nonlinear problems including contact (interfaces) and cables.

The input data for an ANSYS analysis are prepared using a preprocessor. The general preprocessor (PREP7) contains powerful solid modeling and mesh generation capabilities, and is also used to define all other analysis data

(geometric properties (real constants), material properties, constraints, loads, etc.), with the benefit of database definition and manipulation of analysis data. Parametric input, user files, macros and extensive online documentation are also available, providing more tools and flexibility for the analyst to define the problem. Extensive graphics capability is available throughout the ANSYS program, including isometric, perspective, section, edge, and hidden-line displays of 3-D structures, x-y graphs of input quantities and results, and contour displays of solution results.

A graphical user interface is available throughout the program, to guide new users through the learning process and provide more experienced users with multiple windows, pull-down menus, dialog boxes, tool bar, and online documentation.

The analysis results are reviewed using postprocessors, which have the ability to display distorted geometries, stress and strain contours, flow fields, safety factor contours, contours of potential field results (thermal, electric, magnetic), vector field displays mode shapes and time history graphs. The postprocessors can also be used for algebraic operations, database manipulations, differentiation, and integration of calculated results. Root-sum-square operations may be performed on seismic modal results. Response spectra may be generated from dynamic analysis results. Results from various loading modes may be combined for harmonically loaded axisymmetric structures.

1.2. Program Verification

ANSYS is continuously being verified by the developers (ANSYS, Inc.) as new capabilities are added to the program. The verification of the ANSYS program is conducted in accordance with written procedures that form a part of an overall Quality Assurance program at ANSYS, Inc. This manual represents a small subset of the Quality Assurance test case library which is used in full when testing new versions of ANSYS. This test library and the test cases in this manual represent comparisons of ANSYS solutions with known theoretical solutions, experimental results, or other independently calculated solutions.

The test cases explore the functionality of ANSYS in validated results. The test cases are based on published works in the disciplines of structures, dynamics, heat transfer, electromagnetics, and fluid flow. While the ANSYS solution to these test cases has been verified, some differences have been examined and are considered acceptable.

In order to solve some test cases, specific ANSYS products may be required. The test cases appropriate to each product can be determined from the following table. Most test cases can be solved within the limitations of the educational ANSYS product. The test case input listings are available through a hyperlink in the test description.

For ANSYS users who may have further need for formal verification of the program, ANSYS, Inc. has testing services available that allow automated testing of ANSYS on a customer's computer. The user is provided with input data, output data, comparator software, and procedures for automating the testing and reporting process. Readers interested in contracting for such services may contact the ANSYS, Inc. Quality Assurance Group.

1.3. Finding Test Cases of Interest

There are several possible methods of locating a test which contains topics of interest to the user. The Index topics display the related verification problem number. If you are using the online documentation, the verification problem numbers in Section 1.14.3: Index by Element Number are hyperlinks to each verification test case description. You can always do a text search while using the online documentation to find specific information. Finally, the code for each VM problem is contained in an appendix at the end of this manual.

1.4. Accessing Test Case Inputs

In the online help, the input file for each test case is linked to its description in each Overview section labeled "Input Listing." If you select the link, the test case input file appears in the browser window. The input listing may be printed.

To read an input listing into ANSYS, copy the input listing into a text editor, save it as a text file, then select **File>Read Input from...** on the ANSYS main menu to send the input to ANSYS. Nested macros may not function properly unless they are read from a file. Formatting commands will not function interactively if not read from a file.

Additionally, each test case input listing appears in Appendix A:, Verification Test Case Input Listings.

1.5. ANSYS Verification Manual Versus Other Manuals

The test cases in this manual are primarily intended for verification of the ANSYS program. An attempt has been made to include most significant analysis capabilities of the ANSYS program in this manual. Although they are valuable as demonstration problems, the test cases are not presented as step-by-step examples with lengthy data input instructions and printouts. Most users with limited finite element experience should be able to fill in the missing details by reviewing the finite element model and the input data listing with its accompanying comments. Problem sketches and modeling notes are included. The reader should refer to the online help and to this manual for complete input data instructions.

Users desiring more detailed instructions for solving problems or in-depth treatment of specific topics should refer to other ANSYS documentation as described in Guide to the ANSYS Documentation in the *ANSYS Commands Reference*. Introductory documentation such as the *ANSYS Tutorials* should be the first stop for new and existing users needing basic information on using the ANSYS program. Seminar notes on several broad topics are also available. These notes are written in a form designed for classroom instruction, and include theory, ANSYS implementation, exercises, and examples. Broad subjects such as dynamics, heat transfer, nonlinearities, magnetics, and optimization are covered in these notes. *ANSYS Tutorials* are also available for various specific topics. These publications focus on particular features or program areas, supplementing other ANSYS reference documents with theory, procedures, guidelines, examples, and references.

1.6. ANSYS Verification Manual Contents

The intent of this manual is to demonstrate the full scope of the analysis capability available in the ANSYS program. This manual will also assist new users of the ANSYS program in running compact test cases and for understanding basic capability. All report results and input listings correspond to ANSYS 10.0.

ANSYS Verification Manual test cases are available on the ANSYS 10.0 installation media provided to the customer in the **verif** subdirectory under the **data** directory. All test cases also appear in three appendixes at the end of this manual.

1.7. Theoretical Solutions

ANSYS is a program intended for solving practical engineering problems. Many theoretical problems are not realistic in that the assumptions necessary to obtain a closed-form analytical solution make the mathematical model depart from a practical application problem. Examples of these assumptions are: step force changes, step temperature changes, perfectly plastic impacts, infinitely rigid supports, etc. Imposing these conditions in a finite element analysis often requires more effort to duplicate the theoretical result than would be required to solve the "real world" problem.

Theoretical solutions are generally based on a continuous or differential approach. In some cases, an exact comparison with a finite-element solution would require an infinite number of elements and/or an infinite number of iterations separated by an infinitely small step size. Such a comparison is neither practical nor desirable.

The examples in this manual have been modeled to give reasonably accurate comparisons ("engineering accuracy") with a low number of elements and iterations. In some cases, even fewer elements and/or iterations will still yield an acceptable engineering accuracy. A survey of the results comparisons in this manual shows an average accuracy within 1-2% of the target solution.

1.8. Test Case Selection and Method of Solution

The problems solved in this manual and the method of solution were selected with verification as the primary objective. Some problems could have been solved more directly or in a manner other than the way presented. In some cases the same problem is solved in several different ways to demonstrate and verify other elements or capabilities of the program.

Since ANSYS is a program capable of solving very complicated practical engineering problems having no closed-form theoretical solutions, the relatively simple problems solved in this manual do not illustrate the full capability of the ANSYS program.

1.9. Numerical Comparisons

The ANSYS solutions in this manual are compared with solutions from textbooks or technical publications. In some cases noted below, the target (theoretical) answers reported in this manual may differ from those shown in the reference. Any problems having significantly different recalculated values are noted as such. Differences between ANSYS results and target values are reported as ratios (ANSYS:Target) except in cases where the target solution is zero or non-numerical in nature.

Some textbook solutions are based on slide rule accuracy. For example, the reference for problem number 3 reports the stress to be 10,200 psi. Using a hand calculator to recalculate the results shows the result to be 10,152.258 psi. The ANSYS calculation yields 10,152 psi. In problems like this, an appropriate number of significant digits are used in comparing solutions.

Some references have incorrect answers printed and some have incorrect equations. Reference's answers presented without regard to sign are reported with the appropriate sign. Theoretical derivations not having a specific numerical example in the text are solved for a representative numerical example and both the theoretical and ANSYS results are given. In cases where only the results but not the input data are given in the theoretical reference (for example, where only tabular or graphical results are presented), the input data are back-calculated from a convenient solution point. Graphical solution results are reported to an appropriate accuracy.

Different computers and different operating systems may yield slightly different results for some of the test cases in this manual, since numerical precision varies from machine to machine. Solutions which are nonlinear, iterative, have equally-valid alternatives for master degree of freedom selection (**TOTAL** command), or have convergence options activated, are among the most likely to exhibit machine-dependent numerical differences. Because of this, an effort has been made to report an appropriate and consistent number of significant digits in both the target and the ANSYS solution. If you run these test cases on your own computer hardware, be advised that an ANSYS result reported in this manual as 0.01234 may very well show up in your printout as 0.012335271.

It should be noted that only those items corresponding to the given theoretical solution values are reported for each problem. In most cases the same finite element solution also contains a considerable amount of other useful numerical solution data.

1.10. References

The textbooks and references used for the verification tests were chosen for several reasons. Well known and recognized textbooks were used whenever possible; other texts were used if they were readily available to the author. Periodical or technical journal references were used in instances where no textbook solutions could be found for an application of interest. The books should be available for purchase or through most engineering libraries. Periodicals are of the type normally available in university libraries. In most cases the reference listed is not the only source of the theory or of a similar sample problem.

1.11. Test Case Format

Test cases use the following format:

- A description of the test case, including the dimensions, loading, material properties, and other relevant data.
- Theoretical reference(s).
- Figures describing the problem, including either the ANSYS finite element model showing node and element locations, or the ANSYS "solid model," showing keypoints, line segments, areas and/or volumes (as applicable).
- Analysis assumptions, modeling notes, and comments.
- Target results, ANSYS results, and normalized ratio.
- ANSYS input data listing, including comments.
- Graphics displays of the results (optional).
- Additional information containing references to analysis guides with similar problems and other test cases using similar features (optional).

1.12. Symbols and Nomenclature

The majority of the nomenclature used in this manual follows what is considered commonly-used form. Exceptions and special circumstances are described when used. A few specific cases deserve definition, where many authors vary in their usage of nomenclature/symbols and there is no clear "standard."

In the text, vectors are shown by {A} or $\bar{A}$, the former being used primarily when symbolizing vector unknowns. Matrices are shown as [K], and |a| is used to denote absolute value. Natural logarithms use "ln" and base 10 logarithms are shown as "log".

In the figures, node and keypoint locations are denoted by • in the figures. Node numbers are unitalicized (1), keypoint numbers are shown italicized (*1*) and line numbers are shown italicized with prefix "L" (*L2*). Element numbers are enclosed with a circle , area numbers are enclosed with a box , and volume numbers are enclosed with a hexagon .

1.13. Memory Requirements and Run Times

The ANSYS program is supported on many different computers. Memory size, run time, and cost will vary from computer to computer. The test cases in this manual are small enough to require only a minimum memory size.

The test cases generally require a very short run time each, although some are somewhat larger and longer running to allow the inclusion of meaningful tests for some of the more advanced capabilities included in ANSYS.

The benchmark test cases in Section 2.1: Description of the Benchmark Studies are small to moderately-sized tests as well, but the run time for these is very dependent on the parameters chosen for the specific test.

1.14. Abbreviation, Element, and Product Lists

1.14.1. Abbreviation and Symbol List

Abbreviation	Explanation
a	Acceleration
A	Area, Vector magnetic potential, Amplitude
B	Magnetic flux density
B_r	Residual induction
c	Viscous damping constant, Specific heat
C	Thermal capacitance, Fluid conductance
d	Diameter
MDOF	Master Degrees of freedom (See Define Master Degrees of Freedom (for Modal Analysis) and Define Master Degrees of Freedom (for Transient Analysis) in *ANSYS Structural Analysis Guide*
E	Young's modulus of elasticity
f	Frequency of vibration, Friction factor
F	Force
g	Gravitational acceleration
G	Shear modulus
h	Average convection coefficient, Height
H	Magnetic field intensity
H_c	Coercive force
I	Moment of inertia, Electrical current
ITS	Integration time step
J	Torsional moment of inertia, Electrical current density
k	Spring constant, Thermal conductivity
KI	Stress intensity factor
ℓ	Length
L	Inductance, Length
m	Mass
M	Moment
Nu	Nusselt number
P, p	Pressure
Pr	Prandtl number
q	Heat flow rate
$\dddot{q}$	Heat generation rate
r	Radius

Abbreviation	Explanation
R	Electrical resistance, Reaction
Re	Reynolds number
t	Thickness, Time
T	Temperature
u	Displacement
V, v	Velocity, Voltage
w	Flow rate, Width
W	Weight
$\bar{y}$	Centroid location
α	Coefficient of thermal expansion, Thermal diffusivity
γ	Weight density
δ, Δ	Deflection
ε	Strain, Emissivity, Permittivity
ν	Poisson's ratio
Θ	Angle
ξ	Damping ratio
μ	Magnetic permeability, Viscosity, Coefficient of friction
ρ	Mass density, Electrical resistivity
σ_{yp}	Yield stress
τ	Period of vibration, Shear stress
ω	Circular frequency of vibration, Fluid flow rate, Angular velocity
σ	Electrical conductivity, direct stress

Other symbols and abbreviations are defined where used.

1.14.2. Units Abbreviation List

Abbreviation	Units
AbA	AbAmpere
A	Ampere
A	t-Ampere-turns
BTU	British Thermal Unit
cm	centimeter
°C	Centigrade
C	Coulomb
°F	Fahrenheit
F	Farad
ft	feet
G	Gauss
gm	gram
H	Henry

Abbreviation	Units
Hz	Hertz
hr	hour
in	inch
kg	Kilogram
kip	Kilopound (1000 pound force)
ksi	Kilopounds per square inch
m	meter
mm	millimeter
MPa	Megapascal
N	Newton
Oe	Oersted
Pa	Pascal
lb	pound force
psi	pounds per square inch
psig	pounds per square inch (gauge)
rad	radian
rpm	revolutions per minute
sec	second
S	Siemen
T	Tesla
W	Watt
Wb	Weber
Ω	Ohm

1.14.3. Index by Element Number

ANSYS Element and Keywords	Element Options	Test Cases
BEAM3 - 2-D Elastic Beam		
Static Structural		VM2, VM41, VM127, VM136, VM157, VM180
Eigenvalue Buckling	Stress Stiffening	VM127
Modal		VM50, VM52, VM61
Modal, Spectrum		VM70
Transient Dynamic		VM40, VM77
Coupled Field, Modal		VM177
BEAM4 - 3-D Elastic Beam		
Static Structural	Stress Stiffening	VM21
Static Structural		VM36, VM195
Static Structural, Modal	Stress Stiffening	VM59
Modal	Rotary Inertia	VM57

ANSYS Element and Keywords	Element Options	Test Cases
Transient Dynamic, Restart		VM179
Modal Spectrum, Harmonic		VM19
BEAM23 - 2-D Plastic Beam		
Static Structural		VM24, VM133
BEAM24 - 3-D Thin-Walled Plastic Beam		
Static Structural		VM134
BEAM44 - 3-D Elastic Tapered Unsymmetric Beam		
Tapered	Static Structural	VM34
BEAM54 - 2-D Elastic Tapered Unsymmetric Beam		
Static Structural		VM10
Static Structural	Offset - Y	VM14
Static Structural	Elastic Foundation	VM135
BEAM188 - 3-D Finite Strain Beam		
Static Structural		VM216, VM217VM239
Static Structural	Tapered Section	VM34
BEAM189 - 3-D Finite Strain Beam		
Static Structural		VM216, VM217
CIRCU94 - Piezoelectric Circuit		
Transient Piezoelectric - circuit		VM237
CIRCU124 - General Circuit Element		
Current Conduction, Static, Harmonic		VM117, VM207, VM208
Transient		VM226
CIRCU125 - Common or Zener Diode		
Transient		VM226
COMBIN7 - Revolute Joint		
Transient Dynamic	Stops	VM179
Static Structural	Stops	VM195
COMBIN14 - Spring-Damper		
Coupled Field	Longitudinal	VM171
Modal	Longitudinal	VM45, VM52, VM89, VM154
COMBIN37 - Control		
Steady-State Thermal		VM159
COMBIN39 - Nonlinear Spring		
Transient Dynamic		VM156
COMBIN40 - Combination		
Static Structural		VM36
Static Structural	Mass	VM69

ANSYS Element and Keywords	Element Options	Test Cases
Modal, Transient Dynamic	Mass	VM182
Modal, Spectrum	Mass	VM68
Modal, Harmonic Response	Mass	VM183
Transient Dynamic	Mass	VM9, VM79
Transient Dynamic	Mass, Friction	VM73
Transient Dynamic	Mass, Gap	VM81
Transient Dynamic	Mass, Damping, Gap	VM83
Transient Dynamic	Mass, Damping	VM71, VM72, VM74, VM75
Harmonic Response	Mass, Damping	VM86, VM88
Harmonic Response	Mass	VM87
CONTAC12 - 2-D Point-to-Point Contact		
Static Structural	Gap Size by Node Location	VM27
Static Structural	Friction, Nonzero Separated-Interface Stiffness	VM29
CONTAC52 - 3-D Point-to-Point Contact		
Static Structural	Gap Size by Node Location	VM27
CONTA171 - 2–D Surface-to-Surface Contact		
Static Structural		VM211
Thermal Structural Contact		VM229
CONTA172 - 2-D 3-Node Surface-to-Surface Contact		
Static Structural		VM211
CONTA173 - 3-D Surface-to-Surface Contact		
Static Structural		VM211
CONTA174 - 3-D 8-Node Surface-to-Surface Contact		
Static Structural		VM211
CONTA175 - 2-D/3-D Node-to-Surface Contact		
Static Structural, Transient Dynamic		VM191, VM201, VM65, VM23, VM64
CONTA178 - 3-D Node-to-Node Contact		
Static Structural		VM63
FLUID29 - 2-D Acoustic Fluid		
Coupled Field, Modal Analysis	Structure at Interface	VM177
Acoustics, Modal Analysis	No Structure at Interface	VM177
FLUID30 - 3-D Acoustic Fluid		
Coupled Field, Harmonic Response	Structure at Interface	VM177
Acoustics, Harmonic Response	No Structure at Interface	VM177
FLUID38 - Dynamic Fluid Coupling		

ANSYS Element and Keywords	Element Options	Test Cases
Modal		VM154
FLUID79 - 2-D Contained Fluid		
Fluid Flow		VM149
FLUID80 - 3-D Contained Fluid		
Fluid Flow		VM150
FLUID81 - Axisymmetric-Harmonic Contained Fluid		
Modal	Mode 1	VM154
FLUID116 - Thermal Fluid Pipe		
Fluid Flow		VM122
Steady-State Thermal		VM126
Fluid Flow	Flow Losses (Additional Length)	VM123
Fluid Flow	Flow Losses (Loss Coefficient) Pump Head	VM124
FLUID136 - 3-D Squeeze Film Fluid Element		
Harmonic		VM245
FLUID141 - 2-D Fluid-Thermal		
CFD Thermal	Axisymmetric	VM121
CFD Multispecies	Axisymmetric	VM209
CFD Non Newtonian	Axisymmetric	VM219
FLUID142 - 3-D Fluid-Thermal		
CFD, Thermal, Fluid Flow		VM178, VM46
HF119 - 3-D High Frequency Tetrahedral Solid		
Full Harmonic Magnetic		VM214
HF120 - 3-D High Frequency Brick Solid		
Mode-frequency Magnetic		VM212
Full Harmonic Magnetic		VM213
INFIN9 - 2-D Infinite Boundary		
Static Magnetic		VM188
Static Magnetic	AZ Degree of Freedom	VM165
INFIN47 - 3-D Infinite Boundary		
Static Magnetic		VM190
INFIN110 - 2-D Infinite Solid		
Electrostatic, Harmonic		VM49, VM120, VM206, VM207
INFIN111 - 3-D Infinite Solid		
Electrostatic		VM51
INTER115 - 3-D Magnetic Interface		
Static Magnetic		VM189
LINK1 - 2-D Spar (or Truss)		
Static Structural		VM1, VM3, VM4, VM11, VM27, VM194

ANSYS Element and Keywords	Element Options	Test Cases
Static Structural	Initial Strain	VM132
Modal		VM76
Transient Dynamic		VM80, VM84, VM85, VM156
Harmonic Response, Static Response, Modal		VM76
LINK10 -Tension-only (Chain) or Compression-only Spar		
Static Structural	Stress Stiffening	VM31
Static Structural, Modal	Stress Stiffening, Initial Strain	VM53
LINK11 - Linear Actuator		
Static Structural		VM195
LINK31 - Radiation Link		
Steady-State Thermal		VM106, VM107
LINK32 - 2-D Conduction Bar		
Steady-State Thermal		VM92, VM93, VM94,VM110, VM115, VM116, VM125, VM164
Static Magnetic	AUX12	VM147
LINK33 - 3-D Conduction Bar		
Steady-State Thermal		VM95, VM114
LINK34 - Convection Link		
Steady-State Thermal		VM92, VM94, VM95,VM97, VM107, VM109, VM110, VM159
Steady-State Thermal	Temperature-Dependent Film Coefficient	VM116
LINK68 -Thermal-Electric Line		
Current Conduction		VM117
Coupled Field	Multi-field Coupling	VM170
MASS21 - Structural Mass		
Static Structural		VM131
Modal		VM45, VM57, VM89
Modal	Rotary Inertia	VM47, VM48, VM52,VM57
Transient Dynamic		VM65, VM77, VM80,VM81, VM91, VM156
Harmonic Response		VM90
MASS71 - Thermal Mass		
Transient Thermal		VM109, VM159
MATRIX27 - Stiffness, Damping, or Mass Matrix		
Static Structural		VM41
MATRIX50 - Superelement (or Substructure)		
Static Structural, Substructure		VM141
Static Structural, Modal		VM153

ANSYS Element and Keywords	Element Options	Test Cases
Radiation Matrix Substructure	Steady-State Thermal, Substructural	VM125
Steady-State Thermal	AUX12	VM147
MPC184 - Multipoint Constraint Elements		
Static Structural		VM239, VM240
PIPE16 - Elastic Straight Pipe		
Structural		VM12, VM146
Modal		VM48, VM57
PIPE18 - Elastic Curved Pipe (Elbow)		
Static Structural	Static Structural	VM18
PIPE20 - Plastic Straight Pipe		
Static Structural		VM7
PIPE59 - Immersed Pipe or Cable		
Transient Dynamic	Tangential Drag	VM158
PLANE2 - 2-D 6-Node Triangular Structural Solid		
Static Structural, Substructure	Plane Stress with Thickness Input	VM141
Static Structural		VM142, VM180
Static Structural	Axisymmetric	VM63
Modal	Axisymmetric	VM181
PLANE13 - 2-D Coupled-Field Solid		
Coupled Field	Plane Strain with Multi-field Coupling	VM171
Coupled Field	Axisymmetric w/ AZ DOF and Multi-field Coupling	VM172
Coupled Field	Plane Stress with Multi-field Coupling	VM174
Harmonic Magnetic	AZ Degree of Freedom	VM166
Coupled Field	AZ and VOLT Degree of Freedom, Multi-field Coupling	VM185
Transient Magnetic	AZ Degree of Freedom	VM167
Coupled Field	AZ and VOLT Degree of Freedom, Multi-field Coupling	VM186
Static Magnetic	AZ Degree of Freedom	VM165
Coupled Field	Thermal-Structural Coupling	VM23
PLANE25 - 4-Node Axisymmetric-Harmonic Structural Solid		
Static Structural	Mode 1	VM43
Modal	Mode 0 and 2	VM67
PLANE35 - 2-D 6-Node Triangular Thermal Solid		
Steady-State Thermal	Axisymmetric	VM58
Steady-State Radiosity		VM228
PLANE42 - 2-D Structural Solid		
Static Structural	Plane Stress with Thickness Input	VM5, VM64, VM128, VM205

ANSYS Element and Keywords	Element Options	Test Cases
Static Structural	Plane Stress, Surface Stress Printout	VM5, VM16
Static Structural	Axisymmetric	VM32, VM38
Eigenvalue Buckling, Static Structural	Plane Stress with Thickness Input, Stress Stiffening	VM142, VM155, VM191
PLANE53 - 2-D 8-Node Magnetic Solid		
Static Magnetic, Harmonic		VM188, VM206, VM207, VM220
PLANE55 - 2-D Thermal Solid		
Steady-State Thermal	Axisymmetric	VM32, VM102
Transient Thermal	Axisymmetric	VM111
Steady-State Thermal	Axisymmetric, Analogous Flow Field	VM163
Steady-State Thermal		VM98, VM99, VM100,VM105, VM118, VM193
Transient Thermal		VM104, VM113
PLANE67 - 2-D Thermal-Electric Solid		
Coupled Field	Multi-field Coupling	VM119
PLANE75 - Axisymmetric-Harmonic Thermal Solid		
Steady-State Thermal	Mode 1	VM108
PLANE77 - 2-D 8-Node Thermal Solid		
Transient Thermal	Axisymmetric	VM112
Transient Thermal		VM28
Steady-State Radiosity		VM227
PLANE78 - Axisymmetric-Harmonic 8-Node Thermal Solid		
Steady-State Thermal	Mode 2	VM160
PLANE82 - 2-D 8-Node Structural Solid		
Static Structural	Surface Stress Printout	VM5
Static Structural	Axisymmetric	VM25, VM63
Static Structural, Substructuring	Plane Stress with Thickness	VM141
Static Structural	Shifted Midside Nodes	VM143
Static Structural	Plane Stress with Thickness	VM205
PLANE83 - 8-Node Axisymmetric-Harmonic Structural Solid		
Static Structural	Modes 0 and 1	VM140
PLANE121 - 2-D 8-Node Electrostatic Solid		
Electrostatic		VM49, VM120
PLANE145 - 2-D Quadrilateral Structural Solid p-Element		
Static Structural	Plane Stress with Thickness	VM141
PLANE146 - 2-D Triangular Structural Solid p-Element		
Static Structural, Submodeling		VM142
PLANE182 - 2-D Structural Solid		

ANSYS Element and Keywords	Element Options	Test Cases
Static Structural		VM191, VM201, VM211
Creep		VM224
PLANE183 - 2-D 8-Node Structural Solid		
Static Structural		VM56, VM201, VM211, VM243
Creep		VM224
PLANE223 - 2-D 8-Node Coupled-Field Solid		
Static and Transient Piezoelectric		VM237
Static Piezoresistive		VM238
PRETS179 - 2-D/3-D Pretension Solid		
Structural Static, Preload-ing		VM225
SHELL28 - Shear/Twist Panel		
Modal		VM202
SHELL41 - Membrane Shell		
Static Structural		VM20, VM153
Static Structural, Modal		VM153
SHELL43 - Plastic Shell		
Static Structural		VM7
Static Structural, Restart		VM26
SHELL51 - Axisymmetric Structural Shell		
Static Structural		VM13, VM15, VM22
Static Structural	Stress Stiffening, Large Deflection	VM137, VM138
Static Structural, Modal	Stress Stiffening	VM55
SHELL57 - Thermal Shell		
Steady-State Thermal		VM97, VM103
SHELL61 - Axisymmetric-Harmonic Structural Shell		
Static Structural	Mode 1	VM44
Modal, Static Structural	Mode 0, 1, and 2	VM152
Modal	Mode 0, 1, and 2	VM151
SHELL63 - Elastic Shell		
Static Structural		VM34, VM39, VM54,VM139
Static Structural	Snap-Through Buckling	VM17
Modal		VM54, VM62, VM66
Coupled Field, Harmonic Response		VM177
SHELL91 - 16-Layer Structural Shell		
Static Structural	Multi-layer, Interlaminar Shear Printout	VM35
SHELL93 - 8-Node Structural Shell		
Static Structural		VM6, VM42

ANSYS Element and Keywords	Element Options	Test Cases
Static Structural, Substructure		VM141
Modal, Spectrum	Integration Points Printout	VM203
SHELL99 - 100-Layer Structural Shell		
Static Structural	Multi-layer, Interlaminar Stresses, Failure Criterion	VM78
Static Structural	Multi-layer, Orthotropic Properties	VM82
Static Structural	Nodal Stress and Strain Printout, Multi-layer, Node Offset	VM144
Modal	Multi-layer	VM60
SHELL150 - 8-Node Structural Shell p-Element		
Static Structural		VM6
SHELL157 - Coupled Thermal-Electric Shell		
Coupled-Field		VM215
SHELL181 - Finite Strain Shell		
Static Structural		VM242, VM244
Static, Large Deflection		VM26, VM218
SHELL208 - 2-Node Finite Strain Axisymmetric Shell		
Static, Large Deflection		VM218
SOLID5 - 3-D Coupled-Field Solid		
Coupled Field	Multi-field Coupling	VM173
Static Structural	Displacement Field	VM184, VM187
Coupled Field, Modal	Multi-field Coupling, Anisotropic Material Properties	VM175
Coupled Field, Harmonic Response	Multi-field Coupling, Anisotropic Material Properties	VM176
Coupled Field, Modal	Multi-field Coupling	VM33, VM170
Coupled Field	MAG Degree of Freedom	VM168
Static Structural	Multi-field Coupling	VM173
SOLID45 - 3-D Structural Solid		
Static Structural		VM7, VM37, VM143, VM191, VM196
Static Structural	Generalized Plane Strain	VM38
SOLID46 - 3-D Layered Structural Solid		
Static Structural	Multi-layer, Orthotropic Properties	VM82
Static Structural	Nodal Stress and Strain Printout, Multi-layer, Node Offset	VM144
SOLID62 - 3-D Magneto-Structural Solid		
Coupled Field		VM172
SOLID64 - 3-D Anisotropic Structural Solid		
Static Structural	Material Matrix	VM145
SOLID65 - 3-D Reinforced Concrete Solid		

ANSYS Element and Keywords	Element Options	Test Cases
Static Structural	Cracking	VM146
SOLID69 - 3-D Thermal-Electric Solid		
Coupled Field		VM119
SOLID70 - 3-D Thermal Solid		
Steady-State Thermal		VM95, VM101, VM118
Transient Thermal		VM192
SOLID87 - 3-D 10-Node Tetrahedral Thermal Solid		
Steady-State Thermal		VM96
SOLID90 - 3-D 20-Node Thermal Solid		
Steady-State Thermal		VM161, VM162
SOLID92 - 3-D 10-Node Tetrahedral Structural Solid		
Static Structural		VM184, VM187
SOLID95 - 3-D 20-Node Structural Solid		
Static Structural		VM143, VM148, VM210
SOLID96 - 3-D Magnetic-Scalar Solid		
Harmonic Response	CMVP Formulation	VM189
SOLID97 - 3-D Magnetic Solid		
Coupled Field		VM172, VM189
SOLID98 - Tetrahedral Coupled-Field Solid		
Static Structural	Displacement Field	VM184, VM187
Static Magnetic	MAG Degree of Freedom	VM169, VM190
SOLID117 - 3-D 20-Node Magnetic Solid		
Static Magnetic		VM241
SOLID122 - 3-D 20-Node Electrostatic Solid		
Electrostatic		VM51
SOLID147 - 3-D Brick Structural Solid p-Element		
Static Structural		VM184
SOLID148 - 3-D Tetrahedral Structural Solid p-Element		
Static Structural		VM187
SOLID185 - 3-D 8-Node Structural Solid		
Static Structural		VM56, VM143, VM191, VM196, VM201, VM211, VM225, VM240, VM244, VM246
SOLID186 - 3-D 20-Node Structural Solid		
Static Structural		VM56, VM143, VM148, VM210, VM211, VM244, VM246
SOLID187 - 3-D 10-Node Tetrahedral Structural Solid		
Static Structural		VM184, VM187, VM244, VM246
SOLID191 - 3-D 20-Node Layered Structural Solid		
Static Structural	Nodal Stress and Strain Printout, Multi-layer, Node Offset	VM144
SOLSH190 - 3-D Structural Solid Shell		

ANSYS Element and Keywords	Element Options	Test Cases
Static Structural		VM54, VM139, VM143
Modal		VM54, VM66
SOURC36 - Current Source		
Static Magnetic		VM190
SURF151 - 2-D Thermal Surface Effect		
Steady-State Thermal	AUX12	VM147
SURF152 - 3-D Thermal Surface Effect		
Static Structural	No Midside Nodes	VM192
SURF153 - 2-D Structural Surface Effect		
Static Structural	Axisymmetric, No Midside Nodes	VM38
SURF154 - 3-D Structural Surface Effect		
Static Structural	Axisymmetric, No Midside Nodes	VM38
TARGE169 - 2-D Target Segment		
Static Structural		VM211, VM191
Thermal Structural Contact		VM229
TARGE170 - 3-D Target Segment		
Static Structural		VM211
VISCO88 - 2-D 8-Node Viscoelastic Solid		
Static Structural	Axisymmetric	VM200
VISCO89 - 3-D 20-Node Viscoelastic Solid		
Static Structural		VM200
VISCO106 - 2-D Large Strain Solid		
Static Structural	Rate-independent Viscoplasticity	VM198
Static Structural	Rate-dependent Viscoplasticity	VM199
VISCO107 - 3-D Large Strain Solid		
Static Structural	Rate-independent Viscoplasticity	VM198
Static Structural	Rate-dependent Viscoplasticity	VM199
VISCO108 - 2-D 8-Node Large Strain Solid		
Static Structural	Rate-independent Viscoplasticity	VM198
Static Structural	Rate-dependent Viscoplasticity	VM199

VM1: Statically Indeterminate Reaction Force Analysis

Overview

Reference:	S. Timoshenko, *Strength of Material, Part I, Elementary Theory and Problems*, 3rd Edition, D. Van Nostrand Co., Inc., New York, NY, 1955, pg. 26, problem 10.
Analysis Type(s):	Static Analysis (**ANTYPE** = 0)
Element Type(s):	2-D Spar (or Truss) Elements (LINK1)
Input Listing:	vm1.dat

Test Case

A prismatic bar with built-in ends is loaded axially at two intermediate cross-sections by forces F_1 and F_2. Determine the reaction forces R_1 and R_2.

Figure 1.1 Prismatic Bar Problem Sketch

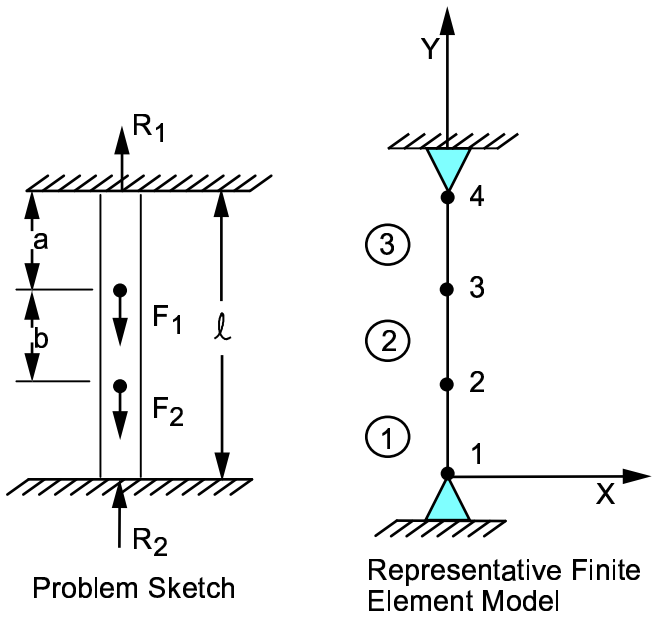

Material Properties	Geometric Properties	Loading
$E = 30 \times 10^6$ psi	$\ell = 10$ in. $a = b = 0.3\ \ell$	$F_1 = 2F_2 = 1000$ lb

Analysis Assumptions and Modeling Notes

Nodes are defined where loads are to be applied. Since stress results are not to be determined, a unit cross-sectional area is arbitrarily chosen.

Results Comparison

	Target	ANSYS	Ratio
R_1, lb	900.0	900.0	1.000

	Target	ANSYS	Ratio
R_2 , lb	600.0	600.0	1.000

VM2: Beam Stresses and Deflections

Overview

Reference:	S. Timoshenko, *Strength of Material, Part I, Elementary Theory and Problems*, 3rd Edition, D. Van Nostrand Co., Inc., New York, NY, 1955, pg. 98, problem 4.
Analysis Type(s):	Static Analysis (**ANTYPE** = 0)
Element Type(s):	2-D Elastic Beam Elements (BEAM3)
Input Listing:	vm2.dat

Test Case

A standard 30" WF beam, with a cross-sectional area A, is supported as shown below and loaded on the overhangs by a uniformly distributed load w. Determine the maximum bending stress σ in the middle portion of the beam and the deflection δ at the middle of the beam.

Figure 2.1 Beam with Cross Section Problem Sketch

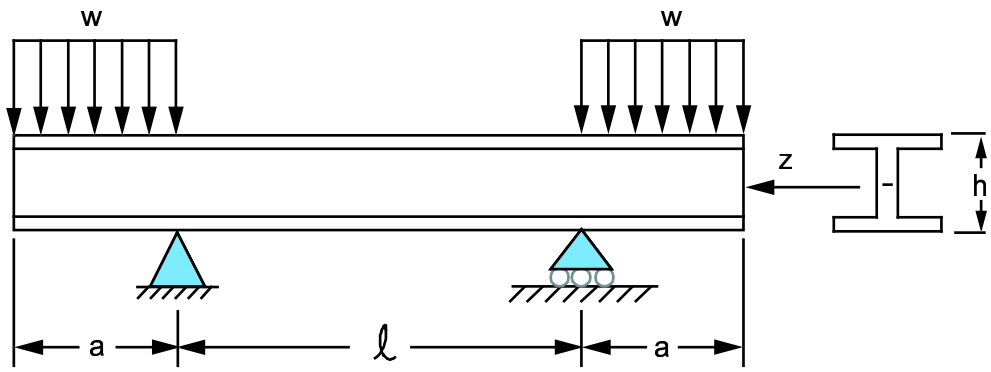

Problem Sketch

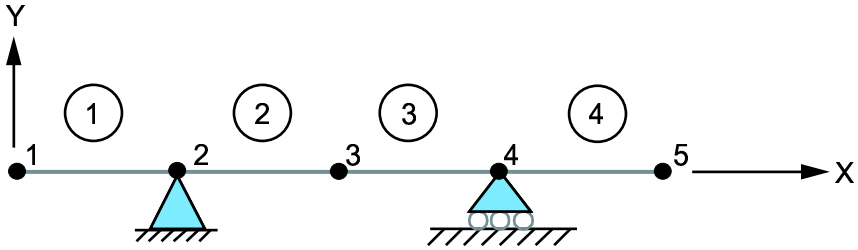

Representative Finite Element Model

Material Properties	Geometric Properties	Loading
E = 30 x 10^6 psi	ℓ = 20 ft = 240 in. a = 10 ft = 120 in. h = 30 in. A = 50.65 in^2 I_z = 7892 in^4	w = 10000 lb/ft = (10000/12) lb/in

Analysis Assumptions and Modeling Notes

Consistent length units (inches) are used. A half-model could also have been used because of symmetry.

Results Comparison

	Target	ANSYS	Ratio
Stress, psi	-11,400	-11,404	1.000
Deflection, in	0.182	0.182	1.003

1. occurs at the bottom flange of the beam

Figure 2.2 Displaced Geometry Display

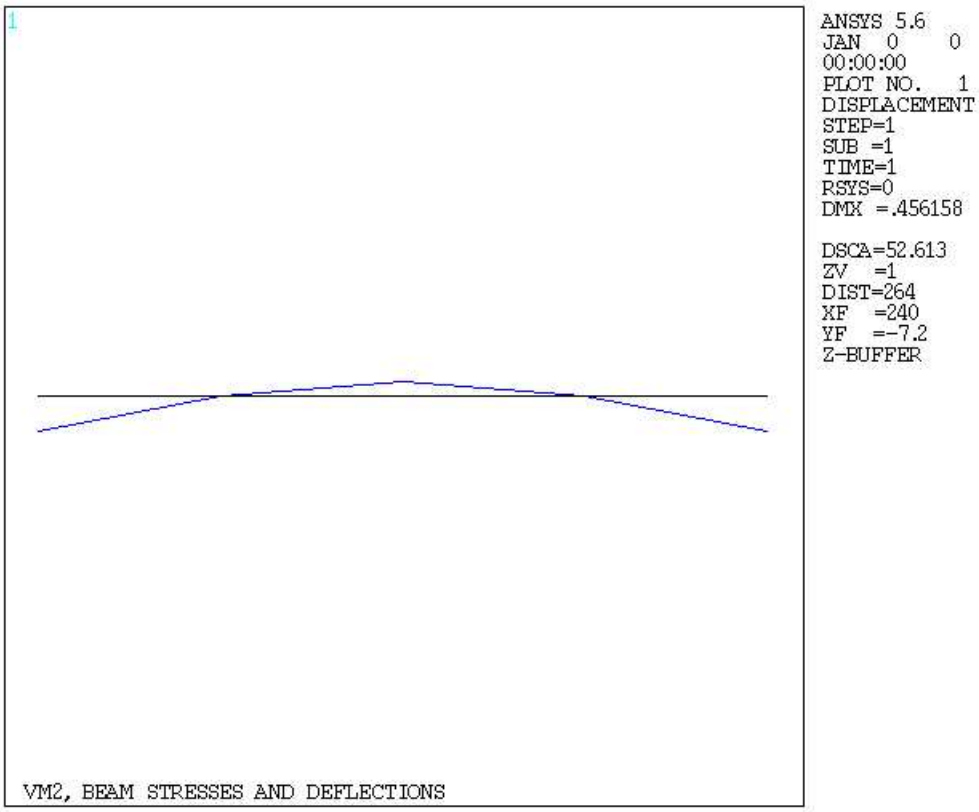

VM3: Thermally Loaded Support Structure

Overview

Reference:	S. Timoshenko, *Strength of Material, Part I, Elementary Theory and Problems*, 3rd Edition, D. Van Nostrand Co., Inc., New York, NY, 1955, pg. 30, problem 9.
Analysis Type(s):	Static, Thermal Stress Analysis (**ANTYPE** = 0)
Element Type(s):	2-D Spar (or Truss) Elements (LINK1)
Input Listing:	vm3.dat

Test Case

Find the stresses in the copper and steel wire structure shown below. The wires have a cross-sectional area of A. The structure is subjected to a load Q and a temperature rise of ΔT after assembly.

Figure 3.1 Support Structure Problem Sketch

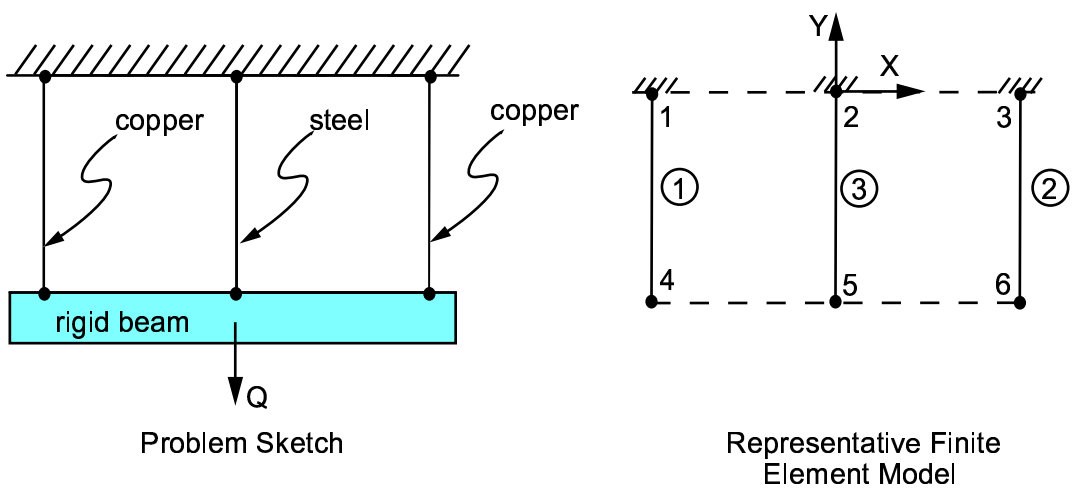

Material Properties	**Geometric Properties**	**Loading**
$E_c = 16 \times 10^6$ psi $\alpha_c = 92 \times 10^{-7}$ in/in-°F $E_s = 30 \times 10^6$ psi $\alpha_s = 70 \times 10^{-7}$ in/in-°F	$A = 0.1$ in^2	Q = 4000 lb $\Delta T = 10$°F

Analysis Assumptions and Modeling Notes

Length of wires (20 in.), spacing between wires (10 in.), and the reference temperature (70°F) are arbitrarily selected. The rigid lower beam is modeled by nodal coupling.

Results Comparison

	Target	ANSYS	Ratio
Stress in steel, psi	19,695.	19,695.	1.000
Stress in copper, psi	10,152.	10,152.	1.000

VM4: Deflection of a Hinged Support

Overview

Reference:	S. Timoshenko, *Strength of Material, Part I, Elementary Theory and Problems*, 3rd Edition, D. Van Nostrand Co., Inc., New York, NY, 1955, pg. 10, problem 2.
Analysis Type(s):	Static Analysis (**ANTYPE** = 0)
Element Type(s):	2-D Spar (or Truss) Elements (LINK1)
Input Listing:	vm4.dat

Test Case

A structure consisting of two equal steel bars, each of length ℓ and cross-sectional area A, with hinged ends is subjected to the action of a load F. Determine the stress, σ, in the bars and the deflection, δ, of point 2. Neglect the weight of the bars as a small quantity in comparison with the load F.

Figure 4.1 Hinged Support Problem Sketch

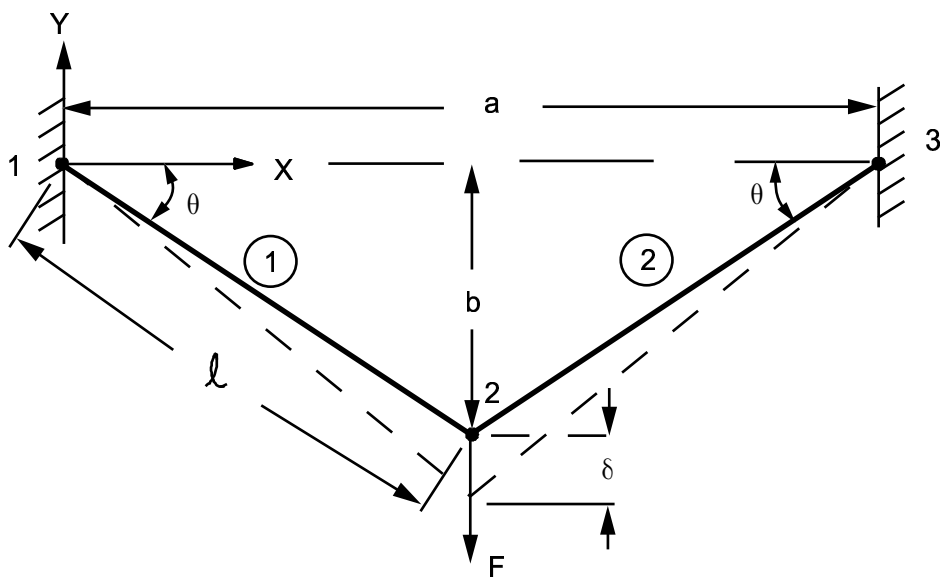

Problem Model

Material Properties	Geometric Properties	Loading
E = 30 x 10^6 psi	ℓ = 15 ft A = .05 in Θ = 30°	F = 5000 lb

Analysis Assumptions and Modeling Notes

Consistent length units are used. The dimensions a and b are calculated parametrically in the input as follows: a = 2 ℓ cos Θ, b = ℓ sin Θ.

Results Comparison

	Target	ANSYS	Ratio
Stress, psi	10,000.	10,000.	1.000
Deflection, in	-0.120	-0.120	1.000

VM5: Laterally Loaded Tapered Support Structure

Overview

Reference:	S. H. Crandall, N. C. Dahl, *An Introduction to the Mechanics of Solids*, McGraw-Hill Book Co., Inc., New York, NY, 1959, pg. 342, problem 7.18.
Analysis Type(s):	Static Analysis (**ANTYPE** = 0)
Element Type(s):	2-D Structural Solid Elements (PLANE42) 2-D 8-Node Structural Solid Elements (PLANE82)
Input Listing:	vm5.dat

Test Case

A cantilever beam of thickness t and length ℓ has a depth which tapers uniformly from d at the tip to 3d at the wall. It is loaded by a force F at the tip, as shown. Find the maximum bending stress at the mid-length (X = ℓ) and the fixed end of the beam.

Figure 5.1 Cantilever Beam Problem Sketch

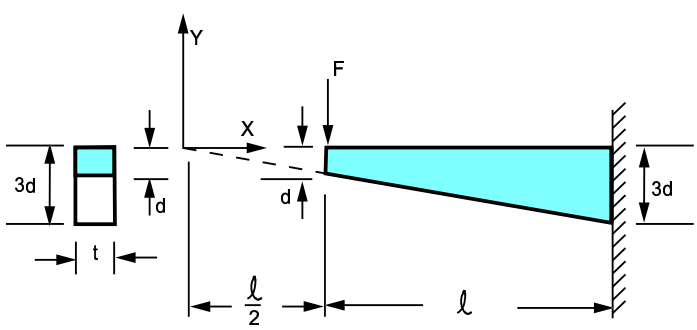

Material Properties	Geometric Properties	Loading
E = 30 x 10^6 psi υ = 0.0	ℓ = 50 in d = 3 in t = 2 in	F = 4000 lb

The PLANE82 model uses the same node numbering at the element corners as the PLANE42 model and has additional midside nodes added to all elements.

Analysis Assumptions and Modeling Notes

Two different solutions are obtained. The first solution uses lower order PLANE42 elements and the second solution uses higher order PLANE82 elements. The 2 inch thickness is incorporated by using the plane stress with thickness option. Poisson's ratio is set to 0.0 to agree with beam theory.

Results Comparison

		Target	ANSYS	Ratio
PLANE42	at mid-length stress, psi	8,333.	8,163.656	.980
	at fixed end stress, psi	7,407.	7,151.096	.965
PLANE82	at mid-length stress, psi	8,333.	8,363.709	1.004

	at fixed end stress, psi	7,407.	7,408.980	1.000

Figure 5.2 Displacement Display

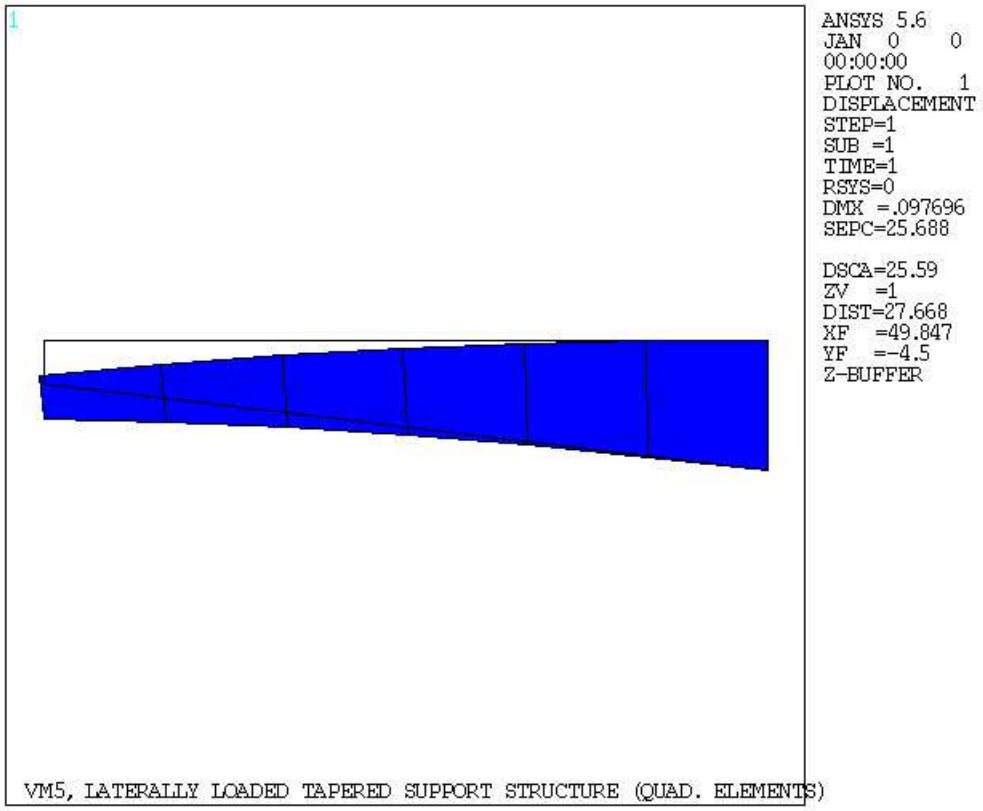

VM6: Pinched Cylinder

Overview

Reference:	R. D. Cook, *Concepts and Applications of Finite Element Analysis*, 2nd Edition, John Wiley and Sons, Inc., New York, NY, 1981, pp. 284-287. H. Takemoto, R. D. Cook, "Some Modifications of an Isoparametric Shell Element", *International Journal for Numerical Methods in Engineering*, Vol. 7 No. 3, 1973.
Analysis Type(s):	Static Analysis (**ANTYPE** = 0)
Element Type(s):	8-Node Shell Elements (SHELL93) 8-Node Structural Shell p-element (SHELL150)
Input Listing:	vm6.dat

Test Case

A thin-walled cylinder is pinched by a force F at the middle of the cylinder length. Determine the radial displacement δ at the point where F is applied. The ends of the cylinder are free edges.

Figure 6.1 Pinched Cylinder Problem Sketch

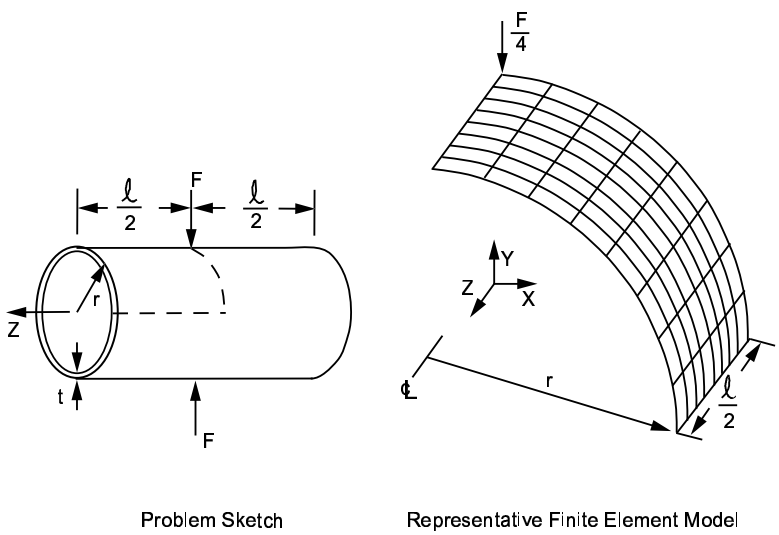

Material Properties	Geometric Properties	Loading
E = 10.5 x 10^6 psi υ = 0.3125	ℓ = 10.35 in r = 4.953 in t = 0.094 in	F = 100 lb

Analysis Assumptions and Modeling Notes

A one-eighth symmetry model is used. One-fourth of the load is applied due to symmetry.

Results Comparison

	Target[1]	ANSYS	Ratio
Deflection, in SHELL93	0.1139	0.1138	0.999

	Target[1]	ANSYS	Ratio
Deflection, in SHELL150	0.1139	0.1149	1.009

1. H. Takemoto, R. D. Cook, “Some Modifications of an Isoparametric Shell Element”.

VM7: Plastic Compression of a Pipe Assembly

Overview

Reference:	S. H. Crandall, N. C. Dahl, *An Introduction to the Mechanics of Solids*, McGraw-Hill Book Co., Inc., New York, NY, 1959, pg. 180, ex. 5.1.
Analysis Type(s):	Static, Plastic Analysis (**ANTYPE** = 0)
Element Type(s):	Plastic Straight Pipe Element (PIPE20) 3-D Structural Solid Elements (SOLID45) 2-D Plastic Large Strain Shell Elements (SHELL43)
Input Listing:	vm7.dat

Test Case

Two coaxial tubes, the inner one of 1020 CR steel and cross-sectional area A_s, and the outer one of 2024-T4 aluminum alloy and of area A_a, are compressed between heavy, flat end plates, as shown below. Determine the load-deflection curve of the assembly as it is compressed into the plastic region by an axial displacement. Assume that the end plates are so stiff that both tubes are shortened by exactly the same amount.

Figure 7.1 Pipe Assembly Problem Sketch

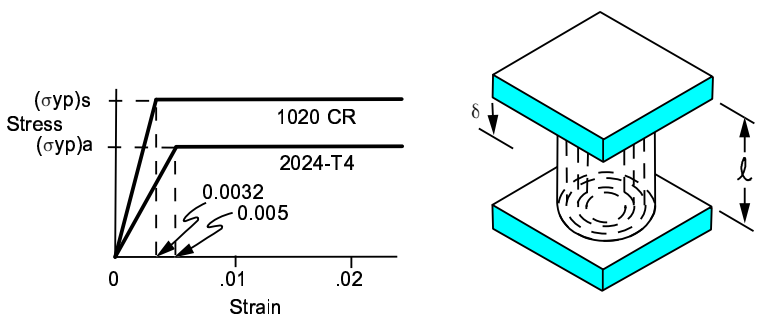

Stress - Strain Curve

Problem Sketch

Figure 7.2 Pipe Assembly Finite Element Models

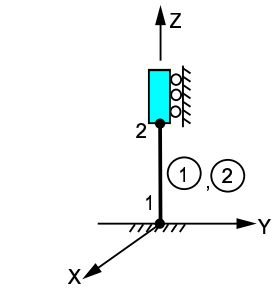

Representative Finite Element Model - PIPE20

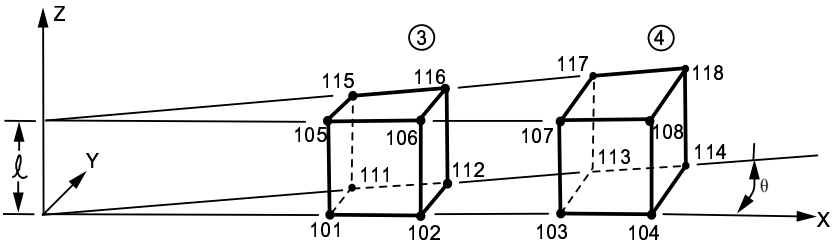

Representative Finite Element Model - SOLID45

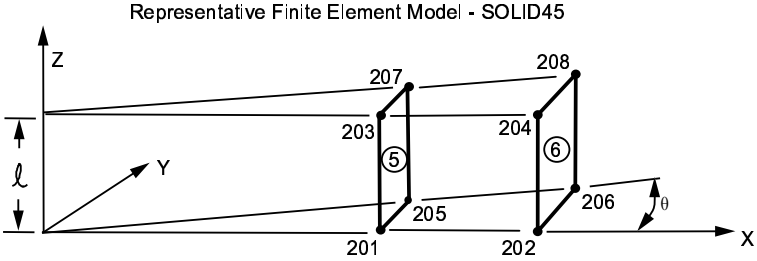

Representative Finite Element Model - SHELL43

Material Properties	Geometric Properties	Loading
E_s = 26,875,000 psi $\sigma_{(yp)s}$ = 86,000 psi E_a = 11,000,000 psi $\sigma_{(yp)a}$ = 55,000 psi υ = 0.3	ℓ = 10 in A_s = 7 in^2 A_a = 12 in^2	1st Load Step: δ = 0.032 in 2nd Load Step: δ = 0.05 in 3rd Load Step: δ = 0.10 in

Analysis Assumptions and Modeling Notes

The following tube dimensions, which provide the desired cross-sectional areas, are arbitrarily chosen. Inner (steel) tube: inside radius = 1.9781692 in., wall thickness = 0.5 in. Outer (aluminum) tube: inside radius = 3.5697185 in., wall thickness = 0.5 in.

The problem can be solved in one of three ways:

- using PIPE20 - the plastic straight pipe element
- using SOLID45 - the 3-D structural solid element
- using SHELL43 - the 2-D plastic large strain shell element

In the SOLID45 and SHELL43 cases, since the problem is axisymmetric, only a one element Θ-sector is modeled. A small angle Θ = 6° is arbitrarily chosen to reasonably approximate the circular boundary with straight sided elements. The nodes at the boundaries have the UX (radial) degree of freedom coupled. In the SHELL43 model, the nodes at the boundaries additionally have the ROTY degree of freedom coupled.

An ANSYS warning message is issued stating that element 1, (PIPE20 pipe element) has a radius to thickness ratio less than 5. Because the model involves only axial loading, this does not affect the accuracy of the results.

Results Comparison

		Target	ANSYS[1]	Ratio
PIPE20	Load, lb for Deflection = 0.032 in	1,024,400	1,024,400	1.000
	Load, lb for Deflection = 0.05 in	1,262,000	1,262,000	1.000
	Load, lb for Deflection = 0.1 in	1,262,000	1,262,000	1.000
SOLID45	Load, lb for Deflection = 0.032 in	1,024,400	1,022,529	0.998
	Load, lb for Deflection = 0.05 in	1,262,000	1,259,695	0.998
	Load, lb for Deflection = 0.1 in	1,262,000	1,259,695	0.998

1. From POST1 FSUM of bottom nodal forces (ΣFZ).

		Target	ANSYS[1]	Ratio
SHELL43	Load, lb for Deflection = 0.032 in	1,024,400	1,023,932	1.000
	Load, lb for Deflection = 0.05 in	1,262,000	1,261,423	1.000
	Load, lb for Deflection = 0.1 in	1,262,000	1,261,423	1.000

1. From POST1 FSUM of bottom nodal forces (ΣFZ) X 360°/6°(Identified as parameter "LOAD").

VM8: Parametric Calculation of Point-to-Point Distances

Overview

Reference:	Any Basic Geometry Text
Analysis Type(s):	Parametric Arithmetic
Element Type(s):	None
Input Listing:	vm8.dat

Test Case

Write a user file macro to calculate the distance *d* between either nodes or keypoints in PREP7. Define abbreviations for calling the macro and verify the parametric expressions by using the macro to calculate the distance between nodes N_1 and N_2 and between keypoints K_3 and K_4.

Figure 8.1 Parametric Calculation Problem Sketch

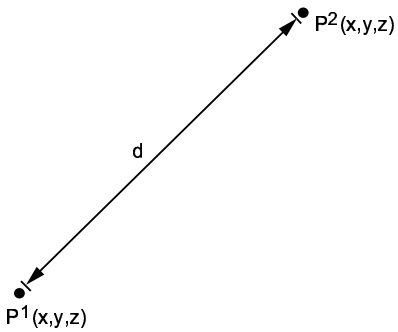

Geometric Properties
N_1 (x, y, z) = 1.5,2.5,3.5
N_2 (x, y, z) = -3.7,4.6,-3
K_3 (x, y, z) = 100,0,30
K_4 (x, y, z) = -200,25,80

Analysis Assumptions and Modeling Notes

The user file is created by the ***CREATE** command within the run. In normal use, this file would most likely already exist locally. Colons are used in the user file to create non-echoing comments (the colon character specifies a branching label in ANSYS). The active coordinate system is saved and restored within the macro to ensure Cartesian coordinates in the distance calculations and to re-establish the active coordinate system after the macro is used. Lowercase input is used throughout. Input case is preserved by ANSYS where appropriate (system-dependent).

Results Comparison

	Target	ANSYS	Ratio
N_1 - N_2 distance (LEN2)	8.5849	8.5849	1.000
K_3 - K_4 distance (LEN1)	305.16	305.16	1.000

VM9: Large Lateral Deflection of Unequal Stiffness Springs

Overview

Reference:	G. N. Vanderplaats, *Numerical Optimization Techniques for Engineering Design with Applications*, McGraw-Hill Book Co., Inc., New York, NY, 1984, pp. 72-73, ex. 3-1.
Analysis Type(s):	Nonlinear Transient Dynamic Analysis (**ANTYPE** = 4)
Element Type(s):	Spring-Damper Elements (COMBIN14) Combination Elements (COMBIN40)
Input Listing:	vm9.dat

Test Case

A two-spring system is subjected to a force F as shown below. Determine the strain energy of the system and the displacements δ_x and δ_y.

Figure 9.1 Unequal Stiffness Springs Problem Sketch

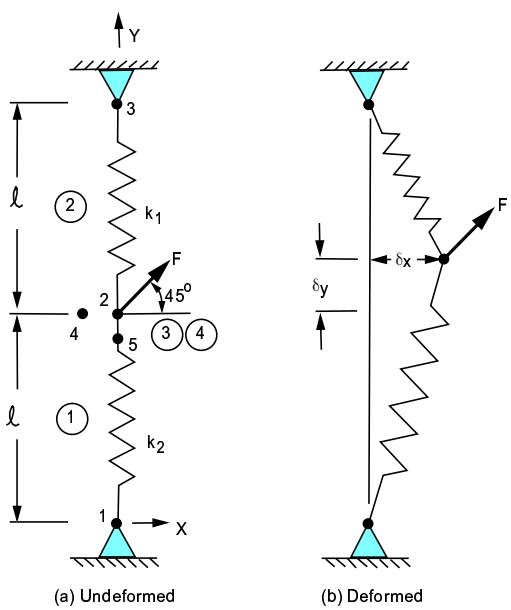

Geometric Properties	Loading
ℓ = 10 cm k_1 = 8 N/cm k_2 = 1 N/cm m = 1	$F = 5\sqrt{2}$ N

Analysis Assumptions and Modeling Notes

The solution to this problem is best obtained by adding mass and using the "slow dynamics" technique with approximately critical damping. Combination elements (COMBIN40) are used to provide damping in the X and Y directions. Approximate damping coefficients c_x and c_y, in the x and y directions respectively, are determined from

$$c_x = 2\sqrt{k_x m}, c_y = 2\sqrt{k_y m}$$

where m is arbitrarily assumed to be unity. k_x and k_y cannot be known before solving so are approximated by $k_y = k_2 = 1$ N/cm and $k_x = k_y/2 = 0.5$ N/cm, hence $c_x = 1.41$ and $c_y = 2.0$. Large deflection analysis is performed due to the fact that the resistance to the load is a function of the deformed position. POST1 is used to extract results from the solution phase.

Results Comparison

	Target	ANSYS	Ratio
Strain Energy, N-cm	24.01	24.02	1.000
Deflection_x , cm	8.631	8.633	1.000
Deflection_y , cm	4.533	4.533	1.000

VM10: Bending of a Tee-Shaped Beam

Overview

Reference:	S. H. Crandall, N. C. Dahl, *An Introduction to the Mechanics of Solids*, McGraw-Hill Book Co., Inc., New York, NY, 1959, pg. 294, ex. 7.2.
Analysis Type(s):	Static Analysis (**ANTYPE** = 0)
Element Type(s):	2-D Elastic Tapered Unsymmetric Beam Element (BEAM54)
Input Listing:	vm10.dat

Test Case

Find the maximum tensile and compressive bending stresses in an unsymmetric T beam subjected to uniform bending M_z, with dimensions and geometric properties as shown below.

Figure 10.1 Tee-Shaped Beam Problem Sketch

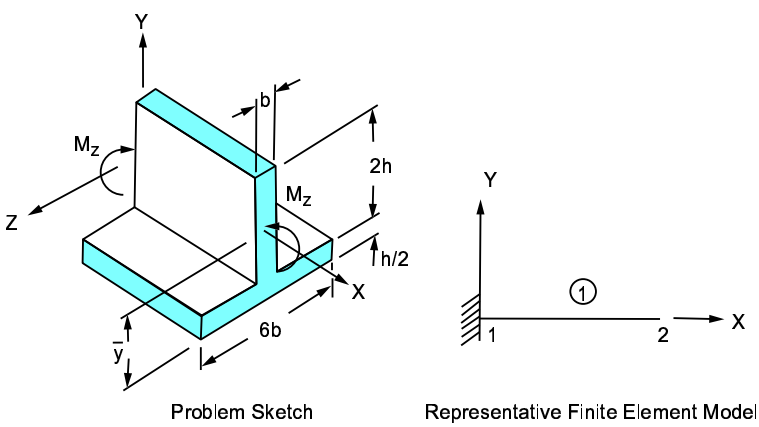

Material Properties	Geometric Properties	Loading
$E = 30 \times 10^6$ psi	b = 1.5 in h = 8 in $\bar{y}$ = 6 in Area = 60 in^2 $I_z = 2000\ in^4$	M_z = 100,000 in-lb

Analysis Assumptions and Modeling Notes

A length of 100 in. is arbitrarily selected since the bending moment is constant. Distances from the centroid ($\bar{y}$) to the top and bottom of the beam are calculated as 14 in. and 6 in. respectively.

Results Comparison

	Target	ANSYS	Ratio
$Stress_{BEND,Bot}$, psi	300.	300.	1.00
$Stress_{BEND,Top}$, psi	-700.	-700.	1.00

VM11: Residual Stress Problem

Overview

Reference:	S. H. Crandall, N. C. Dahl, *An Introduction to the Mechanics of Solids*, McGraw-Hill Book Co., Inc., New York, NY, 1959, pg. 234, problem 5.31.
Analysis Type(s):	Static, Plastic Analysis (**ANTYPE** = 0)
Element Type(s):	2-D Spar (or Truss) Elements (LINK1)
Input Listing:	vm11.dat

Test Case

A chain hoist is attached to the ceiling through three tie rods as shown below. The tie rods are made of cold-rolled steel with yield strength σ_{yp} and each has an area A. Find the deflection δ at load F_1 when the deflections are elastic in all three rods. When the frame is loaded to F_2 (where all three rods become fully plastic), and then unloaded, find the residual stress σ_r in the central rod.

Figure 11.1 Residual Stress Problem Sketch

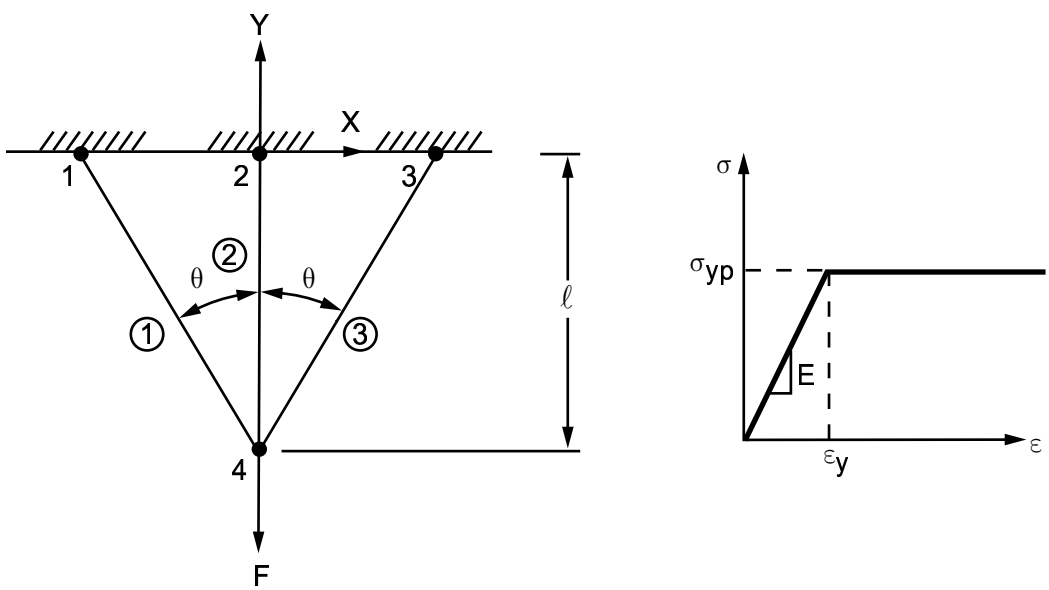

Problem Model

Stress-Strain Curve

Material Properties	Geometric Properties	Loading
σ_{yp} = 30,000 psi E = 30 x 10^6 psi	A = 1 in^2 ℓ = 100 in Θ = 30°	F_1 = 51,961.5 lb F_2 = 81,961.5 lb

Note — F_1 and F_2 values are back-calculated from theoretical relationships.

Analysis Assumptions and Modeling Notes

Automatic load stepping (**AUTOTS**,ON) is used to obtain the nonlinear plastic solution (load steps 2 and 3).

Results Comparison

	Target	ANSYS	Ratio
Deflection at F_1 , in	-0.07533	-0.07534	1.000
$Stress_r$, psi	-5,650.	-5,650.[1]	1.000

1. SAXL in element solution printout for element 2.

VM12: Combined Bending and Torsion

Overview

Reference:	S. Timoshenko, *Strength of Material, Part I, Elementary Theory and Problems*, 3rd Edition, D. Van Nostrand Co., Inc., New York, NY, 1955, pg. 299, problem 2.
Analysis Type(s):	Static Analysis (**ANTYPE** = 0)
Element Type(s):	Elastic Straight Pipe Element (PIPE16)
Input Listing:	vm12.dat

Test Case

A vertical bar of length ℓ is subjected to the action of a horizontal force F acting at a distance d from the axis of the bar. Determine the maximum principal stress σ_{max} and the maximum shear stress τ_{max} in the bar.

Figure 12.1 Combined Bending and Torsion Problem Sketch

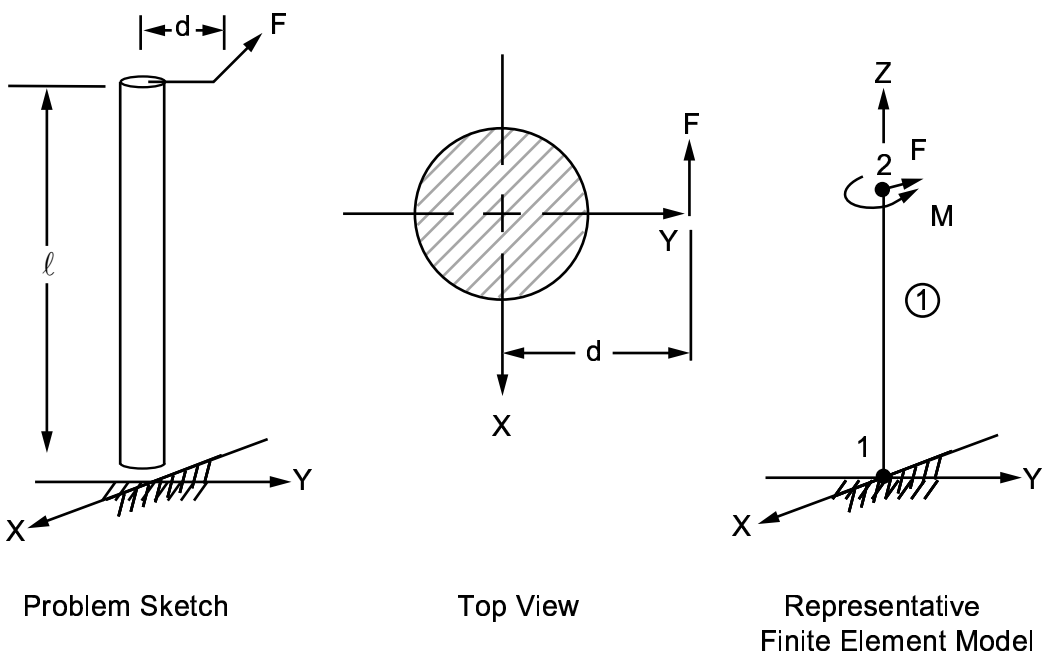

Material Properties	Geometric Properties	Loading
E = 30 x 10^6 psi υ = 0.3	ℓ = 25 ft d = 3 ft Section modulus (I/c) = 10 in^3	F = 250 lb M = Fd = 9000 in-lb

Analysis Assumptions and Modeling Notes

Use consistent length units of inches. Real constants R1 = 4.67017 in. and R2 = 2.33508 in. (pipe O.D. and wall thickness, respectively) are calculated for a solid cross-section from the given section modulus. The offset load is applied as a centroidal force and a moment.

Results Comparison

	Target[1]	ANSYS	Ratio
Principal $stress_{max}$, psi	7527.	7527.[2]	1.000
Shear $stress_{max}$, psi	3777.	3777.[3]	1.000

1. Solution recalculated
2. Corresponds to S1MX in element solution printout
3. Calculated as SINTMX/2 (SINTMX from element solution printout) since SINTMX is defined as twice the maximum shear stress.

VM13: Cylindrical Shell Under Pressure

Overview

Reference:	S. Timoshenko, *Strength of Material, Part I, Elementary Theory and Problems*, 3rd Edition, D. Van Nostrand Co., Inc., New York, NY, 1955, pg. 45, article 11. A. C. Ugural, S. K. Fenster, *Advanced Strength and Applied Elasticity*, Elsevier, 1981.
Analysis Type(s):	Static Analysis (**ANTYPE** = 0)
Element Type(s):	Axisymmetric Structural Shell Element (SHELL51)
Input Listing:	vm13.dat

Test Case

A long cylindrical pressure vessel of mean diameter d and wall thickness t has closed ends and is subjected to an internal pressure P. Determine the axial stress σ_y and the hoop stress σ_z in the vessel at the midthickness of the wall.

Figure 13.1 Cylindrical Shell Problem Sketch

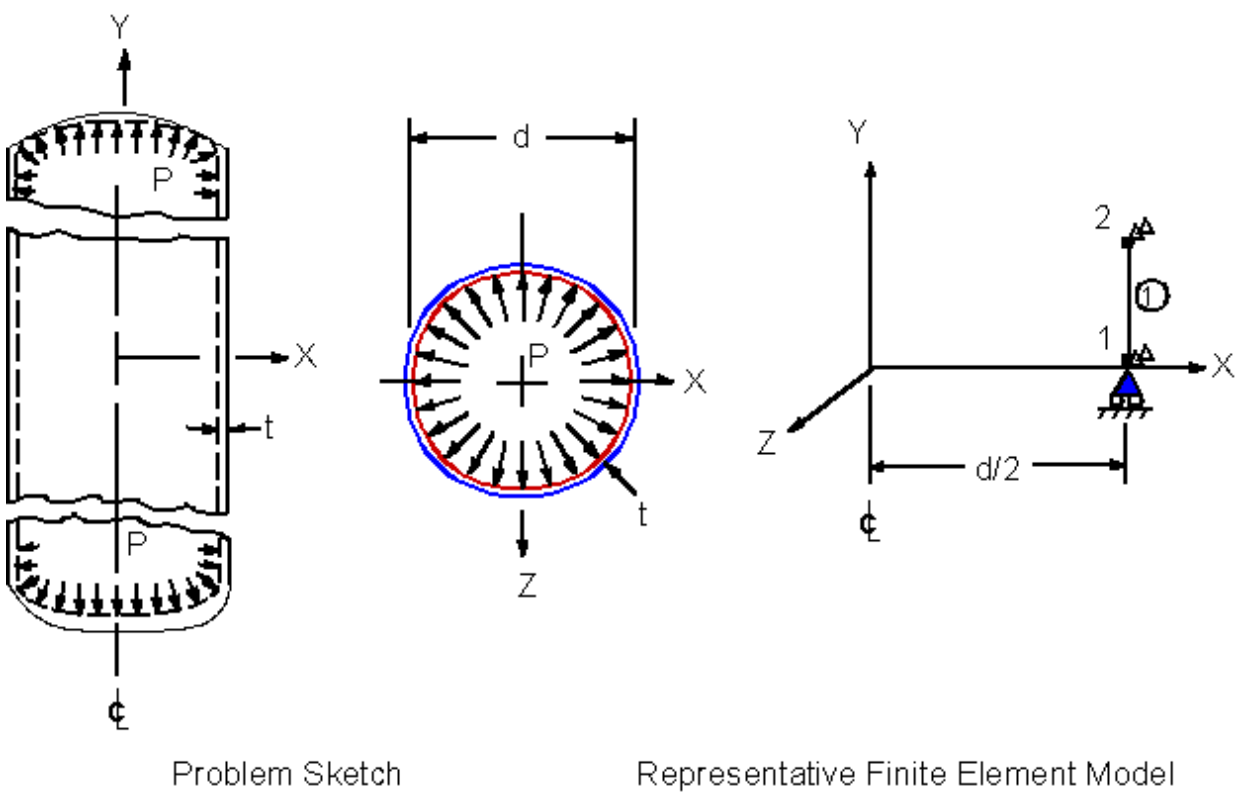

Material Properties	Geometric Properties	Loading
$E = 30 \times 10^6$ psi $\upsilon = 0.3$	t = 1 in d = 120 in	P = 500 psi

Analysis Assumptions and Modeling Notes

An arbitrary axial length of 10 inches is selected. Nodal coupling is used in the radial direction. An axial force of 5654866.8 lb ($(P\pi d^2)/4$) is applied to simulate the closed-end effect.

Results Comparison

	Target[1]	ANSYS	Ratio
$Stress_y$, psi	15,000.	15,000.[2]	1.000
$Stress_z$, psi	29,749.	29,750.	1.000

1. Axial Stress σ_y is calculated (per S. Timoshenko, *Strength of Material, Part I, Elementary Theory and Problems*) using thin shell theory. Since SHELL51 uses thick shell logic to determine stress variations through the thickness, the hoop stress σ_z is calculated per A. C. Ugural, S. K. Fenster, *Advanced Strength and Applied Elasticity*.
2. SX in element solution printout since element X-axis is parallel to global Y-axis.

ANSYS Verification Manual . ANSYS Release 10.0 . 002184 . © SAS IP, Inc.

VM14: Large Deflection Eccentric Compression of a Column

Overview

Reference:	S. Timoshenko, *Strength of Material, Part I, Elementary Theory and Problems*, 3rd Edition, D. Van Nostrand Co., Inc., New York, NY, 1955, pg. 263, problem 1.
Analysis Type(s):	Static, Large Deflection Analysis (**ANTYPE** = 0)
Element Type(s):	2-D Elastic Tapered Unsymmetric Beam Elements (BEAM54)
Input Listing:	vm14.dat

Test Case

Find the deflection Δ at the middle and the maximum tensile and compressive stresses in an eccentrically compressed steel strut of length ℓ. The cross-section is a channel with moment of inertia I, area A, and flange width b. The ends are pinned at the point of load application. The distance between the centroid and the back of the channel is e, and the compressive force F acts in the plane of the back of the channel and in the symmetry plane of the channel.

Figure 14.1 Slender Column Problem Sketch

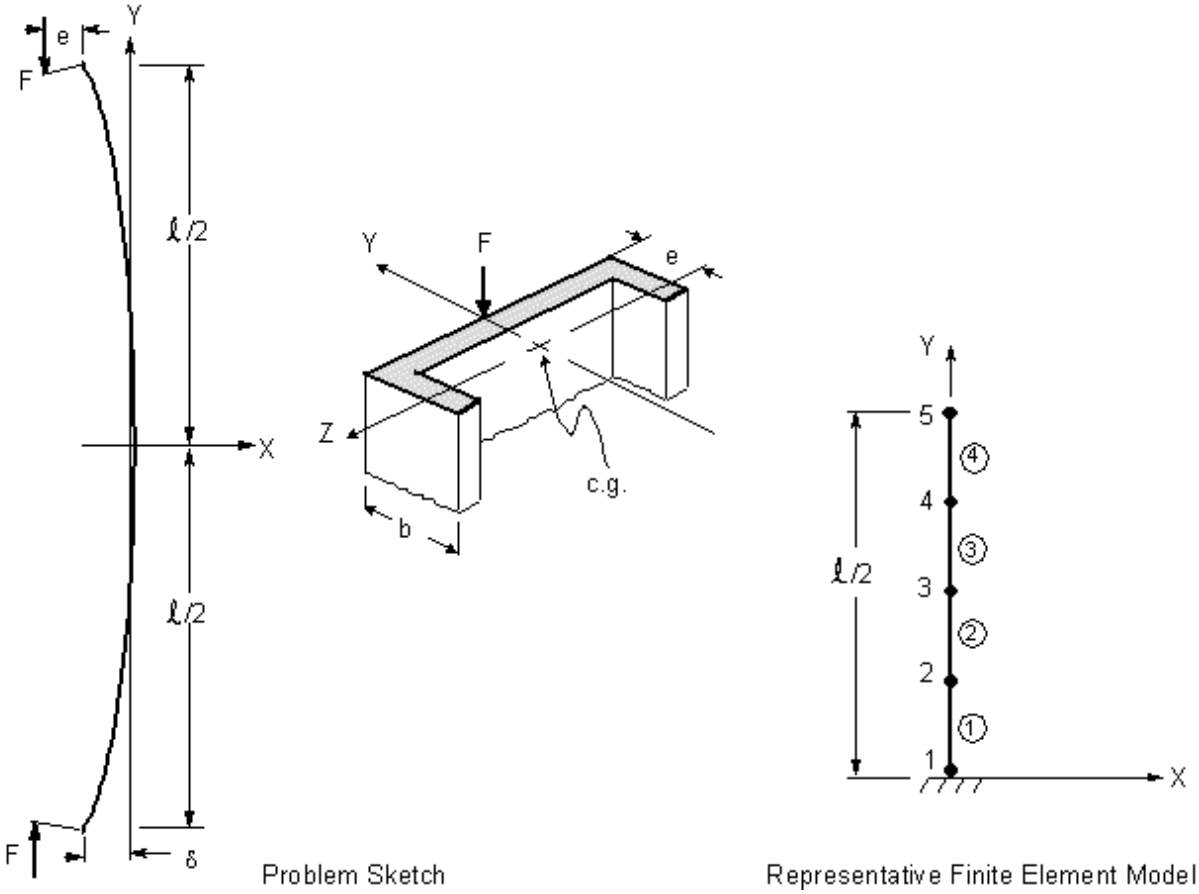

Material Properties	Geometric Properties	Loading
$E = 30 \times 10^6$ psi $\upsilon = 0.3$	$\ell = 10$ ft $I_z = 1.3$ in^4 $A = 3.36$ in^2 e = 0.58 in b = 2.26 in	F = 4,000 lb

Analysis Assumptions and Modeling Notes

Only one-half of the structure is modeled because of symmetry. The boundary conditions for the equivalent half model become fixed-free. Large deflection is needed since the stiffness of the structure and the loading change significantly with deflection. The offset e is defined in the element coordinate system.

Results Comparison

	Target[1]	ANSYS	Ratio
Deflection, in	0.1264	0.1261[2]	0.997
$Stress_{tens}$, psi	2461.	2451.5[3]	0.998
$Stress_{comp}$, psi	-2451.	-2447.8[4]	0.999

1. Solution recalculated
2. Corresponds to negative of X-deflection at node 5
3. SMAX, Element 1, Node I from element solution printout
4. SMIN, Element 1, Node I from element solution printout

ANSYS Verification Manual . ANSYS Release 10.0 . 002184 . © SAS IP, Inc.

VM15: Bending of a Circular Plate Using Axisymmetric Elements

Overview

Reference:	S. Timoshenko, *Strength of Material, Part II, Elementary Theory and Problems*, 3rd Edition, D. Van Nostrand Co., Inc., New York, NY, 1956, pp. 96, 97, and 103.
Analysis Type(s):	Static Analysis (**ANTYPE** = 0)
Element Type(s):	Axisymmetric Structural Shell Elements (SHELL51)
Input Listing:	vm15.dat

Test Case

A flat circular plate of radius r and thickness t is subject to various edge constraints and surface loadings. Determine the deflection δ at the middle and the maximum stress σ_{max} for each case.

Case 1: Uniform loading P, clamped edge.
Case 2: Concentrated center loading F, clamped edge.
Case 3: Uniform loading P/4, simply supported edge.

Figure 15.1 Flat Circular Plate Problem Sketch

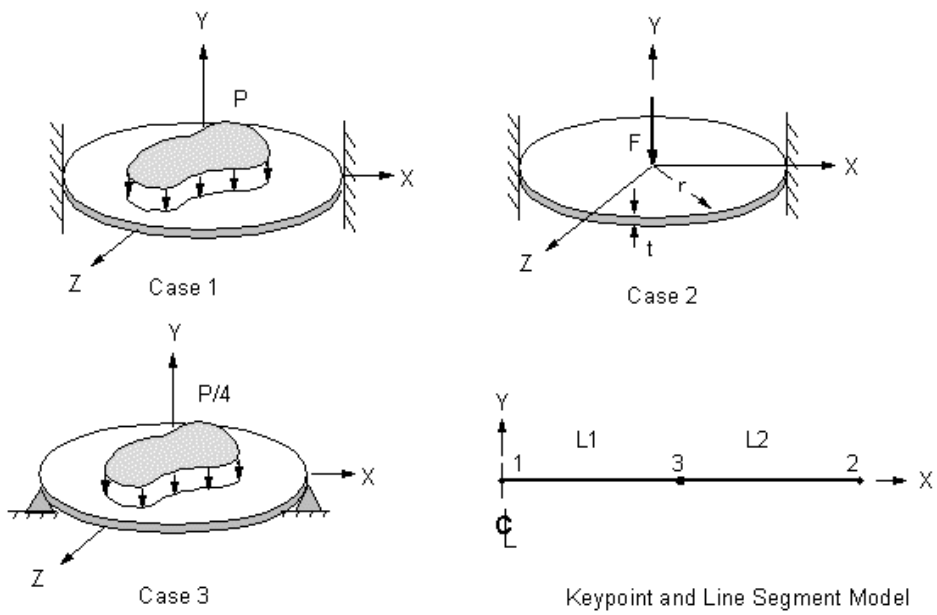

Note that edge constraints apply over the full circumference.

Material Properties	Geometric Properties	Loading
E = 30 x 10^6 psi υ = 0.3	r = 40 in t = 1 in	P = 6 psi F = 7,539.82 lb

Analysis Assumptions and Modeling Notes

The stiffness matrix formed in the first load step is automatically reused in the second load step. A new stiffness matrix is automatically formed in the third load step because of changed boundary constraints. The mesh density is biased near the centerline and outer edge to recover stress values near those points.

Results Comparison

		Target	ANSYS[1]	Ratio
Case 1	Deflection, in	-0.08736	-0.08737	1.000
	$Stress_{max}$, psi	7200.	7040.	0.978
Case 2	Deflection, in	-0.08736	-0.08735	1.000
	$Stress_{max}$, psi[2]	3600.	3568.	0.991
Case 3	Deflection, in	-0.08904	-0.08903	1.000
	$Stress_{max}$, psi	2970.	2968.	0.999

1. Theoretical σ_{max} occurs at a node location; ANSYS results, taken from element solution printout, are at the centroid of the nearest element.
2. This result is at the edge of the plate since point loading causes (theoretically) infinite stresses at the point of load application.

Figure 15.2 Displaced Geometry Displays

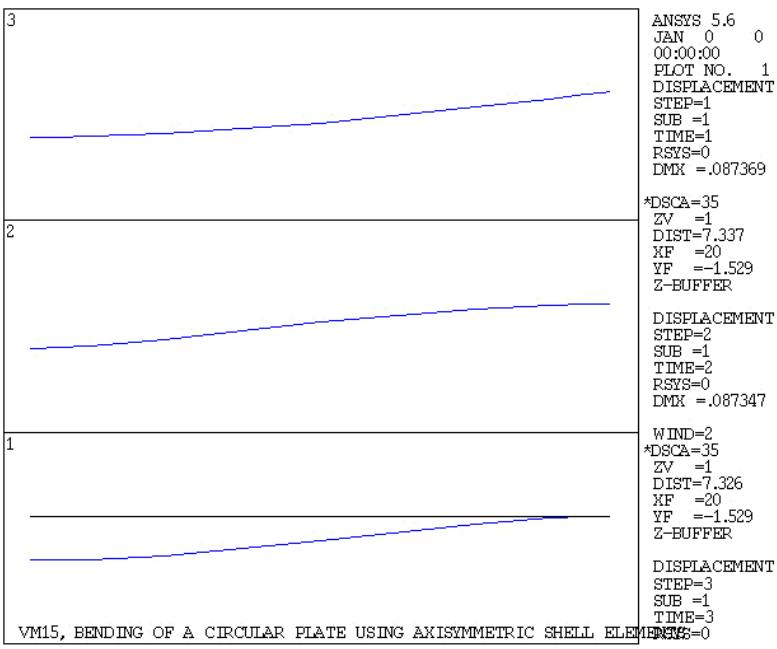

Window 1: Uniform Loading, Clamped Edge
Window 2: Concentrated Loading, Clamped Edge
Window 3: Uniform Loading Simply-supported Edge

VM16: Bending of a Solid Beam (Plane Elements)

Overview

Reference:	R. J. Roark, *Formulas for Stress and Strain*, 4th Edition, McGraw-Hill Book Co., Inc., New York, NY, 1965, pp. 104, 106.
Analysis Type(s):	Static Analysis (**ANTYPE** = 0)
Element Type(s):	2-D Structural Solid Elements (PLANE42)
Input Listing:	vm16.dat

Test Case

A beam of length ℓ and height h is built-in at one end and loaded at the free end with:

- a moment M
- a shear force F

For each case, determine the deflection δ at the free end and the bending stress σ_{Bend} a distance d from the wall at the outside fiber.

Figure 16.1 Bending of a Solid Beam with Plane Elements Problem Sketch

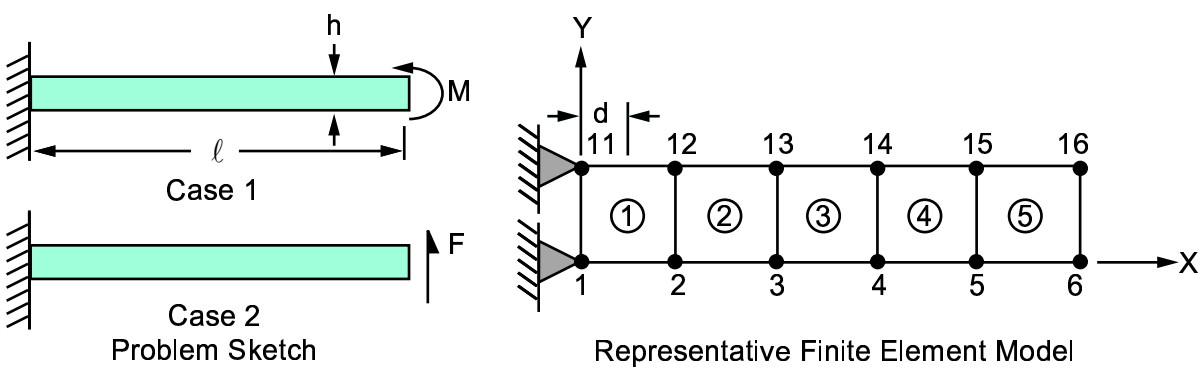

Material Properties	Geometric Properties	Loading
E = 30 x 10^6 psi υ = 0.0	ℓ = 10 in h = 2 in d = 1 in	Case 1, M = 2000 in-lb Case 2, F = 300 lb

Analysis Assumptions and Modeling Notes

The stiffness matrix formed in the first load step is also used in the second load step (automatically determined by ANSYS). The end moment is represented by equal and opposite forces separated by a distance h. The bending stress is obtained from face stresses on element 1.

Results Comparison

		Target	ANSYS	Ratio
Case 1	Deflection, in	0.00500	0.00500	1.000
	$Stress_{Bend}$, psi	3000	3000[1]	1.000

		Target	ANSYS	Ratio
Case 2	Deflection, in	0.00500	0.00505	1.010
	$Stress_{Bend}$, psi	4050	4050[1]	1.000

1. S(PAR) in face printout for element 1 in element solution printout.

VM17: Snap-Through Buckling of a Hinged Shell

Overview

Reference:	C. C. Chang, "Periodically Restarted Quasi-Newton Updates in Constant Arc-Length Method", *Computers and Structures*, Vol. 41 No. 5, 1991, pp. 963-972.
Analysis Type(s):	Static Analysis (**ANTYPE** = 0)
Element Type(s):	Elastic Shell Elements (SHELL63)
Input Listing:	vm17.dat

Test Case

A hinged cylindrical shell is subjected to a vertical point load (P) at its center. Find the vertical displacement (UY) at points A and B for the load of 1000 N.

Figure 17.1 Hinged Shell Problem Sketch

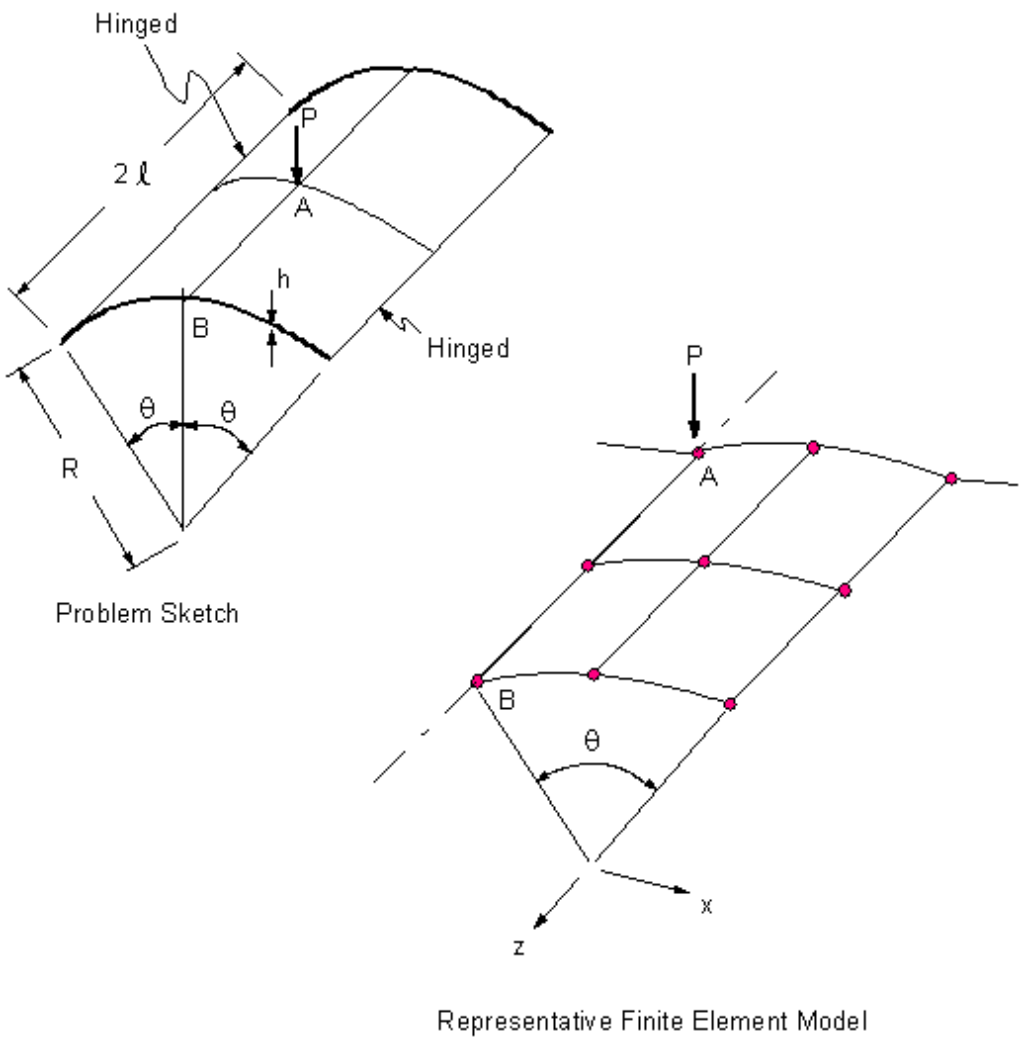

Material Properties	Geometric Properties	Loading
E = 3.10275 kN/mm^2 υ = 0.3	R = 2540 m ℓ = 254 m h = 6.35 m Θ = 0.1 rad	P = 1000 N

Analysis Assumptions and Modeling Notes

Due to symmetry, only a quarter of the structure is analyzed. The structure exhibits the nonlinear postbuckling behavior under the applied load. Therefore, a large deflection analysis is performed using the arc length solution technique. The results are observed in POST26.

Results Comparison

	Target[1]	ANSYS	Ratio
UY @ A, mm	-30.0	-31.7	1.056
UY @ B, mm	-26.0	-25.8	0.994

1. Target results are from graphical solution

Figure 17.2 Deflection and Total Load Plot

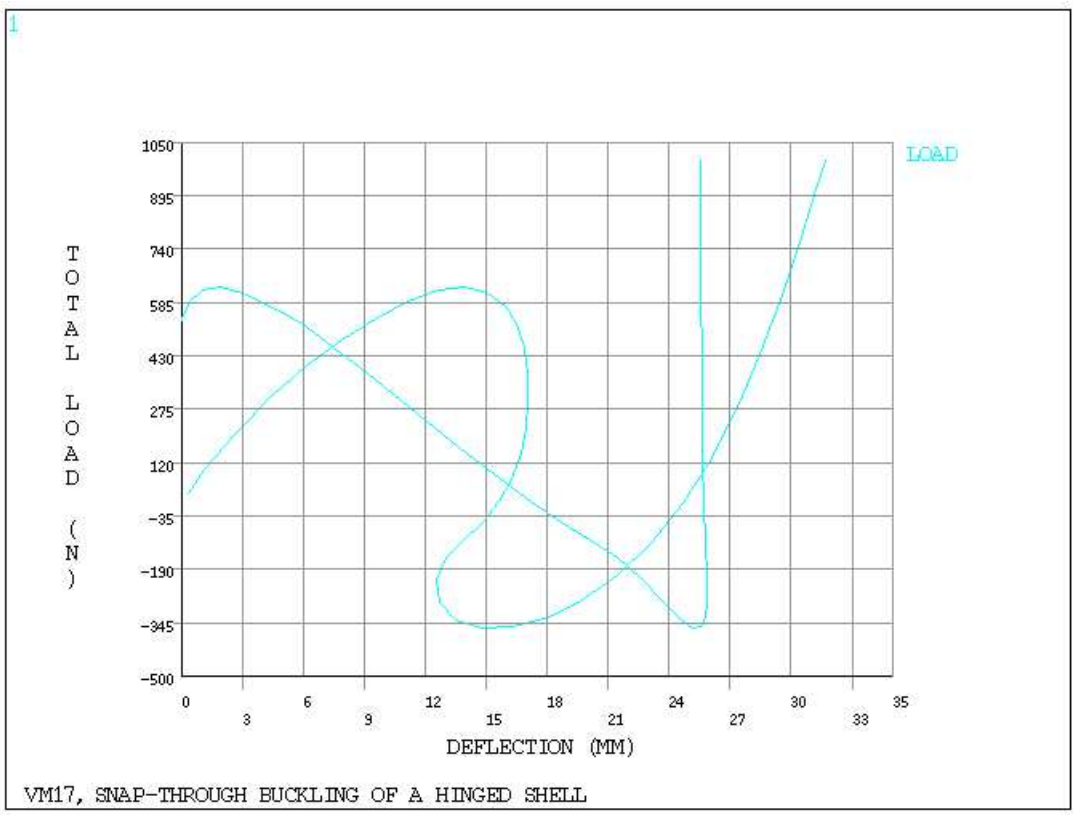

VM18: Out-of-Plane Bending of a Curved Bar

Overview

Reference:	S. Timoshenko, *Strength of Material, Part I, Elementary Theory and Problems*, 3rd Edition, D. Van Nostrand Co., Inc., New York, NY, 1955, pg. 412, eq. 241.
Analysis Type(s):	Static Analysis (**ANTYPE** = 0)
Element Type(s):	Elastic Curved Pipe Element (PIPE18)
Input Listing:	vm18.dat

Test Case

A portion of a horizontal circular ring, built-in at A, is loaded by a vertical (Z) load F applied at the end B. The ring has a solid circular cross-section of diameter d. Determine the deflection δ at end B, the maximum bending stress σ_{Bend}, and the maximum torsional shear stress τ.

Figure 18.1 Curved Bar Problem Sketch

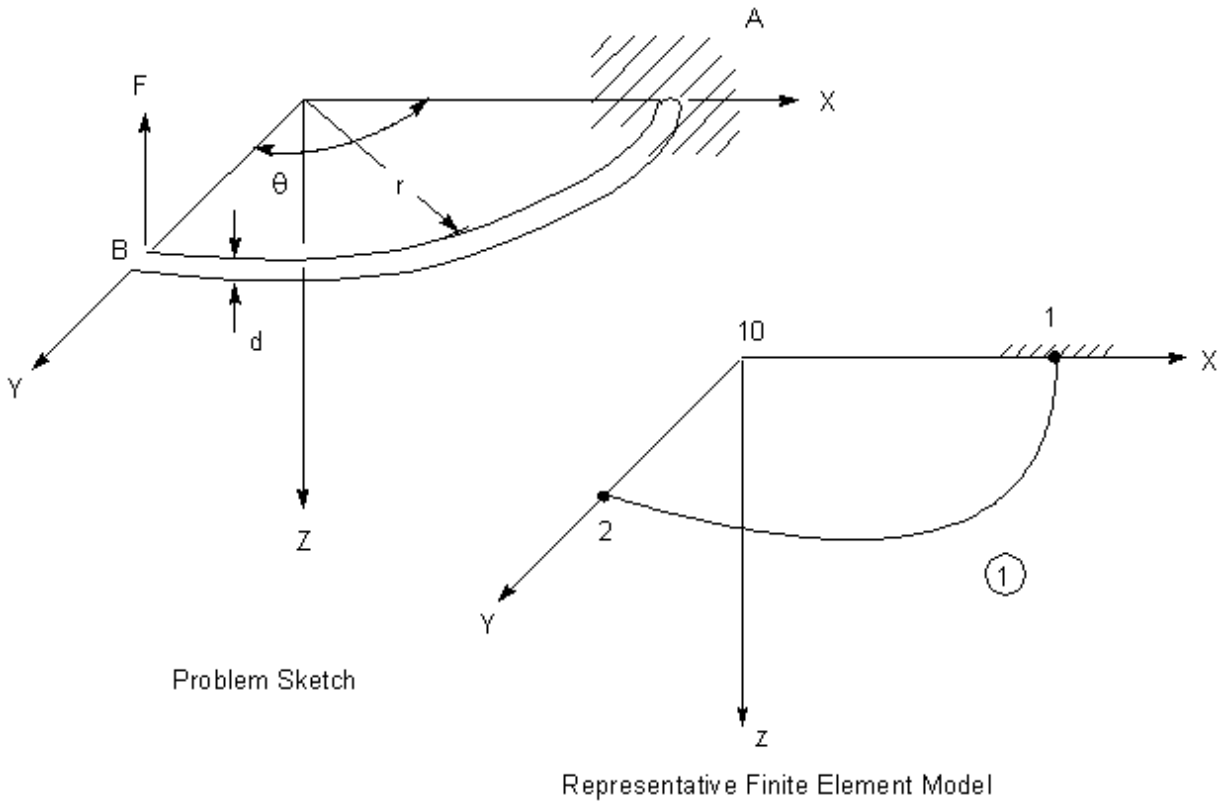

Material Properties	Geometric Properties	Loading
E = 30 x 10^6 psi υ = 0.3	r = 100 in d = 2 in Θ = 90°	F = 50 lb

Analysis Assumptions and Modeling Notes

Node 10 is arbitrarily located on the radius of curvature side of the element to define the plane of the elbow. The wall thickness is set to half the diameter for a solid bar.

Results Comparison

	Target	ANSYS	Ratio
Deflection, in	-2.648	-2.650	1.001
$Stress_{Bend}$, psi	6366.	6366.[1]	1.000
Shear stress, psi	-3183.	-3183.[2]	1.000

1. Corresponds to maximum SAXL at 0° angle location in element solution output.
2. Corresponds to SXH at 0° angle location in element solution output.

ANSYS Verification Manual . ANSYS Release 10.0 . 002184 . © SAS IP, Inc.

VM19: Random Vibration Analysis of a Deep Simply-Supported Beam

Overview

Reference:	NAFEMS, *Selected Benchmarks for Forced Vibration*, Report prepared by W. S. Atking Engineering Sciences, April 1989, Test 5R.
Analysis Type(s):	Mode-frequency, Spectrum Analysis (**ANTYPE** = 8) Harmonic Analysis (**ANTYPE** = 3)
Element Type(s):	3-D Elastic Beam (BEAM4)
Input Listing:	vm19.dat

Test Case

A deep simply-supported square beam of length ℓ, thickness t, and mass density m is subjected to random uniform force power spectral density. Determine the peak response PSD value.

Figure 19.1 Simply-Supported Beam Problem Sketch

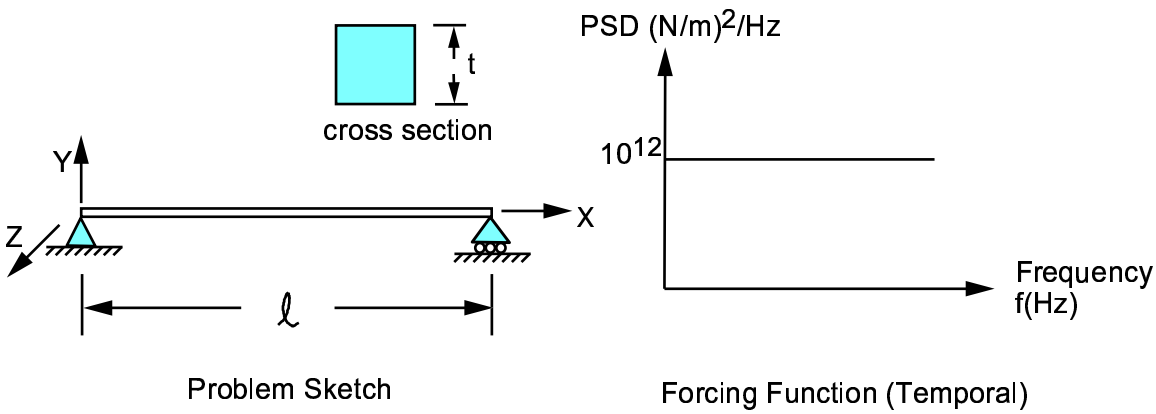

Material Properties	**Geometric Properties**	**Loading**
$E = 200 \times 10^9$ N/m^2 $\upsilon = 0.3$ m = 8000 Kg/m^3	ℓ = 10. m t = 2.0 m	PSD = $(10^6$ N/m$)^2$ /Hz Damping δ = 2%

Analysis Assumptions and Modeling Notes

All degrees of freedom in the Y direction are selected as master degrees of freedom (MDOF). A frequency range of .1 Hz to 70 Hz was used as an approximation of the white noise PSD forcing function frequency.

Results Comparison

	Target	ANSYS	Ratio
Modal Frequency f (Hz)	42.65	42.66	1.00
PSD Freq (Hz)	42.66	42.64	1.00
Peak d PSD(mm^2/Hz)	180.9	179.36[1]	0.99
Peak stress PSD(N/mm^2)^2 /Hz	58516.	58553.[1]	1.00

1. The peak value occurred at frequency 42.64 Hz.

VM20: Cylindrical Membrane Under Pressure

Overview

Reference:	S. Timoshenko, *Strength of Material, Part II, Elementary Theory and Problems*, 3rd Edition, D. Van Nostrand Co., Inc., New York, NY, 1956, pg. 121, article 25.
Analysis Type(s):	Static Analysis (**ANTYPE** = 0)
Element Type(s):	Membrane Shell Element (SHELL41)
Input Listing:	vm20.dat

Test Case

A long cylindrical membrane container of diameter d and wall thickness t is subjected to a uniform internal pressure P. Determine the axial stress σ_1 and the hoop stress σ_2 in the container. See VM13 for the problem sketch.

Figure 20.1 Cylindrical Membrane Problem Sketch

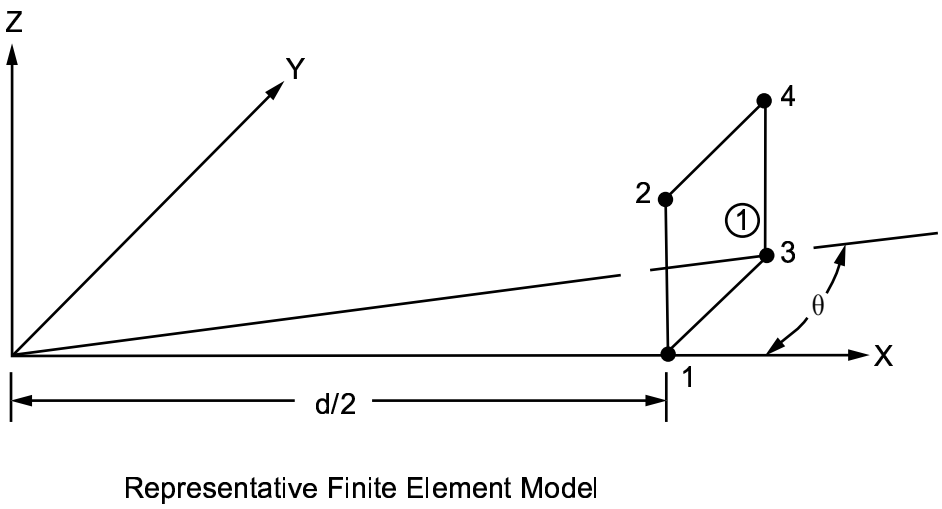

Material Properties	Geometric Properties	Loading
E = 30 x 10^6 psi υ = 0.3	d = 120 in t = 1 in	P = 500 psi

Analysis Assumptions and Modeling Notes

An arbitrary axial length is selected. Since the problem is axisymmetric, only a one element sector is needed. A small angle $\Theta = 10°$ is used for approximating the circular boundary with a straight-sided element. Nodal coupling is used at the boundaries. An axial traction of 15,000 psi is applied to the edge of the element to simulate the closed-end effect. The internal pressure is applied as an equivalent negative pressure on the exterior (face 1) of the element.

Results Comparison

	Target	ANSYS	Ratio
$Stress_1$, psi	15,000	15,000	1.000

	Target	ANSYS	Ratio
$Stress_2$, psi	29,749	29,886	1.005

VM21: Tie Rod with Lateral Loading

Overview

Reference:	S. Timoshenko, *Strength of Material, Part II, Elementary Theory and Problems*, 3rd Edition, D. Van Nostrand Co., Inc., New York, NY, 1956, pg. 42, article 6.
Analysis Type(s):	Static, Stress Stiffening Analysis (**ANTYPE** = 0)
Element Type(s):	3-D Elastic Beam Elements (BEAM4)
Input Listing:	vm21.dat

Test Case

A tie rod is subjected to the action of a tensile force F and a uniform lateral load p. Determine the maximum deflection z_{max}, the slope Θ at the left-hand end, and the maximum bending moment M_{max}. In addition, determine the same three quantities for the unstiffened tie rod (F = 0).

Figure 21.1 Tie Rod Problem Sketch

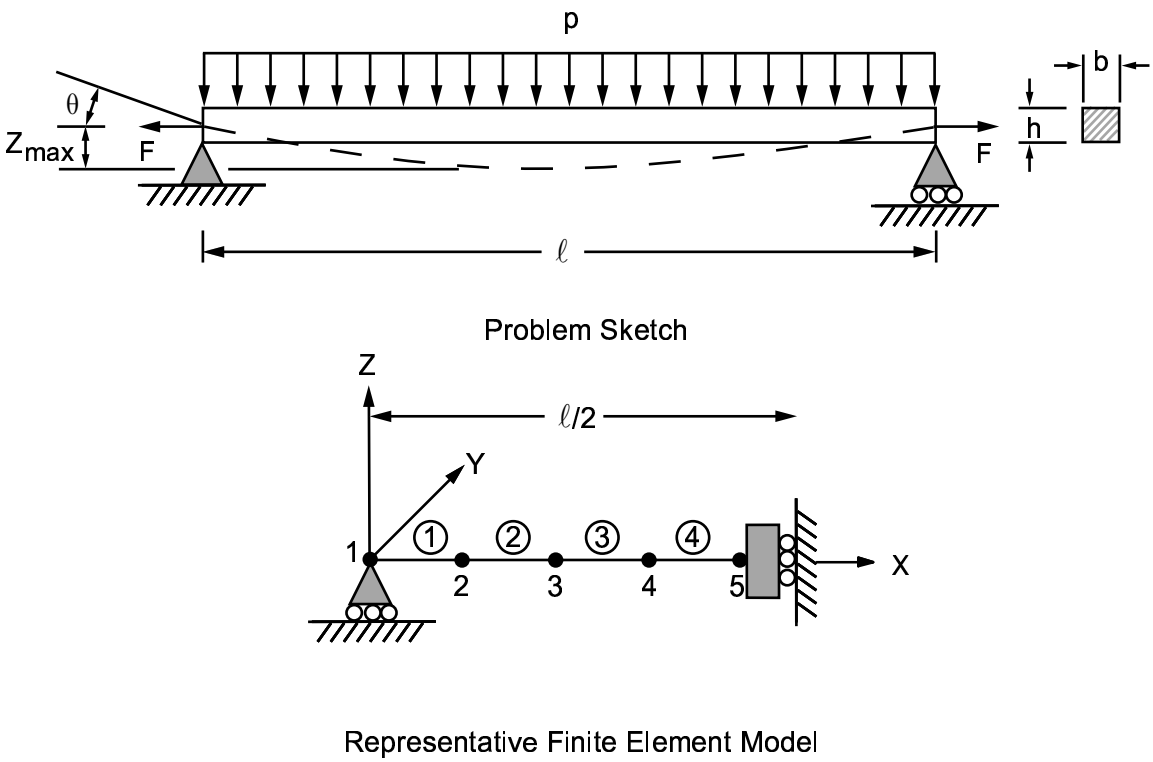

Material Properties	Geometric Properties	Loading
E = 30 x 10^6 psi	ℓ = 200 in b = h = 2.5 in	F = 21,972.6 lb p = 1.79253 lb/in

Analysis Assumptions and Modeling Notes

Due to symmetry, only one-half of the beam is modeled. The full load is applied for each iteration. The first solution represents the unstiffened case. The second solution represents the stiffened case. For b and h of 2.5 in, the area is 6.25 in^2 and I_y is 3.2552 in^4.

Results Comparison

		Target	ANSYS	Ratio
F neq 0 (stiffened)	Z_{max} , in	-0.19945	-0.19946	1.000
	Slope, rad	0.0032352	0.0032353	1.000
	M_{max} , in-lb	-4580.1	-4580.1	1.000
F = 0 (un-stiffened)	Z_{max} , in	-0.38241	-0.38241	1.000
	Slope, rad	0.0061185	0.0061185	1.000
	M_{max} , in-lb	-8962.7	-8962.6	1.000

ANSYS Verification Manual . ANSYS Release 10.0 . 002184 . © SAS IP, Inc.

VM22: Small Deflection of a Belleville Spring

Overview

Reference:	S. Timoshenko, *Strength of Material, Part II, Elementary Theory and Problems*, 3rd Edition, D. Van Nostrand Co., Inc., New York, NY, 1956, pg. 143, problem 2.
Analysis Type(s):	Static Analysis (**ANTYPE** = 0)
Element Type(s):	Axisymmetric Structural Shell Element (SHELL51)
Input Listing:	vm22.dat

Test Case

The conical ring shown below represents an element of a Belleville spring. Determine the deflection y produced by a load F per unit length on the inner edge of the ring.

Figure 22.1 Belleville Spring Problem Sketch

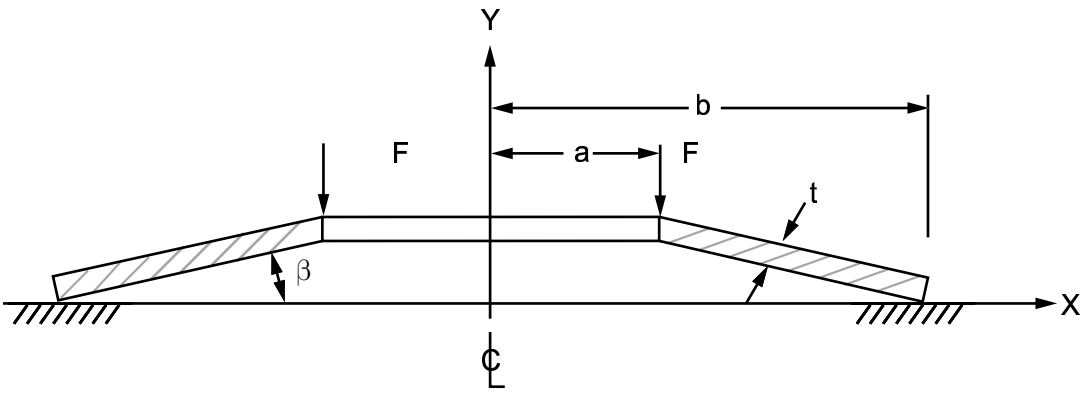

Problem Sketch

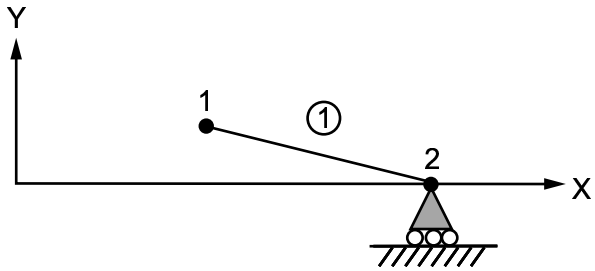

Representative Finite Element Model

Material Properties	**Geometric Properties**	**Loading**
$E = 30 \times 10^6$ psi $\upsilon = 0.0$	a = 1 in b = 1.5 in t = 0.2 in $\beta = 7° = 0.12217$ rad	F = 100 lb/in

Analysis Assumptions and Modeling Notes

The input force, -2 πF = -628.31853 lb., is applied per full circumference.

Results Comparison

	Target	ANSYS	Ratio
y, in	-0.0028205	-0.0028404	1.007

VM23: Thermal-structural Contact of Two Bodies

Overview

Reference:	Any Basic Mechanics Text
Analysis Type(s):	Static Analysis (**ANTYPE** = 0)
Element Type(s):	2-D Coupled-field Solid Elements (PLANE13) 2-D/3-D Node-to-Surface Contact Element (CONTA175) 2-D Target Segment Element (TARGE169)
Input Listing:	vm23.dat

Test Case

Two bodies, A and B, are initially at a temperature of 100°C. A temperature of 500°C is then imposed at the left edge, E_{A1}, of A. Further, the right edge, E_{B2}, of B is heated to attain a temperature of 850°C and is subsequently cooled back to 100°C. Compute the interface temperature (right edge) of A, E_{A2}, and the amount of heat flow through the interface when the right edge of E_{B2} is at 600°C and 850°C, respectively. Also, compute the heat flow through the interface when B is subsequently cooled to 100°C.

Figure 23.1 Contact Problem Sketch

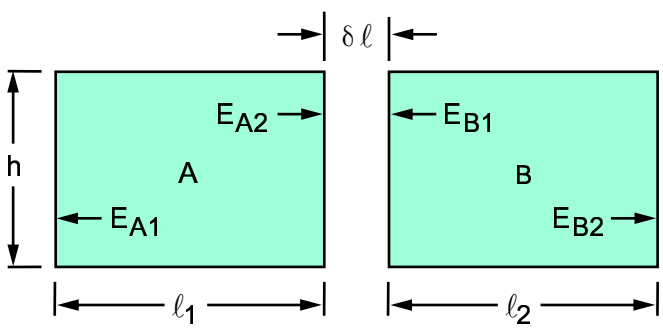

Problem Sketch (not to scale)

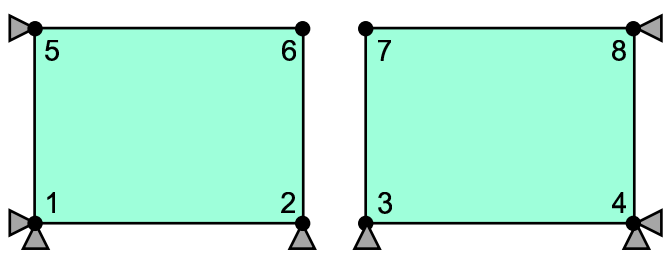

Representative Finite Element Model

Material Properties	**Geometric Properties**	**Loading**
$E = 10 \times 10^6$ N/m^2 K = 250 W/m°C $\alpha = 12 \times 10^{-6}$ m/m°C Contact Conductance = 100 W/°C (per contact element)	h = 0.1 m $\ell_1 = 0.4$ m $\ell_2 = 0.5$ m $\delta\ell = 0.0035$ m	T_{ref} = 100°C Load Step 1 T@E_1 = 500°C Load Step 2 T@E_2 = 850°C Load Step 3 T@E_2 = 100°C

Analysis Assumptions and Modeling Notes

A coupled-field analysis is performed to solve this thermal/structural contact problem. The interface is modeled using CONTA175 and TARGE169 elements with the heat conduction option.

Results Comparison

		Target	ANSYS	Ratio
T @ E_{B2} = 600°C	T @ E_{A2} oC	539.0	539.0	1.000
	Q W	2439.0	2439.0	1.000
T @ E_{B2} = 850°	T @ E_{A2} oC	636.6	636.6	1.000
	Q W	8536.6	8536.6	1.000
T @ E_{B2} = 100°	Q W	0.0	0.0	--

ANSYS Verification Manual . ANSYS Release 10.0 . 002184 . © SAS IP, Inc.

VM24: Plastic Hinge in a Rectangular Beam

Overview

Reference:	S. Timoshenko, *Strength of Material, Part II, Elementary Theory and Problems*, 3rd Edition, D. Van Nostrand Co., Inc., New York, NY, 1956, pg. 349, article 64.
Analysis Type(s):	Static, Plastic Analysis (**ANTYPE** = 0)
Element Type(s):	2-D Plastic Beam Element (BEAM23)
Input Listing:	vm24.dat

Test Case

A rectangular beam is loaded in pure bending. For an elastic-perfectly-plastic stress-strain behavior, show that the beam remains elastic at $M = M_{yp} = \sigma_{yp}\, bh^2/6$ and becomes completely plastic at $M = M_{ult} = 1.5\, M_{yp}$.

Figure 24.1 Plastic Hinge Problem Sketch

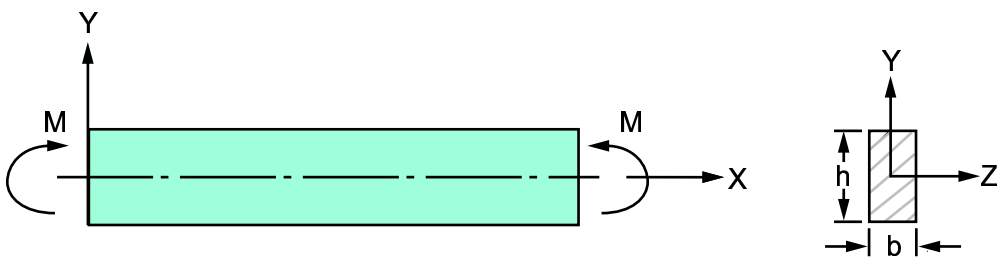

Problem Sketch

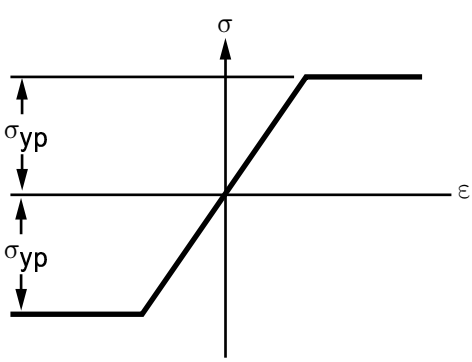

Stress-Strain Curve

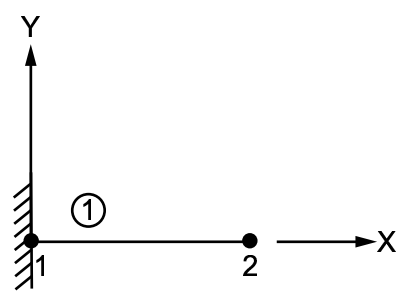

Representative Finite Element Model

Material Properties	Geometric Properties	Loading
$E = 30 \times 10^6$ psi $\upsilon = 0.3$ $\sigma_{yp} = 36000$ psi	$b = 1$ in $h = 2$ in $I_z = b\,h^3/12 = 0.6667$ in^4	$M = 1.0\, M_{yp}$ to $1.5\, M_{yp}$ ($M_{yp} = 24000$ in-lb)

Analysis Assumptions and Modeling Notes

The problem is solved by using two types of plasticity rules:

- the bilinear kinematic hardening (BKIN)
- the bilinear isotropic hardening (BISO)

An arbitrary beam length is chosen. Because of symmetry, only half of the structure is modeled (since length is arbitrary, this means only that boundary conditions are changed). The load is applied in four increments using a do-loop, and convergence status is determined from the axial plastic strain for each load step in POST26.

Results Comparison (for both analyses)

M/M_{yp}	Target	ANSYS	Ratio
1.0	Fully Elastic	Fully Elastic	--
1.1666	Elastic-Plastic	Elastic-Plastic[1]	--
1.3333	Elastic-Plastic	Elastic-Plastic[1]	--
1.5	Fully Plastic	Fully Plastic[2]	--

1. Solution converges
2. Solution does not converge (indicates that the structure has collapsed). Moment ratios slightly less than 1.5 will also show a collapse since plasticity is monitored only at discrete integration points through the cross-section.

VM25: Stresses in a Long Cylinder

Overview

Reference:	S. Timoshenko, *Strength of Material, Part II, Elementary Theory and Problems*, 3rd Edition, D. Van Nostrand Co., Inc., New York, NY, 1956, pg. 213, problem 1 and pg. 213, article 42.
Analysis Type(s):	Static Analysis (**ANTYPE** = 0)
Element Type(s):	2-D 8-Node Structural Solid Elements (PLANE82)
Input Listing:	vm25.dat

Test Case

A long thick-walled cylinder is initially subjected to an internal pressure p. Determine the radial displacement δ_r at the inner surface, the radial stress σ_r, and tangential stress σ_t, at the inner and outer surfaces and at the middle wall thickness. Internal pressure is then removed and the cylinder is subjected to a rotation ω about its center line. Determine the radial σ_r and tangential σ_t stresses at the inner wall and at an interior point located at $r = X_i$.

Figure 25.1 Long Cylinder Problem Sketch

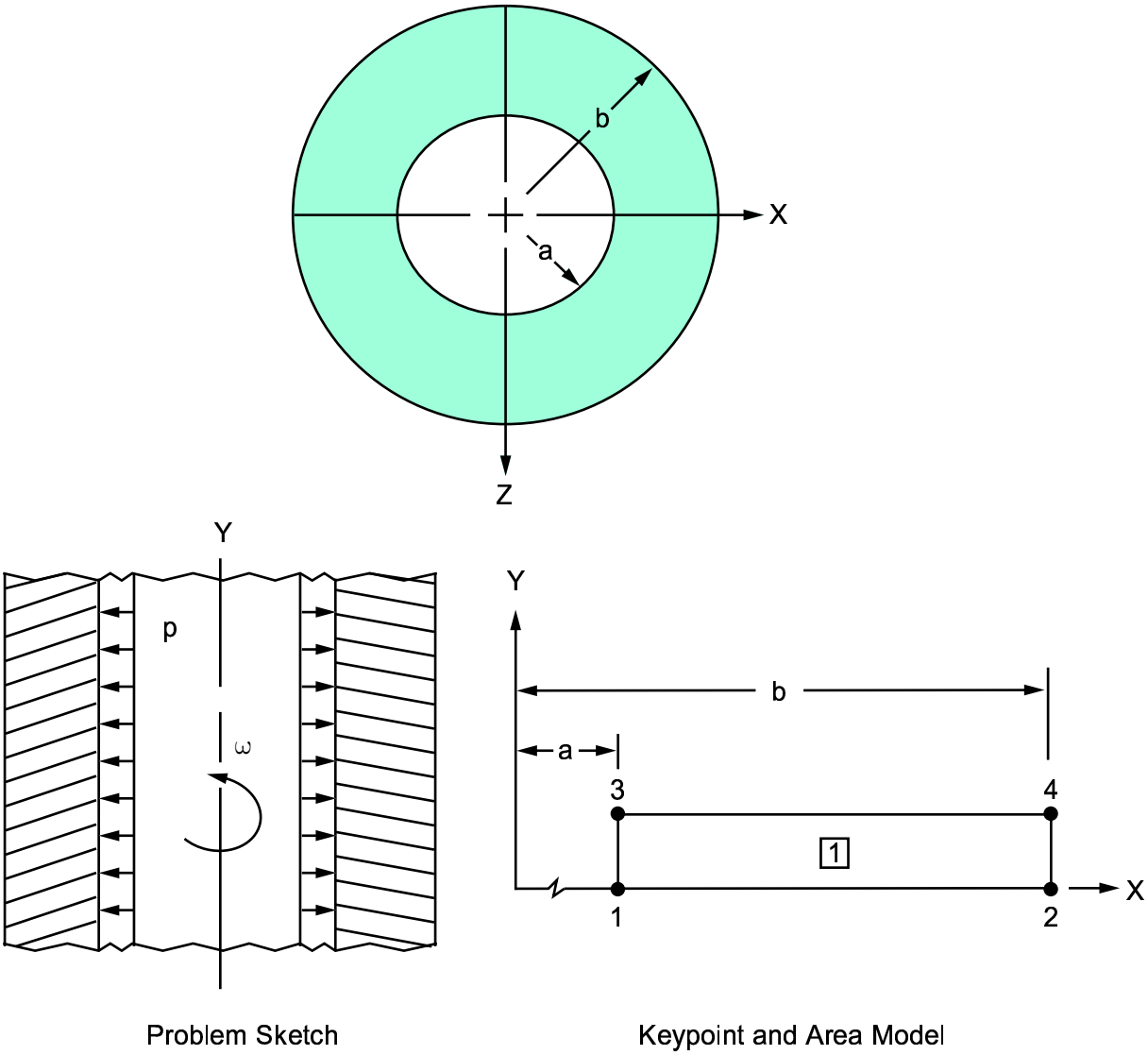

Material Properties	Geometric Properties	Loading
$E = 30 \times 10^6$ psi $\upsilon = 0.3$ $\rho = 0.00073$ lb-sec^2/in^4	a = 4 inches b = 8 inches $X_i = 5.43$ inches	p = 30,000 psi $\omega = 1000$ rad/sec

Analysis Assumptions and Modeling Notes

The axial length is arbitrarily selected. Elements are oriented such that surface stresses may be obtained at the inner and outer cylinder surfaces.

POST1 is used to display linearized stresses through the thickness of the cylinder when it is subjected to an internal pressure.

Results Comparison

		Target	ANSYS	Ratio
p = 30,000 psi	Displacement$_r$, in (r = 4 in)	0.0078666	0.0078667	1.000

	$Stress_r$, psi (r = 4 in)	-30000.	-29908.	0.997
	$Stress_r$, psi (r = 6 in)	-7778.	-7757.	0.997
	$Stress_r$, psi (r = 8 in)	0.	6.734	--
	$Stress_t$, psi (r = 4 in)	50000.	49908.	0.998
	$Stress_t$, psi (r = 6 in)	27778.	27758.	0.999
	$Stress_t$, psi (r = 8 in)	20000.	19993.	1.000
		Target	**ANSYS**	**Ratio**
Rotation = 1000 rad/sec	$Stress_r$, psi (r = 4 in)	0.0	49.380	--
	$Stress_t$, psi (r = 4 in)	40588.	40526.	0.998
	$Stress_r$, psi (r = 5.43 in)	4753.	4745.	0.998
	$Stress_t$, psi (r = 5.43 in)	29436.	29406.	0.999

Figure 25.2 SZ Stresses Along a Section (Internal Pressure)

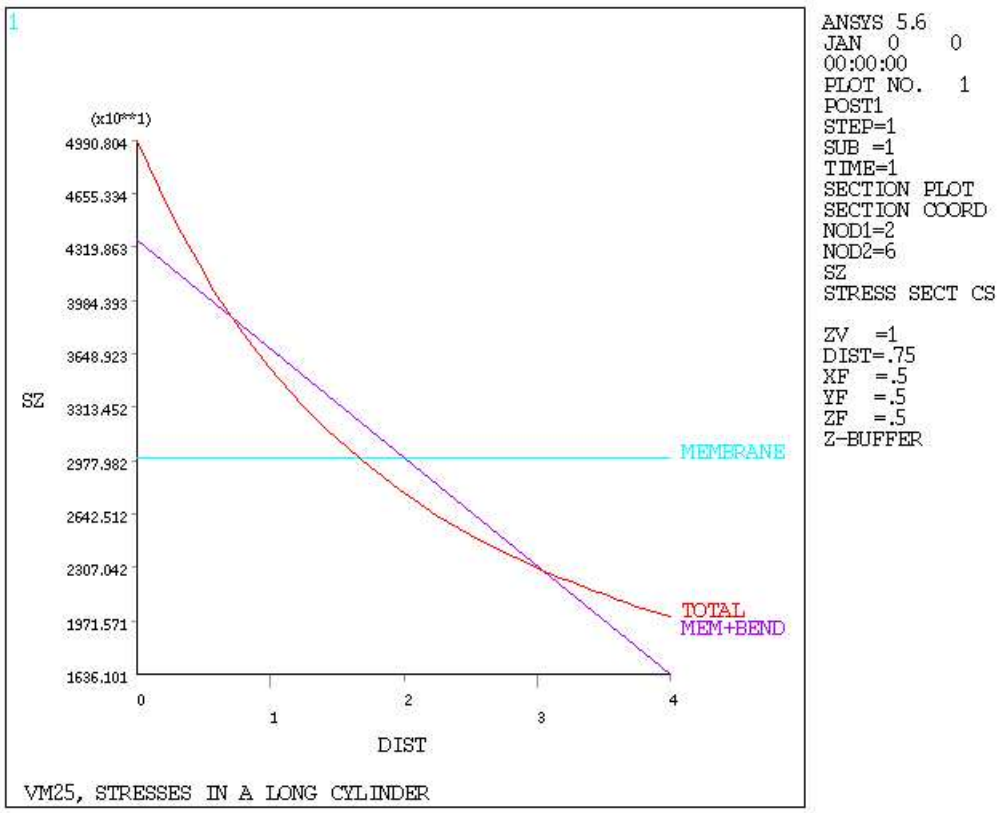

Figure 25.3 SX Stresses Along a Section (Internal Pressure)

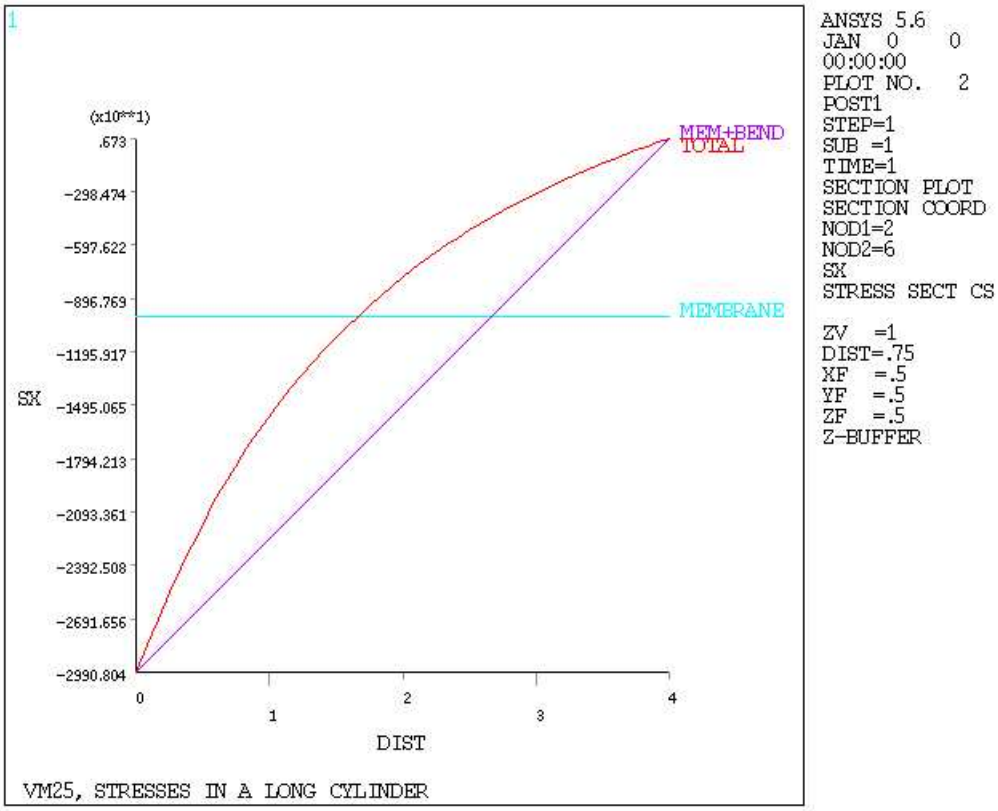

ANSYS 5.6
JAN 0 0
00:00:00
PLOT NO. 2
POST1
STEP=1
SUB =1
TIME=1
SECTION PLOT
SECTION COORD
NOD1=2
NOD2=6
SX
STRESS SECT CS

ZV =1
DIST=.75
XF =.5
YF =.5
ZF =.5
Z-BUFFER

VM26: Large Deflection of a Cantilever

Overview

Reference:	K. J. Bathe, E. N. Dvorkin, "A Formulation of General Shell Elements - The Use of Mixed Interpolation of Tensorial Components", *Int. Journal for Numerical Methods in Engineering*, Vol. 22 No. 3, 1986, pg. 720.
Analysis Type(s):	Static, Large Deflection Analysis (**ANTYPE** = 0)
Element Type(s):	4-Node Plastic Large Strain Shell Elements (SHELL43) 4-Node Finite Strain Shell (SHELL181)
Input Listing:	vm26.dat

Test Case

A cantilevered plate of length ℓ, width b, and thickness t is fixed at one end and subjected to a pure bending moment M at the free end. Determine the true (large deflection) free-end displacements and rotation, and the top surface stress at the fixed end, using shell elements.

Figure 26.1 Cantilever Problem Sketch

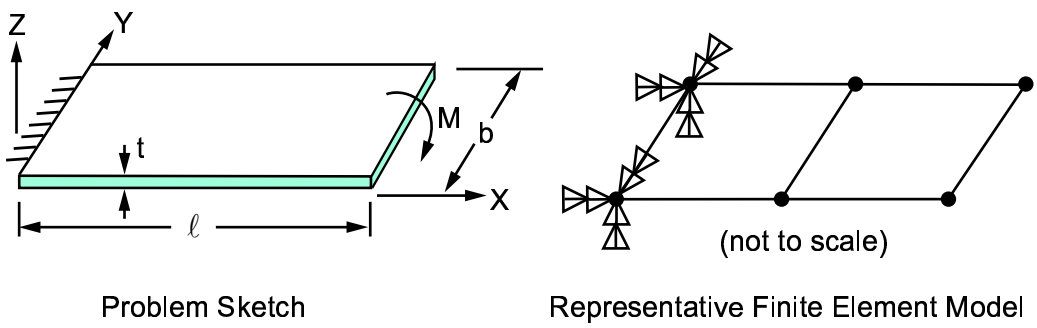

Material Properties	**Geometric Properties**	**Loading**
E = 1800 N/mm^2 υ = 0.0	ℓ = 12 mm b = 1 mm t = 1 mm	M = 15.708 N-mm

Analysis Assumptions and Modeling Notes

The large deflection option is chosen (**NLGEOM**,ON) and shell elements are used to match the reference's assumptions and test case definition. Since the geometry is closer to that of a beam, a shell element is not the usual element type to solve problems of this geometry.

The free-end nodes are coupled in y-rotations so that the bending moment M can be applied to only one end node. The load is applied in two equal increments, using the analysis restart option (solely for validation and demonstration of **ANTYPE**,,REST).

Results Comparison

		Target[1]	ANSYS	Ratio
SHELL43	UX, node 4 (mm)	-2.9	-2.61	0.90

	UZ, node 4 (mm)	-6.5	-6.55	1.01
	ROTY, node 4 (rad)	1.26	1.22	0.97
	$Stress_x$, node 1 (N/mm^2)	94.25	94.25	1.00
		Target[1]	**ANSYS**	**Ratio**
SHELL181	UX, node 4 (mm)	-2.9	-2.77	0.95
	UZ, node 4 (mm)	-6.5	-6.71	1.03
	ROTY, node 4 (rad)	1.26	1.26	1.00
	$Stress_x$, node 1 (N/mm^2)	94.25	94.25	1.00

1. to accuracy of graphical readout

VM27: Thermal Expansion to Close a Gap

Overview

Reference:	C. O. Harris, *Introduction to Stress Analysis*, The Macmillan Co., New York, NY, 1959, pg. 58, problem 8.
Analysis Type(s):	Static, Thermal-stress Analysis (**ANTYPE** = 0)
Element Type(s):	2-D Spar (or Truss) Elements (LINK1) 2-D Point-to-Point Contact Elements (CONTAC12) 3-D Spar (or Truss) Elements (LINK8) 3-D Point-to-Point Contact Elements (CONTAC52)
Input Listing:	vm27.dat

Test Case

An aluminum-alloy bar is fixed at one end and has a gap δ between its other end and a rigid wall when at ambient temperature T_a. Calculate the stress σ, and the thermal strain $\varepsilon_{Thermal}$ in the bar after it has been heated to temperature T.

Figure 27.1 Gap Problem Sketch

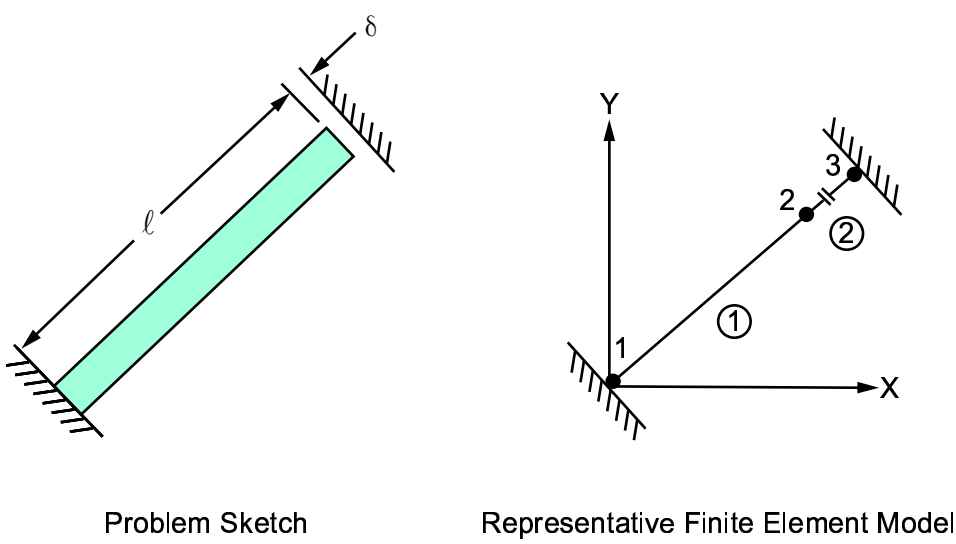

Material Properties	**Geometric Properties**	**Loading**
$E = 10.5 \times 10^6$ psi $\alpha = 12.5 \times 10^{-6}$ in/in-°F	$\ell = 3$ in $\delta = 0.002$ in	$T_a = 70°F$ $T = 170°F$

Analysis Assumptions and Modeling Notes

The problem is solved first in 2-D using LINK1 and CONTAC12 elements, then in 3-D using LINK8 and CONTAC52 elements. Models are created at arbitrary angles. The gap stiffness is arbitrarily selected at a high value (10×10^{10} psi) to approximate the rigid wall. The automatic load stepping procedure (**AUTOTS**,ON) is used.

Results Comparison

		Target	ANSYS	Ratio
2-D Analysis	Stress, psi	-6125.	-6125.	1.000
	$Strain_{Thermal}$	0.00125	0.00125	1.000
3-D Analysis	Stress, psi	-6125.	-6125.	1.000
	$Strain_{Thermal}$	0.00125	0.00125	1.000

ANSYS Verification Manual . ANSYS Release 10.0 . 002184 . © SAS IP, Inc.

VM28: Transient Heat Transfer in an Infinite Slab

Overview

Reference:	J. P. Holman, *Heat Transfer*, 4th Edition, McGraw-Hill Book Co., Inc., New York, NY, 1976, pg. 106.
Analysis Type(s):	Thermal Analysis (**ANTYPE** = 4)
Element Type(s):	2-D 8-Node Thermal Solid Element (PLANE77)
Input Listing:	vm28.dat

Test Case

A semi-infinite solid is initially at temperature T_o. The solid is then suddenly exposed to an environment having a temperature T_e and a surface convection coefficient h. Determine the temperature distribution through the solid after 2000 seconds.

Figure 28.1 Infinite Slab Problem Sketch

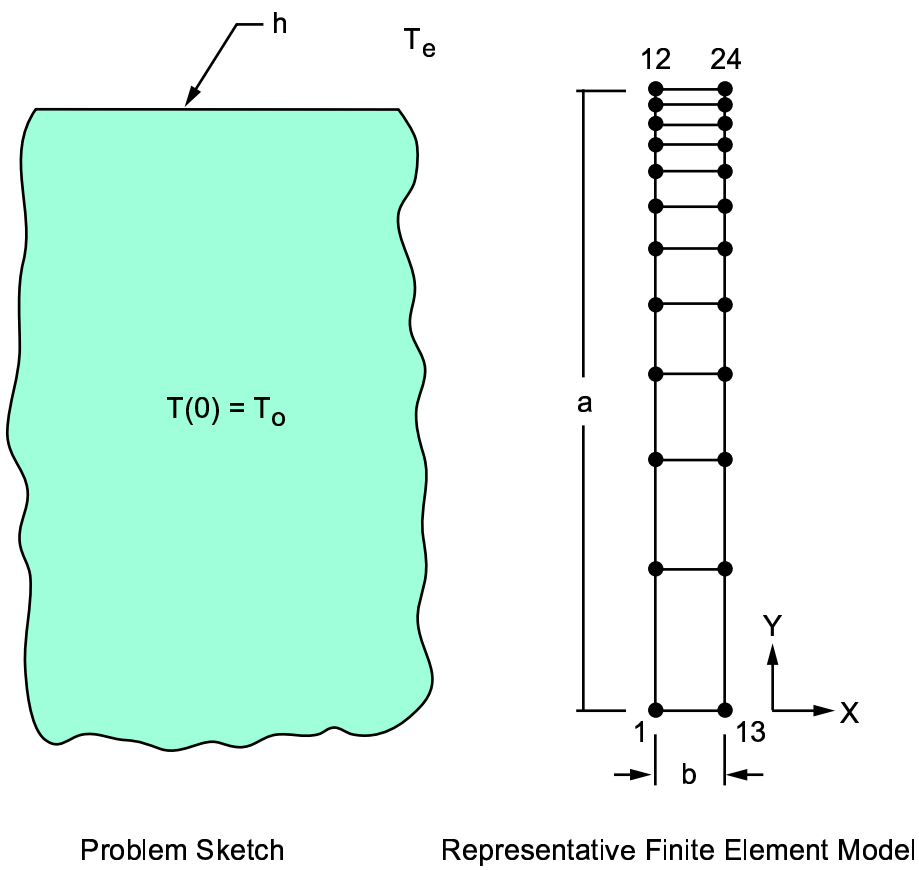

Material Properties	**Geometric Properties**	**Loading**
k = 54 W/m°C ρ = 7833 kg/m^3 c = 465 J/kg-°C	a = 1 m b = 0.1 m	T_o = 0°C T_e = 1000°C h = 50 W/m^2-°C

Analysis Assumptions and Modeling Notes

The width b of 0.1 m is arbitrarily selected for the elements. The model length a (1 meter) is selected to model the infinite boundary such that no significant temperature change occurs at the inside end points (nodes 1, 13) for the time period of interest. The node locations are selected with a higher density near the surface to better model the transient behavior. The automatic time stepping procedure (**AUTOTS**,ON) is used with an initial integration time step of 10 sec (2000 sec/200 max. iterations = 10) to more closely model the thermal shock at the surface.

Results Comparison

Temperature °C	Target	ANSYS	Ratio
@ Y = .9777 (Node 11)	140	141	1.01
@ Y = .9141 (Node9)	98.9	99.1	1.00
@ Y = .8134 (Node 7)	51.8	51.7	0.997
@ Y = .6538 (Node 5)	14.5	14.0	0.968

ANSYS Verification Manual . ANSYS Release 10.0 . 002184 . © SAS IP, Inc.

VM29: Friction on a Support Block

Overview

Reference:	F. P. Beer, E. R. Johnston, Jr., *Vector Mechanics for Engineers, Statics and Dynamics*, McGraw-Hill Book Co., Inc., New York, NY, 1962, pg. 283, problem 8.2.
Analysis Type(s):	Static Analysis (**ANTYPE** = 0)
Element Type(s):	2-D Point-to-Point Contact Elements (CONTAC12)
Input Listing:	vm29.dat

Test Case

A support block is acted upon by forces F_x and F_y. For a given value of F_y determine the smallest value of F_x which will prevent the support block from sliding down the plane. Also determine the normal force F_n and sliding force F_s at the interface.

Figure 29.1 Support Block Problem Sketch

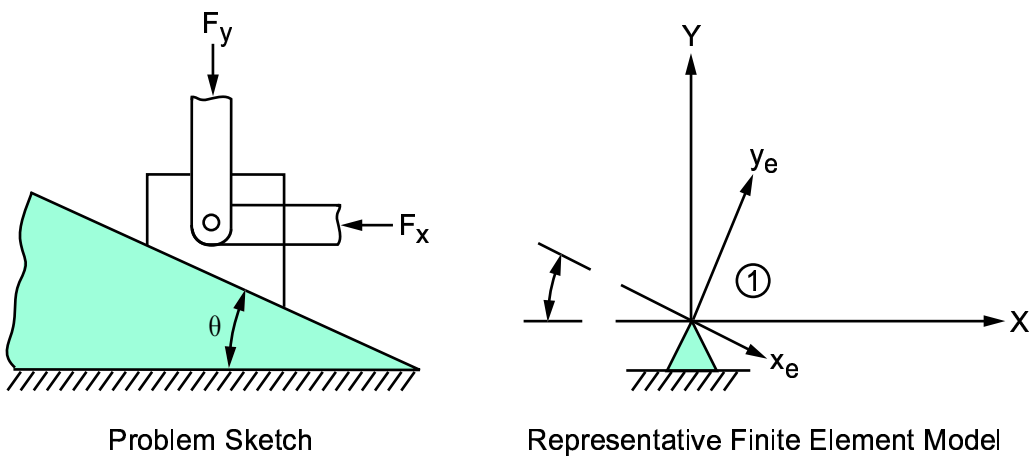

Material Properties	Geometric Properties	Loading
μ = 0.3	Θ = 205	F_y = 100 lb

Analysis Assumptions and Modeling Notes

A real problem of this nature would be solved in a trial-and-error, iterative fashion. In this case the theoretical answer is known, so the solution is verified by the "backward" process described below.

The normal stiffness of the sticking interface is arbitrarily selected at a high value. A value slightly greater than the calculated F_x value of 5.76728 lb is input in the first load step. A slightly lesser value is input in the second load step. The number of substeps is limited to one to prevent divergence due to the free motion of the block.

Results Comparison

Status	Target	ANSYS	Ratio
F_x = 5.76729 lb.	**Sticking**	**Sticking**	**--**
F_n , lb	-95.942	-95.942	1.000

Status	Target	ANSYS	Ratio
F_s , lb	28.783	28.783	1.000
F_x = 5.76720 lb.	**Sliding**	**Sliding**	**--**
F_n , lb	-95.942	-95.942	1.000
F_s , lb	28.783	28.783	1.000

VM30: Solid Model of Surface Fillet

Overview

Reference:	D. R. Hose, I. A. Rutherford, "Benchmarks for Finite Element Pre-processors", *NAFEMS Ref: R0001*, December 1993, pg. 23.
Analysis Type(s):	Solid Modeling Boolean Operations
Element Type(s):	Not Applicable
Input Listing:	vm30.dat

Test Case

A rectangular plate and a trapezoidal plate intersect at an angle of 90° with a common radius fillet of 1 mm. The edge of the fillet lies in a plane. From solid model construction, determine the accuracy of the fillet operation by measuring the out-of-plane deviation of subsequent meshed node locations.

Figure 30.1 Surface Fillet Problem Sketch

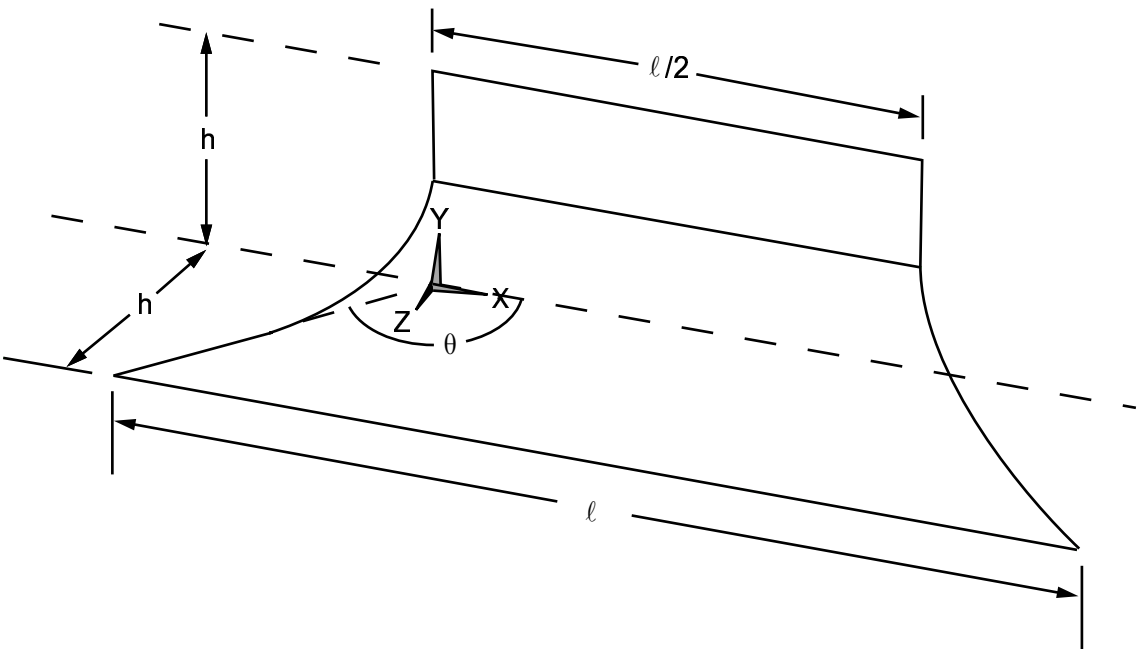

Problem Sketch

Geometric Properties
ℓ = 8 mm
h = 2 mm
Θ = 1355

Analysis Assumptions and Modeling Notes

The model is created using geometric primitives. The fillet is created using an area fillet operation. A glue operation is used to provide continuity for creating the fillet. An arbitrary element type (SHELL93) is defined for meshing purposes. A local coordinate system is created in the plane of the weld. The nodes are listed in that coordinate system to access the maximum out-of-plane deviation. The maximum absolute deviation is reported.

Results Comparison

	Target	ANSYS	Ratio
Maximum Deviation (mm)	0	3.19E-7	--

Figure 30.2 Area Plot

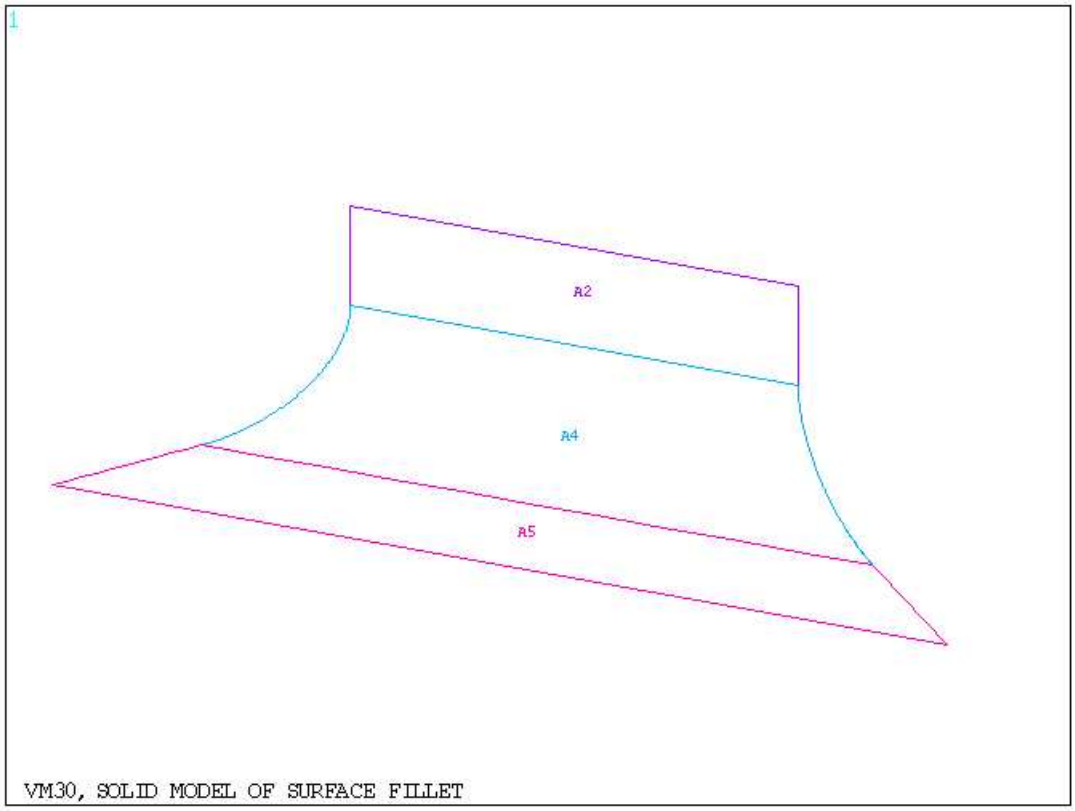

ANSYS Verification Manual . ANSYS Release 10.0 . 002184 . © SAS IP, Inc.

Figure 30.3 Element Plot

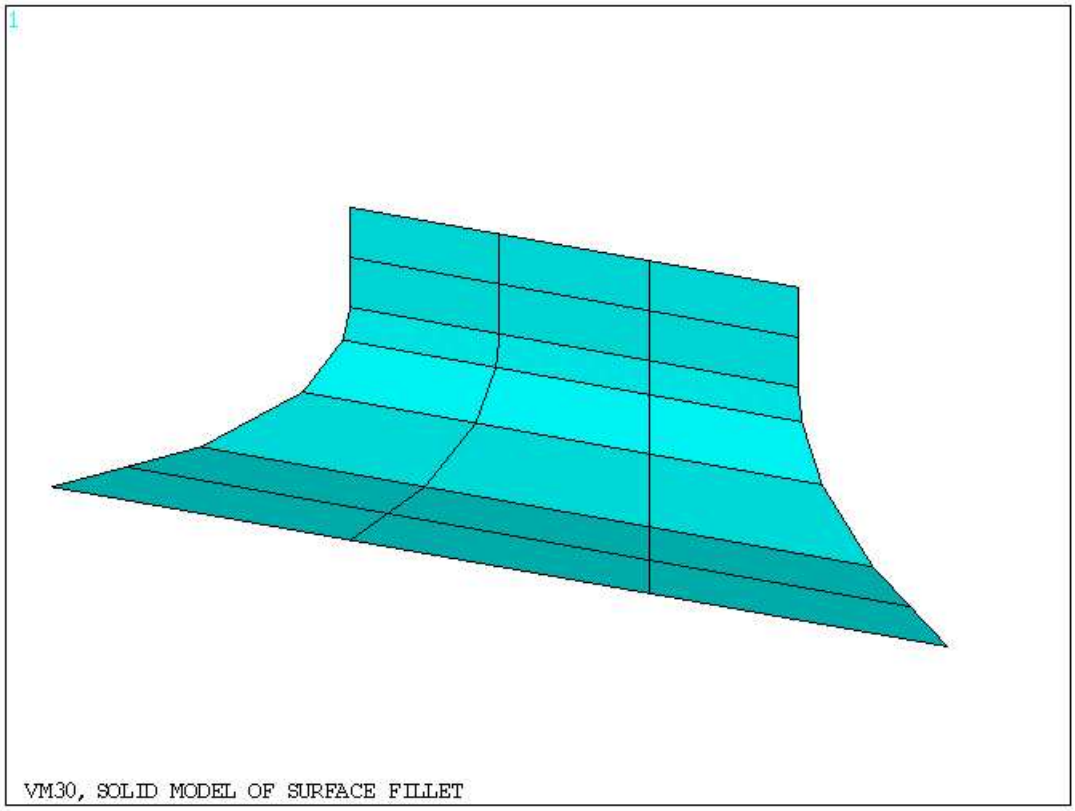

VM31: Cable Supporting Hanging Loads

Overview

Reference:	F. P. Beer, E. R. Johnston, Jr., *Vector Mechanics for Engineers, Statics and Dynamics*, McGraw-Hill Book Co., Inc., New York, NY, 1962, pg. 260, problem 7.8.
Analysis Type(s):	Static, Stress Stiffening Analysis (**ANTYPE** = 0)
Element Type(s):	Tension-only or Compression-only Spar Elements (LINK10)
Input Listing:	vm31.dat

Test Case

The cable AE supports three vertical loads from the points indicated. For the equilibrium position shown, determine the horizontal A_x and vertical A_y reaction forces at point A and the maximum tension T in the cable.

Figure 31.1 Hanging Load Problem Sketch

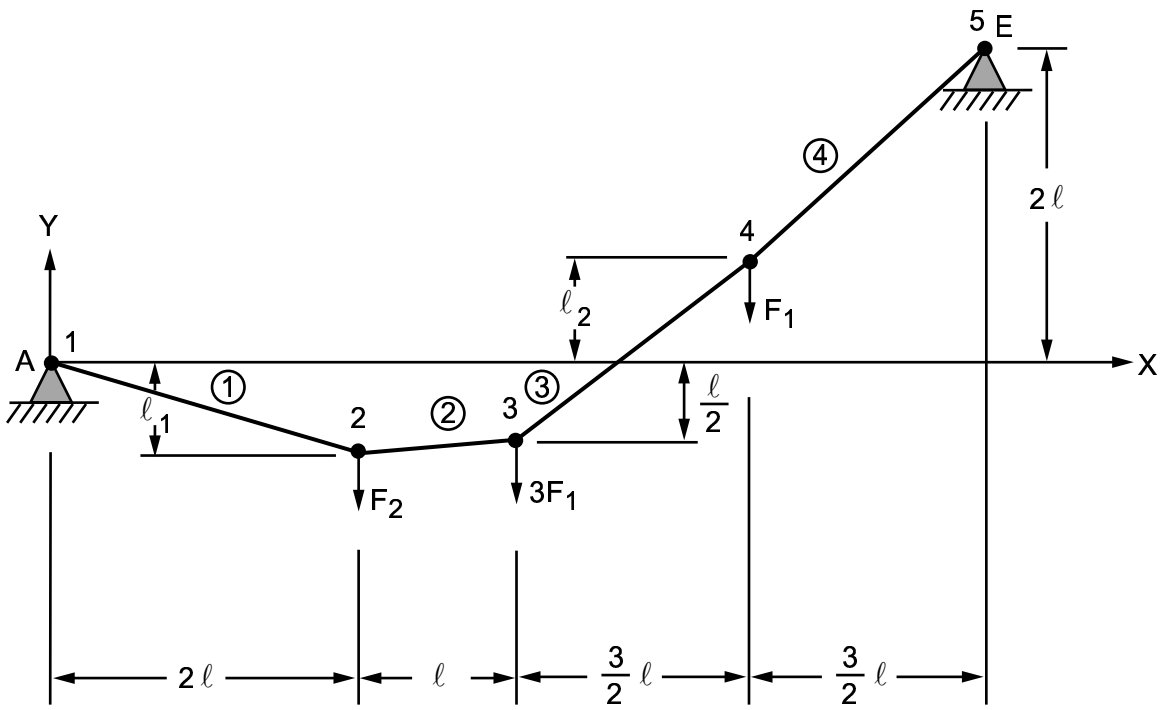

Problem Model

Material Properties	**Geometric Properties**	**Loading**
$E = 20 \times 10^6$ ksi	Area of cable = 0.1 ft^2 ℓ = 10 ft ℓ_1 = 5.56 ft ℓ_2 = 5.83 ft	F_1 = 4 kips F_2 = 6 kips

Analysis Assumptions and Modeling Notes

An iterative solution is required. A small initial strain (1×10^{-8}) is input to give some initial stiffness to the cable.

Results Comparison

	Target[1]	ANSYS	Ratio
A_x , Kips	-18.000	-17.997	1.000
A_y , Kips	5.0000	5.0009	1.000
T, Kips	24.762	24.756[2]	1.000

1. Solution recalculated
2. Corresponds to MFORX for element 4 in element solution output

VM32: Thermal Stresses in a Long Cylinder

Overview

Reference:	S. Timoshenko, *Strength of Material, Part II, Elementary Theory and Problems*, 3rd Edition, D. Van Nostrand Co., Inc., New York, NY, 1956, pg. 234, problem 1.
Analysis Type(s):	Static Analysis (**ANTYPE** = 0)
Element Type(s):	2-D Thermal Solid Elements (PLANE55) 2-D Structural Solid Elements (PLANE42)
Input Listing:	vm32.dat

Test Case

A long thick-walled cylinder is maintained at a temperature T_i on the inner surface and T_o on the outer surface. Determine the temperature distribution through the wall thickness. Also determine the axial stress σ_a and the tangential (hoop) stress σ_t at the inner and outer surfaces.

Figure 32.1 Long Cylinder Problem Sketch

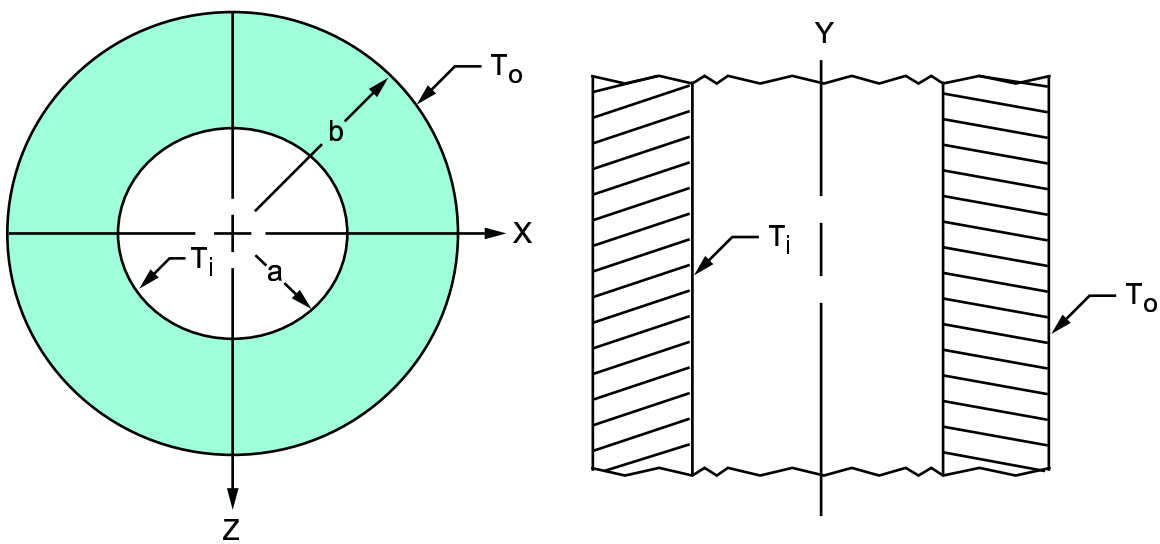

Problem Sketch

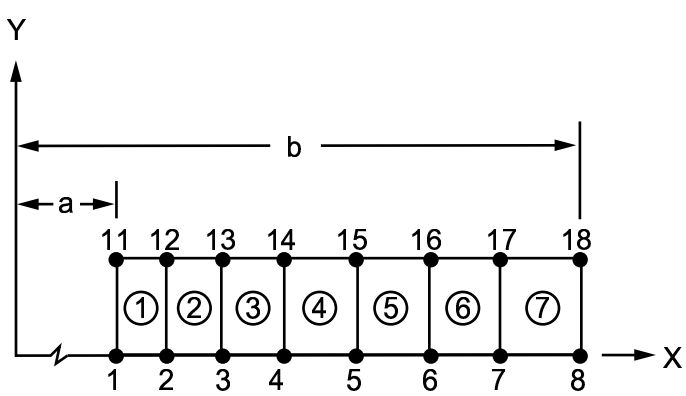

Representative Finite Element Model

Material Properties	Geometric Properties	Loading
$E = 30 \times 10^6$ psi $\alpha = 1.435 \times 10^{-5}$ in/in-°C $\upsilon = 0.3$ k = 3Btu/hr-in-°C	a = 0.1875 inches b = 0.625 inches	T_i = -1°C T_o = 0°C

Analysis Assumptions and Modeling Notes

The axial length is arbitrary. Two element types are defined so that the same model can be used for the thermal and stress solutions. A radial grid with nonuniform spacing ratio (1:2) is used since the largest rate of change of the thermal gradient occurs at the inner surface. Surface stresses are requested on element 1 and 7 to obtain more accurate axial and hoop stresses at the inner and outer radii. Nodal coupling is used in the static stress analysis.

Results Comparison

Thermal Analysis	Target	ANSYS	Ratio
T,°C (at X = 0.1875 in)	-1.0000	-1.0000	1.000
T,°C (at X = 0.2788 in)	-0.67037	-0.67061	1.000
T,°C (at X = 0.625 in)	0.0000	0.0000	-

Static Analysis	Target	ANSYS	Ratio
$Stress_a$, psi (at X = 0.1875 in)	420.42	419.59	0.998
$Stress_t$, psi (at X = 0.1875 in)	420.42	415.00	0.987
$Stress_a$, psi (at X = 0.625 in)	-194.58	-195.43	1.004
$Stress_t$, psi (at X = 0.625 in)	-194.58	-194.52	1.000

VM33: Transient Thermal Stress in a Cylinder

Overview

Reference:	R. J. Roark, W. C. Young, *Formulas for Stress and Strain*, 5th Edition, McGraw-Hill Book Co., Inc., New York, NY, 1975, pg. 585.
Analysis Type(s):	Coupled-field Analysis (**ANTYPE** = 4)
Element Type(s):	3-D Coupled-field Solid Element (SOLID5)
Input Listing:	vm33.dat

Test Case

A long thick-walled cylinder, initially at a uniform temperature T_o, has its outer radius temperature raised at a constant rate of 1.0°/sec to temperature T_f. After a steady state of heat flow has been reached, determine the tangential stress at the inner and outer surfaces. Display the outer-to-inner surface temperature difference and the tangential stress as a function of time.

Figure 33.1 Cylinder Problem Sketch

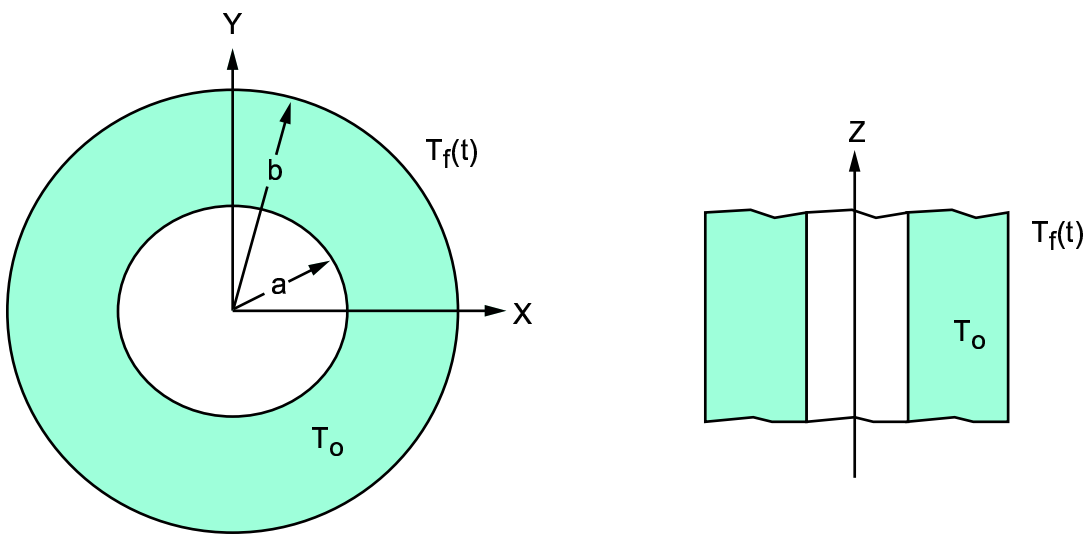

Problem Sketch

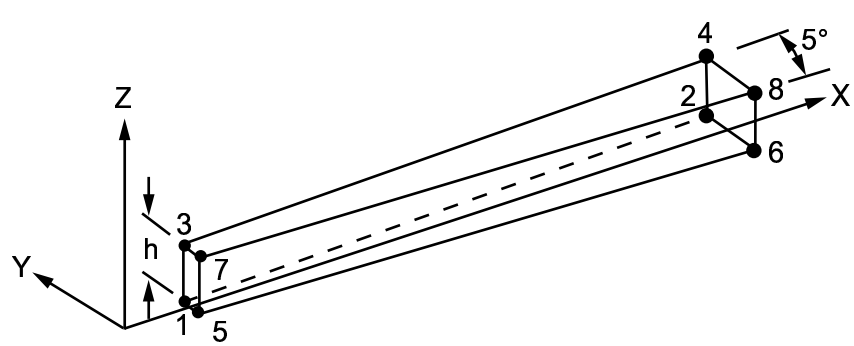

Keypoint and Line Segment Model

Material Properties	Geometric Properties	Loading
$E = 30 \times 10^6$ psi $\upsilon = 0.3$ $\alpha = 8.4 \times 10^{-6}$ in/in-°F k = .000625 BTU/sec in-°F $\rho = 0.284$ lb/in^3 c = .10 BTU/lb-°F	a = 1.0 in b = 3.0 in h = .20 in	$T_b = 500$°F $T_o = 70$°F

Analysis Assumptions and Modeling Notes

Due to symmetry, only a wedge of arbitrary height is required for modeling. A 5° wedge is selected to minimize curved geometry effects when using a lower order element. The thermal steady state condition is satisfied when the inner and outer wall temperature difference is constant. A transient thermal-stress analysis is required with a sufficient time period to allow the steady-state condition to be obtained. A time period of t = 430 sec is selected. The temperature T_f is assigned a value of T = 500°F such that, for a ramped load condition, the constant temperature rise of: T_f-T_o/Δt = 500-70/430 = 1°F/sec is obtained. Since the structural dynamic effects are not of concern, inertial and damping structural effects can be ignored, by specifying time integration for the temperature degree of freedom only. A sufficient number of elements (15) is modeled through the thickness such that an accurate thermal transient and nodal stress results are obtained.

Symmetric structural boundary conditions are used at the radial and bottom planes. Since the cylinder being modeled is long, nodes at z = h are coupled in UZ to enforce a constant axial strain condition. The reported values at t = 430 sec. should be fairly accurate since thermal steady state is achieved.

Results Comparison

Tangential Stress	Target	ANSYS	Ratio
$Stress_y$psi(r=b)	-13396	-13097	0.978
$Stress_y$psi(r=a)	10342	10425	1.008

Figure 33.2 Outer-to-inner Surface Temperature Difference

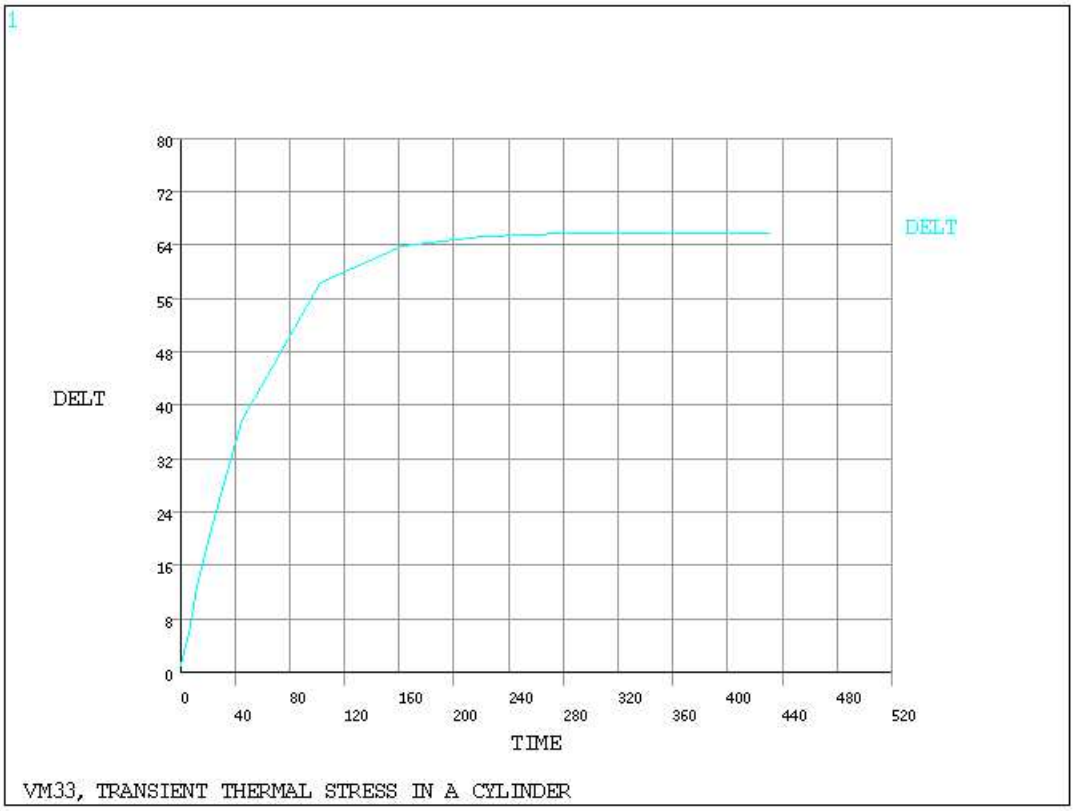

Figure 33.3 Tangential Stress as a Function of Time

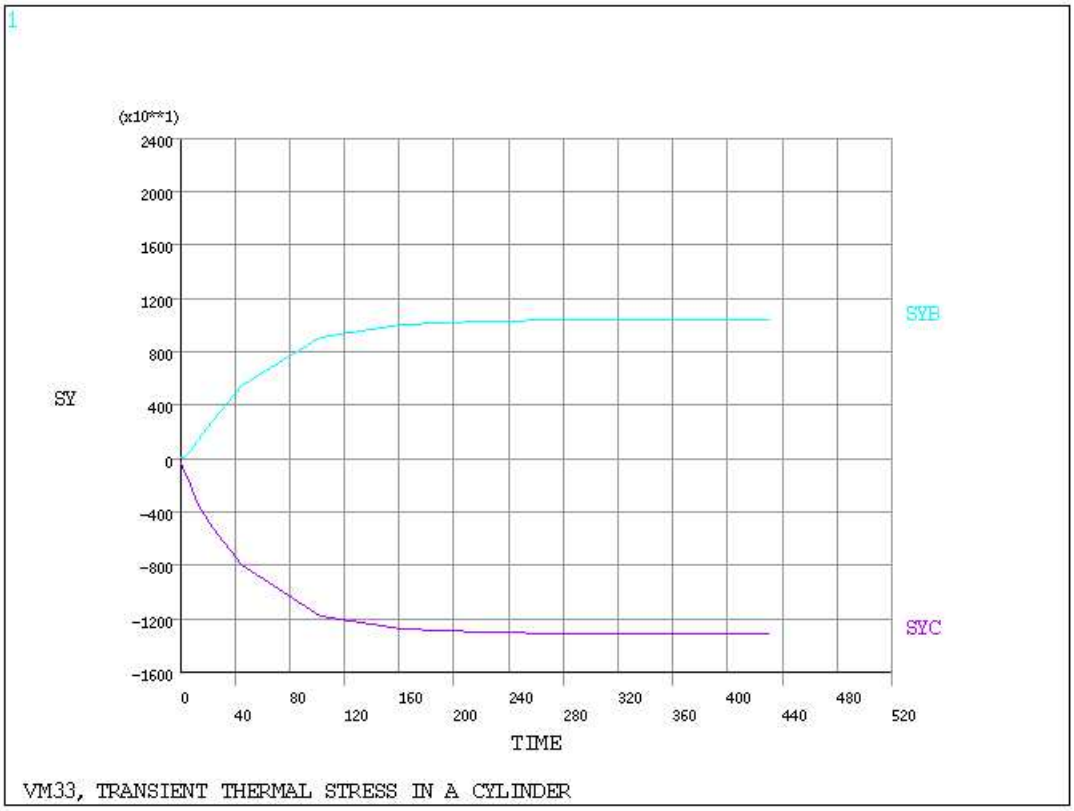

VM34: Bending of a Tapered Plate (Beam)

Overview

Reference:	C. O. Harris, *Introduction to Stress Analysis*, The Macmillan Co., New York, NY, 1959, pg. 114, problem 61.
Analysis Type(s):	Static Analysis (**ANTYPE** = 0)
Element Type(s):	Elastic Shell Elements (SHELL63) 3-D Elastic Tapered Unsymmetric Beam Elements (BEAM44) 3-D Elastic Tapered Unsymmetric Beam Element (BEAM188)
Input Listing:	vm34.dat

Test Case

A tapered cantilever plate of rectangular cross-section is subjected to a load F at its tip. Find the maximum deflection δ and the maximum principal stress σ_1 in the plate.

Figure 34.1 Beam Problem Sketch

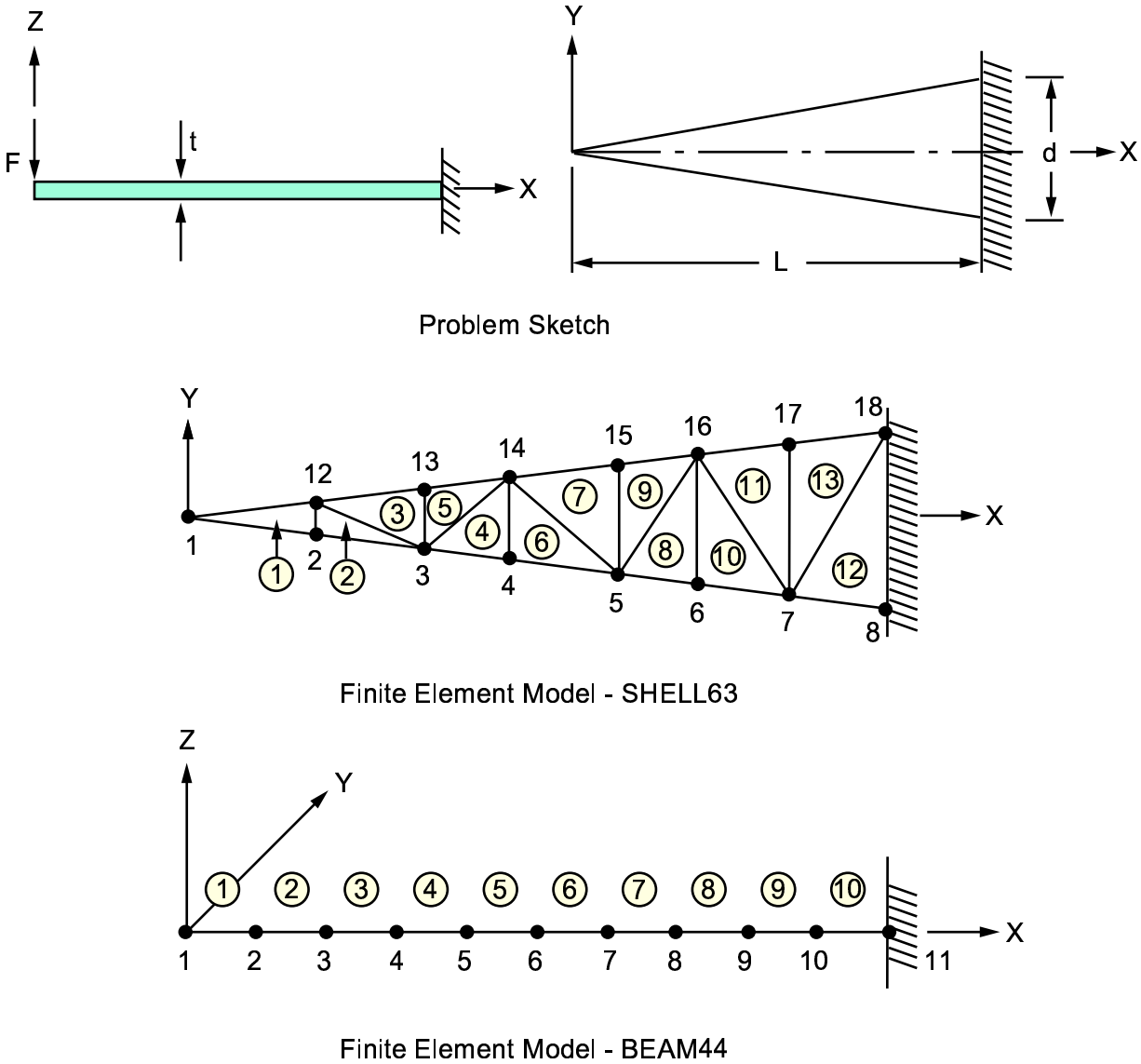

Material Properties	Geometric Properties	Loading
E = 30 x 10^6 psi υ = 0.0	L = 20 in d = 3 in t = 0.5 in	F = 10 lbs

Analysis Assumptions and Modeling Notes

The problem is solved first using quadrilateral shell elements (SHELL63) and then using tapered beam elements (BEAM44). For the quadrilateral shell elements (used in triangular form), nodal coupling is used to ensure symmetry. For the beam elements, the area and Y dimension of the beam are not used and are input as 1.0. Node 12 is arbitrarily located at Z = 1.0 in order to define the orientation of the beam. The problem is also solved using tapered sections beam elements (BEAM188).

Results Comparison

		Target	ANSYS	Ratio
SHELL63	Deflection, in	-0.042667	-0.042667	1.000
	$(Stress_1)_{max}$, psi	1600.00	1600.4	1.000
BEAM44	Deflection, in	-0.042667	-0.043109	1.010
	$(Stress_1)_{max}$, psi	1600.00	1600.00	1.000
BEAM188	Deflection, in	-0.042667	-0.042792	1.003
	$(Stress_1)_{max}$, psi	1600.00	1599.966	1.000

VM35: Bimetallic Layered Cantilever Plate with Thermal Loading

Overview

Reference:	R. J. Roark, W. C. Young, *Formulas for Stress and Strain*, 5th Edition, McGraw-Hill Book Co., Inc., New York, NY, 1975, pp. 113-114.
Analysis Type(s):	Static Analysis (**ANTYPE** = 0)
Element Type(s):	Nonlinear Layered Structural Shell Elements (SHELL91)
Input Listing:	vm35.dat

Test Case

A cantilever beam of length ℓ, width w, and thickness t is built from two equal thickness layers of different metals. The beam is stress free at $T_{ref.}$ The beam is fixed at the centerline of one end (X = 0, Y = w/2), and subjected to a uniform temperature T_a. Determine the deflection at the centerline of the free end (X = ℓ) of the cantilever and the outer fiber bending stress at the fixed end.

Figure 35.1 Cantilever Plate Problem Sketch

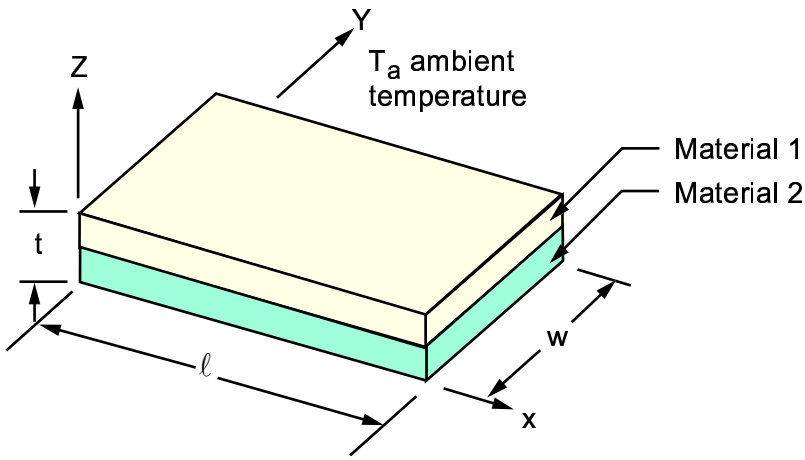

Problem Sketch

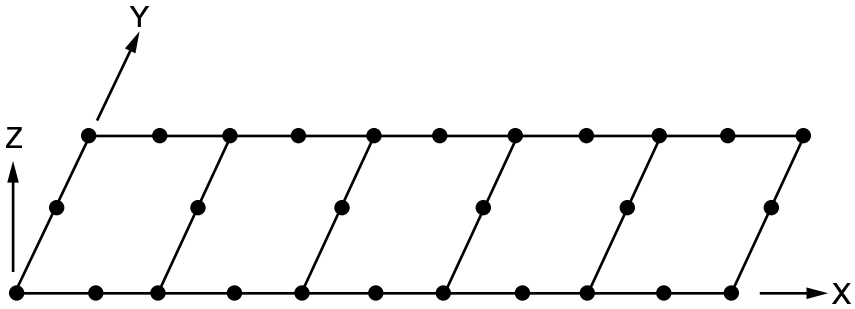

Representative Finite Element Model

Material Properties	Geometric Properties	Loading
$E_1 = E_2 = 3 \times 10^7$ psi $\upsilon_1 = \upsilon_2 = 0.0$ $\alpha_1 = 1 \times 10^{-5}$ in/in-°F $\alpha_2 = 2 \times 10^{-5}$ in/in-°F	$\ell = 10$ in t = 0.1 in	$T_{ref} = 70$°F $T_a = 170$°F

Analysis Assumptions and Modeling Notes

The width w is arbitrary for the solution of this problem and is chosen as 1 to produce reasonably-shaped elements. At the "fixed" end, only the center node is constrained to match the simple beam theory used in the reference, and allow unrestrained bending in the Y-Z plane.

Results Comparison

	Target	ANSYS	Ratio
free-end deflection$_z$, in	0.750	0.750	1.000
free-end deflection$_x$, in	0.015	0.015	1.000
fixed-end top stress$_x$, psi	7500	7500	1.000

VM36: Limit Moment Analysis

Overview

Reference:	S. H. Crandall, N. C. Dahl, *An Introduction to the Mechanics of Solids*, McGraw-Hill Book Co., Inc., New York, NY, 1959, pg. 389, ex. 8.9.
Analysis Type(s):	Static Analysis (**ANTYPE** = 0)
Element Type(s):	Combination Elements (COMBIN40) 3-D Elastic Beam Elements (BEAM4)
Input Listing:	vm36.dat

Test Case

A symmetric cross-section beam of bending stiffness EI_y, and height h, totally fixed at C, simply supported at A, is subjected to a concentrated load P at point B. Verify that a load P which is slightly smaller than the theoretical load limit P_L will cause elastic deformation and that a load which is slightly larger than P_L will cause plastic deformation. Also determine the maximum deflection δ, the reaction force at the left end R_A, and the reaction moment at the right end M_c just prior to the development of a plastic hinge.

Figure 36.1 Limit Moment Problem Sketch

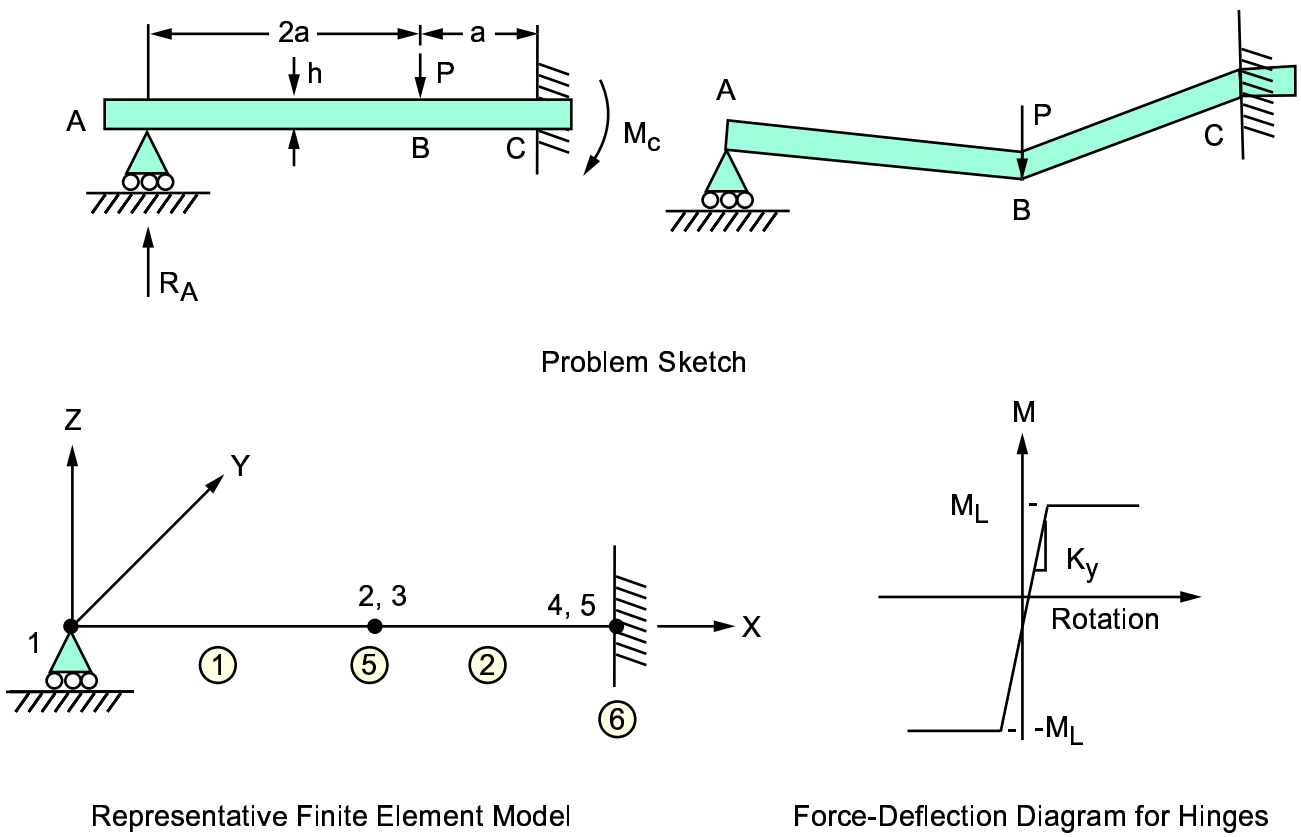

Material Properties	Geometric Properties	Loading
$E = 30 \times 10^6$ psi $\upsilon = .3$ $M_L = 27{,}777.77$ in-lb $K_y = 1 \times 10^{12}$ lb/in	a = 50 in $I_y = 20$ in^4 h/2 = 3.93597 in	P = -1000.0 lb (Load Step #1) P = -1388.8 lb (Load Step #2) P = -1390.0 lb (Load Step #3)

Analysis Assumptions and Modeling Notes

The load required for M_c=M_L (the limiting, or fully plastic bending moment) is calculated to be 1000 lbs. From the reference, the second plastic hinge develops at B when $P_L = 2.5M_L/a = 1388.88$ lb. The beam area is not necessary for this loading and is assumed to be 1.0. The beam half height, h/2, is input as a BEAM4 real constant. K_y is arbitrarily selected to be a large value (1×10^{12}) to minimize the elastic effect of the hinge.

Combination elements are used as breakaway hinge connections, which slide above the M_L value. An extra set of these elements are defined in parallel with an arbitrary low stiffness and a large value of real constant FSLIDE to maintain solution stability after collapse. Sliding status of the combination elements indicates that a plastic hinge has formed.

Results Comparison

		Target	ANSYS	Ratio
P = 1000 lbs (elastic)	Deflection, in	-0.02829	-0.02829	1.00
	R_A lb	148.15	148.15	1.00
	M_c in-lb	27778	27778	1.00
P = 1388.8 lbs	Hinge @ B	Elastic	Elastic	-
	Hinge @ C	Plastic	Sliding	-
P = 1390 lbs	Hinge @ B	Plastic	Sliding	-
	Hinge @ C	Plastic	Sliding	-

VM37: Elongation of a Solid Bar

Overview

Reference:	C. O. Harris, *Introduction to Stress Analysis*, The Macmillan Co., New York, NY, 1959, pg. 237, problem 4.
Analysis Type(s):	Static Analysis (**ANTYPE** = 0)
Element Type(s):	3-D Structural Solid Elements (SOLID45) 3-D Structural Solid Elements (SOLID185) 3-D Structural Solid Shell Elements (SOLSH190)
Input Listing:	vm37.dat

Test Case

A tapered aluminum alloy bar of square cross-section and length L is suspended from a ceiling. An axial load F is applied to the free end of the bar. Determine the maximum axial deflection δ in the bar and the axial stress σ_y at mid-length (Y = L/2).

Figure 37.1 Solid Bar Problem Sketch

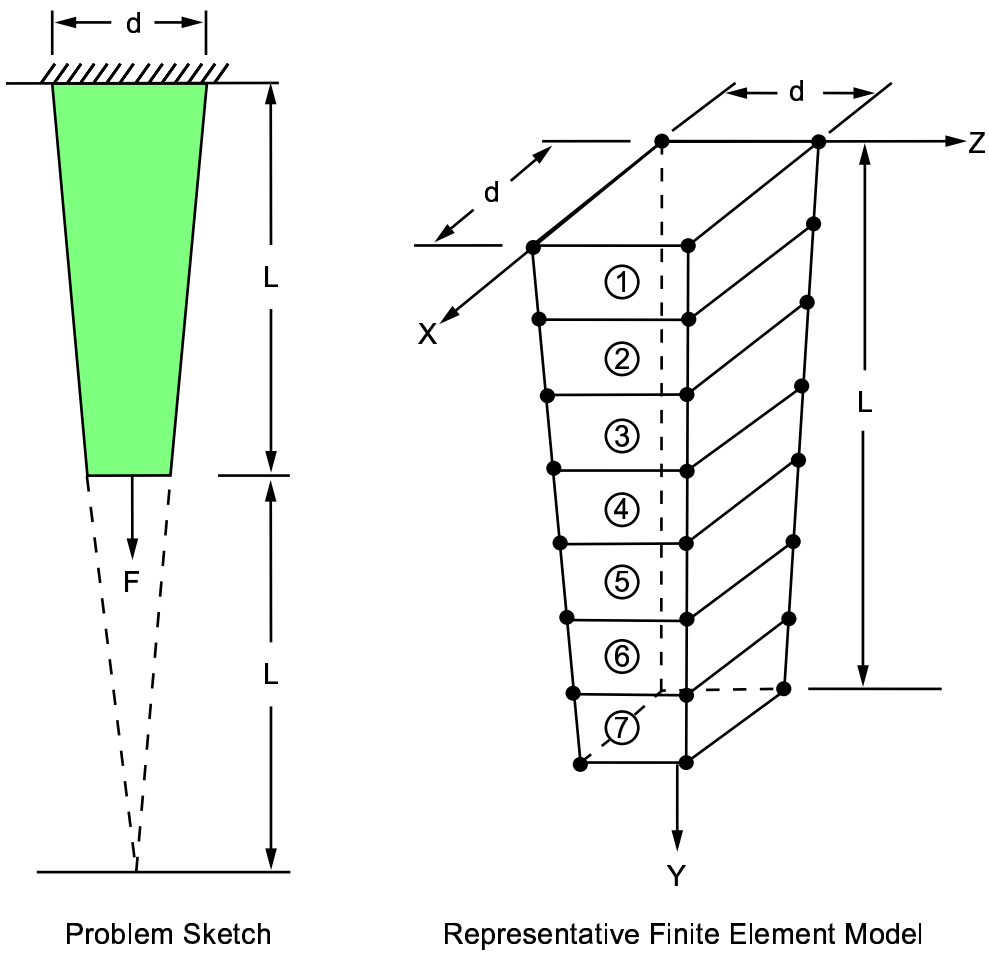

Material Properties	**Geometric Properties**	**Loading**
$E = 10.4 \times 10^6$ psi $\upsilon = .3$	L = 10 in d = 2 in	F = 10,000 lb

Analysis Assumptions and Modeling Notes

The problem is solved in three different ways:

- Using 3-D Structural Solid Elements (SOLID95)
- Using 3-D Structural Solid Elements (SOLID186)
- Using 3-D Structural Solid Shell Elements (SOLSH190)

A single tapered volume is mapped-meshed with seven brick-shaped elements along the length of the bar.

POST1 is used to get the nodal displacements at the free end and the axial stress at mid-length of the bar.

Results Comparison

	Target	ANSYS	Ratio
SOLID45			
d , in	0.0048077	.0047570	0.989
$Stress_y$, psi (elem. 4)	4444.	4441.	0.999
SOLID185			
d , in	0.0048077	.0047570	0.989
$Stress_y$, psi (elem. 4)	4444.	4441.	0.999
SOLSH190			
d , in	0.0048077	.0047801	0.994
$Stress_y$, psi (elem. 4)	4444.	4463.29	1.004

Figure 37.2 Elongation of a Solid-Bar-Axial Stress Contour Display (SOLID45 Model)

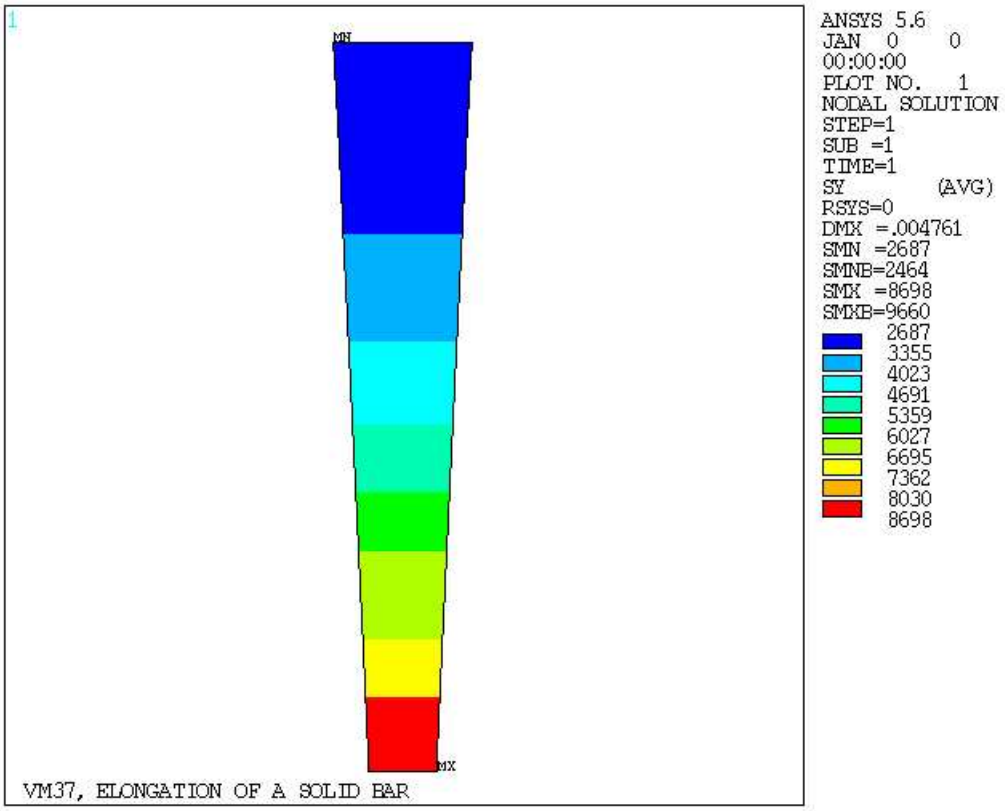

VM38: Plastic Loading of a Thick-Walled Cylinder

Overview

Reference:	S. Timoshenko, *Strength of Material, Part II, Elementary Theory and Problems*, 3rd Edition, D. Van Nostrand Co., Inc., New York, NY, 1956, pg. 388, article 70.
Analysis Type(s):	Static, Plastic Analysis (**ANTYPE** = 0)
Element Type(s):	2-D Structural Solid Elements (PLANE42) 2-D Structural Surface Effect Elements (SURF153) 3-D Structural Solid Elements (SOLID45) 3-D Structural Surface Effect Elements (SURF154)
Input Listing:	vm38.dat

Test Case

A long thick-walled cylinder is subjected to an internal pressure p (with no end cap load). Determine the radial stress, σ_r, and the tangential (hoop) stress, σ_t, at locations near the inner and outer surfaces of the cylinder for a pressure, p_{el}, just below the yield strength of the material, a fully elastic material condition. Determine the effective (von Mises) stress, σ_{eff}, at the same locations for a pressure, p_{ult}, which brings the entire cylinder wall into a state of plastic flow.

Figure 38.1 Thick-Walled Cylinder Problem Sketch

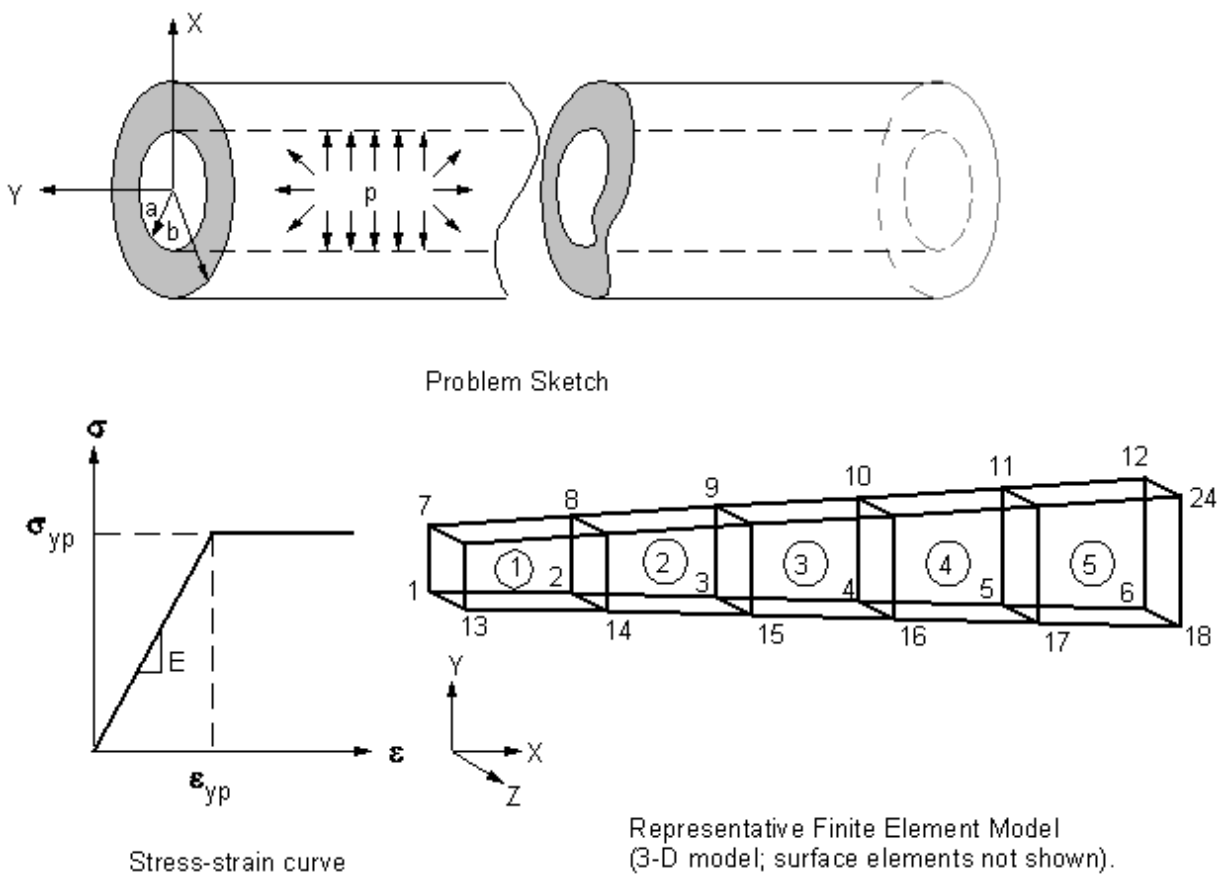

Material Properties	Geometric Properties	Loading
$E = 30 \times 10^6$ psi $\sigma_{yp} = 30{,}000$ psi $\upsilon = 0.3$	a = 4 in b = 8 in	$p_{el} = 12{,}990$ psi $p_{ult} = 24{,}011$ psi

Analysis Assumptions and Modeling Notes

The theory available for this problem is based on the Tresca (maximum shear) yield criterion while ANSYS uses the von Mises yield criterion. The applied p_{ult} pressure is calculated from the Tresca theory by using $T_y = \sigma_{yp}\sqrt{3}$. This procedure is sufficient to calculate approximate loads but the resulting nonlinear stress components should not be compared directly.

The problem is solved first using axisymmetric solid elements (PLANE42) and then using 3-D solid elements (SOLID45). Since the problem is axisymmetric, only a small sector (5°) is modeled with SOLID45. In order to ensure constant axial strain (implied by the "long" cylinder definition), nodal coupling is used with PLANE42 and SOLID45. Extra shapes are suppressed for PLANE42 and SOLID45.

To illustrate the use of surface effect elements, the internal pressure P is applied using 2-D structural surface effect elements (SURF153) in the first analysis, whereas 3-D structural surface effect elements (SURF154) are used in the second analysis. Results are obtained from the solution phase and from the element centroid data.

Results Comparison

		Target	ANSYS	Ratio
PLANE42: Fully Elastic	$Stress_r$, psi (X=4.4 in)	-9,984.	-9,900.	0.992
	$Stress_t$, psi (X=4.4 in)	18,645.	18,820.	1.009
	$Stress_r$, psi (X=7.6 in)	-468.	-458.	0.978
	$Stress_t$, psi (X=7.6 in)	9,128.	9,116.	0.999
PLANE42: Fully Plastic	$Stress_{eff}$, psi (X=4.4 in)	30,000.	29,991.[1]	1.000
	$Stress_{eff}$, psi (X=7.6 in)	30,000.	30,000.[1]	1.000
SOLID45: Fully Elastic	$Stress_r$, psi (X=4.4 in)	-9,984.	-9,891.	0.991
	$Stress_t$, psi (X=4.4 in)	18,645.	18,811.	1.009
	$Stress_r$, psi (X=7.6 in)	-468.	-455.	0.971
	$Stress_t$, psi (X=7.6 in)	9,128.	9,113.	0.998
SOLID45: Fully Plastic	$Stress_{eff}$, psi (X=4.4 in)	30,000.	29,991.[1]	0.999
	$Stress_{eff}$, psi (X=7.6 in)	30,000.	30,000.[1]	1.000

1. Output quantity SEQV

VM39: Bending of a Circular Plate with a Center Hole

Overview

Reference:	S. Timoshenko, *Strength of Material, Part II, Elementary Theory and Problems*, 3rd Edition, D. Van Nostrand Co., Inc., New York, NY, 1956, pg. 111, eq. E and F.
Analysis Type(s):	Static Analysis (**ANTYPE** = 0)
Element Type(s):	Elastic Shell Elements (SHELL63)
Input Listing:	vm39.dat

Test Case

A circular plate of thickness t with a center hole is rigidly attached along the inner edge and unsupported along the outer edge. The plate is subjected to bending by a moment M_a applied uniformly along the outer edge. Determine the maximum deflection δ and the maximum slope Φ of the plate. In addition, determine the moment M and stress σ_x at the top centroidal locations of element 1 (near inner edge) and element 6 (near outer edge).

Figure 39.1 Circular Plate Problem Sketch

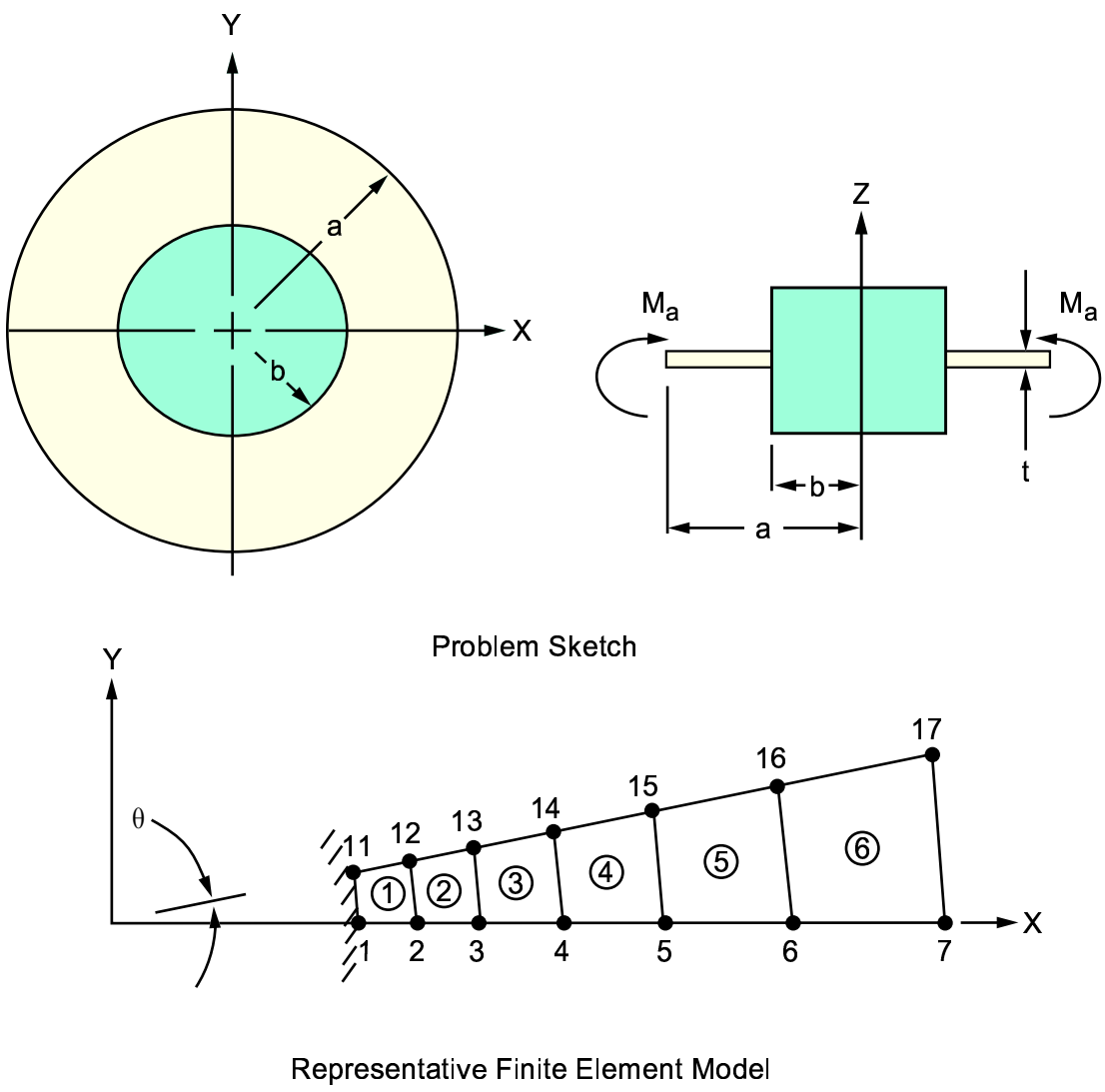

Material Properties	Geometric Properties	Loading
$E = 30 \times 10^6$ psi $\upsilon = .3$	a = 30 in b = 10 in t = .25 in $\Theta = 105$	M_a = 10 in-lb/in = 52.360 in-lb/10° segment

Analysis Assumptions and Modeling Notes

Since the problem is axisymmetric only a small sector of elements is needed. A small angle $\Theta = 10°$ is used for approximating the circular boundary with a straight-edged element. A radial grid with nonuniform (3:1) spacing is used. The calculated load is equally divided and applied to the outer nodes.

Results Comparison

		Target	ANSYS	Ratio
Deflection, in		.049064	.049218	1.003
Slope, rad		-.0045089	-.0045249	1.004
@ x = 10.81 in.	M, in-lb/in	-13.783	-13.675	0.992
	$Stress_x$, psi	-1323.2	-1312.7	0.992
@ x = 27.1 in.	M, in-lb/in	-10.127	-10.133	1.001
	$Stress_x$, psi	-972.22	-972.742	1.001

Figure 39.2 Window 1: UZ Displacement Contours; Window 2: Displaced Shape - Edge View

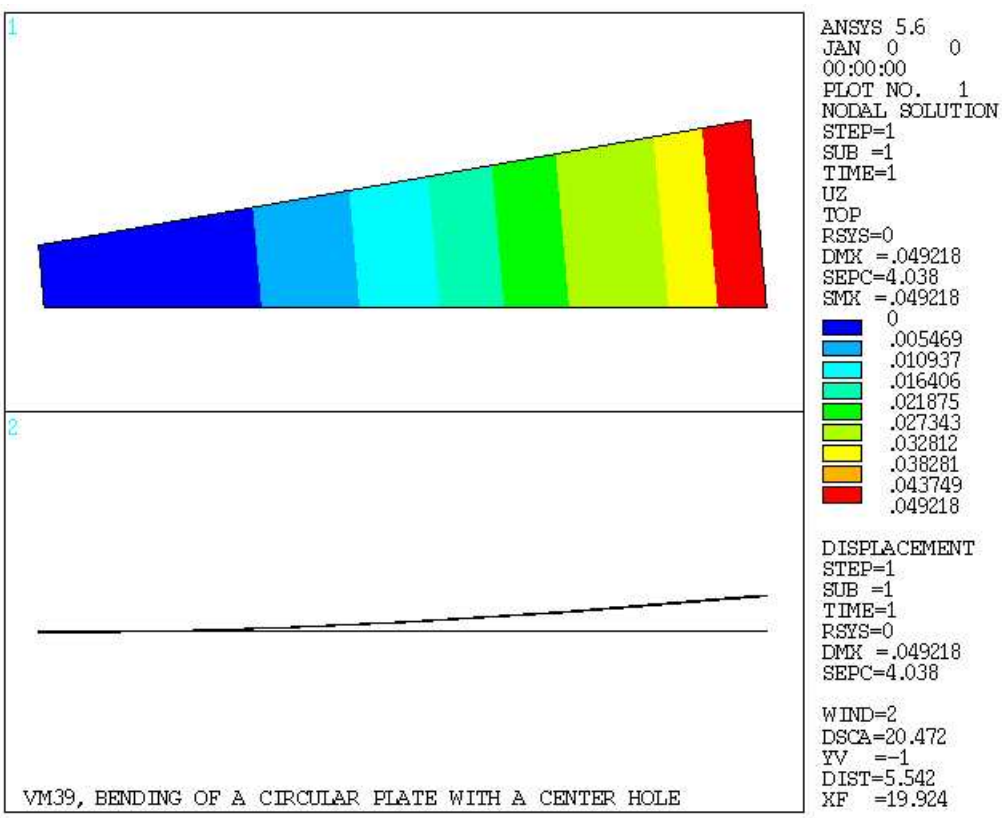

VM40: Large Deflection and Rotation of a Beam Pinned at One End

Overview

Reference:	Any basic mathematics book
Analysis Type(s):	Nonlinear Transient Dynamic Analysis (**ANTYPE** = 4)
Element Type(s):	2-D Elastic Beam Element (BEAM3)
Input Listing:	vm40.dat

Test Case

A massless beam of length L is initially at position AB on a horizontal frictionless table. Point A is pinned to the table and given a large rotation Θ_z through a full revolution at speed ω_z. Determine the position of the beam in terms of δ, and Θ at various angular locations. Show that the beam has no axial stress σ at any position.

Figure 40.1 Beam Problem Sketch

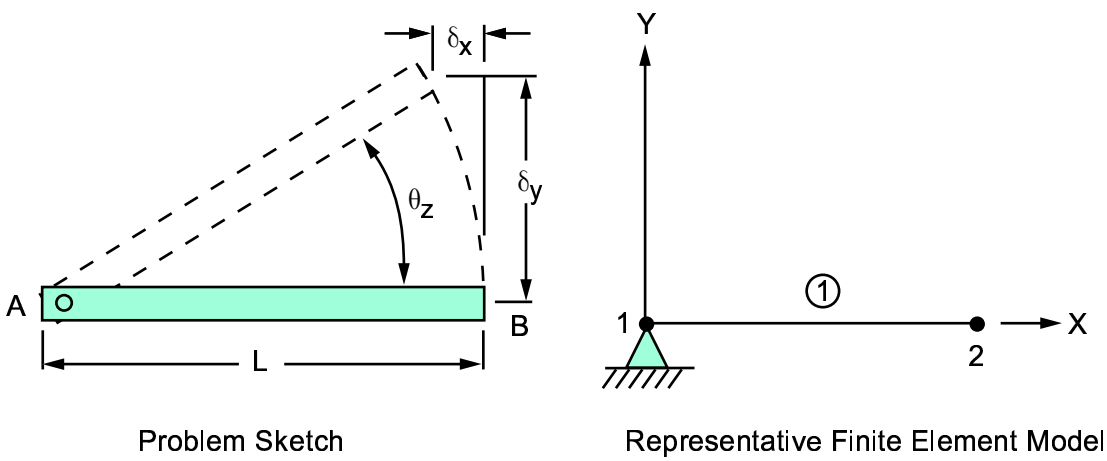

Material Properties	Geometric Properties	Loading
$E = 30 \times 10^6$ psi $\rho = 1 \times 10^{-10}$ lbs/in^3	L = 10 in	ω_z = 400 rpm (ccw)

Analysis Assumptions and Modeling Notes

The beam area, moment of inertia, and thickness have no effect on the solution and are assumed equal to 1.0. Density (ρ) is assigned as nearly zero (1×10^{-10}) to avoid centrifugal effects in the problem. Since this is rigid body motion, the time step is chosen to obtain the solution at discrete locations. The speed of 400 rpm is obtained by rotating one revolution in 0.15 sec (1/400th of a minute).

Results Comparison

Rotation$_z$, deg	Deflection	Target	ANSYS	Ratio
60	Deflection$_x$ (in)	-5.0	-5.0	1.00
90	Deflection$_y$ (in)	10.0	10.0	1.00
180	Deflection$_x$ (in)	-20.0	-20.0	1.00

Rotation$_z$, deg	Deflection	Target	ANSYS	Ratio
210	Deflection$_y$ (in)	-5.0	-5.0	1.00
315	Deflection$_x$ (in)	-2.93	-2.93	1.00
360	Deflection$_y$ (in)	0.0	0.0	-

Note — Axial stress, $\sigma \approx 0$, at each position.

Figure 40.2 Displacement of the Free End

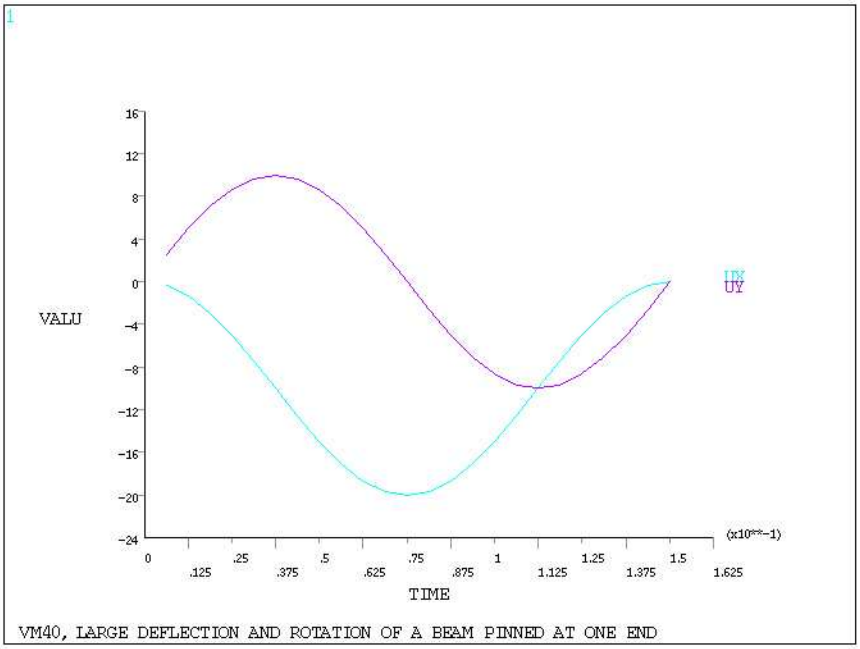

VM41: Small Deflection of a Rigid Beam

Overview

Reference:	Any Basic Statics and Strength of Material Book
Analysis Type(s):	Static Analysis (**ANTYPE** = 0)
Element Type(s):	Stiffness, Damping, or Mass Matrix Element (MATRIX27) 2-D Elastic Beam Element (BEAM3)
Input Listing:	vm41.dat

Test Case

A very stiff beam of length L, subjected to a lateral load F, is initially at position AB on a horizontal table. Point A is pinned to the table and restrained from rotation by a relatively weak torsion spring. Determine the final position of the beam in terms of δ_x, δ_y, and Θ. Show that the bending stress in the beam σ_{bend} is negligible.

Figure 41.1 Rigid Beam Problem Sketch

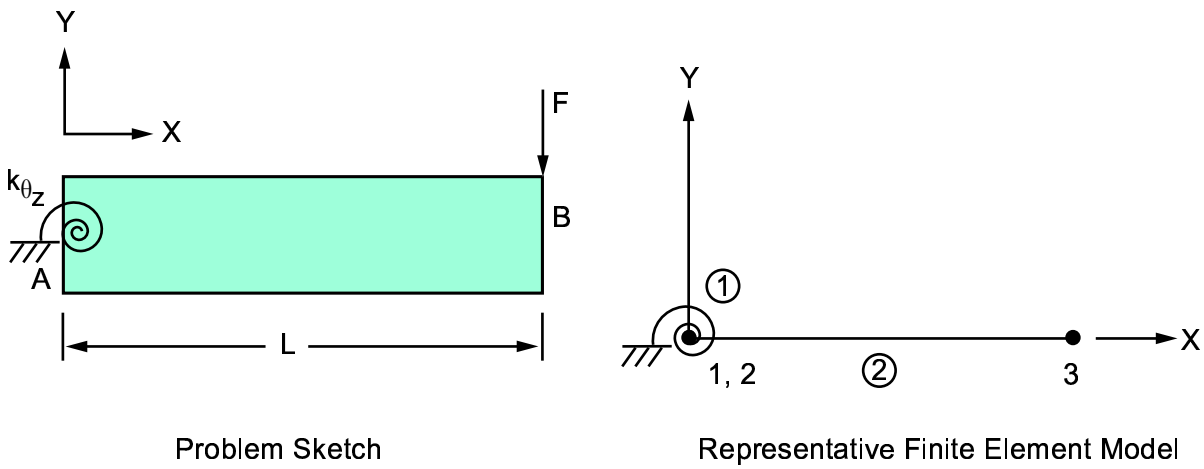

Material Properties	Geometric Properties	Loading
$K_{\theta z}$ = 10,000 in-lb/rad E = 30 x 10^6 psi	L = 10 in	F = 10 lb

Analysis Assumptions and Modeling Notes

The problem is solved using two approaches:

- thick beam geometry approach
- constraint equation approach

In the thick beam approach, the "rigid" beam properties are arbitrarily selected as area = 100 in^2, I = 1000 in^4, thickness = 10 in.

In the constraint equation approach, a constraint equation is used to enforce the assumption of a rigid beam. The constraint equation is of the form: $\delta_y = (L)(\Theta)$. The beam properties are arbitrarily based on a 0.25 square inch cross-section.

Results Comparison

		Target	ANSYS	Ratio
Thick Beam	$Deflection_x$, in	0.0	0.0	-
	$Deflection_y$, in	-0.1	-0.1	1.000
	Angle, rad	-0.01	-0.01	1.000
	$Stress_{bend}$, psi	0.0	0.5[1]	-
Constraint Equation	$Deflection_x$, in	0.0	0.0	-
	$Deflection_y$, in	-0.1	-0.1	1.000
	Angle, rad	-0.01	-0.01	1.000
	$Stress_{bend}$, psi	0.0	0.0	-

1. Small but negligible stress.

VM42: Barrel Vault Roof Under Self Weight

Overview

Reference:	R. D. Cook, *Concepts and Applications of Finite Element Analysis*, 2nd Edition, John Wiley and Sons, Inc., New York, NY, 1981, pp. 284-287.
Analysis Type(s):	Static Analysis (**ANTYPE** = 0)
Element Type(s):	8-Node Structural Shell Elements (SHELL93)
Input Listing:	vm42.dat

Test Case

A cylindrical shell roof of density ρ is subjected to a loading of its own weight. The roof is supported by walls at each end and is free along the sides. Find the x and y displacements at point A and the top and bottom stresses at points A and B. Express stresses in the cylindrical coordinate system.

Figure 42.1 Barrel Vault Roof Problem Sketch

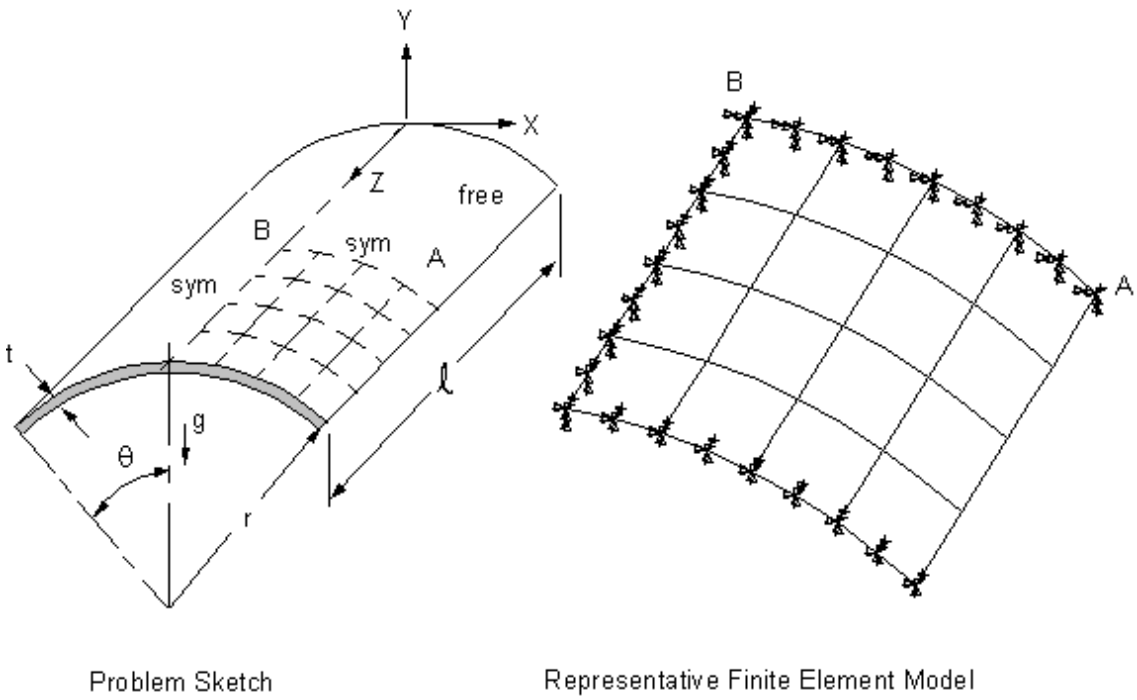

Material Properties	**Geometric Properties**	**Loading**
$E = 4.32 \times 10^8$ N/m^2 $\upsilon = 0.0$ $\rho = 36.7347$ kg/m^3	t = 0.25 m r = 25 m ℓ = 50 m $\Theta = 40°$	g = 9.8 m/s^2

Analysis Assumptions and Modeling Notes

A one-fourth symmetry model is used. Displacements, UX and UY, and the longitudinal rotation, ROTZ, are constrained at the roof end to model the support wall.

Results Comparison

	Target	ANSYS	Ratio
UY_A, m	-.3019	-.3029	1.003
UX_A, m	-.1593	-.1598	1.003
$Stress_z$, Top @ A, Pa	215,570.	216,056	1.002
$Stress_z$, Bot @ A, Pa	340,700.	341,438	1.002
$Stress_{angle}$, Top @ B, Pa	191,230.	190,666	0.997
$Stress_{angle}$, Bot @ B, Pa	-218,740.	-219,515	1.004

ANSYS Verification Manual . ANSYS Release 10.0 . 002184 . © SAS IP, Inc.

VM43: Bending of an Axisymmetric Thick Pipe

Overview

Reference:	R. J. Roark, *Formulas for Stress and Strain*, 4th Edition, McGraw-Hill Book Co., Inc., New York, NY, 1965, pg. 112, no. 33.
Analysis Type(s):	Static Analysis (**ANTYPE** = 0)
Element Type(s):	Axisymmetric-Harmonic 4-Node Structural Solid Elements (PLANE25)
Input Listing:	vm43.dat

Test Case

A long thick-walled pipe is rigidly supported at its ends between two walls. Determine the maximum deflection in the pipe due to gravity loading. Determine the maximum tensile stress σ_{max} at the outer surface of the pipe at Y = 4.16666 in.

Figure 43.1 Axisymmetric Thick Pipe Sketch Problem

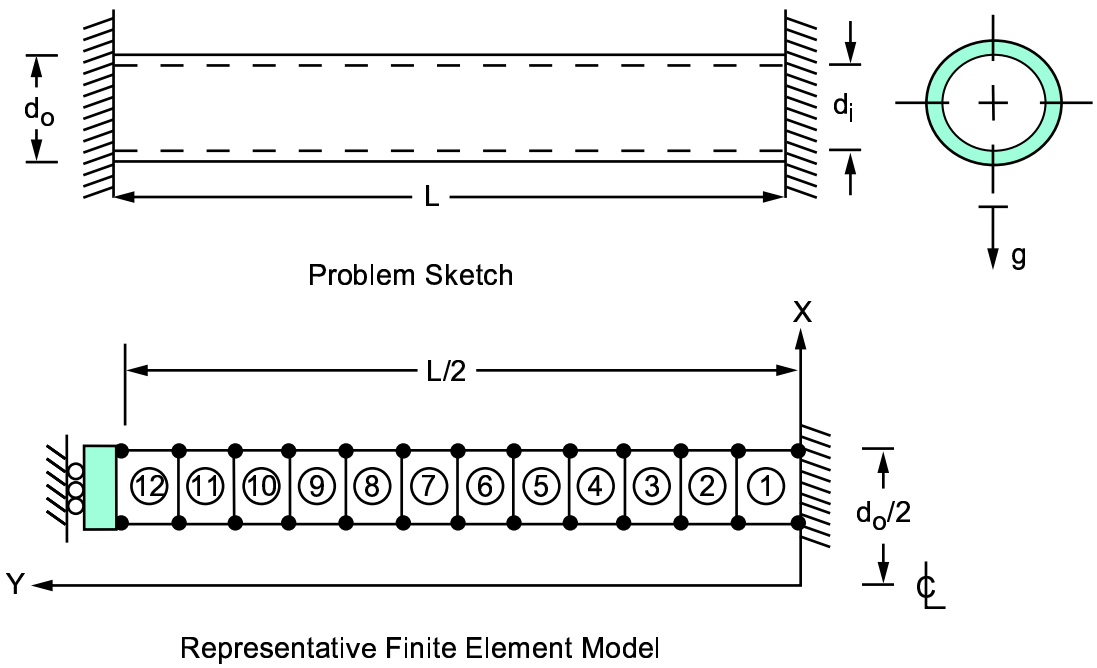

Material Properties	Geometric Properties	Loading
$E = 30 \times 10^6$ $\rho = .00073$ lb-sec^2/in^4 $\upsilon = 0.0$	L = 200 in $d_o = 2$ in $d_i = 1$ in	g = 386 in/sec^2

Analysis Assumptions and Modeling Notes

The loading g, which is constant in magnitude and direction around the circumference of the pipe, is applied as the sum of two harmonically varying loads. Each load has one wave around the circumference and is 90° out of phase with the other.

Results Comparison

	Target	ANSYS	Ratio
Deflection$_x$, in (angle = 0°)	-0.12524	-0.12529	1.000
Deflection$_z$, in (angle = 90°)	0.12524	0.12530	1.000
Stress$_{max}$, psi (angle = 0°)	2637.8	2652.4	1.006

Figure 43.2 Displacement Displays

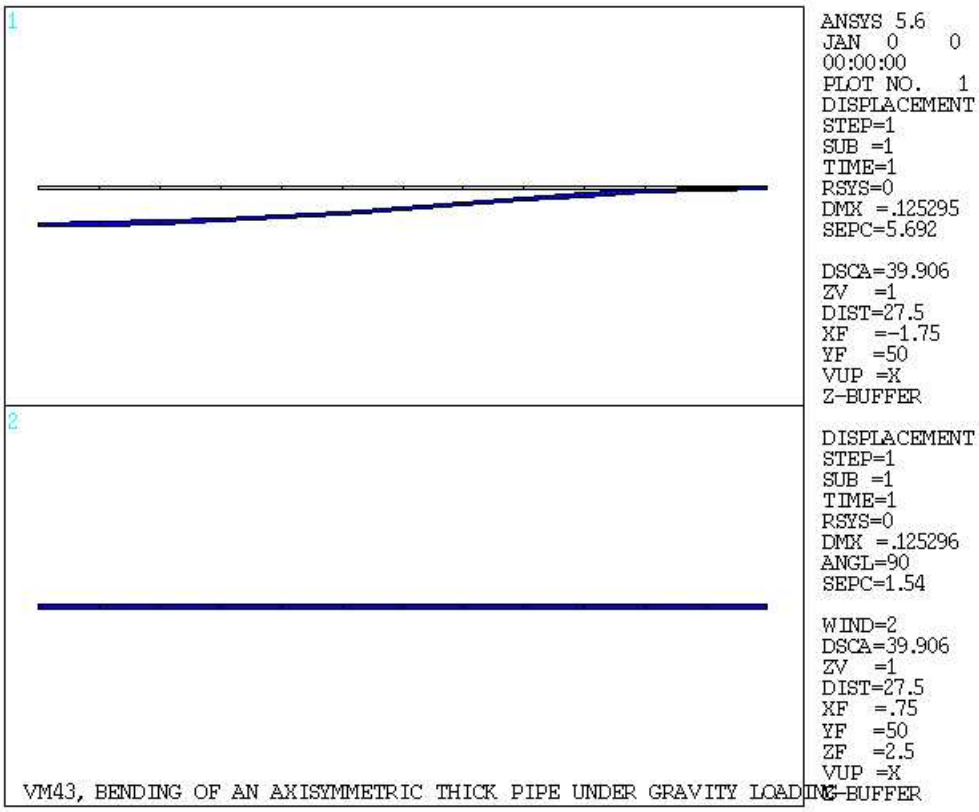

Window 1 Shows a Circumferential Angle of 0°
Window 2 Shows a Circumferential Angle of 90°

VM44: Bending of an Axisymmetric Thin Pipe

Overview

Reference:	R. J. Roark, *Formulas for Stress and Strain*, 4th Edition, McGraw-Hill Book Co., Inc., New York, NY, 1965, pg. 112, no. 33.
Analysis Type(s):	Static Analysis (**ANTYPE** = 0)
Element Type(s):	Axisymmetric Harmonic Structural Shell Elements (SHELL61)
Input Listing:	vm44.dat

Test Case

A long thin-walled pipe is rigidly supported at its ends between two walls. Determine the maximum deflection in the pipe due to gravity loading. Determine the maximum tensile stress σ_{max} at the outer surface of the pipe at Y = 0.

Figure 44.1 Axisymmetric Thin Pipe Problem Sketch

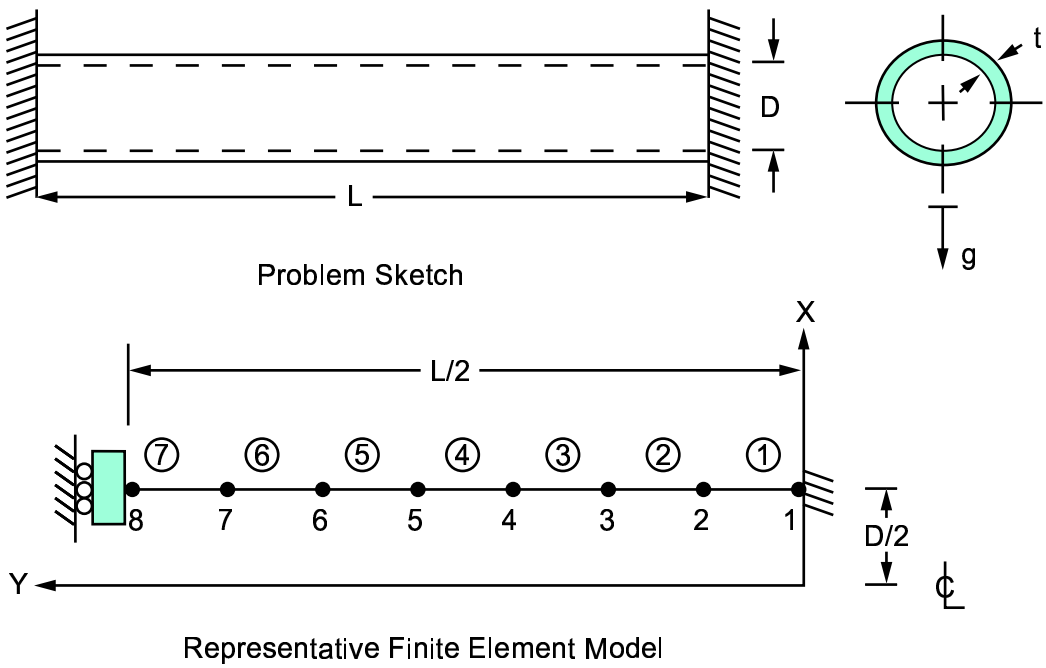

Material Properties	Geometric Properties	Loading
$E = 30 \times 10^6$ psi $\rho = 0.00073$ lb-sec^2/in^4 $\upsilon = 0.0$	L = 250 in D = 2 in t = 0.1 in	g = 386 in/sec^2

Analysis Assumptions and Modeling Notes

The loading g, which is constant in magnitude and direction around the circumference of the pipe, is applied as the sum of two harmonically varying loads. Each load has one wave around the circumference and is 90° out of phase with the other.

Results Comparison

	Target	ANSYS	Ratio
Deflection$_x$, in (angle = 0°)	-0.19062	-0.19079	1.001
Deflection$_z$, in (angle = 90°)	0.19062	0.19079	1.001
Stress$_{max}$, psi (angle = 0°)	3074.3	3059.1[1]	0.995

1. Corresponds to S1 at BOT of element 1 (section at node I).

Figure 44.2 Displacement Displays

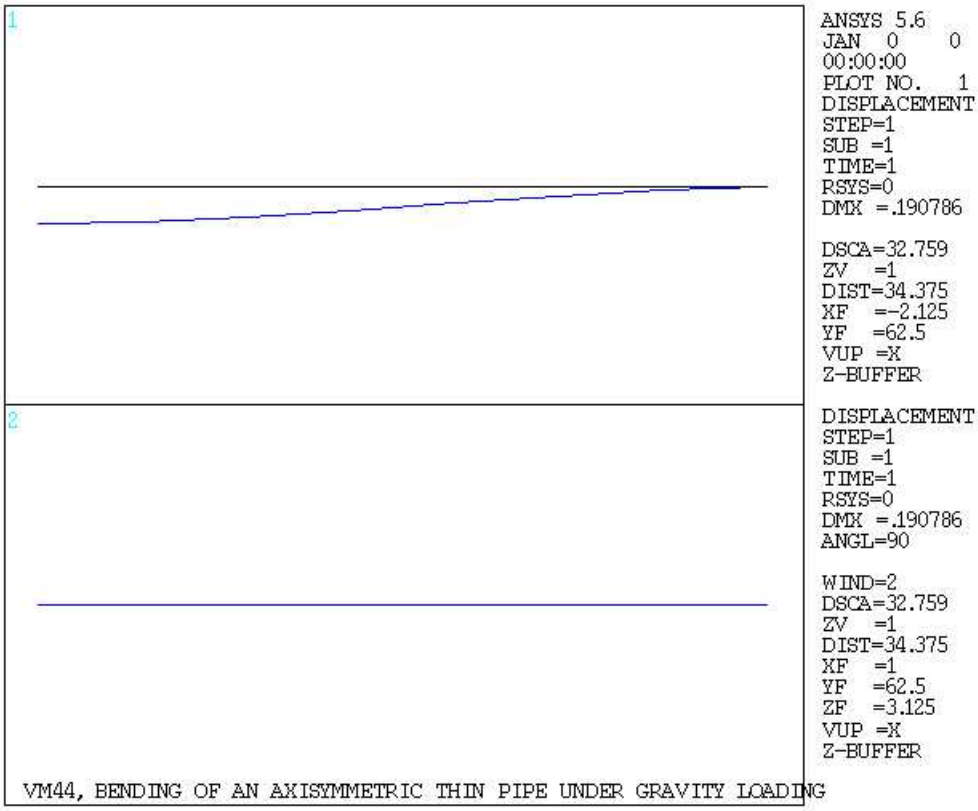

Window 1 Shows a Circumferential Angle of 0°
Window 2 Shows a Circumferential Angle of 90°

VM45: Natural Frequency of a Spring-Mass System

Overview

Reference:	W. T. Thomson, *Vibration Theory and Applications*, 2nd Printing, Prentice-Hall, Inc., Englewood Cliffs, NJ, 1965, pg. 6, ex. 1.2-2.
Analysis Type(s):	Mode-frequency Analysis (**ANTYPE** = 2)
Element Type(s):	Spring-Damper Element (COMBIN14) Structural Mass Element (MASS21)
Input Listing:	vm45.dat

Test Case

An instrument of weight W is set on a rubber mount system having a stiffness k. Determine its natural frequency of vibration f.

Figure 45.1 Spring-mass System Problem Sketch

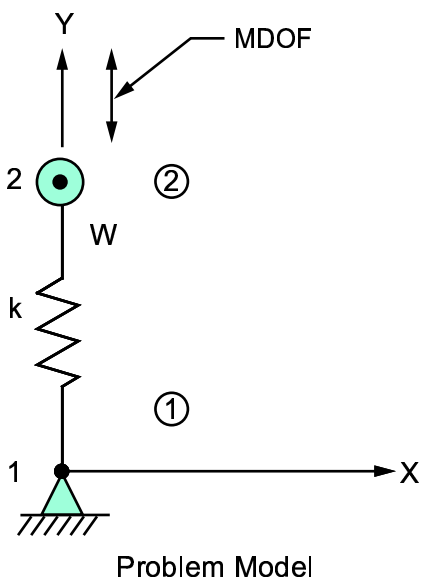

Material Properties	**Loading**
k = 48 lb/in W = 2.5 lb	g = 386 in/sec^2

Analysis Assumptions and Modeling Notes

The spring length is arbitrarily selected. One master degree of freedom is chosen at the mass in the spring length direction. The weight of the lumped mass element is divided by gravity in order to obtain the mass. Mass = W/g = 2.5/386 = .006477 lb-sec^2/in.

Results Comparison

	Target	ANSYS	Ratio
f, Hz	13.701	13.701	1.000

VM46: Flow Between Rotating Concentric Cylinders

Overview

Reference:	F. M. White, *Viscous Fluid Flow*, McGraw-Hill Book Co., Inc., New York, NY, 1991, Section 3-2.3.
Analysis Type(s):	Fluid, Flow Analysis (**FLOTRAN**)
Element Type(s):	3-D Fluid-Thermal Element (FLUID142)
Input Listing:	vm46.dat

Test Case

Consider the steady flow maintained between two infinite concentric cylinders by a constant angular velocity of the inner cylinder while the outer cylinder remains fixed. Determine the velocity distribution between the two cylinders using a rotating reference frame attached to the inner cylinder.

Figure 46.1 Concentric Cylinders Problem Sketch

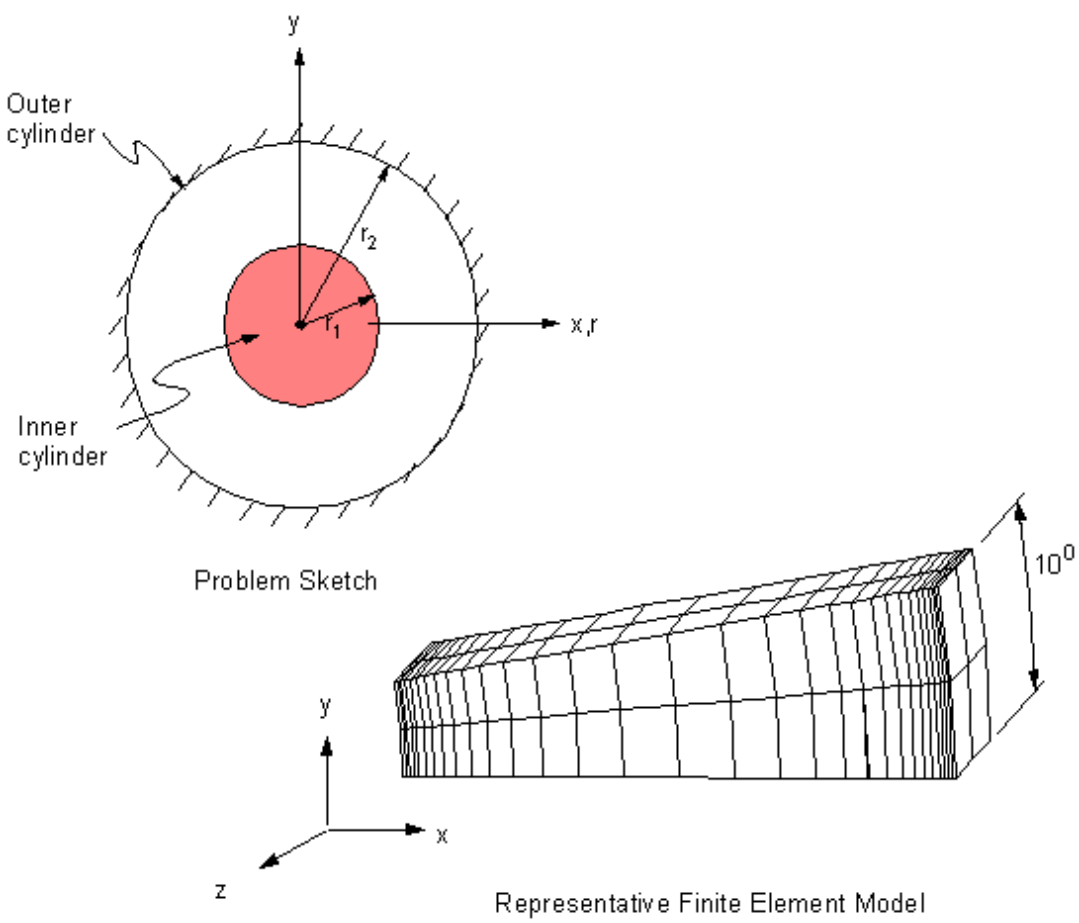

Material Properties	Geometric Properties	Loading
ρ = lb-sec^2/in^4 μ = 1.0 lb-sec/in^2	r_1 = 1.0 in r_2 = 2.0 in	ω = 1.0 rad/sec

Analysis Assumptions and Modeling Notes

The flow is steady-state and incompressible. The periodic nature of the solution permits the use of a model representing 10 degree angular section. The boundary conditions at $\Theta = 0$ are periodic and applied using the macro PERI. The mesh density is skewed at the boundaries to resolve the pressure gradient.

The circumferential velocity (VY) is a function of the radius while the radial and axial components are zero. The circumferential velocity component is given by:

$$VY(r) = \frac{r_2^2\omega}{r_2^2 - r_1^2}[r_1^2/r - r]$$

The pressure distribution is nonlinear, with a steep gradient in the region near the rotating inner cylinder.

Results Comparison

	Target	ANSYS	Ratio
VY (r = 1.5)	-1.111	-1.111	1.0

Figure 46.2 Velocity Distribution

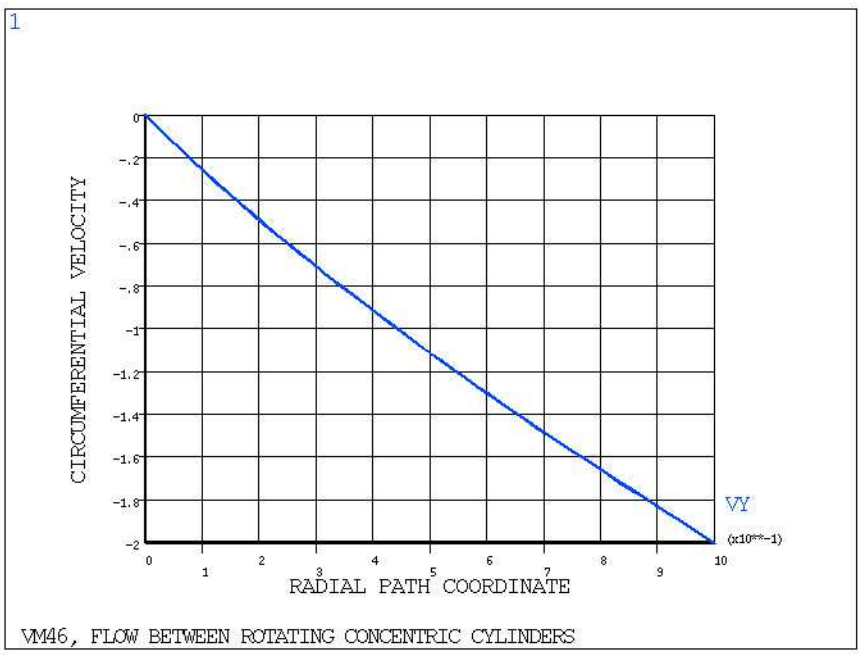

Figure 46.3 Pressure Distribution

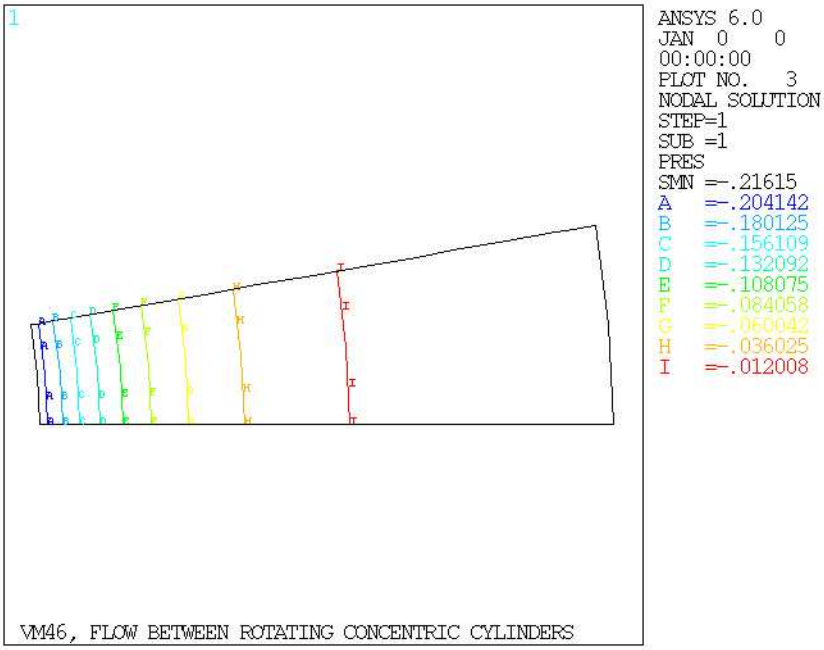

VM47: Torsional Frequency of a Suspended Disk

Overview

Reference:	W. T. Thomson, *Vibration Theory and Applications*, 2nd Printing, Prentice-Hall, Inc., Englewood Cliffs, NJ, 1965, pg. 10, ex. 1.3-2
Analysis Type(s):	Mode-frequency Analysis (**ANTYPE** = 2)
Element Type(s):	Spring-Damper Elements (COMBIN14) Structural Mass Elements (MASS21)
Input Listing:	vm47.dat

Test Case

A disk of mass m which has a polar moment of inertia J is suspended at the end of a slender wire. The torsional stiffness of the wire is k_θ. Determine the natural frequency f of the disk in torsion.

Figure 47.1 Suspended Disk Problem Sketch

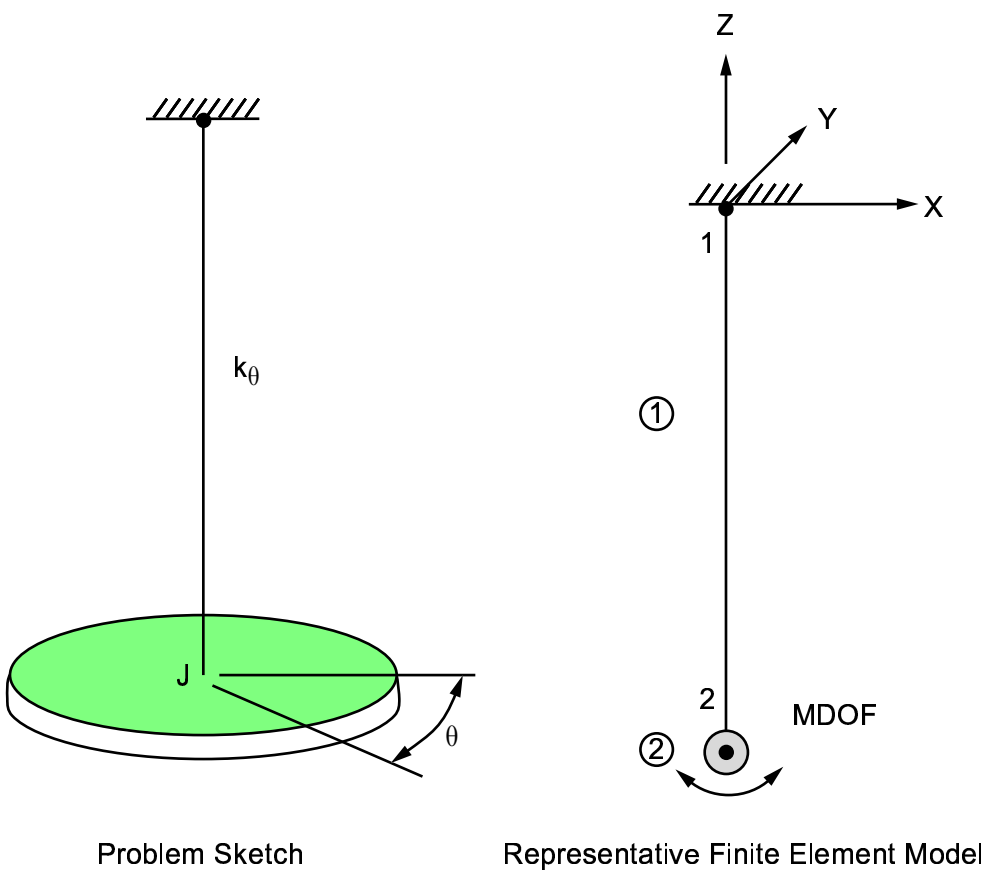

Material Properties	Geometric Properties
m = 1 lb-sec^2/in k_θ = 4.8 in-lb/rad	J = .30312 lb-in-sec^2

Analysis Assumptions and Modeling Notes

The length of the wire is arbitrarily selected. One rotational master degree of freedom at the disk is chosen.

Results Comparison

	Target	ANSYS	Ratio
f, Hz	0.63333	0.63333	1.00

VM48: Natural Frequency of a Motor-Generator

Overview

Reference:	W. T. Thomson, *Vibration Theory and Applications*, 2nd Printing, Prentice-Hall, Inc., Englewood Cliffs, NJ, 1965, pg. 10, ex. 1.3-3
Analysis Type(s):	Mode-frequency Analysis (**ANTYPE** = 2)
Element Type(s):	Elastic Straight Pipe Elements (PIPE16) Structural Mass Elements (MASS21)
Input Listing:	vm48.dat

Test Case

A small generator of mass m is driven off a main engine through a solid steel shaft of diameter d. If the polar moment of inertia of the generator rotor is J, determine the natural frequency f in torsion. Assume that the engine is large compared to the rotor so that the engine end of the shaft may be assumed to be fixed. Neglect the mass of the shaft also.

Figure 48.1 Motor-Generator Problem Sketch

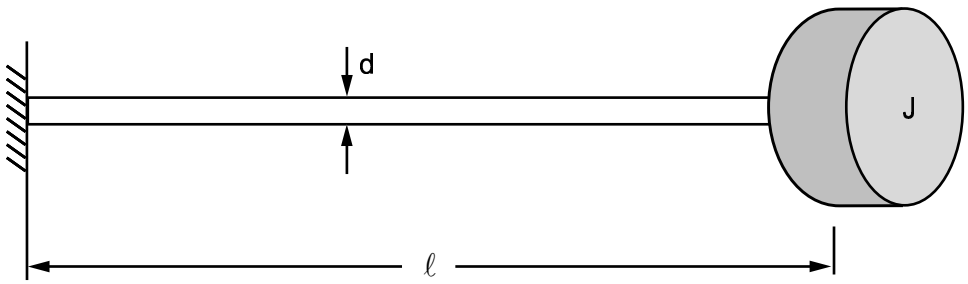

Problem Sketch

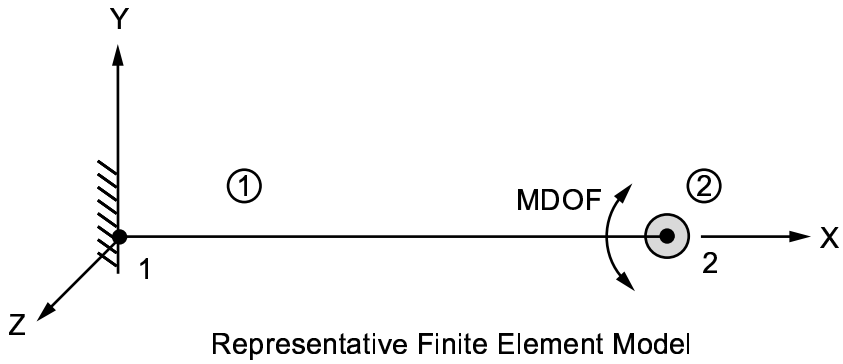

Representative Finite Element Model

Material Properties	Geometric Properties
E = 31.2 x 10^6 psi m = 1 lb-sec^2/in	d = .375 in ℓ = 8.00 in J = .031 lb-in-sec^2

Analysis Assumptions and Modeling Notes

One rotational master degree of freedom is selected at the mass. The wall thickness of the pipe is defined as half the diameter to obtain a solid cross-section.

Results Comparison

	Target	ANSYS	Ratio
f, Hz	48.781	48.781	1.00

ANSYS Verification Manual . ANSYS Release 10.0 . 002184 . © SAS IP, Inc.

VM49: Electrostatic Field Analysis of Quadpole Wires

Overview

Reference:	Any Basic Static and Dynamic Electricity Book
Analysis Type(s):	Static, Electrostatic Analysis (**ANTYPE** = 0)
Element Type(s):	2-D 8-Node Electrostatic Solid Element (PLANE121) 2-D Infinite Solid Element (INFIN110)
Input Listing:	vm49.dat

Test Case

Two wires of quadpole device system of zero radius, carrying positive charge, q_1 are placed along the X-axis with their centers located at positive and negative distances, d from the origin, O. Two wires of the same radius carrying negative charge, q_2, are placed along the Y-axis with their centers at positive and negative distances, d from the origin, O. All wires are extended in the Z direction. Determine the electric potential, V, produced out to a radius of 470 mm measured from the origin, O.

Figure 49.1 Quadpole Wires Problem Sketch

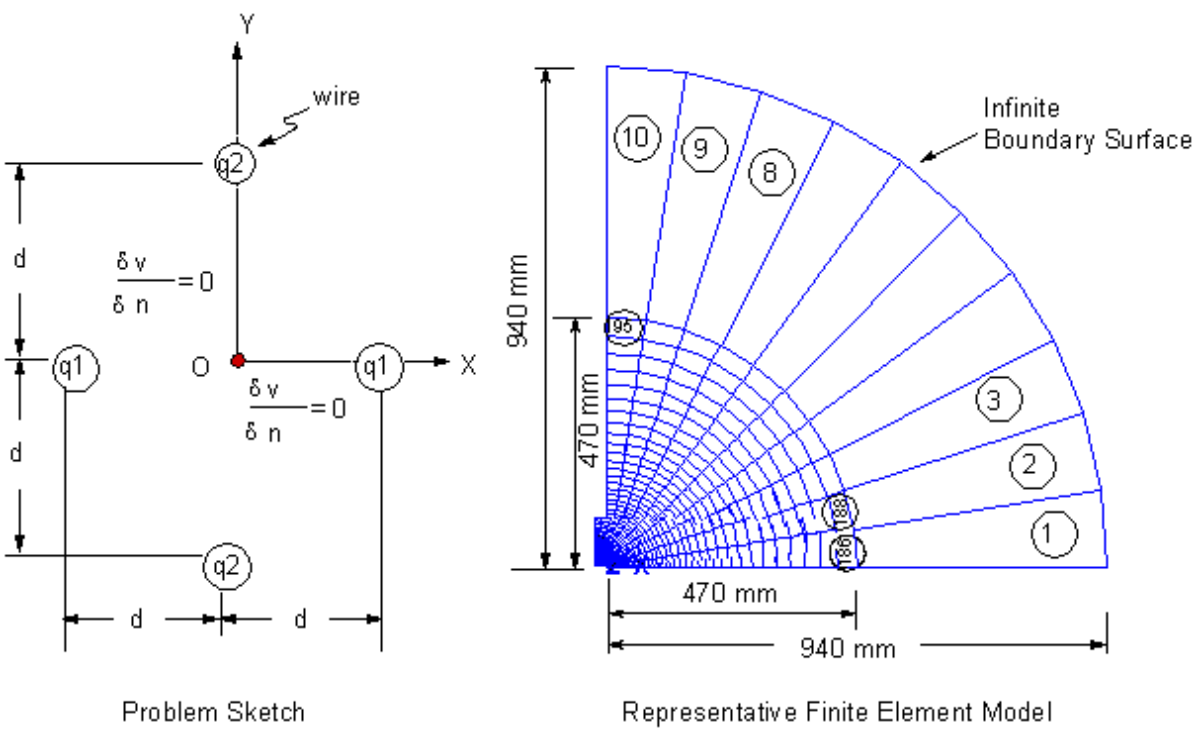

Material Properties	Geometric Properties	Loading
$\varepsilon_o = 8.85 \times 10^{-12}$ F/m	d = 25.4 mm	$q_1 = +10^{-6}$ C/m $q_2 = -10^{-6}$ C/m

Analysis Assumptions and Modeling Notes

Two dimensional quad elements of PLANE121 are used out to the radius of 470 mm. At this radius the INFIN110 (quad elements) with length equal to two times the 470 mm are used. Due to symmetry only one quadrant

(positive X and positive Y), containing one half of each of two wires (carrying half of positive and negative charge magnitude), is modeled with flux-normal boundary conditions at X = 0.0 and Y = 0.0 axes. Note, since 4-node INFIN110 elements are used with 8-node PLANE121, the infinite element domain is required to mesh before the finite element domain to drop off automatically the midside nodes from the PLANE121 element faces at the interface of the finite and infinite element domain. SF command with label, INF is used to flag the exterior surface (at infinity) of the INFIN110 elements. The charge is applied as a point load at the center of each of two wires.

In POST1 electric potential V at angles 0 to 90° (with 10 divisions) on the outer surface of radius 470 mm are retrieved and written by ***VWRITE** command.

Results Comparison

V (Volt)	Target	ANSYS	Ratio
@ Angle 0°	105.05	105.79	1.01
@ Angle 9°	99.90	100.62	1.01
@ Angle 18°	84.98	85.59	1.01
@ Angle 27°	61.74	62.18	1.01
@ Angle 36°	32.46	32.69	1.01
@ Angle 45°	0.0000	0.0000	0.0
@ Angle 54°	-32.46	-32.69	1.01
@ Angle 63°	-61.74	-62.18	1.01
@ Angle 72°	-84.98	-85.59	1.01
@ Angle 81°	-99.98	-100.62	1.01
@ Angle 90°	-105.05	-105.79	1.01

ANSYS Verification Manual . ANSYS Release 10.0 . 002184 . © SAS IP, Inc.

VM50: Fundamental Frequency of a Simply Supported Beam

Overview

Reference:	W. T. Thomson, *Vibration Theory and Applications*, 2nd Printing, Prentice-Hall, Inc., Englewood Cliffs, NJ, 1965, pg. 18, ex. 1.5-1
Analysis Type(s):	Mode-frequency Analysis (**ANTYPE** = 2)
Element Type(s):	2-D Elastic Beam Elements (BEAM3)
Input Listing:	vm50.dat

Test Case

Determine the fundamental frequency f of a simply-supported beam of length ℓ and uniform cross-section as shown below.

Figure 50.1 Simply Supported Beam Problem Sketch

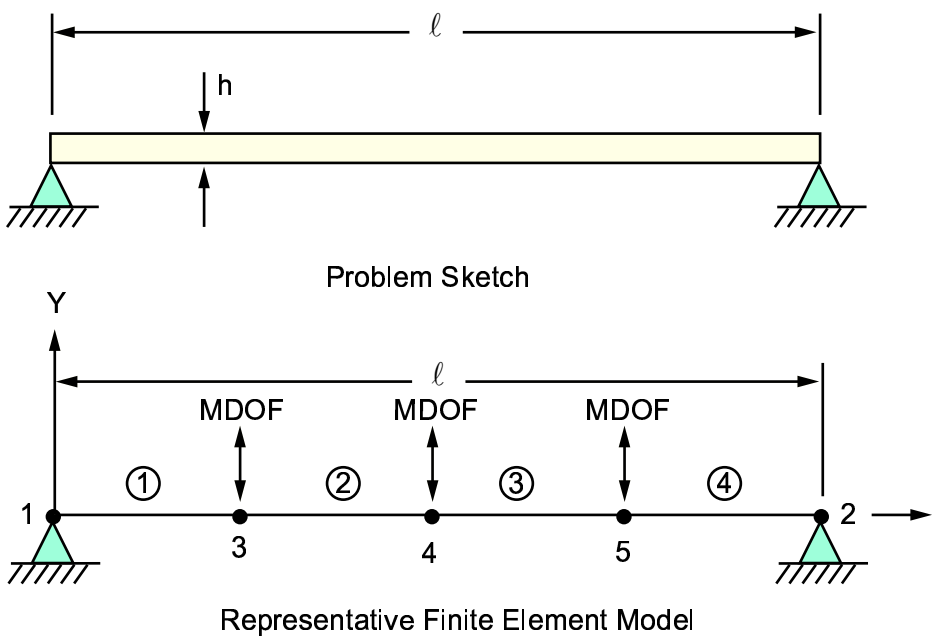

Material Properties	**Geometric Properties**	**Loading**
$E = 30 \times 10^6$ psi w = 1.124 lb/in $\rho = w/Ag = .000728$ lb-sec^2/in^4	ℓ = 80 in A = 4 in^2 h = 2 in I = 1.3333 in^4	g = 386 in/sec^2

Analysis Assumptions and Modeling Notes

Three lateral master degrees of freedom are selected. A partial solution is done to demonstrate the method.

Results Comparison

	Target	ANSYS	Ratio
f, Hz	28.766	28.767	1.00

VM51: Electrostatic Forces Between Charged Spheres

Overview

Reference:	Any General Physics Textbook
Analysis Type(s):	Electrostatic Analysis (**ANTYPE** = 0)
Element Type(s):	3-D 20-Node Electrostatic Solid Element (SOLID122) 3-D Infinite Solid Element (INFIN111)
Input Listing:	vm51.dat

Test Case

Two spheres with radii = 1 m, separated by a distance of 3 m, are subjected to a surface charge. Find the resultant electrostatic force between the spheres.

Figure 51.1 Charged Spheres Problem Sketch

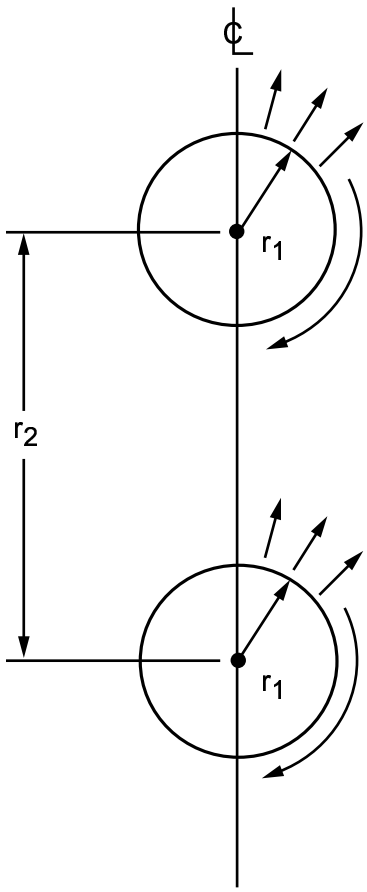

Problem Sketch

Material Properties	Geometric Properties	Loading
ε = 8.854E-12 F/m	r_1 = 1.0 m r_2 = 3.0 m r_3 = 6.0 m r_4 = 1.25 m	Surface charge = 8.854 E-12 C/m^2

Analysis Assumptions and Modeling Notes

The finite element mesh and the infinite element mesh are generated from the solid model. A planar section of the model is meshed with PLANE121 elements and rotated through 30 degrees. The 2-D mesh creates a 3-D mesh of SOLID122 elements. SHELL93 elements are generated over the outer surface of the 3-D mesh and extruded in the radial direction to complete the finite element domain. The process is repeated to extrude the INFIN111 mesh in the radial direction.

It can be assumed that a symmetry plane exists at Y = 0, at which a zero voltage constraint is imposed. Infinite flags are set for the outer surface of the INFIN111 elements.

The theoretical solution is:

$$F = \frac{(q_1 * q_2)}{(4 * \pi * \varepsilon * r_2^2)}$$

where ε = 8.854E-12, $q_1 = q_2 = 4 * \pi * \varepsilon$. This charge corresponds to a surface force of ε on the sphere.

surface charge = q/area = $(4 * \pi * \varepsilon)/4 * \pi * (r_1 **2) = \varepsilon$

Results Comparison

	Target	ANSYS	Ratio
YFORCE	-0.1236E-10	-0.1236E-10	1.000

Figure 51.2 Solid Model

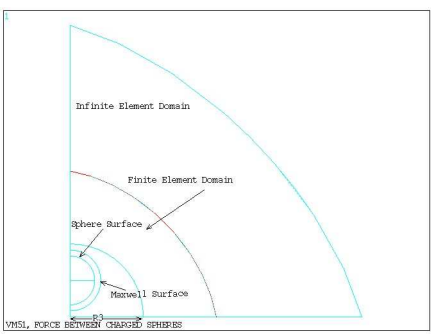

Figure 51.3 FEA Model

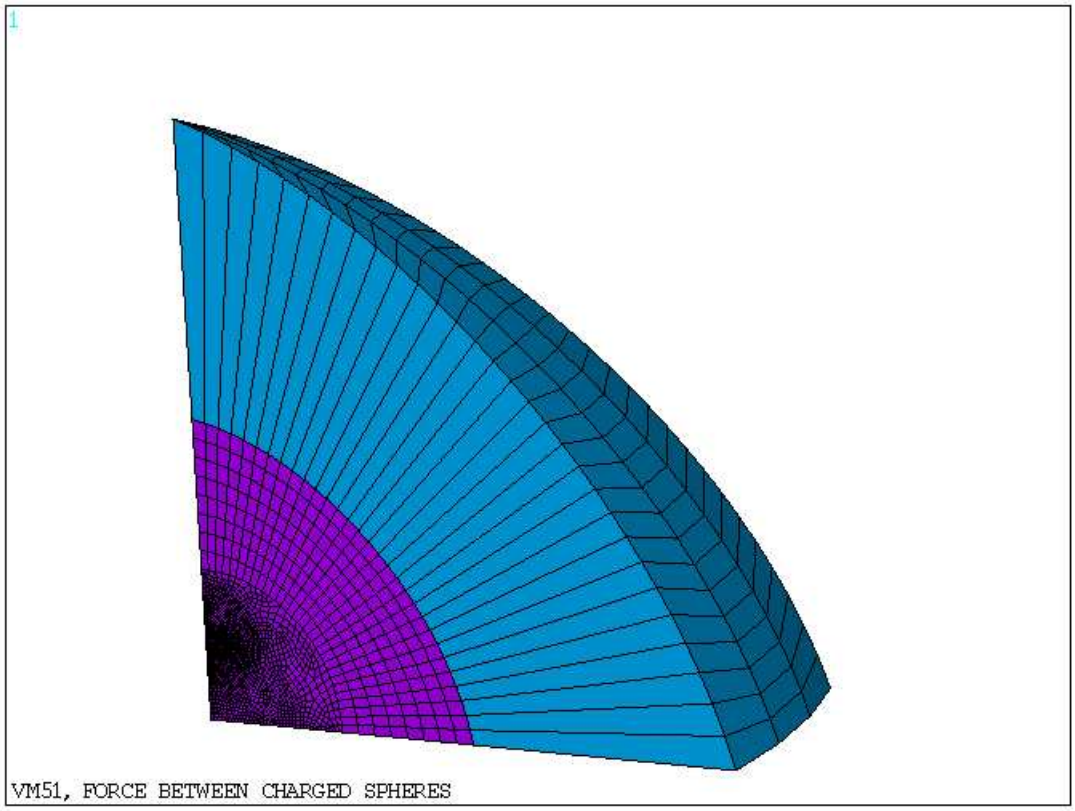

Figure 51.4 Electric Field

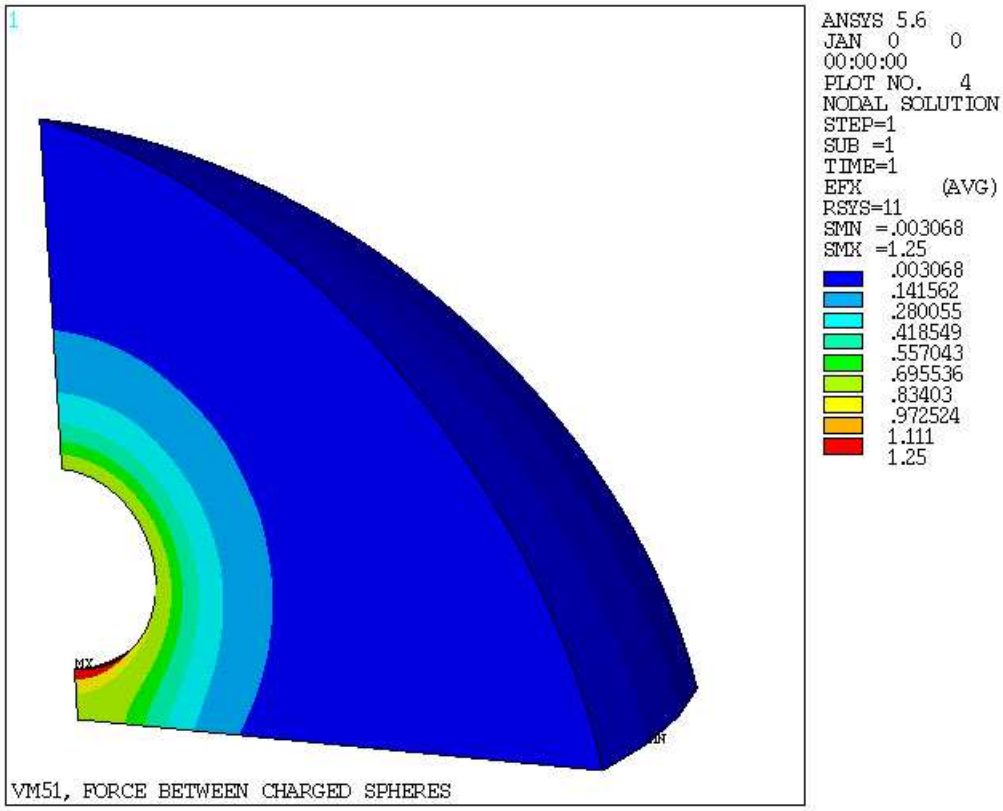

Figure 51.5 Voltage

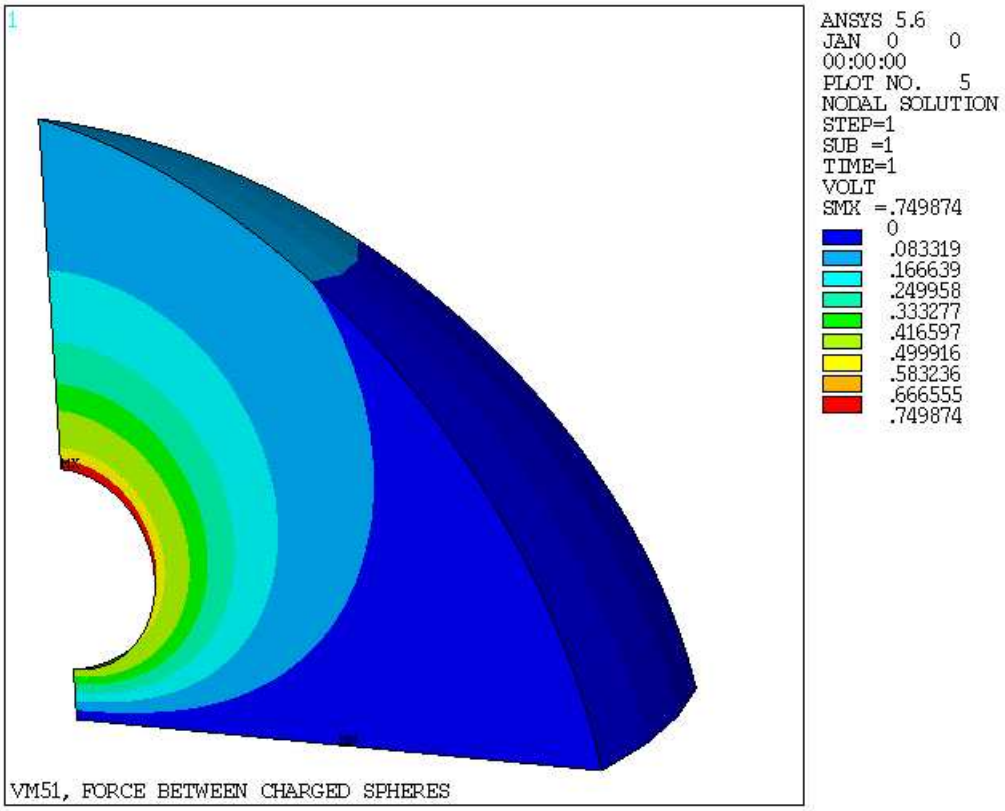

VM52: Automobile Suspension System Vibration

Overview

Reference:	W. T. Thomson, *Vibration Theory and Applications*, 2nd Printing, Prentice-Hall, Inc., Englewood Cliffs, NJ, 1965, pg. 181, ex. 6.7-1
Analysis Type(s):	Mode-frequency Analysis (**ANTYPE** = 2)
Element Type(s):	2-D Elastic Beam Elements (BEAM3) Spring-Damper Elements (COMBIN14) Structural Mass Element (MASS21)
Input Listing:	vm52.dat

Test Case

An automobile suspension system is simplified to consider only two major motions of the system:

- up and down linear motion of the body
- pitching angular motion of the body

If the body is idealized as a lumped mass with weight W and radius of gyration r, determine the corresponding coupled frequencies f_1 and f_2.

Figure 52.1 Automobile Suspension Problem Sketch

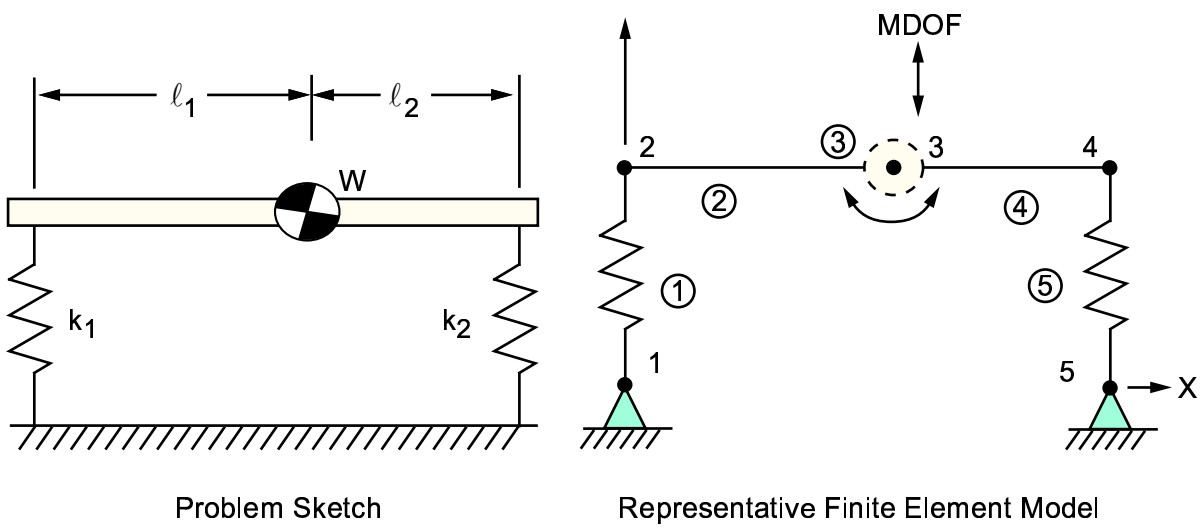

Material Properties	**Geometric Properties**	**Loading**
$E = 4 \times 10^9$ psf w = 3220 lb m = W/g = 100 lb-sec^2/ft k_1 = 2400 lb/ft k_2 = 2600 lb/ft	ℓ_1 = 4.5 ft ℓ_2 = 5.5ft r = 4 ft	g = 32.2 ft/sec^2

Analysis Assumptions and Modeling Notes

The beam geometric properties are input (all as unity) but not used for this solution. The torsional moment of inertia I_T is calculated as $I_T = Wr^2/g = 1600$ lb-sec^2-ft. A lateral master degree of freedom (MDOF) and a rotational MDOF are selected at the mass. The spring length is used only to define the spring direction.

Results Comparison

	Target	ANSYS	Ratio
f_1 , Hz	1.0981	1.0981	1.000
f_2 , Hz	1.4406	1.4406	1.000

ANSYS Verification Manual . ANSYS Release 10.0 . 002184 . © SAS IP, Inc.

VM53: Vibration of a String Under Tension

Overview

Reference:	W. T. Thomson, *Vibration Theory and Applications*, 2nd Printing, Prentice-Hall, Inc., Englewood Cliffs, NJ, 1965, pg. 264, article 8.2.
Analysis Type(s):	Static Analysis (**ANTYPE** = 0) Mode-frequency Analysis (**ANTYPE** = 2)
Element Type(s):	Tension-only or Compression-only Spar Elements (LINK10)
Input Listing:	vm53.dat

Test Case

A flexible string with mass per unit length ρA is fixed at the ends and stretched to an initial strain ε_o. Determine the stress σ and force F in the string under these conditions. Determine the first three natural frequencies f_i of lateral vibration of the stretched string.

Figure 53.1 String Under Tension Problem Sketch

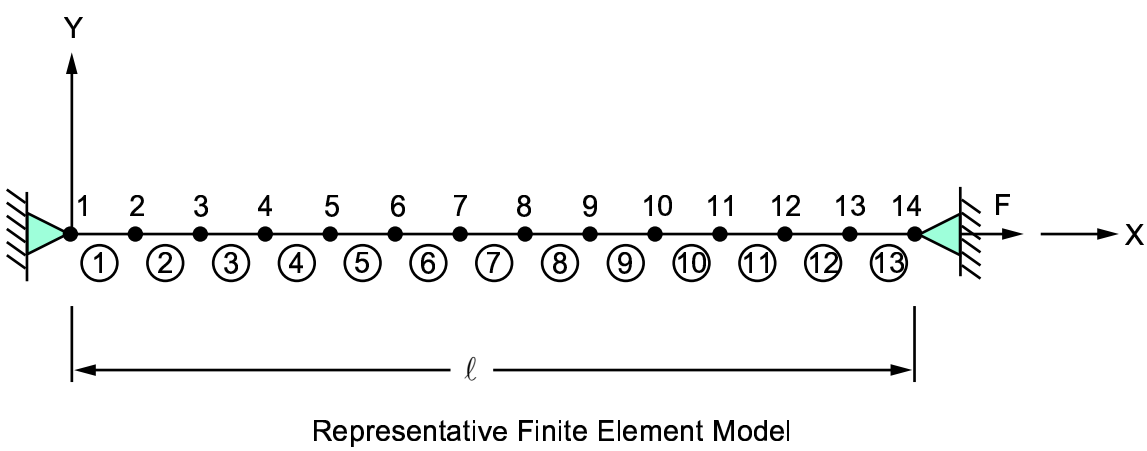

Material Properties	Geometric Properties	Loading
$E = 30 \times 10^6$ psi $\rho = 0.00073$ lb-sec^2/in^4	$\ell = 100$ in $A = 0.00306796$ in^2	$\varepsilon_o = 0.00543228$

Analysis Assumptions and Modeling Notes

Enough elements are selected so that the same model can be used to adequately characterize the dynamic analysis. Prestress effects are turned on during the static and modal solutions.

The subspace method for eigenvalue extraction is chosen solely for the sake of completeness in this manual. Other methods would also be suitable. Only the first three modes are requested.

Results Comparison

		Target	ANSYS	Ratio
Static	F, lb	500.	500.	1.000
	Stress, psi	162,974.	162,970.	1.000

		Target	ANSYS	Ratio
Modal	f_1 , Hz	74.708	75.094	1.005
	f_2 , Hz	149.42	151.29	1.012
	f_3 , Hz	224.12	229.68	1.025

VM54: Vibration of a Rotating Cantilever Blade

Overview

Reference:	W. Carnegie, "Vibrations of Rotating Cantilever Blading", *Journal Mechanical Engineering Science*, Vol. 1 No. 3, 1959, pg. 239
Analysis Type(s):	Static Analysis (**ANTYPE** = 0) Mode-frequency Analysis (**ANTYPE** = 2)
Element Type(s):	Elastic Shell Elements (SHELL63) 3-D Structural Solid Shell Elements (SOLSH190)
Input Listing:	vm54.dat

Test Case

A blade is cantilevered from a rigid rotating cylinder. Determine the fundamental frequency of vibration of the blade, f, when the cylinder is spinning at a rate of Ω .

Figure 54.1 Rotating Cantilever Blade

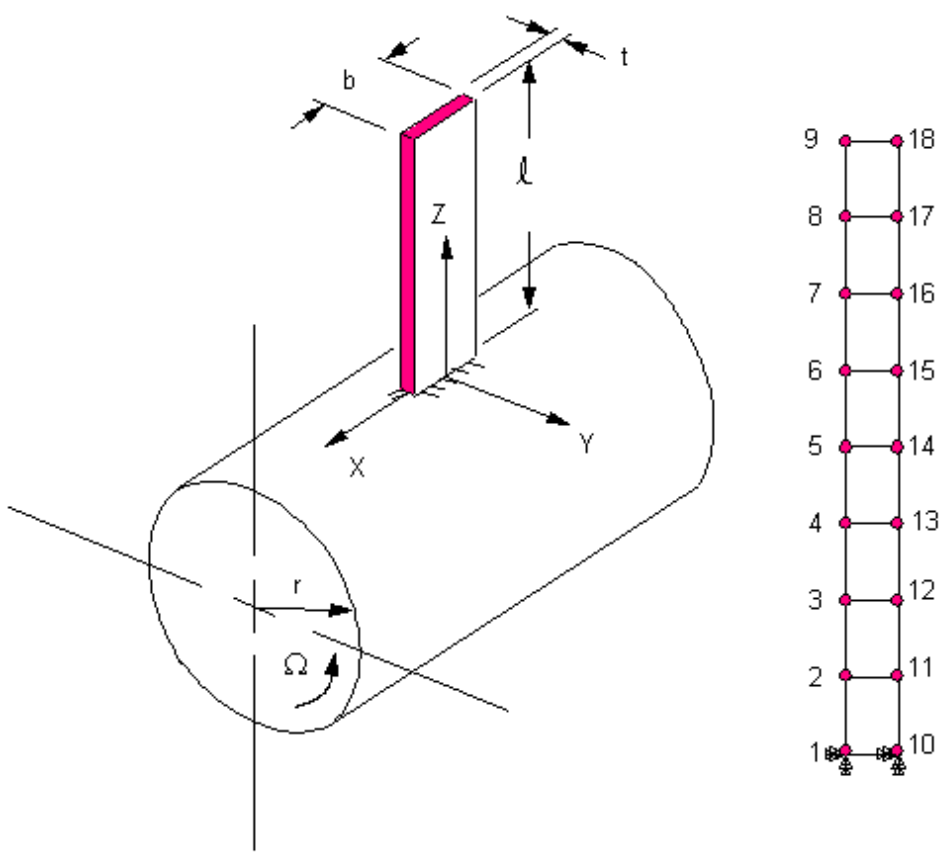

Problem Sketch Representative Finite Element Model

Material Properties	**Geometric Properties**	**Loading**
$E = 217 \times 10^9$ Pa $\rho = 7850$ kg/m^3 $\upsilon = 0.3$	r = 150 mm ℓ = 328 mm b = 28 mm t = 3mm	$\Omega = 100\pi$ rad/sec

Analysis Assumptions and Modeling Notes

The problem is solved in two different ways:

- Using Elastic Shell Elements (SHELL63)
- Using 3-D Solid Shell Elements (SOLSH190)

Spin (centrifugal) softening is used. Since the cylinder is rigid, the base of the blade has its displacements constrained. A static prestress analysis is performed to include the inertial effects resulting from the rotation of the cylinder.

Results Comparison

	Target	ANSYS	Ratio
SHELL63			
f, Hz	52.75	52.01	0.986
SOLSH190			
f, Hz	52.75	51.80	0.982

VM55: Vibration of a Stretched Circular Membrane

Overview

Reference:	S. Timoshenko, D. H. Young, *Vibration Problems in Engineering*, 3rd Edition, D. Van Nostrand Co., Inc., New York, NY, 1955, pg. 439, eq. 182.
Analysis Type(s):	Static Analysis (**ANTYPE** = 0) to Prestress Structure Mode-frequency Analysis (**ANTYPE** = 2)
Element Type(s):	Axisymmetric Structural Shell Elements (SHELL51)
Input Listing:	vm55.dat

Test Case

A circular membrane of radius a, thickness t, and weight per unit area w is simply supported along its edge and subjected to an in-plane radial load of T lb/unit length of circumference. Determine the radial stress σ_r in the membrane and the first three natural frequencies f_i of lateral vibration of the membrane.

Figure 55.1

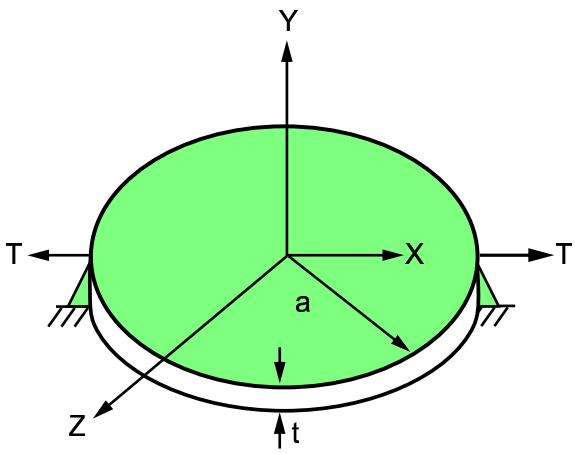

Problem Sketch

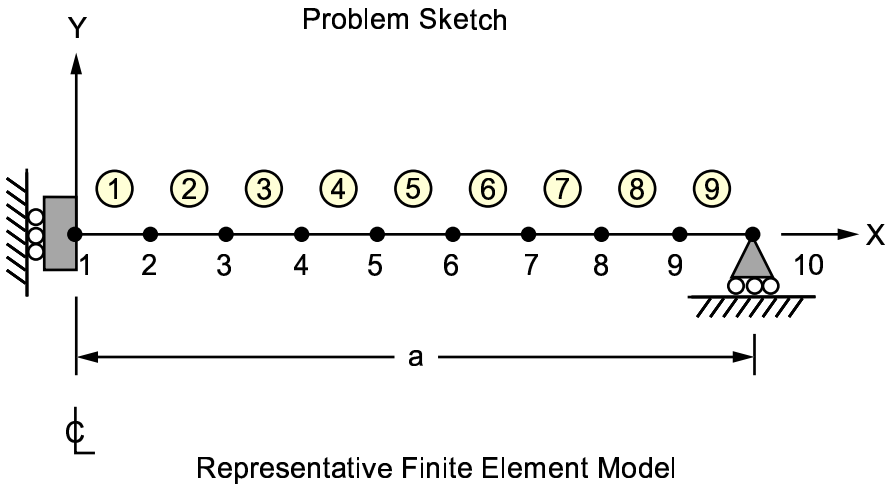

Representative Finite Element Model

Material Properties	Geometric Properties	Loading
E = 30 x 10^6 psi w = 0.0028178 lb/in^2	a = 15 in t = 0.01 in	T = 100 lb/in

Analysis Assumptions and Modeling Notes

The in-plane radial load F is calculated as: F = 2 πa T = 9424.778 lb. The mass density ρ is calculated as w/gt = 0.00073 lb-sec^2/in^4, where g = 386 in/sec^2. Enough elements are defined to adequately characterize the dynamic analysis. Prestress effects are turned on. Since the natural frequency solution accuracy for a distributed mass system depends upon the number of master degrees of freedom (MDOF) selected, all lateral degrees of freedom are selected as MDOF for this model in the modal analysis.

Results Comparison

		Target	ANSYS	Ratio
Static	Stress$_r$, psi	10,000.	10,000.	1.000
Modal	f_1 , Hz	94.406	94.365	1.000
	f_2 , Hz	216.77	217.11	1.002
	f_3 , Hz	339.85	342.46	1.008

ANSYS Verification Manual . ANSYS Release 10.0 . 002184 . © SAS IP, Inc.

VM56: Hyperelastic Thick Cylinder Under Internal Pressure

Overview

Reference:	J. T. Oden, *Finite Elements of Nonlinear Continua*, McGraw-Hill Book Co., Inc., New York, NY, 1972, pp. 325-331.
Analysis Type(s):	Static, Large Deflection Analysis (**ANTYPE** = 0)
Element Type(s):	2-D 8-Node Stuctural Solid Elements (PLANE183) 3-D 8-Node Structural Solid Elements (SOLID185) 3-D 10-Node Tetrahedral Structural Solid Elements (SOLID186)
Input Listing:	vm56.dat

Test Case

An infinitely long cylinder is made of Mooney-Rivlin type material. An internal pressure of P_i is applied. Find the radial displacement at the inner radius and the radial stress at radius R = 8.16 in (center of 1st element).

Figure 56.1 Hyperelastic Thick Cylinder Problem Sketch

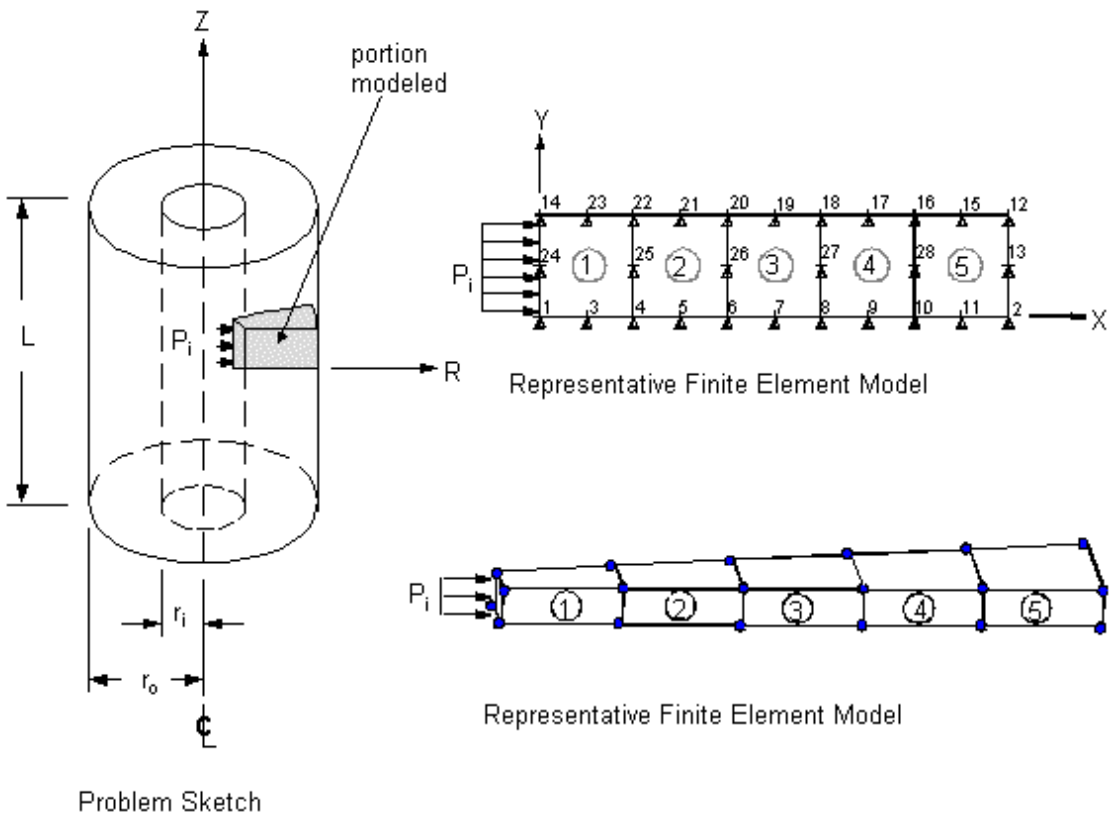

Figure 56.2 Hyperelastic Thick Cylinder Models

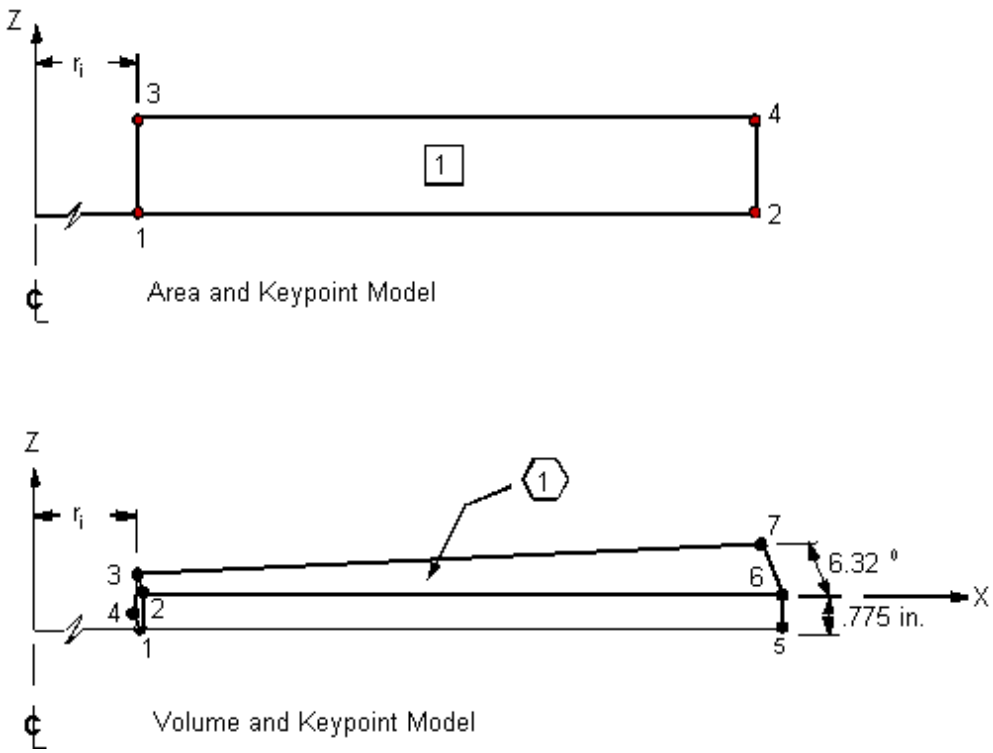

Material Properties	Geometric Properties
υ = .49	r_i = 7.0 in
Mooney-Rivlin material coefficients	r_o = 18.625 in
A = 80 psi	**Loading**
B = 20 psi	P_i = 150 psi

Analysis Assumptions and Modeling Notes

The problem is solved first using PLANE183 and then using SOLID185 / SOLID186. Due to circumferential symmetry, only a small sector need be modeled. The height (and width for SOLID185) of the elements in the finite element model is chosen such that the elements have a reasonable aspect ratio. Only radial degrees of freedom are active. The total pressure is applied in two load increments. To approximate incompressible behavior, Poisson's ratio is set close to 1/2 (0.49) and reduced integration is requested. Temperature-dependent properties are used in the PLANE183 portion solely for verification purposes.

Results Comparison

		Target[1]	ANSYS	Ratio
PLANE183	u_r (inner radius), in	7.180	7.794	1.086
	$Stress_r$ (element 1), psi	-122.0	-122.933	1.008
SOLID185	u_r (inner radius), in	7.180	7.395	1.030
	$Stress_r$ (element 1), psi	-122.0	-123.573	1.013
SOLID186	u_r (inner radius), in	7.180	7.478	1.042

1. Based on fully incompressible assumption, ν = 1/2

VM57: Torsional Frequencies of a Drill Pipe

Overview

Reference:	W. T. Thomson, *Vibration Theory and Applications*, 2nd Printing, Prentice-Hall, Inc., Englewood Cliffs, NJ, 1965, pg. 272, ex. 8.4-5.
Analysis Type(s):	Mode-frequency Analysis (**ANTYPE** = 2)
Element Type(s):	Elastic Straight Pipe Elements (PIPE16) 3-D Elastic Beam Elements (BEAM4) Structural Mass Element (MASS21)
Input Listing:	vm57.dat

Test Case

Determine the first two natural frequencies f_1 and f_2 of an oil-well drill pipe of length ℓ, area A, and polar moment at inertia I_p fixed at the upper end and terminating at the lower end to a drill collar with torsional mass inertia J_o. The drill collar length is small compared to the pipe length.

Figure 57.1 Drill Pipe Problem Sketch

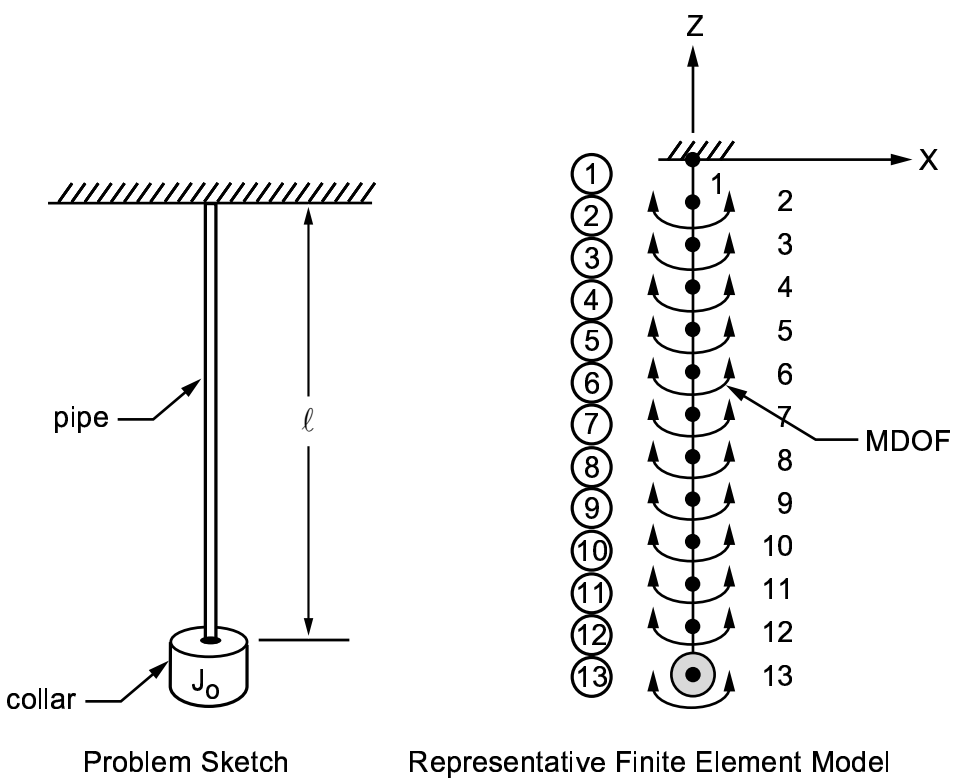

Material Properties	**Geometric Properties**
$G = 12 \times 10^6$ psi	$\ell = 5000$ ft
$\upsilon = 0.3$	OD = 4.5 in = (4.5/12) ft
$\gamma = 490$ lb/ft^3	ID = 3.83 in = (3.83/12) ft
$\rho = \gamma / g = 15.2174$ lb-sec^2/ft^4	$J_o = 29.3$ lb-ft-sec^2
	$I_p = 0.0009226$ ft^4

Analysis Assumptions and Modeling Notes

The drill pipe is modeled first using pipe elements (PIPE16) with the subspace solver and then using beam elements (BEAM4) with the Householder Solver. Young's modulus (E) is calculated as $E = 2G(1 + \upsilon)*144 = 4.4928 \times 10^9 lb/ft^2$ and pipe thickness is calculated as (OD - ID)/2.

In the case of beam elements (BEAM4), the polar moment of inertia could have been omitted since it defaults to $I_{YY} + I_{ZZ}$, both of which must be input.

Twelve torsional master degrees of freedom (MDOF) are selected; one at the collar and eleven along the length of the pipe.

Results Comparison

		Target[1]	ANSYS	Ratio
Pipe Elements	f_1, Hz	0.3833	0.3834	1.000
	f_2, Hz	1.260	1.264	1.003
Beam Elements	f_1, Hz	0.3833	0.3834	1.000
	f_2, Hz	1.260	1.264	1.003

1. Solution recalculated

VM58: Centerline Temperature of a Heat Generating Wire

Overview

Reference:	W. M. Rohsenow, H. Y. Choi, *Heat, Mass and Momentum Transfer*, 2nd Printing, Prentice-Hall, Inc., Englewood Cliffs, NJ, 1963, pg. 106, ex. 6.5.
Analysis Type(s):	Thermal Analysis (**ANTYPE** = 0)
Element Type(s):	2-D 6-Node Triangular Thermal Solid Element (PLANE35) 2-D Thermal Surface Effect Element (SURF151)
Input Listing:	vm58.dat

Test Case

Determine the centerline temperature $T_{\mathbb{C}}$ and the surface temperature T_s of a bare steel wire generating heat at the rate $\ddot{q}$. The surface convection coefficient between the wire and the air (at temperature T_a) is h. Also, determine the heat dissipation rate q.

Figure 58.1 Heat Generating Wire Problem Sketch

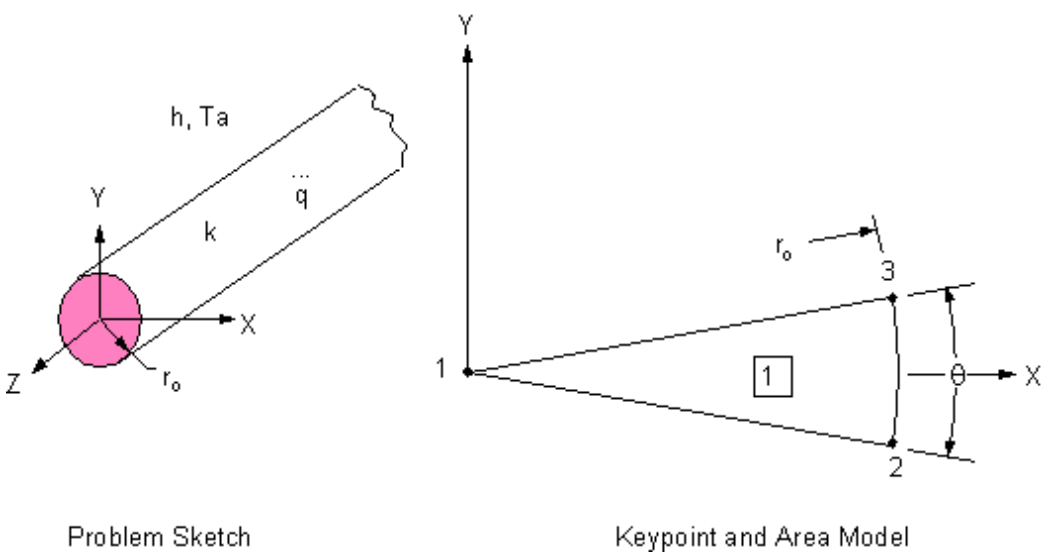

Material Properties	Geometric Properties	Loading
k = 13 Btu/hr-ft-°F h = 5 Btu/hr-ft^2-°F	r_o = 0.375 in = 0.03125 ft	T_a = 70°F $\ddot{q}$ = 111311.7 Btu/hr-ft^3

Analysis Assumptions and Modeling Notes

Since the problem is axisymmetric, only a small sector is needed. An angle Θ= 30° is used for modeling the circular sector. Four mesh divisions are chosen radially for accuracy considerations. Temperatures of the outer nodes are coupled to ensure symmetry. The solution is based on a wire 1 foot long (Z direction). Postprocessing is used to determine $T_{\mathbb{C}}$, T_s, and q.

Results Comparison

	Target	ANSYS	Ratio
Centerline Temperature, °F	419.9	419.9	1.000
Surface Temperature, °F	417.9	417.8	1.000
q, BTU/hr	341.5	341.5[1]	1.000

1. Calculated from heat flow rate per 30° sector x 12 sectors

VM59: Lateral Vibration of an Axially-loaded Bar

Overview

Reference:	S. Timoshenko, D. H. Young, *Vibration Problems in Engineering*, 3rd Edition, D. Van Nostrand Co., Inc., New York, NY, 1955, pg. 374, article 59.
Analysis Type(s):	Static Analysis (**ANTYPE** = 0) Mode-frequency Analysis (**ANTYPE** = 2)
Element Type(s):	3-D Elastic Beam Elements (BEAM4)
Input Listing:	vm59.dat

Test Case

A bar of length ℓ and weight per unit length γA is pinned at its ends and subjected to an axial compressive force F. Determine the stress σ and the axial displacement δ of the bar under these conditions. Determine the first three natural frequencies f_i of lateral vibration of the bar.

Figure 59.1 Axially-Loaded Bar Problem Sketch

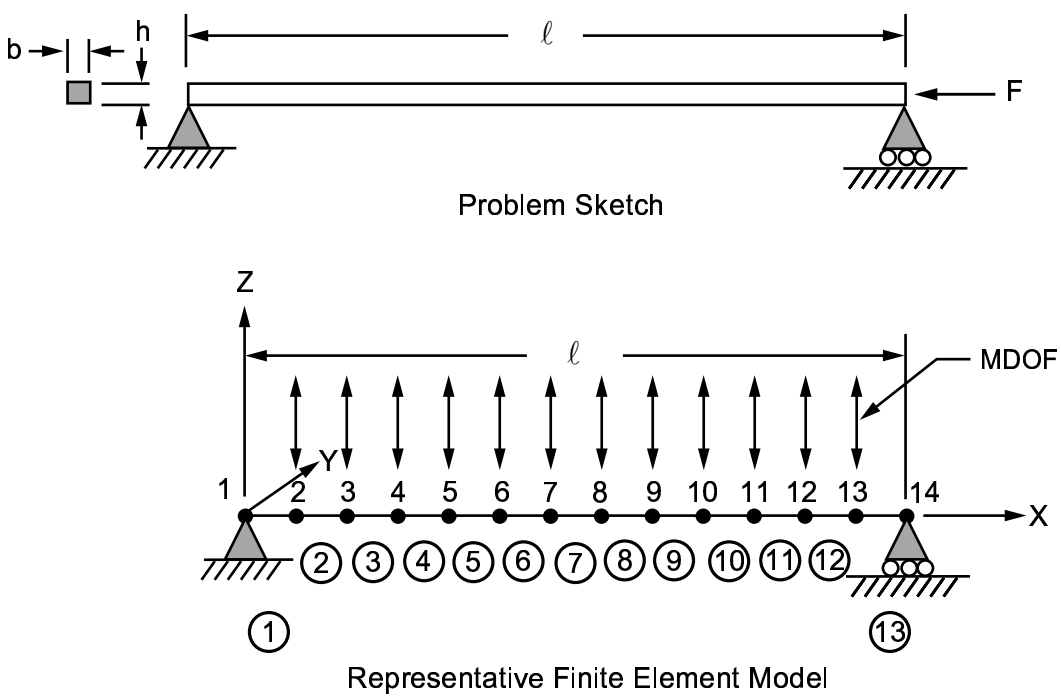

Material Properties	Geometric Properties	Loading
$E = 30 \times 10^6$ psi $\gamma = 0.281$ lb/in^3 $\rho = \gamma / g = 0.000727973$ lb-sec^2/in^4	$b = h = 2$ in $\ell = 80$ in $A = 4$ in^2 $I = bh^3/12 = (4/3)$ in^4	$F = 40{,}000$ lb

Analysis Assumptions and Modeling Notes

Enough elements are selected so that the same model can be used to adequately characterize the dynamic analysis. Prestress effects are turned on in the mode-frequency analysis with the stress state calculated in the

static analysis. Since the solution accuracy in the mode-frequency analysis for a distributed mass system depends upon the number of master degrees of freedom (MDOF) selected, twelve uniformly spaced lateral MDOF are selected.

Results Comparison

		Target	ANSYS	Ratio
Static	Deflection, in	-0.026667	-0.026667	1.000
	Stress , psi	-10,000	-10,000	1.000
Modal	**F = 40,000 lb**			
	f_1 , Hz	17.055	17.052	1.000
	f_2 , Hz	105.32	105.22	0.999
	f_3 , Hz	249.39	248.87	0.998
	F = 0 lb			
	f_1 , Hz [see VM50]	28.766	28.767	1.000

ANSYS Verification Manual . ANSYS Release 10.0 . 002184 . © SAS IP, Inc.

VM60: Natural Frequency of a Cross-ply Laminated Shell

Overview

Reference:	J. N. Reddy, "Exact Solutions of Moderately Thick Laminated Shells", *ASCE Journal Engineering Mechanics*, Vol. 110 No. 5, 1972, pg. 806, tab. 6.
Analysis Type(s):	Mode-frequency Analysis (**ANTYPE** = 2)
Element Type(s):	Linear Layered Structural Shell Elements (SHELL99)
Input Listing:	vm60.dat

Test Case

Determine the first mode natural frequency f of a simply-supported equal-sided sector of a spherical shell of radius r. The shell sector consists of a 0°/90° cross-ply laminate (2 layers of equal thickness, t).

Figure 60.1 Laminated Spherical Shell Problem Sketch

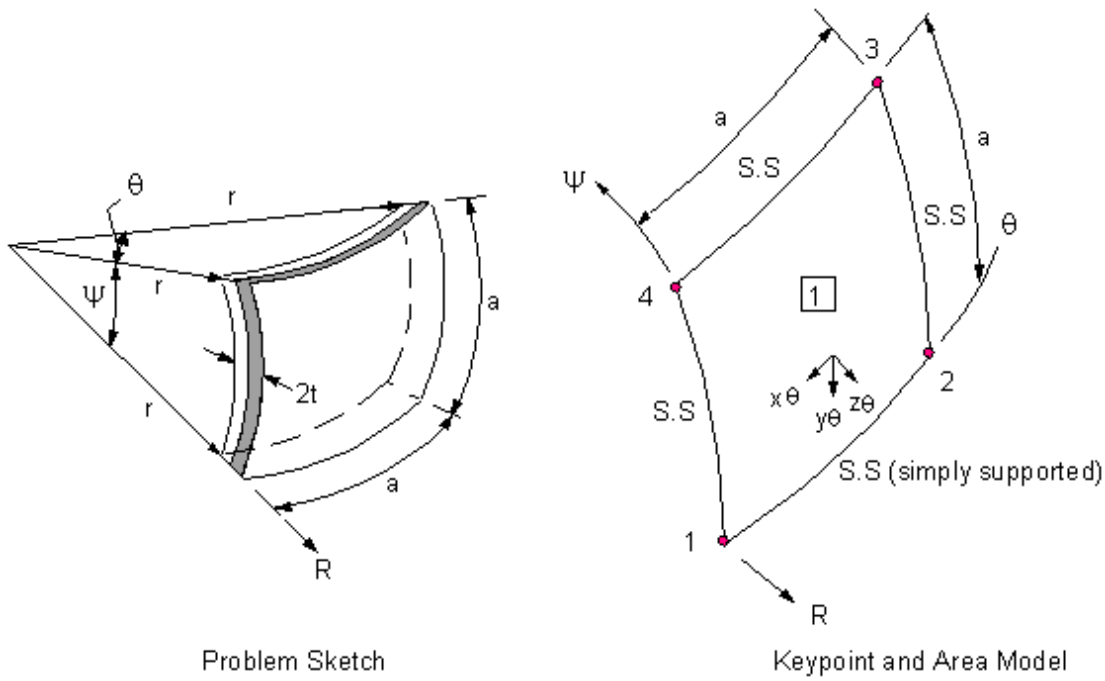

Material Properties	**Geometric Properties**
ρ = 1 gm/mm^3	r = 300 mm
E_x = 25 x 10^6 Pa	a = 100 mm
E_y = 1 x 10^6 Pa	t = 0.5 mm
$G_{xy} = G_{xz}$ = 5 x 10^5 Pa	
G_{yz} = 2 x 10^5 Pa	
υ_{yx} = .25 (major Poisson's ratio)	

Analysis Assumptions and Modeling Notes

Four elements are chosen along each edge of area 1. The reduced method of eigenvalue solution is chosen and the first five modes are extracted. Note that the input value for υ_{xy} is calculated from:

$$v_{xy} = v_{yx}\frac{E_y}{E_x} = .25\frac{1x10^6}{25x10^6} = .01 \quad \text{(minor Poisson's ratio)}$$

The geometric input in spherical coordinates is calculated as:

$$\theta = \psi = \frac{180}{\pi}\frac{100}{300} = 19.0986^\circ$$

The alternate method of Poisson's ratio input (PRXY) could also have been used.

Results Comparison

	Target	ANSYS	Ratio
f, Hz	0.73215	0.73151	0.999

VM61: Longitudinal Vibration of a Free-free Rod

Overview

Reference:	W. T. Thomson, *Vibration Theory and Applications*, 2nd Printing, Prentice-Hall, Inc., Englewood Cliffs, NJ, 1965, pg. 269, ex. 8.3-1.
Analysis Type(s):	Mode-frequency Analysis (**ANTYPE** = 2)
Element Type(s):	2-D Elastic Beam Elements (BEAM3)
Input Listing:	vm61.dat

Test Case

Determine the first three natural frequencies f_i of a free-free rod (a rod with both ends free) having a length ℓ.

Figure 61.1 Rod Problem Sketch

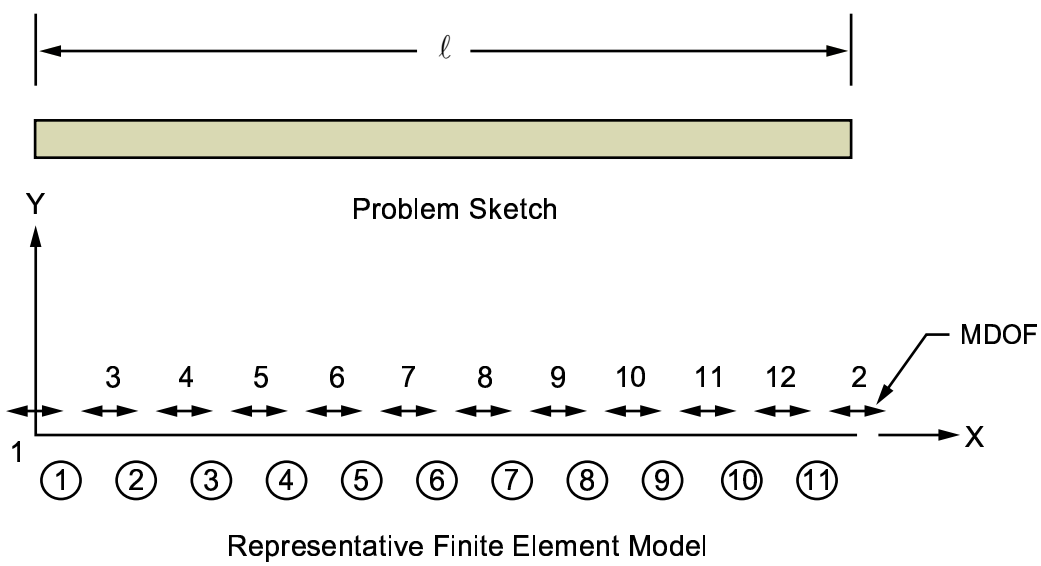

Material Properties	**Geometric Properties**
$E = 30 \times 10^6$ psi $\rho = 0.00073$ lb-sec^2/in^4	$\ell = 800$ in

Analysis Assumptions and Modeling Notes

The beam geometric properties of moment of inertia, area, and thickness are arbitrarily assigned values of 1. Since the solution accuracy for a distributed mass system depends upon the number of master degrees of freedom (MDOF) selected, twelve uniformly spaced longitudinal (axial) MDOF are selected.

Results Comparison

	Target	ANSYS	Ratio
f_1, Hz[1]	0.	0.	-
f_2, Hz	126.70	127.13	1.003
f_3, Hz	253.40	256.86	1.014

1. Rigid body mode

ANSYS Verification Manual . ANSYS Release 10.0 . 002184 . © SAS IP, Inc.

VM62: Vibration of a Wedge

Overview

Reference:	S. Timoshenko, D. H. Young, *Vibration Problems in Engineering*, 3rd Edition, D. Van Nostrand Co., Inc., New York, NY, 1955, pg. 392, article 62.
Analysis Type(s):	Mode-frequency Analysis (**ANTYPE** = 2)
Element Type(s):	Elastic Shell Elements (SHELL63)
Input Listing:	vm62.dat

Test Case

Determine the fundamental frequency of out-of-plane vibration f of a wedge-shaped plate of uniform thickness t, base 2b, and length ℓ.

Figure 62.1 Wedge Vibration Problem Sketch

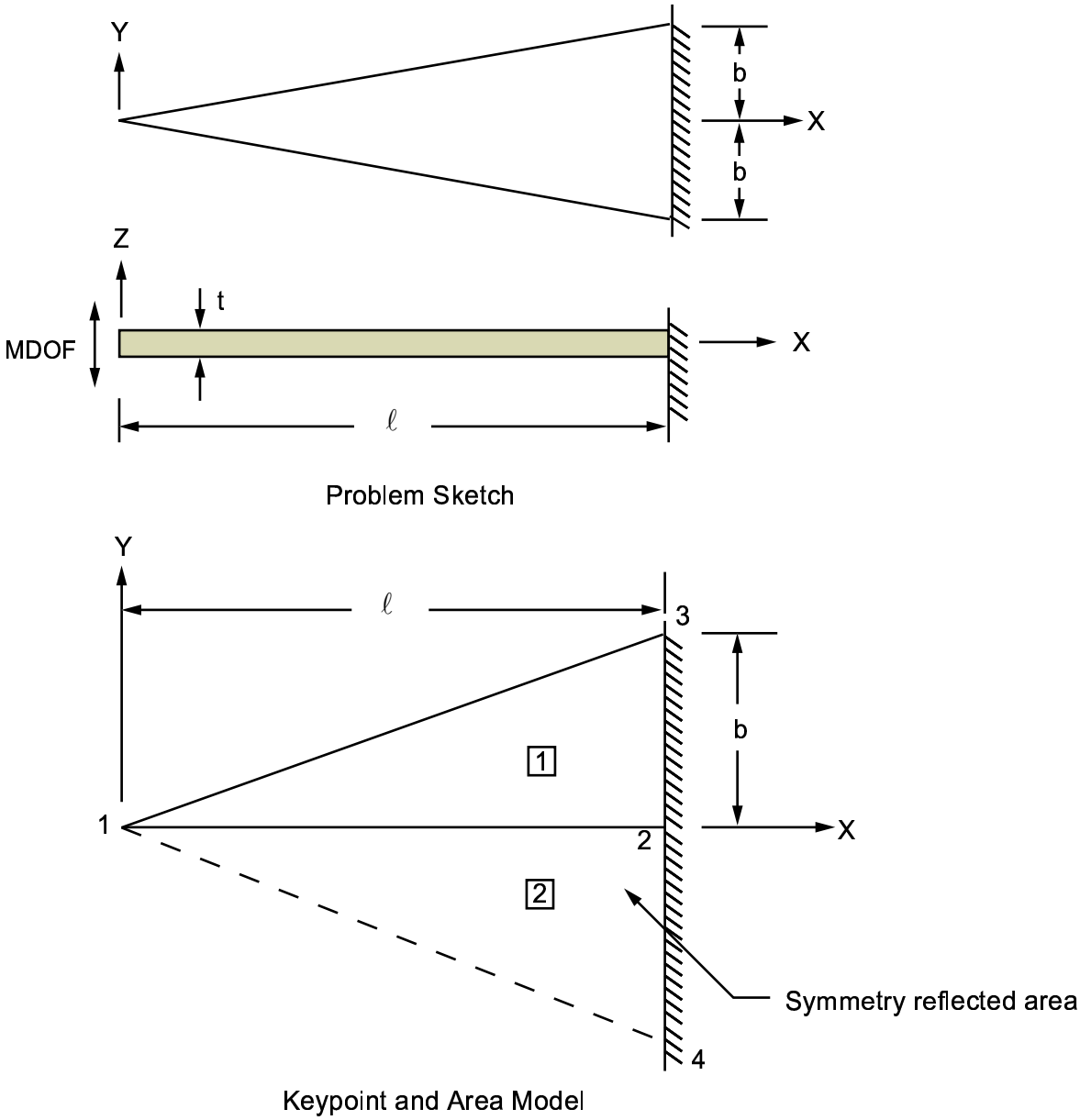

Material Properties	Geometric Properties
$E = 30 \times 10^6$ psi $\rho = 0.000728$ lb-sec^2/in^4 $\upsilon = 0$	t = 1 in b = 2 in ℓ = 16 in

Analysis Assumptions and Modeling Notes

The problem is solved first using "plate" elements (SHELL63 with bending stiffness only) and then using "shell" elements (SHELL63 with bending and membrane stiffness). Two symmetric areas are created to ensure model symmetry about the plate centerline. Out-of-plane (Z-direction) master degrees of freedom (MDOF) are selected along the plate centerline. Each area is meshed with 4 elements along the X axis and 1 element along the Y axis. Poisson's ratio is assumed to be zero.

Results Comparison

		Target	ANSYS	Ratio
Plate Elements	f, Hz	259.16	261.11	1.008
Shell Elements	f, Hz	259.16	261.11	1.008

VM63: Static Hertz Contact Problem

Overview

Reference:	S. Timoshenko, J. N. Goodier, *Theory of Elasticity*, 3rd Edition, McGraw-Hill Book Co., Inc., New York, NY, 1970, pg. 409-413, article 140.
Analysis Type(s):	Static Analysis (**ANTYPE** = 0)
Element Type(s):	2-D 8-Node Structural Solid Elements (PLANE82) 2-D 6-Node Triangular Structural Solid Elements (PLANE2) 3-D Node-to-Node Contact Elements (CONTA178)
Input Listing:	vm63.dat

Test Case

A sphere of radius r is pressed against a rigid flat plane. Determine the contact radius, a, for a given load F.

Figure 63.1 Static Hertz Problem

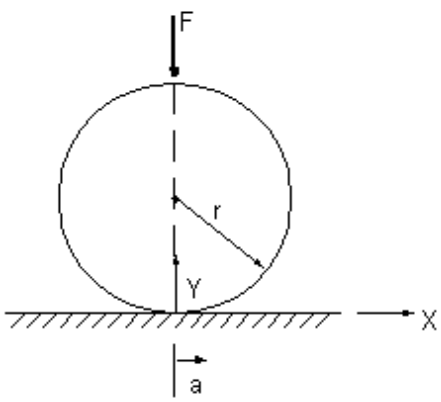

Problem Sketch

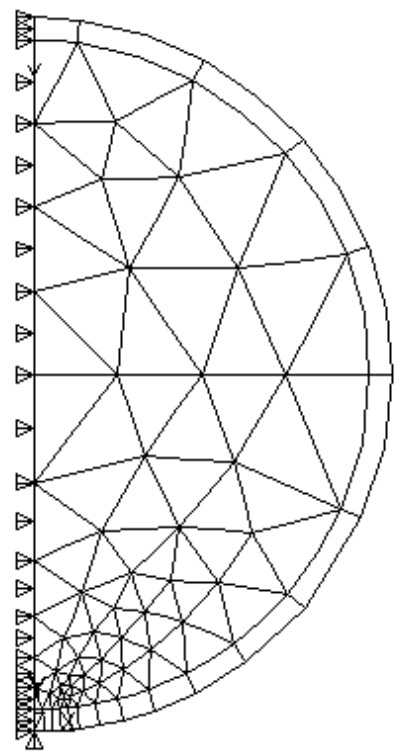

Representative Finite Element Model

Material Properties	**Geometric Properties**
E = 1000 N/mm^2 υ = 0.3	r = 8 mm **Loading** F = (30 x 2 π) N

Analysis Assumptions and Modeling Notes

An axisymmetric model is used. A node is placed near the expected radius of contact. Midside nodes are removed along the surface where contact is likely to occur. The model is comprised of both PLANE82 and PLANE2 for

verification purposes, but could be solved using either element type alone. The model is solved using 3-D node-to-node contact elements (CONTA178).

Results

a, mm	Target	ANSYS	Ratio
CONTA178	1.010	1.011	1.001

VM64: Thermal Expansion to Close a Gap at a Rigid Surface

Overview

Reference:	C. O. Harris, *Introduction to Stress Analysis*, The Macmillan Co., New York, NY, 1959, pg. 58, problem 8.
Analysis Type(s):	Static thermal Stress Analysis (**ANTYPE** = 0)
Element Type(s):	2-D/3-D Node-to-Surface Contact Element (CONTA175) 2-D Target Segment Element (TARGE169) 2-D Structural Solid Elements (PLANE42)
Input Listing:	vm64.dat

Test Case

An aluminum-alloy bar is initially at a temperature of 70°F. Calculate the stresses in the bar after it has been heated to 170°F. The supports are assumed to be rigid.

Figure 64.1 Rigid Surface

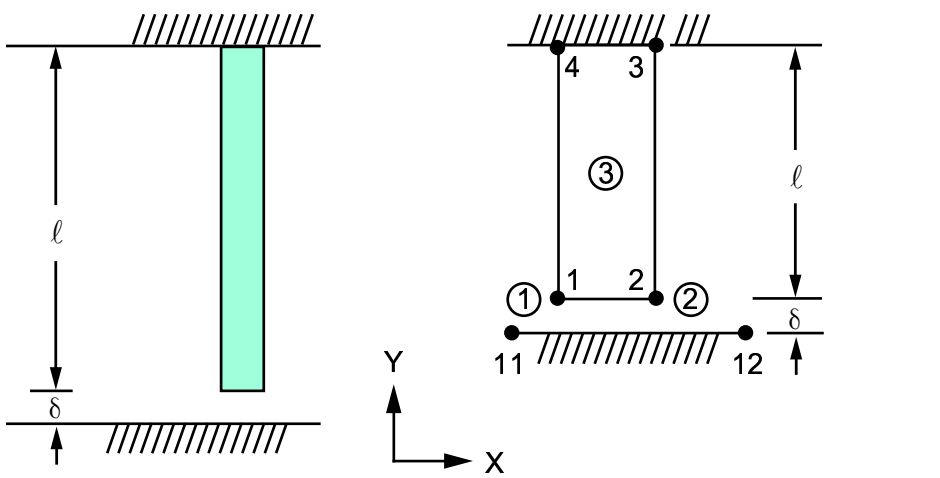

Problem Sketch Representative Finite Element Model

Material Properties	**Geometric Properties**	**Loading**
$E = 10.5 \times 10^6$ psi $\alpha = 12.5\ 10^{-6}$ in/in-°F $\upsilon = 0$	$\ell = 3$ in $\delta = 0.002$ in	$\Delta t = 170° - 70°F$

Results Comparison

	Target	ANSYS	Ratio
$Stress_x$, psi	-13125	-13125	1.000
$Stress_y$, lb	-6125	-6122	0.999

VM65: Transient Response of a Ball Impacting a Flexible Surface

Overview

Reference:	W. T. Thomson, *Vibration Theory and Applications*, 2nd Printing, Prentice-Hall, Inc., Englewood Cliffs, NJ, 1965, pg. 110, ex. 4.6-1.
Analysis Type(s):	Nonlinear Transient Dynamic Analysis (**ANTYPE** = 4)
Element Type(s):	Structural Mass Elements (MASS21) 2-D/3-D Node-to-Surface Contact Elements (CONTA175)
Input Listing:	vm65.dat

Test Case

A rigid ball of mass m is dropped through a height h onto a flexible surface of stiffness k. Determine the velocity, kinetic energy, and displacement y of the ball at impact and the maximum displacement of the ball.

Figure 65.1 Ball Problem Sketch

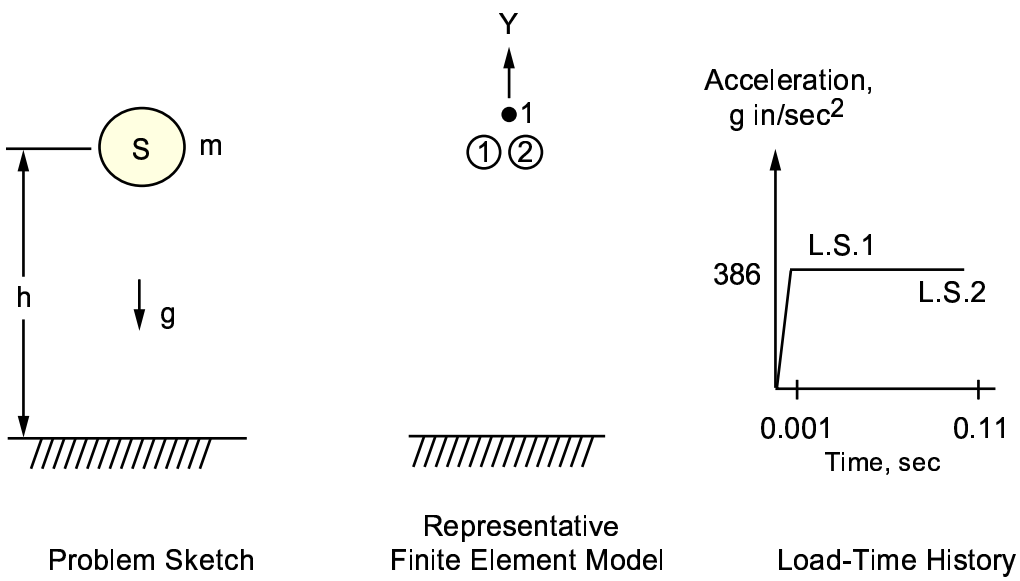

Material Properties	**Geometric Properties**
m = 0.5 lb-sec^2/in k = 1973.92 lb/in	h = 1 in **Loading** g = 386 in/sec^2

Analysis Assumptions and Modeling Notes

The node locations are arbitrarily selected. The final time of 0.11 seconds allows the mass to reach its largest deflection. The integration time step (0.11/110 ≈ 0.001 sec) is based on ≈ 1/100 of the period (during impact), to allow the initial step acceleration change to be followed reasonably well and to produce sufficient printout for the theoretical comparison. At release h, the mass acceleration is 386 in/sec^2. Therefore, a load step with a small time period is used to ramp to the appropriate acceleration while maintaining essentially zero velocity. Displacements and velocities are listed against time in POST26 and stored kinetic energy is obtained in POST1.

The model is solved using the node-to-surface CONTA175 element.

Results

		Target	ANSYS	Ratio
CONTA175 At Impact[1]	time,sec	0.07198	0.072	1.000
	y displacement, in	-1.0000	-0.9991	0.999
	y velocity, in/sec	-27.79	-27.76	0.999
At "Zero" Velocity[2]	time,sec	0.10037	0.10100	1.006
	max. y displacement, in	-1.5506	-1.5503	1.000

1. Target results are for t = 0.07198 sec. ANSYS results are reported for closest time point, t = 0.072 sec.
2. ANSYS results are from the time point closest (reported in POST26) to the change in velocity from negative to positive.

Figure 65.2 Kinetic Energy, Velocity and Displacement vs. Time Display

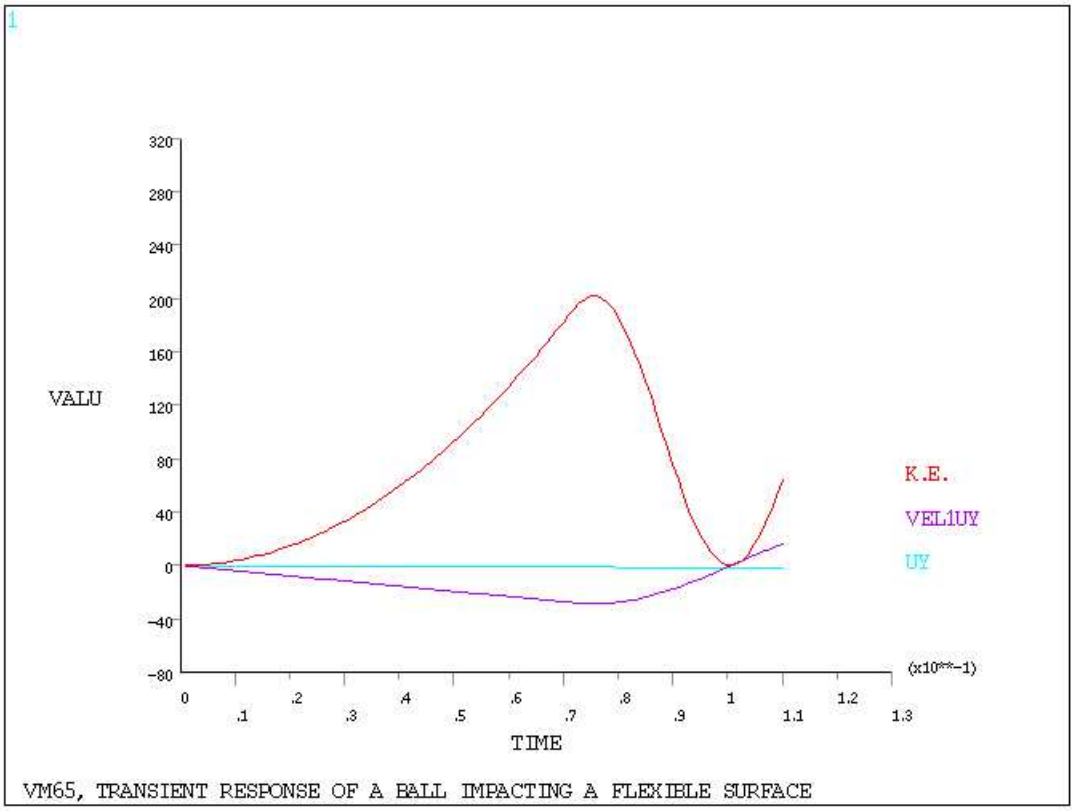

VM66: Vibration of a Flat Plate

Overview

Reference:	S. Timoshenko, D. H. Young, *Vibration Problems in Engineering*, 3rd Edition, D. Van Nostrand Co., Inc., New York, NY, 1955, pg. 338, article 53.
Analysis Type(s):	Mode-frequency Analysis (**ANTYPE** = 2)
Element Type(s):	Elastic Shell Elements (SHELL63) 3-D Structural Solid Shell Elements (SOLSH190)
Input Listing:	vm66.dat

Test Case

Determine the fundamental natural frequency of lateral vibration f of a flat rectangular plate. The plate is of uniform thickness t, width 2b, and length ℓ.

Figure 66.1 Flat Plate Problem Sketch

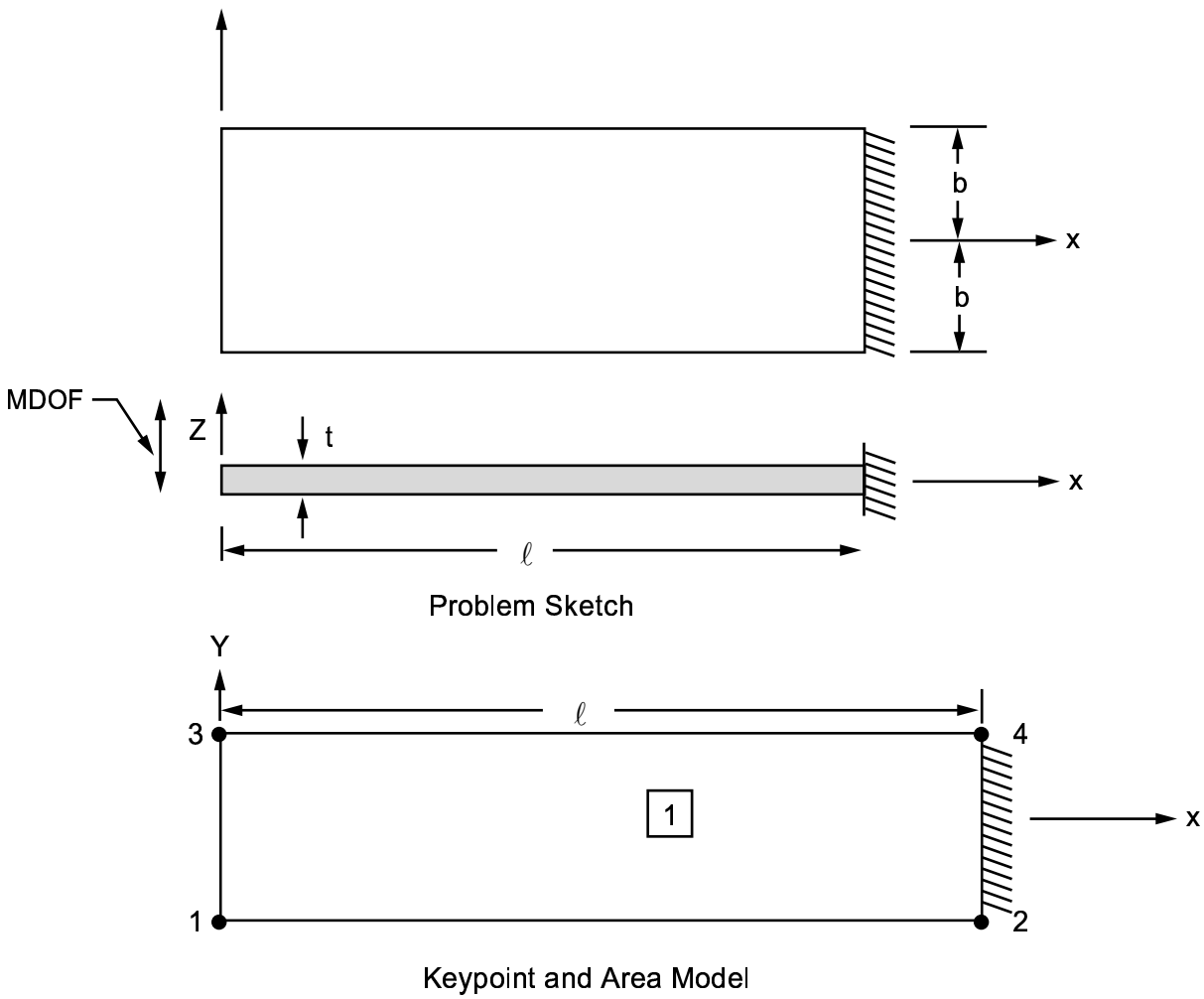

Material Properties	Geometric Properties
$E = 30 \times 10^6$ psi $\rho = 0.000728$ lb-sec^2/in^4 $\upsilon = 0$	t = 1 in b = 2 in ℓ = 16 in

Analysis Assumptions and Modeling Notes

The problem is solved in two different ways:

- Using Elastic Shell Elements (SHELL63)
- Using 3-D Solid Shell Elements (SOLSH190)

All lateral master degrees of freedom (MDOF) are selected along the plate centerline. The area is meshed with 4 elements along the X axis and 2 elements along the Y axis. Poisson's ratio is assumed to be zero.

Results Comparison

	Target	ANSYS	Ratio
SHELL63			
f, Hz	128.09	128.43	1.003
SOLSH190			
f, Hz	128.09	128.72	1.005

VM67: Radial Vibrations of a Circular Ring

Overview

Reference:	S. Timoshenko, D. H. Young, *Vibration Problems in Engineering*, 3rd Edition, D. Van Nostrand Co., Inc., New York, NY, 1955, pg. 425, article 68.
Analysis Type(s):	Mode-frequency Analysis (**ANTYPE** = 2)
Element Type(s):	Axisymmetric-Harmonic 4-Node Structural Solid Elements (PLANE25)
Input Listing:	vm67.dat

Test Case

Determine the fundamental frequency f_o of axisymmetric in-plane radial vibration and the second (extensional) harmonic frequency f_2 of in-plane radial vibration of a circular ring. The cross-section of the ring is square with side length b, at a radius r to the centerline.

Figure 67.1 Ring Axisymmetric Problem Sketch

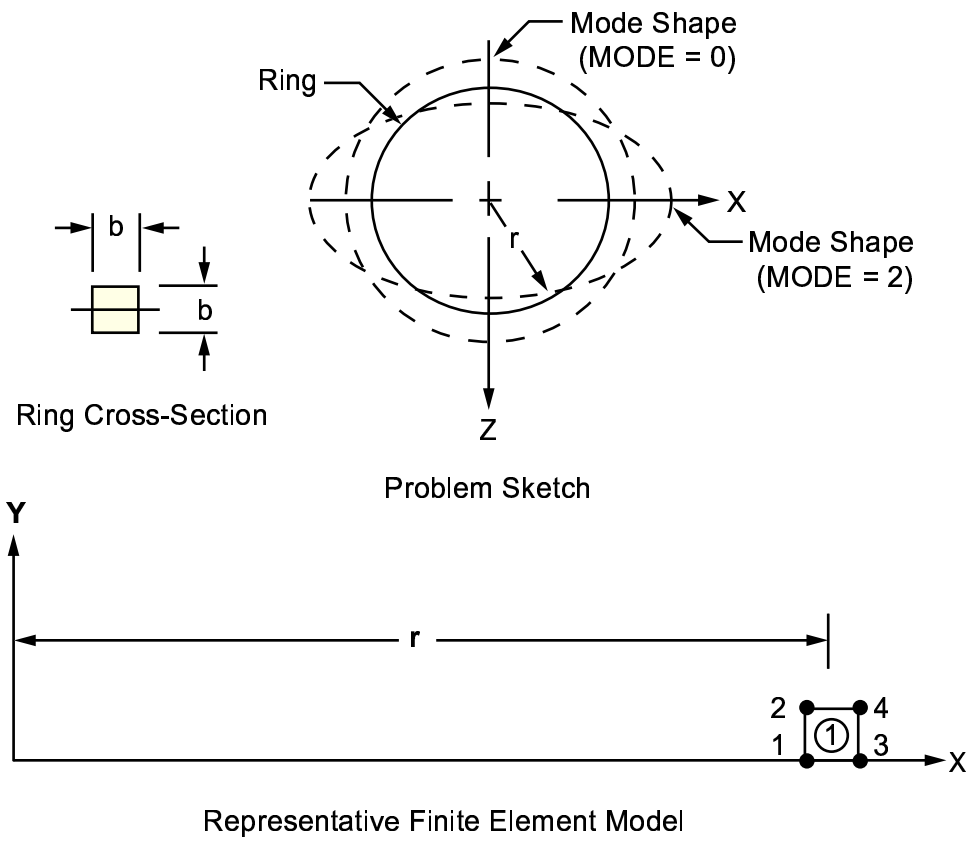

Material Properties	Geometric Properties
$E = 30 \times 10^6$ psi $\rho = 0.00073$ lb-sec^2/in^4 $\upsilon = 0.0$	r = 10 in b = 0.05 in

Analysis Assumptions and Modeling Notes

MODE = 0 for the axisymmetric mode of vibration and MODE = 2 for the second harmonic frequency of vibration. One radial master degree of freedom (MDOF) is selected for the MODE = 0 case and one radial and one tangential MDOF is selected for the MODE = 2 case. Coupling is used to ensure mode symmetry. A local coordinate system is defined at (x, y) = (9.975,0) for convenience.

Results Comparison

	Target	ANSYS	Ratio
f_o, Hz	3226.4	3226.4	1.000
f_2, Hz	12.496	12.496	1.000

ANSYS Verification Manual . ANSYS Release 10.0 . 002184 . © SAS IP, Inc.

VM68: PSD Response of a Two DOF Spring-mass System

Overview

Reference:	R. K. Vierck, *Vibration Analysis*, 2nd Edition, Harper & Row Publishers, New York, NY, 1979, sec. 7-2, 7-14.
Analysis Type(s):	Mode-frequency Analysis (**ANTYPE** = 2) Spectrum Analysis (**ANTYPE** = 8)
Element Type(s):	Combination Elements (COMBIN40)
Input Listing:	vm68.dat

Test Case

Determine the first two natural frequencies, f_1 and f_2, and the response of a damped two degree of freedom system subject to a random acceleration with a spectral density function as shown in the figure below.

Figure 68.1 DOF Spring-mass System Problem Sketch

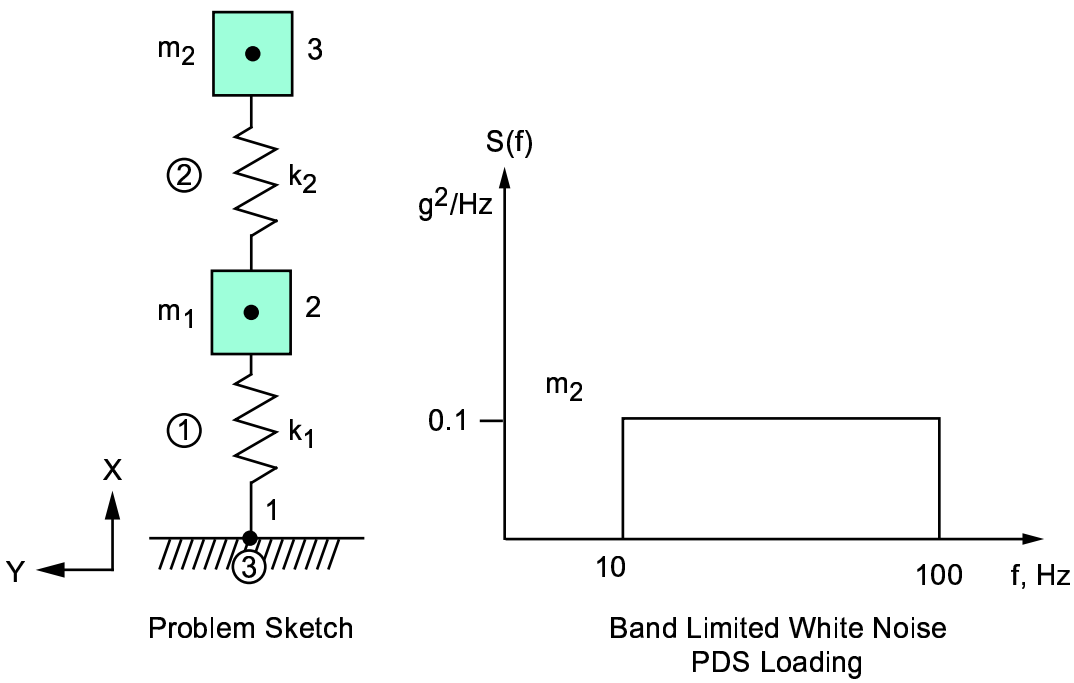

Material Properties
k_1 = 42832 lb/in
k_2 = 32416 lb/in
m_1 = 0.5 lb-sec^2/in
m_2 = 1.0 lb-sec^2/in

Analysis Assumptions and Modeling Notes

The load is applied at node 1 to simulate base excitation. A 2% constant modal damping is assumed. The acceleration results are converted from in/sec^2 to g in POST1.

Results Comparison

	Target	ANSYS	Ratio
f_1 , Hz	20.57	20.57	1.000
f_2 , Hz	64.88	64.88	1.000
Mass 1 - 1 stress Std. dev.	9.059[1]	9.059	1.000
Mass 2 - 1 stress Std. dev.	10.63[1]	10.63	1.000

1. Numerical solution with a uniform frequency spacing equal to 0.001 Hz in the frequency range of 10 to 100 Hz

VM69: Seismic Response

Overview

Reference:	W. T. Thomson, *Vibration Theory and Applications*, 2nd Printing, Prentice-Hall, Inc., Englewood Cliffs, NJ, 1965, pg. 78, ex. 3.11-1
Analysis Type(s):	Mode-frequency, Seismic Analysis (**ANTYPE** = 2)
Element Type(s):	Combination Elements (COMBIN40)
Input Listing:	vm69.dat

Test Case

The spring-mass system shown below represents a vibrometer. Determine its natural frequency f. The displacement response spectrum for the vibrometer is shown for 3 points, based on an input of $u_i = A \cos \omega t$, where u_i is the excitation at the support (node 1). Show that the vibrometer response Δ is 2% in error when operated at frequency ω.

Figure 69.1 Seismic Response Problem Sketch

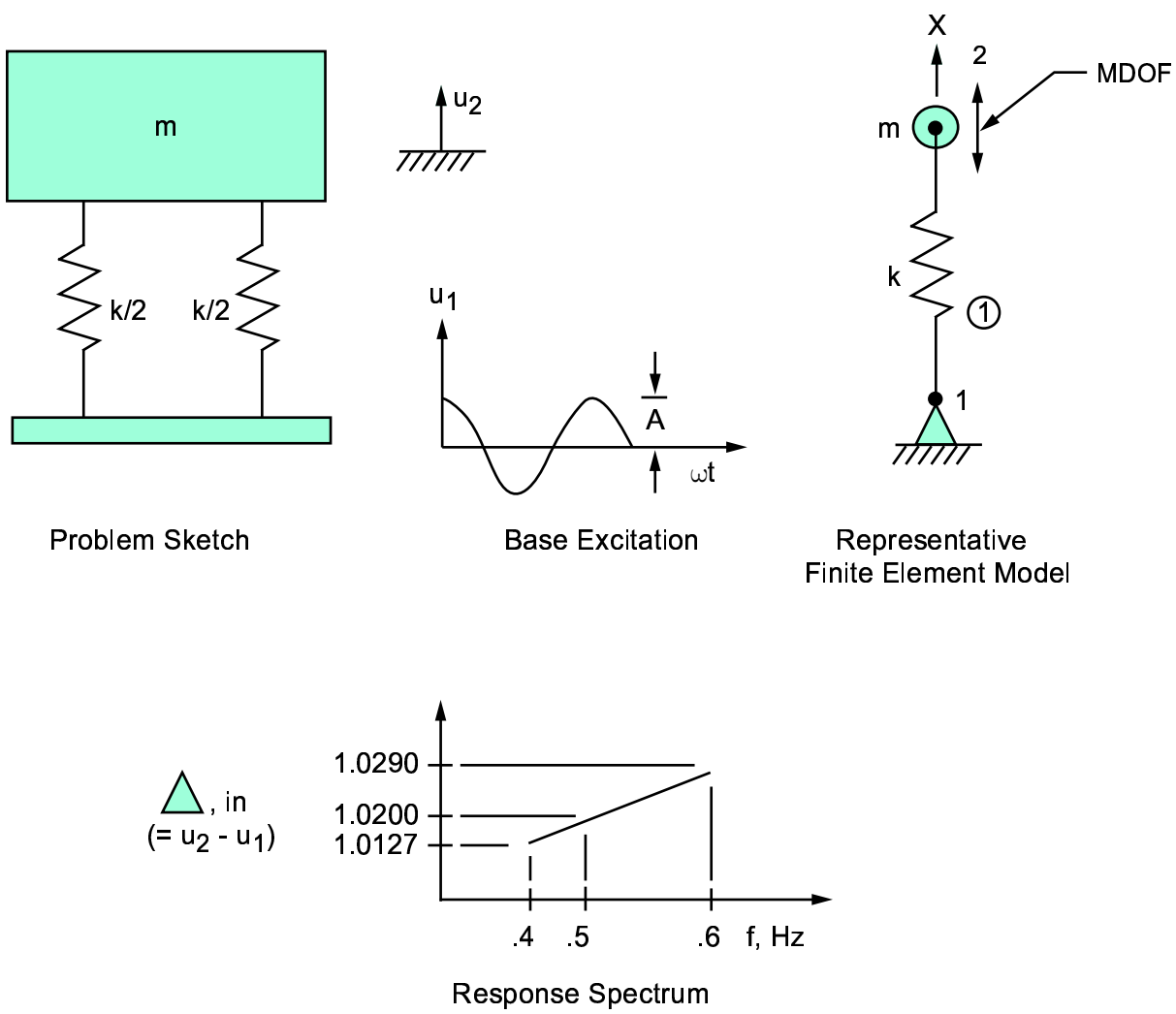

Material Properties	Loading
m = 1 lb-sec^2/in k = 9.8696 lb/in	ω = 22.43537 rad/sec A = 1 in

Analysis Assumptions and Modeling Notes

The node locations are arbitrarily selected. The spring is arbitrarily assumed to vibrate in the X direction. One master degree of freedom (MDOF) is selected at the mass in the vibration direction.

Results Comparison

	Target	ANSYS	Ratio
f, Hz	0.5000	0.5000	1.000
A_e, in[1]	1.0200	1.0200	1.000

1. A_e = expanded mode shape amplitude. Vibrometer accuracy is equal to 100 x (A_e - A)/A = 2%

ANSYS Verification Manual . ANSYS Release 10.0 . 002184 . © SAS IP, Inc.

VM70: Seismic Response of a Beam Structure

Overview

Reference:	J. M. Biggs, *Introduction to Structural Dynamics*, McGraw-Hill Book Co., Inc., New York, NY, 1964, pg. 262, article 6.4.
Analysis Type(s):	Mode-frequency, Seismic Analysis (**ANTYPE** = 2)
Element Type(s):	2-D Elastic Beam Elements (BEAM3)
Input Listing:	vm70.dat

Test Case

A simply supported beam of length ℓ, mass per unit length m, and section properties shown below is subjected to a vertical motion of both supports. The motion is defined in terms of a seismic displacement response spectrum. Determine the fundamental displacement δ, and the corresponding maximum bending stress σ_{max}.

Figure 70.1 Beam Structure Problem Sketch

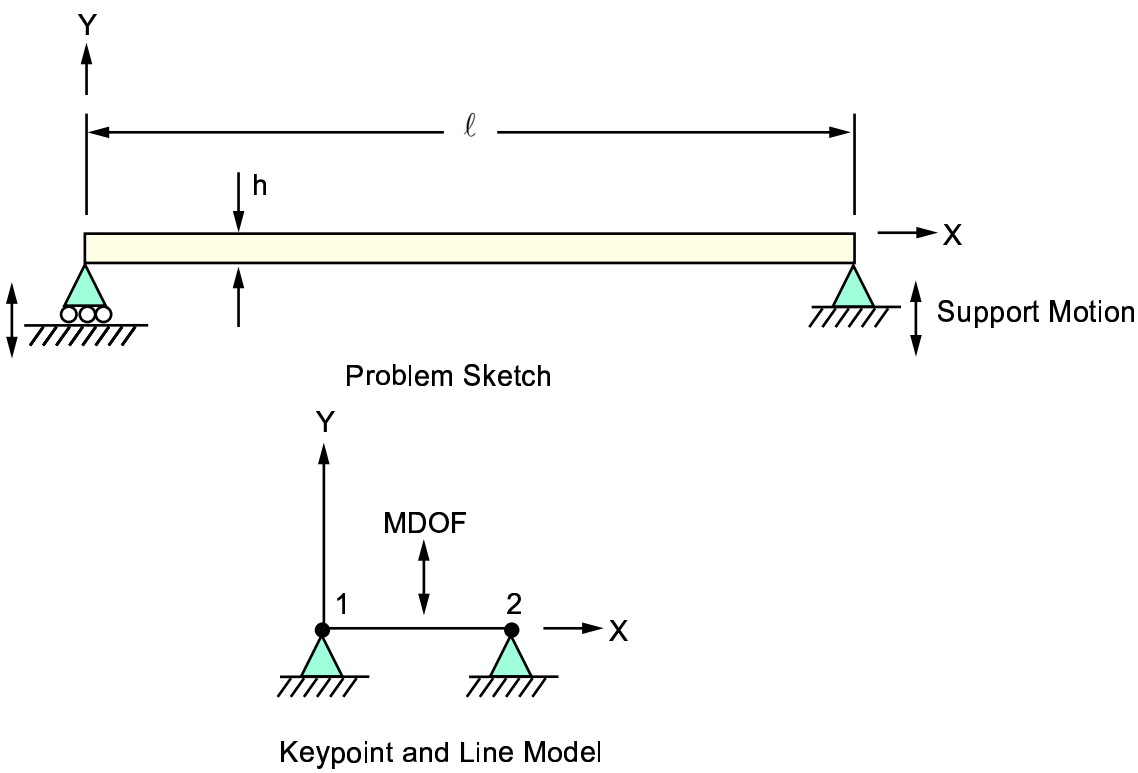

Material Properties	**Geometric Properties**
E = 30 x 10^6 psi	I = (1000/3) in^4
m = 0.2 lb-sec^2/in^2	A = 273.9726 in^2
Response Spectrum	ℓ = 240 in
Frequency, Hz Displacement, in	h = 14 in
0.1 0.44	
10.0 0.44	

Analysis Assumptions and Modeling Notes

All lateral master degrees of freedom (MDOF) are selected for a total of 8 elements used in the model.

Results Comparison

	Target	ANSYS	Ratio
f, H_z	6.0979	6.0974	1.000
Deflection, in	0.56000	0.55301	0.988
$Stress_{max}$, psi	20158.	20156.	1.000

ANSYS Verification Manual . ANSYS Release 10.0 . 002184 . © SAS IP, Inc.

VM71: Transient Response of a Spring-Mass-Damper System

Overview

Reference:	W. T. Thomson, *Vibration Theory and Applications*, 2nd Printing, Prentice-Hall, Inc., Englewood Cliffs, NJ, 1965, pg. 41, ex. 2.2-1.
Analysis Type(s):	Reduced Transient Dynamic Analysis (**ANTYPE** = 4)
Element Type(s):	Combination Elements (COMBIN40)
Input Listing:	vm71.dat

Test Case

A spring-mass system with viscous damping is displaced by a distance Δ and released. Determine the displacement u at time t for four damping ratios:

- $\xi = 2.0$
- $\xi = 1.0$ (critical)
- $\xi = 0.2$
- $\xi = 0.0$ (undamped)

Figure 71.1 Spring-mass-damper System Problem Sketch

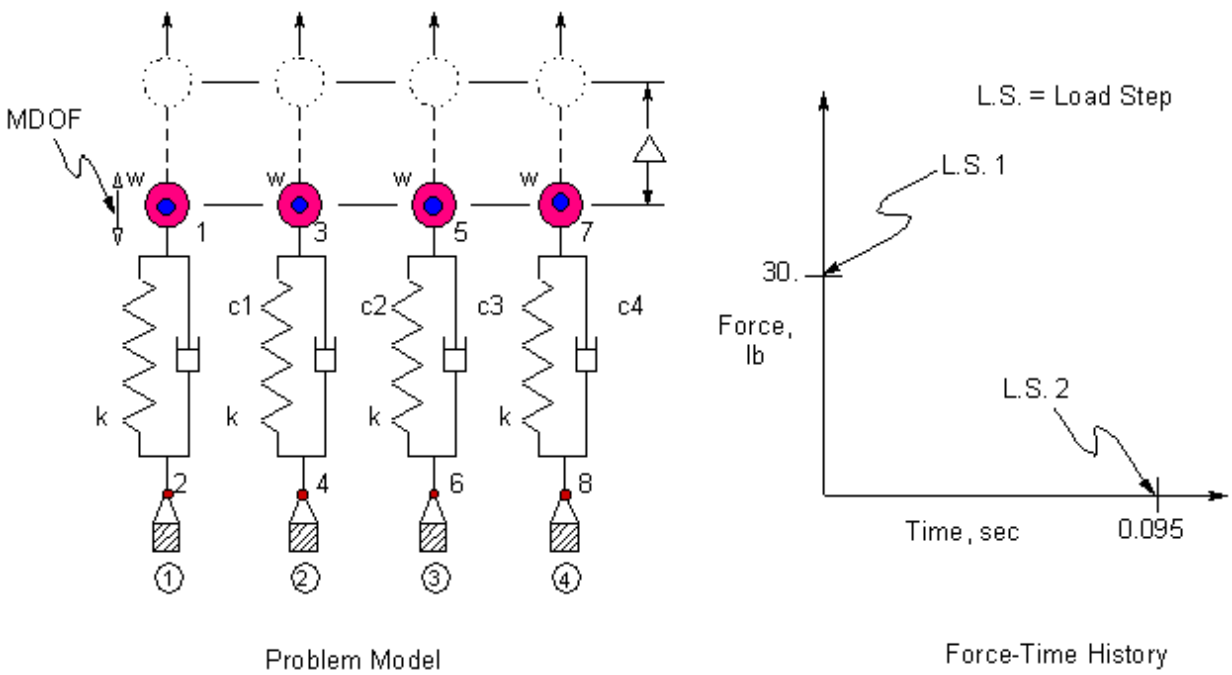

Material Properties	**Loading**
w = 10 lb k = 30 lb/in m = w/g = 0.02590673 lb-sec^2/in	Δ = 1 in g = 386 in/sec^2

Analysis Assumptions and Modeling Notes

The initial static force is calculated as $k\Delta$ = 30 lb and the damping coefficients are calculated as c = 2ξsqrt(km) = 3.52636, 1.76318, 0.352636, and 0.0 lb-sec/in for the four damping ratios (ξ) given in the test case, respectively. The node locations are arbitrarily selected. The integration time step (0.001 sec) is based on ≈ 1/180 of the period to allow the step changes in acceleration to be followed reasonably well and to produce sufficient printout for the theoretical comparison. The maximum time of 0.095 sec covers about 1/2 the period. One master degree of freedom (MDOF) is selected at the mass in the spring direction. A static solution is done at the first load step. POST26 is used to extract results from the solution phase.

Results Comparison

t = 0.09 sec	Target	ANSYS	Ratio
u, in (for damping ratio = 2.0)	0.47420	0.47637	1.005
u, in (for damping ratio = 1.0)	0.18998	0.19245	1.013
u, in (for damping ratio = 0.2)	-0.52108	-0.51951	0.997
u, in (for damping ratio = 0.0)	-0.99688	-0.99498	0.998

Figure 71.2 Displacement vs. Time Display

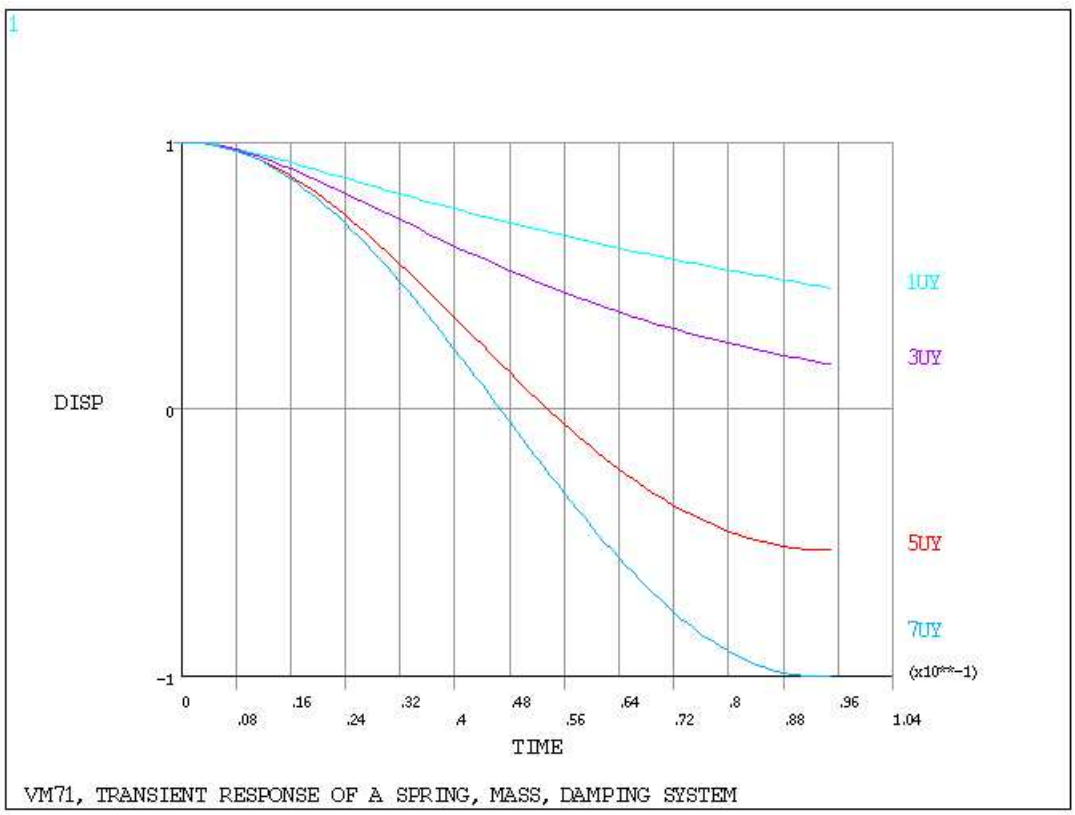

VM72: Logarithmic Decrement

Overview

Reference:	W. T. Thomson, *Vibration Theory and Applications*, 2nd Printing, Prentice-Hall, Inc., Englewood Cliffs, NJ, 1965, pg. 45, ex. 2.3-1.
Analysis Type(s):	Reduced Transient Dynamic Analysis (**ANTYPE** = 4)
Element Type(s):	Combination Elements (COMBIN40)
Input Listing:	vm72.dat

Test Case

Determine the damped natural period τ_d and the ratio R between any two successive amplitudes of the freely vibrating spring-mass-viscous damping system. The system is initially held at rest at the stretched position Δ and then released.

Figure 72.1 Logarithmic Decrement Problem Sketch

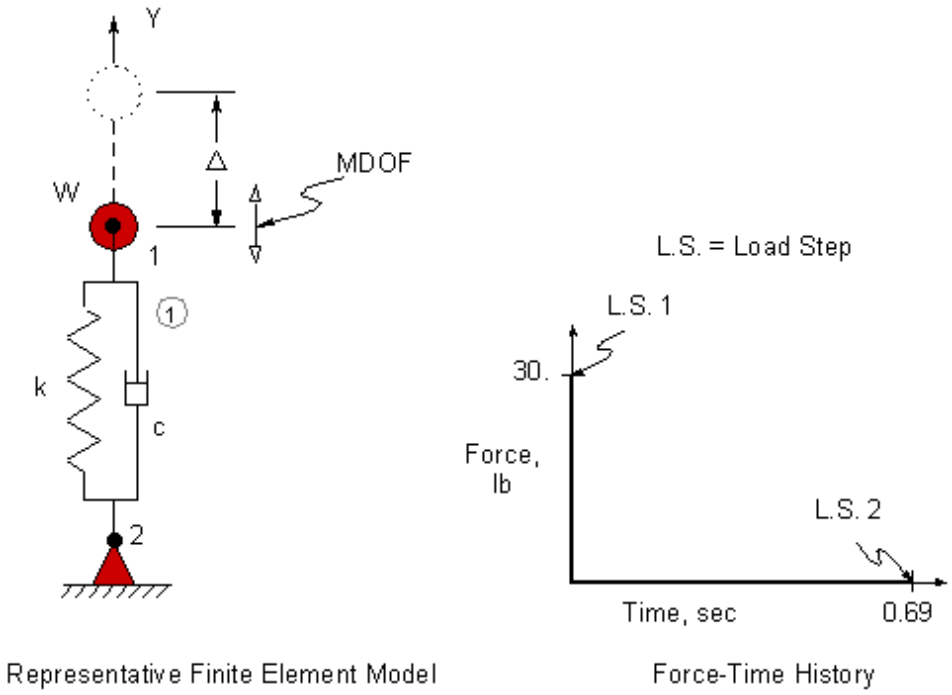

Material Properties	**Loading**
W = 10 lb k = 30 lb/in c = 0.12 lb-sec/in	Δ = 1 in g = 386 in/sec^2

Analysis Assumptions and Modeling Notes

The node locations are arbitrarily selected. The initial static force is k Δ = 30 lb and the mass is m = W/g = 0.02590673 sec^2/in^2 . The integration time step (0.003 sec) is based on $\approx$ 1/60 of the period to allow the step changes in acceleration to be followed reasonably well and to produce sufficient printout for the theoretical comparison. Almost 4 cycles are included in the 0.0 to 0.69 sec time range. One master degree of freedom (MDOF)

is selected at the mass in the spring direction. A static solution is done at the first load step. Results are from the solution phase. POST26 is used to get a displacement versus time display.

Results Comparison

Peak Number[1]	**1**	**2**	**3**	**4**
Max. Amplitude, in	1.0000	0.64981	0.42306	0.27525
Time, sec	0.0000	0.18600	0.37200	0.55800

1. Sequence number of the positive displacement vibration amplitude peaks

	Target	**ANSYS**	**Ratio**
R_{1-2}	1.5350	1.5389	1.003
R_{2-3}	1.5350	1.5360	1.001
R_{3-4}	1.5350	1.5370	1.001
Damped natural period$_{1-2}$	0.18507	0.18600	1.005
Damped natural period$_{2-3}$	0.18507	0.18600	1.005
Damped natural period$_{3-4}$	0.18507	0.18600	1.005

Figure 72.2 Displacement vs. Time Display

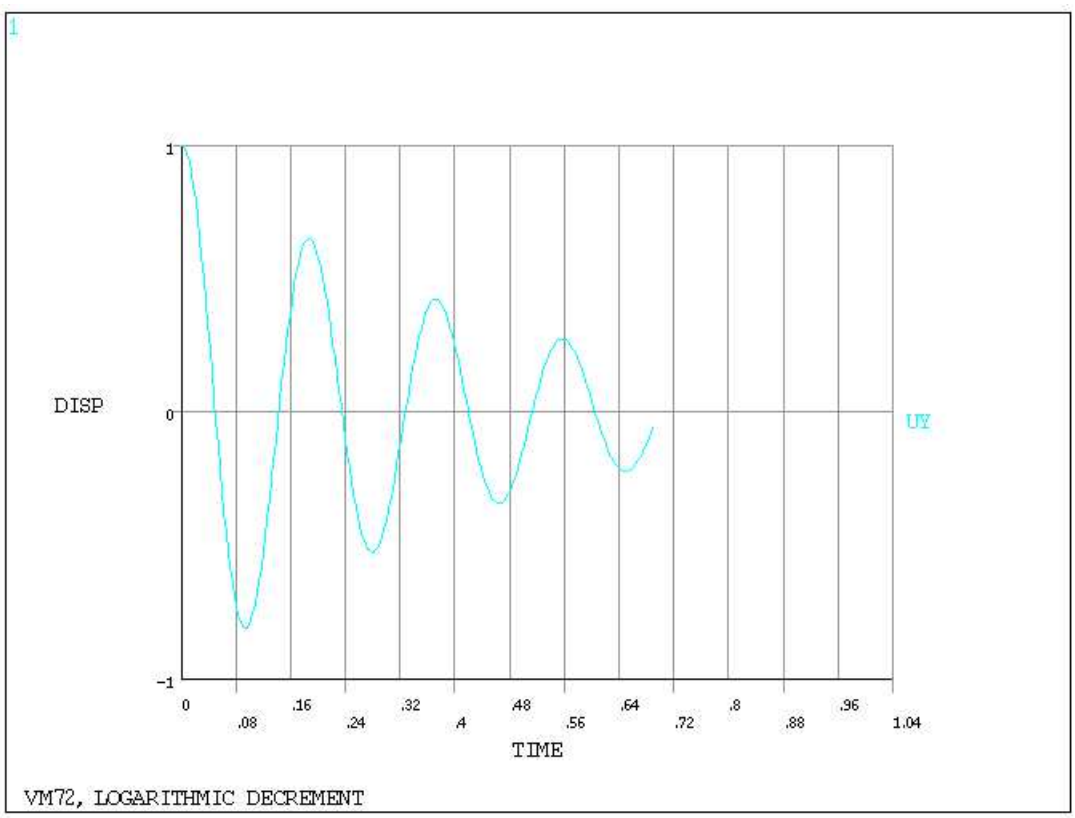

VM73: Free Vibration with Coulomb Damping

Overview

Reference:	F. S. Tse, I. E. Morse, R. T. Hinkle, *Mechanical Vibrations*, Allyn and Bacon, Inc., Boston, MA, 1963, pg. 175, case 1.
Analysis Type(s):	Full Transient Dynamic Analysis (**ANTYPE** = 4)
Element Type(s):	Combination Elements (COMBIN40)
Input Listing:	vm73.dat

Test Case

A spring-mass system with coulomb damping is displaced a distance Δ and released. Dry friction is assumed to act as a limiting sliding force F between the sliding mass and the surface. Determine the displacement u at various times t.

Figure 73.1 Free Vibration Problem Sketch

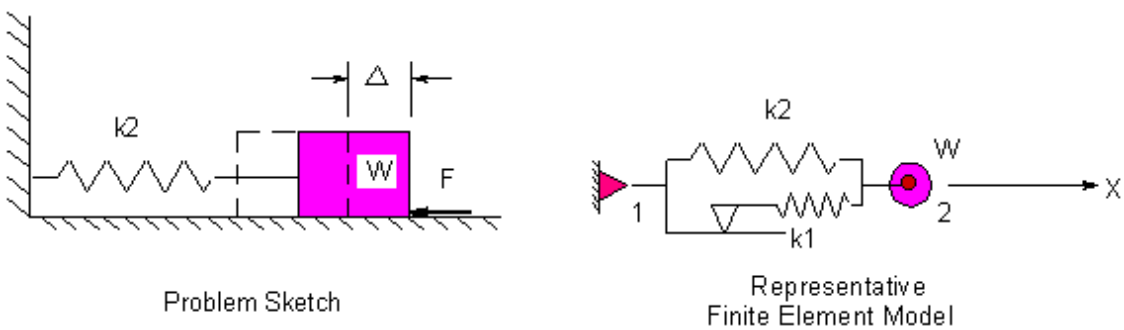

Material Properties	**Loading**
W = 10 lb k_2 = 30 lb/in m = W/g	Δ = -1 in F = 1.875 lb

Initial Conditions		
	Z	$\dot{X}$
t = 0	-1.	0.

Analysis Assumptions and Modeling Notes

One combination element is used with the slider in parallel with the spring. The slider spring constant (k_1 = 10,000 lb/in) is arbitrarily selected high enough to minimize the elastic contact effect but low enough to also allow a practical integration time step size. The integration time step (0.2025/405 = 0.0005 sec) is based on $\approx$ 1/Nf where N = 20 and f is the system natural frequency. At release, the mass acceleration is not necessarily zero. Therefore, a load step with a small time period is used to ramp up to the appropriate acceleration while maintaining an essentially zero velocity. The final time of 0.2025 sec allows one full cycle of motion. POST26 is used to postprocess results from the solution phase.

Results Comparison

	Target	ANSYS	Ratio
u, in (t = 0.09 sec)	0.87208	0.87147	0.999
u, in (t = 0.102 sec)	0.83132	0.83185	1.001
u, in (t = 0.183 sec)	-0.74874	-0.74841	0.999

Figure 73.2 Displacement vs. Time Display

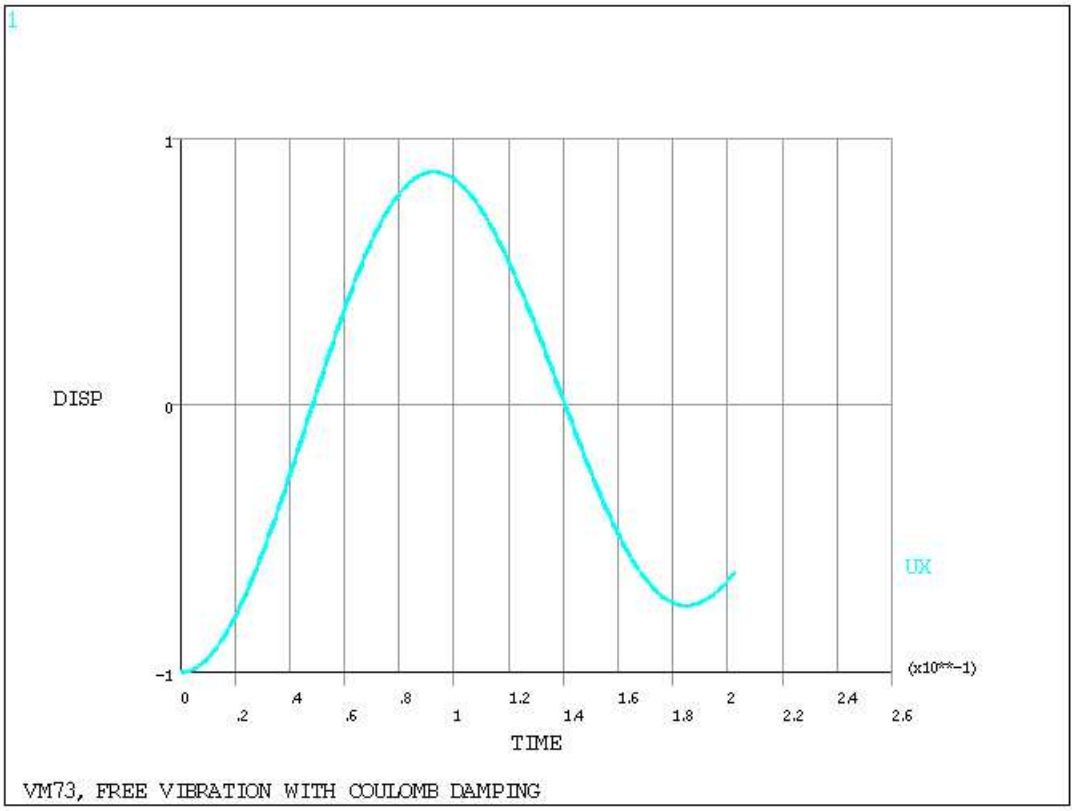

Figure 73.3 Sliding Force vs. Time Display

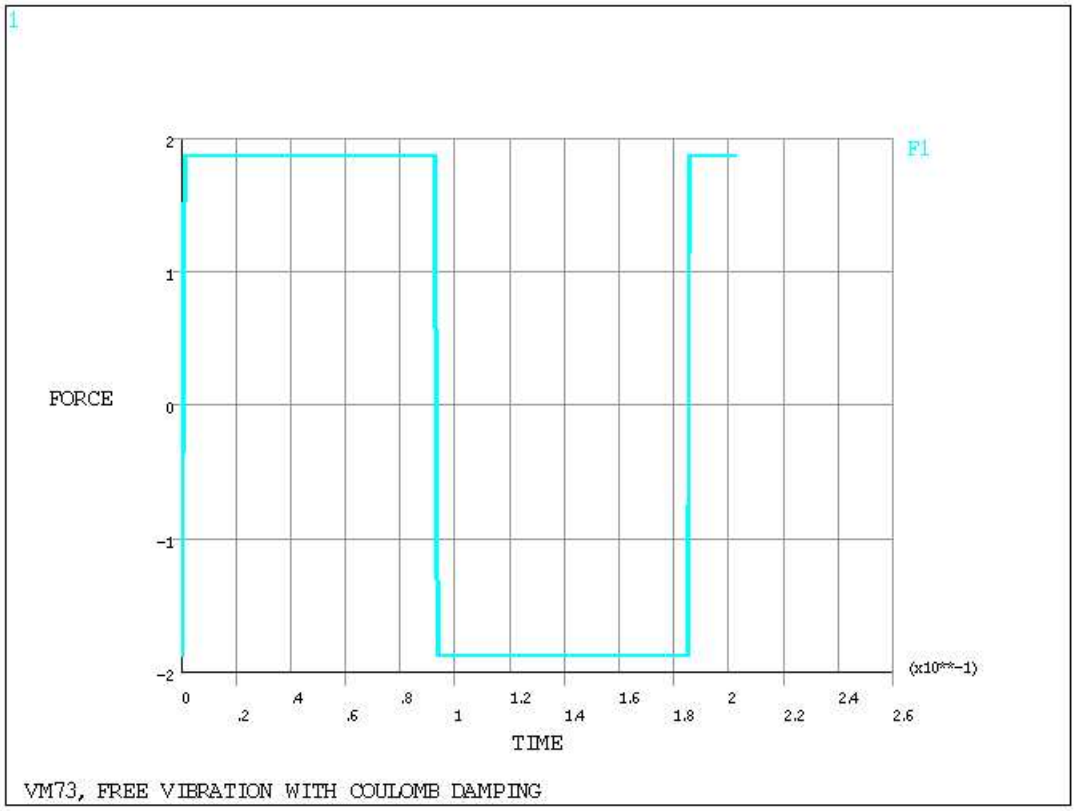

VM74: Transient Response to an Impulsive Excitation

Overview

Reference:	W. T. Thomson, *Vibration Theory and Applications*, 2nd Printing, Prentice-Hall, Inc., Englewood Cliffs, NJ, 1965, pg. 99, article 4.1.
Analysis Type(s):	Reduced Transient Dynamic Analysis (**ANTYPE** = 4)
Element Type(s):	Combination Elements (COMBIN40)
Input Listing:	vm74.dat

Test Case

A mass supported on a spring is subjected to an impulse force F(t) and thereafter undergoes free vibration. Determine the maximum deflection y_{max} of the mass for the undamped case and the deflection y at time t for two damping ratios:

- $\xi = 0.0$ (undamped)
- $\xi = 0.7$.

Figure 74.1 Impulsive Excitation Problem Sketch

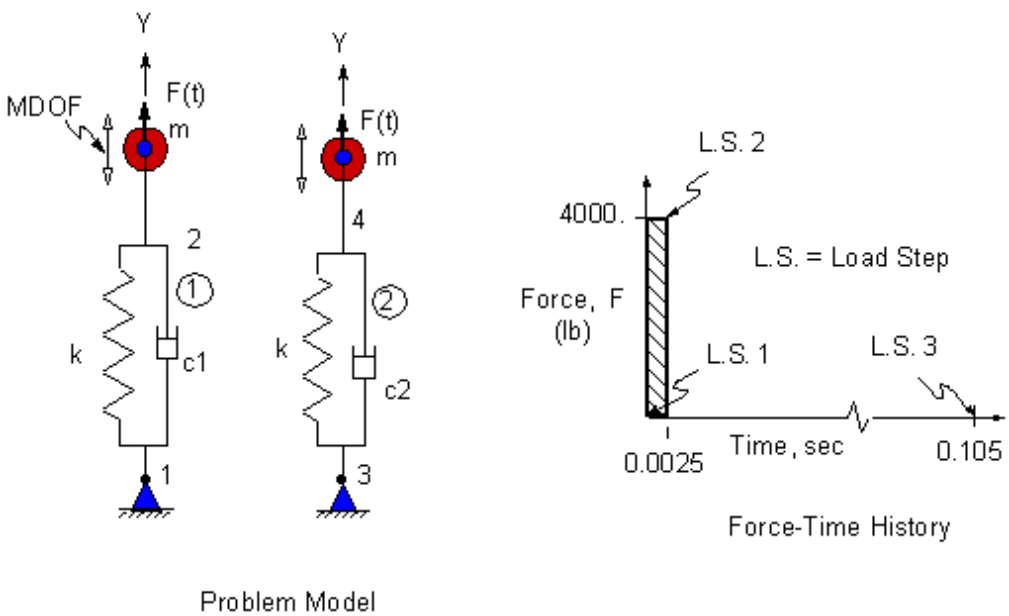

Material Properties	**Loading**
m = 0.5 lb-sec^2/in k = 200 lb/in	(see time history in Figure 74.1: "Impulsive Excitation Problem Sketch")

Analysis Assumptions and Modeling Notes

The node locations are arbitrarily selected. The damping coefficient c is calculated as 2ξsqrt(km) = 0.0 and 14.0 lb-sec/in for $\xi = 0.0$ and $\xi = 0.7$ respectively. A static solution is done at the first load step. The final time of 0.105 sec allows the masses to reach their largest deflections. One master degree of freedom (MDOF) is selected at each mass in the spring direction. The integration time step (0.0025 sec) is based on ≈ 1/120 of the period to allow

the step changes in acceleration to be followed reasonably well and to produce sufficient printout for the theoretical comparison. The impulse is applied over 1 integration time step.

Results Comparison

		Target	ANSYS	Ratio
Time = 0.08 sec Damping ratio = 0.0	$y_{,max}$ in	0.99957	0.99523	0.996
Time = 0.1 sec	y, in (for damping ratio = 0.0)	0.90930	0.92469[1]	1.017
	y, in (for damping ratio = 0.07)	0.34180	0.35167[1]	1.029

1. Based on time = 0.1 + 0.0025 sec to account for finite impulse duration of 0.0025 sec.

VM75: Transient Response to a Step Excitation

Overview

Reference:	W. T. Thomson, *Vibration Theory and Applications*, 2nd Printing, Prentice-Hall, Inc., Englewood Cliffs, NJ, 1965, pg. 102, article 4.3.
Analysis Type(s):	Reduced Transient Dynamic Analysis (**ANTYPE** = 4)
Element Type(s):	Combination Elements (COMBIN40)
Input Listing:	vm75.dat

Test Case

A spring-mass-damping system, initially at rest, is subjected to a step force change F acting on the mass. Determine the maximum deflection u_{max} for the undamped case. Determine the displacement u at time t for two damping ratios:

- $\xi = 0.0$ (undamped)
- $\xi = 0.5$

Figure 75.1 Step Excitation Problem Sketch

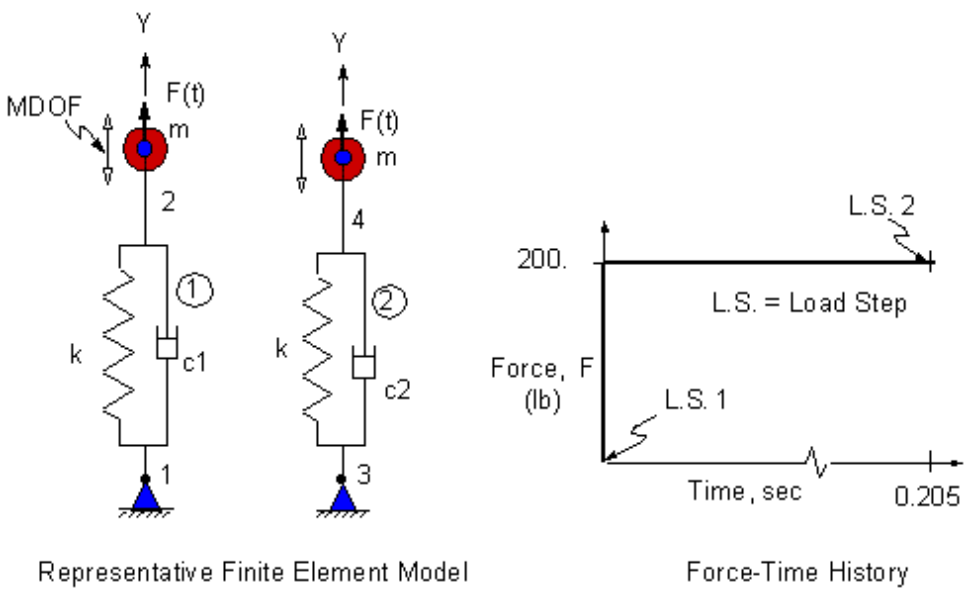

Material Properties	**Loading**
m = 0.5 lb-sec^2/in k = 200 lb/in	F = 200 lb (see Figure 75.2: "Displacement vs. Time Display")

Analysis Assumptions and Modeling Notes

The node locations are arbitrarily selected. The damping coefficient c is calculated as 2ξ sqrt(km) = 0.0 and 10 lb-sec/in for $\xi = 0.0$ and $\xi = 0.5$ respectively. A static solution is done at the first load step. The maximum time of 0.205 sec allows the masses to reach their largest deflections. One master degree of freedom (MDOF) is selected at each mass in the spring direction. The integration time step (0.0025 sec) is based on $\approx$ 1/120 of the period to allow the initial step acceleration change to be followed reasonably well and to produce sufficient printout for

the theoretical comparison. Results are from the solution phase. POST26 is used to get displacement versus time display.

Results Comparison

		Target	ANSYS	Ratio
Time = 0.1575 sec	$u_{max, in}$	2.0000	1.9992	1.000
Time = 0.20 sec	$u_{, in}$ (for Damping ratio = 0.0)	1.6536	1.6723	1.011
	$u_{, in}$ (for Damping ratio = 0.5)	1.1531	1.1544	1.001

Figure 75.2 Displacement vs. Time Display

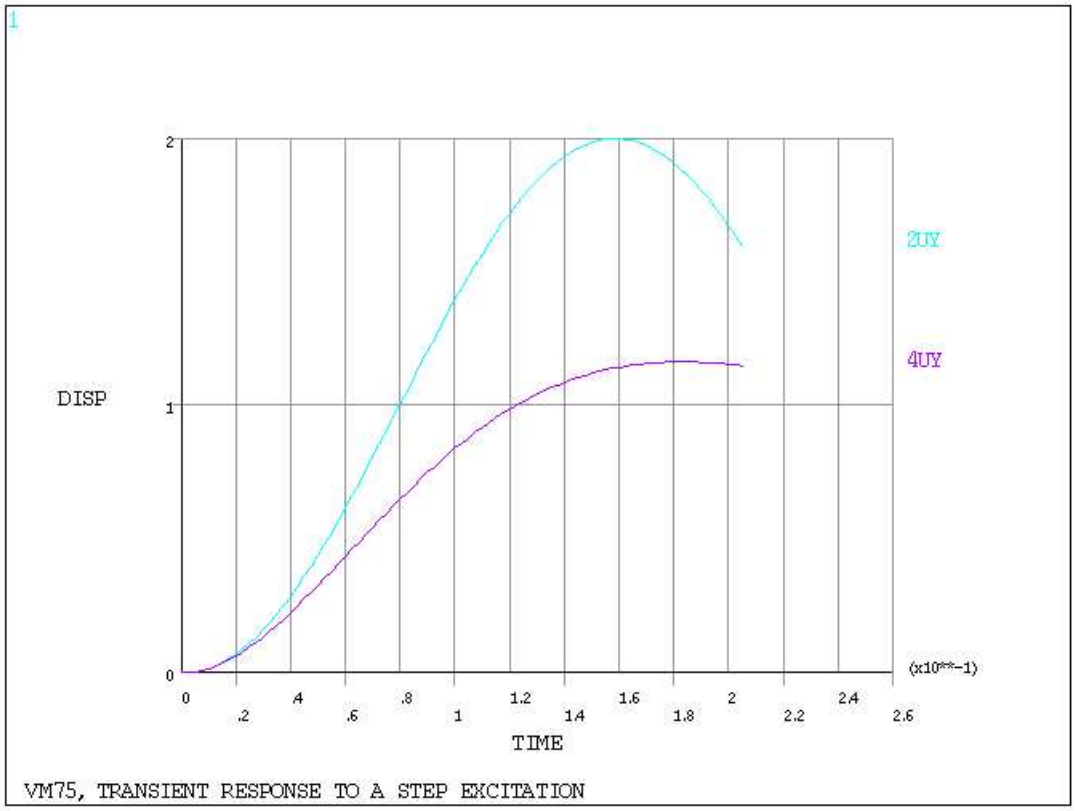

VM76: Harmonic Response of a Guitar String

Overview

Reference:	R. D. Blevins, *Formulas for Natural Frequency and Mode Shape*, Van Nostrand Reinhold Co., New York, NY, 1979, pg. 90, tab. 7-1.
Analysis Type(s):	Static Analysis (**ANTYPE** = 0) Mode-frequency Analysis (**ANTYPE** = 2) Mode Superposition Harmonic Response Analysis (**ANTYPE** = 3)
Element Type(s):	2-D Spar (or Truss) Elements (LINK1)
Input Listing:	vm76.dat

Test Case

A uniform stainless steel guitar string of length ℓ and diameter d is stretched between two rigid supports by a tensioning force F_1, which is required to tune the string to the E note of a C scale. The string is then struck near the quarter point with a force F_2. Determine the fundamental frequency, f_1. Also, show that only the odd-numbered frequencies produce a response at the midpoint of the string for this excitation.

Figure 76.1 Guitar String Problem Sketch

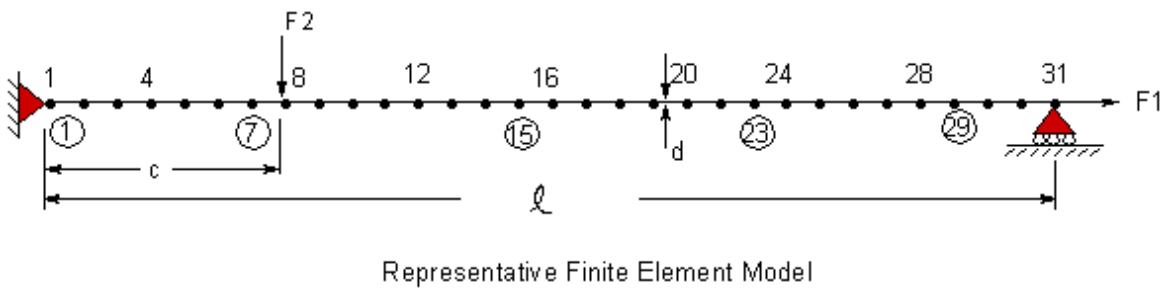

Material Properties	Geometric Properties	Loading
$E = 190 \times 10^9$ Pa $\rho = 7920$ kg/m^3	$\ell = 710$ mm c = 165 mm d = 0.254 mm	$F_1 = 84$ N $F_2 = 1$ N

Analysis Assumptions and Modeling Notes

Enough elements are selected so that the model can be used to adequately characterize the string dynamics. The stress stiffening capability of the element is used. Harmonic response analysis is used to determine the displacement response to the lateral force F_2. The harmonic response is displayed with the time-history postprocessor, POST26, to show the excitation of the odd-numbered frequencies at peak displacement amplitudes.

Results Comparison

		Target	ANSYS	Ratio
Modal	f, Hz	322.2	322.3	1.000
POST26	f_1, (322.2 Hz)	Response	Response, 320 < f < 328	-
	f_2, (644.4 Hz)	No Response	No Response	-

	f_3, (966.6 Hz)	Response	Response, 968 < f < 976	-
	f_4, (1288.8 Hz)	No Response	No Response	-
	f_5, (1611.0 Hz)	Response	Response,1624 < f < 1632	-
	f_6, (1933.2 Hz)	No Response	No Response	-

Figure 76.2 String Midpoint Displacement Amplitude

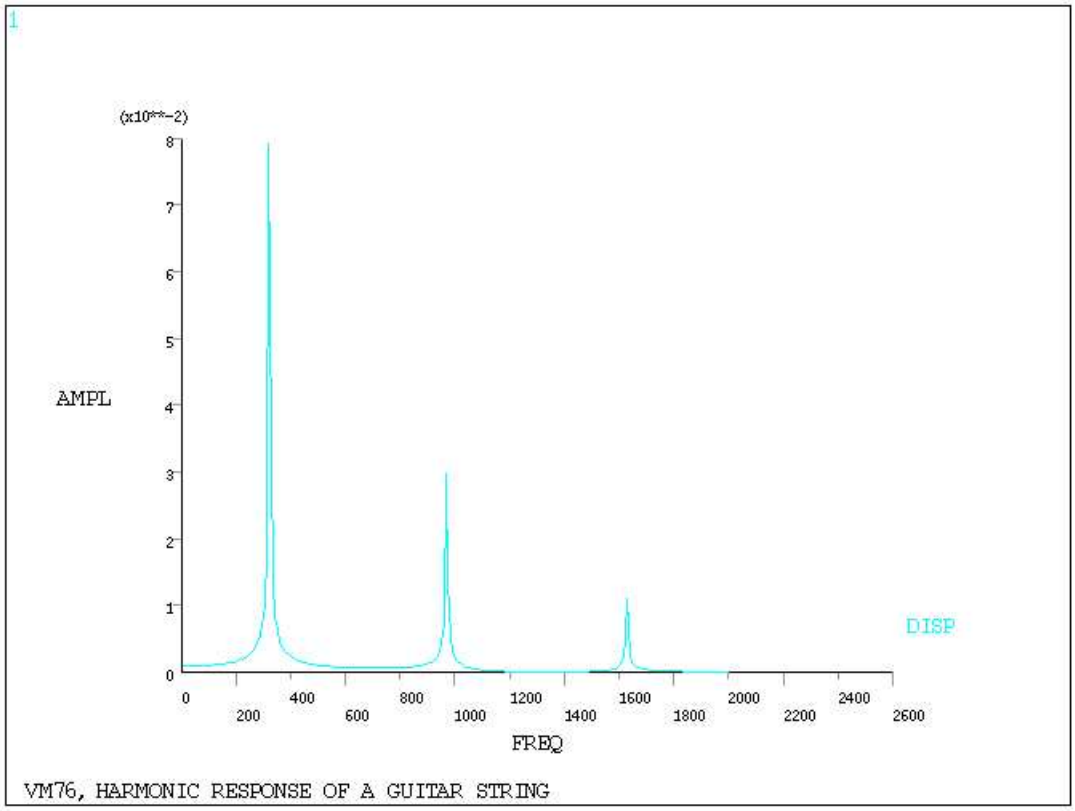

VM77: Transient Response to a Constant Force

Overview

Reference:	J. M. Biggs, *Introduction to Structural Dynamics*, McGraw-Hill Book Co., Inc., New York, NY, 1964, pg. 50, ex. E.
Analysis Type(s):	Reduced Transient Dynamic Analysis (**ANTYPE** = 4)
Element Type(s):	2-D Elastic Beam Elements (BEAM3) Structural Mass Elements (MASS21)
Input Listing:	vm77.dat

Test Case

A steel beam of length ℓ and geometric properties shown below, is supporting a concentrated mass, m. The beam is subjected to a dynamic load F(t) with a rise time t_r and a maximum value F_1. If the weight of the beam is considered negligible, determine the time of maximum displacement response t_{max} and the maximum displacement response y_{max}. Additionally, determine the maximum bending stress σ_{bend} in the beam.

Figure 77.1 Constant Force Problem Sketch

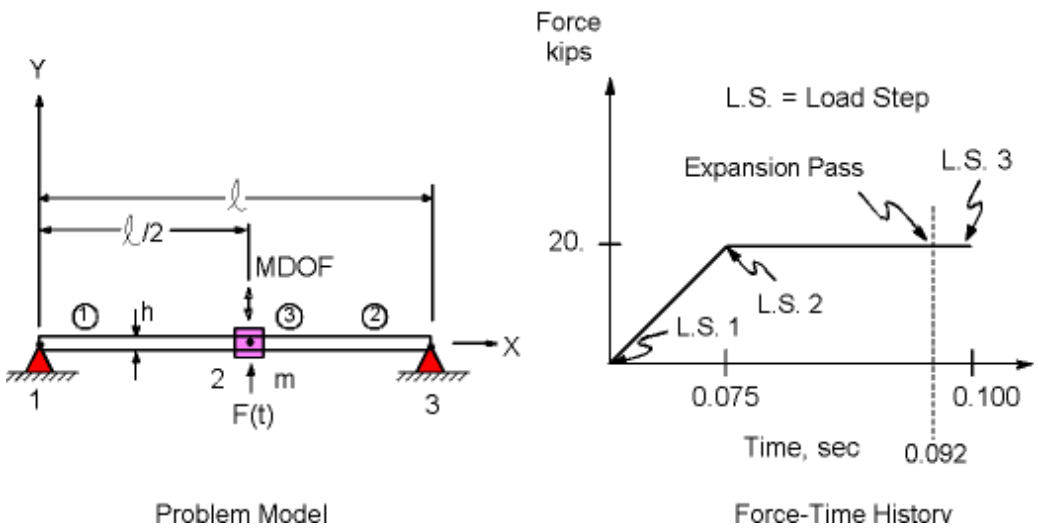

Material Properties	Geometric Properties	Loading
$E = 30 \times 10^3$ ksi $m = 0.0259067$ kips-sec^2/in	$I = 800.6$ in^4 $h = 18$ in $\ell = 20$ ft $= 240$ in	$F_1 = 20$ kips $t_r = 0.075$ sec

Analysis Assumptions and Modeling Notes

The beam area is not used in this solution and is arbitrarily input as unity. The final time of 0.1 sec allows the mass to reach its largest deflection. One master degree of freedom (MDOF) is selected at the mass in the lateral direction. A static solution is done at the first load step. The integration time step (0.004 sec) is based on $\approx 1/25$ of the period to allow the abrupt change in acceleration to be followed reasonably well and to produce sufficient printout for the theoretical comparison. Symmetry could have been used in the model. The time of maximum response (0.092 sec) is selected for the expansion pass calculation.

Results Comparison

		Target[1]	ANSYS	Ratio
Transient	t_{max} , sec	0.092	0.092	1.00
	y_{max} , in	0.331	0.335	1.01
Expansion Pass	$Stress_{bend}$, ksi	-18.6	-18.9	1.01

1. Based on graphical values

VM78: Transverse Shear Stresses in a Cantilever Beam

Overview

Reference:	S. Timoshenko, J. N. Goodier, *Theory of Elasticity*, 2nd Edition, McGraw-Hill Book Co., Inc., New York, NY, 1951, pg. 35, article 20.
Analysis Type(s):	Static Analysis (**ANTYPE** = 0)
Element Type(s):	Linear Layered Structural Shell Elements (SHELL99)
Input Listing:	vm78.dat

Test Case

A cantilever beam of length L, height h, and width w is bent by a force F applied at the free end. Modeling the beam using SHELL99 shell elements having four layers of identical material properties and thickness, determine the shear stress distribution through the beam thickness and the maximum Tsai-Wu failure criterion. The normal and shear failure stresses are $\sigma_x f$ and $\sigma_{xy} f$ respectively.

Figure 78.1 Cantilever Beam Problem Sketch

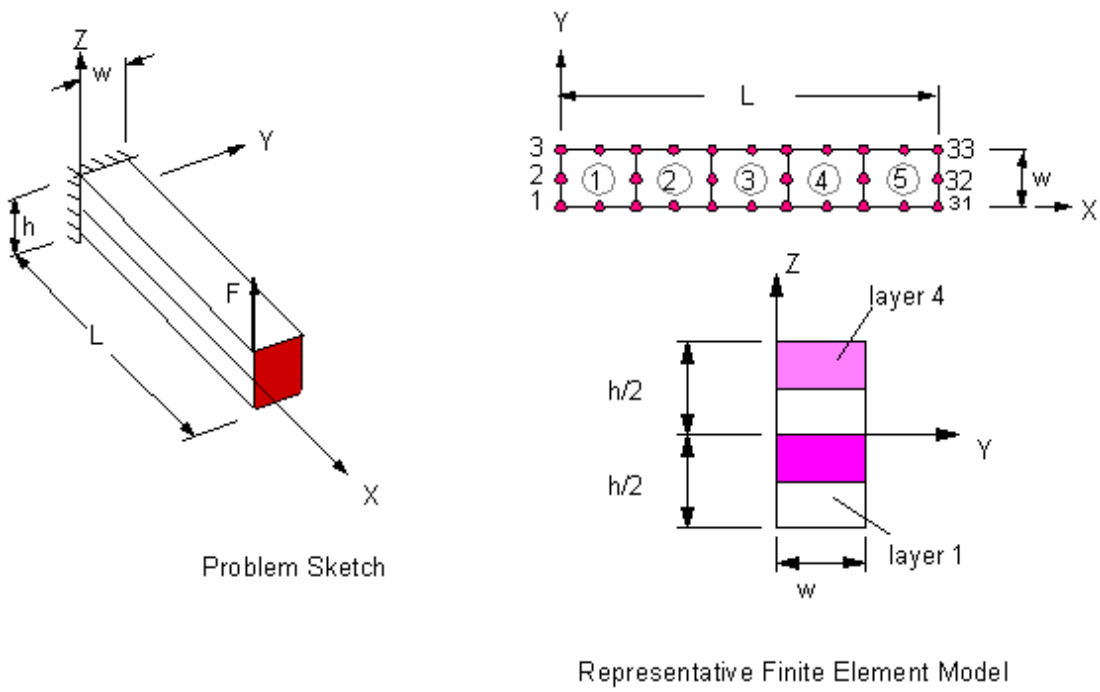

Material Properties	Geometric Properties	Loading
$E = 30 \times 10^6$ psi $\upsilon = 0$ $\sigma_x f = 25000$ psi $\sigma_{xy} f = 500$ psi	L = 10.0 in w = 1.0 in h = 2.0 in	$F_1 = 10000$ lb

Analysis Assumptions and Modeling Notes

Poisson's ratio is set to zero to model the narrow beam assumption. The failure stresses are input in the nonlinear material property table (**TB** commands). Compression values are allowed to default to negative tension values and arbitrary values are assigned to failure stresses in the Y and Z directions. The target solution for the maximum

Tsai-Wu failure criterion (FC3) is obtained from equation 2–92 of the *ANSYS, Inc. Theory Reference*). Since $\sigma_y = \sigma_z = \sigma_{xy} = \sigma_{yx} = 0$, most terms vanish and the equation reduces to:

$$FC3 = \frac{\sigma_x^2}{\sigma_x^{f2}} + \frac{\sigma_{xz}^2}{\sigma_{xz}^{f2}}, \text{where } \sigma_{xz}^f = \sigma_{xy}^f \text{ (by default)}$$

By substituting relations for σ_{xz} (from S. Timoshenko, J. N. Goodier, *Theory of Elasticity*), it can be shown that σ_x and FC3 has a maximum value at the middle plane and:

$$FC3_{max} = \frac{9F^2}{4W^2h^2\sigma_{xy}^{f2}} = 225.0$$

POST1 is used to find the maximum value of the Tsai-Wu failure criterion (FCMX).

Results Comparison

	Target	ANSYS	Ratio
$Stress_{xz}$, psi (z = h/2)	0.0	0.0[1]	1.000
$Stress_{xz}$, psi (z = h/4)	5625.0	5625.0[2]	1.000
$Stress_{xz}$, psi (z = 0)	7500.0	7500.0[3]	1.000
$FC3_{max}$ (FCMX)	225.0	225.0	1.000

1. SXZ for Layer, BOT or Layer 4, TOP (for any element)
2. ILSXZ for Layers 1-2 (or 3-4)
3. ILSXZ for Layers 2-3 (also ILMX)

Poisson's ratio is set to zero to model the narrow beam assumption. The failure stresses are input in the nonlinear material property table (**TB** commands). Compression values are allowed to default to negative tension values and arbitrary.

VM79: Transient Response of a Bilinear Spring Assembly

Overview

Reference:	W. T. Thomson, *Vibration Theory and Applications*, 2nd Printing, Prentice-Hall, Inc., Englewood Cliffs, NJ, 1965, pg. 150, fig. 5.6-1.
Analysis Type(s):	Reduced Transient Dynamic Analysis (**ANTYPE** = 4)
Element Type(s):	Combination Elements (COMBIN40) Gap Condition (GP)
Input Listing:	vm79.dat

Test Case

A mass supported on a nonlinear spring is subjected to an impulsive force F(t) and thereafter undergoes free vibration. The spring stiffness is characterized by the force-deflection curve shown below. Determine the maximum deflection y_{max} of the mass. Compare results with those of VM74.

Figure 79.1 Bilinear Spring Assembly Problem Sketch

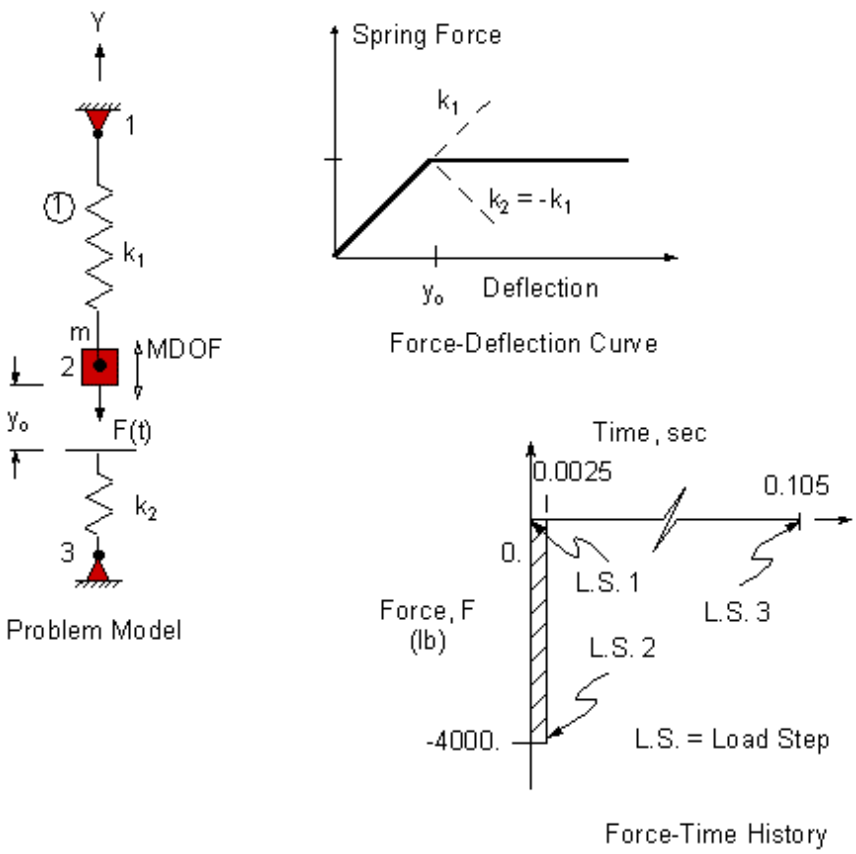

Material Properties	**Geometric Properties**
m = 0.5 lb-sec^2/in k_1 = 200 lb/in	y_o = 0.75 in **Loading** see time history in Figure 79.1: "Bilinear Spring Assembly Problem Sketch"

Analysis Assumptions and Modeling Notes

The node locations are arbitrarily selected. The final time of 0.105 sec allows the mass to reach its largest deflection. A static solution is done at the first load step. A gap condition with a spring constant of $-k_1$ is applied in parallel with k_1 to produce a combined spring stiffness of zero at gap closure. One master degree of freedom (MDOF) is selected at the mass in the spring direction. The integration time step (0.0025 sec) is based on $\approx$ 1/125 of the period to allow the step changes in acceleration to be followed reasonably well and to produce sufficient printout for the theoretical comparison. The impulse is applied over 1 integration time step.

Results Comparison

Time = 0.09 sec	Target	ANSYS	Ratio
Y_{max}, in	-1.0417	-1.0405	0.999

Table 79.1 Comparison of ANSYS Linear and Bilinear Spring Results

Time, sec	0.040	0.070	0.085	0.105
y, in (linear)[1]	-0.68122	-0.97494	-0.99604	-0.88666
y, in (bilinear)	-0.68122	-0.98672	-1.0383	-1.0020

1. From test case VM74 output. Positive displacement direction is reversed for comparison.

VM80: Plastic Response to a Suddenly Applied Constant Force

Overview

Reference:	J. M. Biggs, *Introduction to Structural Dynamics*, McGraw-Hill Book Co., Inc., New York, NY, 1964, pg. 69, article 2.7.
Analysis Type(s):	Full Transient Dynamic, Plastic Analysis (**ANTYPE** = 4)
Element Type(s):	2-D Spar (or Truss) Elements (LINK1) Structural Mass Elements (MASS21)
Input Listing:	vm80.dat

Test Case

A mass m supported on a thin rod of area A and length ℓ is subjected to the action of a suddenly applied constant force F_1. The stress-strain curve for the rod material is shown below. Determine the maximum deflection y_{max} and minimum deflection y_{min} of the mass, neglecting the mass of the rod.

Figure 80.1 Plastic Response Problem Sketch

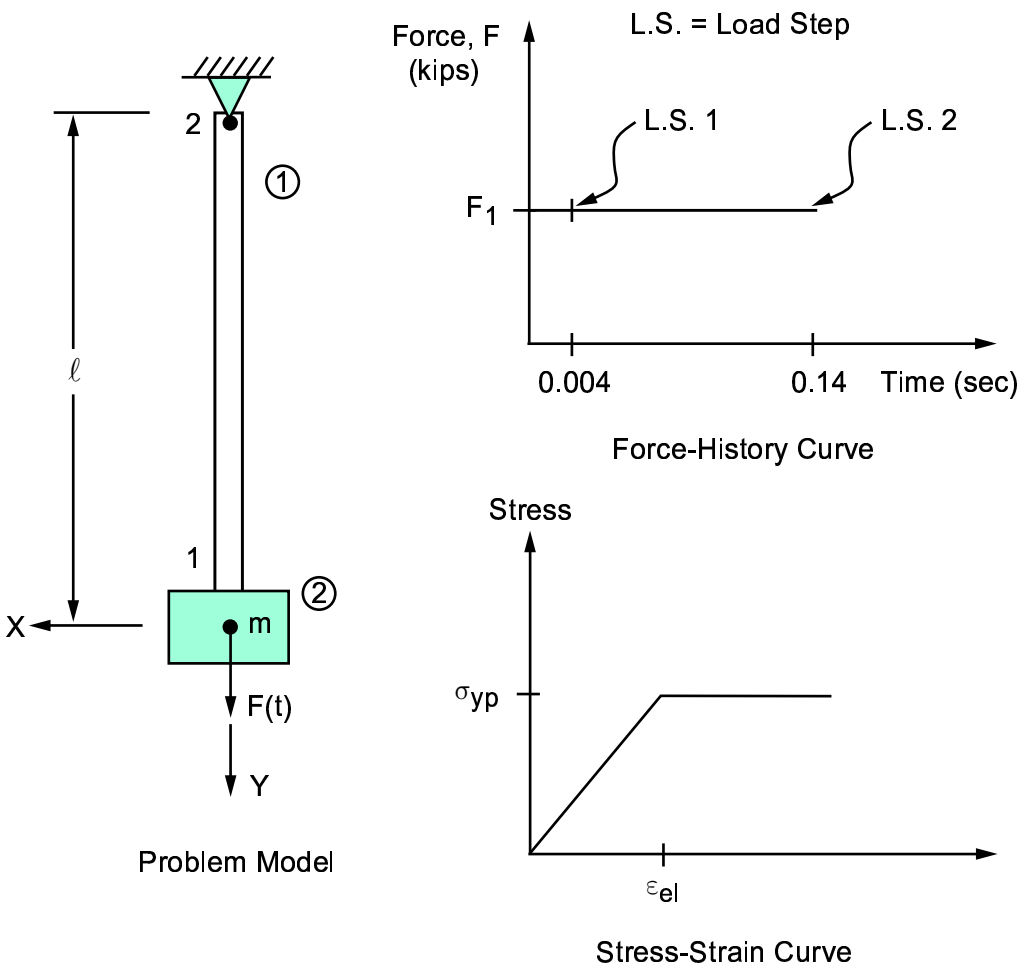

Material Properties	Geometric Properties	Loading
m = 0.0259 kips-sec^2/in E = 30 x 10^3 ksi σ_{yp} = 162.9 ksi	ℓ = 100 in A = 0.278 in^2	F_1 = 30 kips (see time history in Figure 80.1: "Plastic Response Problem Sketch")

Analysis Assumptions and Modeling Notes

The initial integration time step (0.004/10 = 0.0004 sec) is chosen small enough to allow the initial step change in acceleration to be followed reasonably well. The final integration time step ((0.14-.004)/68 = 0.002 sec) is based on ≈ 1/60 of the period to produce sufficient printout for the theoretical comparison. The final time of 0.14 sec allows slightly more than 1 cycle of vibration to be followed. POST26 is used to extract results from the solution phase.

Results Comparison

	Target	ANSYS[1]	Ratio
y_{max}, in	0.806	0.804	0.998
Time, sec	0.0669	0.0680	1.016
y_{min}, in	0.438 [2]	0.438	0.999
Time, sec	0.122 [2]	0.122	1.000

1. ANSYS printout does not occur at theoretical time point given. Comparison (ratio) is therefore made with closest ANSYS time and theoretical time point given.
2. Based on graphical values.

Figure 80.2 Displacement vs. Time Display

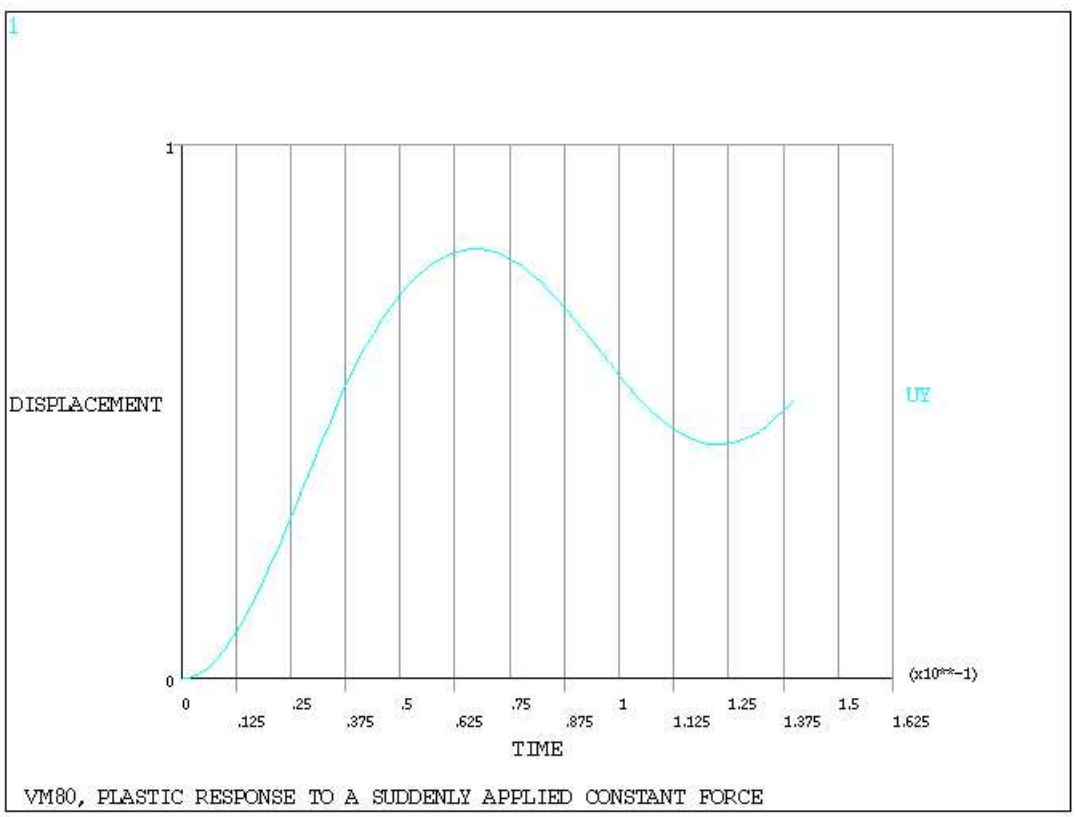

VM81: Transient Response of a Drop Container

Overview

Reference:	W. T. Thomson, *Vibration Theory and Applications*, 2nd Printing, Prentice-Hall, Inc., Englewood Cliffs, NJ, 1965, pg. 110, ex. 4.6-1.
Analysis Type(s):	Full Transient Dynamic Analysis (**ANTYPE** = 4) Reduced Transient Dynamic Analysis (**ANTYPE** = 4)
Element Type(s):	Combination Elements (COMBIN40) Structural Mass Elements (MASS21) Gap Condition (GP)
Input Listing:	vm81.dat

Test Case

A mass m is packaged in a rigid box, as shown below, and dropped through a height h. Determine the velocity and displacement y of the mass at impact and the maximum displacement of the mass. Assume that the mass of the box is large compared to that of the enclosed mass m and that the box remains in contact with the floor after impact.

Figure 81.1 Drop Container Problem Sketch

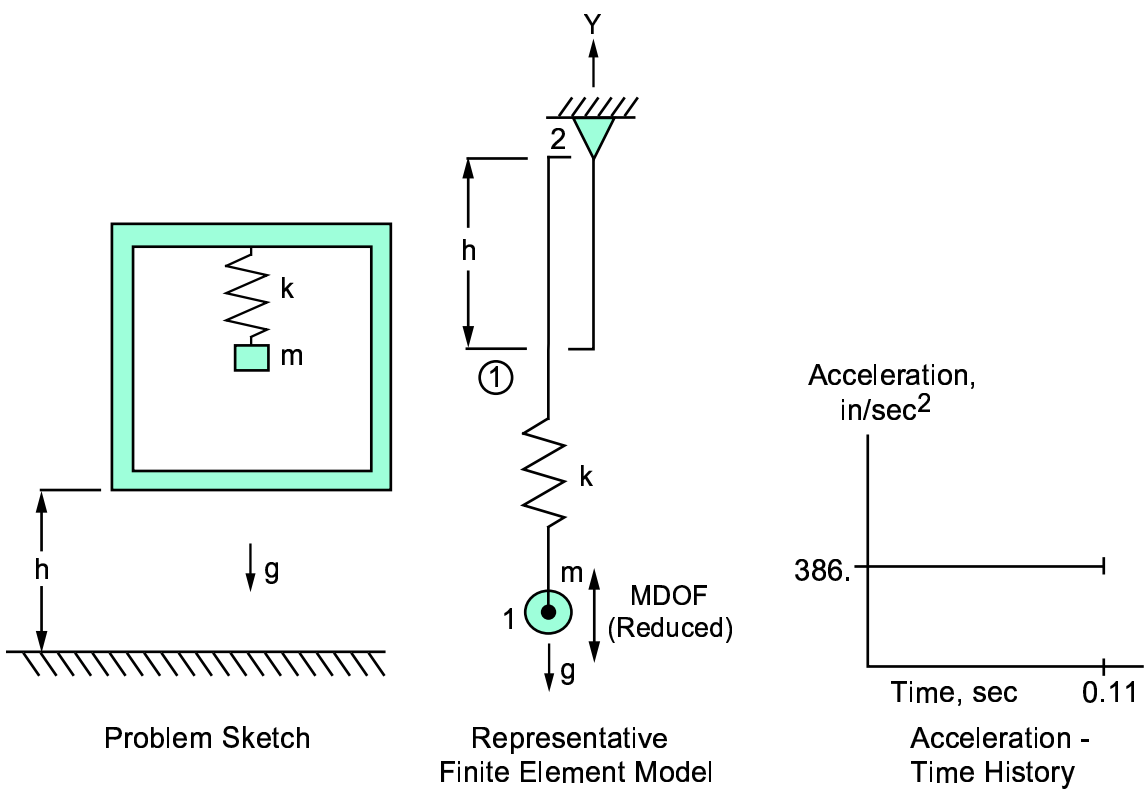

Material Properties	Geometric Properties	Loading
m = 0.5 lb-sec^2/in k = 1973.92 lb/in	h = 1 in	g = 386 in/sec^2

Analysis Assumptions and Modeling Notes

The node locations are arbitrarily selected. The final time of 0.11 sec allows the mass to reach its largest deflection. The integration time step (0.11/110 = 0.001 sec) is based on $\approx$ 1/100 of the period (during impact), to allow the initial step acceleration change to be followed reasonably well, and to produce sufficient printout for the theoretical comparison.

The problem is solved first using the full method in a nonlinear transient dynamic analysis and then using the reduced transient dynamic analysis. The COMBIN40 gap cannot be used in a reduced transient dynamic analysis and is replaced by a mass and a gap condition. One master degree of freedom is selected at the mass in the spring direction. POST26, the time-history postprocessor, is used to extract results from the solution phase.

Results Comparison

At Impact			
Full Transient Dynamic	**Target**	**ANSYS**	**Ratio[1]**
Time, sec	0.07198	0.072	1.000
y, in	-1.00	-1.0005	1.001
vel, in/sec	-27.79	-27.78	1.000
At zero velocity (theoretical y_{max} = -1.5506 in, at time = 0.100366 sec)			
Full Transient Dynamic	**Target[2]**	**ANSYS**	**Ratio**
t = 0.100 sec y, in	-1.5505	-1.5503	1.000
t = 0.101 sec y, in	-1.5502	-1.5502	1.000
At Impact			
Reduced Transient Dynamic	**Target**	**ANSYS**	**Ratio[1]**
Time, sec	0.07198	0.072	-
y, in	-1.00	-0.987	0.987
vel, in/sec	-27.79	-27.59	0.993
At zero velocity (theoretical y_{max} = -1.5506 in, at time = 0.100366 sec)			
Reduced Transient Dynamic	**Target[2]**	**ANSYS**	**Ratio**
t = 0.100 sec y, in	-1.5505	-1.5495	0.999
t = 0.101 sec y, in	-1.5502	-1.5503	1.000

1. ANSYS printout does not occur at theoretical time point given. Comparisons (ratios) of the nearest time results are made with the theoretical time point given.
2. Comparisons are made at the two time points bracketing the theoretical time of zero velocity.

VM82: Simply Supported Laminated Plate Under Pressure

Overview

Reference:	J. N. Reddy, "Exact Solutions of Moderately Thick Laminated Shells", *ASCE Journal Engineering Mechanics*, Vol. 110 No. 5, 1972, pg. 805.
Analysis Type(s):	Static Analysis (**ANTYPE** = 0)
Element Type(s):	Linear Layered Structural Shell Elements (SHELL99) 3-D 8-node Layered Structural Solid Elements (SOLID46)
Input Listing:	vm82.dat

Test Case

A simply-supported square cross-ply laminated plate is subjected to a uniform pressure p_o. The stacking sequence of the plies is symmetric about the middle plane. Determine the center deflection δ (Z-direction) of the plate due to the pressure load.

Figure 82.1 Simply Supported Laminated Plate Problem Sketch

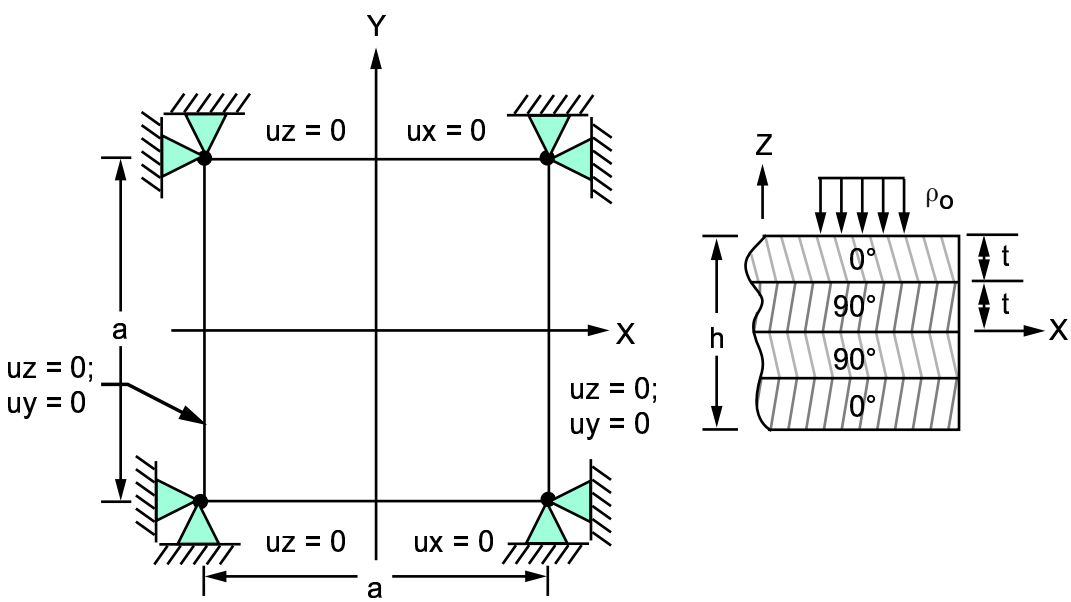

Problem Sketch

Material Properties	Geometric Properties	Loading
$E_x = 25 \times 10^6$ N/m^2 $E_y = 1 \times 10^6$ N/m^2 $\upsilon_{xy} = 0.25$ (Major Poisson's ratio) $G_{xy} = G = 0.5 \times 10^6$ N/m^2 $G_{yz} = 0.2 \times 10^6$ N/m^2	a = 10 m h = 0.1 m t = 0.025 m	$p_o = 1.0$ N/m^2

Analysis Assumptions and Modeling Notes

A quarter of the plate is modeled due to symmetry in geometry, material orientation, loading, and boundary conditions. Two models using SHELL99 and SOLID46 elements, respectively, are analyzed. Note that PRXY is used to directly input the major Poisson's ratio. EZ (explicitly input) is assumed to be equal to EY.

Results Comparison

	Target	ANSYS	Ratio
Deflection, m (SHELL99)	0.0683	0.0692	1.013
Deflection, m (SOLID46)	0.0683	0.0676	0.990
Deflection, m (SOLID191)	0.0683	0.0683	1.00

VM83: Impact of a Block on a Spring Scale

Overview

Reference:	F. P. Beer, E. R. Johnston, Jr., *Vector Mechanics for Engineers, Statics and Dynamics*, McGraw-Hill Book Co., Inc., New York, NY, 1962, pg. 531, problem 14.6.
Analysis Type(s):	Full Transient Dynamic Analysis (**ANTYPE** = 4)
Element Type(s):	Combination Elements (COMBIN40)
Input Listing:	vm83.dat

Test Case

A block of weight W_B is dropped from a height h onto a spring scale pan of weight W_P. Determine the maximum deflection δ of the pan and the maximum fall of the block y. Assume the impact to be perfectly plastic as a theoretical approximation.

Figure 83.1 Spring Scale Problem Sketch

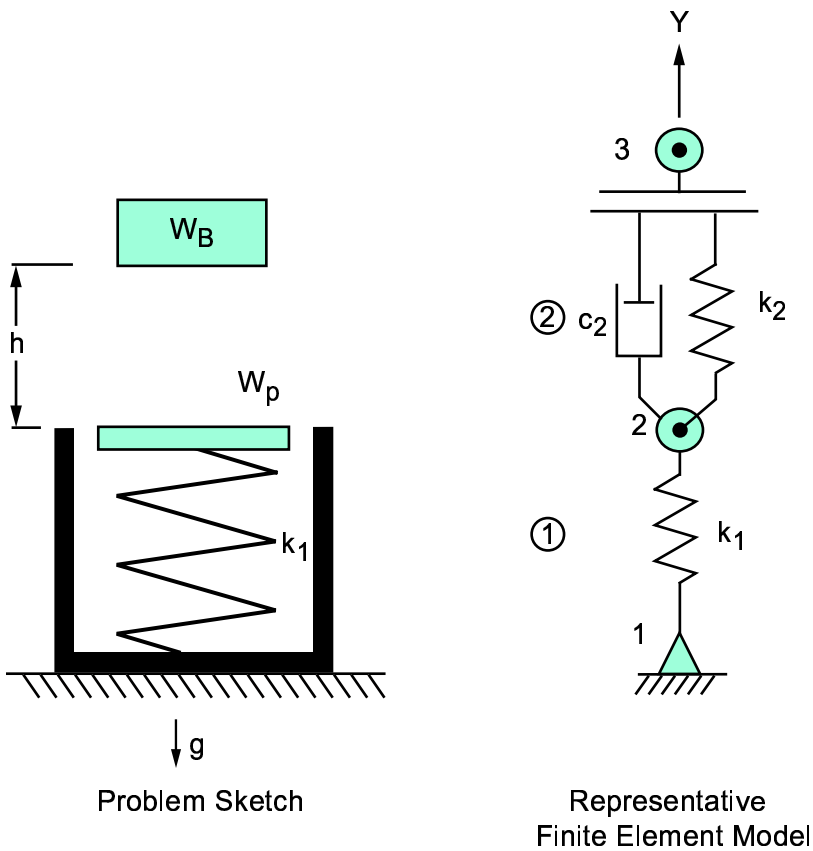

Material Properties	Geometric Properties	Loading
k_1 = 100 lb/in W_B = 50 lb W_P = 25 lb	h = 6 ft = 72 in	g = 386 in/sec^2

Analysis Assumptions and Modeling Notes

The mass of the block (m_B) and the mass of the pan (m_P) are calculated as $m_B = W_B/g = (50/386)$ lb-sec^2/in and $m_P = W_P/g = (25/386)$ lb-sec^2/in respectively. Deflection of the pan due to gravity is $W_P/k_1 = 0.25$ in, hence the initial gap becomes (72-0.25) = 71.75 inches.

The spring length is chosen arbitrarily. The closed-gap spring constant (k_2 = 10,000 lb/in) is arbitrarily selected high enough to minimize the elastic contact effect but low enough to also allow a practical integration time step size. The integration time step (0.0005 sec) is based on < 1/30 of the period of the contact spring to minimize the numerical damping effect, and to allow the acceleration change to be followed reasonably well.

Automatic time stepping is used to reduce the total number of iterations needed to solve the problem. A static solution is done at the first load step to produce the initial pan condition before the start of the transient analysis. The maximum time of 0.7 sec allows the pan to reach its largest deflection.

To model the "plastic impact" a damper (C_2) is used which has the value of critical damping to prevent oscillation of the contact spring. Also, the two masses are locked together after initial contact by use of KEYOPT(1) = 1 on combination element type 1 (COMBIN40). Natural frequency of the closed gap is $f_2 = \text{sqrt}(k_2 m_p)/(2\pi) = 62.54$ Hz. Critical damping is calculated as $C_2 = k_2/\pi f_2 = 10000 / (62.54\pi) = 50.90$ lb-sec/in. POST26 is used to extract results from the solution phase.

Results Comparison

Time = 0.689 sec	Target	ANSYS	Ratio
Deflection, in	-7.7000	-7.612	0.989
y, in	-79.450[1]	-79.41	1.000

1. Based on a perfectly plastic analytical solution.

Figure 83.2 Displacements of Block and Pan

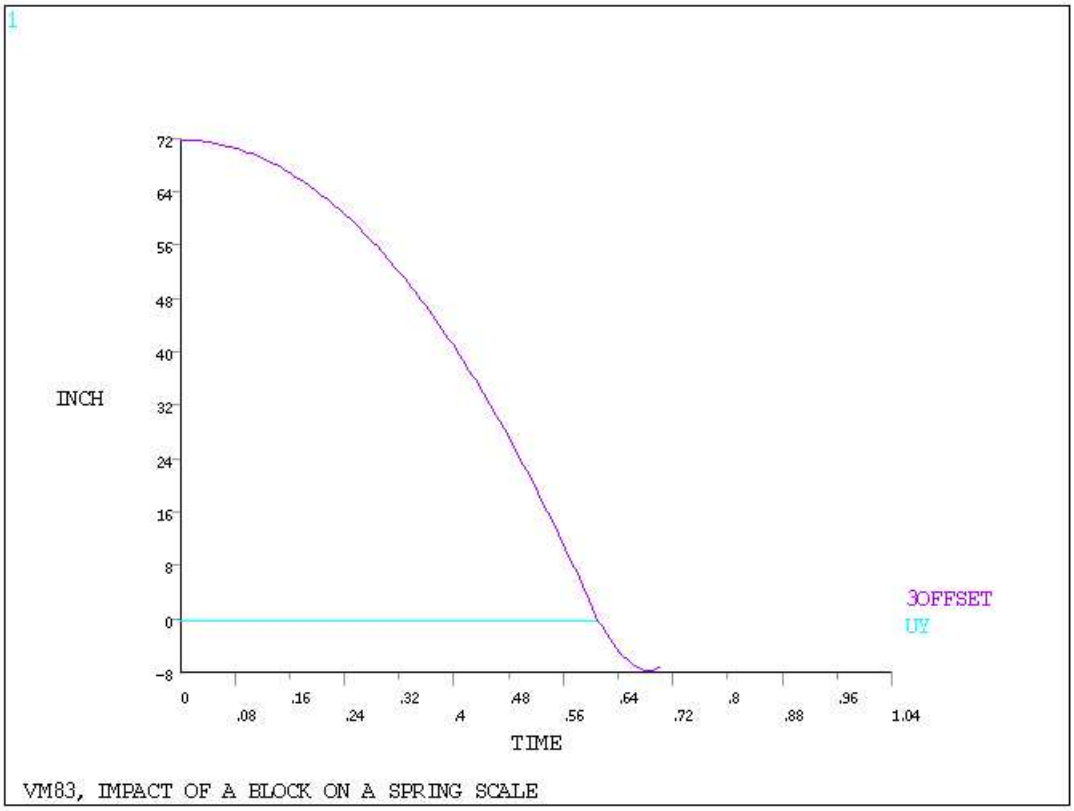

VM84: Displacement Propagation Along a Bar with Free Ends

Overview

Reference:	S. Timoshenko, D. H. Young, *Vibration Problems in Engineering*, 3rd Edition, D. Van Nostrand Co., Inc., New York, NY, 1955, pg. 311, problem 2.
Analysis Type(s):	Reduced Transient Dynamic Analysis (**ANTYPE** = 4)
Element Type(s):	2-D Spar (or Truss) Elements (LINK1)
Input Listing:	vm84.dat

Test Case

A drill stem is a steel bar 4000 ft long. Considering it as a bar with free ends, find the displacement δ of the end ($x = \ell$) at $t = \tau/2$ produced by a force F_1 suddenly applied to this end.

Figure 84.1 Bar with Free Ends Problem Sketch

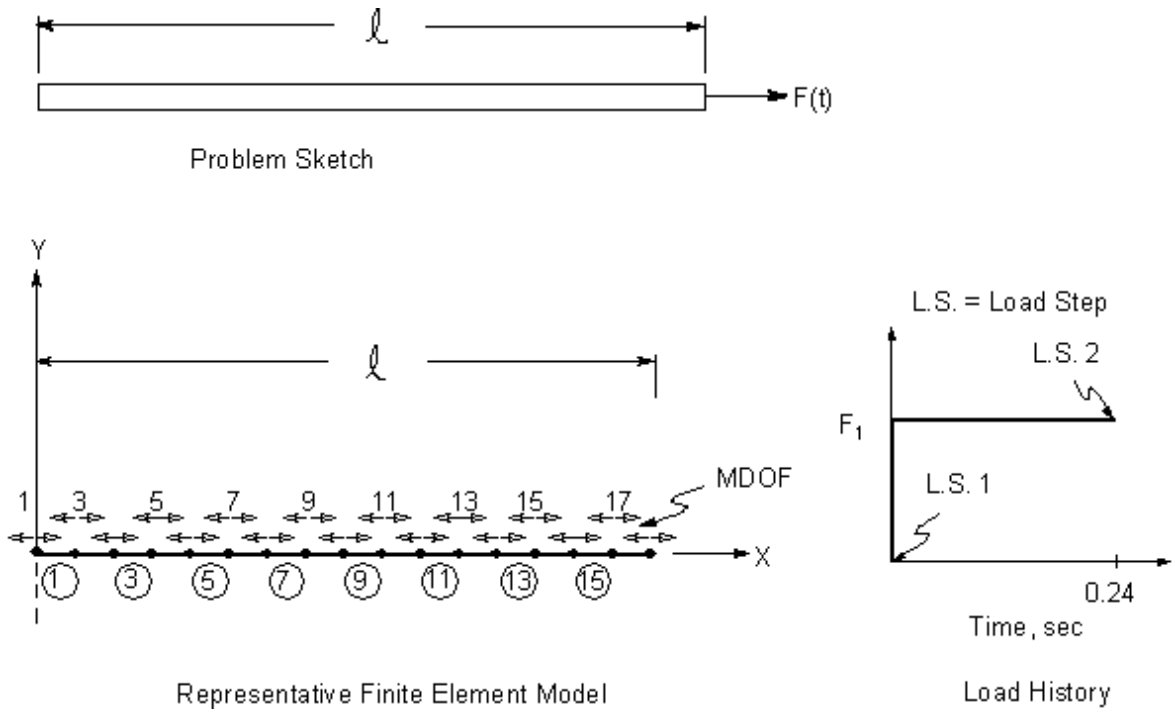

Material Properties	**Geometric Properties**	**Loading**
$E = 30 \times 10^6$ psi $\gamma = 0.278$ lb/in^3 $\rho = \gamma / g = 0.0007202$ lb-sec^2/in^4	$A = 2$ in^2 $g = 386$ in/sec^2 $\ell = 4000 \times 12 = 48{,}000$ in	$F_1 = 6000$ lb (see load history in Figure 84.1: "Bar with Free Ends Problem Sketch")

Analysis Assumptions and Modeling Notes

A static solution is done at the first load step. The fundamental period of vibration (τ) is 0.47937 sec. The final time of 0.24 sec includes 1/2 of the fundamental period of vibration. All longitudinal master degrees of freedom (MDOF) are selected along the length of the bar. The integration time step (0.005 sec) is based on $\approx$ 1/10 of the

shortest period, to allow the initial step change in acceleration to be followed reasonably well, and to produce sufficient printout for the theoretical comparison. POST26 is used to extract results from the solution phase.

Results Comparison

	Target	ANSYS	Ratio
Displacement, in[1]	4.8000	4.8404	1.008

1. Target results are for t = 0.23969 sec (t/2). ANSYS results are reported from the closest time point, t = 0.240 sec.

Figure 84.2 Displacement vs. Time Graph

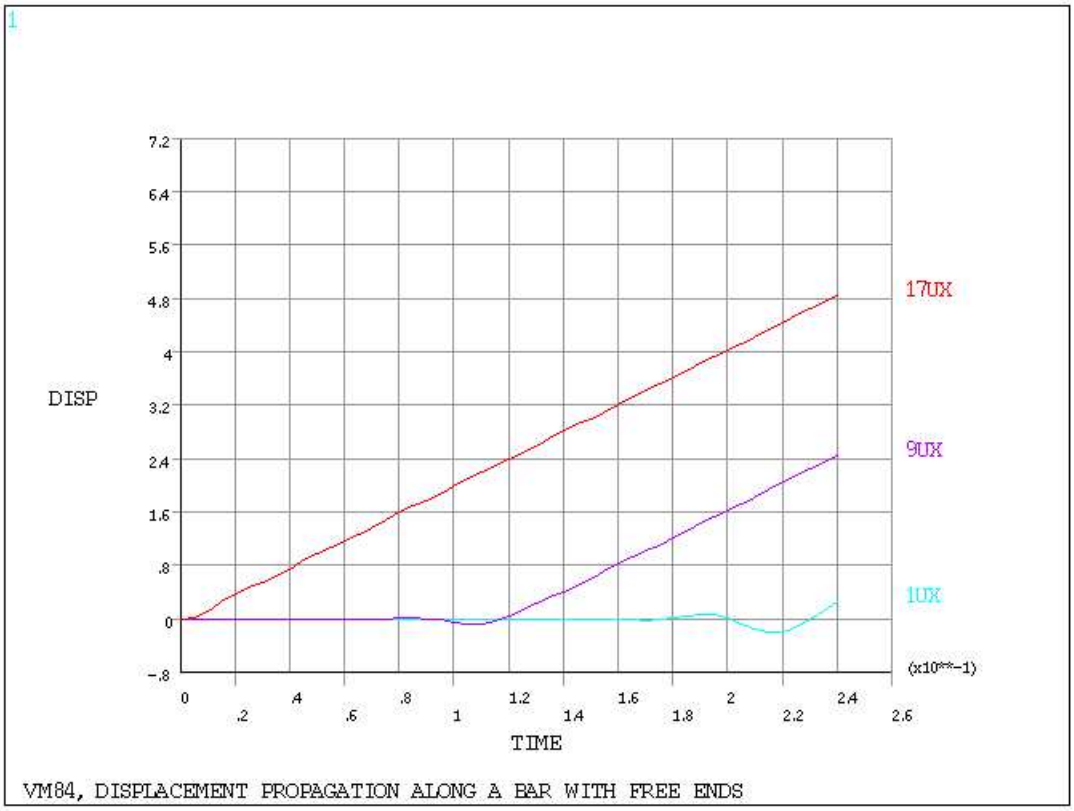

Figure 84.3 Velocity vs. Time Graph

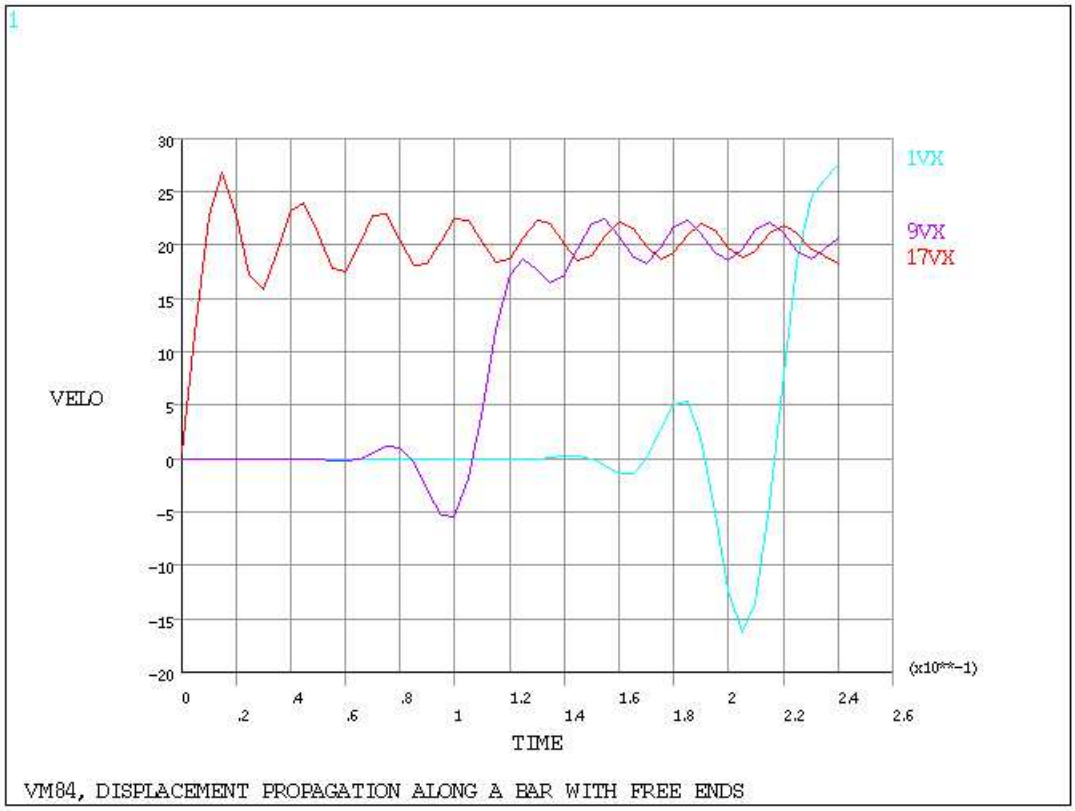

VM85: Transient Displacements in a Suddenly Stopped Moving Bar

Overview

Reference:	S. Timoshenko, D. H. Young, *Vibration Problems in Engineering*, 3rd Edition, D. Van Nostrand Co., Inc., New York, NY, 1955, pg. 305, problem 3.
Analysis Type(s):	Reduced Transient Dynamic Analysis (**ANTYPE** = 5)
Element Type(s):	2-D Spar (or Truss) Elements (LINK1) Gap Condition (GP)
Input Listing:	vm85.dat

Test Case

A steel bar moving along the X-axis with a constant velocity v_o is suddenly stopped at the end X = 0. Determine the displacement δ at the free end and the axial stress σ_x near the stopped end of the bar at time $t_1 = \ell/a$, where a is the speed of sound in the bar.

Figure 85.1 Moving Bar Problem Sketch

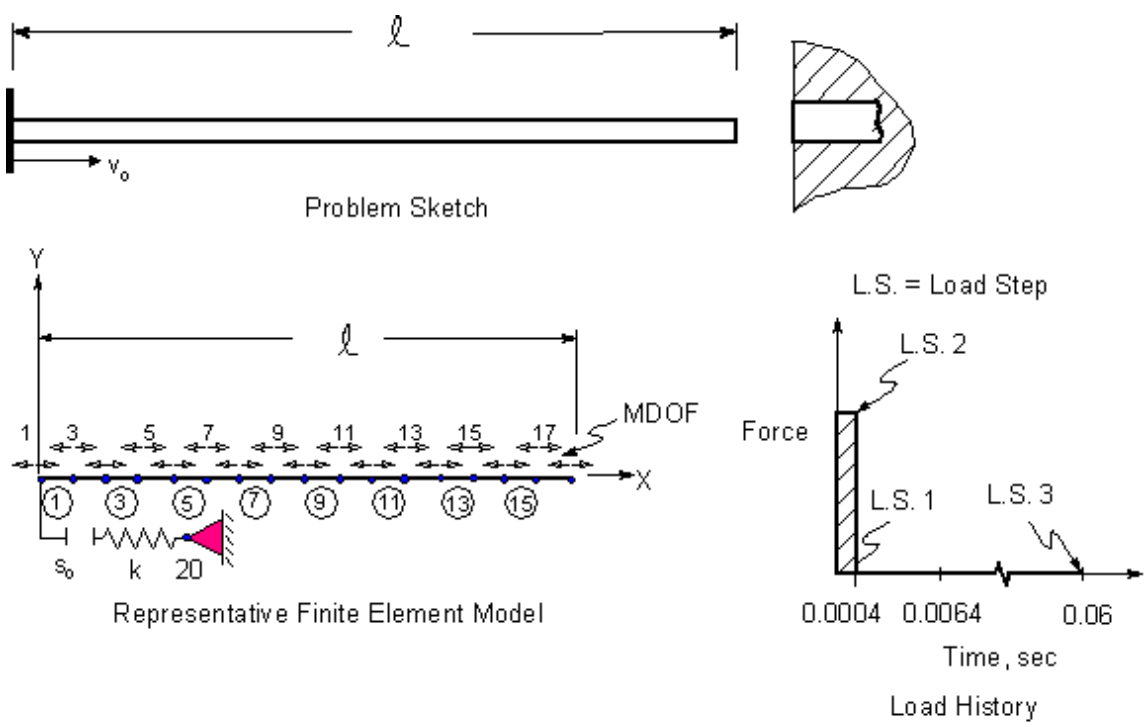

Material Properties	Geometric Properties	Loading
$E = 30 \times 10^6$ psi $r = 0.00073$ lb-sec^2/in^4	$\ell = 10000$ in $A = 1$ in^2 $s_o = 0.64$ in	$v_o = 100$ in/sec

Analysis Assumptions and Modeling Notes

The speed of sound in the bar is $a = \sqrt{E/g}$ = 202,721 in/sec, hence time $t_1 = \ell/a$ = 0.0493288 sec. A static solution is done at the first load step. The final time of 0.06 sec allows the bar to impact (at t_o = 0.0064 sec) and reach its maximum deflection (at $t = t_o + t_1$). The gap stiffness (k = 30,000,000 lb/in) is arbitrarily selected high enough to minimize the elastic contact deformation but low enough to also allow a practical integration time step size.

Seventeen longitudinal master degrees of freedom (MDOF) are selected along the length of the bar. The integration time step size (ITS = 0.0001 sec) is based on the shortest period (during contact) to allow the abrupt changes in acceleration to be followed reasonably well, and to produce sufficient printout for the theoretical comparison.

The initial velocity is produced by a force = $v_o \rho A \ell$ / ITS = 1,825,000 lb acting over 4 ITS and distributed among the MDOF. A "coasting" period of 60 ITS is allowed before the gap (s_o = 0.64 in) closes at impact. An expansion pass is done at $t = t_o + t_1$ to obtain the stress solution. POST26 is used to get the displacement solution and displays versus time.

Results Comparison

		Target[1]	ANSYS[2]	Ratio
Reduced Transient Dynamic	d, in (t = 0.05573 sec)	4.9329	-	-
	d, in (t = 0.0544 sec)	-	4.7734[3]	0.968
	d, in (t = 0.0557 sec)	-	4.7474[4]	0.962
Expansion Pass	$stress_x$, psi (t = 0.05573 sec)	14799.	-	-
	$stress_x$, psi (t = 0.0557 sec)	-	14820.[5]	1.001

- t is time before contact (0.0064 sec) included.
- d is relative displacement between the ends of the bar.

1. Assumes an infinitely rigid stop.
2. Uses a high, but finite stiffness for the stop.
3. Peak displacement.
4. Displacement at the time closest to the theoretical time point given.
5. From Element 1.

Figure 85.2 Displacements at Center and Ends of Bar

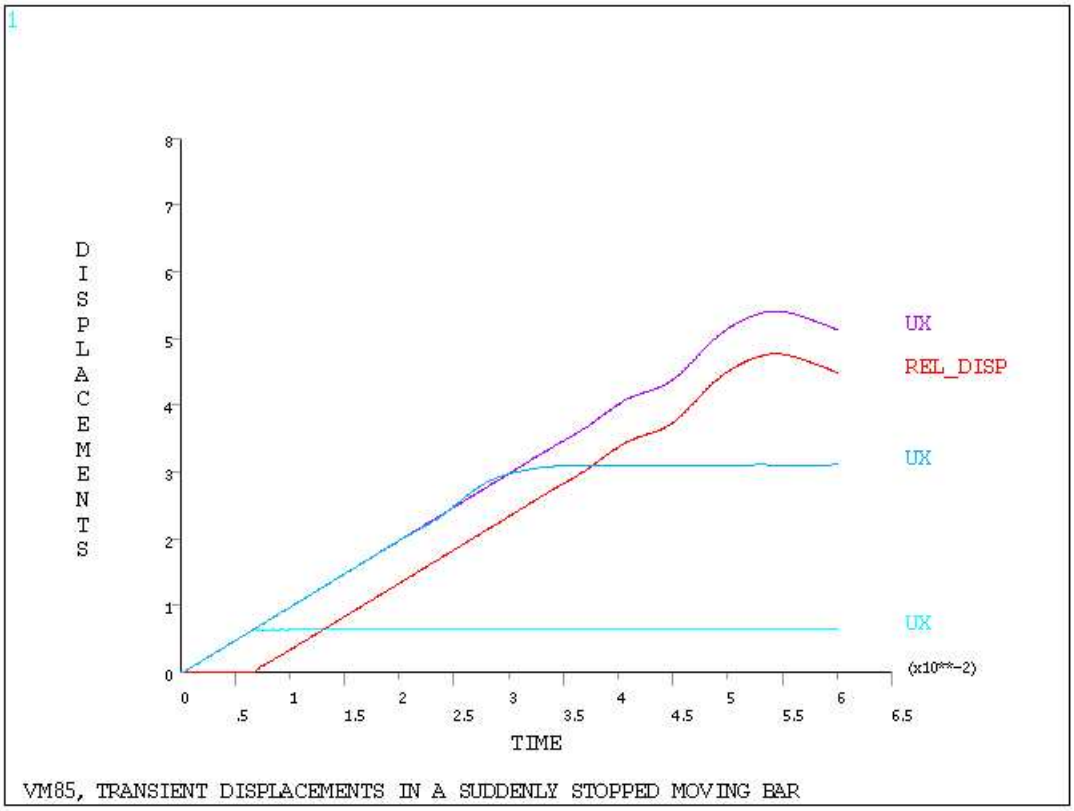

Figure 85.3 Velocities at Center and Ends of Bar

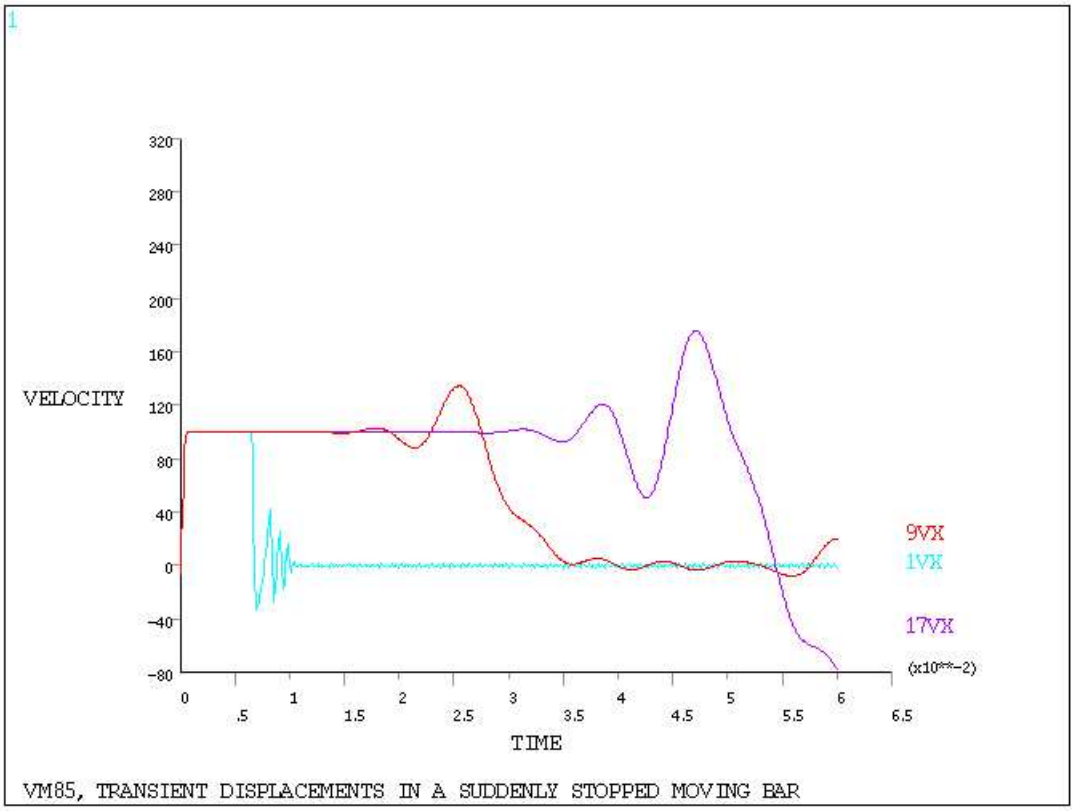

VM86: Harmonic Response of a Dynamic System

Overview

Reference:	W. T. Thomson, *Vibration Theory and Applications*, 2nd Printing, Prentice-Hall, Inc., Englewood Cliffs, NJ, 1965, pg. 56, ex. 3.1-2.
Analysis Type(s):	Reduced Harmonic Response Analysis (**ANTYPE** = 3)
Element Type(s):	Combination Elements (COMBIN40)
Input Listing:	vm86.dat

Test Case

A machine of weight W is supported on springs of total stiffness k. If a harmonic disturbing force of magnitude F_1 and frequency f (equal to the natural frequency of the machine, f_n) acts on the machine, determine the displacement response in terms of the peak amplitude A_o and phase angle Φ. Assume a viscous damping coefficient c.

Figure 86.1 Dynamic System Problem Sketch

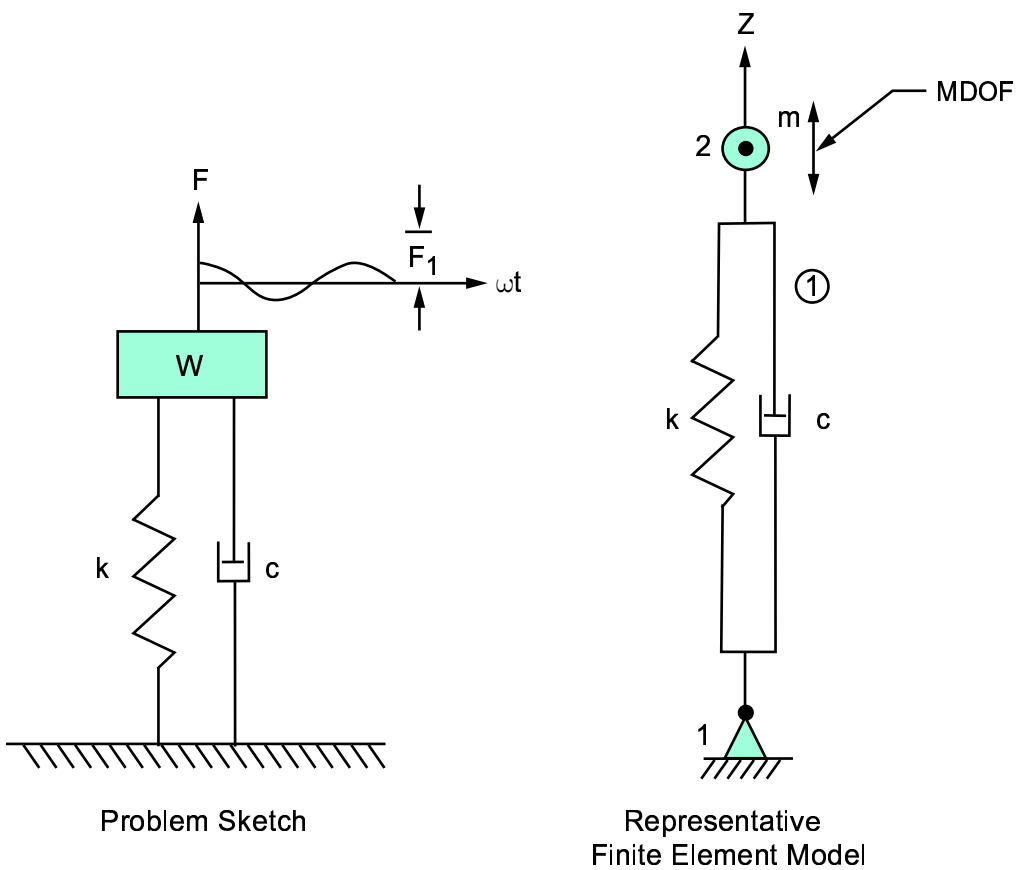

Material Properties	**Loading**
W = 193 lb k = 200 lb/in c = 6 lb-sec/in	g = 386 in/sec^2 F_1 = 10 lb

Analysis Assumptions and Modeling Notes

The mass of the machine is m = W/g = 0.5 lb-sec^2/in. Hence the frequency of the disturbing force (f) becomes f = f_n = sqrt(km)/2π = 3.1831 Hz. The node locations are arbitrarily selected. One master degree of freedom is selected at the mass in the force direction.

Results Comparison

	Target	ANSYS	Ratio
A_o, in	0.0833	0.0833	1.000
angle, deg	-90.0	-90.0	1.000

VM87: Equivalent Structural Damping

Overview

Reference:	W. T. Thomson, *Vibration Theory and Applications*, 2nd Printing, Prentice-Hall, Inc., Englewood Cliffs, NJ, 1965, pg. 72, article 3.9 and pg. 56, ex. 3.1-2.
Analysis Type(s):	Reduced Harmonic Response Analysis (**ANTYPE** = 3)
Element Type(s):	Combination Elements (COMBIN40)
Input Listing:	vm87.dat

Test Case

Test case description is the same as that for VM86 except for the assumption on damping. Assume that all damping is in the form of equivalent structural damping and there is no element damping.

Figure 87.1 Structural Damping Problem Sketch

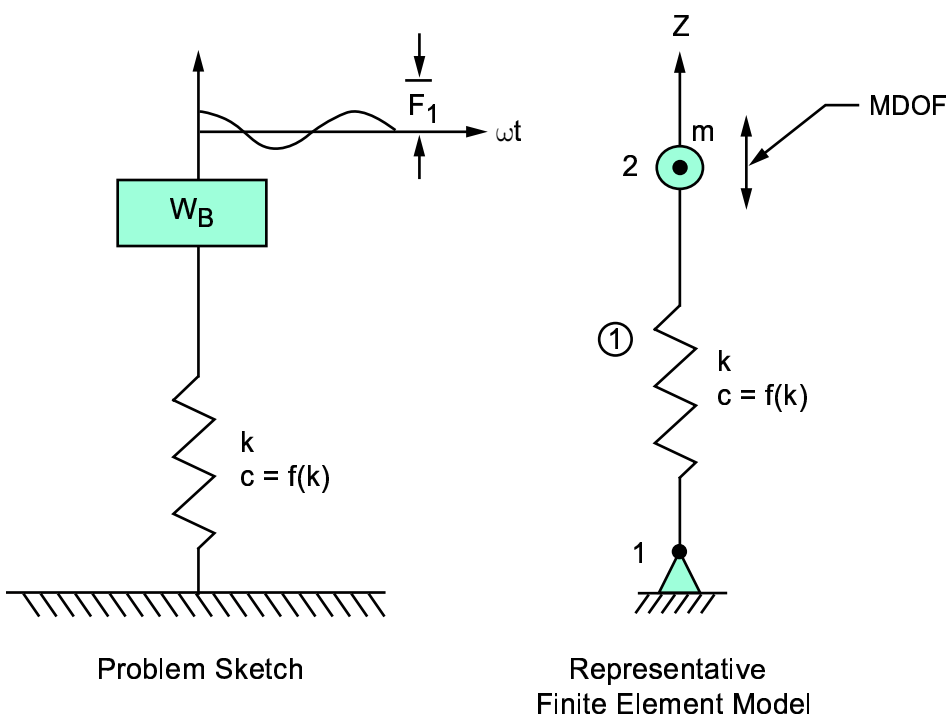

Analysis Assumptions and Modeling Notes

The structural damping factor is $\gamma = 2\,\xi\,\omega/\omega_n$ where ξ is the damping ratio and is equal to $c/2m\,\omega_n$. Therefore, $\gamma = c/(m\,\omega_n) = 6/(0.5 \times 20) = 0.6$ since $\omega = \omega_n$. The frequency-dependent multiplier β is calculated as $\beta = 2\,\xi/\omega_n = \gamma/\omega = 0.6/20 = 0.03$ seconds. The node locations are arbitrarily selected. One master degree of freedom (MDOF) is selected at the mass in the force direction.

Results Comparison

	Target	ANSYS	Ratio
Amp, in	0.083333	0.083333	1.000

	Target	ANSYS	Ratio
angle, deg	-90.000	-90.000	1.000

VM88: Response of an Eccentric Weight Exciter

Overview

Reference:	W. T. Thomson, *Vibration Theory and Applications*, 2nd Printing, Prentice-Hall, Inc., Englewood Cliffs, NJ, 1965, pg. 60, ex. 3.3-1.
Analysis Type(s):	Reduced Harmonic Response Analysis (**ANTYPE** = 3)
Element Type(s):	Combination Elements (COMBIN40)
Input Listing:	vm88.dat

Test Case

A counter-rotating eccentric weight exciter of mass m having a mass unbalance m_u on an eccentricity e is used to produce forced oscillation of a spring-supported mass. For a viscous damping factor c, determine the amplitude and phase angle Φ of the displacement response when the rotating frequency f is (1) the resonant frequency f_n, and (2) $f >> f_n$.

Figure 88.1 Eccentric Weight Exciter Problem Sketch

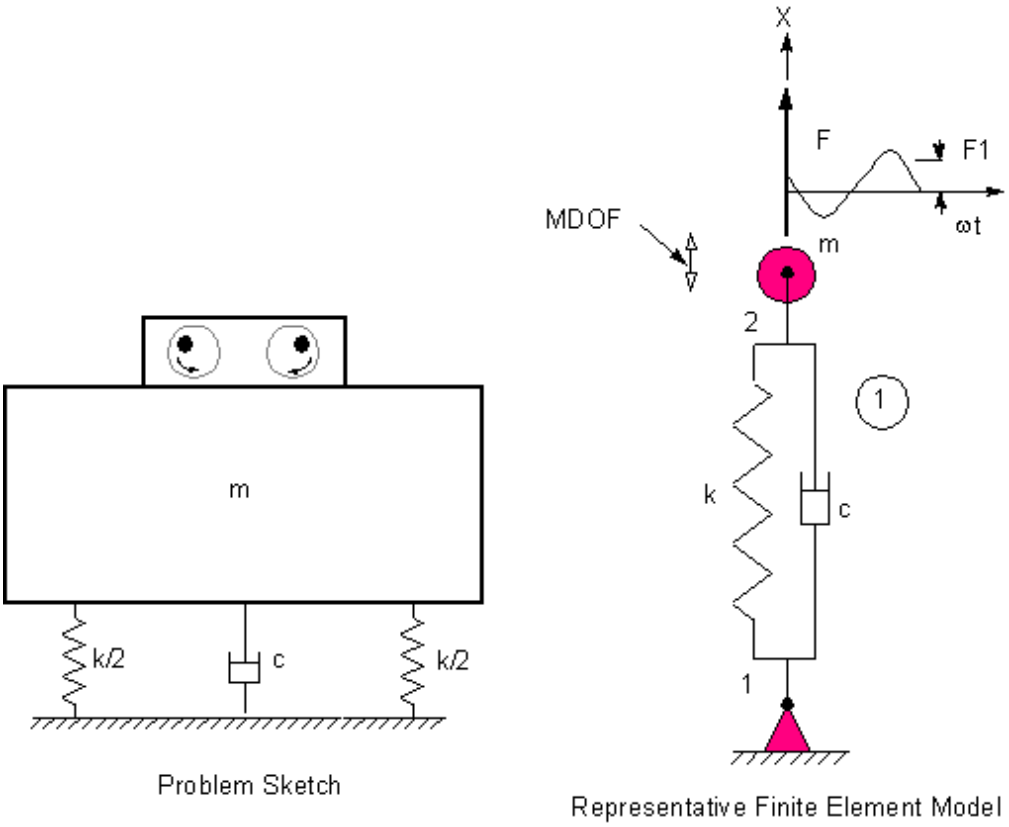

Material Properties

m = 0.02590673 lb-sec^2/in
c = 0.11754533 lb-sec/in
m_u = 0.08 x m
k = 30 lb/in

Analysis Assumptions and Modeling Notes

The node locations are arbitrarily selected. When the rotating frequency f is equal to the resonant frequency f_n, the force $F_1 = m_u\omega^2 = 2.4$ lb where $\omega = \omega_n$ = sqrt(k/m) = 34.0294 rad/sec is the resonant circular frequency. When f >> f_n, it is assumed that f = 100 f_n = 541.5947 Hz and the corresponding force F_1 = 24000 lb.

Results Comparison

		Target	ANSYS	Ratio
f = f_n	Amp, in	0.60000	0.60000	1.000
	angle, deg	-90.000	-90.000	1.000
f =100 f_n	Amp, in	0.080000[1]	0.080008	1.000
	angle, deg	-180.00	-179.92	1.000

1. Based on f = ∞

VM89: Natural Frequencies of a Two-mass-spring System

Overview

Reference:	W. T. Thomson, *Vibration Theory and Applications*, 2nd Printing, Prentice-Hall, Inc., Englewood Cliffs, NJ, 1965, pg. 163, ex. 6.2-2.
Analysis Type(s):	Mode-frequency Analysis (**ANTYPE** = 2)
Element Type(s):	Spring-Damper Elements (COMBIN14) Structural Mass Elements (MASS21)
Input Listing:	vm89.dat

Test Case

Determine the normal modes and natural frequencies of the system shown below for the values of the masses and spring stiffnesses given.

Figure 89.1 Two-mass-spring System Problem Sketch

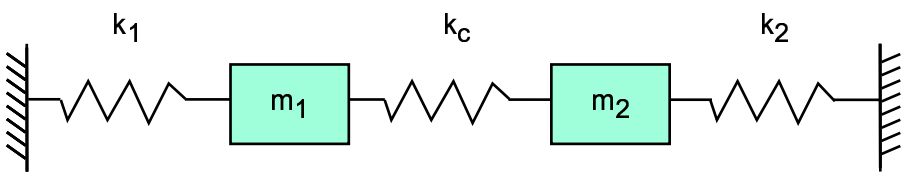

Problem Sketch

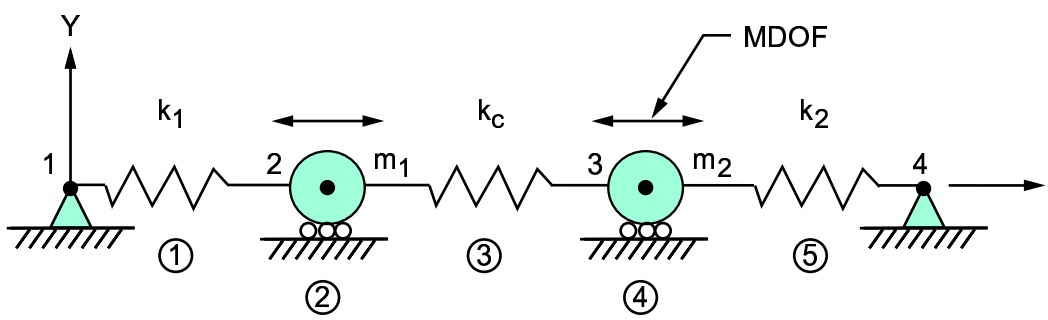

Representative Finite Element Model

Material Properties

$m_2 = 2m_1 = 1.0$ lb-sec^2/in

$k_2 = k_1 = 200$ lb/in

$k_c = 4k_1 = 800$ lb/in

Analysis Assumptions and Modeling Notes

The spring lengths are arbitrarily selected and are used only to define the spring direction. Two master degrees of freedom (MDOF) are selected at the masses in the spring direction.

Results Comparison

	Target[1]	ANSYS	Ratio
f_1, Hz	2.5814	2.5814	1.000
f_2, Hz	8.3263	8.3263	1.000
$(A1/A2)_1$[2]	0.92116	0.92116	1.000
$(A1/A2)_2$[2]	-2.1711	-2.1712	1.000

1. Solution Recalculated
2. Normal Modes (UX of node 2 / UX of node 3)

ANSYS Verification Manual . ANSYS Release 10.0 . 002184 . © SAS IP, Inc.

VM90: Harmonic Response of a Two-Mass-Spring System

Overview

Reference:	W. T. Thomson, *Vibration Theory and Applications*, 2nd Printing, Prentice-Hall, Inc., Englewood Cliffs, NJ, 1965, pg. 178, ex. 6.6-1.
Analysis Type(s):	Reduced Harmonic Response Analysis (**ANTYPE** = 3)
Element Type(s):	Spring-Damper Elements (COMBIN14) Structural Mass Elements (MASS21)
Input Listing:	vm90.dat

Test Case

Determine the response amplitude (X_i) and phase angle (Φ_i) for each mass (m_i) of the system in Figure 90.1: "Two-mass-spring System Problem Sketch" when excited by a harmonic force ($F_1 \sin \omega t$) acting on mass m_1.

Figure 90.1 Two-mass-spring System Problem Sketch

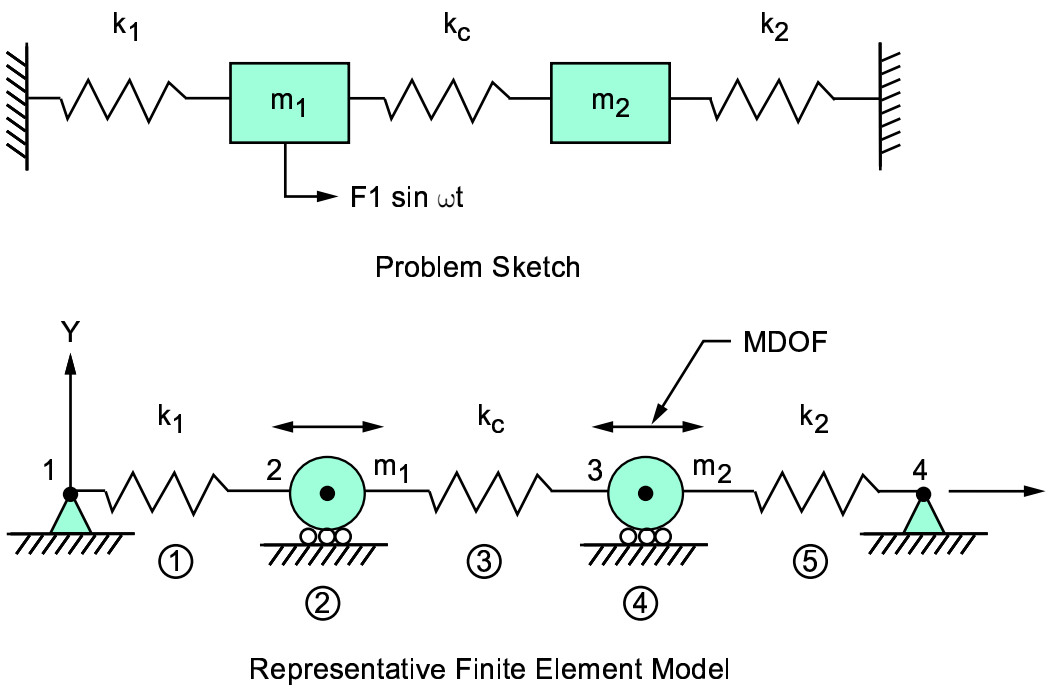

Material Properties	**Loading**
$m_1 = m_2 = 0.5$ lb-sec^2/in $k_1 = k_2 = k_c = 200$ lb/in	$F_1 = 200$ lb

Analysis Assumptions and Modeling Notes

The spring lengths are arbitrarily selected and are used only to define the spring direction. Two master degrees of freedom (MDOF) are selected at the masses in the spring direction. A frequency range from zero to 7.5 Hz with a solution at 7.5/30 = 0.25 Hz intervals is chosen to give an adequate response curve. POST26 is used to get an amplitude versus frequency display.

Results Comparison

	Target	ANSYS	Ratio
X_1 , in (f = 1.5 Hz)[1]	0.82272	0.82272	1.000
$Angle_1$, deg (f = 1.5 Hz)	0.0000	0.0000	-
X_2 , in (f = 1.5 Hz)[1]	0.46274	0.46274	1.000
$Angle_2$, deg (f = 1.5 Hz)	0.000	0.0000	-
X_1 , in (f = 4.0 Hz)	0.51145	0.51146	1.000
$Angle_1$, deg (f = 4.0 Hz)	180.00	180.00	1.000
X_2 , in (f = 4.0 Hz)	1.2153	1.2153	1.000
$Angle_2$, deg (f = 4.0 Hz)	180.00	180.00	1.000
X_1 , in (f = 6.5 Hz)	0.58513	0.58512	1.000
$Angle_1$, deg (f = 6.5 Hz)	180.00	180.00	1.000
X_2 , in (f = 6.5 Hz)	0.26966	0.26965	1.000
$Angle_2$, deg (f = 6.5 Hz)	0.0000	0.0000	-

1. X_1 = UX @ m_1 (node 2) X_2 = UX @ m_2 (node 3)

Figure 90.2 Amplitude vs. Frequency

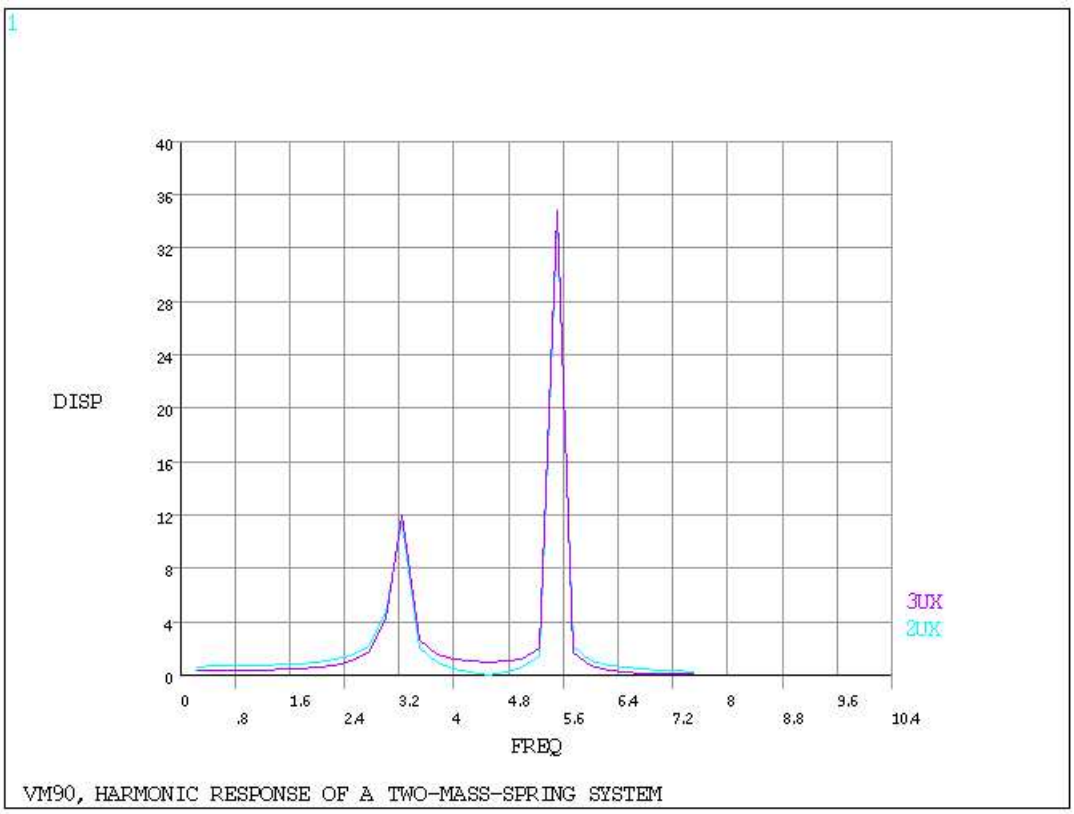

VM91: Large Rotation of a Swinging Pendulum

Overview

Reference:	W. T. Thomson, *Vibration Theory and Applications*, 2nd Printing, Prentice-Hall, Inc., Englewood Cliffs, NJ, 1965, pg. 138, ex. 5.4-1.
Analysis Type(s):	Full Transient Dynamic Analysis (**ANTYPE** = 4)
Element Type(s):	3-D Spar (or Truss) Elements (LINK8) Structural Mass Element (MASS21)
Input Listing:	vm91.dat

Test Case

A pendulum consists of a mass m supported by a rod of length ℓ and cross-sectional area A. Determine the motion of the pendulum in terms of the displacement of the mass from its initial position Θ_o in the x and y directions, δ_x and δ_y, respectively. The pendulum starts with zero initial velocity.

Figure 91.1 Pendulum Swing Problem Sketch

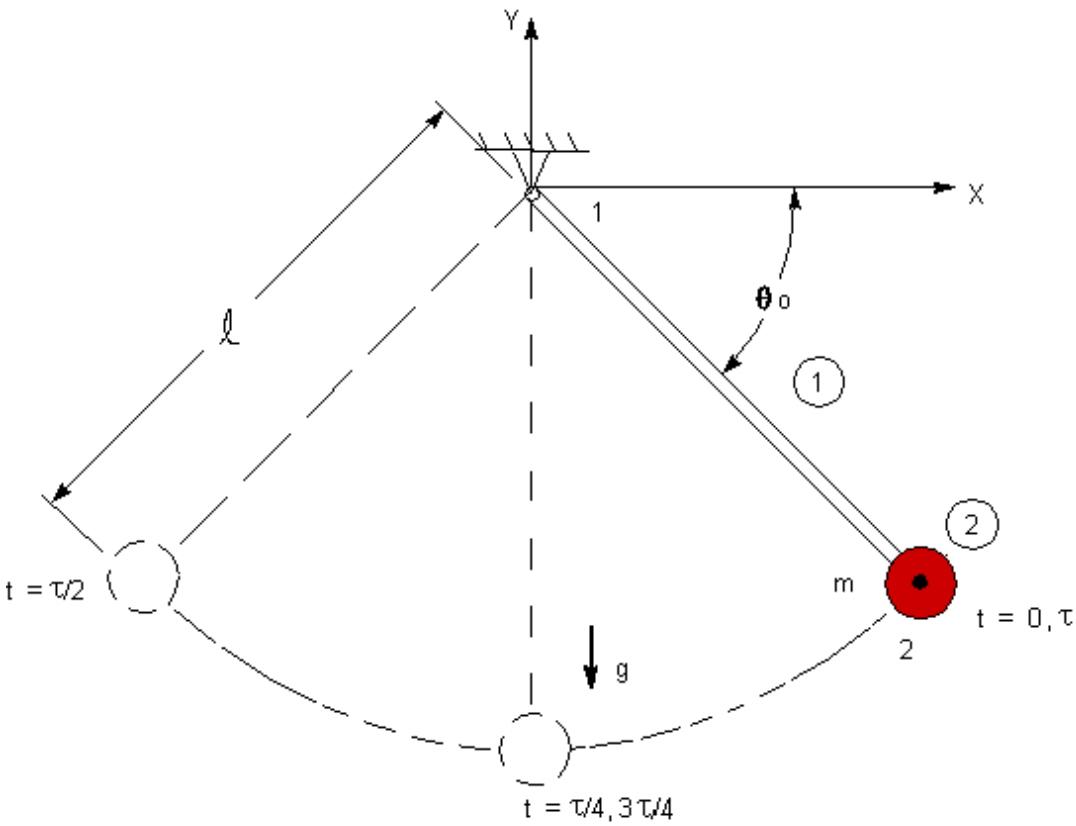

Problem Model

Material Properties	Geometric Properties	Loading
$E = 30 \times 10^6$ psi $m = 0.5$ lb-sec^2/in	$\ell = 100$ in $\Theta_o = 53.135$ $A = 0.1$ in^2	$g = 386$ in/sec^2

Analysis Assumptions and Modeling Notes

A large deflection solution is required. An initial time step is defined over a small time increment (.01/5 = .002 sec) to allow an initial step change in acceleration to be attained. Subsequent integration time steps (1.64142/8 = .205 sec) are based on $\approx$ 1/24 of the period to allow the initial step change in acceleration to be followed reasonably well.

Several load steps are defined for clearer comparison with theoretical results. POST26 is used to process results from the solution phase.

Results Comparison

	Target	ANSYS	Ratio
Deflection$_x$, in(t=period/4)	-60.000	-59.244	0.987
Deflection$_y$, in(t=period/4)	-20.000	-20.004	1.000
Deflection$_x$, in(t=period/2)	-120.00	-119.82	0.999
Deflection$_y$, in(t=period/2)	0.0000	-0.1315	-
Deflection$_x$, in(t=3period/4)	-60.000	-61.871	1.031
Deflection$_y$, in(t=3period/4)	-20.000	-19.993	0.999
Deflection$_x$, in(t=period)	0.0000	-0.0772	-
Deflection$_y$, in(t=period)	0.0000	-0.0682	-
Deflection$_x$, in(t=period/4)	-60.000	-59.372	0.990
Deflection$_y$, in(t=period/4)	-20.000	-20.004	1.000
Deflection$_x$, in(t=period/2)	-120.00	-119.91	0.999
Deflection$_y$, in(t=period/2)	0.0000	-0.0643	0.000
Deflection$_x$, in(t=3period/4)	-60.000	-61.811	1.030
Deflection$_y$, in(t=3period/4)	-20.000	-19.991	1.000
Deflection$_x$, in(t=period)	0.0000	-0.2200	0.000
Deflection$_y$, in(t=period)	0.0000	-0.1749	0.000

ANSYS Verification Manual . ANSYS Release 10.0 . 002184 . © SAS IP, Inc.

Figure 91.2 Pendulum Swing

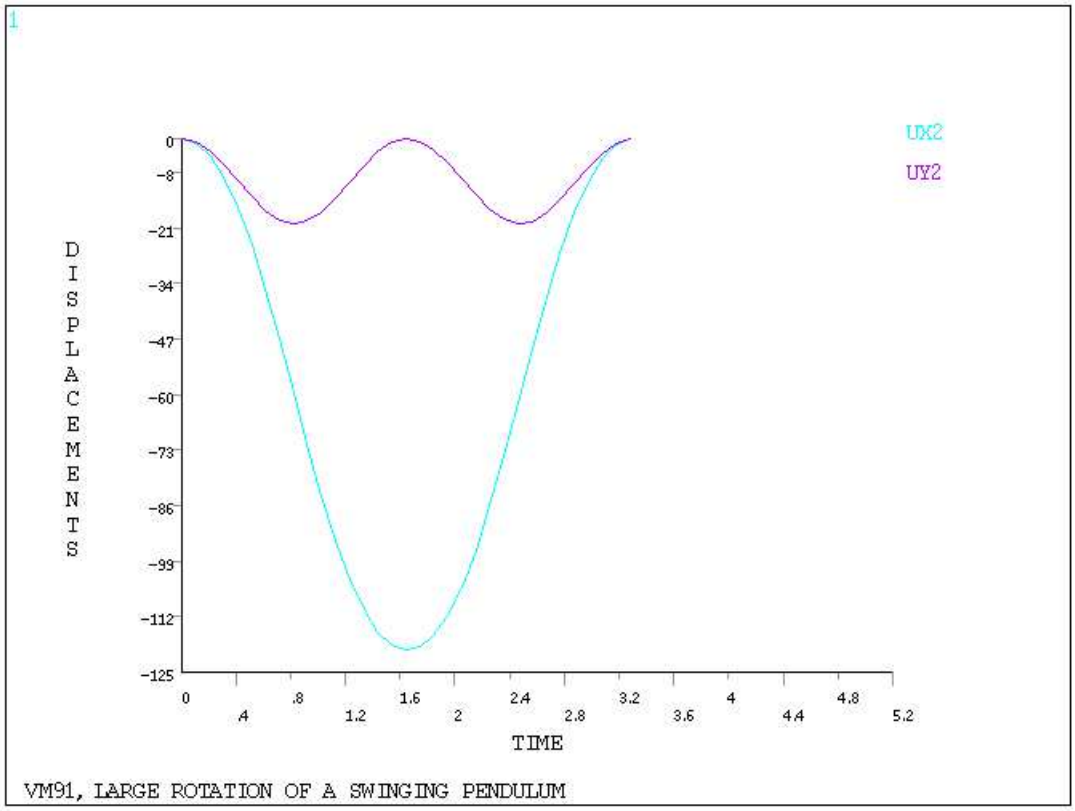

VM92: Insulated Wall Temperature

Overview

Reference:	F. Kreith, *Principles of Heat Transfer*, 2nd Printing, International Textbook Co., Scranton, PA, 1959, pg. 32, ex. 2-5.
Analysis Type(s):	Thermal Analysis (**ANTYPE** = 0)
Element Type(s):	Convection Link Elements (LINK34) 2-D Conduction Bar Elements (LINK32)
Input Listing:	vm92.dat

Test Case

A furnace wall consists of two layers, firebrick and insulating brick. The temperature inside the furnace is T_f and the inner surface convection coefficient is h_i. The ambient temperature is T_a and the outer surface convection coefficient is h_o. Neglect the thermal resistance of the mortar joints and determine the rate of heat loss through the wall q, the inner surface temperature T_i, and the outer surface temperature T_o.

Figure 92.1 Insulated Wall Temperature Problem Sketch

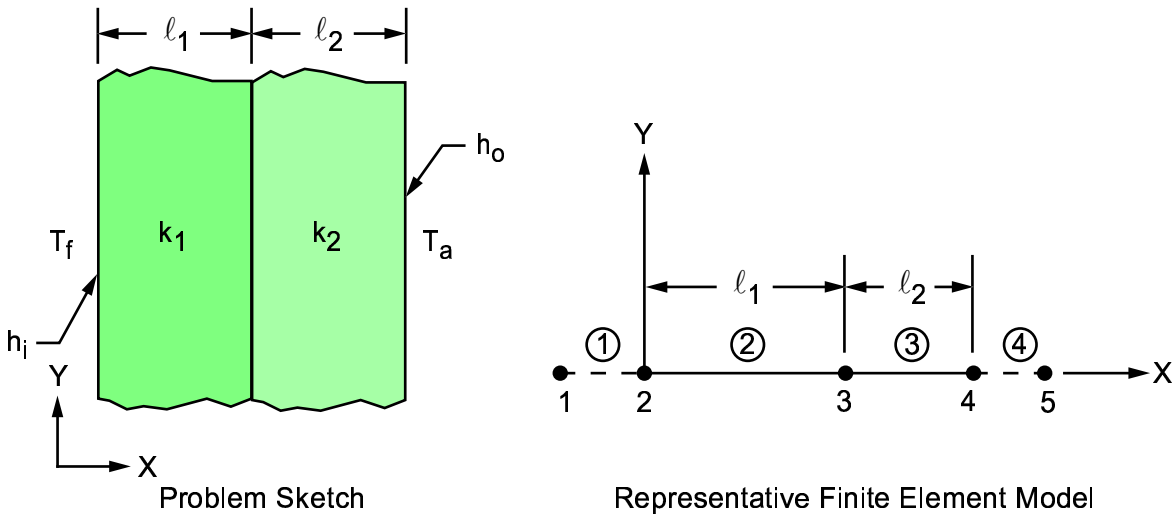

Material Properties	Geometric Properties	Loading
k_1 = 0.8 Btu/hr-ft-°F k_2 = 0.1 Btu/hr-ft-°F h_i = 12 Btu/hr-ft^2-°F h_o = 2 Btu/hr-ft^2-°F	ℓ_1 = 9 in = 0.75 ft ℓ_2 = 5 in = 5/12 ft	T_f = 3000°F T_a = 80°F

Analysis Assumptions and Modeling Notes

A 1 ft^2 area is used for the convection and conduction elements. Nodes 1 and 5 are given arbitrary locations. Feet units are input as (inches/12) for convenience. POST1 is used to extract results from the solution phase.

Results Comparison

	Target[1]	ANSYS	Ratio
q, Btu/hr	513.	513.	1.001
T_i , °F	2957.	2957.	1.000
T_o , °F	336.	337.	1.002

1. Rounded-off values (normalized)

VM93: Temperature Dependent Conductivity

Overview

Reference:	F. Kreith, *Principles of Heat Transfer*, 2nd Printing, International Textbook Co., Scranton, PA, 1959, pg. 25, ex. 2-2
Analysis Type(s):	Thermal Analysis (**ANTYPE** = 0)
Element Type(s):	2-D Conduction Bar Elements (LINK32)
Input Listing:	vm93.dat

Test Case

The conductivity of an 85% magnesia insulating material is given by $k(T) = C_0 + C_1 T$ for $100°F \leq T \leq 300°F$. Determine the rate of heat flow q between these temperatures for a slab of thickness t.

Figure 93.1 Conductivity Problem Sketch

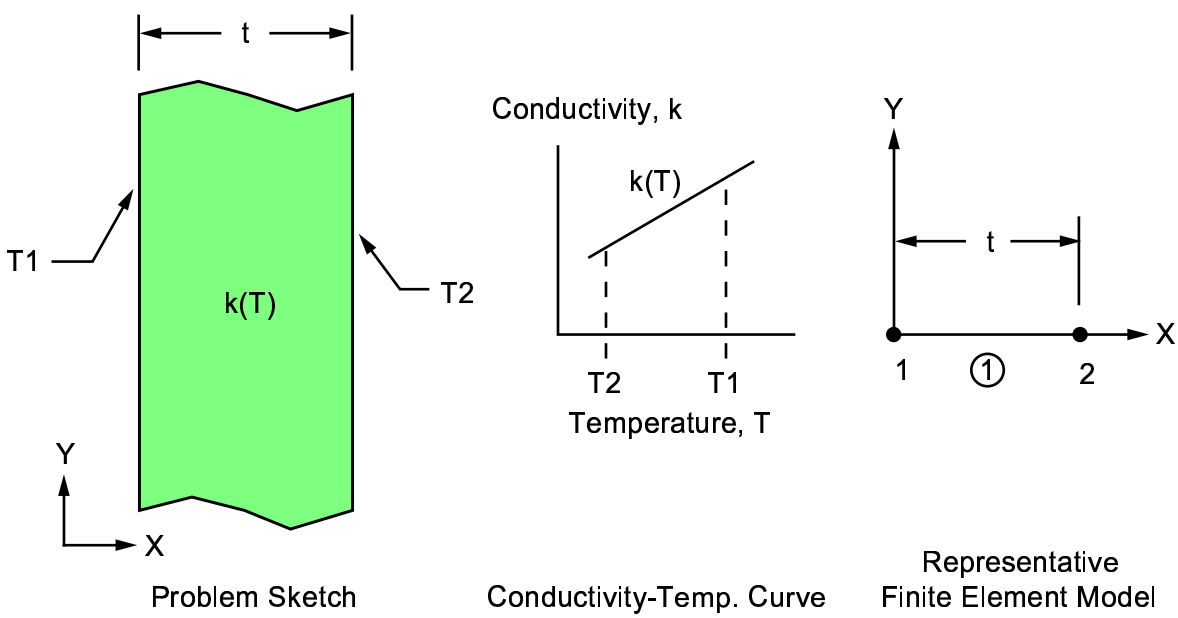

Material Properties	Geometric Properties	Loading
C_0 = 0.031 Btu/hr-ft-°F C_1 = 0.000031 Btu/hr-ft-°F^2	t = 3 in = 0.25 ft	T_1 = 300°F T_2 = 100°F

Analysis Assumptions and Modeling Notes

A 1 ft^2 area is used for the conduction element.

Results Comparison

	Target[1]	ANSYS	Ratio
q, Btu/hr	29.760	29.760	1.000

1. Solution recalculated.

VM94: Heat-generating Plate

Overview

Reference:	F. Kreith, *Principles of Heat Transfer*, 2nd Printing, International Textbook Co., Scranton, PA, 1959, pg. 42, ex. 2-9.
Analysis Type(s):	Thermal Analysis (**ANTYPE** = 0)
Element Type(s):	2-D Conduction Bar Elements (LINK32) Convection Link Elements (LINK34)
Input Listing:	vm94.dat

Test Case

A well-mixed fluid is heated by a long iron plate of conductivity k and thickness t. Heat is generated uniformly in the plate at the rate $\dddot{q}$. If the surface convection coefficient is h and the fluid temperature is T_f, determine the temperature at the center of the plate T_c and the heat flow rate to the fluid q_f.

Figure 94.1 Plate Problem Sketch

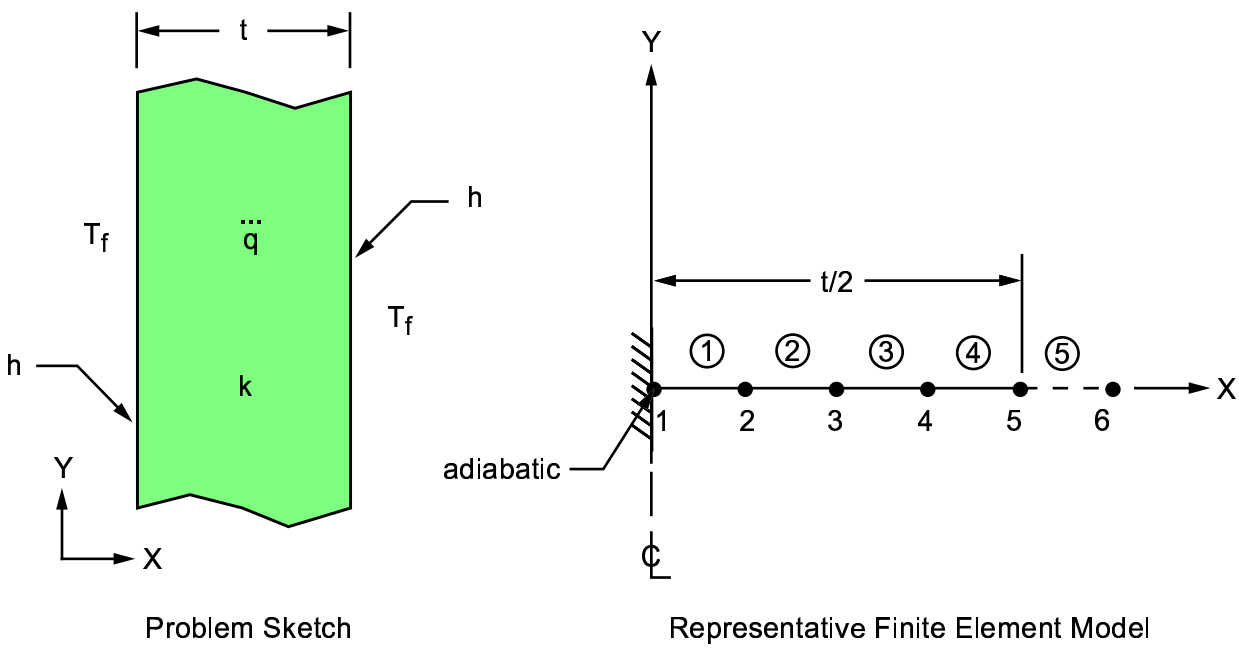

Material Properties	**Geometric Properties**	**Loading**
k = 25 Btu/hr-ft-°F h = 13.969738 Btu/hr-ft^2-°F	t = 1/2 in = 0.041666 ft	$\dddot{q}$ = 100,000 Btu/hr-ft^3 T_f = 150°F

Analysis Assumptions and Modeling Notes

A 1 ft^2 area is used for the conduction and convection elements. Only one half of the plate is modeled because of symmetry. Node 6 is given an arbitrary location. POST1 is used to process results from the solution phase.

Results Comparison

	Target	ANSYS	Ratio
q_f,Btu/hr	2083.3	2083.3	1.000
T_c, °F	299.1	300.0	1.003

ANSYS Verification Manual . ANSYS Release 10.0 . 002184 . © SAS IP, Inc.

VM95: Heat Transfer from a Cooling Spine

Overview

Reference:	F. Kreith, *Principles of Heat Transfer*, 2nd Printing, International Textbook Co., Scranton, PA, 1959, pg. 48, eq. 2-44, 45.
Analysis Type(s):	Heat Transfer Analysis (**ANTYPE** = 0)
Element Type(s):	3-D Conduction Bar Elements (LINK33) Convection Link Elements (LINK34) 3-D Thermal Solid Elements (SOLID70)
Input Listing:	vm95.dat

Test Case

A cooling spine of square cross-sectional area A, length ℓ, and conductivity k extends from a wall maintained at temperature T_w. The surface convection coefficient between the spine and the surrounding air is h, the air temperature is T_a, and the tip of the spine is insulated. Determine the heat conducted by the spine q and the temperature of the tip T_ℓ.

Figure 95.1 Cooling Spine Problem Sketch

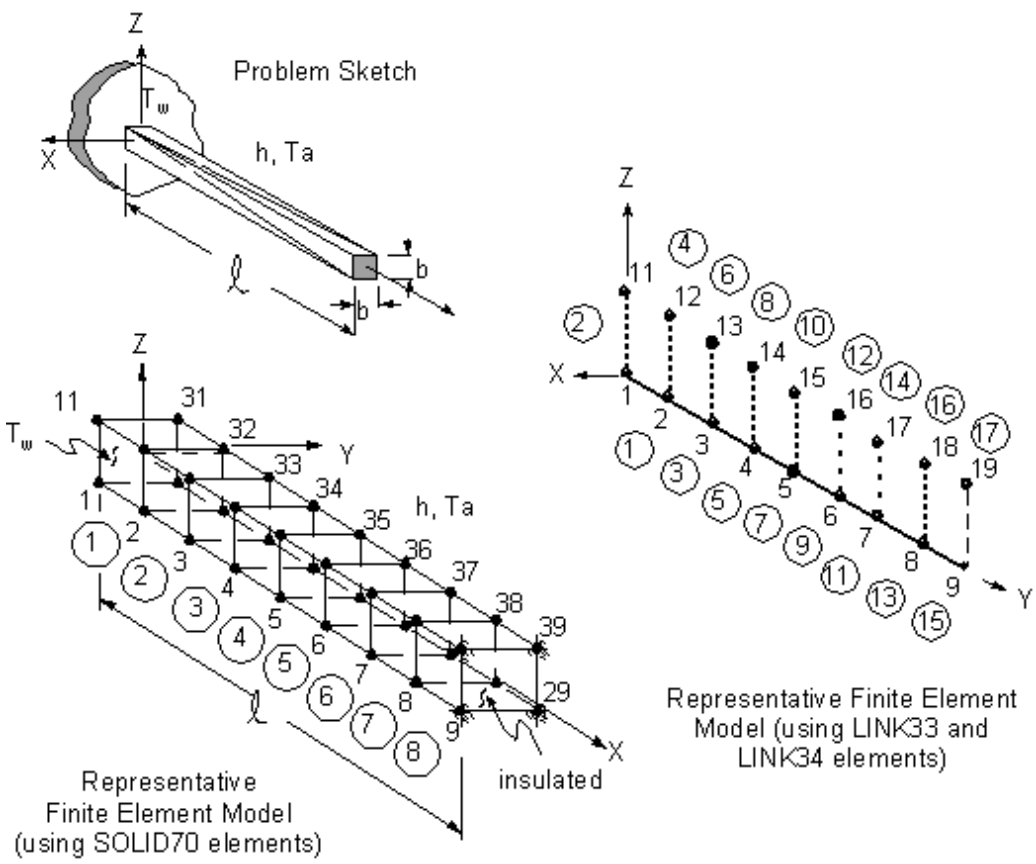

Material Properties	Geometric Properties	Loading
k = 25 Btu/hr-ft-°F h = 1 Btu/hr-ft^2-°F	A = 1 in^2 = (1/144) ft^2 ℓ = 8 in = (2/3) ft b = 1 in = (1/12) ft	T_a = 0°F T_w = 100°F

Analysis Assumptions and Modeling Notes

The problem is solved first using conducting line elements (LINK33) and convection elements (LINK34) and then using conducting solid elements (SOLID70). The surface convection area is 4 in^2 (4/144 ft^2) per inch of length.

In the first case, the convection elements at the end are given half the surface area of the interior convection elements. Nodes 11 through 19 are given arbitrary locations.

In the second case, coupled nodal temperatures are used to ensure symmetry.

Unit conversions are done by input expressions. POST1 is used to process results from the solution phase.

Results Comparison

		Target	ANSYS	Ratio
LINK33 and LINK34	T_{length}, °F	68.594	68.618	1.000
	q, Btu/hr	17.504	17.528	1.001
SOLID70	T_{length}, °F	68.594	68.618	1.000
	q, Btu/hr	17.504	17.528	1.001

ANSYS Verification Manual . ANSYS Release 10.0 . 002184 . © SAS IP, Inc.

VM96: Temperature Distribution in a Short, Solid Cylinder

Overview

Reference:	P. J. Schneider, *Conduction Heat Transfer*, 2nd Printing, Addison-Wesley Publishing Co., Inc., Reading, MA, 1957, pg. 134, fig. 6-7.
Analysis Type(s):	Thermal Analysis (**ANTYPE** = 0)
Element Type(s):	3-D 10-Node Tetrahedral Thermal Solid Elements (SOLID87)
Input Listing:	vm96.dat

Test Case

A short, solid cylinder is subjected to the surface temperatures shown. Determine the temperature distribution within the cylinder

Figure 96.1 Short, Solid Cylinder Problem Sketch

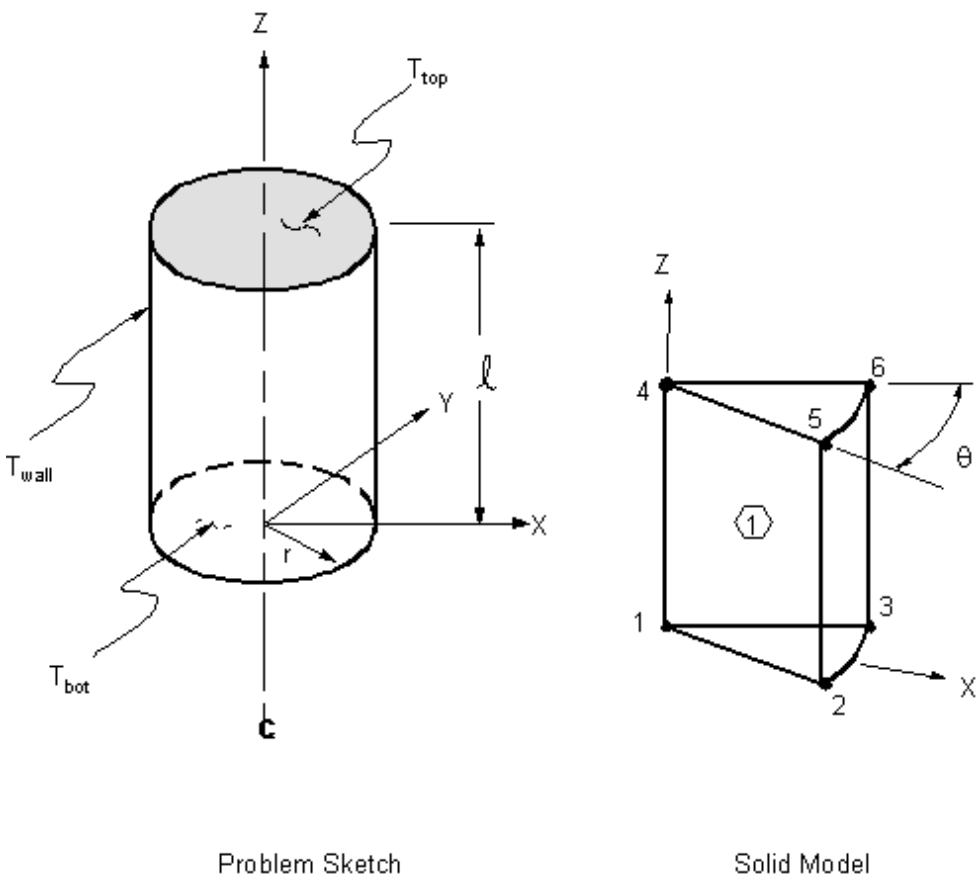

Material Properties	**Geometric Properties**	**Loading**
k = 1.0 Btu/hr-ft-°F	r = ℓ = 0.5 ft	T_{top} = 40°F T_{bot} = T_{wall} = 0°F

Analysis Assumptions and Modeling Notes

Since the problem is axisymmetric, the entire cylinder geometry is not required. An angle $\Theta = 45°$ is arbitrarily chosen. Postprocessing is used to print temperatures at the centerline in geometric order. A finer mesh density (than required for reasonable results) is used to produce a smooth isosurface plot.

Results Comparison

At Centerline		Target	ANSYS	Ratio
z = 0.0 ft	T, °F	0.0	0.0	--
z = 0.125 ft	T, °F	6.8	6.8	1.007
z = 0.25 ft	T, °F	15.6	15.4	0.984
z = 0.375 ft	T, °F	26.8	26.6	0.991
z = 0.5 ft	T, °F	40.0	40.0	1.00

Figure 96.2 Temperature Isosurface Display with Annotation

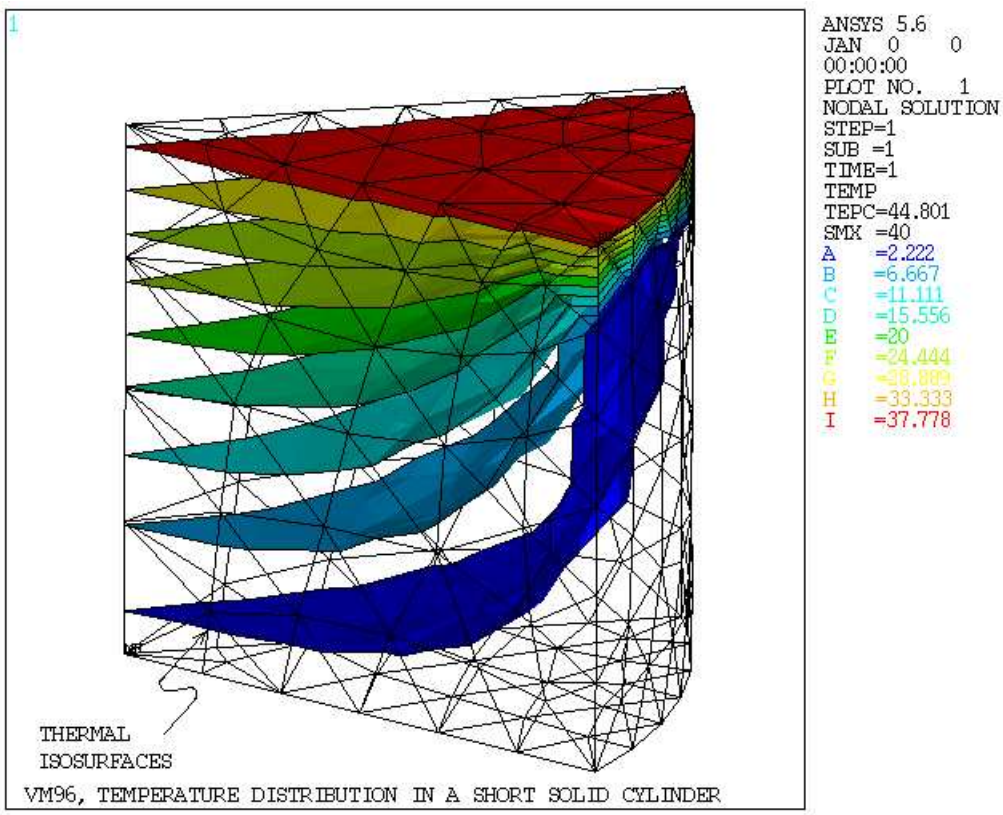

VM97: Temperature Distribution Along a Straight Fin

Overview

Reference:	F. Kreith, *Principles of Heat Transfer*, 2nd Printing, International Textbook Co., Scranton, PA, 1959, pg. 57, ex. 2-13.
Analysis Type(s):	Thermal Analysis (**ANTYPE** = 0)
Element Type(s):	4-Node Layered Thermal Shell Elements (SHELL131) Convection Link Elements (LINK34)
Input Listing:	vm97.dat

Test Case

A straight rectangular stainless steel cooling fin dissipates heat from an air-cooled cylinder wall. The wall temperature is T_w, the air temperature is T_a, and the convection coefficient between the fin and the air is h. Determine the temperature distribution along the fin and the heat dissipation rate q.

Figure 97.1 Straight Fin Problem Sketch

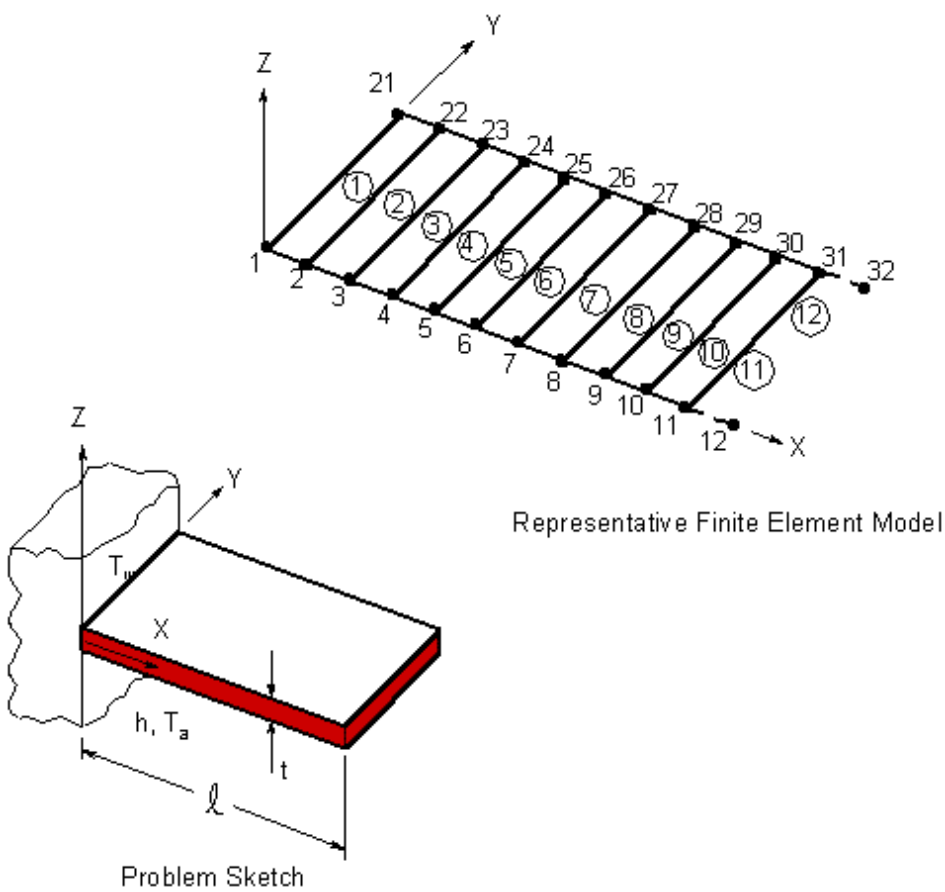

Material Properties	**Geometric Properties**	**Loading**
k = 15 Btu/hr-ft-°F	t = 1 in = (1/12 ft)	T_w = 1100°F
h = 15 Btu/hr-ft^2-°F	ℓ = 4 in = (4/12) ft	T_a = 100°F

Analysis Assumptions and Modeling Notes

Convection from the tip of the fin is modeled with the two convection elements (LINK34). One half of the cross-sectional area is assigned to each element. The depth of the fin (Y-direction) is arbitrarily selected to be 1 foot. POST1 is used to extract results from the solution phase.

Results Comparison

	Target[1]	ANSYS	Ratio
T, °F (at x/length = 0.0)	1100.	1100.	1.000
T, °F (at x/length = 0.1)	955.	958.	1.00
T, °F (at x/length = 0.2)	835.	838.	1.00
T, °F (at x/length = 0.3)	740.	738.	1.00
T, °F (at x/length = 0.4)	660.	655.	0.99
T, °F (at x/length = 0.5)	595.	587.	0.99
T, °F (at x/length = 0.6)	535.	532.	1.00
T, °F (at x/length = 0.7)	490.	489.	1.00
T, °F (at x/length = 0.8)	460.	456.	0.99
T, °F (at x/length = 0.9)	430.	432.	1.01
T, °F (at x/length = 1.0)	416.	417.	1.00
q, Btu/hr	5820.	5840.	1.00

1. Based on graphical readings

VM98: Temperature Distribution Along a Tapered Fin

Overview

Reference:	F. Kreith, *Principles of Heat Transfer*, 2nd Printing, International Textbook Co., Scranton, PA, 1959, pg. 57, ex. 2-13.
Analysis Type(s):	Thermal Analysis (**ANTYPE** = 0)
Element Type(s):	2-D Thermal Solid Elements (PLANE55)
Input Listing:	vm98.dat

Test Case

A tapered rectangular stainless steel cooling fin dissipates heat from an air-cooled cylinder wall. The wall temperature is T_w, the air temperature is T_a, and the convection coefficient between the fin and the air is h. Determine the temperature distribution along the fin and the heat dissipation rate q.

Figure 98.1 Tapered Fin Problem Sketch

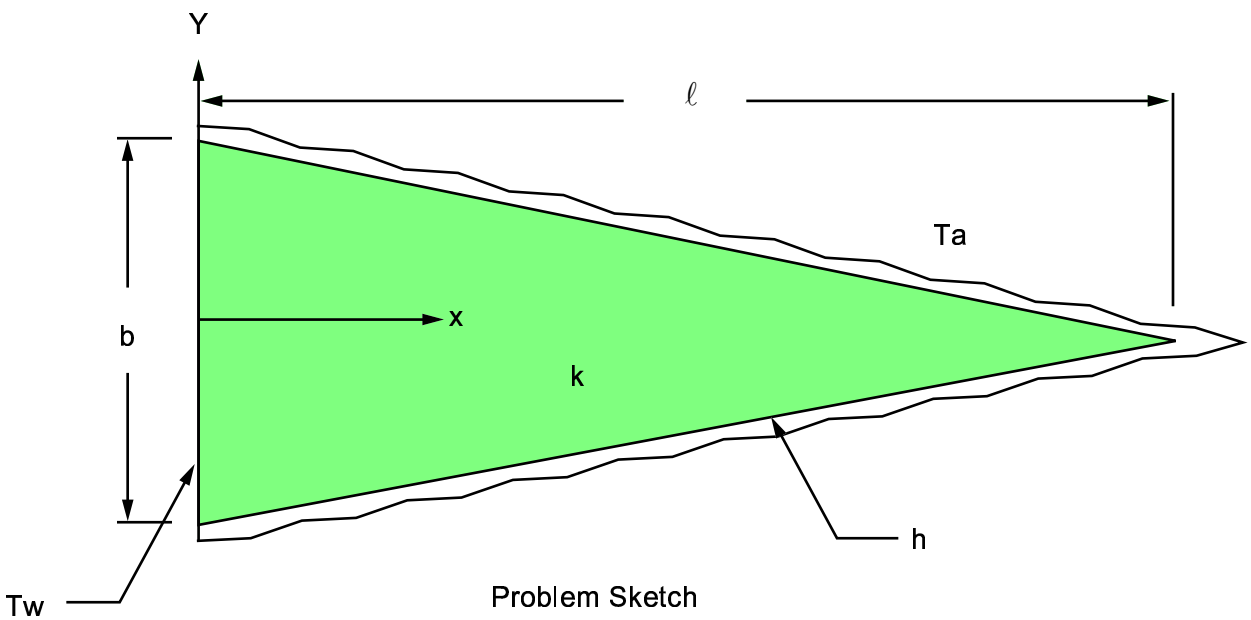

Problem Sketch

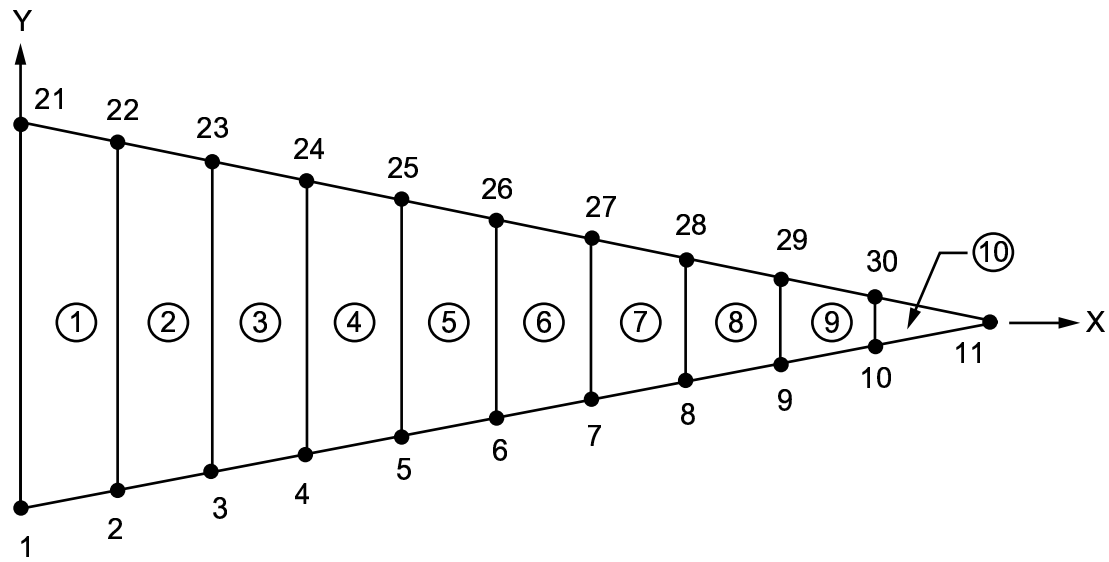

Representative Finite Element Model

Material Properties	Geometric Properties	Loading
k = 15 Btu/hr-ft-°F	b = 1 in = (1/12) ft	T_w = 1100°F
h = 15 Btu/hr-ft^2-°F	ℓ = 4 in = (4/12) ft	T_a = 100°F

Analysis Assumptions and Modeling Notes

The solution is based on a fin of unit depth (Z-direction). POST1 is used to extract results from the solution phase.

Results Comparison

	Target[1]	ANSYS	Ratio
T, °F (at x/length = 0.0)	1100.	1100.	1.000
T, °F (at x/length = 0.1)	970.	971.	1.001

	Target[1]	ANSYS	Ratio
T, °F (at x/length = 0.2)	850.	854.	1.004
T, °F (at x/length = 0.3)	750.	748.	0.998
T, °F (at x/length = 0.4)	655.	653.	0.997
T, °F (at x/length = 0.5)	575.	568.	0.988
T, °F (at x/length = 0.6)	495.	492.	0.994
T, °F (at x/length = 0.7)	430.	424.	0.987
T, °F (at x/length = 0.8)	370.	364.	0.984
T, °F (at x/length = 0.9)	315.	311.	0.988
T, °F (at x/length = 1.0)	265.	267.	1.006
q, Btu/hr	5050.	5109.	1.012

1. Based on graphical estimates.

VM99: Temperature Distribution in a Trapezoidal Fin

Overview

Reference:	P. J. Schneider, *Conduction Heat Transfer*, 2nd Printing, Addison-Wesley Publishing Co., Inc., Reading, MA, 1957, pg. 164, Article 7-8.
Analysis Type(s):	Thermal Analysis (**ANTYPE** = 0)
Element Type(s):	2-D Thermal Solid Elements (PLANE55)
Input Listing:	vm99.dat

Test Case

A rectangular cooling fin with a trapezoidal cross-section dissipates heat from a wall maintained at a temperature T_w. The surrounding air temperature is T_a and the convection coefficient between the fin and the air is h. Determine the temperature distribution within the fin and the heat dissipation rate q.

Figure 99.1 Trapezoidal Fin Problem Sketch

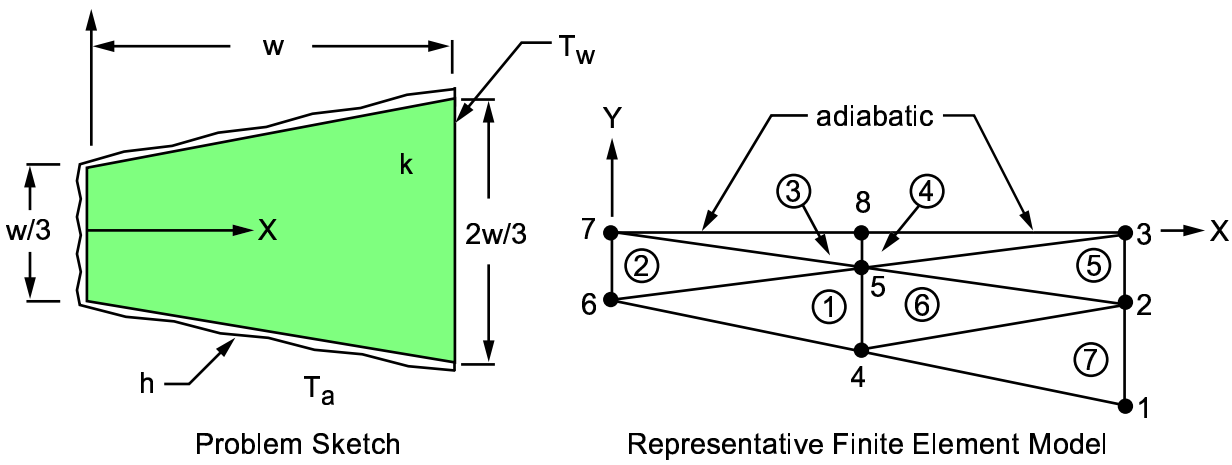

Material Properties	**Geometric Properties**	**Loading**
k = 18 Btu/hr-ft-°F	w = 0.96 in = 0.08 ft	T_w = 100°F
h = 500 Btu/hr-ft^2-°F		T_a = 0°F

Analysis Assumptions and Modeling Notes

The finite element model is made the same as the reference's relaxation model for a direct comparison. The solution is based on a fin of unit depth (Z-direction). Only half of the fin is modeled due to symmetry. POST1 is used to extract results from the solution phase.

Results Comparison

	Target[1]	ANSYS	Ratio
T, °F (at Node 4)	27.6	27.8	1.01
T, °F (at Node 5)	32.7	32.8	1.00
T, °F (at Node 6)	9.5	9.5	1.00
T, °F (at Node 7)	10.7	10.7	1.00

	Target[1]	ANSYS	Ratio
q, Btu/hr	3545.[2]	3482.	0.982

1. Based on a numerical relaxation method.
2. Solution recalculated.

VM100: Heat Conduction Across a Chimney Section

Overview

Reference:	F. Kreith, *Principles of Heat Transfer*, 2nd Printing, International Textbook Co., Scranton, PA, 1959, pg. 102, ex. 3-4.
Analysis Type(s):	Thermal Analysis (**ANTYPE** = 0)
Element Type(s):	2-D Thermal Solid Elements (PLANE55)
Input Listing:	vm100.dat

Test Case

Determine the temperature distribution and the rate of heat flow q per foot of height for a tall chimney whose cross-section is shown in Figure 100.1: "Heat Conduction Across a Chimney Section Problem Sketch". Assume that the inside gas temperature is T_g, the inside convection coefficient is h_i, the surrounding air temperature is T_a, and the outside convection coefficient is h_o.

Figure 100.1 Heat Conduction Across a Chimney Section Problem Sketch

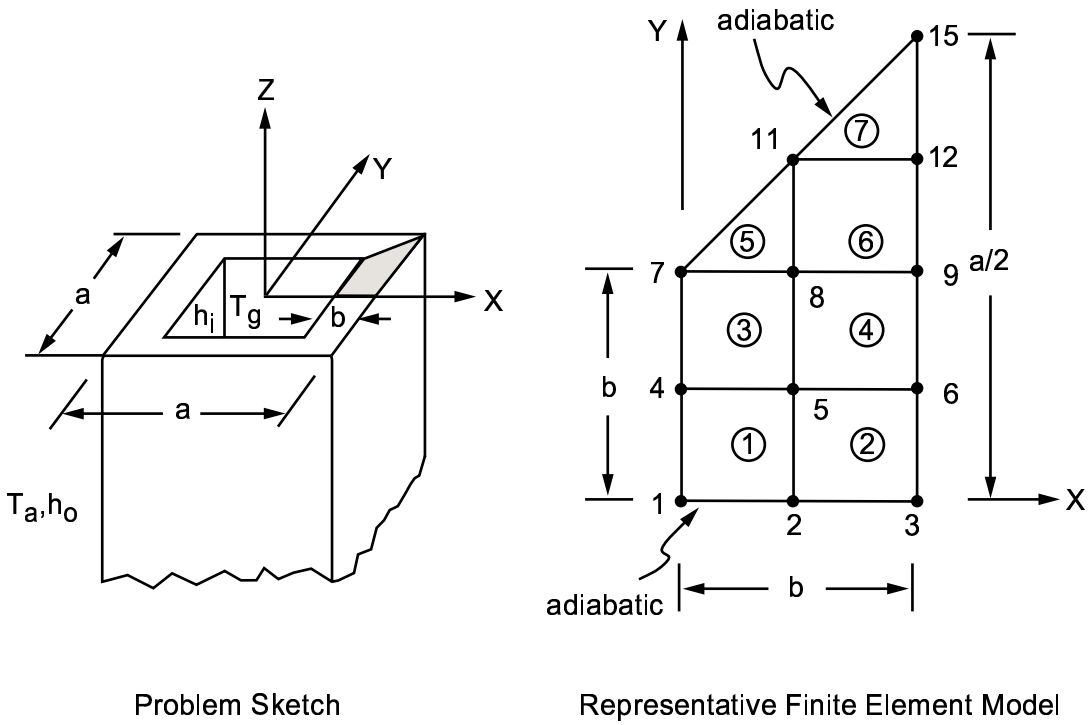

Material Properties	Geometric Properties	Loading
k = 1.0 Btu/hr-ft-°F h_i = 12 Btu/hr-ft^2-°F h_o = 3 Btu/hr-ft^2-°F	a = 4 ft b = 1 ft	T_g = 100°F T_a = 0°F See Figure 100.2: "Temperature Contour Display".

Analysis Assumptions and Modeling Notes

Due to symmetry, a 1/8 section is used. The finite element model is made the same as the reference's relaxation model for a direct comparison. The solution is based on a fin of unit depth (Z-direction). POST1 is used to obtain results from the solution phase.

Results Comparison

	Target[1]	ANSYS	Ratio
T, °F (at Node 1)	93.7	93.6	1.00
T, °F (at Node 2)	56.3	56.8	1.01
T, °F (at Node 3)	22.2	22.1	0.99
T, °F (at Node 4)	93.2	93.2	1.00
T, °F (at Node 5)	54.6	54.9	1.01
T, °F (at Node 6)	21.4	21.1	0.98
T, °F (at Node 7)	87.6	87.8	1.00
T, °F (at Node 8)	47.5	47.7	1.01
T, °F (at Node 9)	18.3	17.3	0.95
T, °F (at Node 11)	29.6	27.6	0.93
T, °F (at Node 12)	11.7	12.5	1.07
T, °F (at Node 15)	4.7	5.0	1.07
q, Btu/hr	775.2	773.5[2]	1.00

1. Based on a numerical relaxation method.
2. From heat rates at elements 1 and 3 multiplied by 8.

Figure 100.2 Temperature Contour Display

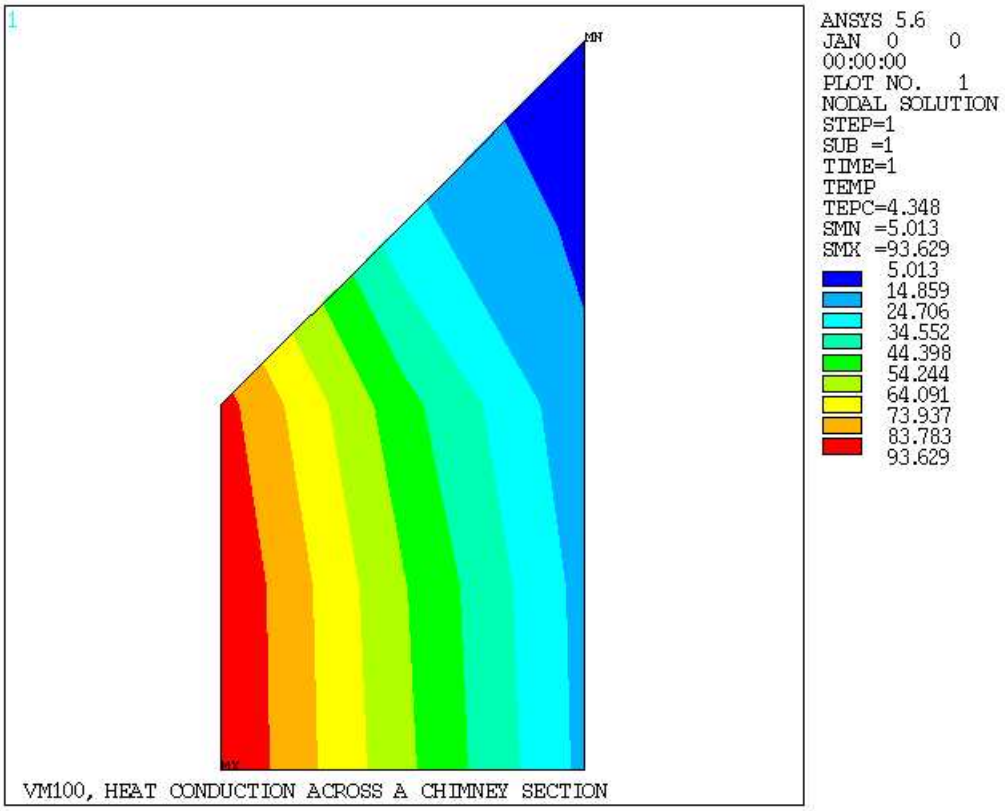

VM101: Temperature Distribution in a Short Solid Cylinder

Overview

Reference:	P. J. Schneider, *Conduction Heat Transfer*, 2nd Printing, Addison-Wesley Publishing Co., Inc., Reading, MA, 1957, pg. 134, fig. 6-7.
Analysis Type(s):	Thermal Analysis (**ANTYPE** = 0)
Element Type(s):	3-D Thermal Solid Elements (SOLID70)
Input Listing:	vm101.dat

Test Case

A short solid cylinder is subjected to the surface temperatures shown. Determine the temperature distribution within the cylinder.

Figure 101.1 Short Solid Cylinder Problem Sketch

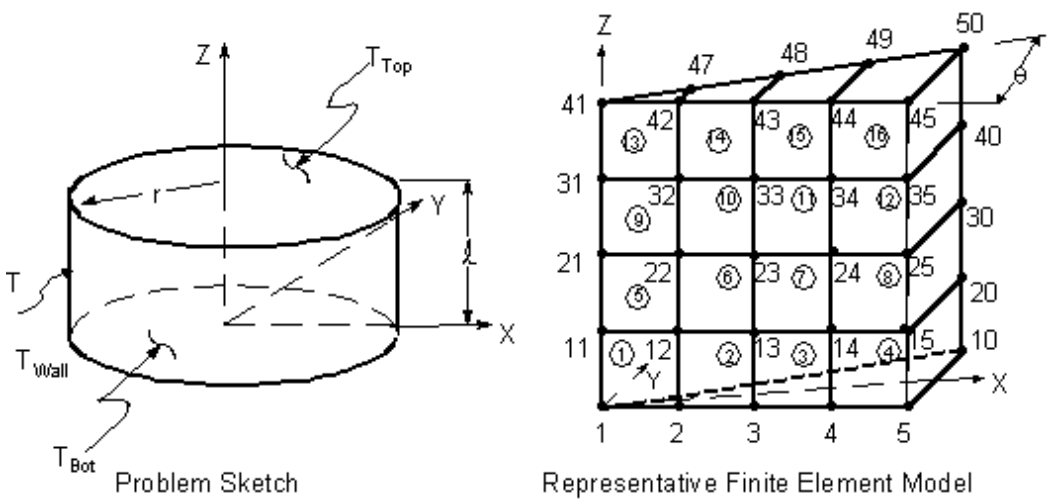

Material Properties	**Geometric Properties**	**Loading**
k = 1.0 Btu/hr-ft-°F	r = ℓ = 6 in = 0.5 ft	T_{Top} = 40°F T_{Bot} = T_{Wall} = 0°F

Analysis Assumptions and Modeling Notes

Since the problem is axisymmetric only a sector (one element wide) is modeled. A small angle Θ=10° is used for approximating the circular boundary with a straight-sided element. Note that circumferential symmetry is automatically ensured due to default adiabatic boundary conditions. POST1 is used to report centerline and mid-radius temperatures to compare results.

Results Comparison

		Target[1]	ANSYS	Ratio
T, °F (centerline)	Node 11	6.8	7.4	1.09
	Node 21	15.6	16.4	1.05
	Node 31	26.8	27.4	1.02

		Target[1]	ANSYS	Ratio
T, °F (mid-radius)	Node 13	5.2	5.3	1.02
	Node 23	12.8	13.0	1.02
	Node 33	24.0	24.8	1.03

1. Based on a graphical estimate.

Figure 101.2 Temperature Contour Display

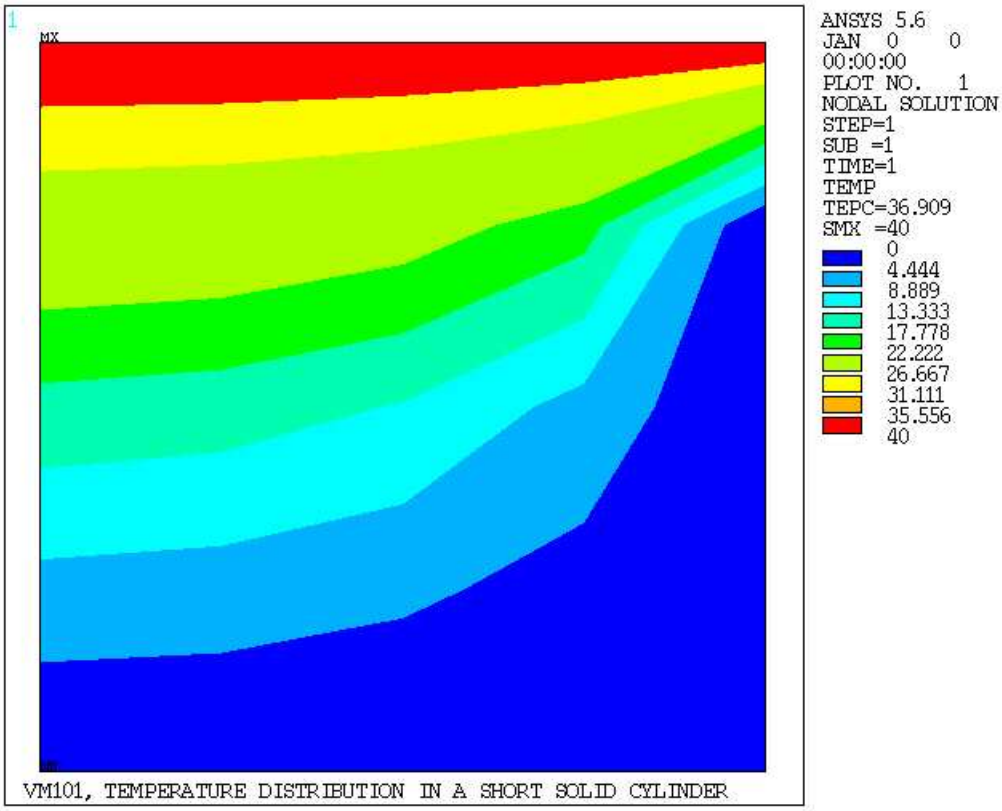

VM102: Cylinder with Temperature Dependent Conductivity

Overview

Reference:	P. J. Schneider, *Conduction Heat Transfer*, 2nd Printing, Addison-Wesley Publishing Co., Inc., Reading, MA, 1957, pg. 166, article 7-9.
Analysis Type(s):	Thermal Analysis (**ANTYPE** = 0)
Element Type(s):	2-D Thermal Solid Elements (PLANE55)
Input Listing:	vm102.dat

Test Case

A long hollow cylinder is maintained at temperature T_i along its inner surface and T_o along its outer surface. The thermal conductivity of the cylinder material is known to vary with temperature according to the linear function $k(T) = C_0 + C_1 T$. Determine the temperature distribution in the cylinder for two cases:

- k = constant, (i.e. $C_1 = 0$)
- k = k (T).

Figure 102.1 Cylinder Problem Sketch

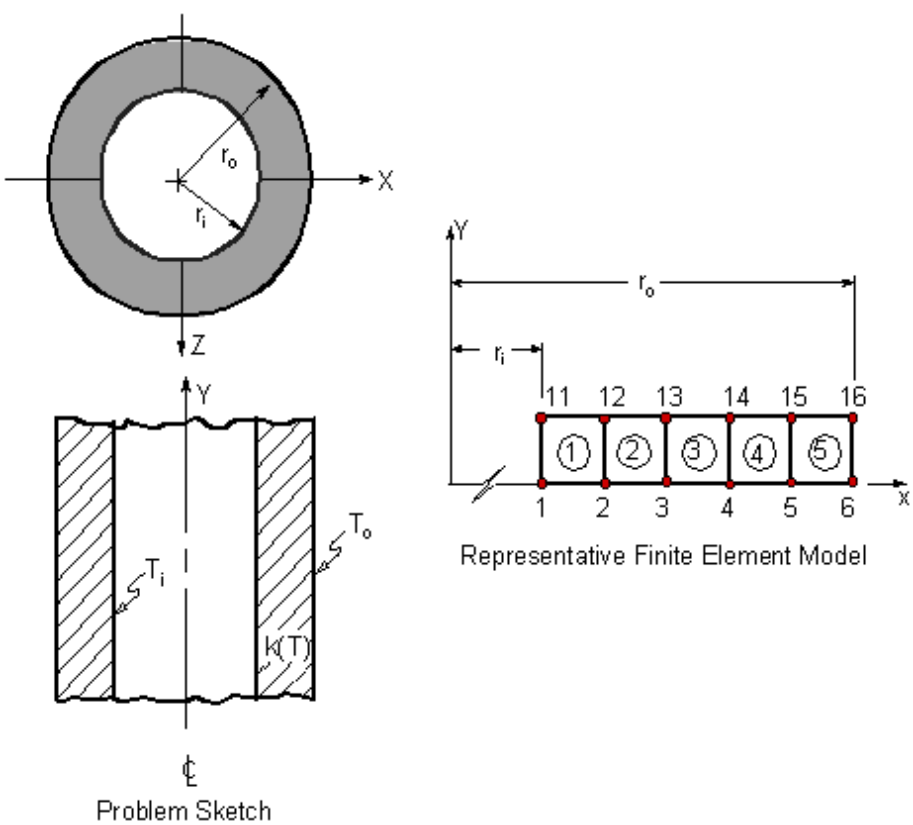

Material Properties	Geometric Properties	Loading
C_0 = 50 Btu/hr-ft-°F	r_i = 1/2 in = (1/24) ft	T_i = 100°F
C_1 = 0.5 Btu/hr-ft-°F^2	r_o = 1 in = (1/12) ft	T_o = 0°F

Analysis Assumptions and Modeling Notes

The axial length of the model is arbitrarily chosen to be 0.01 ft. Note that axial symmetry is automatically ensured by the adiabatic radial boundaries. The problem is solved in two load steps. The first load step uses the constant k. The **MP** command is reissued in the second load step to specify a temperature-dependent k.

Results Comparison

		Target[1]	ANSYS	Ratio
T, °F (k = constant); first load step	Node 2	73.8	73.7	1.000
	Node 3	51.5	51.5	1.000
	Node 4	32.2	32.2	1.000
	Node 5	15.3	15.2	0.99
T, °F (k = k(T)); second load step	Node 2	79.2	79.2	1.000
	Node 3	59.6	59.5	1.000
	Node 4	40.2	40.2	1.000
	Node 5	20.8	20.7	0.99

1. Based on a numerical relaxation method.

ANSYS Verification Manual . ANSYS Release 10.0 . 002184 . © SAS IP, Inc.

VM103: Thin Plate with Central Heat Source

Overview

Reference:	P. J. Schneider, *Conduction Heat Transfer*, 2nd Printing, Addison-Wesley Publishing Co., Inc., Reading, MA, 1957, pg. 173, article 8-1.
Analysis Type(s):	Thermal Analysis (**ANTYPE** = 0)
Element Type(s):	4-Node Layered Thermal Shell Elements (SHELL131)
Input Listing:	vm103.dat

Test Case

Determine the temperature distribution in the thin infinite plate with a cylindrical heat source $\dddot{q}$ shown in the following table. The plate also gains heat on the top face from an ambient gas at a temperature T_T and loses heat on the bottom face to an ambient gas at temperature T_B. Assume that no temperature gradient exists through the thickness of the plate.

Figure 103.1 Thin Plate Problem Sketch

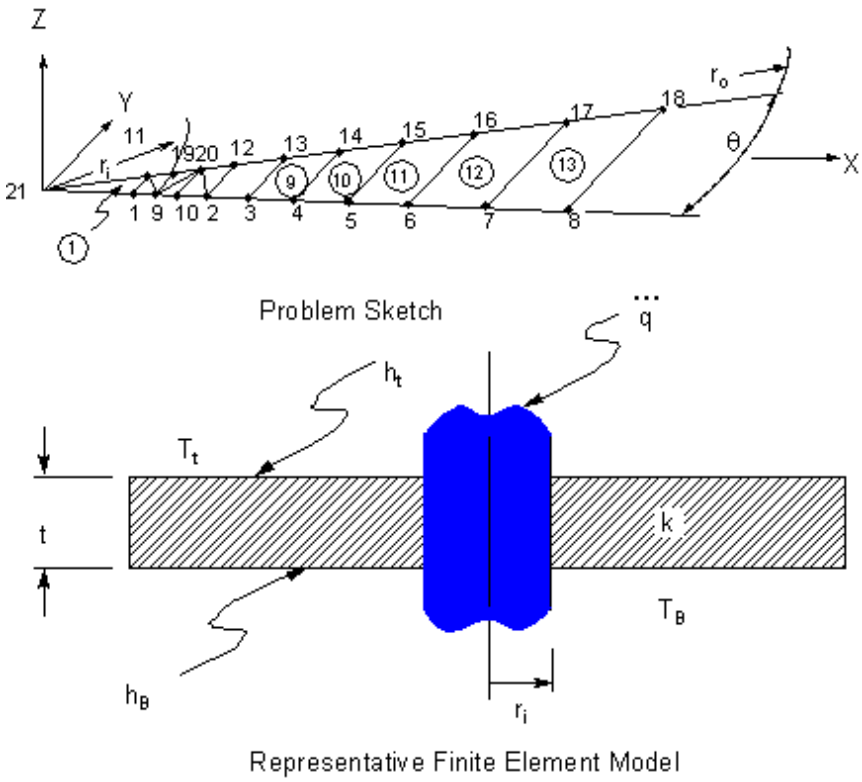

Material Properties	Geometric Properties	Loading
k = 5 Btu/hr-ft-°F h_T = 30 Btu/hr-ft^2-°F h_B = 20 Btu/hr-ft^2-°F	t = 0.1 ft r_i = 0.1 ft	T_T = 100°F T_B = 0°F $\dddot{q}$ = 250,000 Btu/hr-ft^3

Analysis Assumptions and Modeling Notes

Since the problem is axisymmetric only a one-element sector is needed. A small angle $\Theta = 10°$ is used for approximating the circular boundary with a straight-sided element. The outer radius r_o is arbitrarily selected at a point where the heat source should have negligible effect. Small elements are used adjacent to the heat source where the temperature gradient is the largest. Nodal coupling is used to ensure circumferential symmetry. Triangular and quadrilateral elements are used.

Results Comparison

	Target[1]	ANSYS	Ratio
T, °F (at Node 1)	226.3	227.0	1.00
T, °F (at Node 9)	173.1	164.9	0.95
T, °F (at Node 10)	130.7	126.8	0.97
T, °F (at Node 2)	103.2	102.4	0.99
T, °F (at Node 3)	73.8	73.6	1.00
T, °F (at Node 4)	65.8	64.6	0.98
T, °F (at Node 5)	62.8	61.6	0.98
T, °F (at Node 6)	60.8	60.6	1.00
T, °F (at Node 7)	60.2	60.2	1.00
T, °F (at Node 8)	60.0	60.2	1.00

1. Based on graphical estimate

ANSYS Verification Manual . ANSYS Release 10.0 . 002184 . © SAS IP, Inc.

VM104: Liquid-Solid Phase Change

Overview

Reference:	J. A. Dantzig, "Modeling Liquid-Solid Phase Changes with Melt Convection", *Int. Journal Numerical Methods in Engineering*, Vol. 28, 1989, pg. 1774, problem I.
Analysis Type(s):	Thermal Analysis (with phase change) (**ANTYPE** = 4)
Element Type(s):	2-D Thermal Solid Elements (PLANE55)
Input Listing:	vm104.dat

Test Case

A layer of liquid (of depth a), covering an insulated surface and initially at its freezing temperature T_o, is suddenly subjected to a free surface temperature T_s (less than T_o). Determine the time, t_f, taken for the liquid to solidify completely, and the temperature distribution in the solid phase at time t_1 seconds.

Figure 104.1 Liquid-Solid Phase Change Problem Sketch

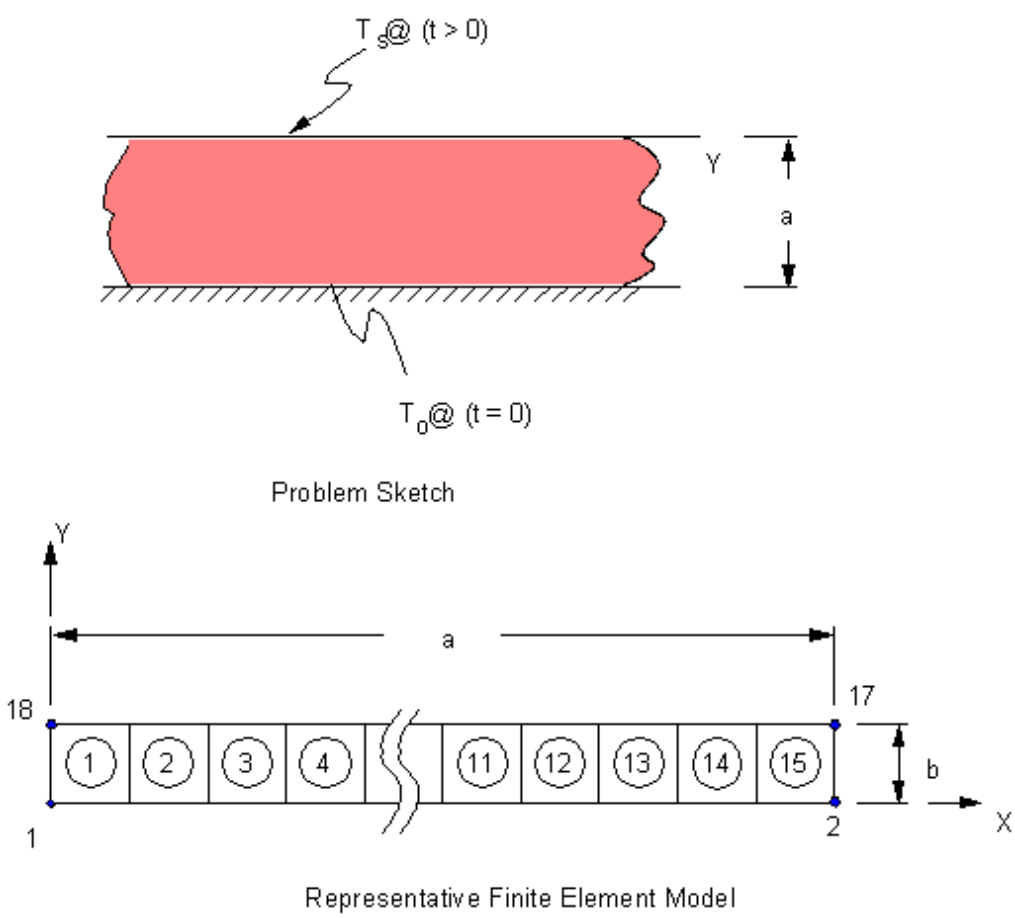

Material Properties	Geometric Properties	Loading
ρ = 1000 kg/m^3 C_p = 4200.0 J/kg-°C k = 0.60 W/m-°C L_f = Latent heat of fusion = 42000. J/kg	a = 0.01 m b = 0.001 m	T_o = 0°C (t = 0) T_s = -5°C (x = 0; t > 0) t_1 = 500 sec

Analysis Assumptions and Modeling Notes

The problem is formulated in two dimensions, with all faces insulated, except the face representing the liquid surface. The latent heat effect (accompanying change in phase from liquid to solid), is approximated by specifying a rapid variation in enthalpy (material property ENTH), over the "mushy" zone in a temperature range of ΔT (taken as 1.0°C). The enthalpy (H) variation is computed from the equation $H = \rho c \int dT$. An adjusted specific heat of $L_f/\Delta T$ = 42000.0 J/kg-°C, is used in the freezing zone, resulting in a slope discontinuity, as shown in Figure 104.3: "Temperature Distribution at Time = 501 Seconds". For the given case, a time step of 3.0 seconds is found to be adequate to give more than one time step through the freezing zone. Automatic time stepping is used.

POST1 is used to obtain the temperature distribution through the two phases and POST26 is used to display the temperature history of points in each of the phases.

Figure 104.2 Enthalpy vs. Temperature

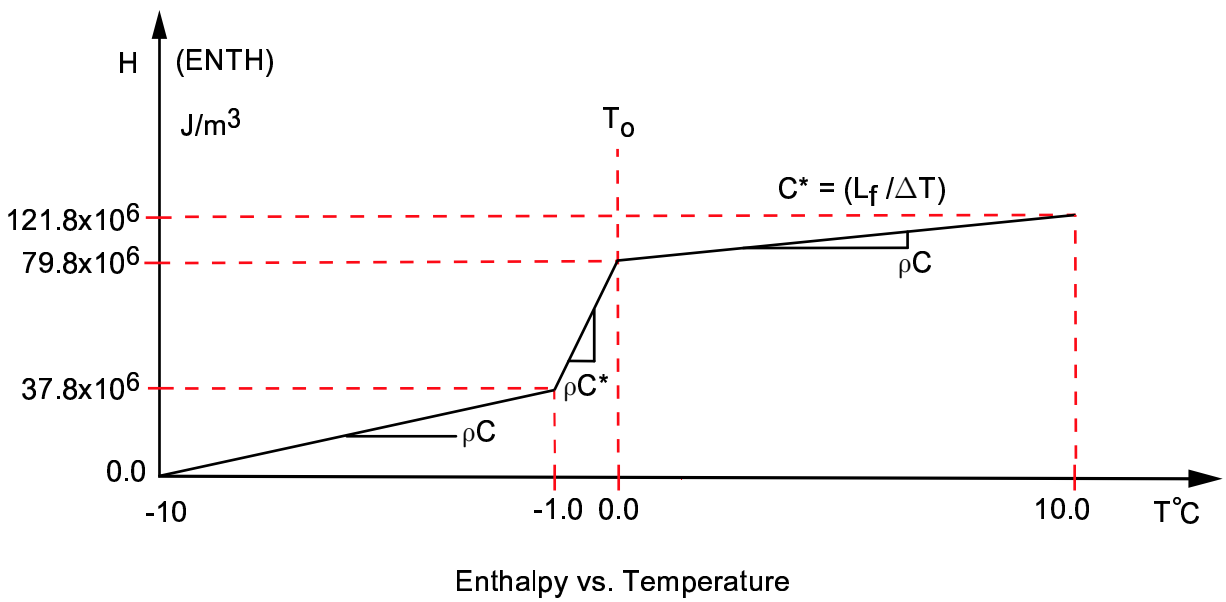

Results Comparison

	Target[1]	ANSYS	Ratio
t_f, seconds	810.0	between (787 to 797) [2]	-
At t = 500 seconds			
T , °C (x = 0.002m)	-3.64	-3.71	1.019
T , °C (x = 0.004m)	-2.32	-2.46	1.059

1. From Equations 20-31, in J. A. Dantzig, “Modeling Liquid-Solid Phase Changes with Melt Convection”.
2. Corresponds to the time interval at which Node 2 temperature crosses the $\Delta T = 1°C$ freezing zone.

Figure 104.3 Temperature Distribution at Time = 501 Seconds

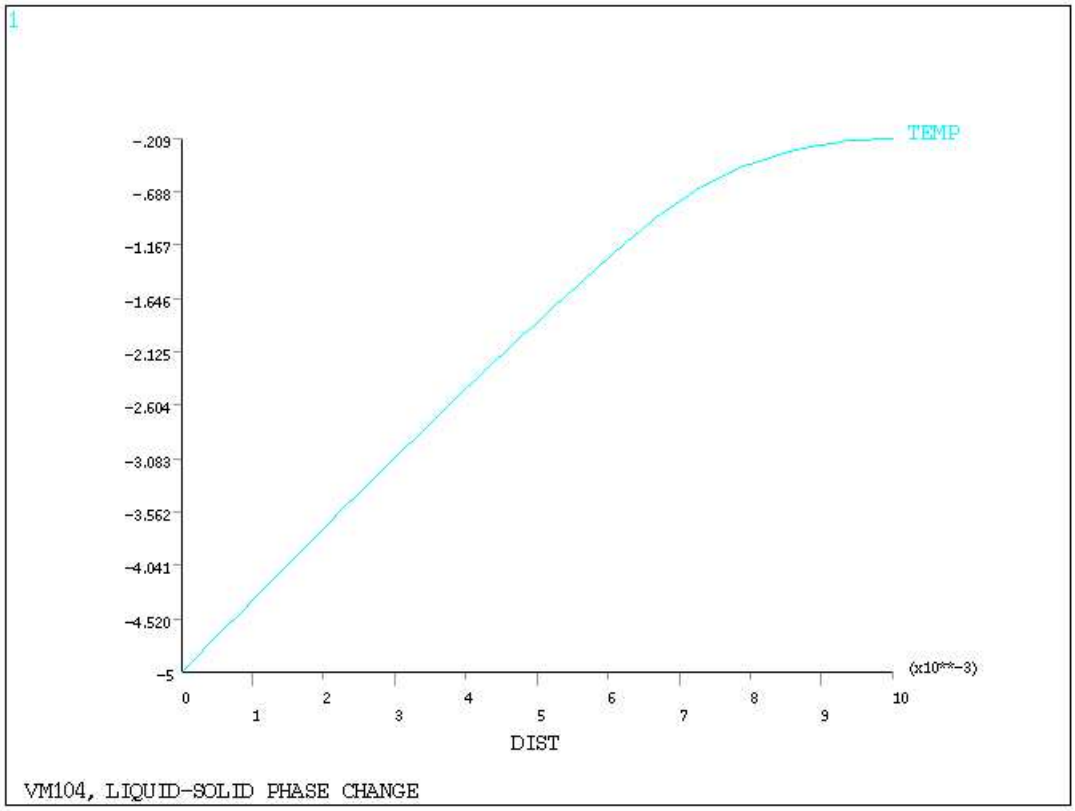

Figure 104.4 Temperature History of Solidification

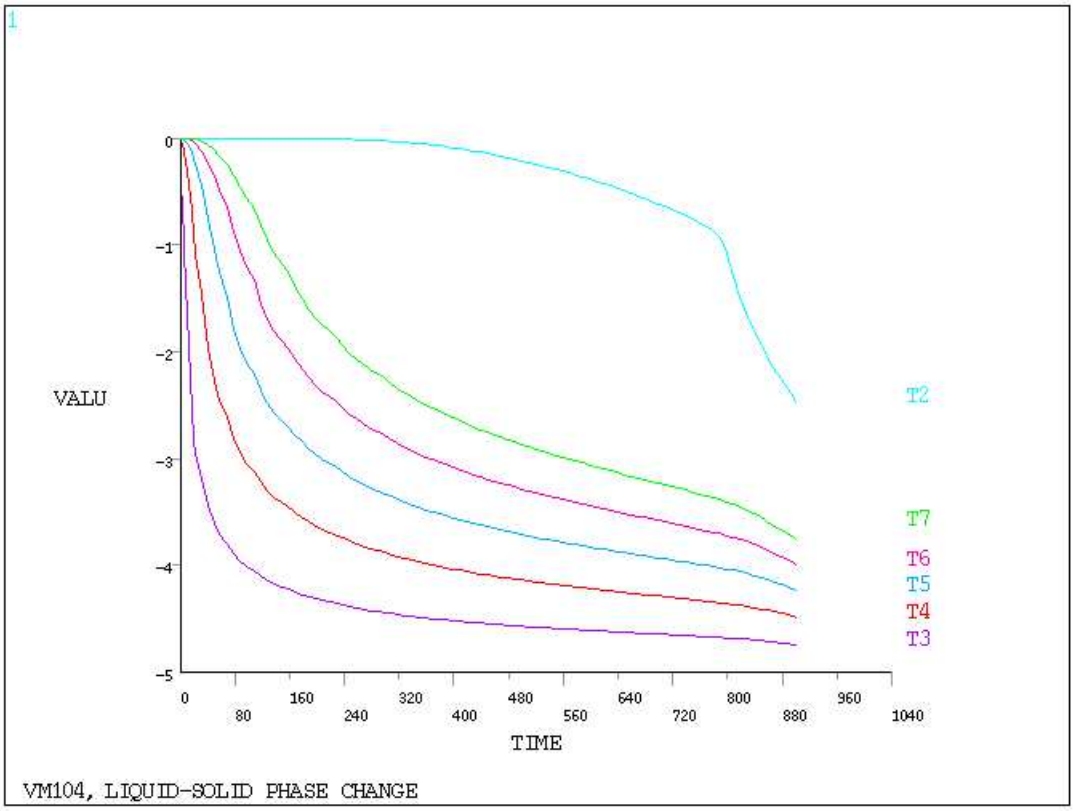

VM105: Heat Generating Coil with Temperature Conductivity

Overview

Reference:	P. J. Schneider, *Conduction Heat Transfer*, 2nd Printing, Addison-Wesley Publishing Co., Inc., Reading, MA, 1957, pg. 193, article 8-8
Analysis Type(s):	Thermal Analysis (**ANTYPE** = 0)
Element Type(s):	2-D Thermal Solid Elements (PLANE55)
Input Listing:	vm105.dat

Test Case

A long hollow generator coil has its inner and outer surface temperatures maintained at temperature T_o while generating Joule heat at a uniform rate $\dot{\dot{q}}$. The thermal conductivity of the coil material varies with temperature according to the function $k(T) = C_0 + C_1 T$. Determine the temperature distribution in the coil.

Figure 105.1 Heat Generating Coil Problem Sketch

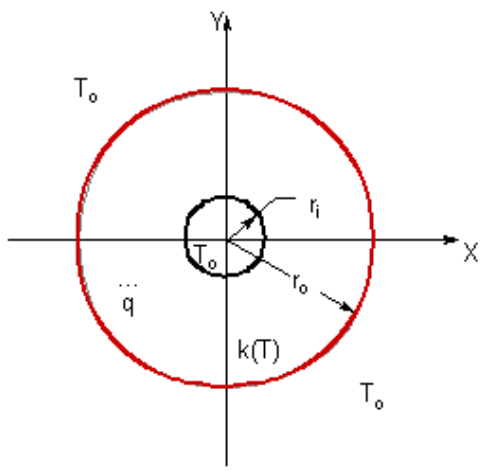

Problem Sketch

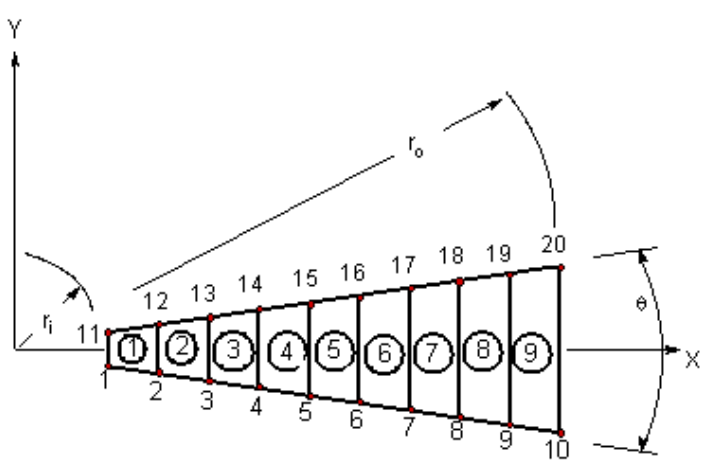

Representative Finite Element Model

Material Properties	Geometric Properties	Loading
C_0 = 10 Btu/hr-ft-°F C_1 = 0.075 Btu/hr-ft-°F^2	r_i = 1/4 in = 1/48 ft r_o = 1 in = 1/12 ft	T_o = 0°F $\ddot{q}$ = 1 x 10^6 Btu/hr-ft^3

Analysis Assumptions and Modeling Notes

Since the problem is axisymmetric only a symmetry sector (one-element wide) is needed. A small angle (Θ=10°) is used for approximating the circular boundary with a straight-sided element. Adiabatic boundary conditions are assumed at the symmetry edges. The steady-state convergence procedures are used. Note that this problem can also be modeled using the axisymmetric option as in VM102.

Results Comparison

T, °F	Target	ANSYS	Ratio
Node 2	23.3	23.0	0.989
Node 3	35.9	35.5	0.990
Node 4	42.2	41.8	0.991
Node 5	44.0	43.7	0.992
Node 6	42.2	41.9	0.992
Node 7	37.0	36.8	0.993
Node 8	28.6	28.4	0.991
Node 9	16.5	16.4	0.991

Figure 105.2 Variation of Temperature in the Radial Direction

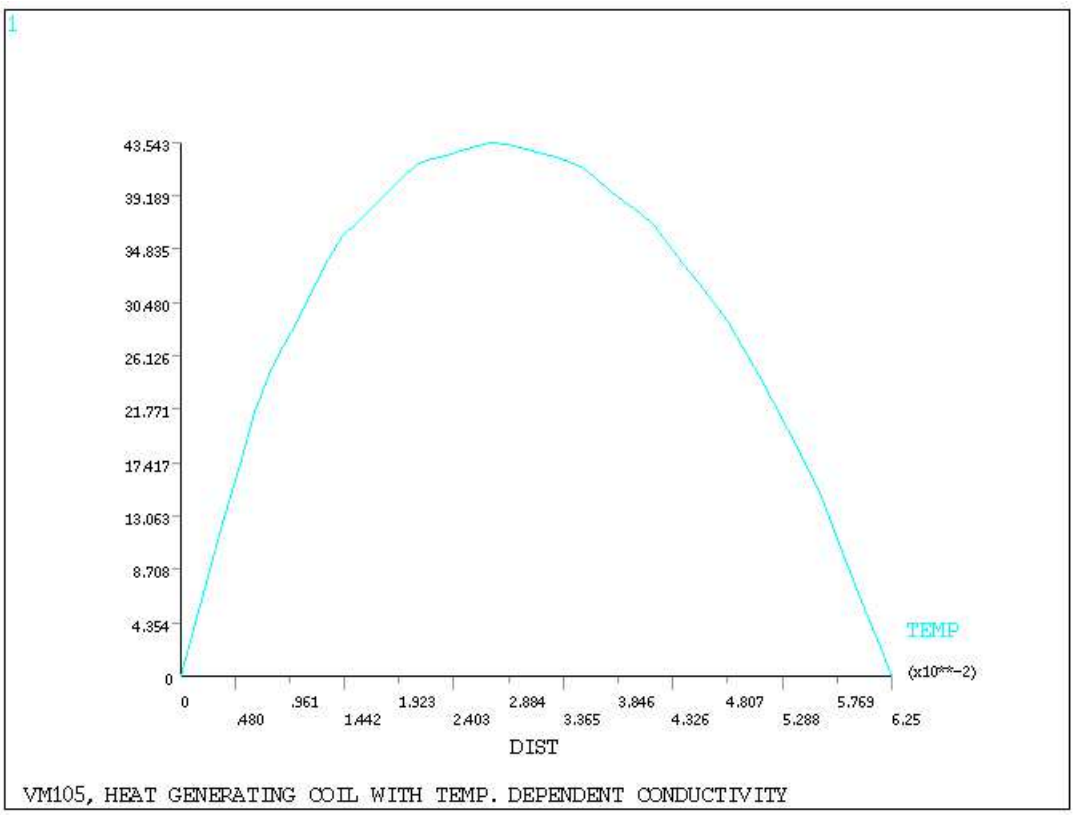

VM106: Radiant Energy Emission

Overview

Reference:	F. Kreith, *Principles of Heat Transfer*, 2nd Printing, International Textbook Co., Scranton, PA, 1959, pg. 22, problem 1-8(b).
Analysis Type(s):	Thermal Analysis (**ANTYPE** = 0)
Element Type(s):	Radiation Link Elements (LINK31)
Input Listing:	vm106.dat

Test Case

Determine the rate of radiant heat emission q in Btu/hr from a black body of unit area A at a temperature T, when ambient temperature is T_a.

Figure 106.1 Radiant Energy Emission Problem Sketch

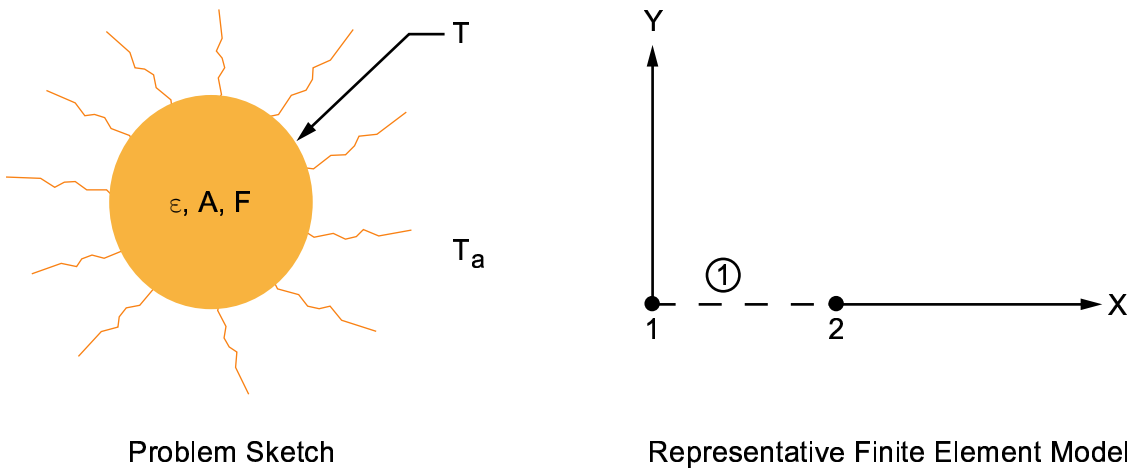

Material Properties	Geometric Properties	Loading
ε = emissivity = 1.0	A = 1 ft^2 F = form factor = 1.0	T = 3000°F T_a = 0°F

Analysis Assumptions and Modeling Notes

A conversion factor of 144 in^2/ft^2 is included in the area input to convert the default Stefan-Boltzmann constant to feet units. The temperature offset of 460°F is required to convert the input Fahrenheit temperature to an absolute (Rankine) temperature. The node locations are arbitrarily selected as coincident.

Results Comparison

	Target	ANSYS[1]	Ratio
q, Btu/hr	2.4559×10^5	2.4552×10^5	1.000

1. Element heat rate

VM107: Thermocouple Radiation

Overview

Reference:	A. J. Chapman, *Heat Transfer*, The Macmillan Co, New York, NY, 1960, pg. 396, article 13.5.
Analysis Type(s):	Thermal analysis (**ANTYPE** = 0)
Element Type(s):	Radiation Link Elements (LINK31) Convection Link Elements (LINK34)
Input Listing:	vm107.dat

Test Case

A thermocouple is used to measure the temperature T_g of a gas flowing within a duct. The duct wall temperature is T_w and the thermocouple is placed at right angles to the flow. If the conduction effects are negligible, determine the thermocouple reading T_t and the heat flow rate q due to convection and radiation.

Figure 107.1 Thermocouple Radiation Problem Sketch

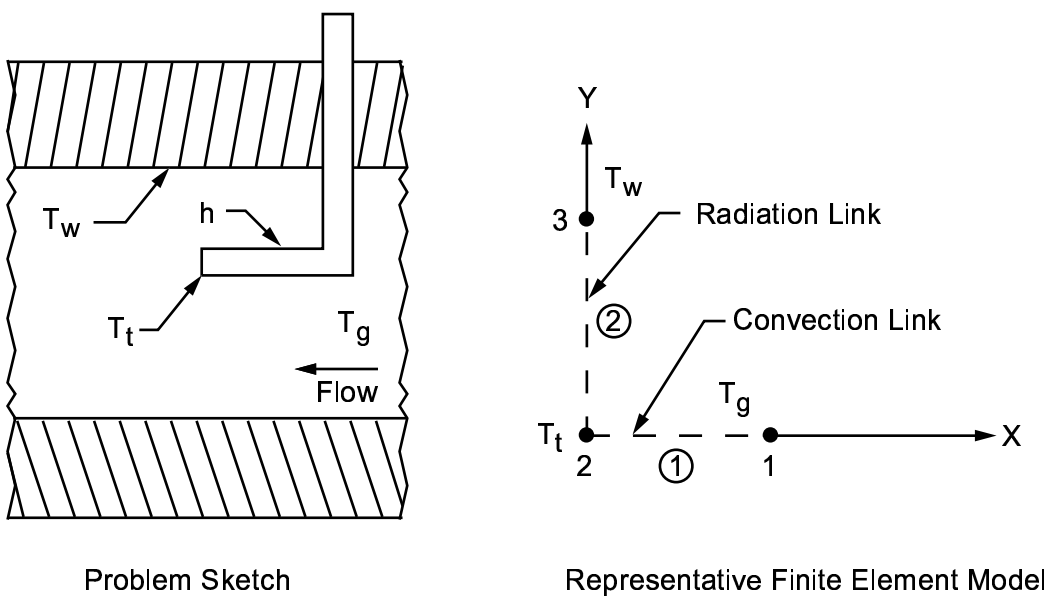

Material Properties	**Loading**
ε = emissivity = 0.5 h = 11.85 Btu/hr-ft^2-°F Stefan-Boltzmann constant[1] = 0.174 x 10^{-8} Btu/hr-ft^2-°R^4	T_w = 300°F T_g = 1309°F

1. As given in A. J. Chapman, *Heat Transfer*.

Analysis Assumptions and Modeling Notes

The temperature offset of 460°F is required to convert the input Fahrenheit temperatures to absolute (Rankine) temperatures. The node locations are arbitrarily selected (coincident).

Results Comparison

	Target	ANSYS[1]	Ratio
T_t, °F	1000.00	999.95	1.000
q, Btu/hr	3661.65	3662.24	1.000

1. At node 2

VM108: Temperature Gradient Across a Solid Cylinder

Overview

Reference:	F. B. Hildebrand, *Advanced Calculus for Applications*, 2nd Edition, Prentice-Hall, Inc., Englewood, NJ, 1976, pg. 447, eqs. 38-44.
Analysis Type(s):	Thermal Analysis (**ANTYPE** = 0)
Element Type(s):	Axisymmetric-Harmonic 4-Node Thermal Solid Elements (PLANE75)
Input Listing:	vm108.dat

Test Case

Heat is conducted across the diameter of a long solid cylinder. The temperature loading along the circumference is antisymmetric about the Y-Z plane and varies sinusoidally with peaks occurring at $\Theta = 0°$ and $\Theta = 180°$. Determine the temperature distribution along the radius at $\Theta = 0°$.

Figure 108.1 Solid Cylinder Problem Sketch

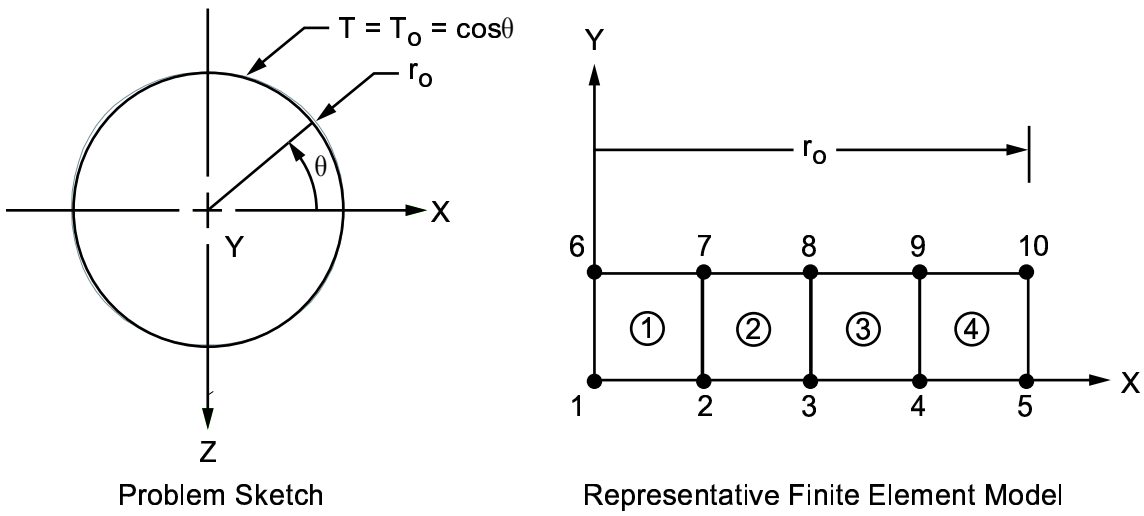

Material Properties	Geometric Properties	Loading
k = 1 Btu/hr-ft-°F	r_o = 20 ft	T_o = 80°F

Analysis Assumptions and Modeling Notes

The axial length of the model is arbitrarily chosen to be 5 ft. The temperature loading is applied as a harmonic function (mode = 1) around the periphery of the cylinder. To obtain the theoretical solution, equations 43 and 44 in F. B. Hildebrand, *Advanced Calculus for Applications* are used. Applying the temperature boundary condition and the requirement that $T(r,\Theta)$ should be finite and single-valued leads to the following solution: $T(r,\Theta) = T_0 * (r/r_0) * \cos\Theta$.

Results Comparison

Mode = 1 (angle =0°)	Target	ANSYS	Ratio
Node 1 T, °F	0.0	0.0	-
Node 2 T, °F	20.0	20.0	1.00

Mode = 1 (angle =0°)	Target	ANSYS	Ratio
Node 3 T, °F	40.0	40.0	1.00
Node 4 T, °F	60.0	60.0	1.00

VM109: Temperature Response of a Suddenly Cooled Wire

Overview

Reference:	F. Kreith, *Principles of Heat Transfer*, 2nd Printing, International Textbook Co., Scranton, PA, 1959, pg. 120, ex. 4-1.
Analysis Type(s):	Thermal Analysis (**ANTYPE** = 4)
Element Type(s):	Convection Link Elements (LINK34) Thermal Mass Elements (MASS71)
Input Listing:	vm109.dat

Test Case

Determine the temperature response of a copper wire of diameter d, originally at temperature T_o, when suddenly immersed in air at temperature T_{air}. The convection coefficient between the wire and the air is h.

Figure 109.1 Cooled Copper Wire Problem Sketch

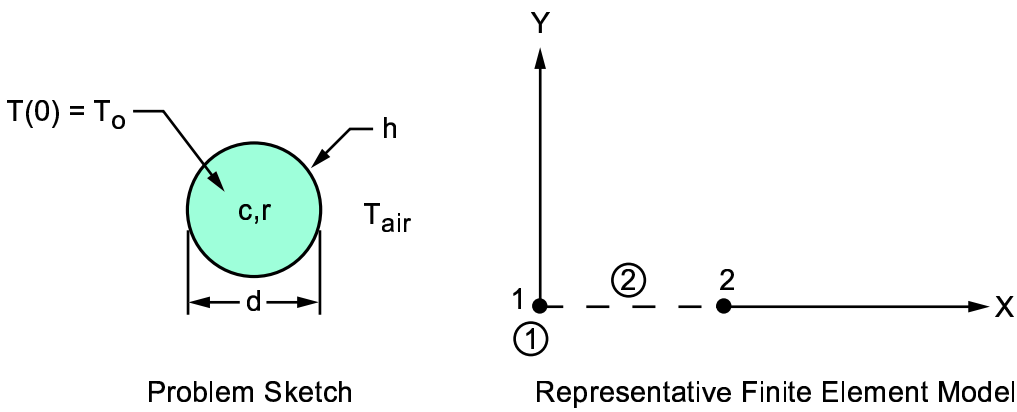

Material Properties	Geometric Properties	Loading
ρ = 558 lb/ft^3 c = 0.091 Btu/lb-°F h = 2 Btu/hr-ft^2-°F	d = 1/32 in	T_{air} = 100°F T_o = 300°F (at t=0)

Analysis Assumptions and Modeling Notes

The node locations are arbitrary (coincident). The final time of 0.05 hr (180 sec) is sufficient for the theoretical response comparison. An initial integration time step of 0.05/40 = 0.00125 hr is used. Automatic time stepping is used. The thermal capacitance C, and the surface area of the wire A_s, are calculated based on a unit length as follows:

$$C = \rho c V = 558 \times 0.091 \times \frac{\pi}{4} \times \left(\frac{1}{32 \times 12}\right)^2 = 2.7046 \times 10^{-4} \text{ BTU/°F}$$

$$A = \pi d = \frac{\pi}{32 \times 12} = 8.1812 \times 10^{-3} \text{ ft}^2$$

Results Comparison

	Target	ANSYS	Ratio
T, °F @ 0.0125hr	193.89	196.48	1.013
T, °F @ 0.0325hr	128.00	130.05	1.016
T, °F @ 0.05hr	109.71	110.83	1.010

1. POST26, Node 1 temperature history

Figure 109.2 Temperature vs. Time Display

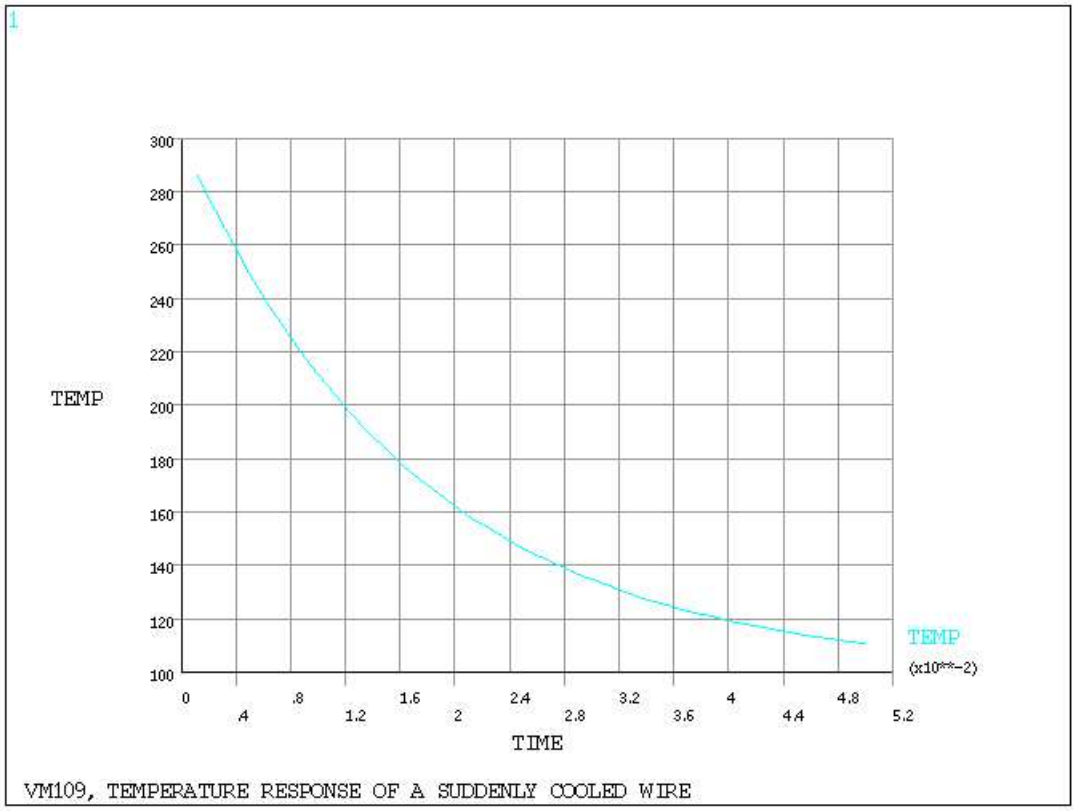

VM110: Transient Temperature Distribution in a Slab

Overview

Reference:	F. Kreith, *Principles of Heat Transfer*, 2nd Printing, International Textbook Co., Scranton, PA, 1959, pg. 140, ex. 4-4.
Analysis Type(s):	Thermal Analysis (**ANTYPE** = 4)
Element Type(s):	2-D Conduction Bar Elements (LINK32) Convection Link Elements (LINK34)
Input Listing:	vm110.dat

Test Case

A concrete wall, originally at temperature T_o, is suddenly exposed on one side to a hot gas at temperature T_g. If the convection coefficient on the hot side is h and the other side is insulated, determine the temperature distribution in the slab after 14.5 hours, and the total heat Q transferred to the wall per square foot of surface area.

Figure 110.1 Slab Problem Sketch

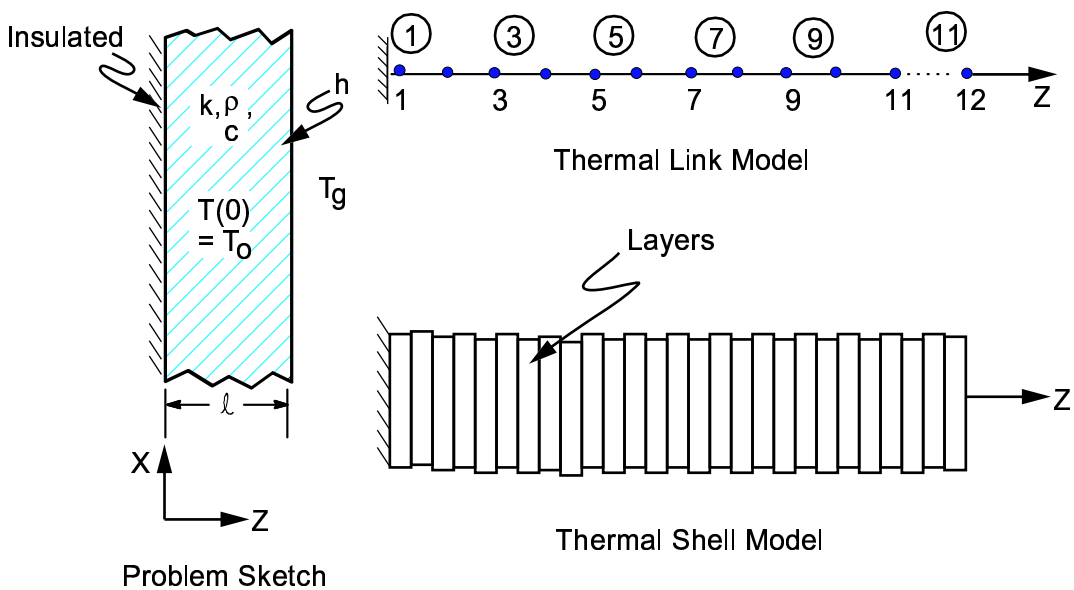

Material Properties	**Geometric Properties**
k = 0.54 Btu/hr-ft-°F	ℓ = 1 ft
ρ = 144 lb/ft^3	**Loading**
c = 0.2 Btu/lb-°F	T_o = 100°F
h = 5 Btu/hr-ft^2-°F	T_g = 1600°F

Analysis Assumptions and Modeling Notes

The problem is first solved using LINK32 elements. A 1 ft^2 area is used for the convection and conduction elements. Node 12 is given an arbitrary location. Automatic time stepping is used. The initial integration time step (ITS) chosen (14.5/80 = 0.18125 hr) is larger than the minimum ITS recommended; ITS $\approx \delta^2/4\alpha$, where δ is the conduction element length (0.1 ft) and a is the thermal diffusivity ($k/\rho c$ = 0.01875 ft^2/hr). POST26 is used to obtain the total heat transferred to the wall.

Results Comparison

Time = 14.5 hr	Target[1]	ANSYS	Ratio[1]
T, °F (node 1)	505.	507.	1.00
T, °F (node 3)	550.	549.	1.00
T, °F (node 5)	670.	675.	1.01
T, °F (node 7)	865.	874.	1.01
T, °F (node 9)	1135	1134.	1.00
T, °F (node 11)	1435.	1433.	1.00
Q[2], BTU/ft^2	-20,736.	-20,662.	1.00

1. Based on graphical estimates
2. $Q = \int q\,dt$, from POST26

VM111: Cooling of a Spherical Body

Overview

Reference:	F. Kreith, *Principles of Heat Transfer*, 2nd Printing, International Textbook Co., Scranton, PA, 1959, pg. 143, ex. 4-5.
Analysis Type(s):	Thermal Analysis (**ANTYPE** = 4)
Element Type(s):	2-D Thermal Solid Elements (PLANE55)
Input Listing:	vm111.dat

Test Case

Determine the temperature at the center of a spherical body, initially at a temperature T_o, when exposed to an environment having a temperature T_e for a period of 6 hours. The surface convection coefficient is h.

Figure 111.1 Spherical Body Problem Sketch

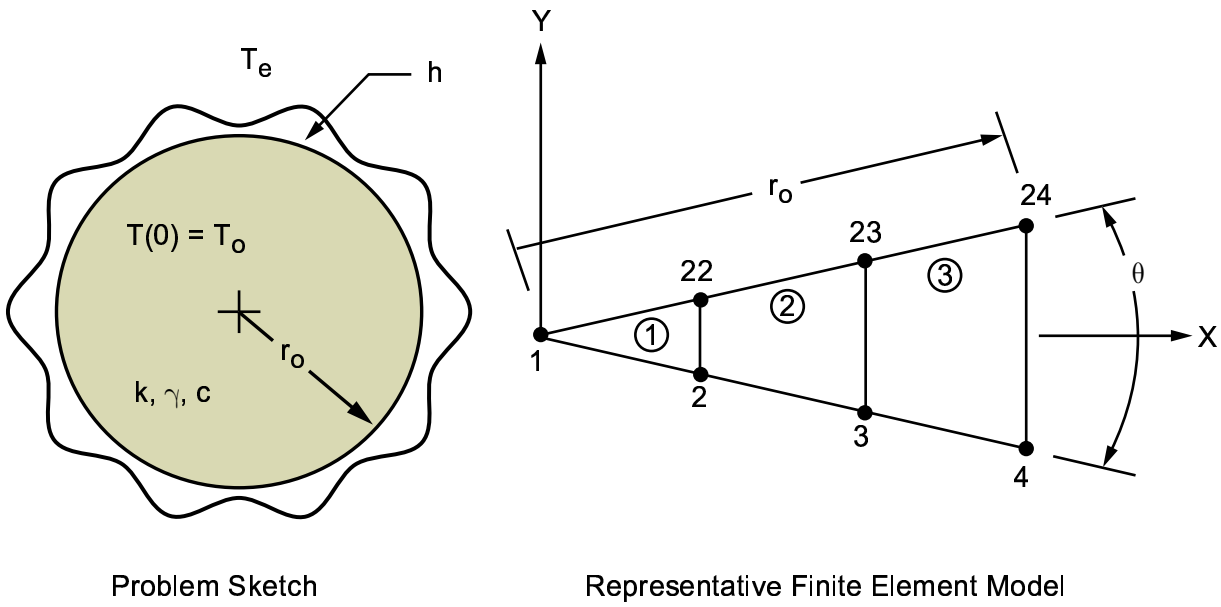

Material Properties	**Geometric Properties**
K=(1/3) BTU/hr-ft-°F	r_o = 2 in = (1/6) ft
γ = 62 lb/ft^3	**Loading**
c = 1.075 Btu/lb-°F	T_o = 65°F
h = 2 Btu/hr-ft^2-°F	T_e = 25°F

Analysis Assumptions and Modeling Notes

Since the problem is axisymmetric, only a one-element sector is needed. A small angle Θ = 15° is used for approximating the circular boundary with a straight-side element. Nodal coupling is used to ensure circumferential symmetry. Automatic time stepping is used. The initial integration time step (6/40 = 0.15 hr) is based on $\approx \delta^2/4\alpha$, where δ is the element characteristic length (0.0555 ft) and α is the thermal diffusivity ($k/\gamma c$ = 0.005 ft^2/hr). POST1 is used to extract results from the solution phase.

Results Comparison

Time = 6 hr	Target[1]	ANSYS	Ratio
T, °F	28.0	28.66	1.024

1. Based on graphical estimates.

VM112: Cooling of a Spherical Body

Overview

Reference:	F. Kreith, *Principles of Heat Transfer*, 2nd Printing, International Textbook Co., Scranton, PA, 1959, pg. 143, ex. 4-5.
Analysis Type(s):	Thermal Analysis (**ANTYPE** = 4)
Element Type(s):	2-D 8-Node Thermal Solid Elements (PLANE77)
Input Listing:	vm112.dat

Test Case

See VM111 for test case description, geometric and material properties, and loading.

Figure 112.1 Spherical Body Problem Sketch

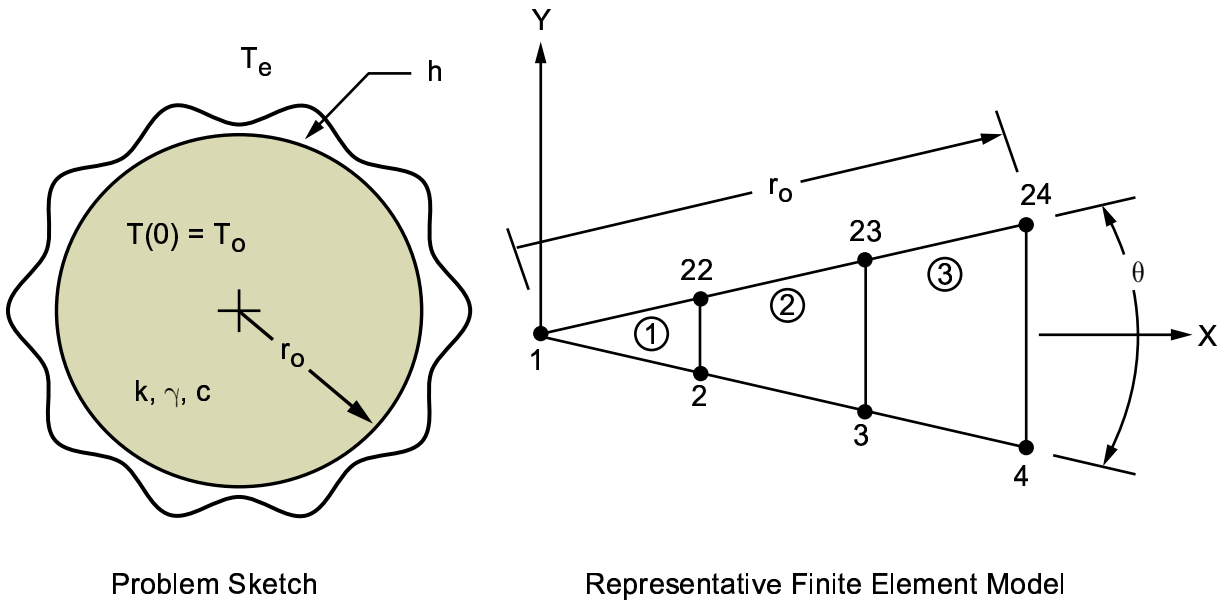

Analysis Assumptions and Modeling Notes

Since the problem is axisymmetric, only a one-element sector is needed. A small angle $\Theta = 15°$ is used for approximating the circular boundary with a curved-side element. Nodal coupling is used to ensure circumferential symmetry. Automatic time stepping is used. The initial integration time step (6/40 = 0.15 hr) is based on $\approx \delta^2/4\alpha$, where δ is the element characteristic length (0.0555 ft) and α is the thermal diffusivity ($k/\gamma c = 0.005$ ft^2/hr). POST1 is used to extract results from the solution phase.

Results Comparison

Time = 6 hr.	Target[1]	ANSYS	Ratio
T, °F	28.0	29.0	1.035

1. Based on graphical estimates.

VM113: Transient Temperature Distribution in an Orthotropic Metal Bar

Overview

Reference:	P. J. Schneider, *Conduction Heat Transfer*, 2nd Printing, Addison-Wesley Publishing Co., Inc., Reading, MA, 1957, pg. 261, ex. 10-7.
Analysis Type(s):	Thermal Analysis (**ANTYPE** = 4)
Element Type(s):	2-D Thermal Solid Elements (PLANE55)
Input Listing:	vm113.dat

Test Case

A long metal bar of rectangular cross-section is initially at a temperature T_o and is then suddenly quenched in a large volume of fluid at temperature T_f. The material conductivity is orthotropic, having different X and Y directional properties. If the surface convection coefficient is h, determine the temperature distribution in the slab after 3 seconds in the following locations of the bar:

- center
- corner edge
- face centers of the bar

Figure 113.1 Orthotropic Metal Bar Problem Sketch

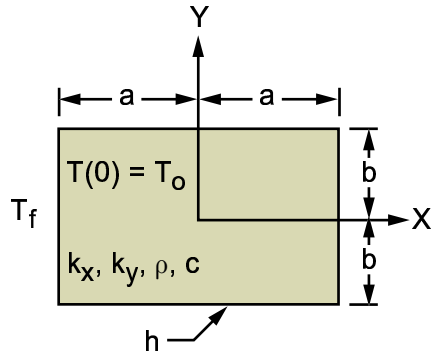

Problem Sketch

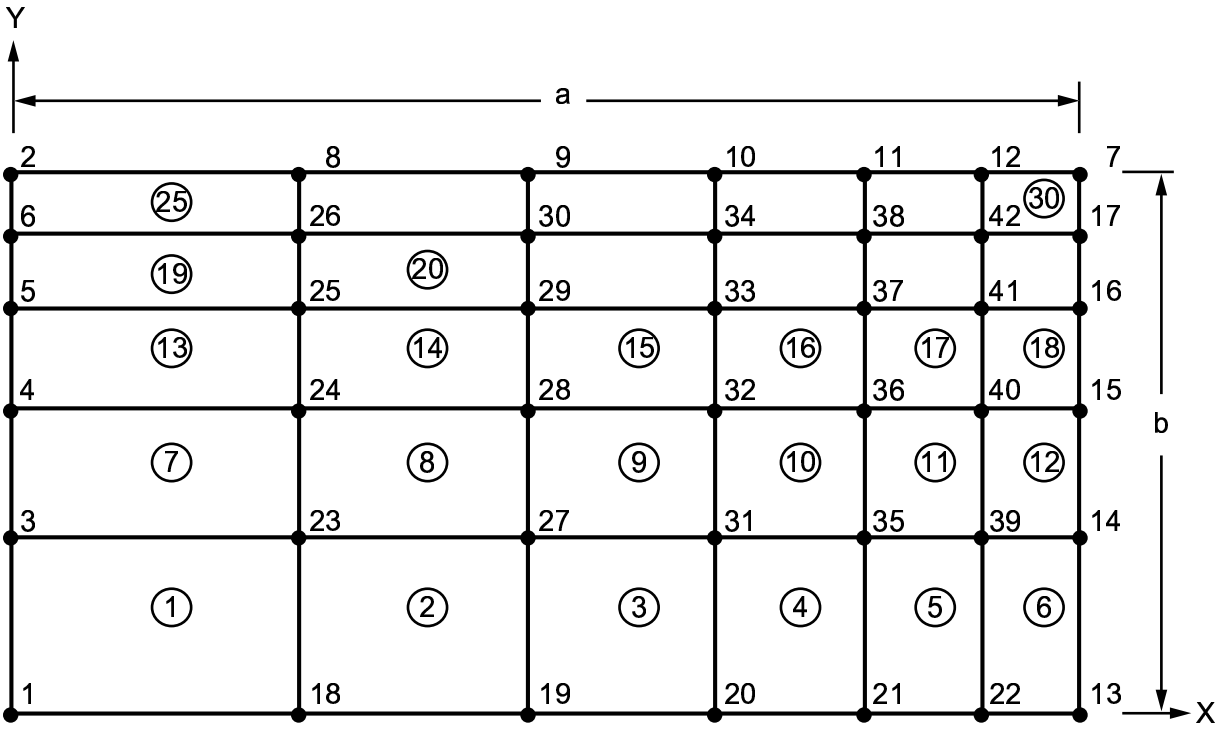

Representative Finite Element Model

Material Properties	**Geometric Properties**
k_x = 20 Btu/hr-ft-°F	a = 2 in = (2/12) ft
k_y = 3.6036 Btu/hr-ft-°F	b = 1 in = (1/12) ft
γ = 400 lb/ft^3	**Loading**
c = 0.009009 Btu/lb-°F	T_o = 500°F
h = 240 Btu/hr-ft^2-°F	T_f = 100°F

Analysis Assumptions and Modeling Notes

A nonuniform grid (based on a geometric progression) is used in both X and Y directions to model a quarter of the bar cross-section. Automatic time stepping is used. The initial integration time step = (3/3600)(1/40) is greater than ($\delta^2/4\alpha$), where δ is the shortest element length (0.0089 ft) and α is the thermal diffusivity ($k_y/\gamma c$ = 1.0 ft^2/hr).

Results Comparison

Time = 3 sec. (=0.0008333 hr.)	Target[1]	ANSYS	Ratio
T, °F (Node 1)	459.	457.	1.00
T, °F (Node 7)	151.	158.	1.05
T, °F (Node 13)	279.	288.	1.03
T, °F (Node 2)	202.	204.	1.01

1. Based on graphical estimates.

VM114: Temperature Response to Increasing Temperature

Overview

Reference:	P. J. Schneider, *Conduction Heat Transfer*, 2nd Printing, Addison-Wesley Publishing Co., Inc., Reading, MA, 1957, pp. 274-275, article 11-2, eq. 11-9.
Analysis Type(s):	Thermal Analysis (**ANTYPE** = 4)
Element Type(s):	3-D Conduction Bar Elements (LINK33)
Input Listing:	vm114.dat

Test Case

A semi-infinite solid, initially at a temperature T_o, is subjected to a linearly rising surface temperature $T_s = 3600$ t, where T_s is in °F and t is time in hours. Determine the temperature distribution in the solid at t = 2 min.

Figure 114.1 Linearly-rising Surface Temperature Problem Sketch

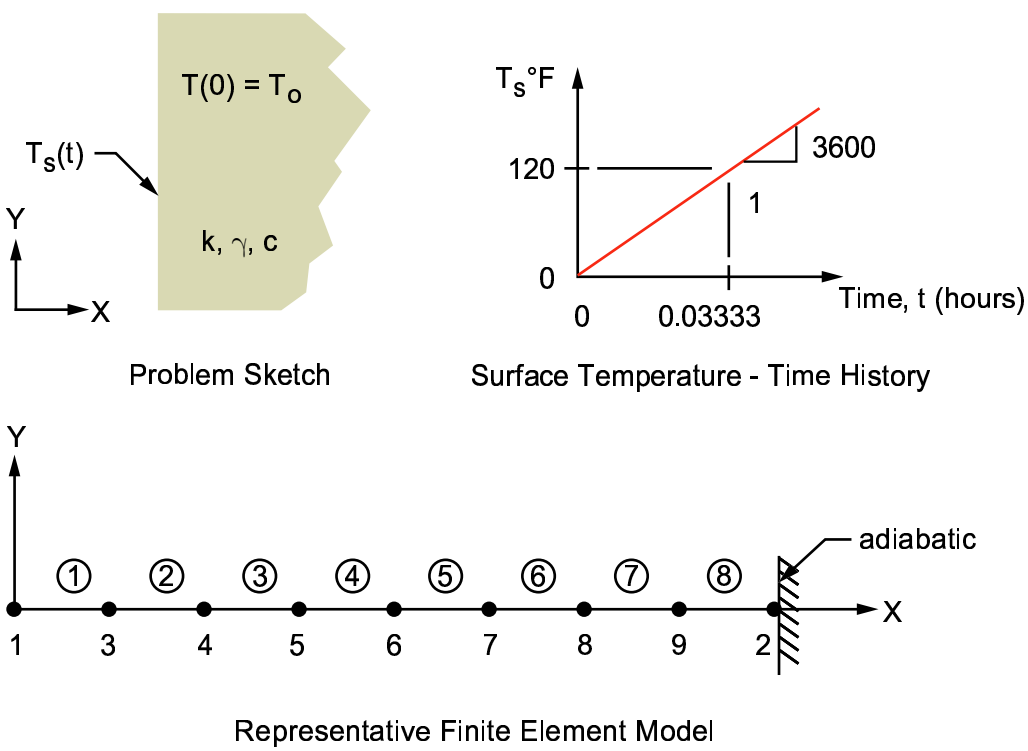

Material Properties	**Loading**
k = 10 Btu/hr-ft-°F γ = 500 lb/ft^3 c = 0.2 Btu/lb-°F	T_o = 0°F @ t = 0 T_s = 120°F @ t = 2 (ramped) (see Figure 114.2: "Temperature vs. Time Plot")

Analysis Assumptions and Modeling Notes

A nonuniform mesh is used to model the nonlinear thermal gradient through the solid. An arbitrary area of 1 ft^2 is used for the elements. The length of the model is taken as 0.3 ft assuming that no significant temperature change occurs at the interior end point (Node 2) during the time period of interest (2 min). This assumption is validated by the temperature of node 2 at the end of the transient analysis.

Automatic time stepping is used with an initial integration time step (0.03333/20 = 0.001666 hr) greater than $\delta^2/4\alpha$, where δ = minimum element conducting length (0.0203 ft) and α = thermal diffusivity (= k/ γc = 0.1 ft^2/hr).

Note that the KBC key (not input) defaults to zero, resulting in the surface temperature load being ramped linearly to its final value.

POST26 and POST1 are used to obtain the temperature history at the node locations, and the temperature distribution at t = 0.03333 hr, respectively.

Results Comparison

Time = 0.03333 hr		Target	ANSYS	Ratio
T, °F (Node 1)	@ x = 0.0 ft	120.00	120.00	1.000
T, °F (Node 3)	@ x = 0.0203 ft	79.32	79.07	0.997
T, °F (Node 4)	@ x = 0.0441 ft	46.62	46.35	0.994
T, °F (Node 5)	@ x = 0.0719 ft	23.44	23.25	0.992
T, °F (Node 6)	@ x = 0.1044 ft	9.51	9.52	1.00
T, °F (Node 2)	@ x = 0.3 ft	0.0	0.03	-

Figure 114.2 Temperature vs. Time Plot

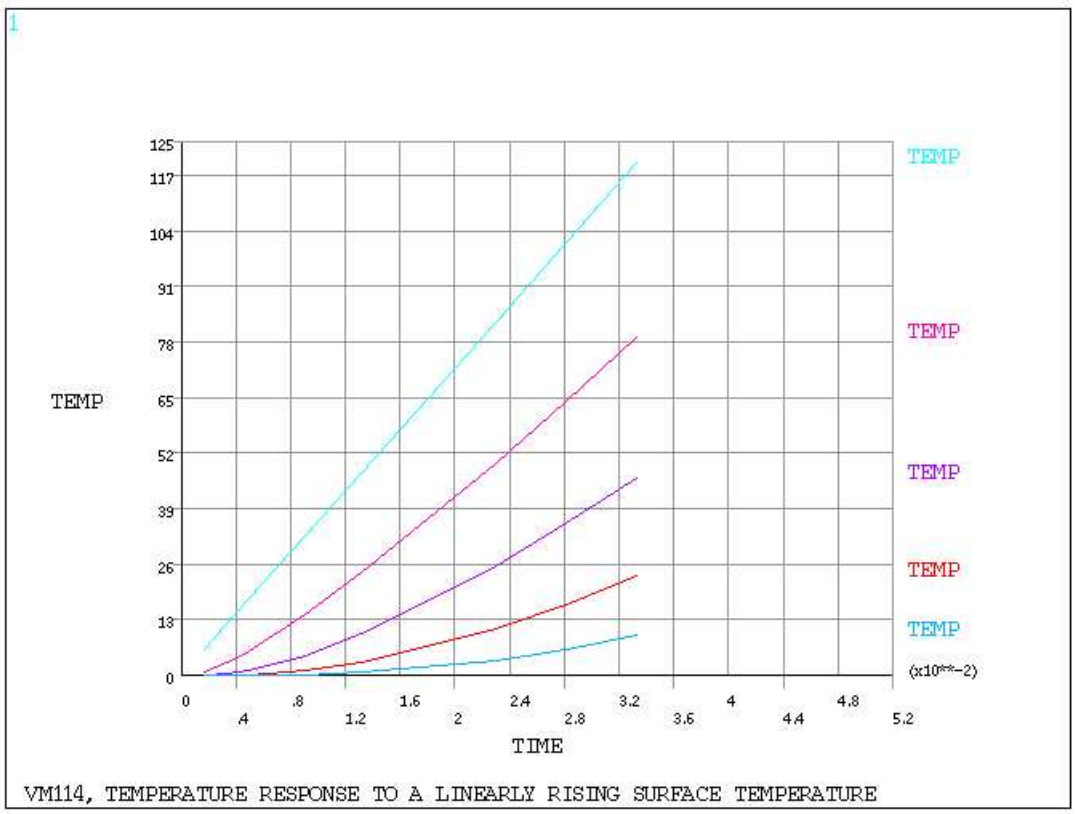

VM115: Thermal Response of a Heat-generating Slab

Overview

Reference:	P. J. Schneider, *Conduction Heat Transfer*, 2nd Printing, Addison-Wesley Publishing Co., Inc., Reading, MA, 1957, pg. 283, article 11-4, eq. (11-21) and pg. 309, article 12-8.
Analysis Type(s):	Thermal Analysis (**ANTYPE** = 4)
Element Type(s):	2-D Conduction Bar Elements (LINK32)
Input Listing:	vm115.dat

Test Case

An infinite plate of thickness ℓ, initially at a uniform temperature T_o, is subjected to a sudden uniformly distributed heat generation rate $\dddot{q}$ and a surface temperature T_s. Determine the temperature distribution in the plate after 12 minutes.

Figure 115.1 Heat-Generating Slab Problem Sketch

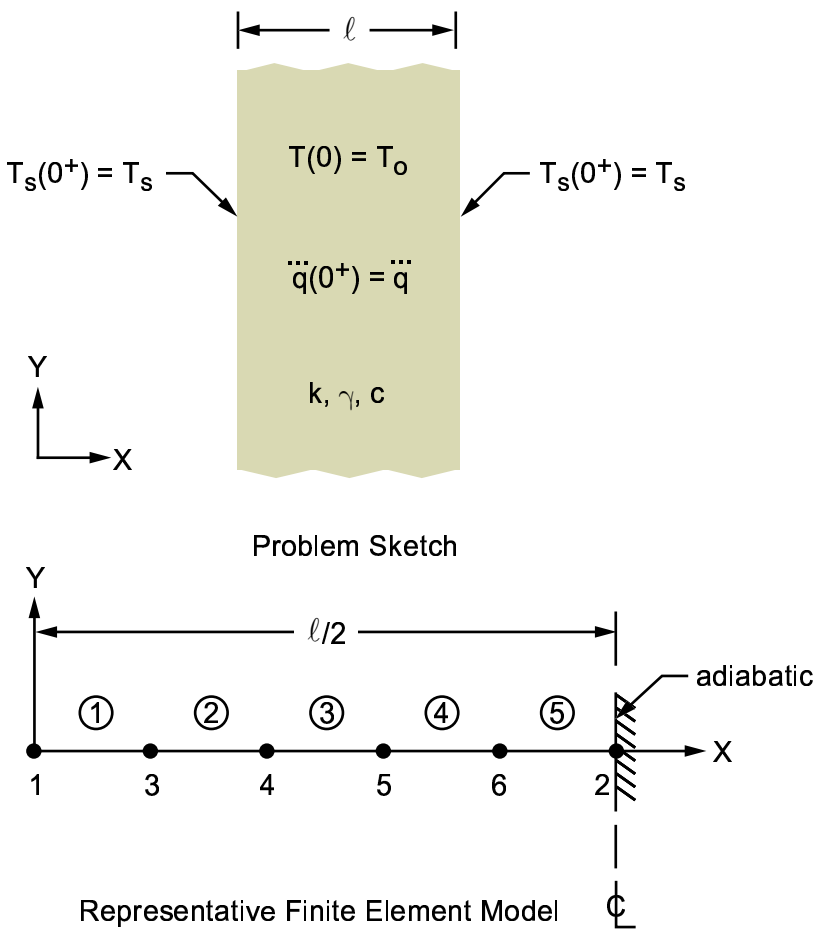

Material Properties	Geometric Properties	Loading
k = 20 Btu/hr-ft-°F γ = 500 lb/ft^3 c= 0.2 Btu/lb-°F	ℓ = 1 ft	T_o = 60°F T_s = 32°F (t>0) $\dddot{q}$ = 4 x 10^4 Btu/hr-ft^3

Analysis Assumptions and Modeling Notes

A 1 ft^2 area is used for the conduction elements. Due to symmetry only half of the plate is modeled. Automatic time stepping is used. The initial integration time step (0.01 hr) is based on $\approx \delta^2/4\alpha$, where δ is the element length (0.1 ft) and α is the thermal diffusivity ($k/\gamma c$ = 0.2 ft^2/hr).

Results Comparison

Time = 0.2 hr	Target	ANSYS	Ratio
T, °F (Node 1)	32.00	32.00	1.000
T, °F (Node 3)	75.75	75.37	0.995
T, °F (Node 4)	103.99	103.26	0.993
T, °F (Node 5)	120.80	119.79	0.992
T, °F (Node 6)	129.46	128.27	0.991
T, °F (Node 2)	132.10	130.85	0.991

Using up to three terms of the infinite series solution in equation 11-21 of P. J. Schneider, *Conduction Heat Transfer*.

VM116: Heat Conducting Plate with Sudden Cooling

Overview

Reference:	F. Kreith, *Principles of Heat Transfer*, 2nd Printing, International Textbook Co., Scranton, PA, 1959, pg. 161, ex. 4-11.
Analysis Type(s):	Thermal Analysis (**ANTYPE** = 4)
Element Type(s):	Convection Link Elements (LINK34) 2-D Conduction Bar Elements (LINK32)
Input Listing:	vm116.dat

Test Case

A large plate of thickness ℓ initially has its left surface at temperature T_1 and the other surface at temperature T_2. The left surface is suddenly subjected to an environment temperature of $T^\infty = T_2$. The convection coefficient on this side is given by $h = 2.0 + 0.02\,(T - T^\infty)$ where T is the surface temperature (function of time). Determine T after 7 hours. Graphically display the variation of T with time and the temperature distribution across the plate at 7 hours.

Figure 116.1 Heat Conducting Plate Problem Sketch

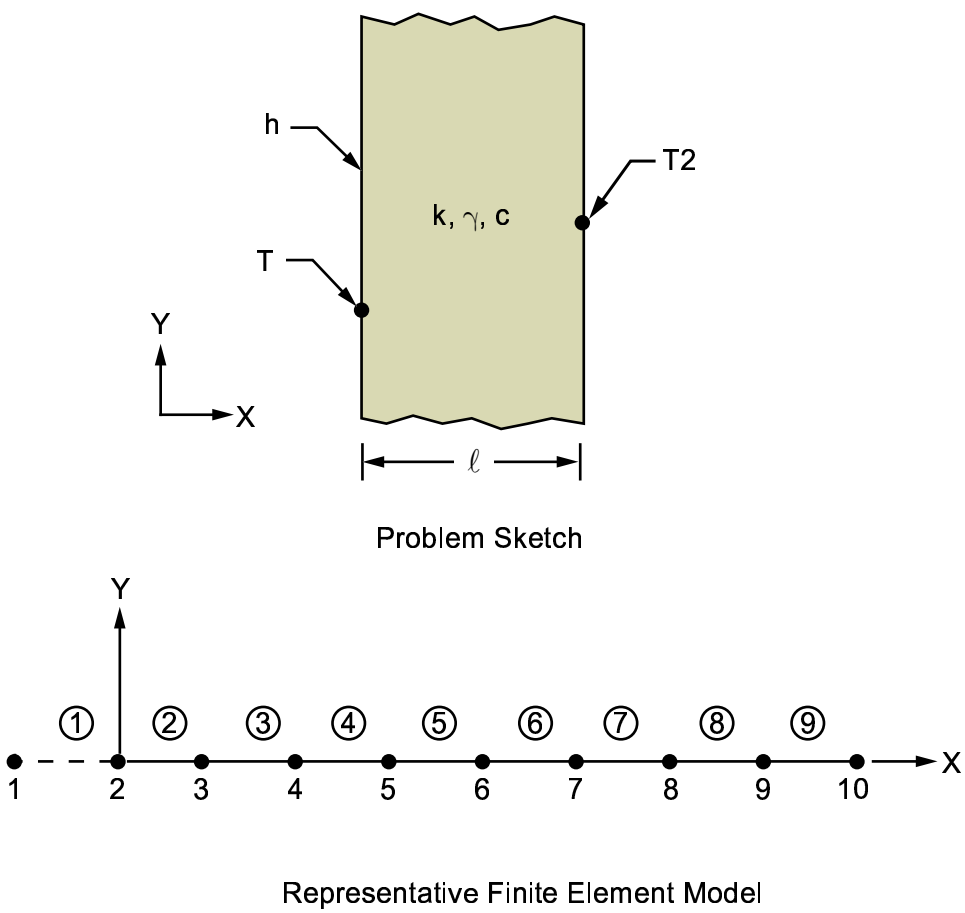

Material Properties	Geometric Properties	Loading
k = 2 Btu/hr-ft-°F γ = 800 lb/ft^3 c = 0.833 Btu/lb-°F	ℓ = 8 in = (8/12) ft	T_1 = 500°F T_2 = 100°F

Analysis Assumptions and Modeling Notes

A 1 ft^2 area is assumed for the conduction elements. The length of the convection element is taken as zero (arbitrarily selected). The finite element model is made the same as the theoretical model for a direct comparison. A steady-state solution is done in the first load step. Automatic time stepping is used. The initial integration time step (7/20 = 0.35 hr) is based on $\approx \delta^2/4\alpha$, where δ is the nodal distance within the element (1/12 ft), and α is the thermal diffusivity $k/\gamma c$ = 0.003 ft^2/hr). POST26 and POST1 are used to obtain the surface temperature history and the temperature distribution at the final time step, respectively.

Results Comparison

Time = 7 hr	Target	ANSYS	Ratio
T, °F (at X = 0.0 in)	285.[1]	293.[2]	1.03

1. Based on graphical estimates
2. Temperature at Node 2

Figure 116.2 Surface Temperature History Plot

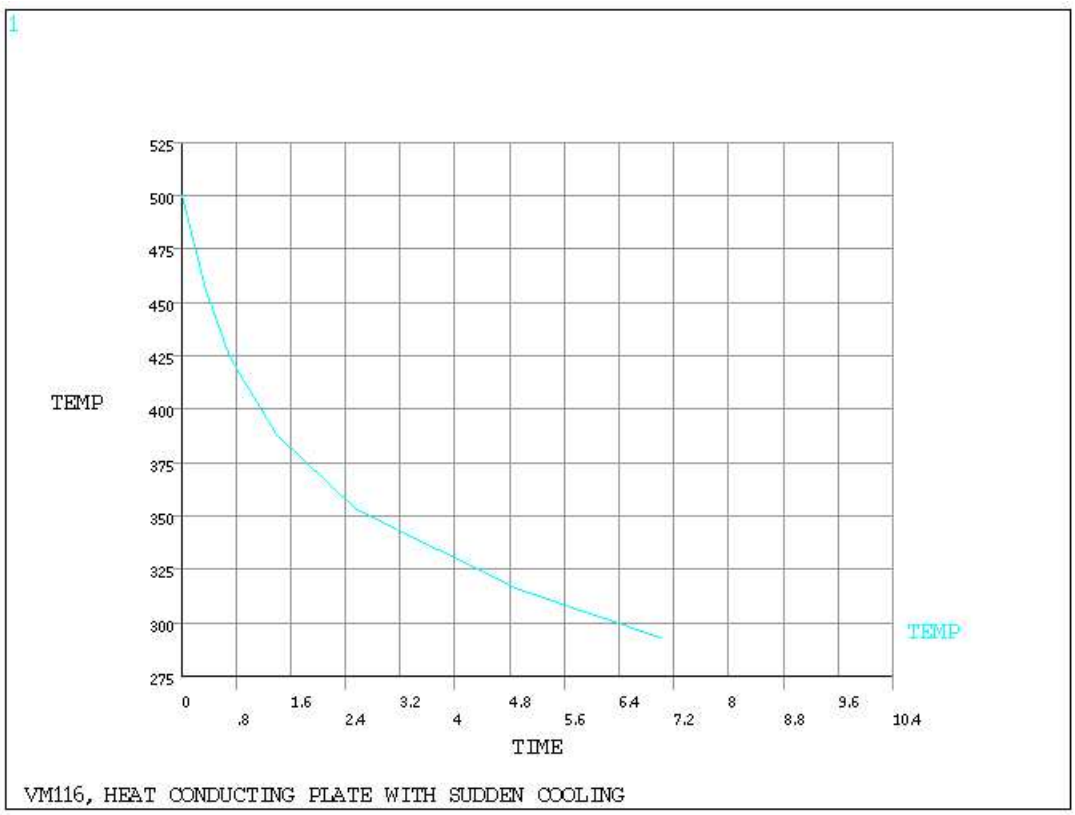

Figure 116.3 Temperature Distribution Across Thickness Plot

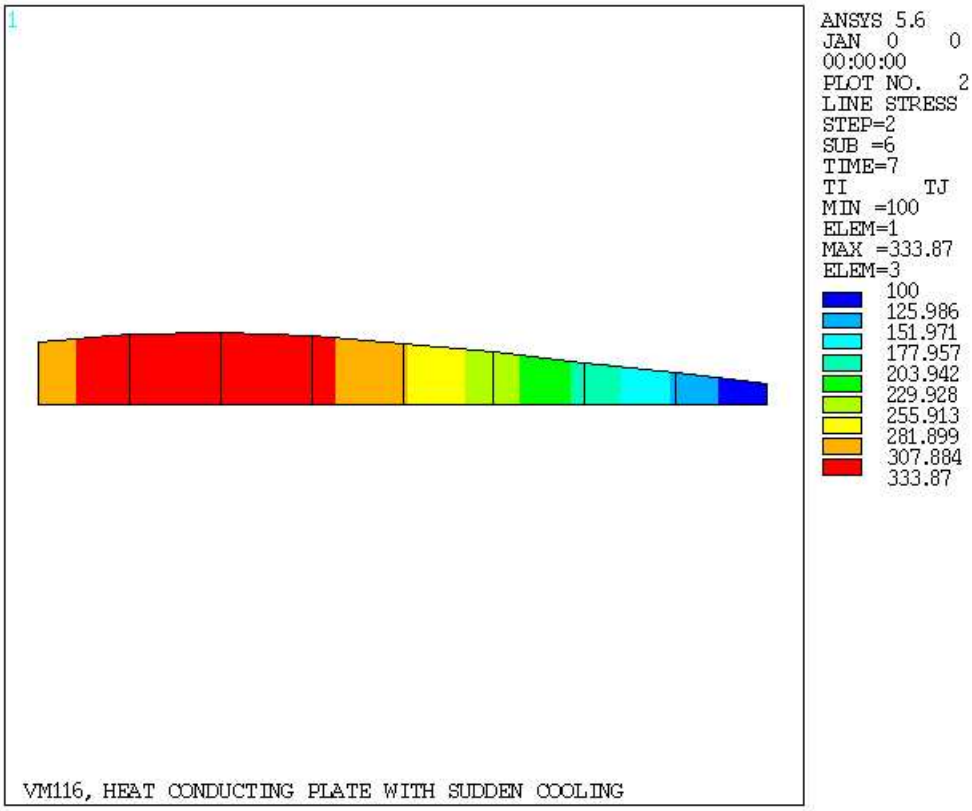

VM117: Electric Current Flowing in a Network

Overview

Reference:	A. E. Fitzgerald, D. E. Higginbotham, *Basic Electrical Engineering*, 2nd Edition, McGraw-Hill Book Co., Inc., New York, NY, 1957, pg. 22, ex. 1-11.
Analysis Type(s):	Thermal (electrical) Analysis (**ANTYPE** = 0)
Element Type(s):	Coupled Thermal-Electric Line Elements (LINK68) Electric Circuit Element (CIRCU124)
Input Listing:	vm117.dat

Test Case

The network shown below is that of an unbalanced bridge used in measuring resistance. With the circuit parameters as specified, determine the current $I_{a\text{-}b}$ flowing in each branch (from a to b) and the voltage at each node.

Figure 117.1 Electric Current Problem Sketch

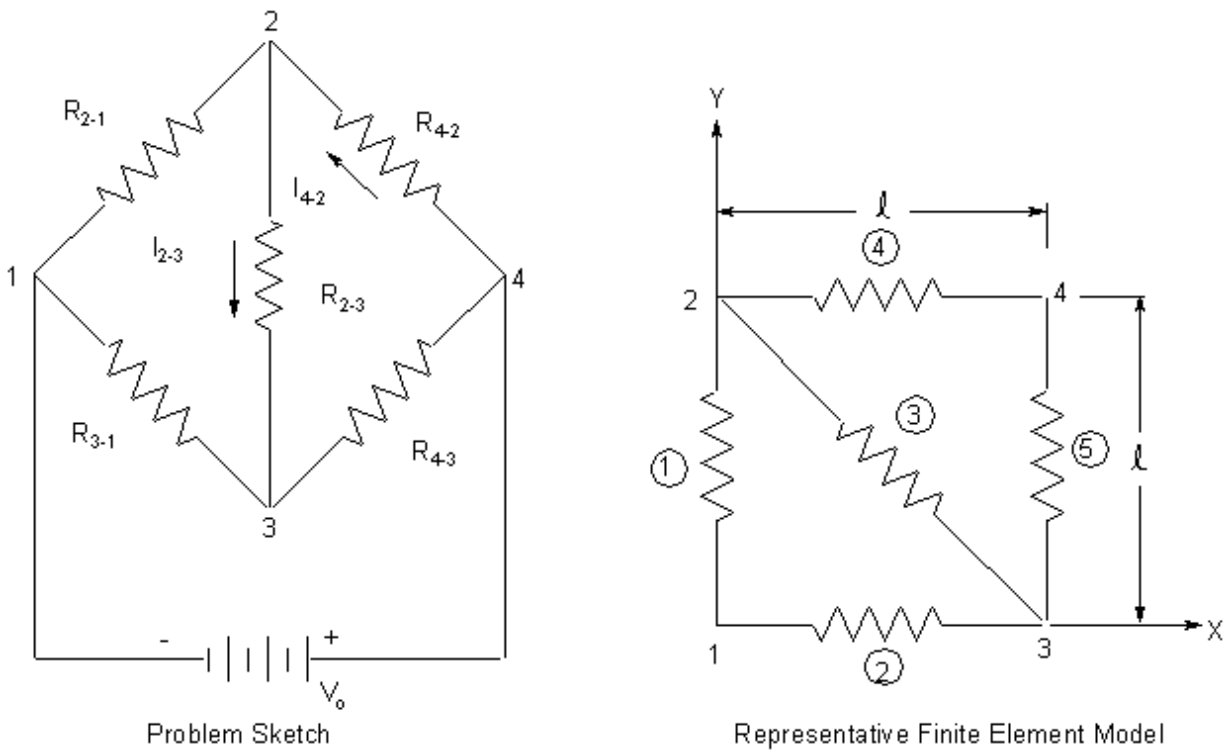

Material Properties	**Loading**
$R_{2\text{-}1} = 20\ \Omega$	$V_o = 100$ volts
$R_{3\text{-}1} = 10\ \Omega$	
$R_{2\text{-}3} = 9\ \Omega$	
$R_{4\text{-}2} = 30\ \Omega$	
$R_{4\text{-}3} = 90\ \Omega$	

Analysis Assumptions and Modeling Notes

The branch resistance is implicitly input as the element area (real constant). A convenient geometric configuration is assumed (ℓ = 1 ft) and the material resistivity is taken as 1 ohm-ft (input as material property RSVX). The areas are calculated from the relation: $A = \rho \ell / R$, where A = area of element (ft^2), ℓ = length of element (ft), ρ = resistivity (ohm-ft), R = given resistance (ohm).

Node 1 is assumed to be the ground node for reference. POST1 is used to extract the currents in each branch. A negative value indicates that current flow is opposite to the assumed direction (Node I to J of the element).

Results Comparison

LINK68	Target	ANSYS	Ratio
V_1, volts	0.0	0.0	-
V_2, volts	28.0	28.0	1.00
V_3, volts	19.0	19.0	1.00
V_4, volts	100.0	100.0	1.00
I_{2-1}, amps	1.4	1.4	1.00
I_{3-1}, amps	1.9	1.9	1.00
I_{2-3}, amps	1.0	1.0	1.00
I_{4-2}, amps	2.4	2.4	1.00
I_{4-3}, amps	0.9	0.9	1.00
I_{1-4}, amps	3.3	3.3	1.00

CIRCU124	Target	ANSYS	Ratio
V_1, volts	0.0	0.0	-
V_2, volts	28.0	28.0	1.00
V_3, volts	19.0	19.0	1.00
V_4, volts	100.0	100.0	1.00
I_{2-1}, amps	1.4	1.4	1.00
I_{3-1}, amps	1.9	1.9	1.00
I_{2-3}, amps	1.0	1.0	1.00
I_{4-2}, amps	2.4	2.4	1.00
I_{4-3}, amps	0.9	0.9	1.00
I_{1-4}, amps	3.3	3.3	1.00

VM118: Centerline Temperature of a Heat-generating Wire

Overview

ANSYS 10.0

Reference:	W. M. Rohsenow, H. Y. Choi, *Heat, Mass and Momentum Transfer*, 2nd Printing, Prentice-Hall, Inc., Englewood Cliffs, NJ, 1963, pg. 106, ex. 6.5.
Analysis Type(s):	Thermal Analysis (CIRCU124 = 0)
Element Type(s):	2-D Thermal Solid Elements (PLANE55) 3-D Thermal Solid Elements (SOLID70)
Input Listing:	vm118.dat

Test Case

Determine the centerline temperature $T_{\mathbb{C}}$ and the surface temperature T_s of a bare steel wire generating heat at the rate $\dddot{q}$. The surface convection coefficient between the wire and the air (at temperature T_a) is h. Also determine the heat dissipation rate q.

Figure 118.1 Heat-generating Wire Problem Sketch

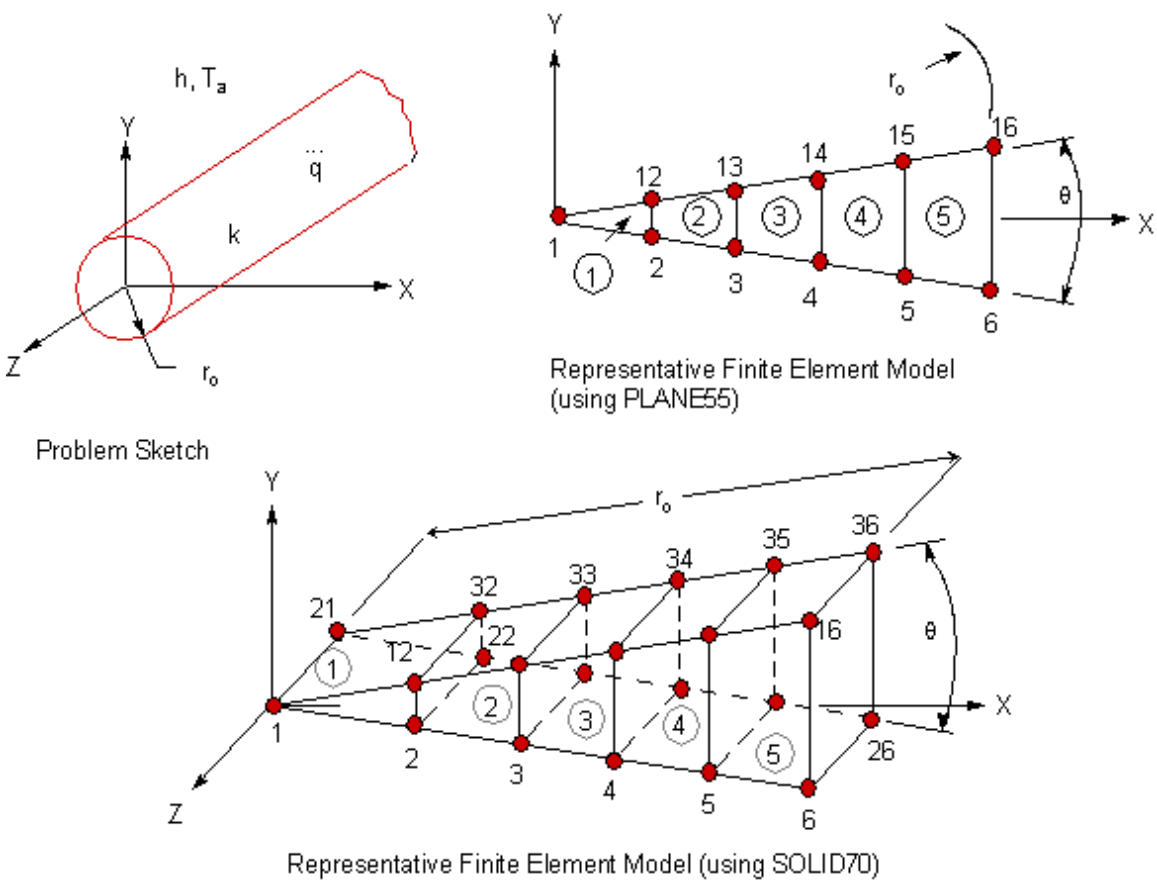

Material Properties	**Geometric Properties**	**Loading**
k = 13 Btu/hr-ft-°F h = 5 Btu/hr-ft^2-°F	r_o = 0.375 in = 0.03125 ft	T_a = 70°F $\dddot{q}$ = 111311.7 Btu/hr-ft^3

Analysis Assumptions and Modeling Notes

The problem is solved first using conducting area elements (PLANE55) and then using conducting solid elements (SOLID70). Since the problem is axisymmetric, only a one-element sector is needed. A small angle $\Theta = 10°$ is used for approximating the circular boundary with a straight-sided element. Nodal coupling is used to ensure circumferential symmetry. The solution is based on a wire 1 foot long (Z-direction). POST1 is used to extract results from the solution phase. Total heat dissipation is computed parametrically at the outer surface as HRATE using q = h.area.(T_s - T_a).

Results Comparison

		Target	ANSYS	Ratio
PLANE55	Centerline Temperature, °F	419.9	418.6	0.997
	T_s, °F	417.9	416.5	0.997
	q, Btu/hr	341.5	339.8	0.995
SOLID70	Centerline Temperature, °F	419.9	418.6	0.997
	T_s, °F	417.9	416.5	0.997
	q, Btu/hr	341.5	339.8	0.995

VM119: Centerline Temperature of an Electrical Wire

Overview

Reference:	W. M. Rohsenow, H. Y. Choi, *Heat, Mass and Momentum Transfer*, 2nd Printing, Prentice-Hall, Inc., Englewood Cliffs, NJ, 1963, pg. 106, ex. 6.5.
Analysis Type(s):	Thermal Analysis (**ANTYPE** = 0)
Element Type(s):	2-D Coupled Thermal-Electric Solid Elements (PLANE67) 3-D Coupled Thermal-Electric Solid Elements (SOLID69) 2-D Coupled-Field Solid Elements (PLANE223) 3-D Coupled-Field Solid Elements (SOLID226)
Input Listing:	vm119.dat

Test Case

Determine the centerline temperature $T_{\mathbb{C}}$ and the surface temperature T_s of a bare steel wire carrying a current I and having a resistance R. The surface convection coefficient between the wire and the air (at temperature T_a) is h. Also determine the heat dissipation rate q.

Figure 119.1 Electrical Wire Problem Sketch

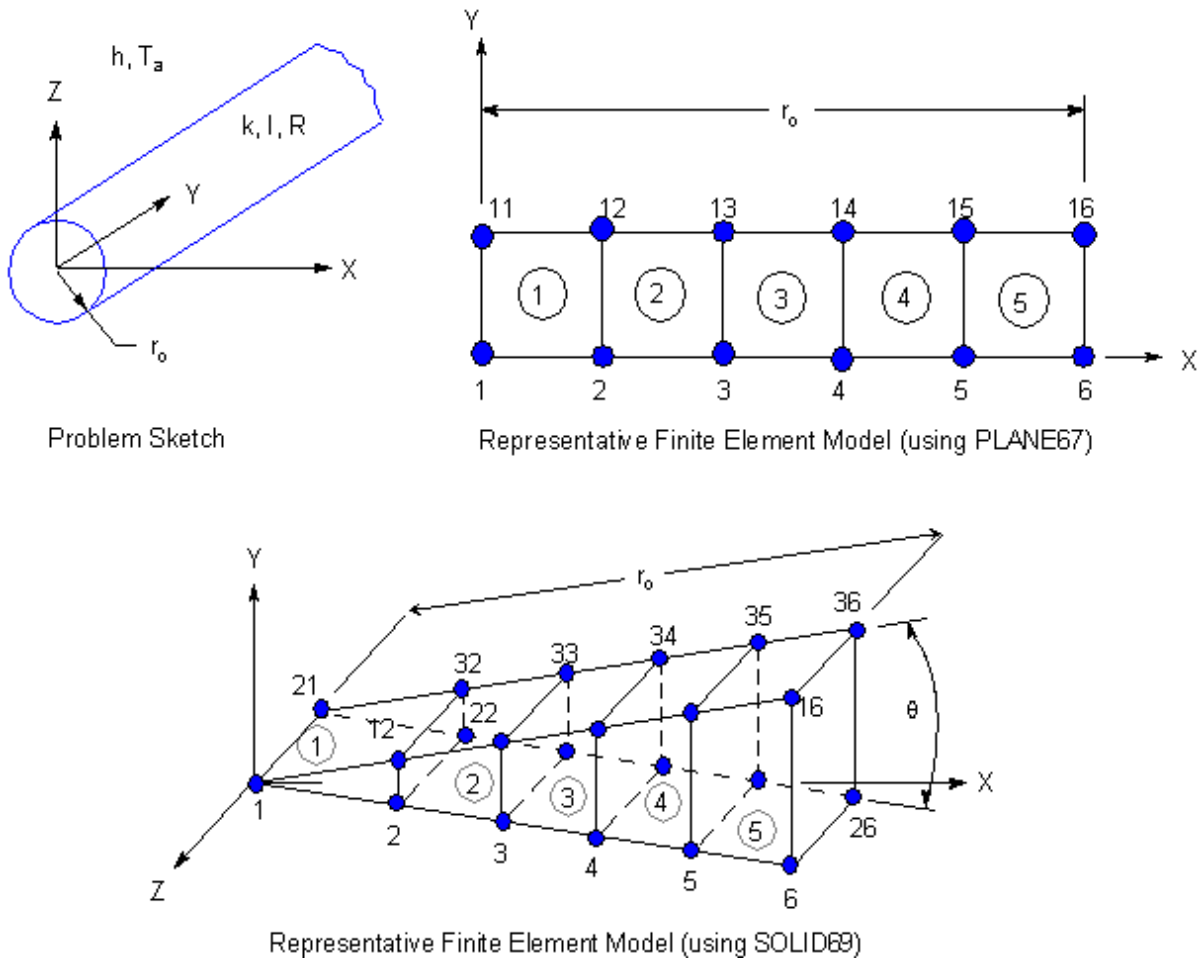

Material Properties	Geometric Properties	Loading
k = 13 Btu/hr-ft °F h = 5 Btu/hr-ft^2-°F R = 0.0001 Ω/ft	r_o = 0.375 in = 0.03125 ft	T_a = 70°F I = 1000 A

Analysis Assumptions and Modeling Notes

The problem is solved first using thermal-electric axisymmetric elements (PLANE67, PLANE223) and then using thermal-electric solid elements (SOLID69, SOLID226).

A 1 foot axial length is chosen for convenience. Nodal coupling is used to ensure axial symmetry (as well as circumferential symmetry in the case of (SOLID69). The voltage drop per foot is IR = 0.1 volt/ft. The resistivity ρ is calculated as $\rho = RA/L = (0.0001)(\pi)(0.03125)^2/(1) = 3.06796 \times 10^{-7}$ Ω-ft.

A conversion factor 3.415 (Btu/hr)/W must be included in the resistivity ρ so that the Joule heat units match the thermal units $\rho/3.415 = 8.983782 \times 10^{-8}$. Current printout is divided by 3.415 to get electrical (amp) units. The steady-state convergence procedures are used.

For the thermal-electric axisymmetric elements (SOLID69), nodes 1 through 16 are assumed to be ground nodes for reference. The solution is based on a unit radian model. Since the problem is axisymmetric, only a one-element sector is needed. A small angle Θ = 10° is used for approximating the circular boundary with a straight-sided element.

POST1 is used to extract results from the solution phase. Total heat dissipation is computed parametrically at the outer surface as HRATE using $q = h.area.(T_s-T_a)$.

Results Comparison

		Target[1]	ANSYS	Ratio
PLANE67	Centerline Temperature, °F	419.9	420.0	1.000
	T_s, °F	417.9	417.8	1.000
	q, Btu/hr	341.5	341.5[2]	1.000
SOLID69	Centerline Temperature, °F	419.9	418.6	0.997
	T_s, °F	417.9	416.5	0.997
	q, Btu/hr	341.5	339.8[3]	0.995
PLANE223	Centerline Temperature, °F	419.9	420.0	1.000
	T_s, °F	417.9	417.8	1.000
	q, Btu/hr	341.5	341.5	1.000
SOLID226	Centerline Temperature, °F	419.9	418.6	0.997
	T_s, °F	417.9	416.5	0.997
	q, Btu/hr	341.5	339.8	0.995

1. Solution recalculated
2. Total Joule heat rate/radian x 2 π

3. Calculated from heat flow rate per 10° sector x 36 sectors

VM120: Microstrip Transmission Line Capacitance

Overview

Reference:	J. Beren, R. Kaires, "EMGAP Solves Electromagnetic Problems Using Finite Element Analysis", *Tektronix Internal Publication*, Beaverton, OR, May 1983.
Analysis Type(s):	Electrostatic Analysis (**ANTYPE** = 0)
Element Type(s):	2-D 8-Node Electrostatic Solid Element (PLANE121)
Input Listing:	vm120.dat

Test Case

A shielded microstrip transmission line consists of a substrate, microstrip, and a shield. The strip is at a potential V_1, and the shield is at a potential V_0. Determine the capacitance of the transmission line.

Figure 120.1 Microstrip Transmission Line Problem Sketch

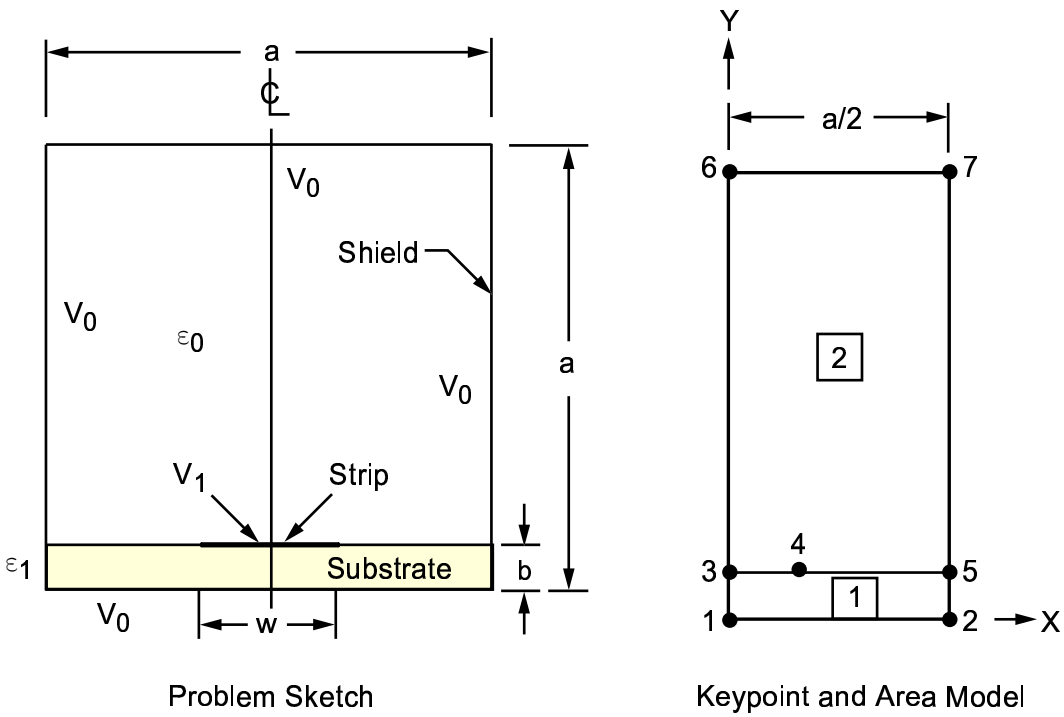

Material Properties	Geometric Properties	Loading
$\varepsilon_0 = 8.85 \times 10^{-12}$ F/m $\varepsilon_1 = 8.85 \times 10^{-11}$ F/m	a = 10 cm b = 1 cm w = 1 cm	$V_1 = 1.5$ v $V_0 = 0.5$ v

Analysis Assumptions and Modeling Notes

The capacitance of the device can be calculated from electrostatic energy and the applied potential difference as $W_e = 1/2\ C\ (V_1\text{-}V_o)^2$ where W_e is the electrostatic energy and C is the capacitance. The electrostatic energy is available by summing the energies for all the elements in the model in POST1. Additional postprocessing includes displaying equipotential lines and the electric field as vectors.

Results Comparison

	Target	ANSYS	Ratio
Capacitance, pF/m	178.1	179.5	1.008

VM121: Laminar Flow Through a Pipe with Uniform Heat Flux

Overview

Reference:	F. M. White, *Fluid Mechanics*, McGraw-Hill Book Co., Inc., New York, NY, 1979. F. P. Incropera, D. P. DeWitt, *Fundamentals of Heat Transfer*, John Wiley & Sons, 1981.
Analysis Type(s):	CFD Thermal Analysis (**FLOTRAN**)
Element Type(s):	2-D Fluid-Thermal Element (FLUID141)
Input Listing:	vm121.dat

Test Case

Pressure-driven flow in a straight duct of circular cross-section with radius R. Inlet and outlet boundaries have uniform, dissimilar pressure boundary conditions. The mean fluid temperature at the inlet is $T_{m,i}$. The pipe is subjected to a uniform wall heat flux, q'', throughout its length, L.

From the Velocity Field Determine

VX_c = centerline axial velocity

VX_m = mean axial velocity

Re = Reynolds number

$\dot{m}$ = mass flow rate

τ_w = wall shear stress

From the Temperature Field Determine

$L_{E,T}$ = thermal entry length

$T_{m,o}$ = outlet mean temperature

$T_{w,o}$ = outlet wall temperature

$T_{c,o}$ = outlet centerline temperature

Fluid Properties	**Geometric Properties**
Mercury (Hg) at 300K	R = 2.5 mm
ρ = 13,529 kg/m^3	L = 0.1 m
μ = 1.523 x 10^{-3} kg/m-sec	**Loading**
k = 8.54 W/m-K	ΔP = 1.0 Pa
C_p = 139.3 J/kg-K	$T_{m,i}$ = 300 K
Pr = 0.025 (liquid metal)	q''= 5000 W/m^2

Figure 121.1 Pipe with Uniform Heat Flux Problem Sketch

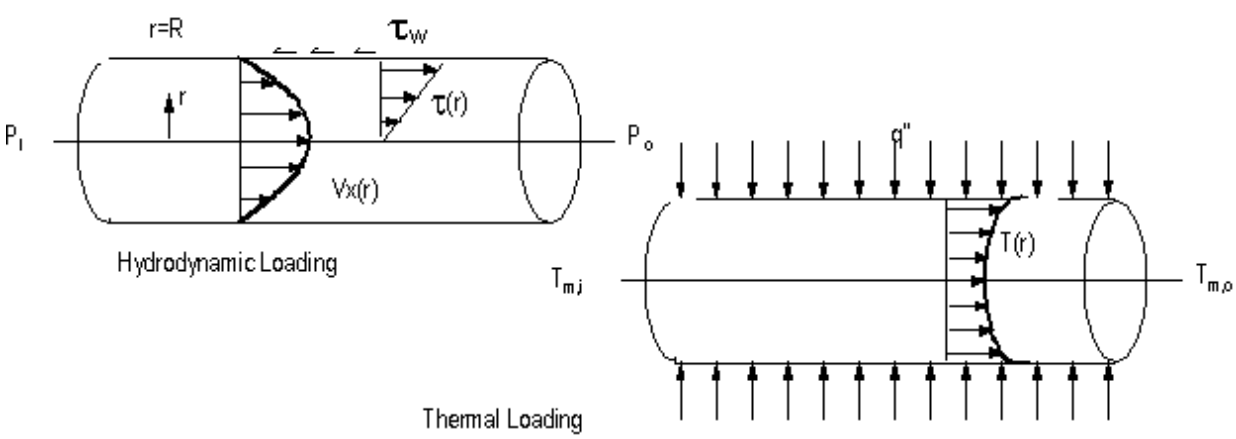

Assumptions

- steady-state flow
- incompressible fluid
- radial (VY) and circumferential (VZ) velocities are zero
- axial (VX) velocity is a function of radius (Y) only
- axial pressure gradient, $\Delta P/L$, is a negative constant
- pipe wall has negligible thermal resistance
- no body forces
- fluid properties are constant

Velocity Solution

For steady-state conditions, the velocity field for this problem is fully-developed throughout the pipe. The velocity profile follows the "Hagen-Poiseuille" paraboloid, given by F. M. White, *Fluid Mechanics*:

$$VX(r) = \frac{R^2}{4\mu}(-\Delta P/L)\left[1-\left(\frac{r}{R}\right)^2\right]$$

From the above, the centerline velocity is:

$$VX_c = VX(r)_{r=0} = 1.026\,\mathrm{cm/sec}$$

The mean velocity is defined as:

$$VX_m \equiv \int_{A_F} \frac{VX(r)dA_F}{A}$$

$$= \frac{2}{R^2}\int_0^R VX(r)\,r\,dr \qquad \text{(integrated in POST1)}$$

$$= \frac{1}{2}VX_c = 0.513\,\mathrm{cm/sec}$$

where:

A_F = flow area

The flow Reynold's number is:

$$Re = \frac{2\rho\,VX_m\,R}{\mu} = 228 \qquad \text{(laminar flow)}$$

The mass flow rate is:

$$\dot{m} = \rho\,VX_m\,A_F = 0.00136\,\mathrm{kg/sec}$$

The wall shear stress is:

$$\tau_w = \mu \frac{d\,VX(r)}{dr}$$
$$= \frac{1}{2}\frac{\Delta P}{L} R = 0.0125\,\text{Pa}$$

Temperature Solution

As the uniform-temperature fluid enters the pipe, convection heat transfer occurs and a thermal boundary layer begins development along the pipe wall. Since the surface heat flux is constant, a thermally-developed flow condition is eventually reached downstream. For laminar flow, this thermal entry length may be expressed by F. P. Incropera, D. P. DeWitt, *Fundamentals of Heat Transfer* as:

$$L_{E,T} \approx 0.05\,\text{Re}\,\text{Pr}\,D = 0.143\,\text{cm} = (1.4\%\,\text{of}\,L)$$

where:

D = 2R

The mean temperature at any cross-section is defined by F. P. Incropera, D. P. DeWitt, *Fundamentals of Heat Transfer* as:

$$T_m = \frac{2}{VX_m R^2}\int_0^R VX(r)\,T(r)\,r\,dr \quad \text{(integrated in POST1)}$$

Applying conservation of energy, the heat input from the applied flux should balance the heat removed through fluid mass transport, or:

$$q'' A_s = \dot{m} C_p (T_{m,o} - T_{m,i})$$

where:

A_s = wall surface area

The outlet mean temperature is then:

$$T_{m,o} = T_{m,i} + \frac{q'' A_s}{\dot{m} C_p} = 341.4\,\text{K}$$

To determine the outlet wall temperature, we employ Newton's law of cooling (see F. P. Incropera, D. P. DeWitt, *Fundamentals of Heat Transfer*):

$$q'' = h(T_{w,o} - T_{m,o})$$

where:

h = convection film coefficient

For laminar, thermally-developed conditions in a circular pipe with a constant heat flux, the Nusselt number is constant, independent of Re, Pr and axial location. It is known to be:

$$\text{Nu} \equiv \frac{hD}{k} = 4.36$$

The outlet wall temperature is then:

$$T_{w,o} = T_{m,o} + \frac{q'' A_s}{h} = 342.1K$$

where:

$$h = \frac{4.36K}{D}$$

For the thermally-developed region with constant surface heat flux, the temperature profile is of the form as described in F. P. Incropera, D. P. DeWitt, *Fundamentals of Heat Transfer*:

$$T(r) = T_w - \frac{2VX_m R^2}{\alpha}\left(\frac{dT_m}{dx}\right)\left[\frac{3}{16} + \frac{1}{16}\left(\frac{r}{R}\right)^4 - \frac{1}{4}\left(\frac{r}{R}\right)^2\right]$$

where:

$$\alpha = \frac{k}{\rho Cp}$$

Since

$$L_{E,T} \ll L, \left(\frac{dT_m}{dx}\right)$$

is assumed constant over the entire pipe length, or:

$$\frac{dT_m}{dx} = \frac{(T_{m,o} - T_{m,i})}{L} = 414K/m$$

The outlet centerline temperature is then:

$$T_{c,o} = T(r)_{r=0} = 341.0K$$

Results Comparison

		Target	ANSYS	Ratio
VX_c	(cm/sec)	1.026	1.030	1.004
VM_m	(cm/sec)	0.513	0.512	0.998
Mass Flow Rate	(kg/sec)	0.00136	0.00136	1.000
Wall Shear Stress	(Pa)	0.0125	0.01214	0.971
$T_{m,o}$	(K)	341.4	340.8	0.998
$T_{w,o}$	(K)	342.1	341.4	0.998
$T_{c,o}$	(K)	341.0	340.4	0.998

Figure 121.2 Laminar Flow Through a Pipe with Uniform Heat Flux

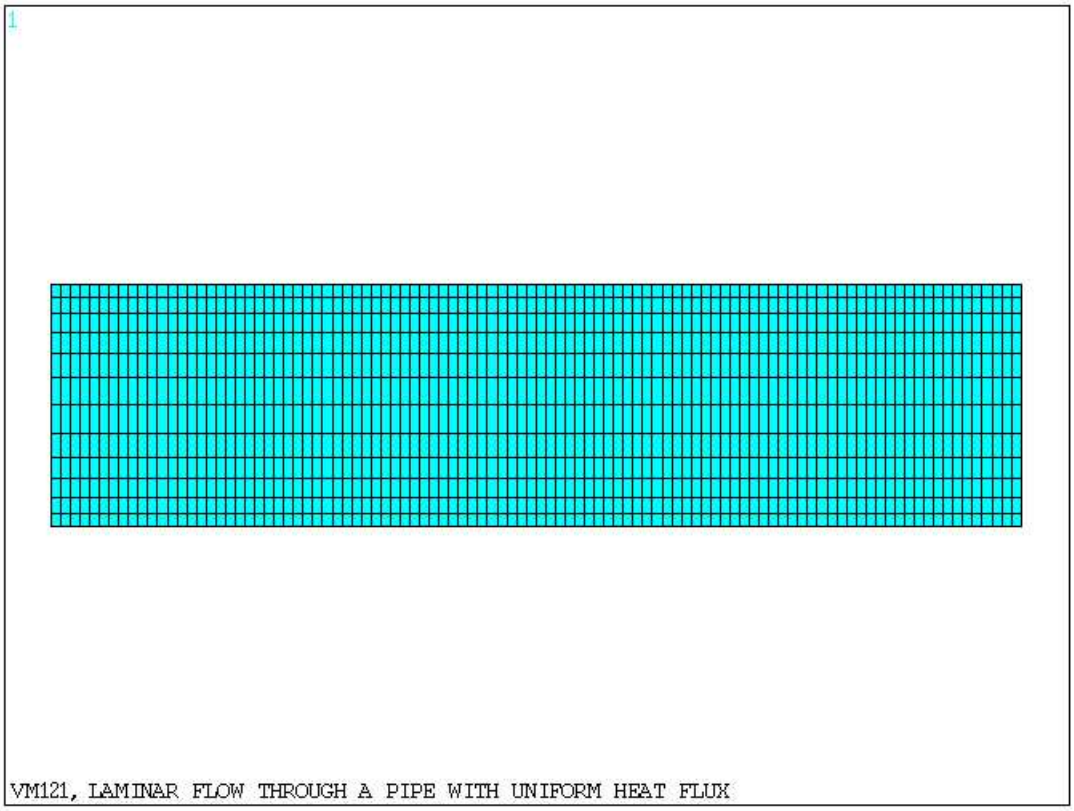

Figure 121.3 Contours of Axial Velocity

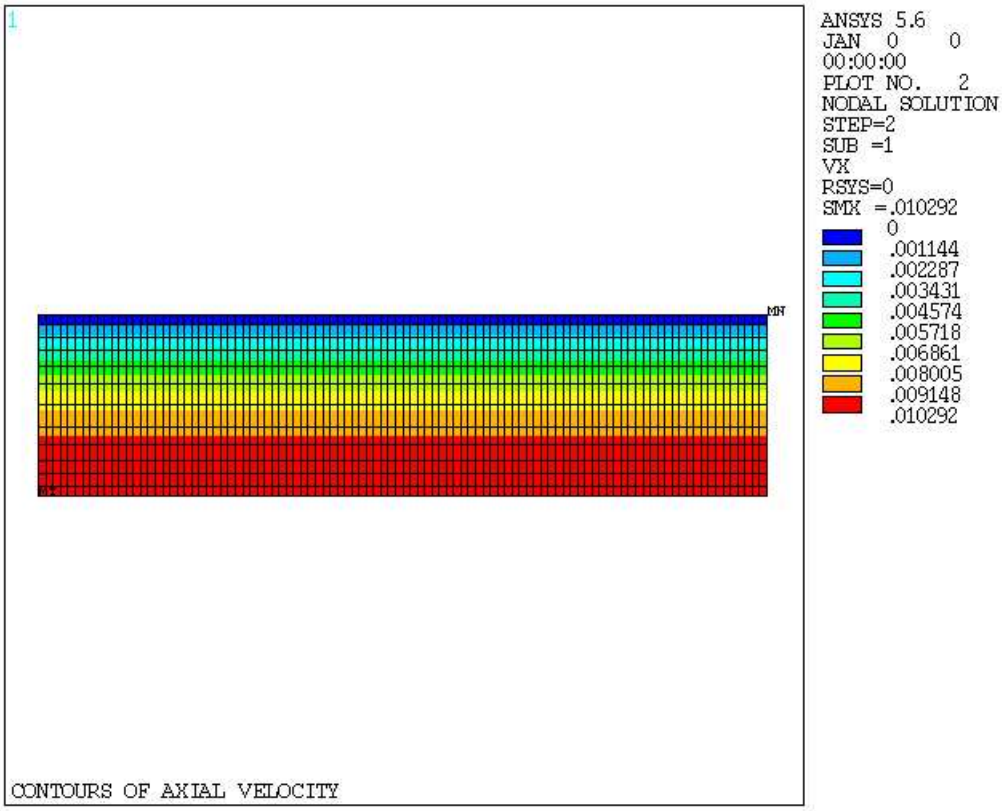

Figure 121.4 Contours of Wall Shear Stress

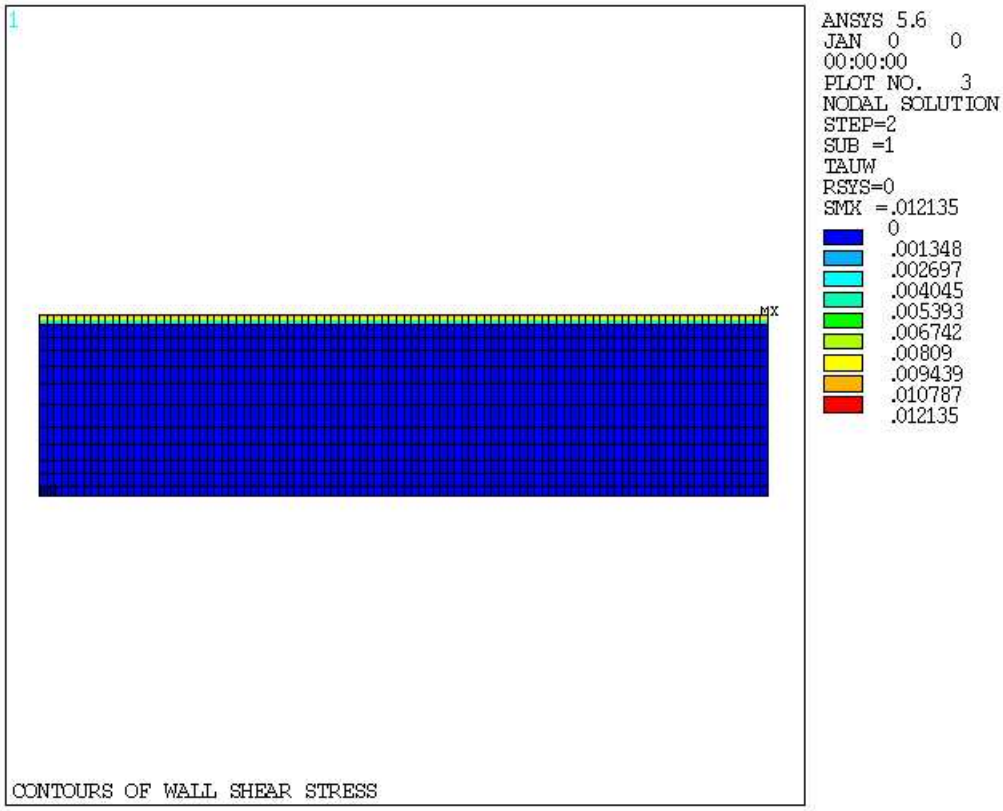

Figure 121.5 Contours of Temperature

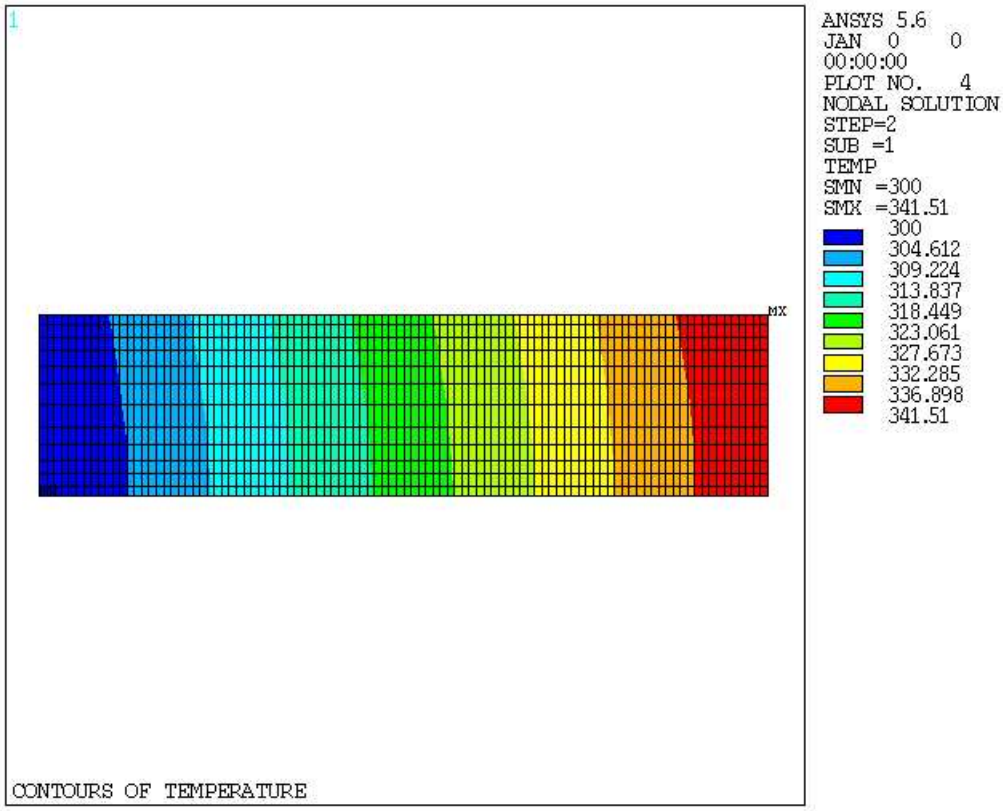

Figure 121.6 Axial Velocity Profile, VX(R)

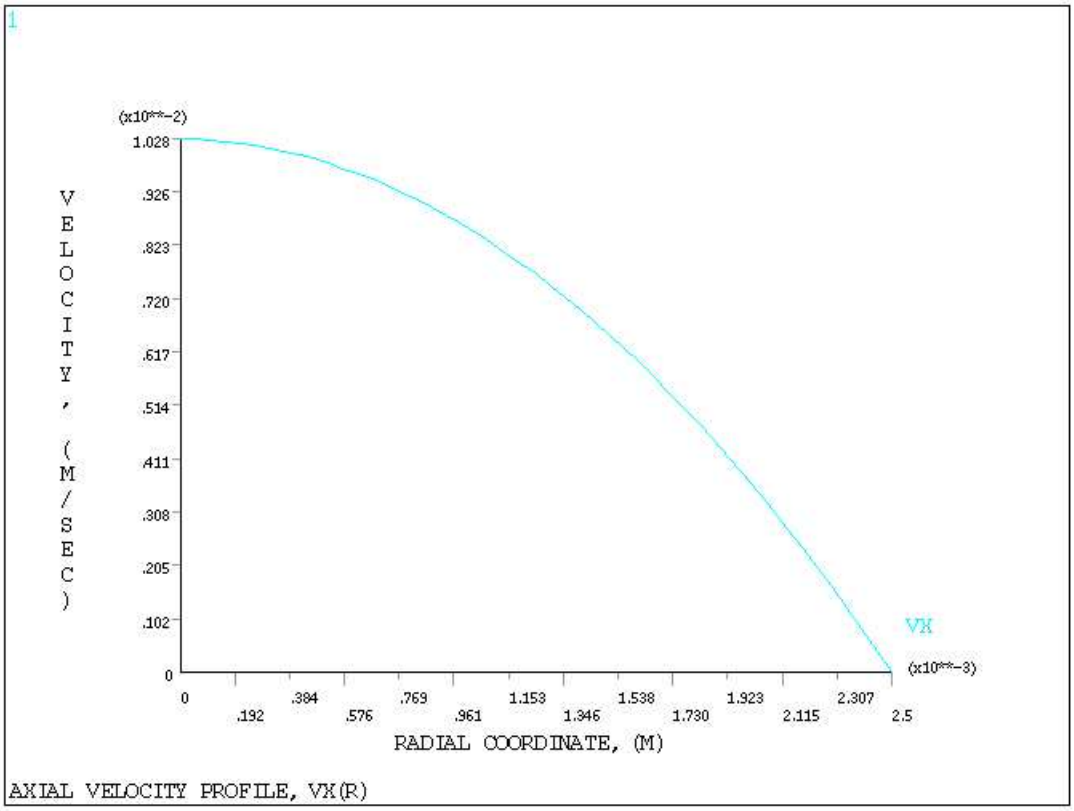

Figure 121.7 Outlet Temperature Profile, T(R)

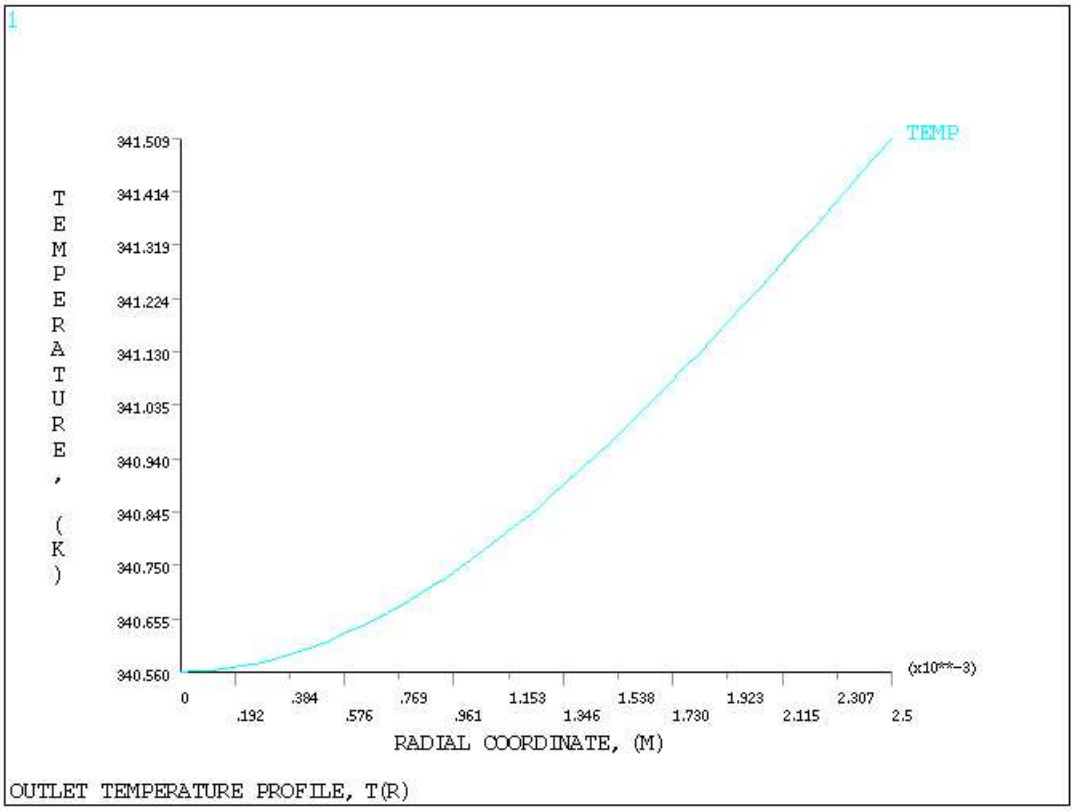

VM122: Pressure Drop in a Turbulent Flowing Fluid

Overview

Reference:	R. C. Binder, *Fluid Mechanics*, 3rd Edition, 3rd Printing, Prentice-Hall, Inc., Englewood Cliffs, NJ, 1956, pg. 118, article 8-6.
Analysis Type(s):	Thermal (pressure) Analysis (**ANTYPE** = 0)
Element Type(s):	Coupled Thermal-Fluid Pipe Elements (FLUID116)
Input Listing:	vm122.dat

Test Case

Benzene at 50°F flows through a horizontal commercial steel pipe of diameter d, with an average velocity v. Determine the pressure drop, Δp, in a length ℓ of pipe. The pipe friction factor is f.

Figure 122.1 Turbulent Flowing Fluid Problem Sketch

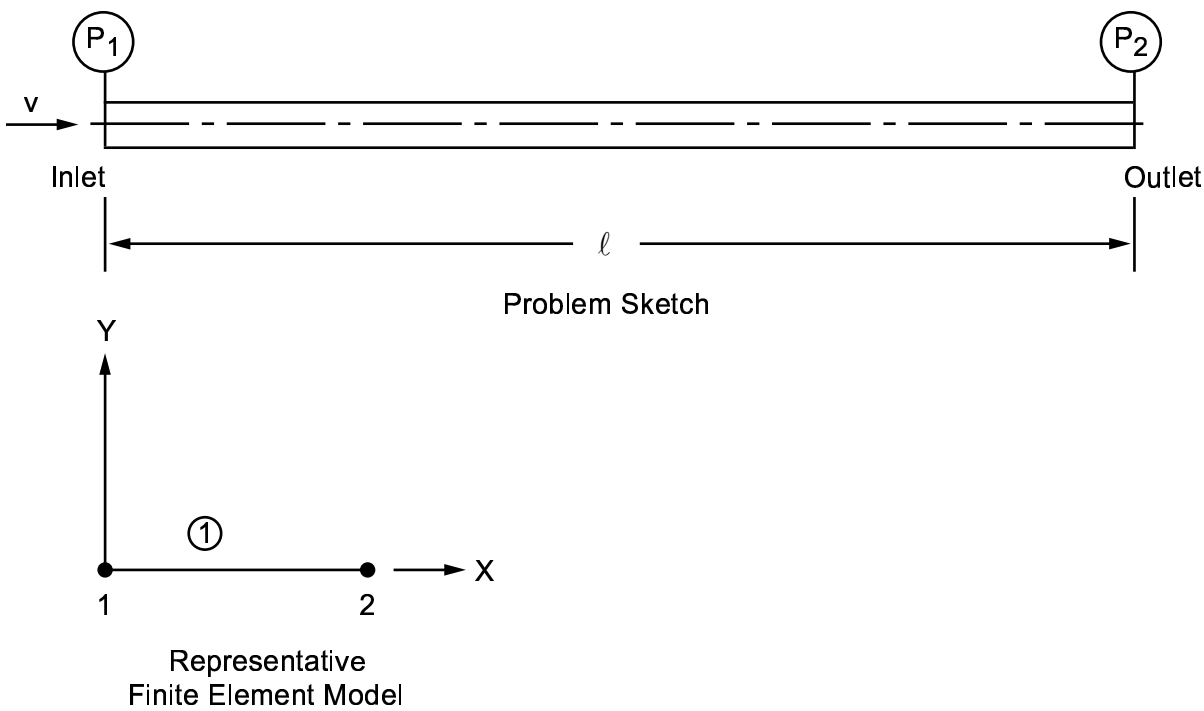

Material Properties	Geometric Properties	Loading
f = 0.016 sp. gr. (specific gravity) = 0.9	ℓ = 200 ft = 2400 in d = 6 in	v = 132 in/sec

Analysis Assumptions and Modeling Notes

The inlet flow rate w is input as a nodal quantity. The outlet pressure is defined to be zero for reference. An iterative solution is required to find the pressure drop. The following quantities are required for input and are calculated from the given data:

$$\rho = \text{mass density} = \text{sp. gr.} \times \rho H_2 0 = 0.9 \times 62.4$$

$$= /(386.4 \times 12^3) = 8.411 \times 10^{-5}\ lb_f\text{-}sec^2/in^4$$

$$w = \text{mass flow rate} = \rho vA = 8.411 \times 10^{-5} \times 132 \times \pi \times 6\ 2/4$$

$$= .3138\ lb_f/sec/in$$

Results Comparison

	Target	ANSYS	Ratio
Pressure Drop , psi	4.69	4.69[1]	1.00

1. Pressure drop Δp is given by PRES degree of freedom at node 1.

VM123: Laminar Flow in a Piping System

Overview

Reference:	Crane Company Engineering Division, "Flow of Fluids through Valves, Fittings, and Pipe", Technical Paper No. 410, Chicago, IL, 1969, pg. 4-5, ex. 4-9.
Analysis Type(s):	Thermal (pressure) Analysis (**ANTYPE** = 0)
Element Type(s):	Coupled Thermal-Fluid Pipe Elements (FLUID116)
Input Listing:	vm123.dat

Test Case

S.A.E. 70 lube oil at 0°F is flowing through a horizontal 5" schedule 40 piping system (of diameter d) at a flow rate w. Determine the pressure drop, Δp, and the Reynold's number Re. Assume that the friction factor is determined by the laminar flow relationship for smooth pipes. The equivalent length of elbow and valves to account for flow losses is ℓ_a.

Figure 123.1 Laminar Flow Problem Sketch

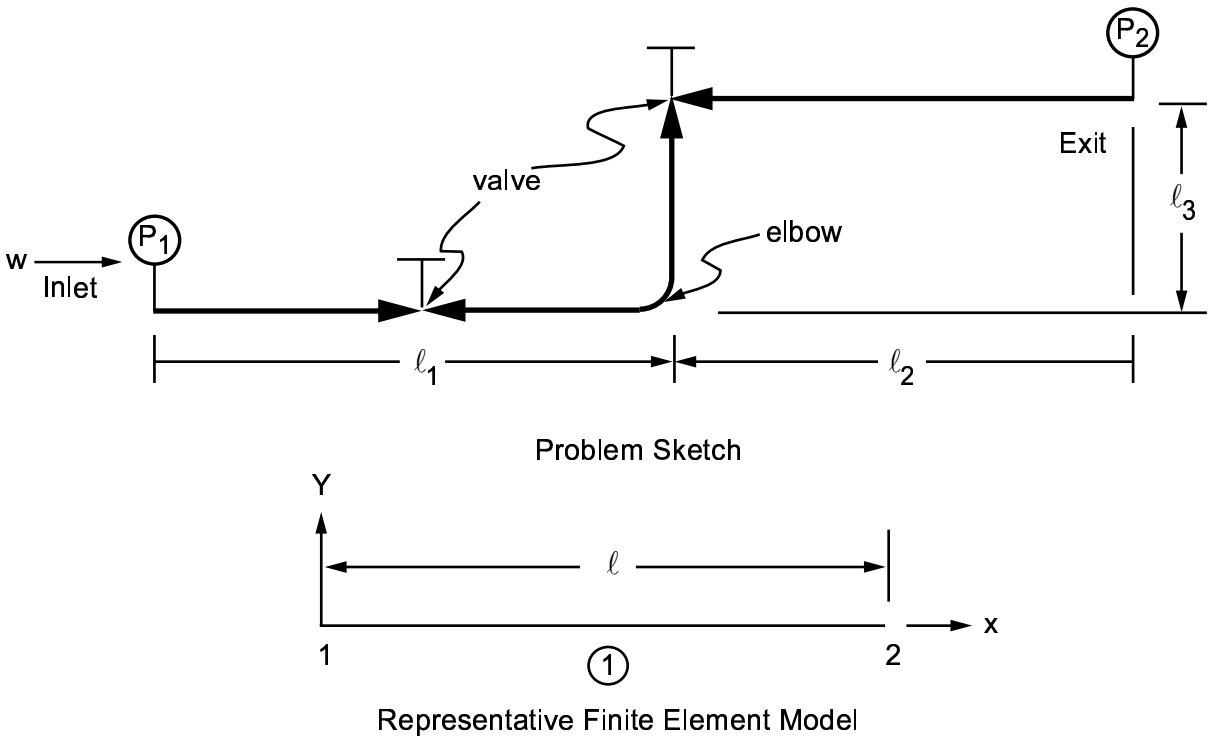

Material Properties	Geometric Properties	Loading
μ = viscosity = 0.010032 lb-sec/ft^2 ρ = 1.7546 lb-sec^2/ft^4	d = 0.4206 ft ℓ_1 = 175 ft ℓ_2 = 75 ft ℓ_3 = 50 ft ℓ_a = 53 ft	w = 2.345 slugs/se/sec

Analysis Assumptions and Modeling Notes

The piping system is modeled using a single element of length $\ell = \ell_1 + \ell_2 + \ell_3 = 300$ ft. The flow, w, is input at the inlet node. The exit pressure is defined to be zero for reference. An iterative solution is required. A friction factor of 0.05 (input for MU) is assumed for a starting value.

Results Comparison

	Target	ANSYS	Ratio
Pressure Drop, lb/ft^2	6160.	6164.[1]	1.001
Re	708.	708.	1.000

1. Pressure drop Δp is given by the PRES degree of freedom at node 1.

ANSYS Verification Manual . ANSYS Release 10.0 . 002184 . © SAS IP, Inc.

VM124: Discharge of Water from a Reservoir

Overview

Reference:	K. Brenkert, Jr., *Elementary Theoretical Fluid Mechanics*, John Wiley and Sons, Inc., New York, NY, 1960, pg. 224, ex. 4.
Analysis Type(s):	Thermal (pressure) Analysis (**ANTYPE** = 0)
Element Type(s):	Coupled Thermal-Fluid Pipe Elements (FLUID116)
Input Listing:	vm124.dat

Test Case

Water (density ρ, viscosity μ) flows from a large reservoir into a long piping system. Determine the Reynold's number Re and the flow rate w for pipes of friction factor f and diameter d. The loss coefficients for the sharp-edged entrance and 90° elbow are K_1 and K_2, respectively.

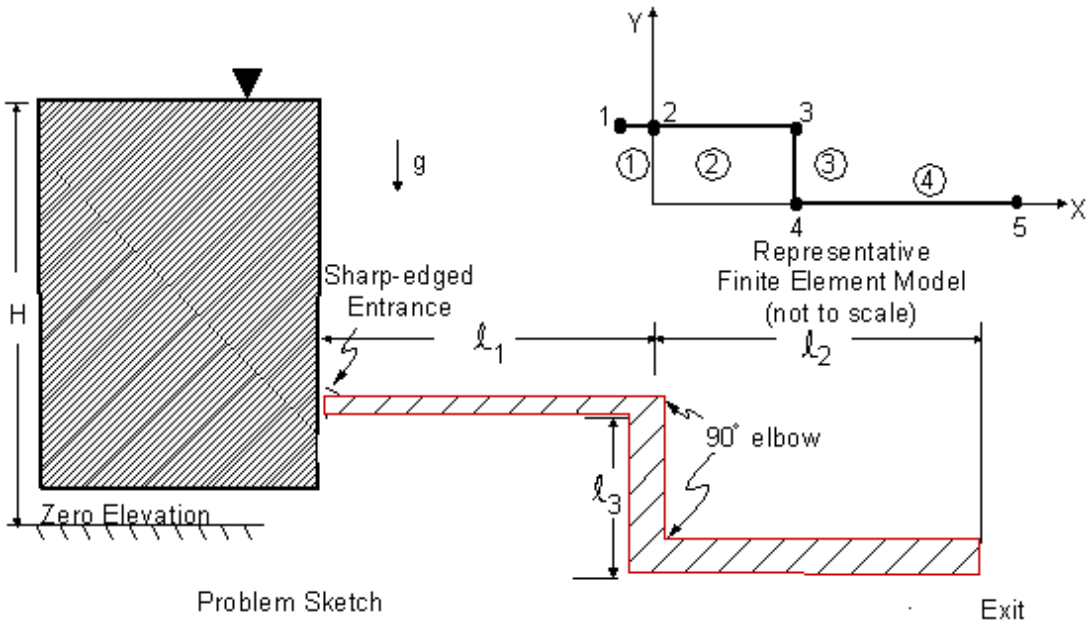

Material Properties	**Geometric Properties**	**Loading**
ρ = 1.94 lb-sec^2/ft^4 μ = 2.36 x 10^{-5} lb-sec/ft^2	H = 20 ft ℓ_1 = 20 ft ℓ_2 = 70 ft ℓ_3 = 10 ft d = 0.25 ft	K_1 = 0.5 K_3 = 0.9 f = 0.028 for $10^5 < Re < 10^6$ g = 32.2 ft/sec^2

Analysis Assumptions and Modeling Notes

The reservoir head is given by (H - ℓ_3) = 10 ft. This is applied as a pump head within a short (0.01 ft, to minimize friction) horizontal element. The acceleration input accounts for the vertical flow. The exit pressure and the water surface pressure is defined to be zero. An iterative solution is required. A friction factor of 0.025 (input for MU) is assumed for a starting value.

Results Comparison

	Target	ANSYS	Ratio
w, lb_fsec/ft	0.898	0.930[1]	1.04
Re	1.94×10^5	2.01×10^5	1.04

1. w is given by nodal flow at node 1.

VM125: Radiation Heat Transfer Between Concentric Cylinders

Overview

Reference:	F. Kreith, *Principles of Heat Transfer*, 2nd Printing, International Textbook Co., Scranton, PA, 1959, pg. 260.
Analysis Type(s):	Thermal Analysis (**ANTYPE** = 0) AUX12 (Radiation View Factor Utility)
Element Type(s):	2-D Conduction Bar Elements (LINK32) Superelement (or Substructure) (MATRIX50)
Input Listing:	vm125.dat

Test Case

Two long concentric cylinders are held at constant temperatures T_1 and T_2. Determine the rate of radiative heat transfer between the cylinders.

Figure 125.1 Concentric Cylinders Problem Sketch

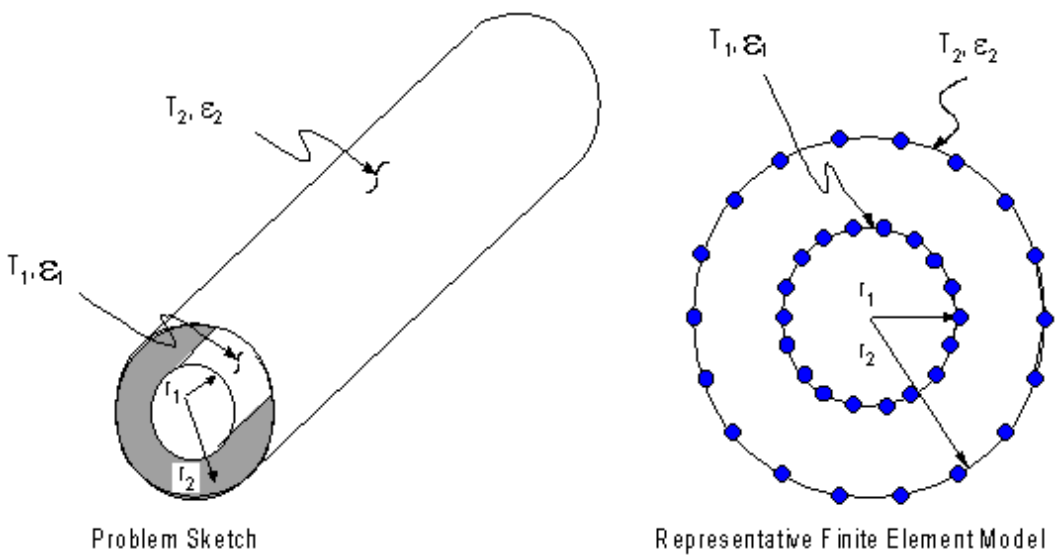

Material Properties	**Geometric Properties**	**Loading**
$\varepsilon_1 = 0.7$	$r_1 = 1$ in	$T_1 = 1000°R$
$\varepsilon_2 = 0.5$	$r_2 = 2$ in	$T_2 = 460°R$

Analysis Assumptions and Modeling Notes

The cylinders are assumed to be sufficiently long enough to neglect end losses. A 2-D model is used to determine the heat transfer rate per unit depth. The thermal conductivity and cross-sectional areas of the conducting bars are arbitrarily set equal to 1. The Stefan-Boltzmann constant defaults to 0.119×10^{-10} Btu/hr-in^2-°R^4 (value given in reference).

Results Comparison

	Target	ANSYS	Ratio
Q, Btu/hr-in	37.0[1]	36.4	0.984

1. Based on two cylinders 100 inches long.

VM126: Heat Transferred to a Flowing Fluid

Overview

Reference:	W. M. Rohsenow, H. Y. Choi, *Heat, Mass and Momentum Transfer*, 2nd Printing, Prentice-Hall, Inc., Englewood Cliffs, NJ, 1963, pg. 168, ex. 7.5
Analysis Type(s):	Thermal (fluid flow) Analysis (**ANTYPE** = 0)
Element Type(s):	Coupled Thermal-Fluid Pipe Elements (FLUID116)
Input Listing:	vm126.dat

Test Case

Heat is transferred to air at 14.7 psi, and temperature T_i, flowing at a rate w inside a round tube of length ℓ and diameter d having a uniform tube wall temperature T_w. Determine the heat flow in terms of the inlet (q_{in}) and outlet (q_{out}) heat transport rates. Also determine the air outlet temperature T_o. The convection coefficient is given by the expression $Nu = 0.08\ Re^{0.7}\ Pr^{0.35} + 1.63$. The tube is nearly frictionless.

Figure 126.1 Flowing Fluid Problem Sketch

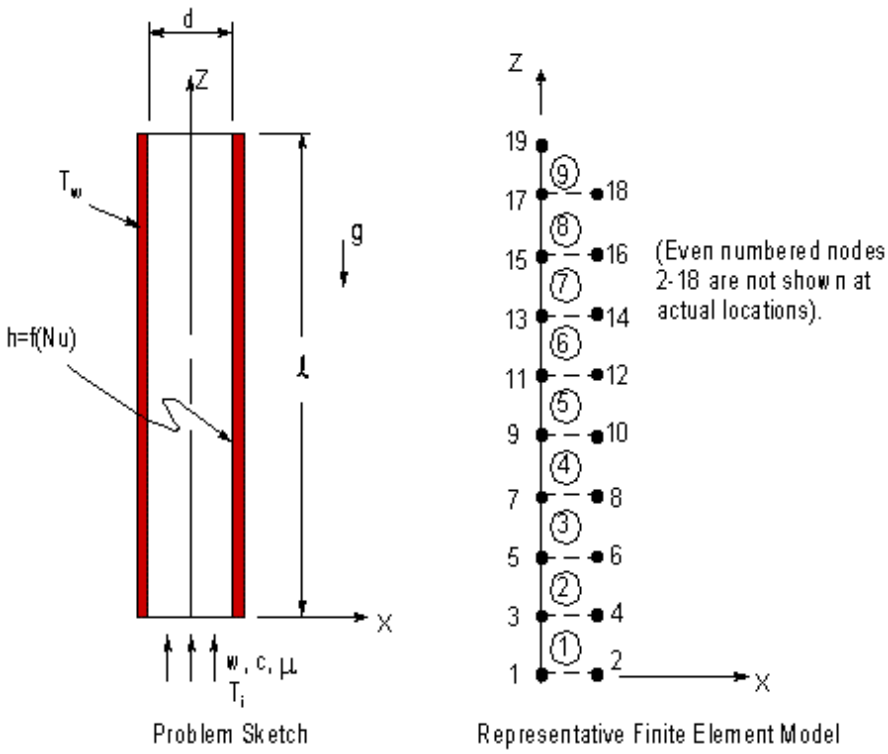

Material Properties	**Geometric Properties**
k = 0.017 BTU/hr-ft-°F	d = 1 in = (1/12) ft
c = 1.002 x 18^8 BTU -ft/lb_f-hr^{2-}°F	ℓ = 5 in = (5/12) ft
$\mu = 1.17418 \times 10^{-10}\ lb_f\ hr/ft^4$	**Loading**
$\rho = 1.4377 \times 10^{-10}\ lb_f\text{-}hr^2/ft^4$	T_i = 100°F
f = 0.001 for 0 < Re < 5 x 10^4	T_w = 200°F
	w = 1.131 x 10^{-8} lb_f hr/ft

Analysis Assumptions and Modeling Notes

The convection node locations are arbitrarily selected as coincident. The flow rate (w) is input as a real constant, so MU is not required to be input. The nonlinear material property table is used to input the friction factor table and the flow-dependent film coefficient. Since the heat transport rate is calculated at the element inlet, an extra element is extended beyond the tube exit to obtain q_{out}. POST1 is used to report the required quantities.

Results Comparison

	Target	ANSYS	Ratio
T_o , °F	123.0	122.55[1]	1.00
q_{in} , Btu/hr	113.28	113.44[2]	1.001
q_{out} , Btu/hr	139.33	139.02[2]	1.000

1. Temperature at Node 17.
2. q_{in} and q_{out} are obtained from the heat transport rates of elements 1 and 9, respectively.

ANSYS Verification Manual . ANSYS Release 10.0 . 002184 . © SAS IP, Inc.

VM127: Buckling of a Bar with Hinged Ends (Line Elements)

Overview

Reference:	S. Timoshenko, *Strength of Material, Part II, Elementary Theory and Problems*, 3rd Edition, D. Van Nostrand Co., Inc., New York, NY, 1956, pg. 148, article 29.
Analysis Type(s):	Buckling Analysis (**ANTYPE** = 1) Static (prestress) Analysis (**ANTYPE** = 0)
Element Type(s):	2-D Elastic Beam Elements (BEAM3)
Input Listing:	vm127.dat

Test Case

Determine the critical buckling load of an axially loaded long slender bar of length ℓ with hinged ends. The bar has a cross-sectional height h, and area A.

Figure 127.1 Buckling Bar Problem Sketch

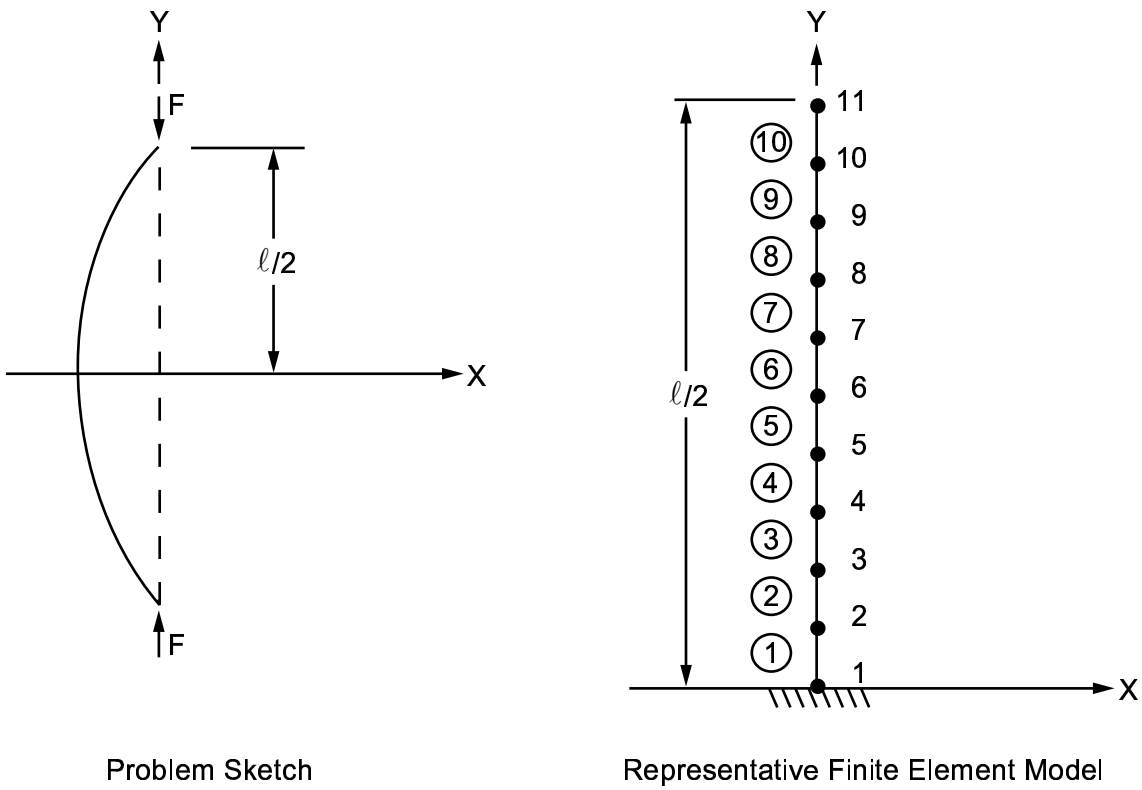

Material Properties	**Geometric Properties**	**Loading**
E = 30 x 10^6 psi	ℓ = 200 in A = 0.25 in^2 h = 0.5 in	F = 1 lb

Analysis Assumptions and Modeling Notes

Only the upper half of the bar is modeled because of symmetry. The boundary conditions become free-fixed for the half symmetry model. A total of 10 master degrees of freedom in the X-direction are selected to characterize the buckling mode. The moment of inertia of the bar is calculated as $I = Ah^2/12 = 0.0052083\ in^4$.

Results Comparison

	Target	ANSYS	Ratio
F_{cr}, lb	38.553	38.553[1]	1.000

1. F_{cr} = Load Factor (1st mode).

ANSYS Verification Manual . ANSYS Release 10.0 . 002184 . © SAS IP, Inc.

VM128: Buckling of a Bar with Hinged Ends (Area Elements)

Overview

Reference:	S. Timoshenko, *Strength of Material, Part II, Elementary Theory and Problems*, 3rd Edition, D. Van Nostrand Co., Inc., New York, NY, 1956, pg. 148, article 29.
Analysis Type(s):	Buckling Analysis (**ANTYPE** = 1) Static (Prestress) Analysis (**ANTYPE** = 0)
Element Type(s):	2-D Structural Solid Elements (PLANE42)
Input Listing:	vm128.dat

Test Case

Determine the critical buckling load of an axially loaded long slender bar of length ℓ with hinged ends. The bar has a cross-sectional height h, and area A.

Figure 128.1 Buckling Bar Problem Sketch

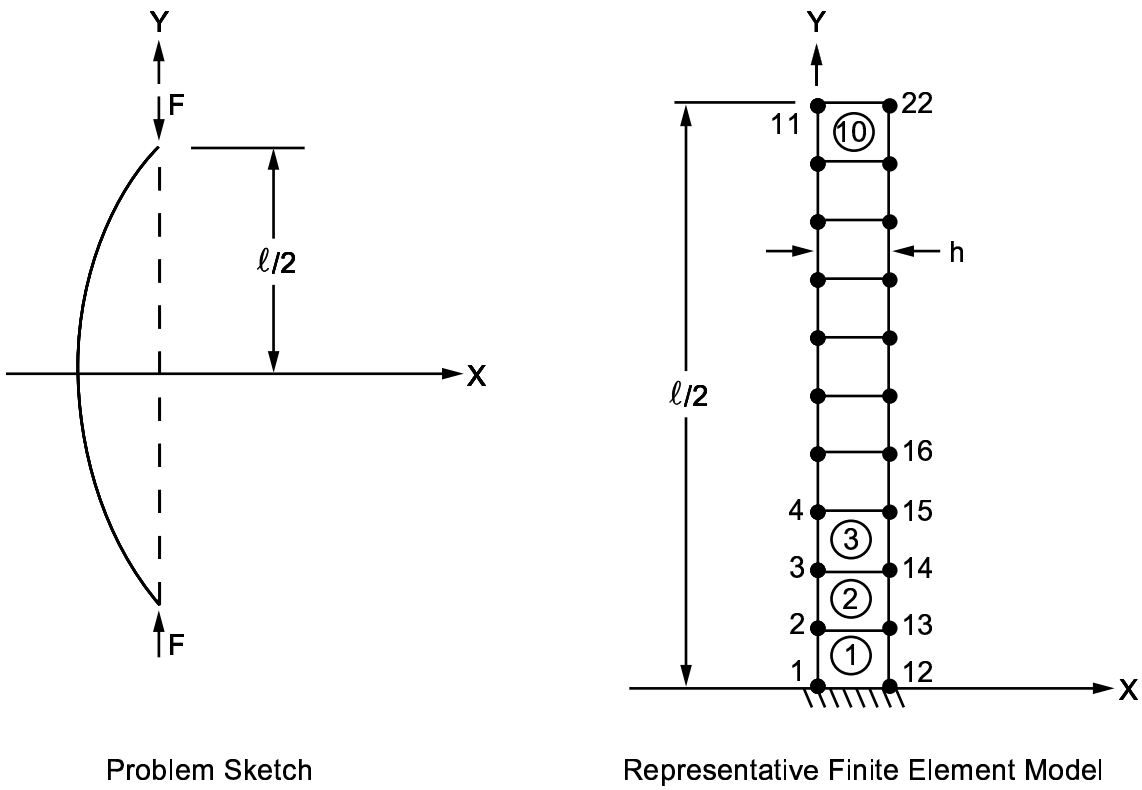

Material Properties	Geometric Properties	Loading
E = 30 x 10^6 psi	ℓ = 200 in A = 0.25 in 2 h = 0.5 in	F = 1 lb

Analysis Assumptions and Modeling Notes

Only the upper half of the bar is modeled because of symmetry. The boundary conditions become free-fixed for the half symmetry model. The bar is assumed to have a rectangular cross-section (thickness = A/h = 0.5 in).

Results Comparison

	Target	ANSYS	Ratio
F_{cr}, lb subspace	38.553	38.714[1]	1.004
F_{cr}, lb Block-Lanczos	38.553	38.712[1]	1.004

1. F_{cr} = Load Factor (1st mode).

VM129: Numerical Differentiation and Integration

Overview

Reference:	Any Basic Calculus Book
Analysis Type(s):	First and Second Derivatives and Integrals Using APDL
Element Type(s):	None
Input Listing:	vm129.dat

Test Case

Given a sine wave f(t) = A sin ωt, find the maximum value of the first and second derivatives. For the same sine wave, find the values of the two integrals:

$$I_1 = \int_0^{36} f(t)dt \quad \text{and} \quad I_2 = \int_0^{36} \left[\int f(t)dt\right]dt$$

Figure 129.1 Numerical Differentiation and Integration

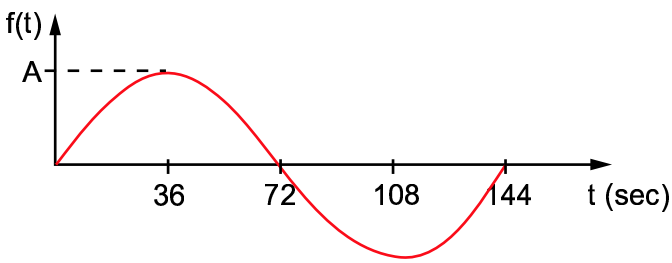

Problem Sketch

Definitions:

A = 1.2732
ω = frequency = π/72 rad/sec

Analysis Assumptions and Modeling Notes

Arrays for one cycle of 145 data points (one data point per second) are generated, starting from a value of 0 up to 144 (representing time, t, in sec). The ***VOPER** command is used to obtain the first and second derivatives, and the single and double integrals.

Results Comparison

	Target	ANSYS	Ratio
df/dt (Max)	5.555×10^{-2}	5.554×10^{-2}	1.000
d^2f/dt^2 (Max)	2.424×10^{-3}	2.422×10^{-3}	0.999
I_1	29.18	29.17	1.000
I_2	381.7	381.7	1.000

max df/dt is obtained as DERIV1 array parameter E.

max d^2f/dt^2 is obtained as DERIV2 array parameter G

$$I_1 = \int_0^{36} f\,dt \qquad \text{and} \qquad I_2 = \int_0^{36} \left[\int f\,dt\right] dt$$

I_1 and I_2 are obtained from array parameters F and H (at row 37 corresponding to t = 36 sec)

ANSYS Verification Manual . ANSYS Release 10.0 . 002184 . © SAS IP, Inc.

VM130: Fourier Series Generation for a Saw Tooth Wave

Overview

Reference:	S. Timoshenko, D. H. Young, *Vibration Problems in Engineering*, D. Van Nostrand Co., Inc., New York, NY, 1955, pg. 102, problem 2.
Analysis Type(s):	Fourier Coefficients Generated and Series Evaluated Using APDL
Element Type(s):	None
Input Listing:	vm130.dat

Test Case

For the saw tooth wave shown below, determine the coefficients of the Fourier series approximating this wave. Plot both the given wave and the wave as evaluated from the calculated series.

Figure 130.1 Saw Tooth Wave Problem Sketch

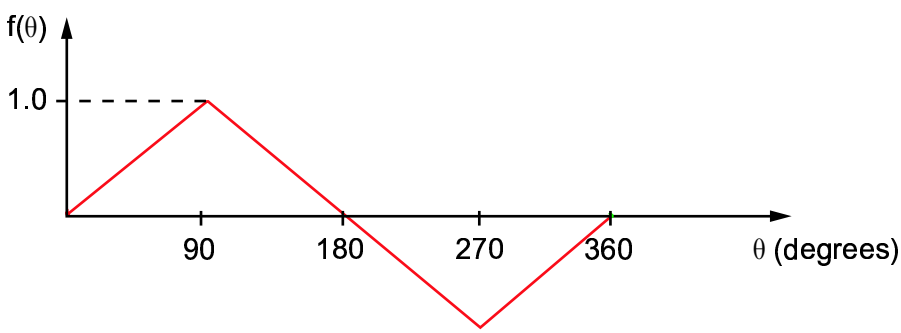

Problem Sketch

Analysis Assumptions and Modeling Notes

The wave is described by 121 points (arbitrary). Twenty four terms are assumed to be sufficient for the series. Since the wave is antisymmetric, only sine terms with odd modes are chosen.

Results Comparison

	Target	ANSYS	Ratio
Mode 1 Coefficient	0.811	0.811	1.000
Mode 3 Coefficient	-0.901×10^{-1}	-0.902×10^{-1}	1.002
Mode 5 Coefficient	0.324×10^{-1}	0.326×10^{-1}	1.006
Mode 7 Coefficient	-0.165×10^{-1}	-0.167×10^{-1}	1.014

Figure 130.2 Fourier Display

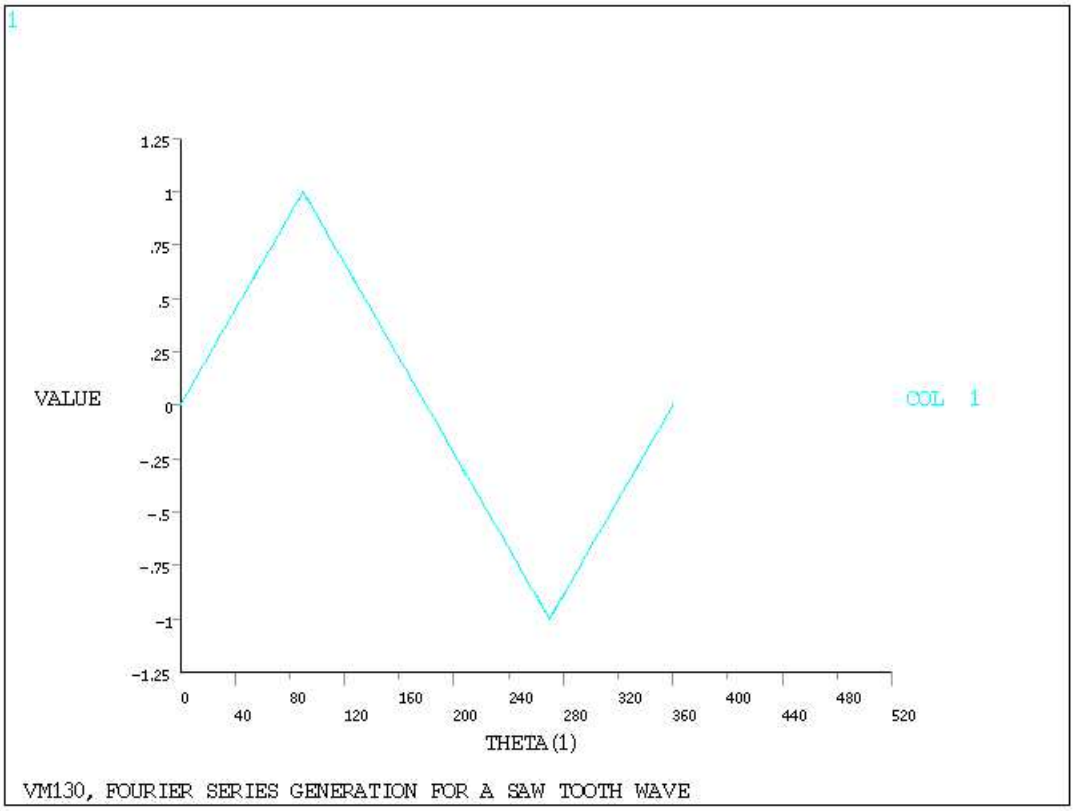

VM131: Acceleration of a Rotating Crane Boom

Overview

Reference:	F. P. Beer, E. R. Johnston, Jr., *Vector Mechanics for Engineers, Statics and Dynamics*, 5th Edition, McGraw-Hill Book Co., Inc., New York, NY, 1962, pg. 616, problem 15.13.
Analysis Type(s):	Static Analysis (**ANTYPE** = 0)
Element Type(s):	Structural Mass Elements (MASS21)
Input Listing:	vm131.dat

Test Case

Determine the acceleration at the tip P of a crane boom that has a constant angular velocity cab rotation (Ω) while being raised with a constant angular velocity (ω).

Figure 131.1 Rotating Crane Boom Problem Sketch

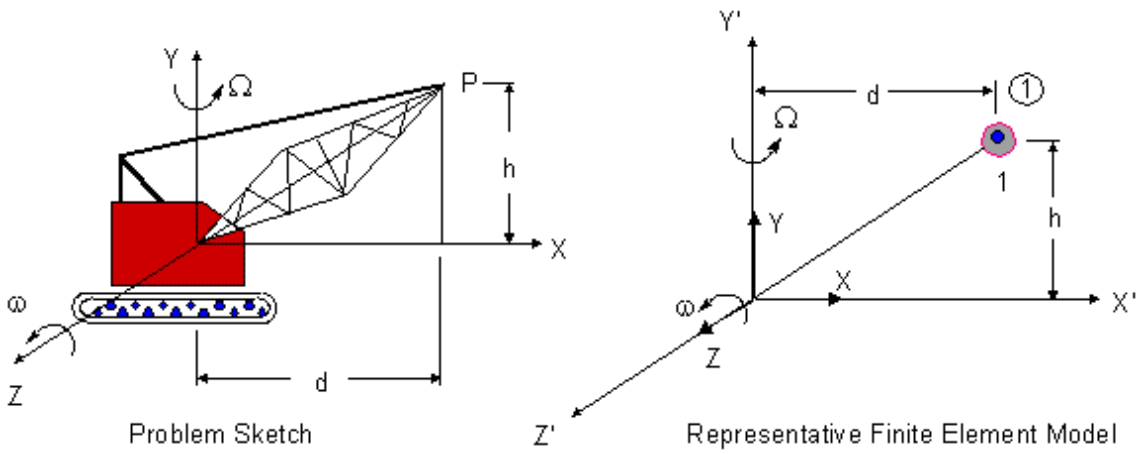

Geometric Properties	**Loading**
d = 34.64 ft	Ω = 0.3 rad/sec
h = 20 ft	ω = 0.5 rad/sec

Analysis Assumptions and Modeling Notes

Consider X', Y', Z' as the fixed reference coordinate system. The global Cartesian coordinate system (XYZ) is taken as attached to the cab which rotates at an angular velocity of Ω about the Y'-axis of the reference coordinate system. The boom angular velocity ω is applied about the global Z-axis. The Coriolis effect due to the rotation of the cab is modeled by putting a mass of 1 lb-sec^2/ft (without rotary inertia) at point P, and constraining its degrees of freedom. The reaction forces at the mass then give the acceleration components.

Results Comparison

	Target	ANSYS[1]	Ratio
a_x , ft/sec^2	-11.78	-11.78	1.00
a_y , ft/sec^2	-5.00	-5.00	1.00

	Target	ANSYS[1]	Ratio
a_z , ft/sec^2	6.00	6.00	1.00

1. a_x , a_y , a_z are given by the reaction forces at node 1 (FX, FY, FZ respectively).

VM132: Stress Relaxation of a Tightened Bolt Due to Creep

Overview

Reference:	S. Timoshenko, *Strength of Material, Part II, Elementary Theory and Problems*, 3rd Edition, D. Van Nostrand Co., Inc., New York, NY, 1956, pg. 531, article 93.
Analysis Type(s):	Static Analysis (**ANTYPE** = 0) (with creep properties and initial strain)
Element Type(s):	2-D Spar (or Truss) Elements (LINK1)
Input Listing:	vm132.dat

Test Case

A bolt of length ℓ and cross-sectional area A is tightened to an initial stress σ_o. The bolt is held for a long period of time t_1 at an elevated temperature T_o. The bolt material has a creep strain rate given by $d\varepsilon/dt = k\sigma^n$. Determine the stress σ in the bolt at various times during creep relaxation.

Figure 132.1 Tightened Bolt Problem Sketch

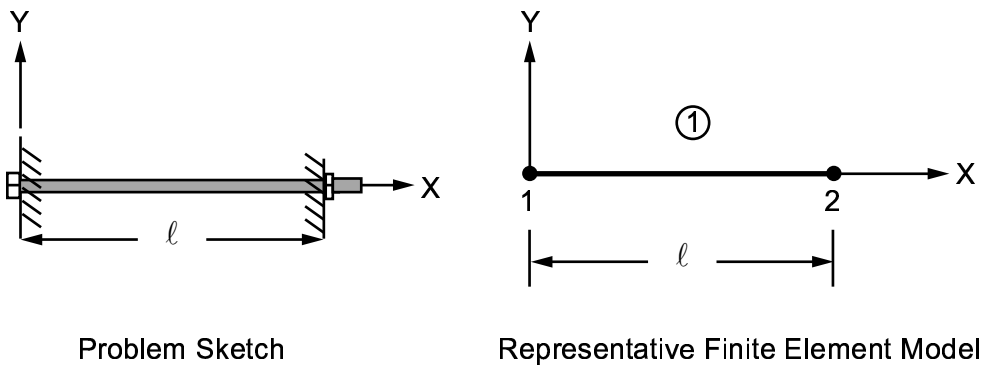

Material Properties	Geometric Properties	Loading
$E = 30 \times 10^6$ psi $n = 7$ $k = 4.8 \times 10^{-30}$/hr	$\ell = 10$ in $A = 1$ in^2	$\sigma_o = 1000$ psi $T_o = 900°F$ $t_1 = 1000$ hr

Analysis Assumptions and Modeling Notes

An integration time step of 10 hours over the 1000 hour time range (i.e., 100 iterations) is used. The initial strain is calculated by $\sigma_o/E = (1000 \text{ psi})/(30 \times 10^6 \text{ psi}) = 1/30000$.

Results Comparison

	Target	ANSYS(1)	Ratio
Stress, psi @t = 190 hr	975.	976.	1.00
Stress, psi @t = 420 hr	950.	951.	1.00
Stress, psi @t = 690 hr	925.	926.	1.00
Stress, psi @t = 880 hr	910.	911.	1.00
Stress, psi @t = 950 hr	905.	905.	1.00

1. Stress (σ) corresponds to the quantity SIG in POST26 listing.

ANSYS Verification Manual . ANSYS Release 10.0 . 002184 . © SAS IP, Inc.

VM133: Motion of a Rod Due to Irradiation Induced Creep

Overview

Reference:	Any basic calculus book
Analysis Type(s):	Static Analysis (with creep properties) (**ANTYPE** = 0)
Element Type(s):	2-D Plastic Beam Elements (BEAM23)
Input Listing:	vm133.dat

Test Case

A rod of length ℓ and square cross-sectional area A is held at a constant stress σ_o at a temperature T_o. The rod is also subjected to a constant neutron flux Φ. The rod material has an irradiation induced creep strain rate given by the relationship $d\varepsilon_{cr} / dt = k_1\sigma\Phi e - (\Phi t / k_2)$. Determine the amount of creep strain ε_{cr} accumulated up to 5 hours.

Figure 133.1 Rod Motion Problem Sketch

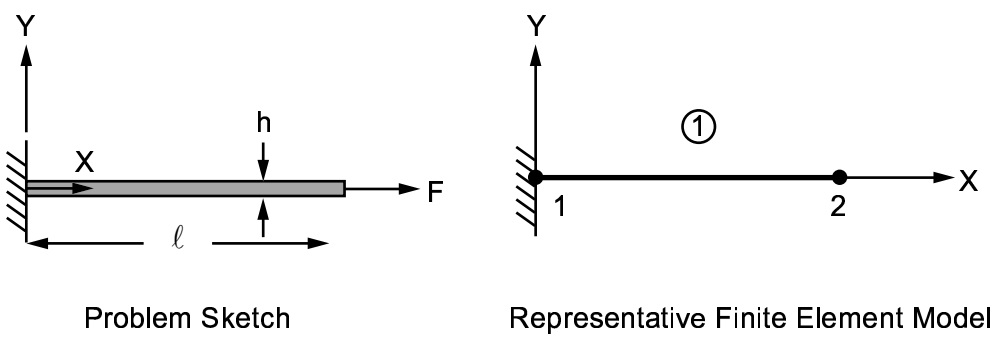

Material Properties	**Geometric Properties**	**Loading**
E = 300 psi	ℓ = 1 in	σ_o = 1 psi
$k_1 = 0.5 \times 10^{-12}$ in^4/lb neutron	A = 0.25 in^2	T_o = 1000°F
$k_2 = 1 \times 10^{10}$ neutron/in^2	h = 0.5 in	
$\Phi = 1 \times 10^{10}$ neutron/in^2-hr		

Analysis Assumptions and Modeling Notes

A ramp fluence is required to be input for a constant flux (since time increases linearly). Two load steps are used so that the fluence can be ramped while the temperature is held constant. An integration time step of 0.1 hr is assumed over the 5 hour time range (50 substeps). The irradiation induced creep equation is accessed using C_{66} = 5 in the nonlinear material table. POST26 is used to obtain the variation of creep strain with time. The following quantities are required for input:

Maximum fluence = $5\ \Phi = 5 \times 10^{10}$ neutron/in^2
$F = \sigma_o$
A = 0.25 lb
$h = \sqrt{A}$
I = moment of inertia = $A^2/12$ = 0.0052083 in^4

Results Comparison

	Target	ANSYS	Ratio
Creep Strain (t = 0.0 hr)	0.00000	0.00000	-
Creep Strain (t = 0.5 hr)	0.00197	0.00197	0.998
Creep Strain (t = 1.0 hr)	0.00316	0.00316	1.000
Creep Strain (t = 5.0 hr)	0.00497	0.00496	0.999

ANSYS Verification Manual . ANSYS Release 10.0 . 002184 . © SAS IP, Inc.

VM134: Plastic Bending of a Clamped I-Beam

Overview

Reference:	N. J. Hoff, *The Analysis of Structures*, John Wiley and Sons, Inc., New York, NY, 1956, pg. 388, article 4.5.
Analysis Type(s):	Static, Plastic Analysis (**ANTYPE** = 0)
Element Type(s):	3-D Thin-walled Beam Elements (BEAM24)
Input Listing:	vm134.dat

Test Case

A wide-flanged I-beam of length ℓ, with clamped ends, is uniformly loaded as shown. Investigate the behavior of the beam at load w_1 when yielding just begins at the ends, at load w_2, when the midpoint begins to yield, and at load w_3, when pronounced plastic yielding has occurred. The beam's cross-section is shown in Figure 134.1: "Clamped I-Beam Problem Sketch".

Figure 134.1 Clamped I-Beam Problem Sketch

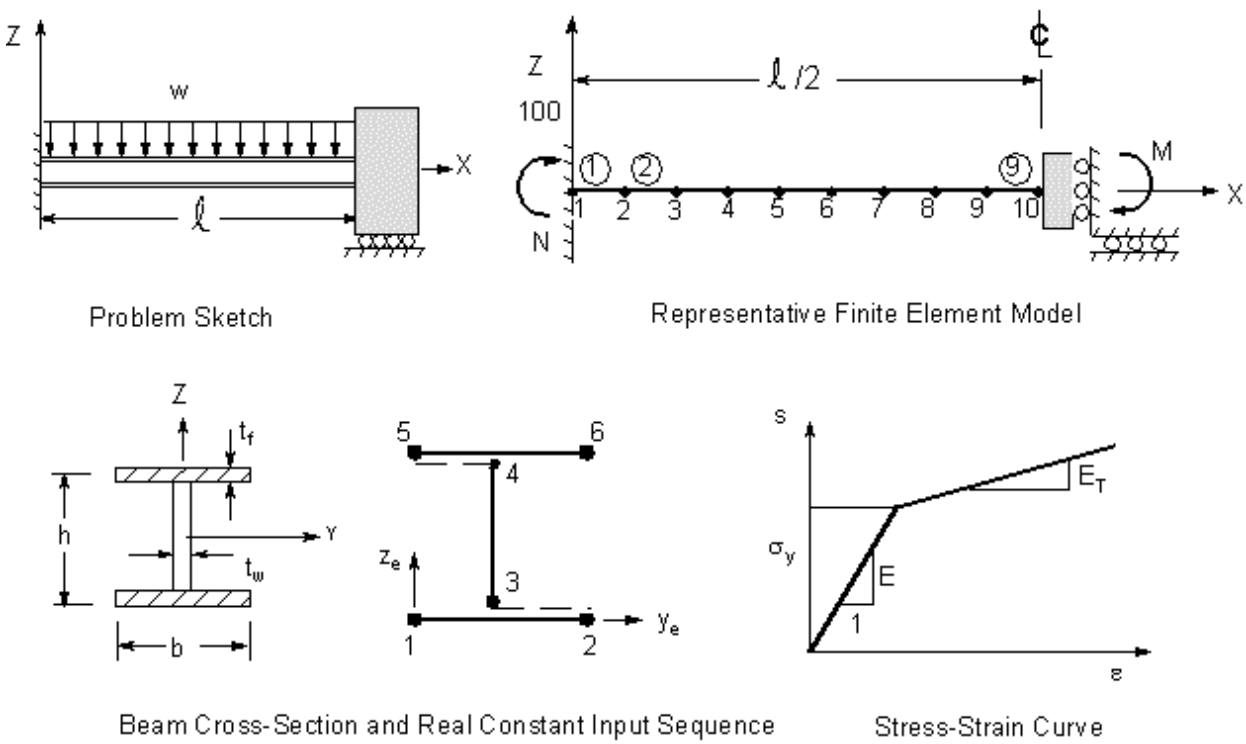

Material Properties	Geometric Properties	Loading
$E = 29 \times 10^6$ psi	$\ell = 144$ in	$w_1 = 2190$ lb/in
$E_T = 5.8 \times 10^6$ psi	$b = 10$ in	$w_2 = 3771$ lb/in
$\sigma_y = 38{,}000$ psi	$h = 10.6$ in	$w_3 = 9039$ lb/in
	$t_f = 0.9415$ in	
	$t_w = 0.0001$ in	

Analysis Assumptions and Modeling Notes

The beam cross-section is modeled as an idealized section to compare with the assumptions of the analytical solution. The loading is assumed to be applied through the centroid of the element cross-section (the neutral axis). Only half the beam is modeled, taking advantage of symmetry. Classical bilinear kinematic hardening behavior is used.

Results Comparison

		Target	ANSYS	Ratio
w_1 = 2190 lb/in	Midspan Deflection , in	-0.160	-0.160	1.00
	End Moment N, in-lb	-3.784×10^6	-3.784×10^6	1.00
	Mid Moment M, in-lb	-1.892×10^6	-1.892×10^6	1.00
	End Status	At Yield	At Yield	-
	Mid Status	Elastic	Elastic	-
w_2 = 3771 lb/in	Midspan Deflection , in	-0.357	-0.359	1.01
	End Moment N, in-lb	-5.98×10^6	-5.97×10^6	1.00
	Mid Moment M, in-lb	-3.78×10^6	-3.80×10^6	1.01
	End Status	Plastic	Plastic	-
	Mid Status	At Yield	At Yield	-
w_3 = 9039 lb/in	Midspan Deflection , in	-2.09	-2.11	1.01
	End Moment N, in-lb	-1.51×10^7	-1.50×10^7	0.99
	Mid Moment M, in-lb	-8.36×10^6	-8.45×10^6	1.01
	End Status	0.0200	0.0206	1.03
	Mid Status	0.0089	0.0089	1.00

Note — δ_{mid} (midspan deflection) is UZ at node 10.

N (fixed-end moment and M (midspan moment) are obtained from the reaction moments MY at nodes 1 and 10 respectively. The end and mid status are determined by comparing SAXL to the yield stress (σ_y).

The total end strain is obtained y adding the quantities EPELAXL and EPPLAXL for element 1 (end I). The total mid strain is obtained by adding EPELAXL and EPPLAXL for element 9 (end J).

ANSYS Verification Manual . ANSYS Release 10.0 . 002184 . © SAS IP, Inc.

VM135: Bending of a Beam on an Elastic Foundation

Overview

Reference:	S. Timoshenko, *Strength of Material, Part II, Elementary Theory and Problems*, 3rd Edition, D. Van Nostrand Co., Inc., New York, NY, 1956, pg. 12, article 2.
Analysis Type(s):	Static Analysis (**ANTYPE** = 0)
Element Type(s):	2-D Elastic Tapered Unsymmetric Beam Elements (BEAM54)
Input Listing:	vm135.dat

Test Case

A long (semi-infinite) beam on an elastic foundation is bent by a force F and a moment M applied at the end as shown. Determine the lateral end deflection of the beam δ_{end}. The elastic foundation stiffness k is based on 0.3 inches deflection under 10,000 lb loads spaced 22 inches apart.

Figure 135.1 Beam Problem Sketch

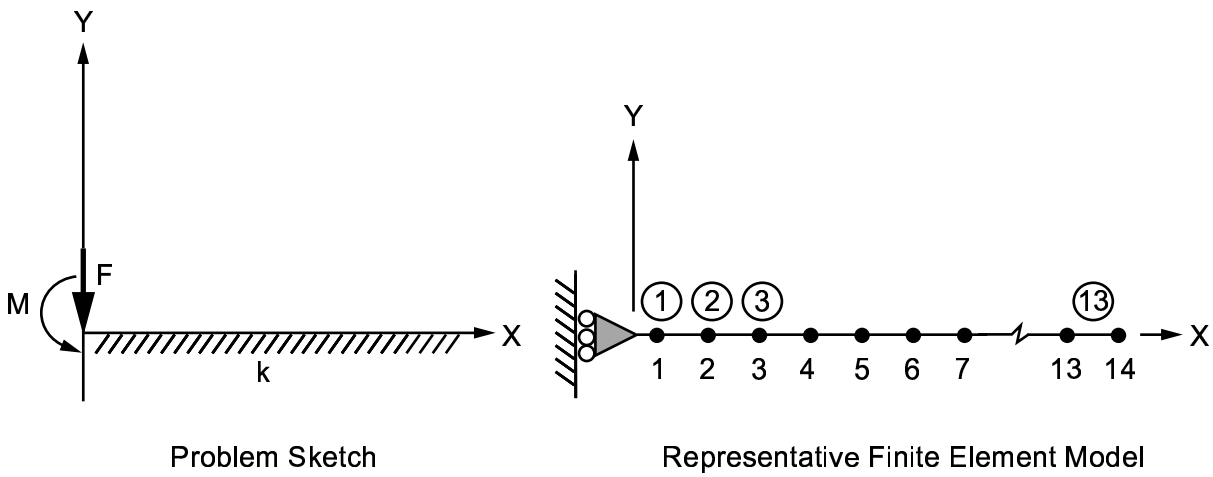

Material Properties	Geometric Properties	Loading
k = 1515.15 lb/in^2 E = 30 x 10^6 psi	A = 23 in^2 I = 44 in^4	F = 1000 lb M = 10,000 in-lb

Analysis Assumptions and Modeling Notes

A nodal spacing of 22 inches is selected to match the discrete foundation locations upon which the stiffness is based. The beam length is arbitrarily selected to be 286 in. The height of the beam cross-section h is arbitrarily taken as 5 inches (should not affect the end displacement).

Results Comparison

	Target	ANSYS	Ratio
Deflection$_{end}$, in	-0.03762	-0.03761[1]	1.000

1. UY at Node 1.

VM136: Large Deflection of a Buckled Bar (the Elastica)

Overview

Reference:	S. Timoshenko, J. M. Gere, *Theory of Elastic Stability*, 2nd Edition, McGraw-Hill Book Co. Inc., New York, NY, 1961, pg. 78, article 2.7.
Analysis Type(s):	Static Analysis (**ANTYPE** = 0) with Large Deflection
Element Type(s):	2-D Elastic Beam Elements (BEAM3)
Input Listing:	vm136.dat

Test Case

A slender bar of cross-sectional height h, and area A, fixed at the base and free at the upper end, is loaded with a value larger than the critical buckling load. Determine the displacement (ΔX, ΔY, Θ) of the free end and display the deformed shape of the bar at various loadings.

Figure 136.1 Buckled Bar Problem Sketch

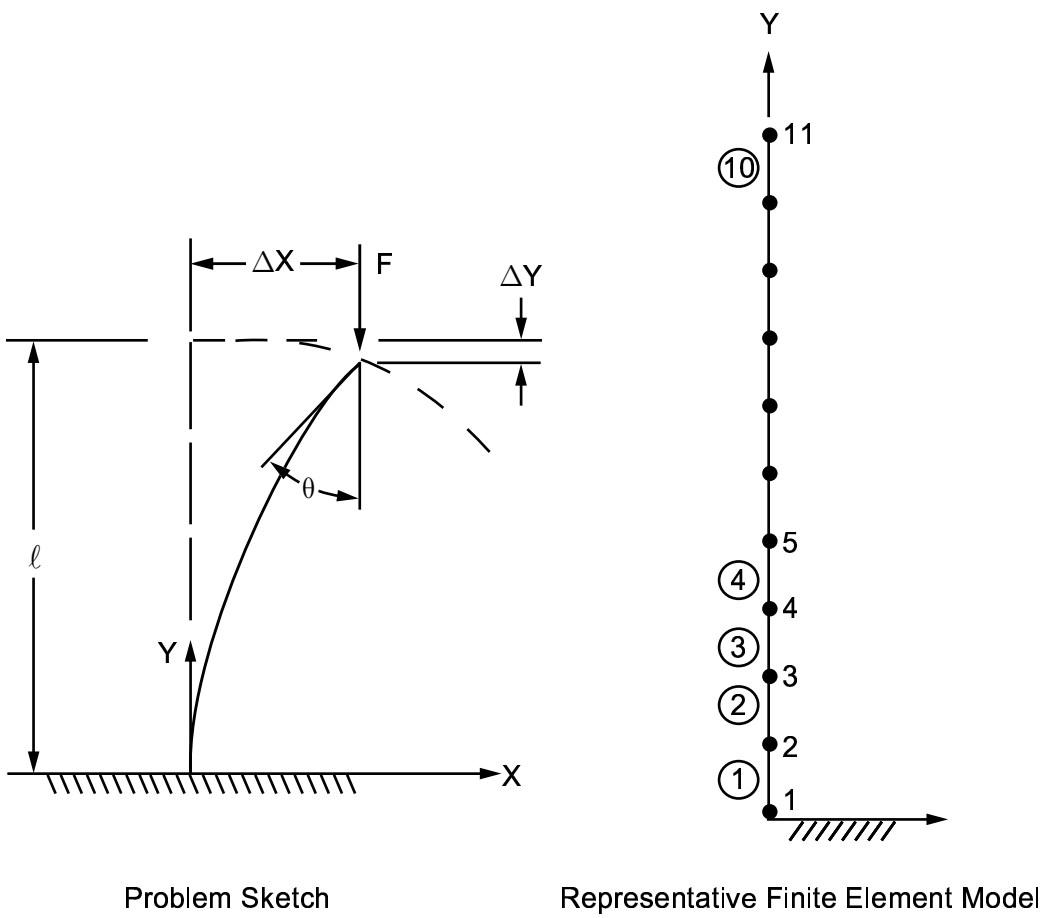

Material Properties	Geometric Properties	Loading
$E = 30 \times 10^6$ psi	$\ell = 100$ in $A = 0.25$ in^2 $h = 0.5$ in	$F/F_{cr} = 1.015; 1.063; 1.152; 1.293; 1.518$ and 1.884

Analysis Assumptions and Modeling Notes

The moment of inertia of the beam, $I = Ah^2/12 = 0.0052083\ in^4$, is used for input and the critical force, $F_{cr} = \pi^2 EI/4\ell^2 = 38.553$ lb, is used for calculation of the applied load F.

A small perturbing force is introduced in the first load step to produce lateral, rather than pure compressive, motion. The number of equilibrium iterations for convergence increases significantly as the loading approaches the critical load (i.e. for solutions with Θ near zero). The six displacement solutions are overlaid by displaying with the **/NOERASE** option set.

Results Comparison

		Target	ANSYS	Ratio
F = 44.413 lb	Angle, deg[1]	-60.0	-59.4	0.990
Load Step 3	DeflectionX, in	59.3	58.9	0.993
	DeflectionY, in	-25.9	-25.3	0.977
F = 49.849 lb	Angle, deg[1]	-80.0	-79.5	0.994
Load Step 4	DeflectionX, in	71.9	71.8	0.998
	DeflectionY, in	-44.0	-43.5	0.989
F = 58.523 lb	Angle, deg[1]	-100.0	-99.8	0.998
Load Step 5	DeflectionX, in	79.2	79.2	1.000
	DeflectionY, in	-65.1	-64.8	0.995
F = 72.634 lb	Angle, deg[1]	-120.0	-120.0	1.000
Load Step 6	DeflectionX, in	80.3	80.4	1.002
	DeflectionY, in	-87.7	-87.5	0.997

1. Angle (Θ) = ROTZ * (180/π), where ROTZ is the node rotation in radians.

Figure 136.2 Deformed Shapes at Various Loads

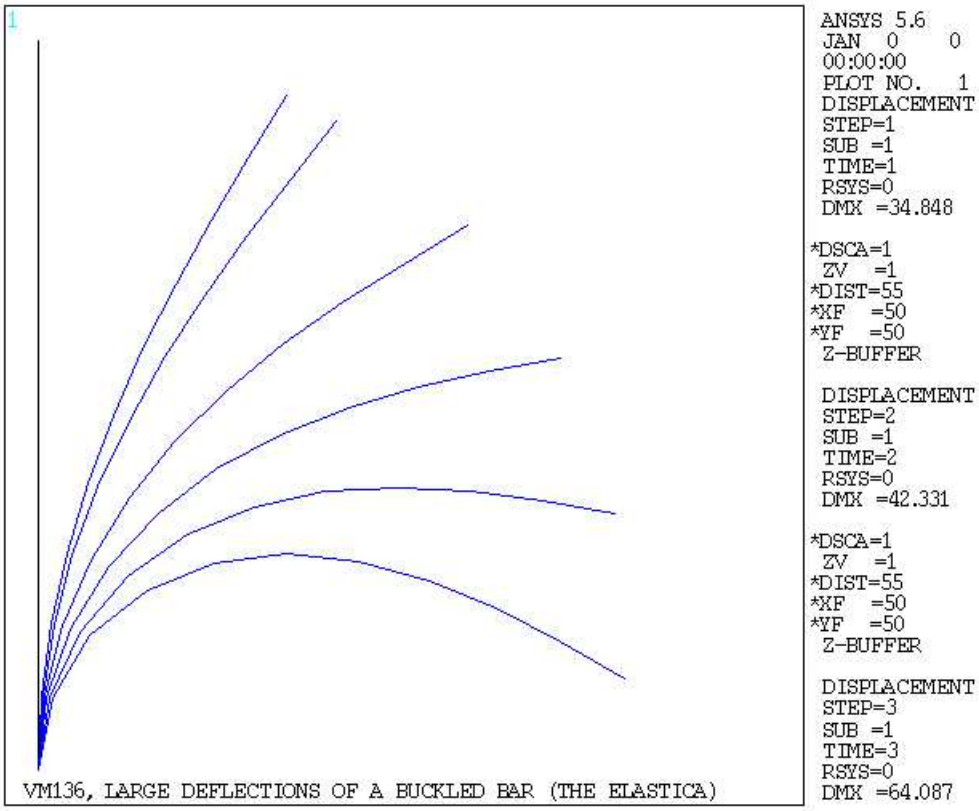

VM137: Large Deflection of a Circular Membrane

Overview

Reference:	S. Timoshenko, S. Woinowsky-Knieger, *Theory of Plates and Shells*, McGraw-Hill Book Co., Inc., New York, NY, 1959, pg. 404, eq. 236.
Analysis Type(s):	Static Analysis (**ANTYPE** = 0) with Large Deflection and Stress Stiffening
Element Type(s):	Axisymmetric-Structural Shell Elements (SHELL51)
Input Listing:	vm137.dat

Test Case

A circular membrane (of radius a and thickness t), clamped around its outer rim, is loaded with a uniform pressure p. Determine the deflection δ at the center, the radial stress σ_o at the center, and the radial stress σ_a at the rim.

Figure 137.1 Circular Membrane Problem Sketch

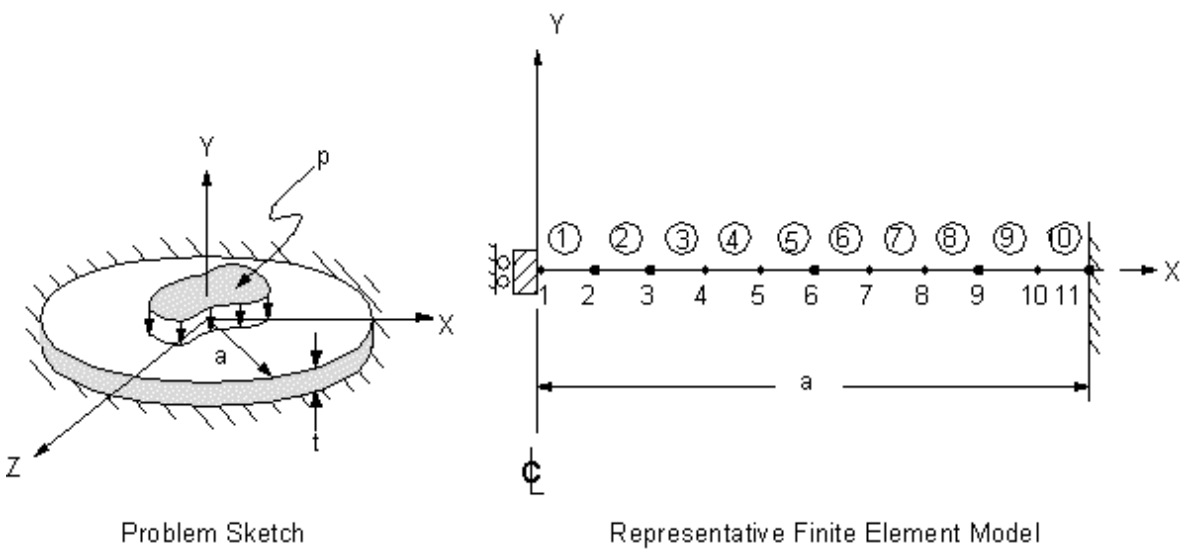

Material Properties	Geometric Properties	Loading
E = 30 x 10^6 psi α = 1 x 10^{-5} in/in-°F υ = 0.25	a = 10 in t = 0.0001 in	p = 0.1 psi

Analysis Assumptions and Modeling Notes

Since there is no significant bending stiffness, the membrane is cooled by -50°F (arbitrary) in the first load step to induce a thermal prestress for stability. The pressure load is applied in the second load step. The cooling load is removed in the third load step. Moment convergence is removed by specifying force convergence, since the moments are not significant to the solution, thereby speeding convergence.

Results Comparison

Load Step 3	Target	ANSYS	Ratio
Deflection, in (UY @ Node 1)	-0.459	-0.463	1.009

Load Step 3	Target	ANSYS	Ratio
$Stress_o$, psi	61,010	61,165[1]	1.003
$Stress_a$, psi	47,310	48,257[2]	1.020

1. Near center at x = 0.5 in (SM stress at MID for element 1)
2. Near rim at x = 9.5 in (SM stress at MID for element 10)

VM138: Large Deflection Bending of a Circular Plate

Overview

Reference:	S. Timoshenko, S. Woinowsky-Knieger, *Theory of Plates and Shells*, McGraw-Hill Book Co., Inc., New York, NY, 1959, pg. 401, eq. 232.
Analysis Type(s):	Static Analysis (**ANTYPE** = 0) with Large Deflection and Stress Stiffening
Element Type(s):	Axisymmetric-Structural Shell Elements (SHELL51)
Input Listing:	vm138.dat

Test Case

A circular plate (radius a and thickness t) built-in around its outer rim is loaded with a uniform pressure p. Determine the deflection δ at the center of the plate.

Figure 138.1 Circular Plate Problem Sketch

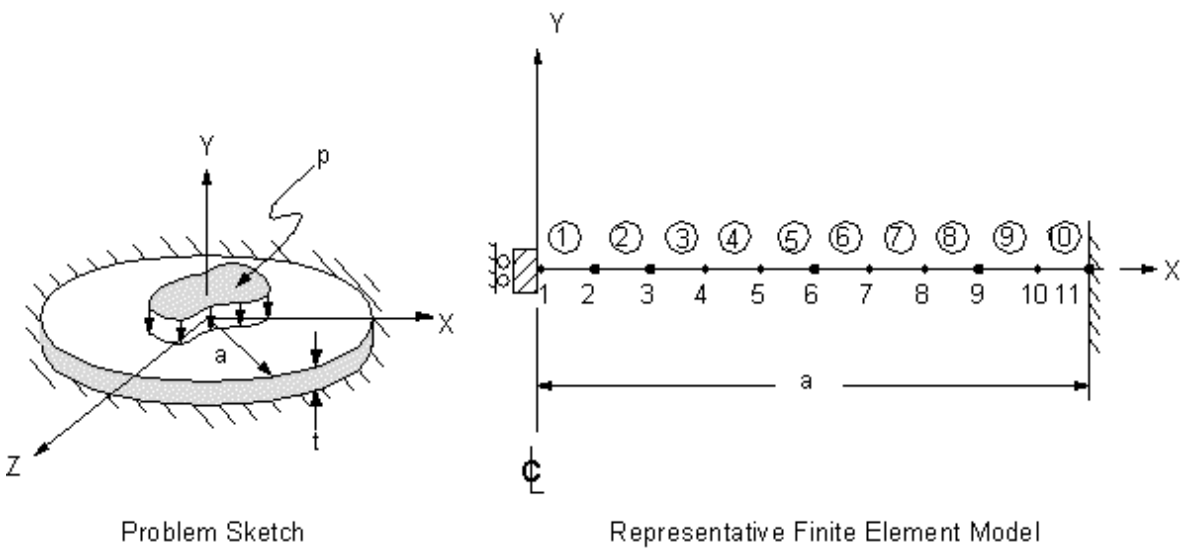

Material Properties	Geometric Properties	Loading
$E = 2 \times 10^{11}$ N/m^2 $\upsilon = 0.3$	a = 0.25 m t = 0.0025 m	p = 6585.175 N/m^2

Results Comparison

	Target	ANSYS	Ratio
Deflection, m	-0.00125	-0.00124[1]	0.992

1. UY @ Node 1

VM139: Bending of a Long Uniformly Loaded Rectangular Plate

Overview

Reference:	S. Timoshenko, *Strength of Material, Part II, Elementary Theory and Problems*, 3rd Edition, D. Van Nostrand Co., Inc., New York, NY, 1956, pg. 80, article 14.
Analysis Type(s):	Static Analysis (**ANTYPE** = 0) with Large Deflection and Stress Stiffening
Element Type(s):	Elastic Shell Elements (SHELL63) 3-D Structural Solid Shell Elements (SOLSH190)
Input Listing:	vm139.dat

Test Case

A rectangular plate whose length is large compared to its width is subjected to a uniform pressure p as shown. The shorter edges are simply-supported. Determine the direct stress σ_x (MID) at the middle of the plate and the maximum combined stress (direct plus bending) σ_x (BOT) at the bottom of the plate.

Figure 139.1 Rectangular Plate Problem Sketch

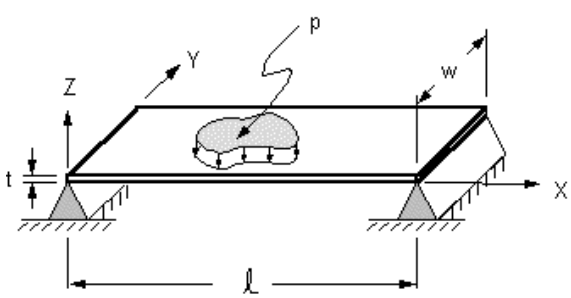

Problem Sketch

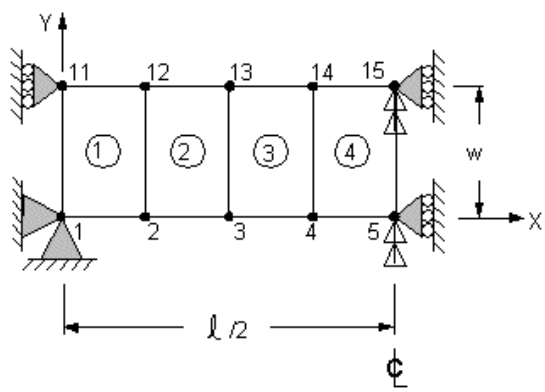

Representative Finite Element Model

Material Properties	Geometric Properties	Loading
$E = 30 \times 10^6$ psi $\upsilon = 0.3$	$\ell = 45$ in w = 9 in t = 0.375 in	$p = 10$ lb/in^2

Analysis Assumptions and Modeling Notes

Since the plate ends are "immovable" along the X-axis, a small lateral displacement due to the pressure load induces membrane stresses. The stress stiffening and large deflection capabilities are used to model this effect. The geometric and loading symmetry is used to model only half the plate with appropriate symmetry boundary conditions at the midspan.

Two analysis solutions are performed. The first solution (without large deflection and stress stiffening) results in a small deflection static solution (with no coupling between in-plane and transverse deflections). The second solution (with large deflection and stress stiffening) results in a converged solution with the coupling effects. POST1 is used to report nodal stresses along the plate middle and bottom. Note that these stresses are based on the original geometry and include the element rotations, due to the large deflection option.

The above two solutions are repeated using 3-D Solid Shell Element (SOLSH190). Two layers of SOLSH190 elements are used across the thickness and appropriate symmetry boundary conditions are applied at mid-thickness. Solid model adopts an approximate method for simulating shell simple support, leading to difference in stress Y component within a small boundary region.

Results Comparison

		Target	ANSYS	Ratio
SHELL63				
Small Deflection Solution	$Stress_x$ (MID), psi	0.0	0.0	-
	$Stress_x$ (BOT), psi	108,000.	107,489.[1]	0.995
Large Deflection Solution	$Stress_x$ (MID), psi	11,240.	10,964.[1]	0.975
	$Stress_x$ (BOT), psi	25,280.	25,012.[1]	0.989
SOLSH190				
Small Deflection Solution	$Stress_x$ (MID), psi	0.0	0.0	-
	$Stress_x$ (BOT), psi	108,000.	107,791[1]	1.000
Large Deflection Solution	$Stress_x$ (MID), psi	11,240	11,193 [1]	0.996
	$Stress_x$ (BOT), psi	25,280	24,605 [1]	0.973

1. POST1 maximum nodal stresses.

VM140: Stretching, Twisting and Bending of a Long Shaft

Overview

Reference:	S. Timoshenko, *Strength of Material, Part I, Elementary Theory and Problems*, 3rd Edition, D. Van Nostrand Co., Inc., New York, NY, 1955, pg. 296, article 65.
Analysis Type(s):	Static Analysis (**ANTYPE** = 0)
Element Type(s):	Axisymmetric-Harmonic 8-Node Structural Solid Elements (PLANE83)
Input Listing:	vm140.dat

Test Case

A long solid circular shaft of length ℓ and diameter d is built-in at one end and loaded at the other end by a twisting moment, an axial force, and a vertical force as shown. Determine the maximum shear stress τ at the wall due to the moment. Determine the maximum normal stress σ_y at the wall and at one inch from the wall due to the forces. Also determine the maximum combined stress σ_1 at the wall due to both the moment and the forces.

Figure 140.1 Shaft Problem Sketch

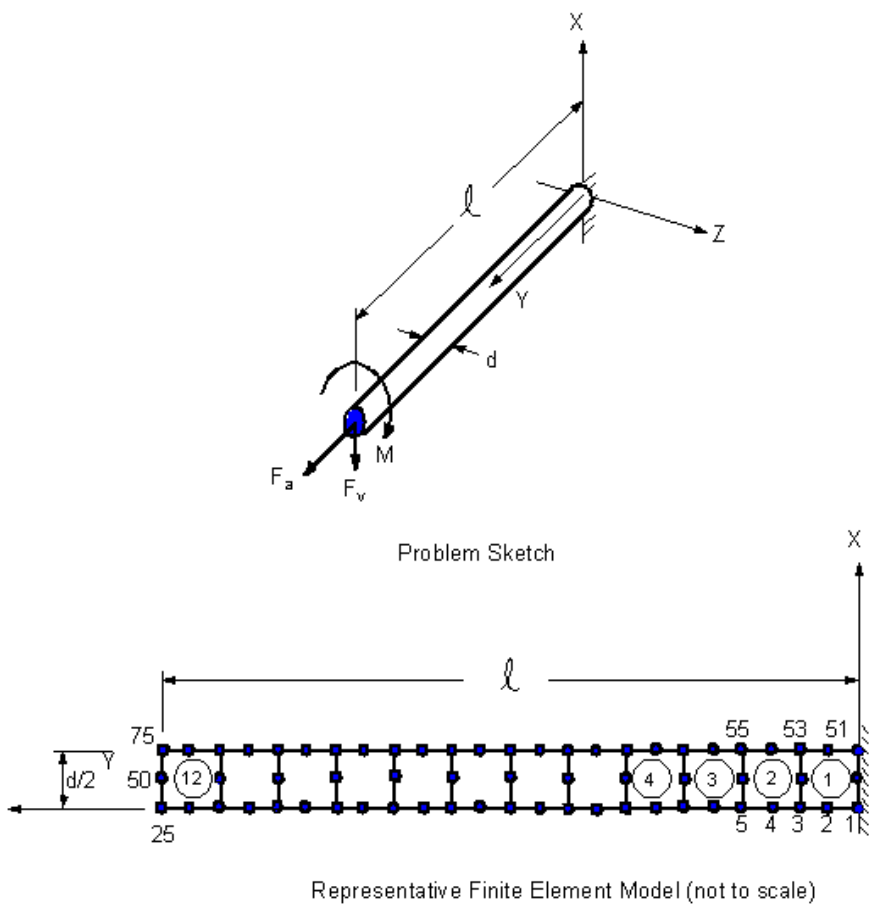

Material Properties	Geometric Properties	Loading
$E = 30 \times 10^6$ psi $\upsilon = 0.0$	$\ell = 24$ in d = 1 in	$F_v = -25$ lb M = -200 in-lb $F_a = 100$ lb

Analysis Assumptions and Modeling Notes

The loads are applied at only one node (node 75) for convenience since the cross section of interest (at the wall) is far from the load. Nodal forces are applied on full circumference basis and are calculated for symmetric mode 1 as follows:

FZ = -2M/d = 400

FX = 2_{Fv} = -50 (see Triangle, Prism and Tetrahedral Elements in *ANSYS Elements Reference*)

FY = F_a = 100

Poisson's ratio is taken as zero to avoid the stress concentration at the built-in end due to the axial force. The nonaxisymmetric loading capability of this element type (PLANE83) is used to model the bending effect. POST1 is used to report maximum stresses at the wall.

Results Comparison

Maximum Stresses	Target	ANSYS	Ratio
TORSION shear stress, psi	1018.6	1018.6[1]	1.000
AXIAL + BENDING $Stress_y$, psi (at y = 0)	6238.9	6239.9[1]	1.000
COMBINED $Stress_1$, psi	6401.0	6402.1[1]	1.000

1. POST1 nodal stresses at node 51

VM141: Diametral Compression of a Disk

Overview

Reference:	S. Timoshenko, J. N. Goodier, *Theory of Elasticity*, 2nd Edition, McGraw-Hill Book Co., Inc., New York, NY, 1951, pg. 107, article 37.
Analysis Type(s):	Static Analysis (**ANTYPE** = 0) Substructure Analysis (**ANTYPE** = 7)
Element Type(s):	2-D 6-Node Triangular Structural Solid (PLANE2) 2-D 8-Node Structural Solid Plane Stress Elements (PLANE82) 8-Node Structural Shell Elements (SHELL93) Superelement (or Substructure) (MATRIX50) 2-D Quadrilateral Structural Solid p-Elements (PLANE145)
Input Listing:	vm141.dat

Test Case

Two equal and opposite forces act along the vertical diameter of a disk as shown. Determine the compressive stress at the center of the disk and on the major horizontal diameter at 0.1 in. from the center.

Figure 141.1 Disk Problem Sketch

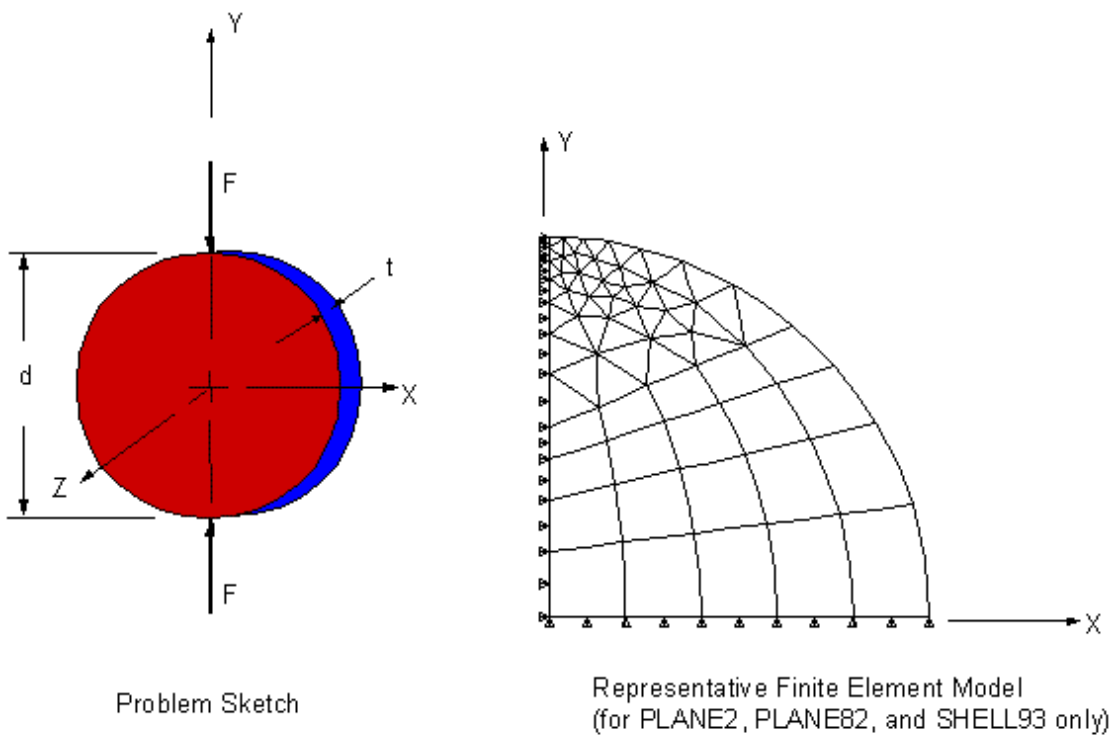

Material Properties	Geometric Properties	Loading
$E = 30 \times 10^6$ psi $\upsilon = 0.3$	d = 2 in t = 0.2 in	F = 2000 lb

Analysis Assumptions and Modeling Notes

The problem is solved first using plane stress elements (PLANE2 and PLANE82), then using shell elements (SHELL93) with the substructure analysis and expansion pass. A third solution is done using plane stress p-elements (PLANE145). In the second case, the model is created as a superelement only to illustrate the procedure for substructure capability. A more coarse mesh is defined for the p-element.

A one-fourth symmetry model is used. Three element types and the corresponding element type modifications are used only for various printout control purposes. One half of the load is applied because of symmetry. POST1 is used to extract results from the solution phase. Since the midside nodal stresses are not available in POST1, path operations are performed to get the compressive stress at 0.1 in. from the center of the disk. The P-method allows specific results to be extracted directly so no path operations are needed.

Results Comparison

		Target	ANSYS	Ratio
PLANE82 and PLANE2	$Stress_y$, psi (at x = 0.0, y = 0.0)	-9549.	-9649.	1.010
	$Stress_y$, psi (at x = 0.1, y = 0.0)	-9298.	-9139.	0.983
SHELL93	$Stress_y$, psi (at x = 0.0, y = 0.0)	-9549.	-9649.	1.010
	$Stress_y$, psi (at x = 0.1, y = 0.0)	-9298.	-9149.	0.983
PLANE145	$Stress_y$, psi (at x = 0.0, y = 0.0)	-9549.	-9528.	0.998
	$Stress_y$, psi (at x = 0.1, y = 0.0)	-9298.	-9297.	1.000

VM142: Stress Concentration At a Hole in a Plate

Overview

Reference:	R. J. Roark, *Formulas for Stress and Strain*, 4th Edition, McGraw-Hill Book Co., Inc., New York, NY, 1965, pg. 384.
Analysis Type(s):	Static Analysis (**ANTYPE** = 0), Submodeling
Element Type(s):	2-D 6-Node Triangular Structural Solid Elements (PLANE2) 2-D Structural Solid Elements (PLANE42) 2-D Triangular Structural Solid p-Elements (PLANE146)
Input Listing:	vm142.dat

Test Case

Determine the maximum stress at a circular hole cut into a square plate loaded with uniform tension P.

Figure 142.1 Plate Problem Sketch

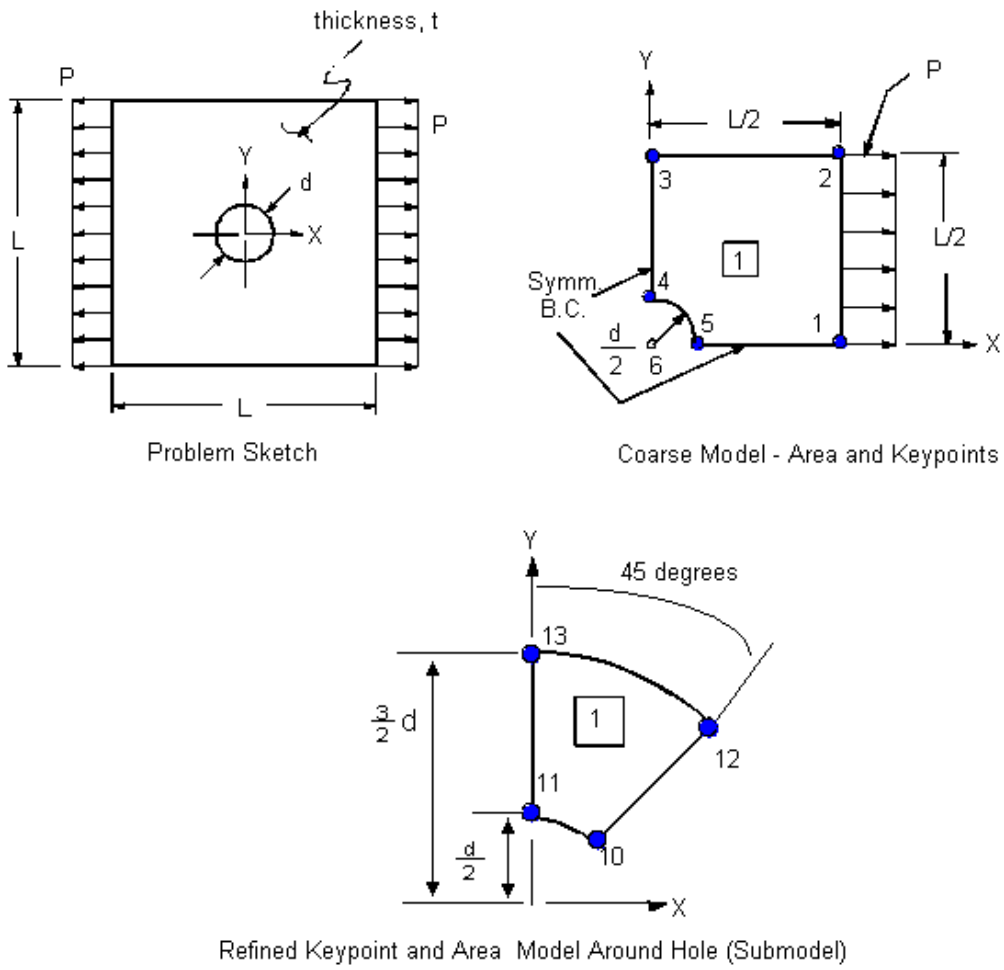

Material Properties	**Geometric Properties**	**Loading**
$E = 30 \times 10^6$ psi $\upsilon = 0.3$	L = 12 in d = 1 in t = 1 in	P = 1000 psi

Analysis Assumptions and Modeling Notes

Due to symmetry, only a quarter sector of the plate is modeled. Mesh generation is used for node and element creation. The area around the hole is remodeled with a fine mesh and boundary conditions are interpolated from the first model by use of the cut-boundary interpolation capability (**CBDOF**) in POST1.

Results Comparison

		Target	ANSYS	Ratio
Coarse Model	$stress_x$ max PLANE2	3018	2721	0.902
Submodel	$stress_x$ max	3018	2979	0.987
Coarse Model	$stress_x$ max PLANE146	3018	2919	0.967

Max σ_x based on estimated bounds due to discretization error for the coarse model and submodel are 2855. and 3076. respectively.

The coarse PLANE2 model is offered for comparison with the submodel. Coarse PLANE2 results may vary across platforms.

Figure 142.2 Stress Concentration at a Hold in a Plate

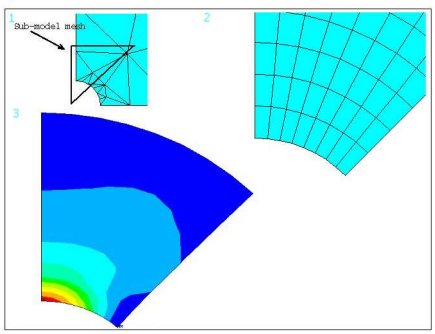

Window 1: Element Displays of Coarse and Refined Models, Overlaid.

Window 2: SX Stress Contours in Coarse Model.

Window 3: SX Stress Contours in Refined Model.

VM143: Fracture Mechanics Stress for a Crack in a Plate

Overview

Reference:	W. F. Brown, Jr., J. E. Srawley, "Plane Strain Crack Toughness Testing of High Strength Metallic Materials", *ASTM STP-410*, 1966.
Analysis Type(s):	Static Analysis (**ANTYPE** = 0)
Element Type(s):	3-D 20-Node Structural Solid Elements (SOLID95) 3-D Structural Solid Elements (SOLID45) 2-D 8-Node Structural Solid Elements (PLANE82) 3-D 20-Node Structural Solid Elements (SOLID186) 3-D Structural Solid Elements (SOLID185)
Input Listing:	vm143.dat

Test Case

A long plate with a center crack is subjected to an end tensile stress σ_o as shown in the problem sketch. Determine the fracture mechanics stress intensity factor KI.

Figure 143.1 Finite Width Plate Problem Sketch

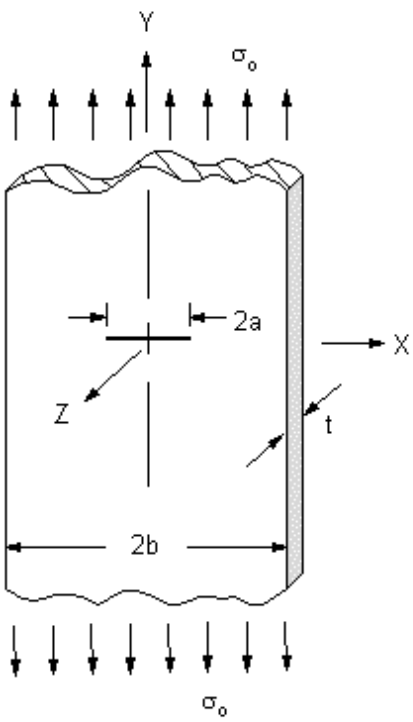

Problem Sketch

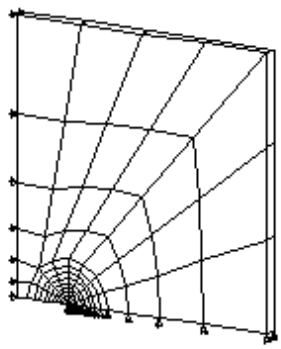

Representative Finite Element Model
(3_D Model with SOLID95 and SOLID45)

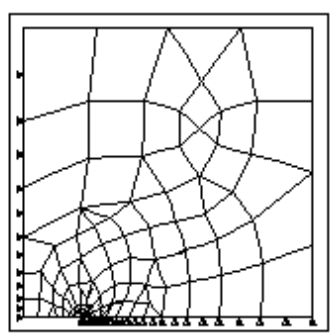

Representative Finite Element Model
(2-D Model with PLANE82)

Material Properties	Geometric Properties	Loading
$E = 30 \times 10^6$ psi $\upsilon = 0.3$	a = 1 in b = 5 in h = 5 in t = 0.25 in	$\sigma_o = 0.5641895$ psi

Analysis Assumptions and Modeling Notes

The problem is solved first using 3-D solid (SOLID95) and 3-D solid (SOLID45) elements and then using 2-D plane strain elements (PLANE82). A third solution is performed using 3-D solid (SOLID186) and 3-D solid (SOLID185) elements. A one-quarter model is used because of symmetry. The macro FRACT is used to create the SOLID95 crack tip elements from the SOLID45 model and SOLID186 crack tip elements from the SOLID185 model using a weighted midside node position (quarter point location).

In the 3-D analysis, the plane strain condition is achieved by constraining UZ degrees of freedom of all the nodes (displacements in the Z-direction). Only the back plane of nodes are shown numbered in the enlargements of the 3-D model. The simpler 2-D model using PLANE82 is created by automatic mesh generation. The **KSCON** command is used to create 2-D crack tip elements with nodal singularity.

POST1 is used to get fracture mechanics stress intensity factor (KI) by displacement extrapolation (**KCALC** command), and J-Integral methods. A user file **JIN1** is created in the input. It consists of path operations necessary to compute the J-Integral. In general usage, the user file would be available in the local directory rather than being created in the input.

Results Comparison

KI	Target	ANSYS	Ratio
Using SOLID95 and SOLID45 (3-D Analysis)			
By Displacement Extrapolation[1]	1.0249	1.0620	1.036
By J-Integral[2]	1.0249	1.0458	1.020
Using PLANE82 (2-D Analysis)			
By Displacement Extrapolation[1]	1.0249	1.0587	1.033
By J-Integral[2]	1.0249	1.0561	1.030
Using SOLID186 and SOLID185 (3-D Analysis)			
By Displacement Extrapolation1]	1.0249	1.0595	1.034
By J-Integral2]	1.0249	1.0493	1.024

1. As parameter KI1 by **KCALC** command
2. As parameter KI2

VM144: Bending of a Composite Beam

Overview

Reference:	R. J. Roark, W. C. Young, *Formulas for Stress and Strain*, McGraw-Hill Book Co., Inc., New York, NY, 1975, pg. 112-114, article 7.2.
Analysis Type(s):	Static Analysis (**ANTYPE** = 0)
Element Type(s):	Linear Layered Structural Shell Elements (SHELL99) 3-D 8-Node Layered Structural Solid Elements (SOLID46)
Input Listing:	vm144.dat

Test Case

A beam of length ℓ and width w, made up of two layers of different materials, is subjected to a uniform rise in temperature from T_{ref} to T_o and a bending moment M_y at the free-end. Determine the free-end displacement δ (in the Z-direction) and the X- direction stresses at the top and bottom surfaces of the layered beam. E_i and α_i correspond to the Young's modulus and thermal coefficient of expansion for layer i, respectively.

Figure 144.1 Composite Beam Problem Sketch

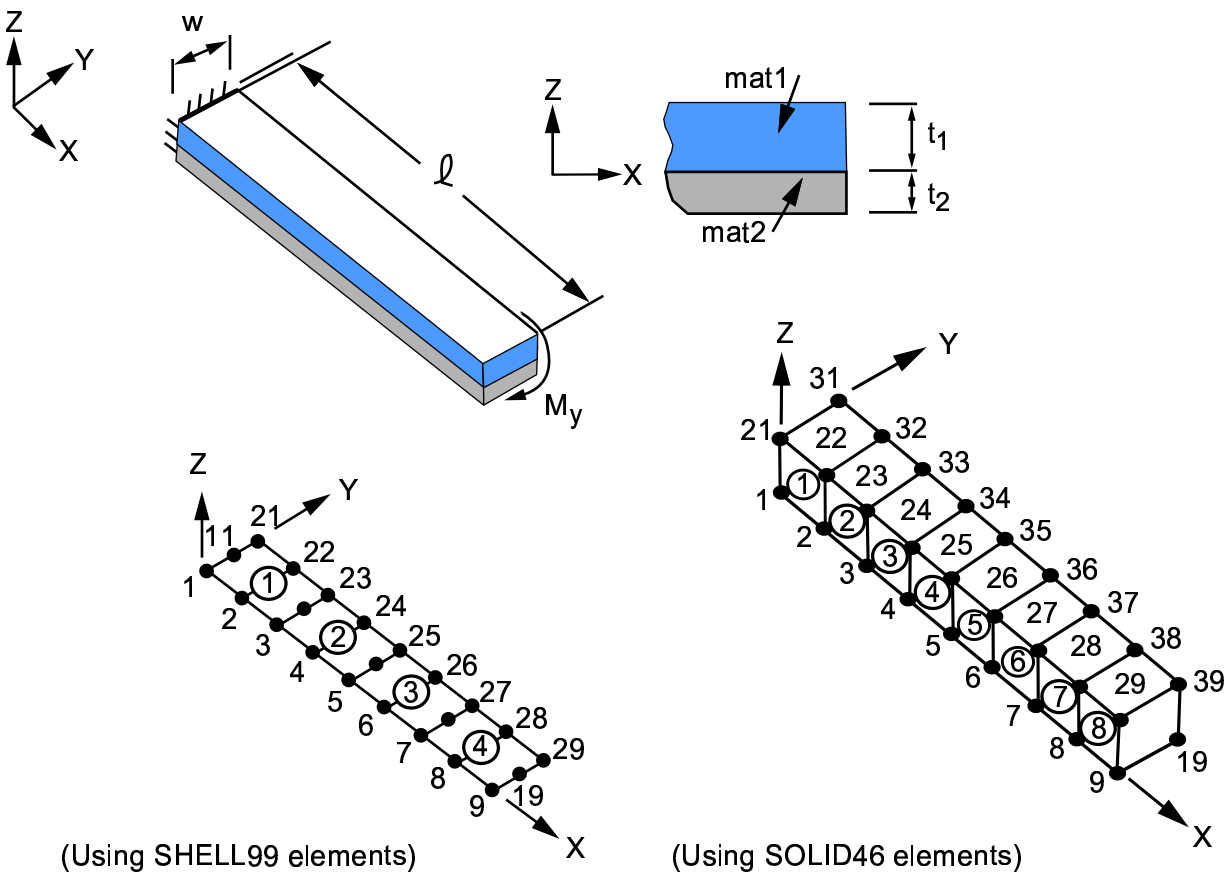

Material Properties	Geometric Properties	Loading
MAT1: $E_1 = 1.2 \times 10^6$ psi $\alpha_1 = 1.8 \times 10^{-4}$ in/in/°F MAT2: $E_2 = 0.4 \times 10^6$ psi $\alpha_2 = 0.6 \times 10^{-4}$ in/in/°F	$\ell = 8$ in w = 0.5 in $t_1 = 0.2$ in $t_2 = 0.1$ in	$T_o = 100$°F $T_{ref} = 0$°F $M_y = 10.0$ in-lb

Analysis Assumptions and Modeling Notes

The beam is idealized to match the theoretical assumptions by taking $\nu = \alpha_y = \alpha_z = 0$. Three models are used for verification of results as described below. Nodal coupling of the ROTY degree of freedom is used for the SHELL99 models to apply the uniform edge moment. Opposing nodal forces are applied at the top and bottom edges of the free end for the SOLID46 model to apply the end moment. The magnitude of these applied nodal forces is calculated as: $FX = M_y/(2 * (t_1+t_2)) = 10/0.6 = (100/6)$. POST1 is used to obtain the nodal stresses and displacements.

The first model uses four SHELL99 elements (each with 2 layers).

The second model is a variation of the first model to verify the node offset option for SHELL99 elements. In this model, two sets of four overlapping elements (a total of eight SHELL99 elements) are used. Each set represents a single layer. The set of four elements representing the lower layer has its nodal plane located on the "top" face whereas the set of elements corresponding to the top layer has its nodal plane located on the "bottom" face. The combination of overlapping elements thus defines a two-layered beam with its nodal plane at the interface between the layers (offset from the middle plane).

The third model uses eight SOLID46 elements (each with 2 layers), similar to the first SHELL99 model.

Results Comparison

		Target	ANSYS	Ratio
SHELL99 model	Displacement, in	0.832	0.832[1]	1.000
	$Stress_x$TOP , psi	2258.	2258.	1.000
	$Stress_x$BOT , psi	1731.	1731.	1.000
SHELL99 model (with node offset)	Displacement, in	0.832	0.832[1]	1.000
	$Stress_x$TOP , psi	2258.	2258.[2]	1.000
	$Stress_x$BOT , psi	1731.	1731.[2]	1.000
SOLID46 model	Displacement, in	0.832	0.832[1]	1.000
	$Stress_x$TOP , psi	2258.	2258.	1.000
	$Stress_x$BOT , psi	1731.	1731.	1.000
SOLID191 model	Disp	.832	.832	1.00
	PRS TP	2258	2257.57	1.00
	RRS BTM	1731	1730.57	1.00

1. UZ at Nodes 9, 19, 29
2. Corresponding shell TOP stresses for selected elements representing the top layer
3. Corresponding shell BOT stresses for selected elements representing the bottom layer

VM145: Stretching of an Orthotropic Solid

Overview

Reference:	S. H. Crandall, N. C. Dahl, *An Introduction to the Mechanics of Solids*, McGraw-Hill Book Co., Inc., New York, NY, 1959, pg. 225. Section 14.64: SOLID64 - 3-D Anisotropic Structural Solid in the *ANSYS, Inc. Theory Reference*
Analysis Type(s):	Static Analysis (**ANTYPE** = 0)
Element Type(s):	3-D Anisotropic Structural Solid Elements (SOLID64)
Input Listing:	vm145.dat

Test Case

A unit cube of side ℓ, having orthotropic material properties, is subjected to forces FX and FY as shown. Three orthogonal faces are supported and the opposite three faces are free. Determine the translational displacements (ΔX, ΔY, and ΔZ) of the free faces.

Figure 145.1 Orthotropic Solid Problem Sketch

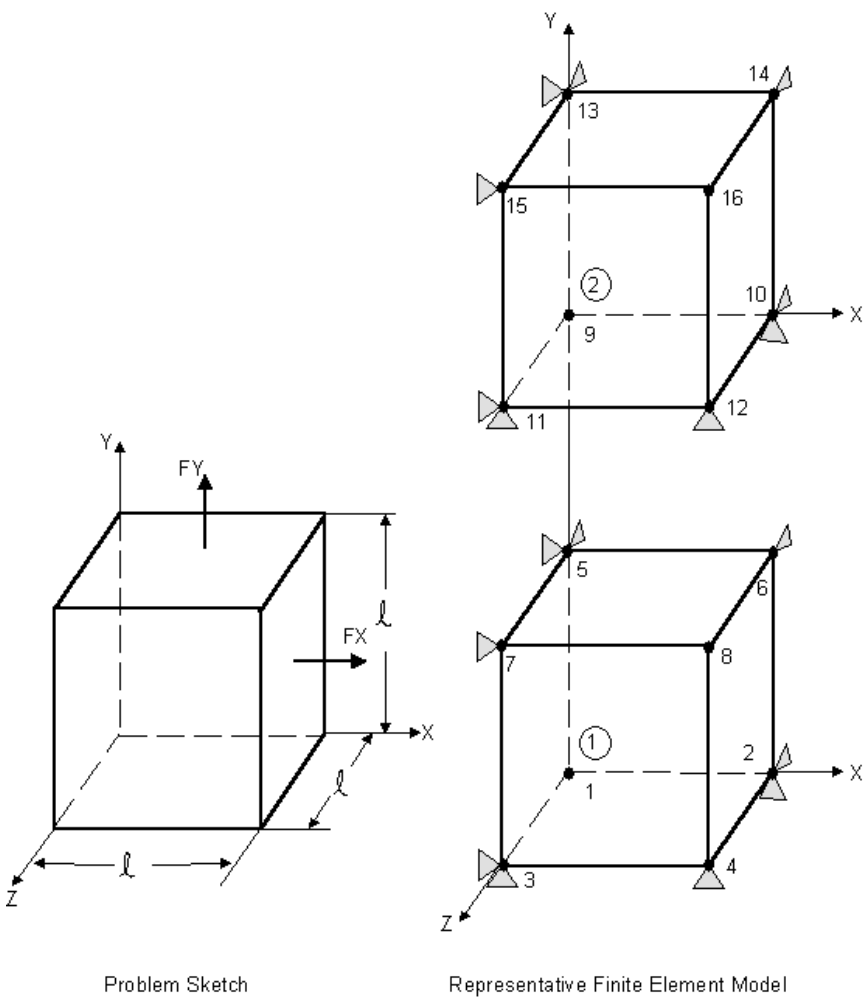

Material Properties	Geometric Properties	Loading
$E_x = 10 \times 10^6$ psi $E_y = 20 \times 10^6$ psi $E_z = 40 \times 10^6$ psi $\upsilon_{xy} = 0.1$ $\upsilon_{yz} = 0.2$ $\upsilon_{xz} = 0.3$ $G_{xy} = G_{xz} = G_{yz} = 10 \times 10^6$ psi	$\ell = 1.0$ in	FX = 100 lb FY = 200 lb

Analysis Assumptions and Modeling Notes

Two independent one-element models are used. Element 1 uses the material property data input in the nonlinear material table (material 1) in a matrix form that is to be inverted by the program. Element 2 uses directly labeled material property input.

The matrix input is defined as shown in Equation 2–4 of the *ANSYS, Inc. Theory Reference* with matrix term numbers 1, 2, 3, 7, 8, 12, 16, 19 and 21. Set *TBOPT* = 1 on the **TB** command to input the stiffness matrix in flexibility form. The same terms are input with the **TBDATA** command as described in the *ANSYS Elements Reference*.

Results Comparison

	Target	ANSYS[1]	Ratio
UX, in	0.9×10^{-5}	0.9×10^{-5}	1.000
UY, in	0.95×10^{-5}	0.95×10^{-5}	1.000
UZ, in	-0.175×10^{-5}	-0.175×10^{-5}	1.000

1. for Nodes 8 and 16

VM146: Bending of a Reinforced Concrete Beam

Overview

Reference:	S. Timoshenko, *Strength of Material, Part I, Elementary Theory and Problems*, 3rd Edition, D. Van Nostrand Co., Inc., New York, NY, 1955, pg. 221, article 48.
Analysis Type(s):	Static Analysis (**ANTYPE** = 0)
Element Type(s):	3-D Reinforced Concrete Solid Elements (SOLID65) 3-D Spar (or Truss) Elements (LINK8) Elastic Straight Pipe Elements (PIPE16)
Input Listing:	vm146.dat

Test Case

A concrete beam reinforced with steel rods (of cross-sectional area A) is subjected to a pure bending load M. Determine the depth of the crack δ_{ck} from the bottom surface, the maximum tensile stress σ_t in the steel, and the maximum compressive stress σ_c in the concrete, assuming the cracking tensile strength of concrete σ_{ct} to be zero.

Figure 146.1 Reinforced Concrete Beam Problem Sketch

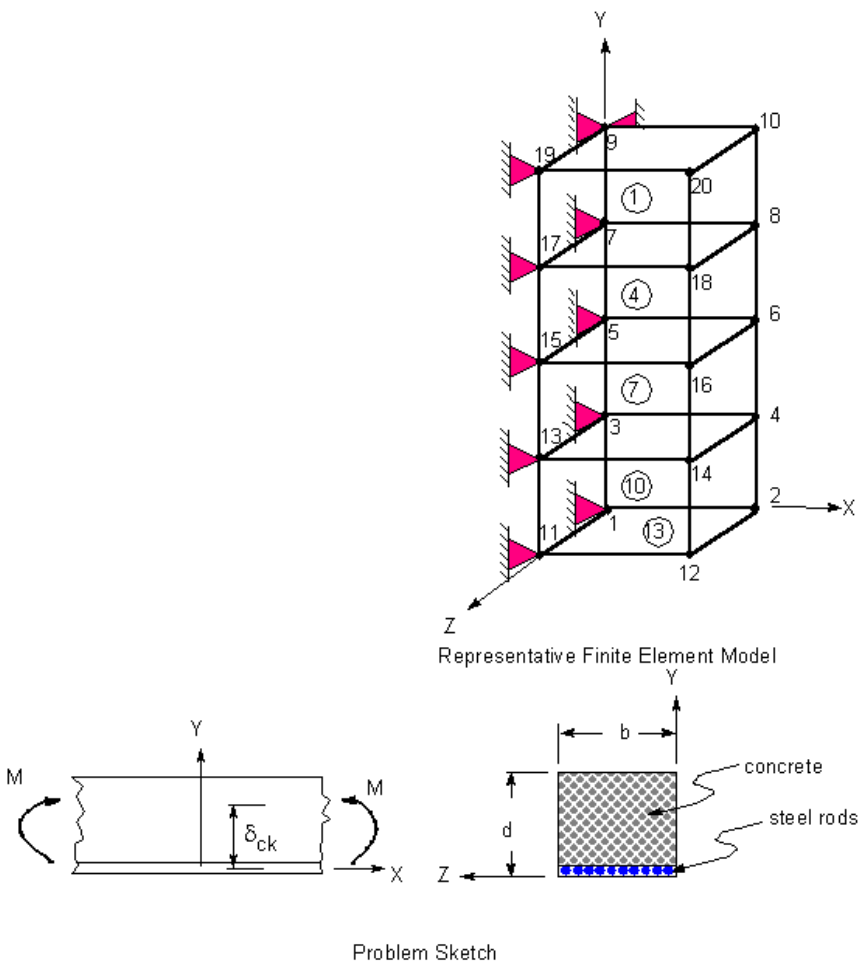

Material Properties	Geometric Properties
Concrete (material 1) $E = 2 \times 10^6$ psi $\sigma_{ct} = 0.0$ psi $\upsilon = 0.0$ **Steel (material 2)** $E = 30 \times 10^6$ psi $\upsilon = 0.3$	b = 5 in d = 6 in $A = 0.30$ in^2 **Loading** M = 600 in-lb

Analysis Assumptions and Modeling Notes

The bottom concrete element is lined with two spar elements to match the assumption given in the reference of discrete (rather than smeared) reinforcement. A zero Poisson's ratio and an infinite crushing strength are also assumed for the concrete to match the reference assumptions. An element width (in the X-direction) of 1.5 in. is arbitrarily selected. Constraint equations are used along the beam depth to conveniently apply the load and match the reference assumption that cross-sections remain plane. Dummy PIPE16 pipe elements are used to "line" the constraint equation region to provide the necessary rotational degrees of freedom at the nodes. Up to five substeps are specified with automatic load stepping to allow convergence of the crack nonlinearity.

Results Comparison

	Target	ANSYS	Ratio
$Depth_{ck}$, in	3.49	Between 3.32 - 4.18[1]	-
$Stress_t$, psi	387.28	387.25[2]	1.000
$Stress_c$, psi	-18.54	-18.49[3]	0.997

1. Five sets of integration points (each set consisting of 4 points parallel to the X-Z plane) below 3.49 in. crack open, including one set at 3.32 in. from the bottom. Three sets of integration points above 3.32 in. remain closed, including one set at 4.18 in. from the bottom. Note that the integration points are printed only if the element has cracked. A more exact comparison with theory could be obtained with more elements along the depth of the beam (and thus a closer spacing of integration points).
2. $Stress_t$ = SAXL in the spars (elements 13 and 14).
3. $Stress_c$ = SX in element 1 at nodes 9, 10, 19, or 20.

VM147: Gray-Body Radiation within a Frustum of a Cone

Overview

Reference:	R. Siegel, J. R. Howell, *Thermal Radiation Heat Transfer*, 2nd Edition, Hemisphere Publishing Corporation, 1981, pg. 277, prob. 9.
Analysis Type(s):	Thermal Analysis (**ANTYPE** = 0) AUX12 (Radiation View Factor Utility)
Element Type(s):	2-D Conduction Bar Elements (LINK32) 2-D Thermal Surface Effect Elements (SURF151) Superelement (or Substructure) Elements (MATRIX50)
Input Listing:	vm147.dat

Test Case

A frustum of a cone has its base heated (q_1) as shown. The top is held at temperature T_3, while the side is perfectly insulated. All the surfaces are diffuse-gray (with emissivities ε_1, ε_2, ε_3, respectively). Determine the temperature T_1, achieved by surface 1 as a result of radiation exchange within the enclosure.

Figure 147.1 Gray-Body Radiation Problem Sketch

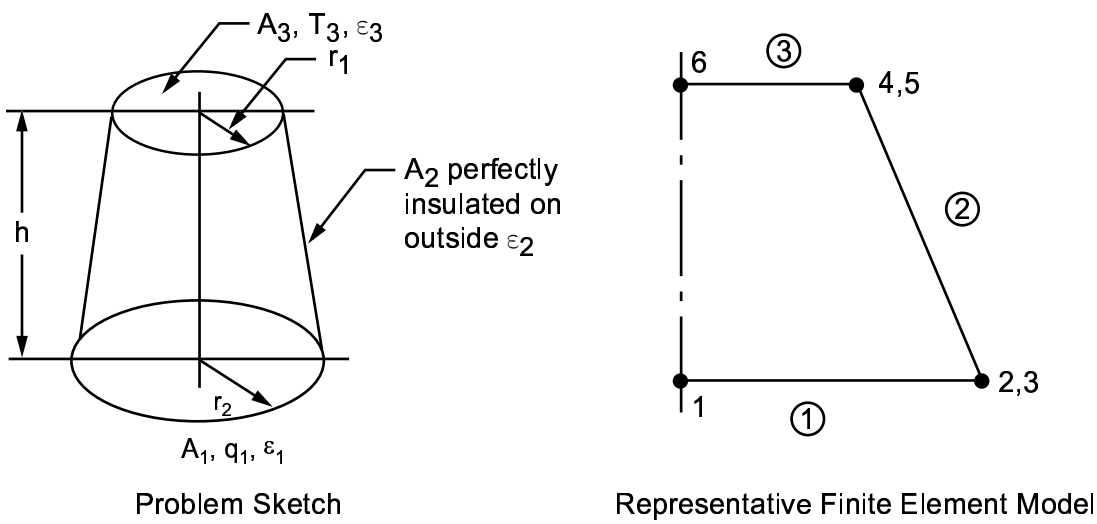

Material Properties	Geometric Properties	Loading
$\varepsilon_1 = .06$	$r_i = 0.050$ m	$T_3 = 550$ K
$\varepsilon_2 = 0.8$	$r_2 = 0.075$ m	$q_1 = 6000$ W/m^2
$\varepsilon_3 = 0.5$	h = 0.075 m	

Analysis Assumptions and Modeling Notes

An axisymmetric model is used for the cone. The radiating surfaces are modeled using three LINK32 elements. The non-hidden method (**VTYPE**) is used since there are no blocking or obscuring surfaces within the enclosure (i.e. all radiating surfaces fully "see" each other). The radiation matrix is written using 50 circumferential divisions (**GEOM**). Since all the radiating surfaces form an enclosure, no space node is specified. Heat flux on the bottom surface is applied using SURF151 (surface effect element). The value of Stefan-Boltzmann constant is specified in consistent units as 5.6696E-8 W/m^2-K.

Results Comparison

Non-hidden method	Target	ANSYS	Ratio
T_1 , K	904	907	1.003

VM148: Bending of a Parabolic Beam

Overview

Reference:	S. Timoshenko, *Strength of Material, Part I, Elementary Theory and Problems*, 3rd Edition, D. Van Nostrand Co., Inc., New York, NY, 1955, pg. 210, article 46.
Analysis Type(s):	Static Analysis (**ANTYPE** = 0)
Element Type(s):	3-D 20-Node Structural Solid Elements (SOLID95) 3-D 20-Node Structural Solid Elements (SOLID186)
Input Listing:	vm148.dat

Test Case

A beam having a parabolic depth-to-length variation is subjected to an end load as shown. The other end is supported at a wall. Determine the deflection δ at the tip of the beam.

Figure 148.1 Parabolic Beam Problem Sketch

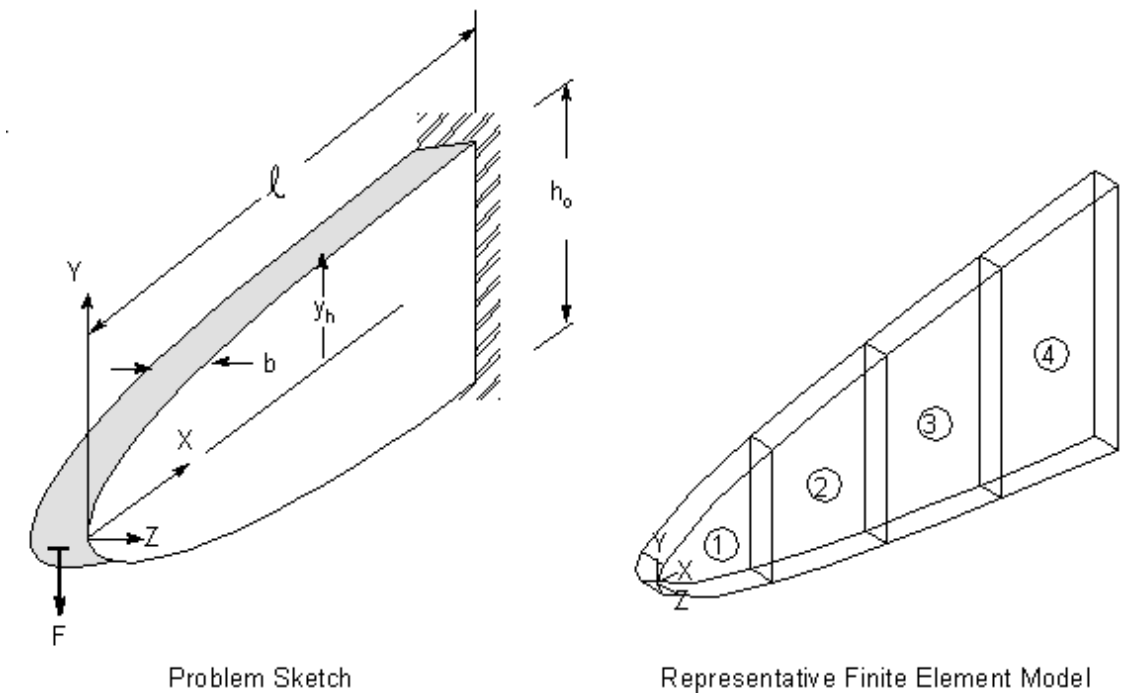

Material Properties	Geometric Properties	Loading
$E = 30 \times 10^6$ psi $G = 1.5 \times 10^8$ psi $\upsilon = 0.0$	$\ell = 4$ in $h_o = 2$ in $b = 0.2$ in	$F = -1000$ lb

Analysis Assumptions and Modeling Notes

The problem is solved first using 3-D solid (SOLID95) and then using 3-D solid SOLID186 elements.

A large shear modulus G is assumed (1.5×10^8) and the Poisson's ratio is taken as zero to match the theoretical assumptions. The six nodes at the top and bottom edges near the tip of element 1 are defined closer to the tip

so that the two mid-edge nodes (11 and 71) are not improperly located. Other nodes along the parabolic edge are generated with parametric input, at uniform spacing along the axis, using the equation:

$$Y_h = (h_o / 2)^* Y_h = (h_o / 2)^* \sqrt{x / \ell}$$

Results Comparison

	Target	ANSYS	Ratio
SOLID95			
Deflection, in	-0.01067	-0.01062[1]	0.995
SOLID186			
Deflection, in	-0.01067	-0.01076	1.009

1. UY at node 11 or 71.

VM149: Rotation of a Tank of Fluid

Overview

Reference:	K. Brenkert, Jr., *Elementary Theoretical Fluid Mechanics*, John Wiley and Sons, Inc., New York, NY, 1960, pg. 54, article 18.
Analysis Type(s):	Static Analysis (**ANTYPE** = 0)
Element Type(s):	2-D Contained Fluid Elements (FLUID79)
Input Listing:	vm149.dat

Test Case

A large cylindrical tank is partially filled with an incompressible liquid. The tank rotates at a constant angular velocity ω about its vertical axis as shown. Determine the elevation δ of the liquid surface relative to the center (lowest) elevation for various radial positions. Also determine the pressure ρ in the fluid near the bottom corner of the tank.

Figure 149.1 Fluid Tank Problem Sketch

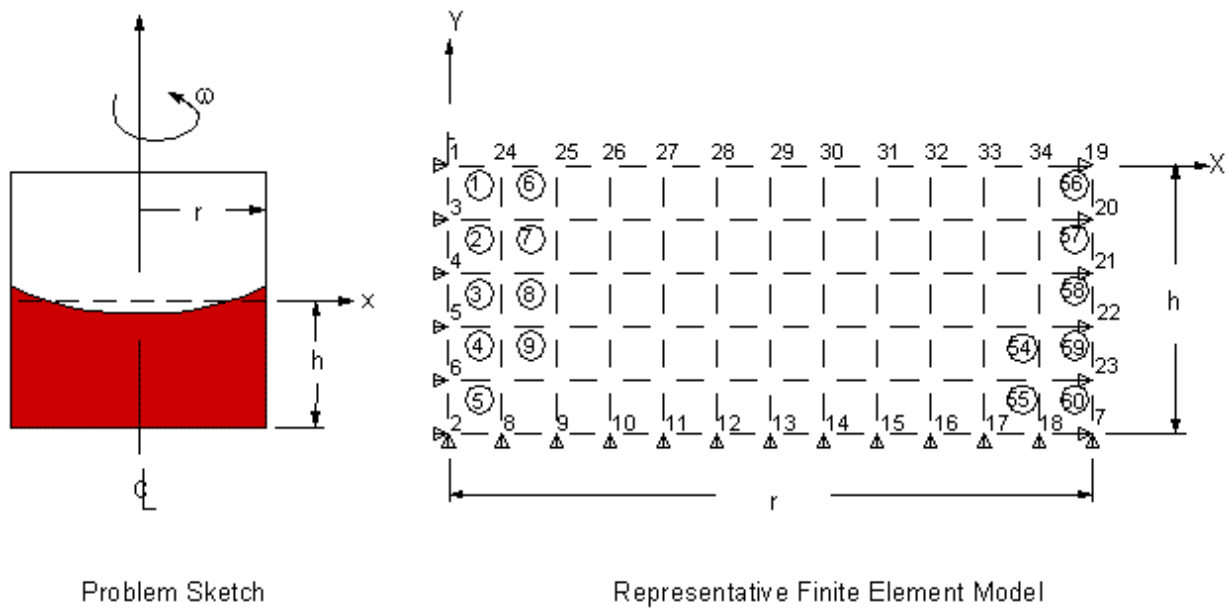

Material Properties	Geometric Properties	Loading
$\rho = 0.9345 \times 10^{-4}$ lb-sec^2/in^4 $\beta = 30 \times 10^4$ psi	r = 48 in h = 20 in	ω = 1 rad/sec g = 386.4 in/sec^2

Analysis Assumptions and Modeling Notes

The axisymmetric option is used for the model. The bulk modulus $\beta = 30 \times 10^4$ psi is taken to be characteristic of the fluid rather than infinite (incompressible) since it is used for shear stability as well as for compressibility effects. POST1 is used to select and print the radial surface elevations and the pressure near the bottom corner of the tank.

Results Comparison

	Target	ANSYS	Ratio
Deflection, in (at X = 12)	0.186	0.197[1]	1.057
Deflection, in (at X = 24)	0.745	0.756[1]	1.014
Deflection, in (at X = 40)	2.070	2.081[1]	1.005
p, psi (at X = 46, Y = -18)	0.695	0.695[2]	1.000

1. Deflection at the three locations corresponds to the parameters UY26, UY29 and UY33 in POST1. These are obtained by subtracting the UY displacement at node 1 from the UY displacements at nodes 26, 29 and 33, respectively.
2. p is obtained from the centroidal pressure of element 60 (parameter PR60 in POST1).

VM150: Acceleration of a Tank of Fluid

Overview

Reference:	K. Brenkert, Jr., *Elementary Theoretical Fluid Mechanics*, John Wiley and Sons, Inc., New York, NY, 1960, pg. 50, article 17.
Analysis Type(s):	Static Analysis (**ANTYPE** = 0)
Element Type(s):	3-D Contained Fluid Elements (FLUID80)
Input Listing:	vm150.dat

Test Case

A large rectangular tank is partially filled with an incompressible liquid. The tank has a constant acceleration a to the right as shown. Determine the elevation δ of the liquid surface relative to the zero acceleration elevation along the Y-axis. Also determine the slope Θ of the free surface and the pressure p in the fluid near the bottom left corner of the tank.

Figure 150.1 Fluid Tank Problem Sketch

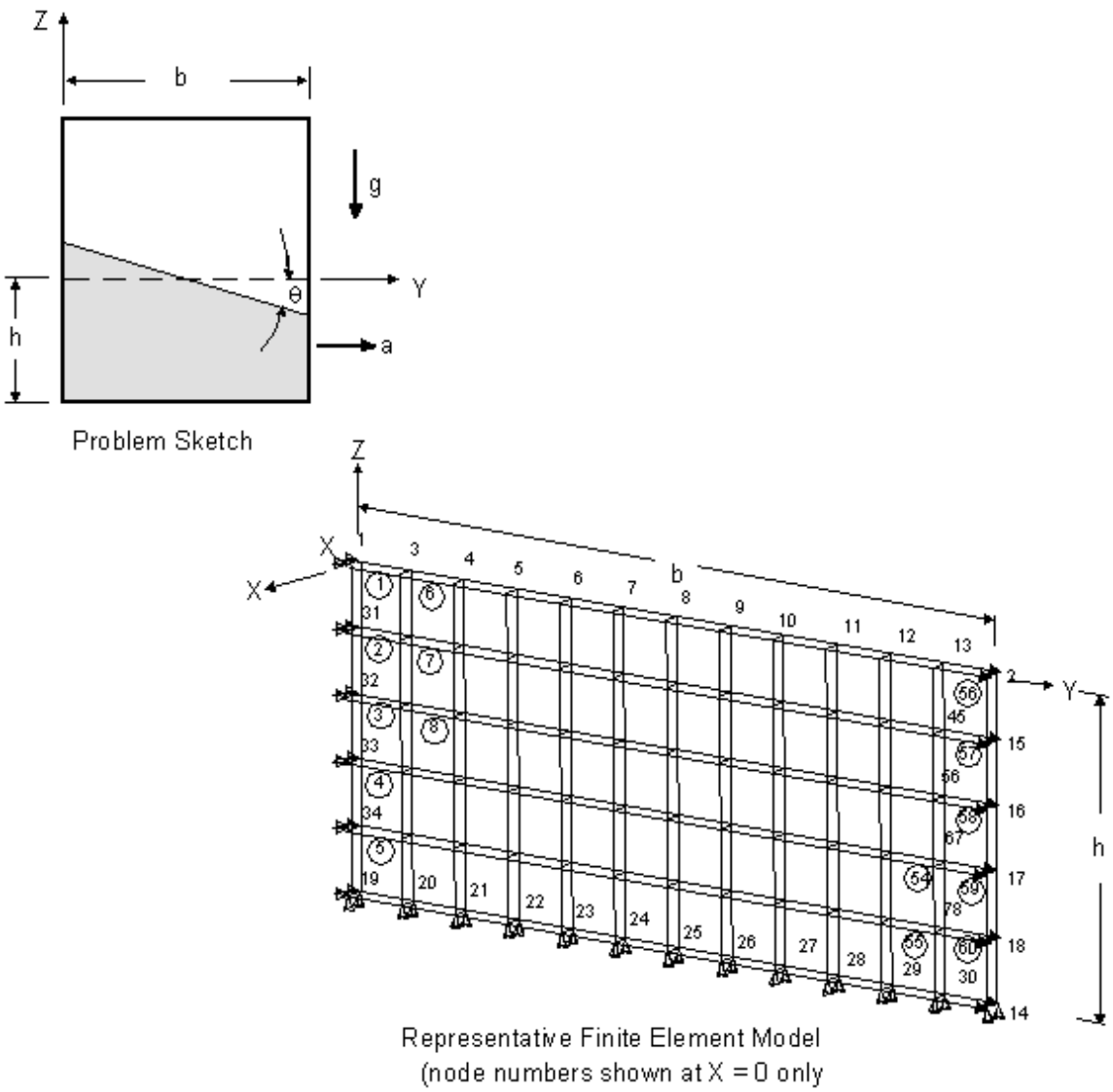

Material Properties	Geometric Properties	Loading
$\rho = 0.9345 \times 10^{-4}$ lb-sec^2/in^4 $\beta = 30 \times 10^4$ psi	b = 48 in h = 20 in	a = 45 in/sec^2 g = 386.4 in/sec^2

Analysis Assumptions and Modeling Notes

The bulk modulus $\beta = 30 \times 10^4$ is taken to be characteristic of the fluid rather than infinite (incompressible) since it is used for shear stability as well as for compressibility effects. A unit thickness is assumed for the solid elements. POST1 is used to obtain the elevations, slope, and corner pressure.

Results Comparison

	Target	ANSYS	Ratio
Displacement, in (at Y = 8)	1.863	1.863[1]	1.000
Displacement, in (at Y = 24)	0.0	0.0[1]	-
Displacement, in (at Y = 40)	-1.863	-1.863[1]	1.000
Slope	-0.1164	-0.1164[2]	1.000
p, psi (at Y = 2, Z = -18)	0.7425	0.7425[3]	1.000

1. Displacement δ at the three locations are UZ displacements at nodes 4, 8 and 12, respectively.
2. Slope Θ is the parameter SLOPE in POST1 given by $\Delta Z/\Delta Y$ based on locations Y = 8 and Y = 40 on the free surface.
3. p is obtained from the centroidal pressure of element 5 (**ETABLE** item PREL in POST1).

VM151: Nonaxisymmetric Vibration of a Circular Plate

Overview

Reference:	R. J. Blevins, *Formulas for Natural Frequency and Mode Shape*, Van Nostrand Reinhold Co., New York, NY, 1979, pg. 240, no. 2.
Analysis Type(s):	Mode-frequency Analysis (**ANTYPE** = 2)
Element Type(s):	Axisymmetric-Harmonic Structural Shell Elements (SHELL61)
Input Listing:	vm151.dat

Test Case

A circular plate with a simply supported edge is allowed to vibrate freely. Determine the natural frequencies $f_{i,j}$ for the first mode of vibration (j = 1 = no. of nodal circles, including the boundary) for the first three harmonics (i = 0,1,2 = no. of harmonic indices).

Figure 151.1 Circular Plate Problem Sketch

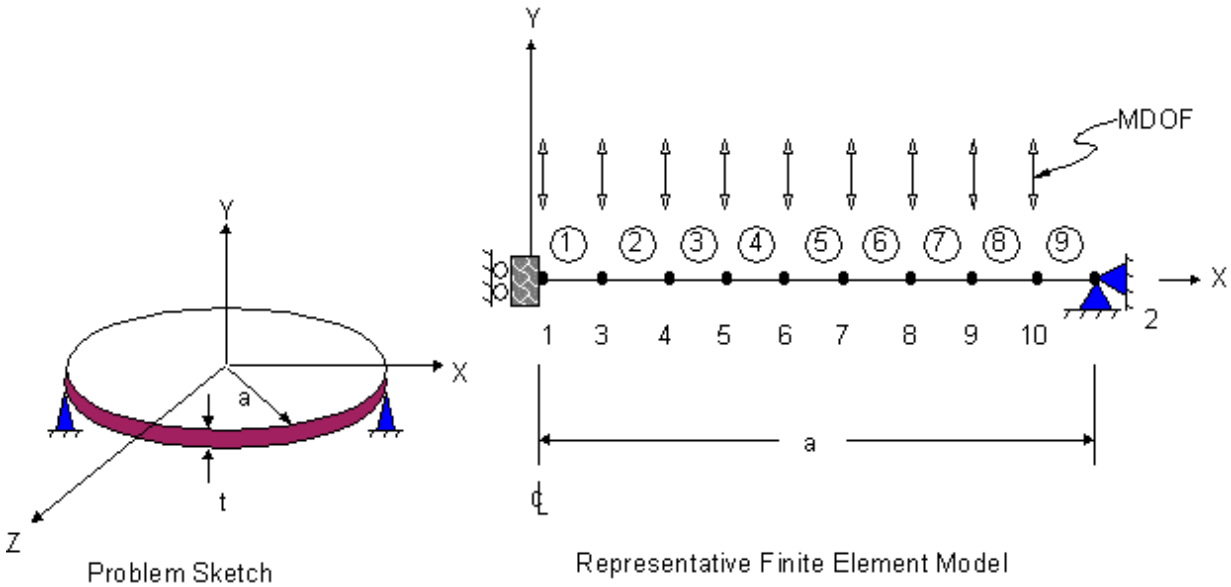

Material Properties	**Geometric Properties**
$E = 30 \times 10^6$ psi $\upsilon = 0.3$ $\rho = 0.00073$ lb-sec^2/in^4	a = 3 in t = 0.05 in

Analysis Assumptions and Modeling Notes

Poisson's ratio defaults to 0.3 and is not defined with the input data. A total of 9 elements is selected for meshing. All lateral degrees of freedom are selected as masters (MDOF) for good theoretical comparisons.

Results Comparison

	Target	ANSYS	Ratio
$f_{o,1}$, Hz	269.96	267.67	0.992

	Target	ANSYS	Ratio
$f_{1,1}$, Hz	756.13	753.74	0.997
$f_{2,1}$, Hz	1391.3	1388.9	0.998

Figure 151.2 Mode Shape Displays

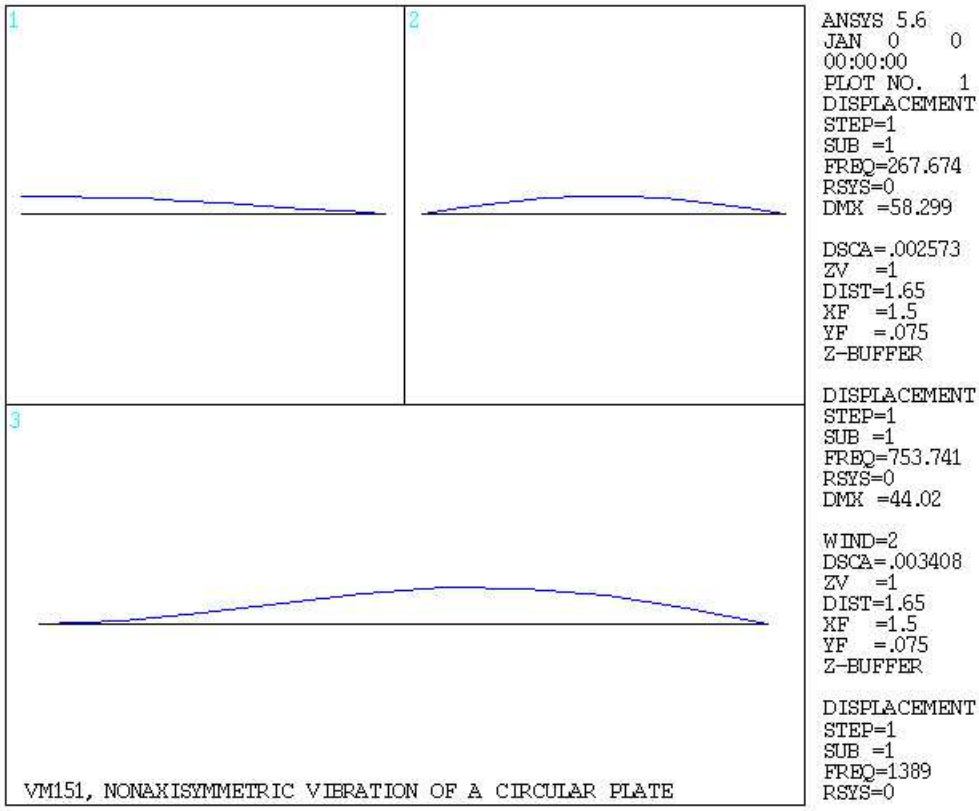

Window 1 - $f_{0,1}$; Window 2 - $f_{1,1}$; Window 3 - $f_{2,1}$

VM152: 2-D Nonaxisymmetric Vibration of a Stretched Membrane

Overview

Reference:	S. Timoshenko, D. H. Young, *Vibration Problems in Engineering*, 3rd Edition, D. Van Nostrand Co., Inc., New York, NY, 1955, pp. 438-439, article 69.
Analysis Type(s):	Mode-frequency Analysis (**ANTYPE** = 2) Static Analysis, Prestress (**ANTYPE** = 0)
Element Type(s):	Axisymmetric-Harmonic Structural Shell Elements (SHELL61)
Input Listing:	vm152.dat

Test Case

A circular membrane under a uniform tension S is allowed to vibrate freely. The edge of the membrane is simply supported. Determine the natural frequencies $f_{i,j}$ for the first mode of vibration (j = 1 = no. of nodal circles, including the boundary) for the first three harmonic (i = 0,1,2 = no. of harmonic indices). Also determine the next highest axisymmetric frequency $f_{0,2}$. See VM153 for a 3-D solution of this problem.

Figure 152.1 Circular Membrane Problem Sketch

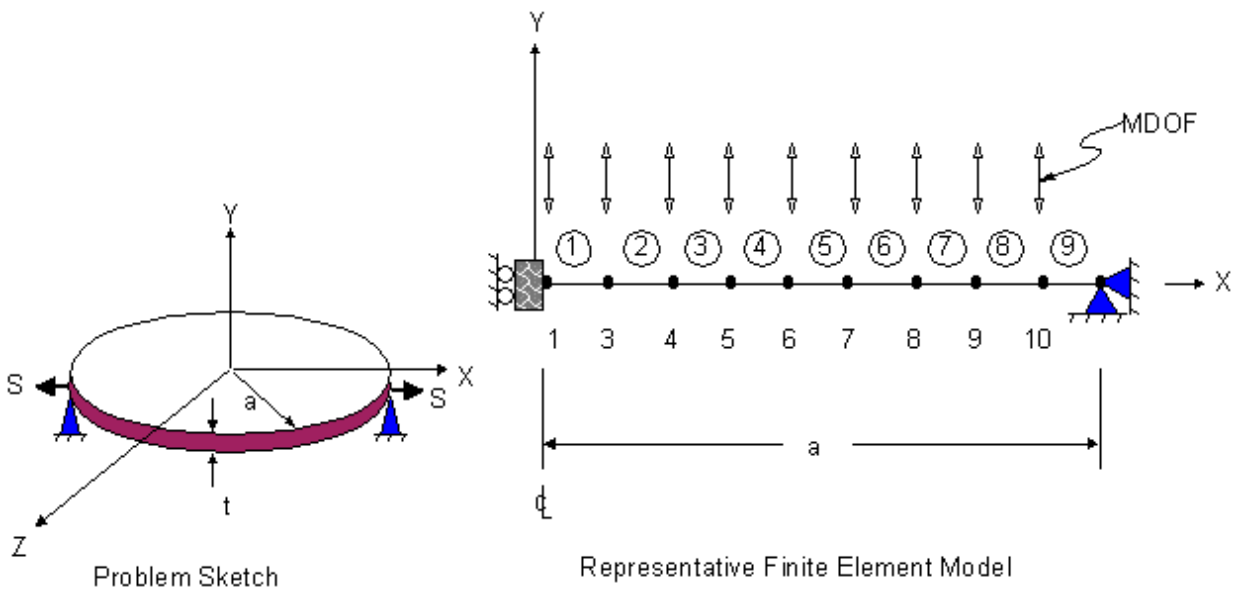

Material Properties	Geometric Properties	Loading
E = 30 x 10^6 psi υ = 0.0 ρ = 0.00073 lb-sec^2/in^4 α = 1 x 10^{-5} in/in-°F	a = 3 in t = 0.00005 in	S = 0.1 lb/in of boundary ΔT = -6.6666°F

Analysis Assumptions and Modeling Notes

All available lateral degrees of freedom are selected as masters (MDOF) for good theoretical comparisons. A total of 9 elements is selected for meshing. The prestress is induced by cooling the membrane. The necessary temperature difference, ΔT, is calculated from S = -E αt(ΔT).

Results Comparison

	Target	ANSYS	Ratio
$f_{o,1}$, Hz (L.S. 1, ITER 1)	211.1	211.2	1.001
$f_{1,1}$, Hz (L.S. 2, ITER 1)	336.5	336.6	1.000
$f_{2,1}$, Hz (L.S. 3, ITER 1)	450.9	451.3	1.001
$f_{0,2}$, Hz (L.S. 1, ITER 2)	484.7	486.2	1.003

Figure 152.2 Mode Shape Displays

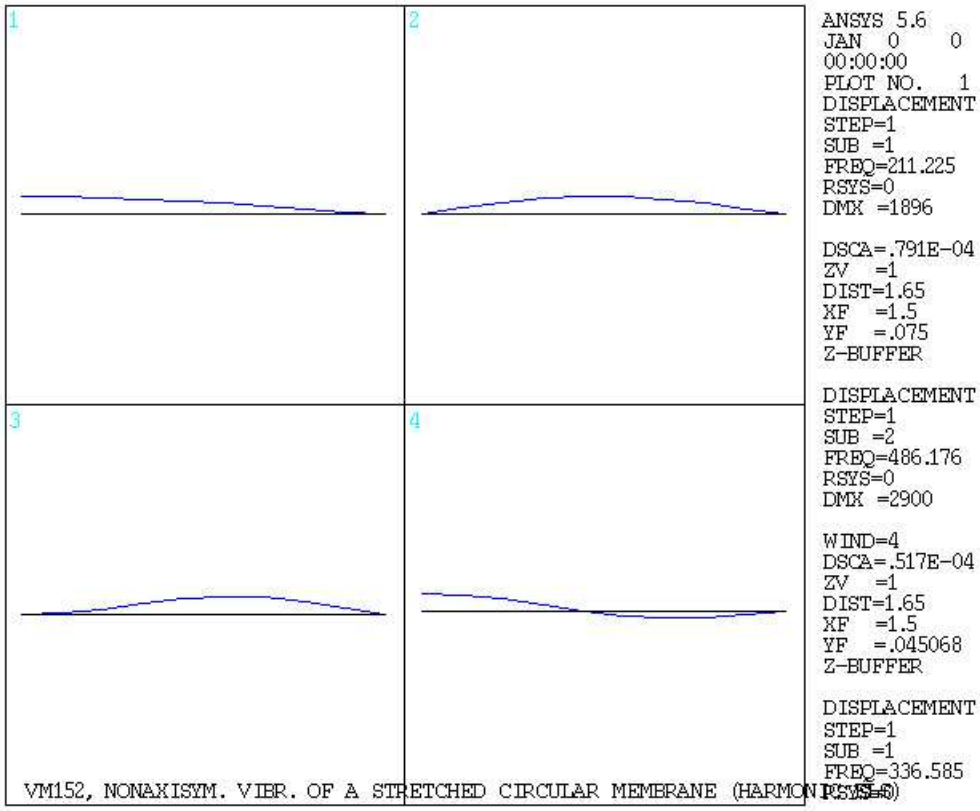

Window 1 - $f_{0,1}$; Window 2 - $f_{1,1}$; Window 3 - $f_{2,1}$; Window 4 - $f_{0,2}$;

VM153: 3-D Nonaxisymmetric Vibration of a Stretched Membrane

Overview

Reference:	S. Timoshenko, D. H. Young, *Vibration Problems in Engineering*, 3rd Edition, D. Van Nostrand Co., Inc., New York, NY, 1955, pg. 439, article 69.
Analysis Type(s):	Mode-frequency Analysis (**ANTYPE** = 2) Prestress Static Analysis (**ANTYPE** = 0) Substructure Cyclic Symmetry Matrix (Macro)
Element Type(s):	Membrane Shell Elements (SHELL41)
Input Listing:	vm153.dat

Test Case

A circular membrane under a uniform tension S is allowed to vibrate freely. The edge of the membrane is simply supported. Determine the natural frequencies $f_{i,j}$ for the first two modes of vibration (j = 1, 2 = no. of nodal circles, including the boundary) for the first two harmonics (i = 0, 1 = no. of harmonic indices). See VM152 for a 2-D solution of this problem.

Figure 153.1 Circular Membrane Problem Sketch

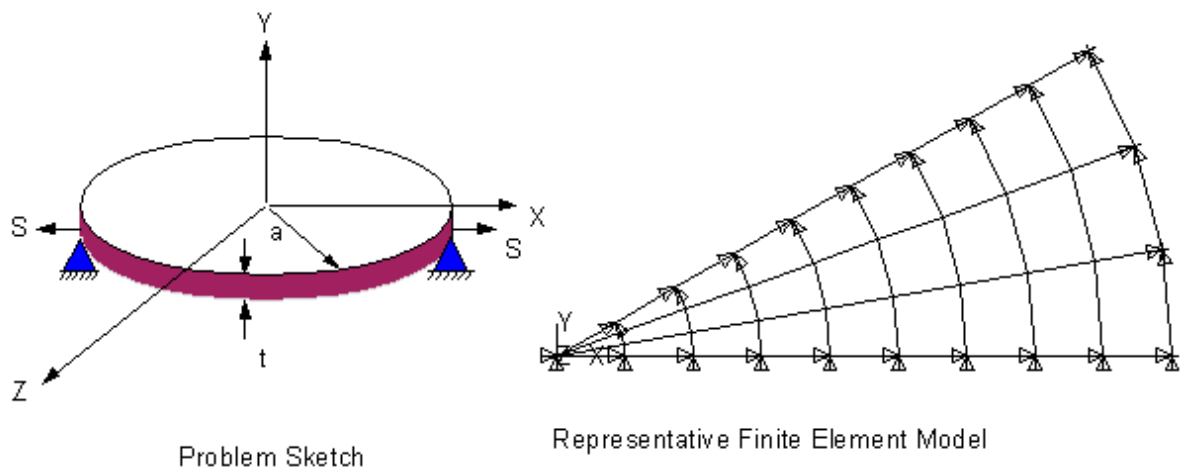

Material Properties	Geometric Properties	Loading
$E = 30 \times 10^6$ psi $\upsilon = 0.0$ $\rho = 0.00073$ lb-sec^2/in^4 $\alpha = 1 \times 10^{-5}$ in/in-°F	a = 3 in t = 0.00005 in	S = 0.1 lb/in of boundary $\Delta T = -6.6666$°F

Analysis Assumptions and Modeling Notes

A 30° sector is used with cyclic symmetry to model the membrane. The prestress is induced by uniform cooling. The temperature difference, ΔT, is calculated from $S = E\,\alpha t\,(\Delta T)$. The low angle edge of the sector is defined as a component for cyclic symmetry analyses. Block Lanczos is used in the modal analysis to extract the first four frequencies.

Results Comparison

	Target	ANSYS	Ratio
$f_{o,1}$, Hz	211.1	212.1	1.005
$f_{o,2}$, Hz	484.7	491.7	1.014
$f_{1,1}$, Hz	336.5	338.9	1.007
$f_{1,2}$, Hz	616.1	629.0	1.021

VM154: Vibration of a Fluid Coupling

Overview

Reference:	R. J. Fritz, "The Effect of Liquids on the Dynamic Motions of Immersed Solids", *ASME, J. of Engr. for Industry*, Vol. 94, Feb. 1972, pp. 167-173.
Analysis Type(s):	Mode-frequency Analysis (**ANTYPE** = 2)
Element Type(s):	Dynamic Fluid Coupling Element (FLUID38) Spring-Damper Elements (COMBIN14) Axisymmetric-Harmonic Contained Fluid Elements (FLUID81)
Input Listing:	vm154.dat

Test Case

A long cylinder is immersed in a circular hole as shown. The cylinder is separated from the containment surface by a frictionless, incompressible liquid annulus. A spring restraint is attached to the cylinder from ground. Determine the natural frequency f of the system based upon the hydrodynamic mass of the liquid annulus.

Figure 154.1 Fluid Coupling Problem Sketch

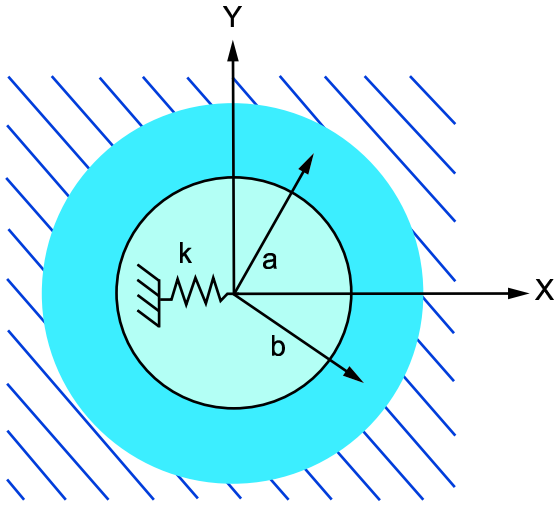

Problem Sketch

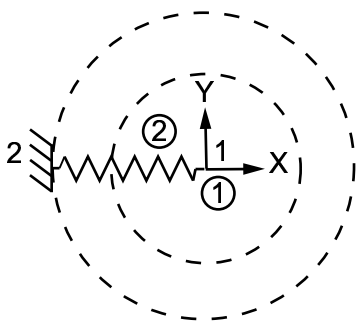

Representative Finite Element Model
(using FLUID38)

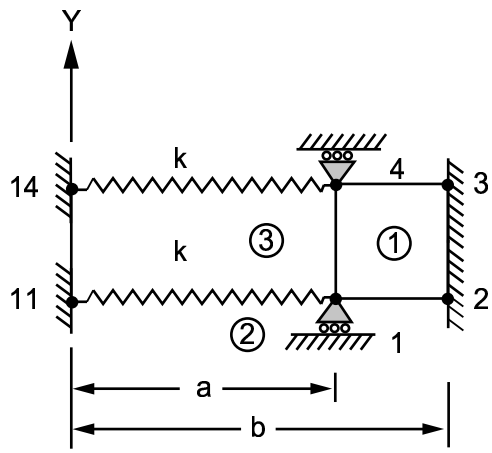

Representative Finite Element Model
(using FLUID81)

Material Properties	**Geometric Properties**
ρ = 0.0000934 lb-sec^2/in^4 k = 10 lb/in β = 30 x 10^4 psi	a = 7 in b = 8 in

Analysis Assumptions and Modeling Notes

The problem is solved first using the fluid coupling element (FLUID38) and then using the harmonic fluid element (FLUID81).

The total length of the assembly is assumed to be long in comparison with its radius. The solution is based upon radial motion of a unit length of the assembly. The cylinder is assumed to be massless so that all mass effects are from liquid annulus. For the fluid coupling element (FLUID38), the nodes are defined as coincident but are shown apart for clarity. For the harmonic fluid element (FLUID81), the bulk modulus (β) should be characteristic of the fluid since it is used for shear stability as well as for compressibility effects. An effective harmonic spring constant, k=10 lb/in is used for each spring to produce equivalent spring force.

Results Comparison

	Target	ANSYS	Ratio
f, Hz (FLUID38)	1.5293	1.5293	1.000
f, Hz (FLUID81)	1.5293	1.5228	0.996

VM155: Shape Optimization of a Cantilever Beam

Overview

Reference:	B. Prasad, R. T. Haftka, "Optimal Structural Design with Plate Finite Elements", *ASCE, J. Structural Div.*, Vol. 105, No. ST11, Nov. 1979.
Analysis Type(s):	Optimization (/OPT) Static Analysis (**ANTYPE** = 0)
Element Type(s):	2-D Structural Solid Elements (PLANE42)
Input Listing:	vm155.dat

Test Case

Minimize the weight (volume) of a cantilever beam subject to an end moment, M. The stress σ_{max} may not exceed 30,000 psi anywhere nor may the deflection δy_{max} be greater than 0.5 in. The thickness of the beam may vary along the length, with the thickness at the point of load application held constant at a value t.

Figure 155.1 Cantilever Beam Problem Sketch

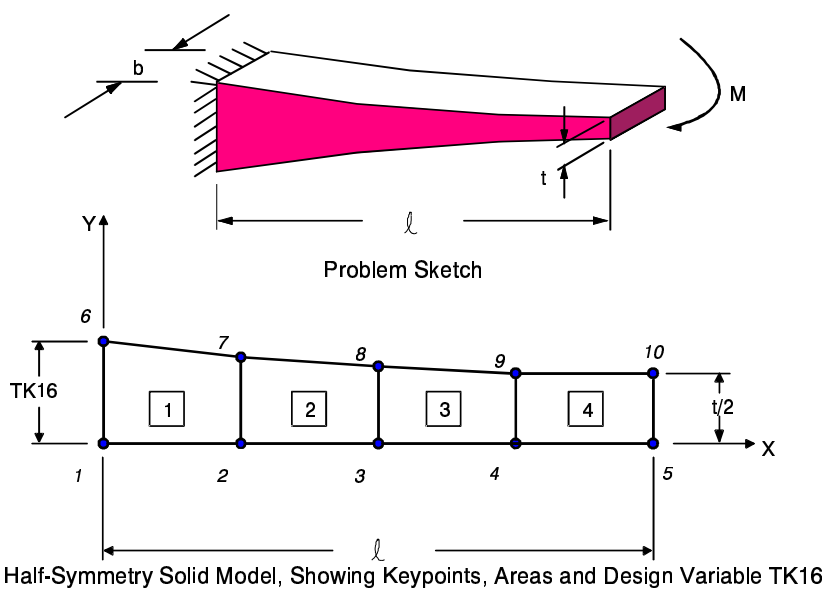

Half-Symmetry Solid Model, Showing Keypoints, Areas and Design Variable TK16

Material Properties	**Geometric Properties**
E = 10 x 10^6 psi υ = 0.3 **Loading** M = 450 in-lb	ℓ = 10 in b = 1 in t = 0.3 in

Analysis Assumptions and Modeling Notes

The keypoints defining the outer fiber are connected with a cubic spline. A half model with antisymmetric boundary conditions is used. The summed element volumes are multiplied by two for the objective function. Maximum sorted deflection and maximum sorted principal stress (S1) are defined as state variables.

The problem is solved independently using the subproblem approximation method and the first order method, both using the same starting design. Three geometric state variables are defined to ensure a left-to-right taper in the subproblem approximation method. These additional state variables are not used in the first order method to demonstrate the robustness of the algorithm.

Results Comparison

Subproblem Approximation Method	Target[1]	ANSYS[2]	Ratio
(TVOL) Volume, in^3	3.60	3.62	1.004
(DEFL) $(Deflection_y)_{max}$, in	0.500	0.499	0.998
(STRS) $Stress_{max}$, psi	30000	29740	0.991

First Order Method	Target[1]	ANSYS[3]	Ratio
(TVOL) Volume, in^3	3.60	3.61	1.003
(DEFL) $(Deflection_y)_{max}$, in	0.5	0.5	1.001
(STRS) $Stress_{max}$, psi	30000	29768	0.992

1. Based on an integrated solution
2. Converged to within chosen tolerances after 11 iterations.
3. Converged to within chosen tolerances after 15 iterations.

Figure 155.2 Subproblem Approximation Method

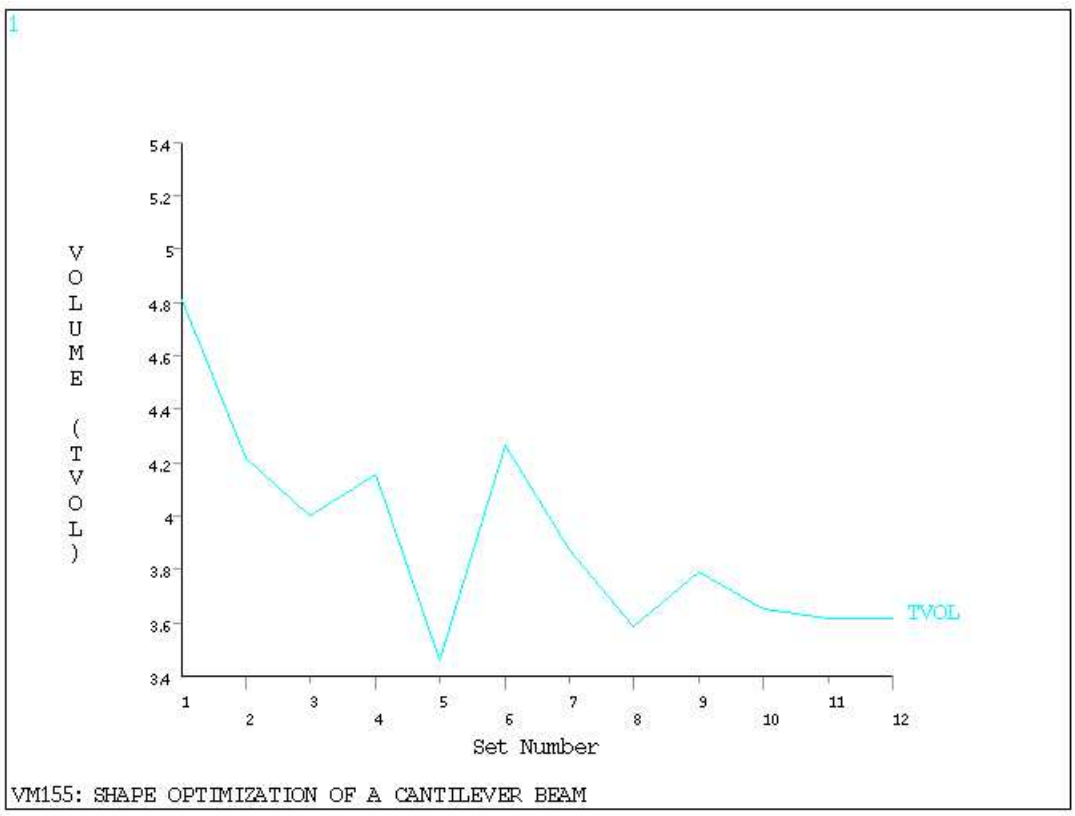

Figure 155.3 First Order Method

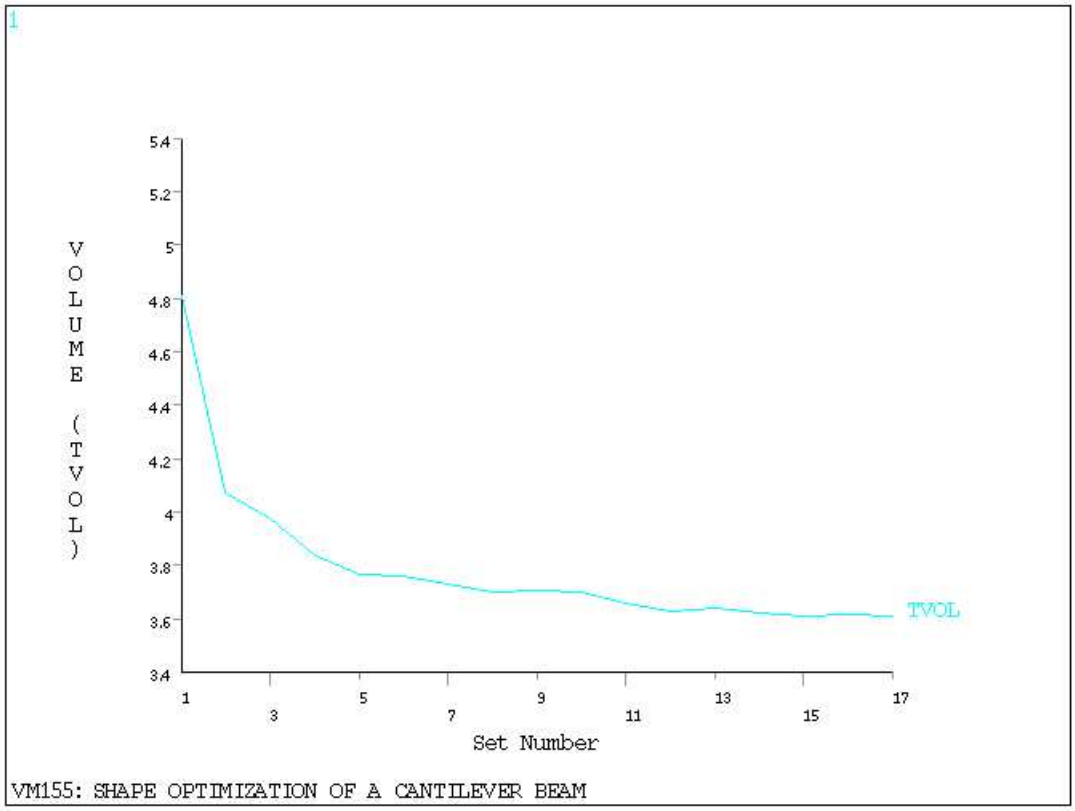

VM156: Natural Frequency of a Nonlinear Spring-Mass System

Overview

Reference:	S. Timoshenko, D. H. Young, *Vibration Problems in Engineering*, 3rd Edition, D. Van Nostrand Co., Inc., New York, NY, 1955, pg. 141.
Analysis Type(s):	Full Transient Dynamic Analysis (**ANTYPE** = 4)
Element Type(s):	Nonlinear Spring Elements (COMBIN39) 2-D Spar (or Truss) Elements (LINK1) Structural Mass Elements (MASS21)
Input Listing:	vm156.dat

Test Case

A mass is supported from a spring having the nonlinear characteristics shown. The mass is displaced an amount δ from its equilibrium position and released (with no initial velocity). Find the corresponding period of vibration τ.

Figure 156.1 Nonlinear Spring-Mass System Problem Sketch

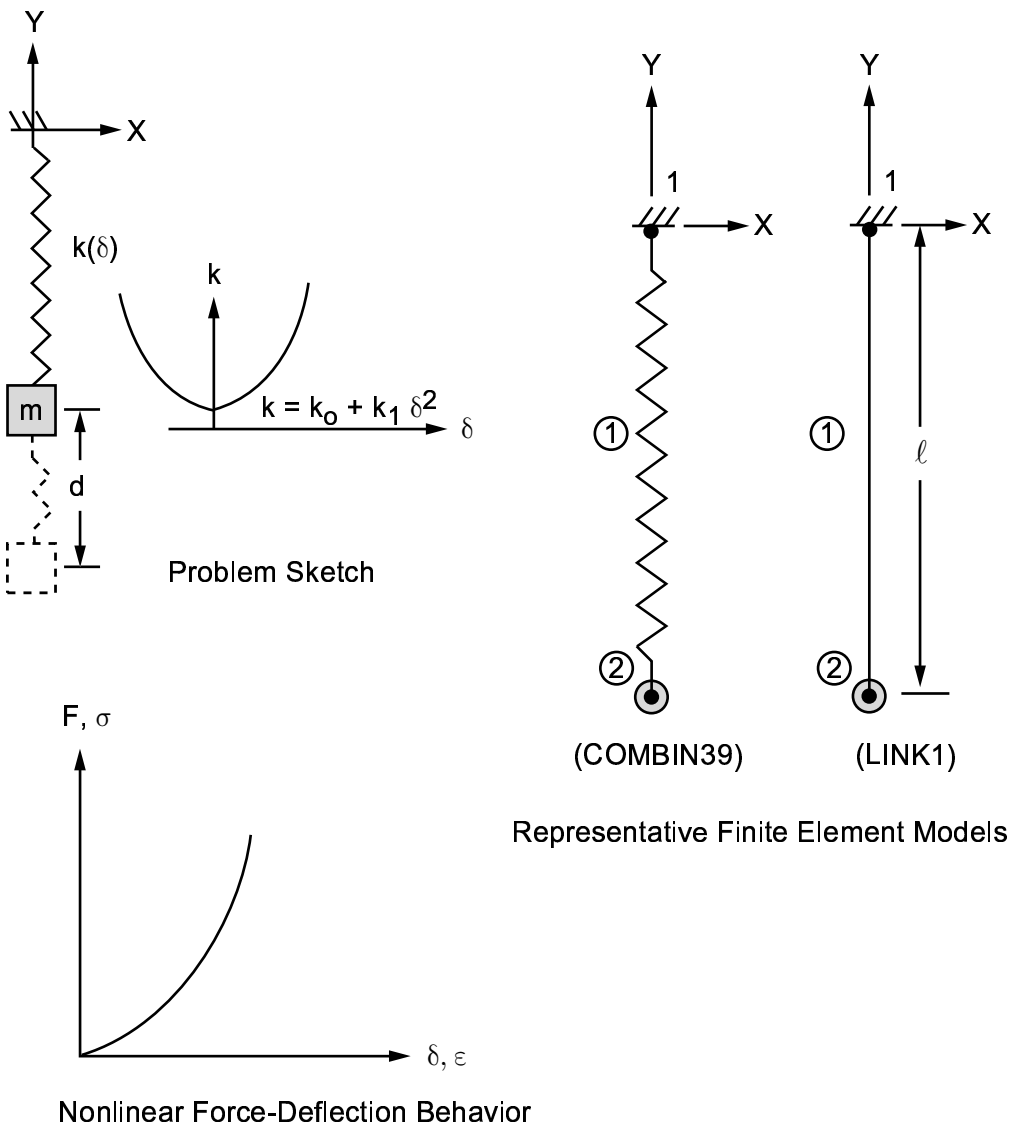

Material Properties	Geometric Properties
m = 1/386.4 = 0.002588 lb-sec^2/in k_o = 2 lb/in k_1 = 4 lb/in^3 see force-deflection curve in Figure 156.1: "Nonlinear Spring-Mass System Problem Sketch"	A = 0.01 in^2 ℓ = 100 in **Loading** δ = -1 in

Analysis Assumptions and Modeling Notes

The problem is solved first using the nonlinear spring element (COMBIN39) and then using a spar element (LINK1) with nonlinear elastic material (nonlinear table).

For the nonlinear spring element (COMBIN39), the nonlinear spring constant is converted to eleven discrete force-deflection points by $F = k\delta$ for δ = 0.0 to 1.0 in steps of 0.1 in.

For the spar element (LINK1) with nonlinear elastic material, the nonlinear spring constant is converted to six discrete stress-strain points by $\sigma = k\delta/A$ and $\varepsilon = \delta/L$ for δ = 0.0 to 1.0 in steps of 0.2 in. The elastic modulus EX on the **MP** command must be greater than the maximum of σ/ε (= kL/A) and hence is assigned a value of 2kL/A = 12 x 10^4 psi.

The **IC** command is used to impose the initial displacement and velocity configuration. The first load step is defined over a very small time step (.0002 sec) to allow the initial step change in acceleration to be attained. The integration time step for the second load step is based on 1/30 of the period to produce a fine resolution for the theoretical comparison. A final time of 0.18 sec is arbitrarily selected.

Area and length parameters are used only with the spar element (LINK1) where the nonlinear spring is treated as a leaf spring with zero mass. The nodes for the nonlinear spring element (COMBIN39) are defined as coincident but are shown apart in the model for clarity.

POST26 is used to extract results from the solution phase. The period is determined by the time when the mass is closest to the original released position after it passes through the spring's equilibrium position.

Results Comparison

		Target	ANSYS	Ratio
COMBIN39	Vibration, sec	0.1447	0.1440	0.995
LINK1	Vibration, sec	0.1447	0.1440	0.995

VM157: Optimization of a Frame Structure

Overview

Reference:	B. H. V. Topping, D. J. Robinson, "Selecting Non-Linear Optimization Techniques for Structural Design", *Intl J. for Computer Aided Engineering and Software: Engineering Computations*, Vol. 1 No. 3, Sept. 1984.
Analysis Type(s):	Optimization (**/OPT**) Static Analysis (**ANTYPE** = 0)
Element Type(s):	2-D Elastic Beam Elements (BEAM3)
Input Listing:	vm157.dat

Test Case

Minimize the volume of a symmetric four member frame subject to four bending moment constraints of the form 825000 $(d_j)^3 - |M_{ij}| \geq 0$ where M_{ij} is the bending moment at end i of member j and d_j is the depth of member j. Cross sections of each member must be rectangular, with depth equal to half the height.

Figure 157.1 Frame Structure Problem Sketch

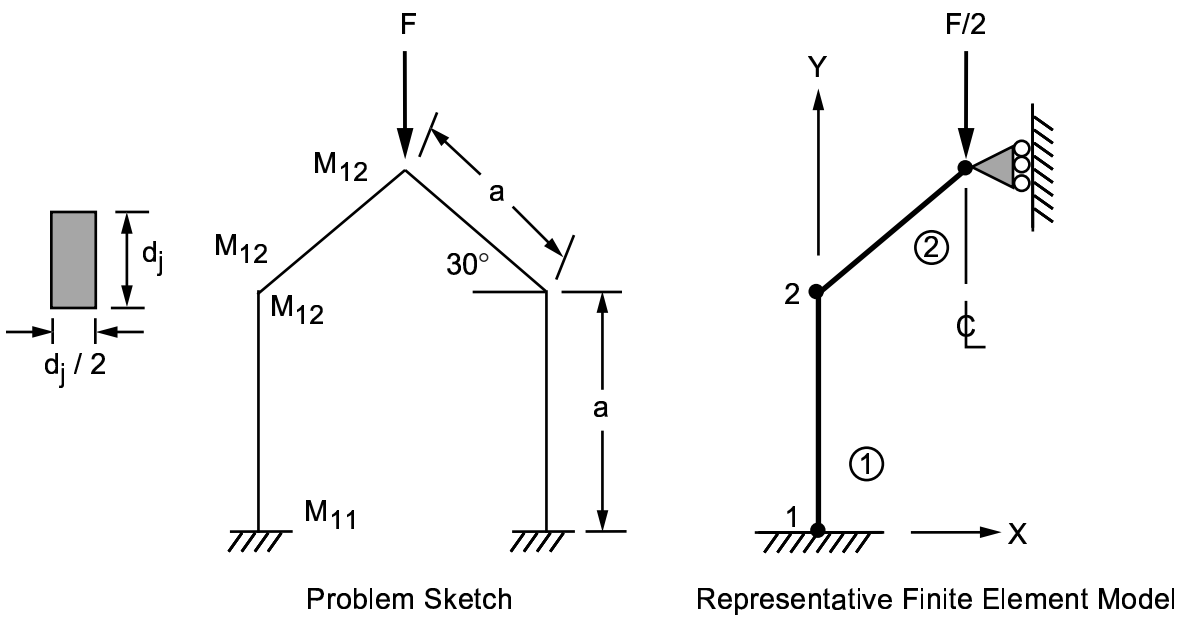

Material Properties	Geometric Properties	Loading
E = 1 x 10^{10} Pa	a = 2.5 m	F = 4000 N

Analysis Assumptions and Modeling Notes

Areas and moments of inertia are input as parametric expressions of the design variables; $A_j = 1/2\ d_j2$, $I_j = 1/24\ d_j4$.

Use half symmetry. An upper bound of 2000 is chosen for the state variables to provide a reasonable feasible design space. Likewise, the design variable limits between .05 m and 0.5 m are chosen as reasonable ranges for member sizes. The starting design is as given in the reference, and is infeasible.

Results Comparison

	Target	ANSYS[1]	Ratio
Volume, m^3	0.0764	0.0772	1.010
d_1, m	0.118	0.1196	1.013
d_2, m	0.129	0.1288	0.998

1. From converged solution, 9th design set

VM158: Motion of a Bobbing Buoy

Overview

Reference:	K. Brenkert, Jr., *Elementary Theoretical Fluid Mechanics*, John Wiley and Sons, Inc., New York, NY, 1960, pg. 37, article 14.
Analysis Type(s):	Full Transient Dynamic Analysis (**ANTYPE** = 4)
Element Type(s):	Immersed Pipe or Cable Elements (PIPE59)
Input Listing:	vm158.dat

Test Case

A cylindrical buoy is initially held at the position shown (above its equilibrium position) and then released (with no initial velocity). Determine the equilibrium position δ of the top of the buoy relative to the water surface.

Figure 158.1 Buoy Problem Sketch

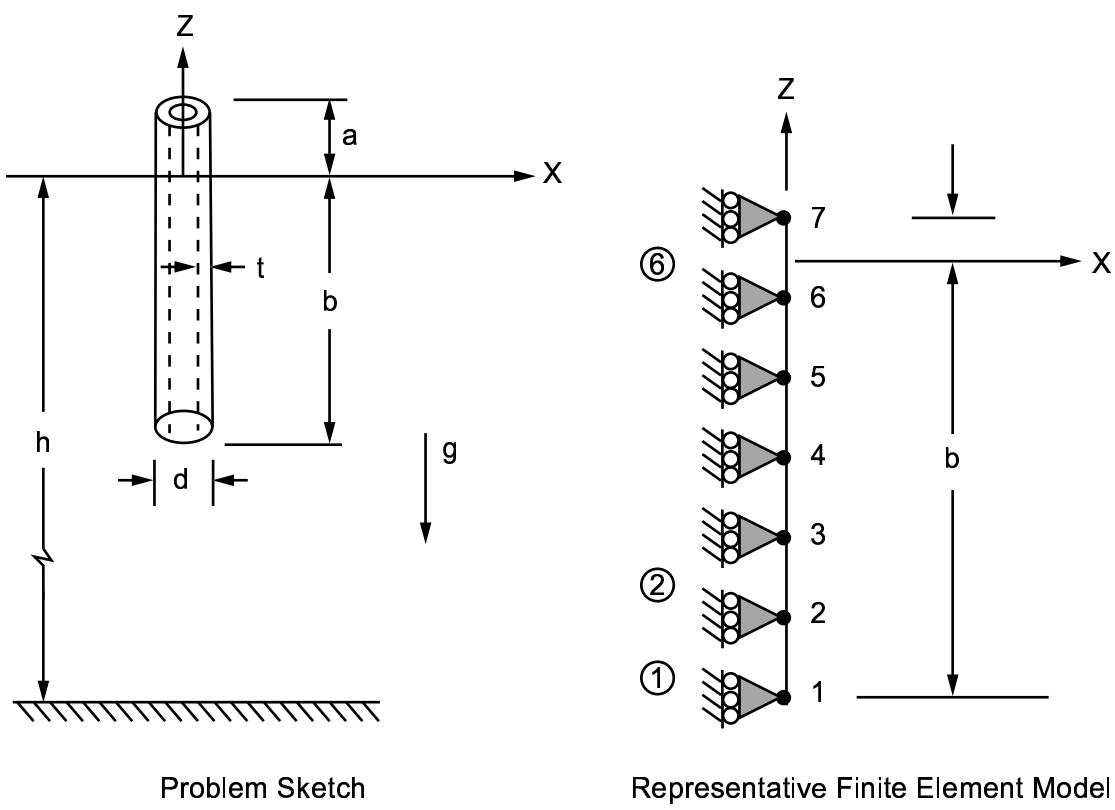

Material Properties	Geometric Properties	Loading
ρ = 8000 kg/m^3 ρ_w = 1000 kg/m^3	a = 1 m b = 9 m d = 1 m t = .03 m h = 30 m tangential drag coefficient = 0.3	g = 9.807 m/sec^2

Analysis Assumptions and Modeling Notes

The static solution to this problem is best obtained by the "slow dynamics" technique with damping, since the buoy is initially subjected to free fall. An arbitrary time to steady state of 30 sec and 1.5 seconds per time step is selected for the slow dynamics. The mass damping value α determines the bouncing (if any) before the final steady state solution. An approximate α value is determined from F/MV where the force F = CV and damping C = αM. The force F is the out-of-balance force (buoyancy force $(1/4\rho_W g\pi d^2 b)$ minus the buoy weight) for the initial position pushing the buoy into the water, M is the mass of the buoy, and V is an estimated average velocity (0.1 m/sec). Based upon these approximations, $\alpha \approx 3\ \text{sec}^{-1}$.

Results Comparison

	Target	ANSYS	Ratio
Deflection , m	-.312	-.312	1.000

Figure 158.2 Displacement vs. Time Display

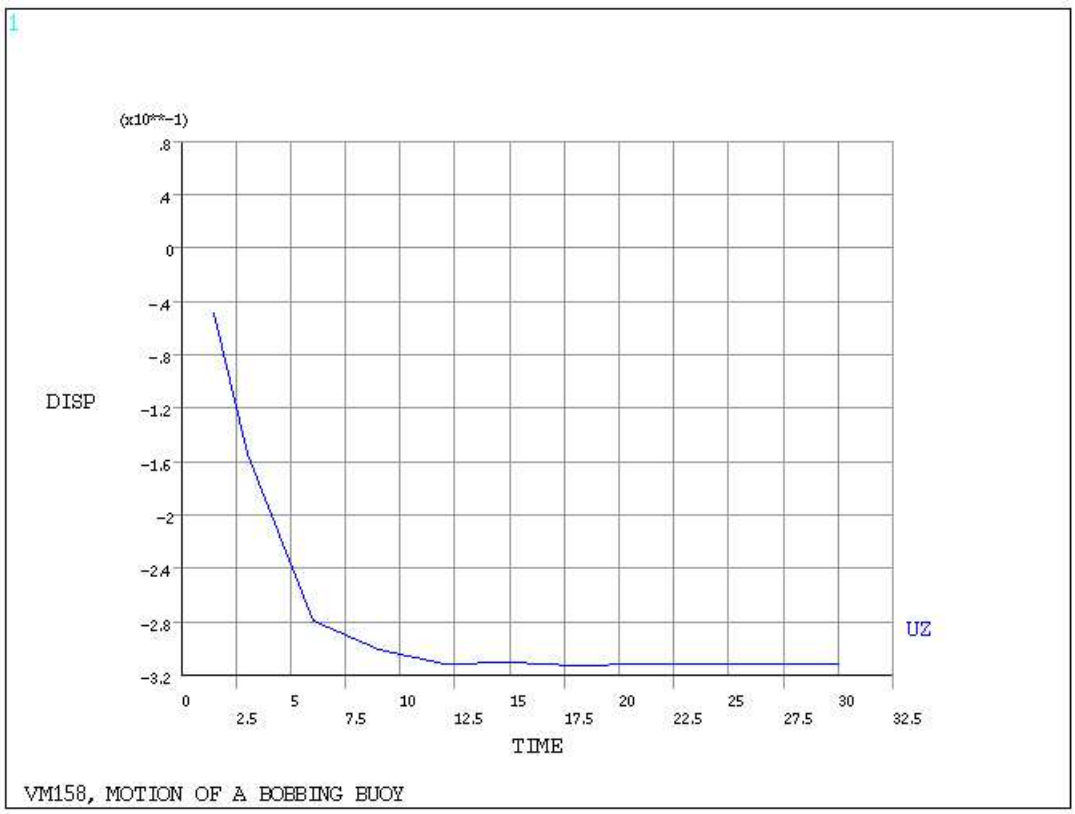

VM159: Temperature-controlled Heater

Overview

Reference:	Self-checking (Response Follows Input Request)
Analysis Type(s):	Transient Thermal Analysis (**ANTYPE** = 4)
Element Type(s):	Control Elements (COMBIN37) Convection Link Elements (LINK34) Thermal Mass Elements (MASS71)
Input Listing:	vm159.dat

Test Case

An assembly consisting of a heater with capacitance C_1 and surface area A_1 is surrounded by a box having capacitance C_2 and surface area A_2. The box is initially at a uniform temperature T_o. The heater, which supplies heat at a rate q, is turned on and remains on until the surrounding box temperature reaches a value T_{off}. The heater then switches off until the box temperature lowers to T_{on} and then switches on again. Determine the temperature response of the box and the heater status vs. time.

Figure 159.1 Temperature-controlled Heater Problem Sketch

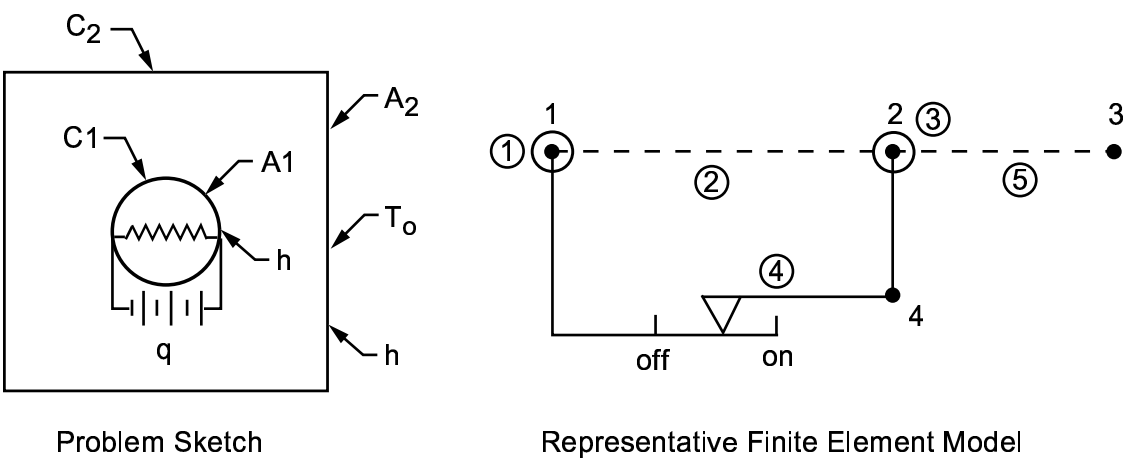

Material Properties	Geometric Properties	Loading
$C_1 = 2.7046 \times 10^{-4}$ Btu/°F $C_2 = 2.7046 \times 10^{-3}$ Btu/°F h = 4 Btu/hr-ft^2-°F	$A_1 = 8.1812 \times 10^{-3}$ ft $A_2 = 4.1666 \times 10^{-2}$ ft	q = 10 Btu/hr T_{on} = 100°F T_{off} = 125°F T_o = 70°F

Analysis Assumptions and Modeling Notes

The conductivity resistance is assumed to be small compared with the thermal capacitance for both the heater and the box. A time of 12 min (0.2 hr) is arbitrarily selected to allow several cycles of response. The integration time step is chosen to be 0.001 and automatic time stepping is used to reduce the number of substeps. The nodes are arbitrarily located at the origin.

Results Comparison

	Target	ANSYS	Ratio
First “off” temp,°F	125	Between 124.842 - 125.003	-
First “on” temp,°F	100	Between 100.854 - 99.564	-

Figure 159.2 Box Temperature vs. Time

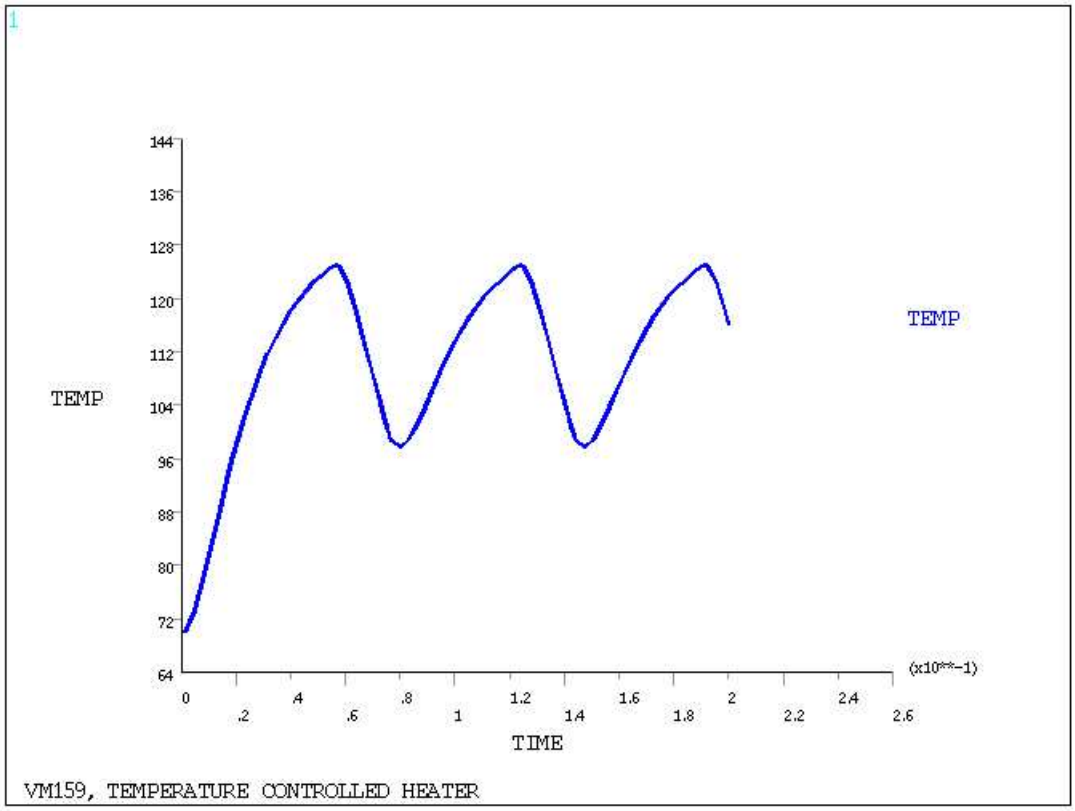

Figure 159.3 Control Status vs. Time

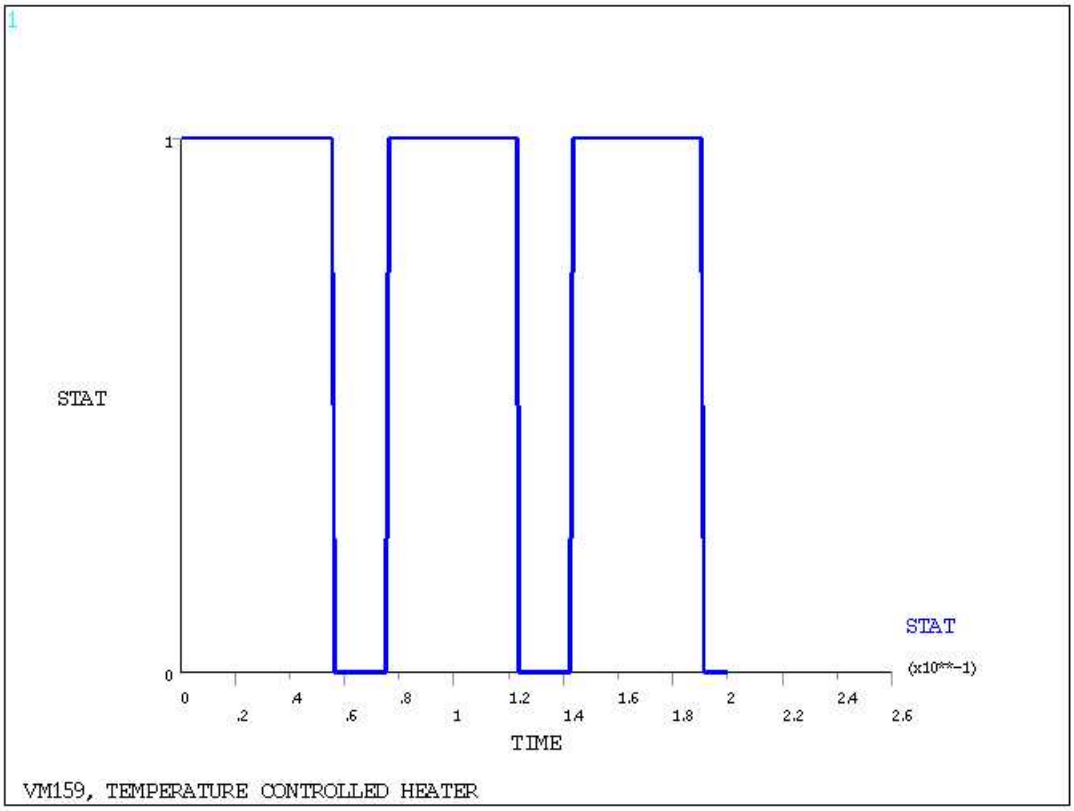

VM160: Solid Cylinder with Harmonic Temperature Load

Overview

Reference:	F. B. Hildebrand, *Advanced Calculus for Applications*, 2nd Edition, Prentice-Hall, Inc., Englewood, NJ, 1976, pg. 447, equations 38-44.
Analysis Type(s):	Thermal Analysis (**ANTYPE** = 0)
Element Type(s):	Axisymmetric-Harmonic 8-Node Thermal Solid Elements (PLANE78)
Input Listing:	vm160.dat

Test Case

A long solid cylinder has a harmonically-varying temperature load along its circumference represented by a cosine function with positive peaks at $\Theta = 0°$ and 180° and negative peaks at $\Theta = 90°$ and 270°. Determine the temperature distribution along the radius at $\Theta = 0$ and $\Theta = 90°$.

Figure 160.1 Solid Cylinder Problem Sketch

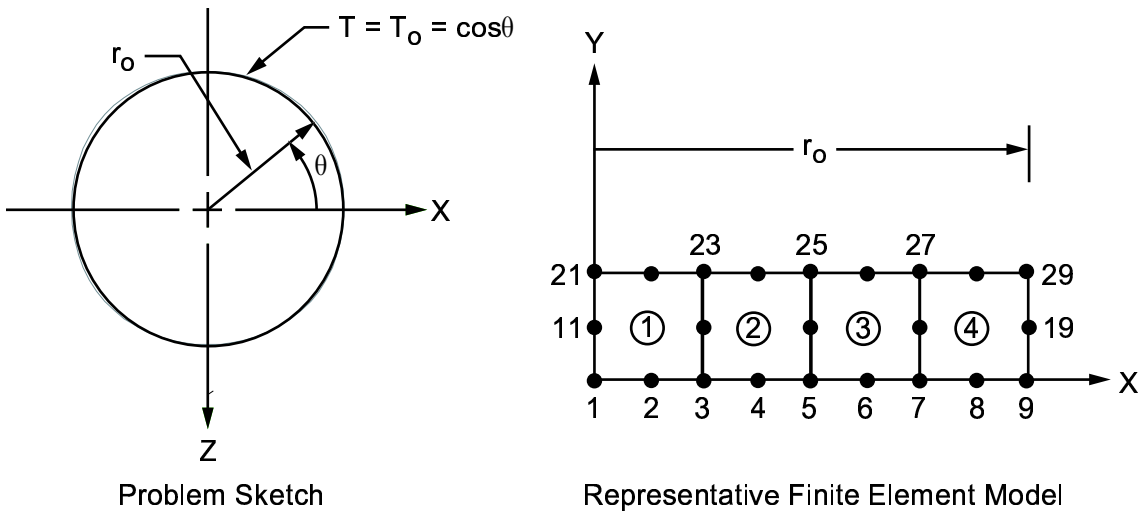

Problem Sketch Representative Finite Element Model

Material Properties	**Geometric Properties**	**Loading**
k = 1 Btu/hr-ft-°F	r_o = 20 ft	T_o = 80°F

Analysis Assumptions and Modeling Notes

The axial length of the model is arbitrarily chosen to be 5 ft. The temperature loading is applied as a symmetric harmonic function (Mode 2) around the periphery of the cylinder. To obtain the theoretical solution, equations 43 and 44 in F. B. Hildebrand, *Advanced Calculus for Applications* are used. Applying the temperature boundary condition and the requirement that $T(r, \Theta)$ should be finite and single-valued leads to the solution: $T(r, \Theta) = T_o * (r/r_o)^2 * \cos(2\Theta)$.

Results Comparison

		Target	ANSYS	Ratio
Mode = 2 Angle = 0°	T, °F (Node 1)	0.0	0.0	1.00
	T, °F (Node 3)	5.0	5.0	1.00

	T, °F (Node 5)	20.0	20.0	1.00
	T, °F (Node 7)	45.0	45.0	1.00
		Target	**ANSYS**	**Ratio**
Mode = 2 Angle = 90°	T, °F (Node 1)	0.0	0.0	1.00
	T, °F (Node 3)	-5.0	-5.0	1.00
	T, °F (Node 5)	-20.0	-20.0	1.00
	T, °F (Node 7)	-45.0	-45.0	1.00

VM161: Heat Flow From an Insulated Pipe

Overview

Reference:	F. Kreith, *Principles of Heat Transfer*, 2nd Printing, International Textbook Co., Scranton, PA, 1959, pg. 36, ex. 2-7.
Analysis Type(s):	Thermal Analysis (**ANTYPE** = 0)
Element Type(s):	3-D 20-Node Thermal Solid Elements (SOLID90)
Input Listing:	vm161.dat

Test Case

A pipe, covered with a layer of insulation, transports a fluid at a temperature T_i. For a given ambient air temperature T_o, determine the heat loss q across the outer surface per lineal foot of pipe.

Figure 161.1 Insulated Pipe Problem Sketch

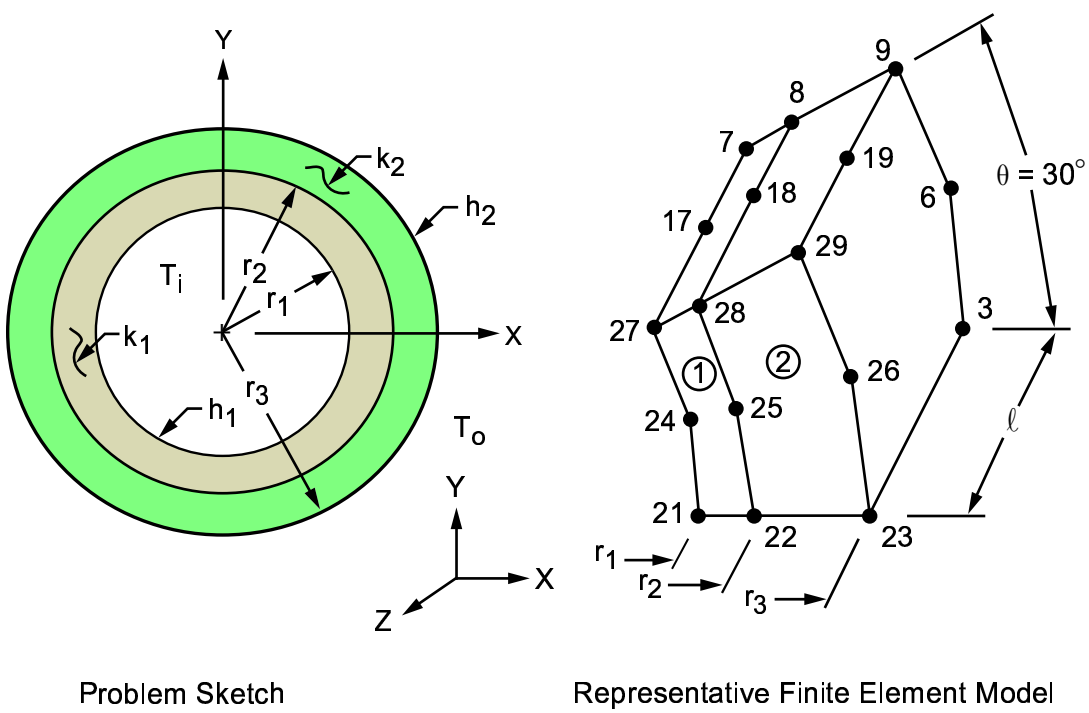

Problem Sketch Representative Finite Element Model

Material Properties	Geometric Properties	Loading
k_1 = 25 Btu/hr-ft-°F	r_1 = 1.535 in = 0.1279166 ft	T_i = 300°F
k_2 = 0.11 Btu/hr-ft-°F	r_2 = 1.75 in = 0.1458333 ft	T_o = 80°F
h_1 = 40 Btu/hr-ft^2-°F	r_3 = 2.25 in = 0.1875 ft	
h_2 = 4 Btu/hr-ft^2-°F	ℓ = 1 ft	

Analysis Assumptions and Modeling Notes

An arbitrary 30° sector, of unit length ℓ, is used for the axisymmetric model.

Results Comparison

	Target	ANSYS	Ratio
q, Btu/hr	362.0	362.0	1.000

Calculated from the surface heat flow rate of 30.17 x 360°/30°.

VM162: Cooling of a Circular Fin of Rectangular Profile

Overview

Reference:	P. J. Schneider, *Conduction Heat Transfer*, 2nd Printing, Addison-Wesley Publishing Co., Inc., Reading, MA, 1957, pg. 82, article 4-10.
Analysis Type(s):	Thermal Analysis (**ANTYPE** = 0)
Element Type(s):	3-D 20-Node Thermal Solid Elements (SOLID90)
Input Listing:	vm162.dat

Test Case

A circular cooling fin of rectangular profile is attached to a cylindrical surface having a temperature T_1. Determine the temperature T_2 at the tip of the fin if the fin is surrounded by cooling air at temperature T_o having a convective film coefficient h.

Figure 162.1 Circular Fin Problem Sketch

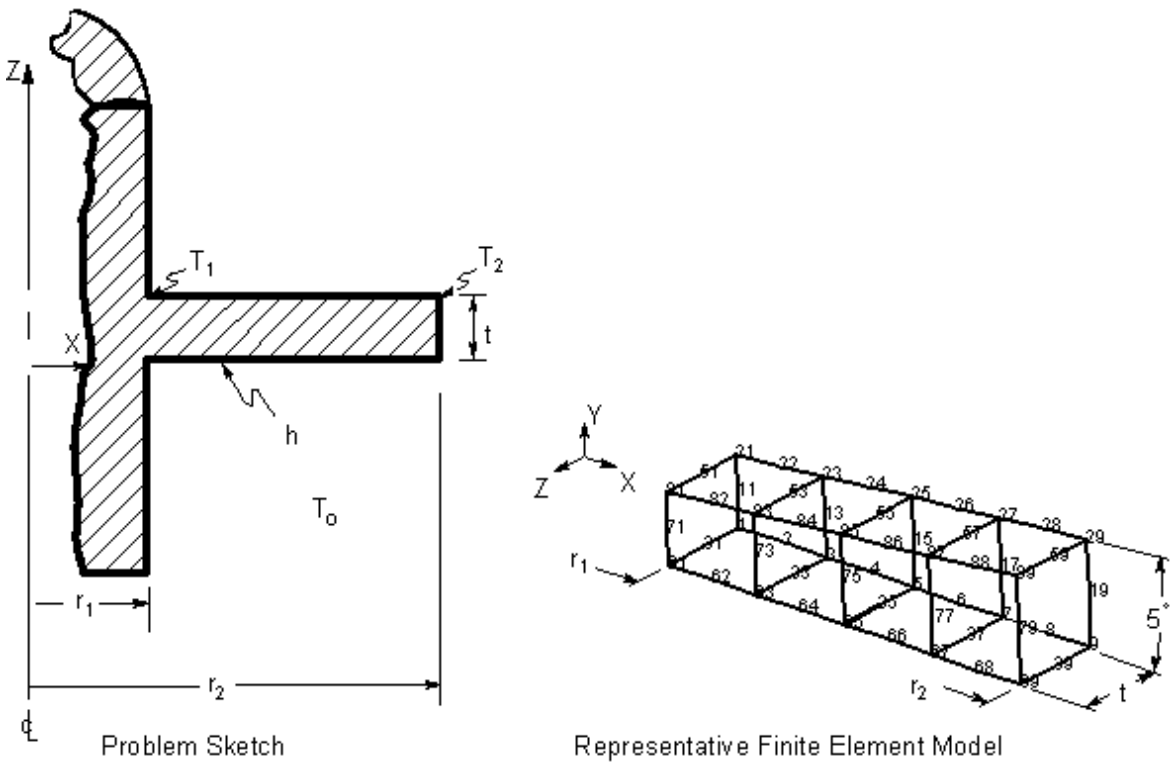

Material Properties	Geometric Properties	Loading
h = 100 Btu/hr-ft^2-°F	r_1 = 0.5 in = 0.04167 ft	T_1 = 100°F
k = 15 Btu/hr-ft-°F	r_2 = 0.75 in = 0.0625 ft	T_o = 0°F
	t = 0.0625 in = 0.005208 ft	

Analysis Assumptions and Modeling Notes

An arbitrary 5° sector is used to model the axisymmetric fin.

Results Comparison

	Target[1]	ANSYS	Ratio
T_2, °F	53.22	52.37	.984
q, Btu/hr	102.05	101.70[2]	.997

1. Based on interpolation with Bessel function tables.
2. Obtained from the reaction heat flow summation of 1.41246 x 360°/5°.

ANSYS Verification Manual . ANSYS Release 10.0 . 002184 . © SAS IP, Inc.

VM163: Groundwater Seepage (Permeability Analogy)

Overview

Reference:	D. R. J. Owen, E. Hinton, *A Simple Guide to Finite Elements*, Pineridge Press Ltd., Swansea, U. K., 1980, pg. 89, article 7.4.
Analysis Type(s):	Thermal Analysis (**ANTYPE** = 0), with Analogous Seepage Variables
Element Type(s):	2-D Thermal Solid Elements (PLANE55)
Input Listing:	vm163.dat

Test Case

An opened top and bottom circular steel caisson separates a low level excavation from the surrounding ground. Determine the groundwater seepage flow rate q beneath the caisson for fully saturated soil. The pressure head is T_1 with respect to a datum T_o at the bottom of the caisson. Show the pressure contours and the flow path.

Figure 163.1 Groundwater Seepage Problem Sketch

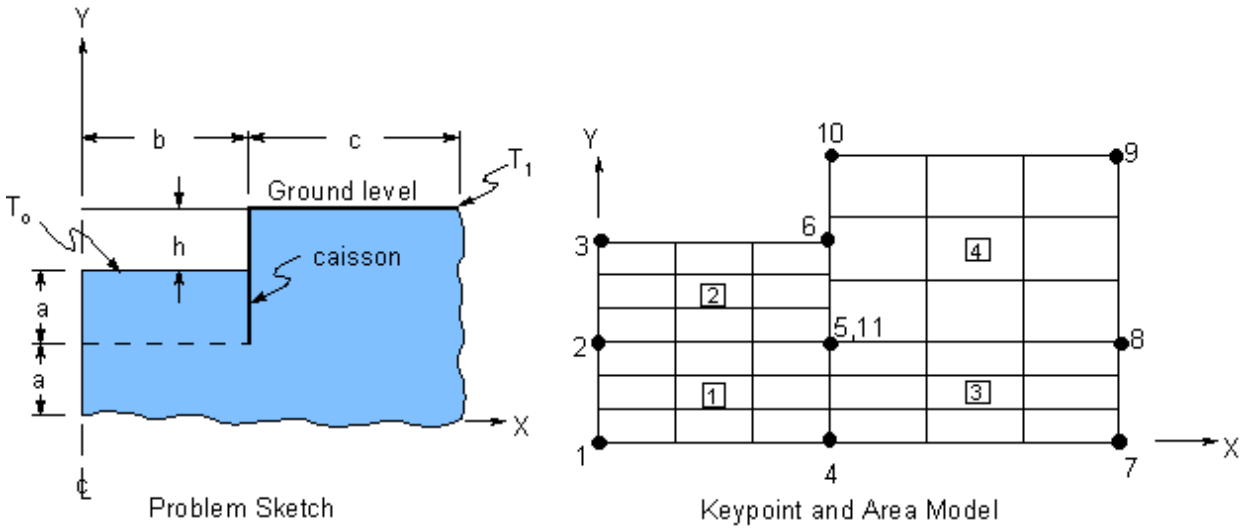

Material Properties	Geometric Properties	Loading
k = permeability = 0.864 m/day	a = 3.5 m b = 8 m c = 10 m h = 3 m	T_o = 0 m (at Y = 7 m) T_1 = 3 m (at Y = 10 m)

Analysis Assumptions and Modeling Notes

The thermal analysis, which solves the Laplace equation, is used to solve this problem since the seepage flow is also governed by the Laplace equation. The following mental substitution of input and output variables (thermal : flow) are used:

- (temperature : flow potential (or pressure head))
- (heat flow rate : fluid flow rate)
- (thermal conductivity : permeability coefficient)

The bottom and side of the model are assumed to be far enough away from the caisson to be treated as impermeable.

Results Comparison

	Target	ANSYS[1]	Ratio
q, m^3/day (per radian)	8.6	8.6	1.0

1. POST1 results for q are on a full circumference basis.

Figure 163.2 Pressure Contours

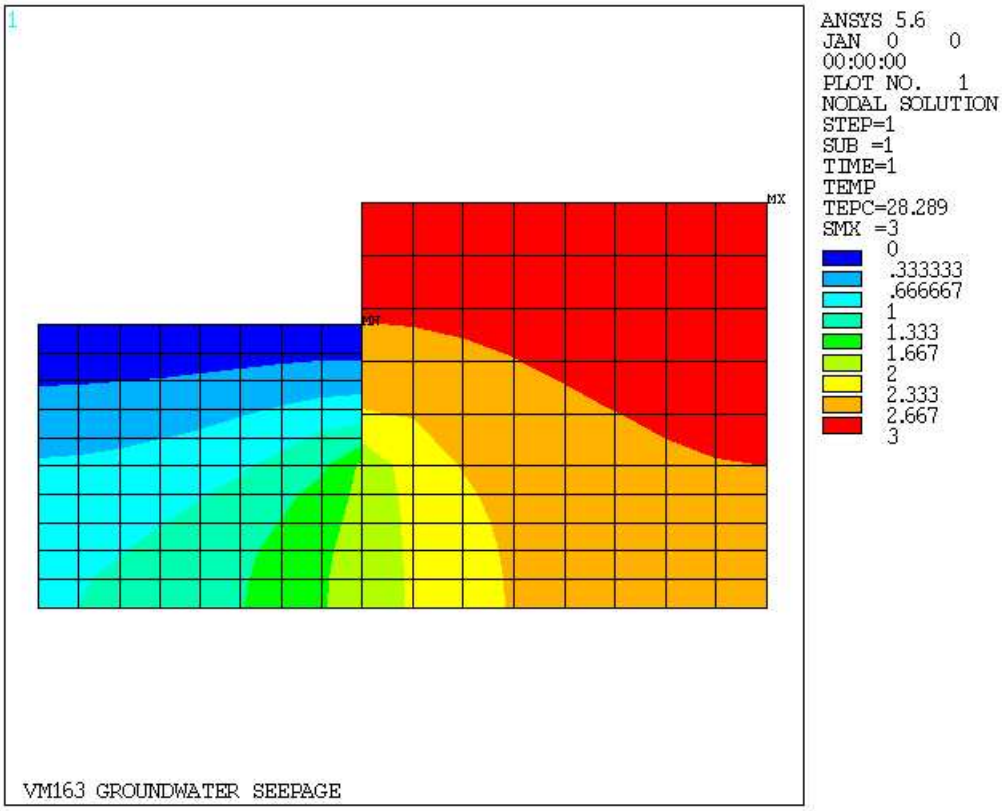

Figure 163.3 Flow Gradients

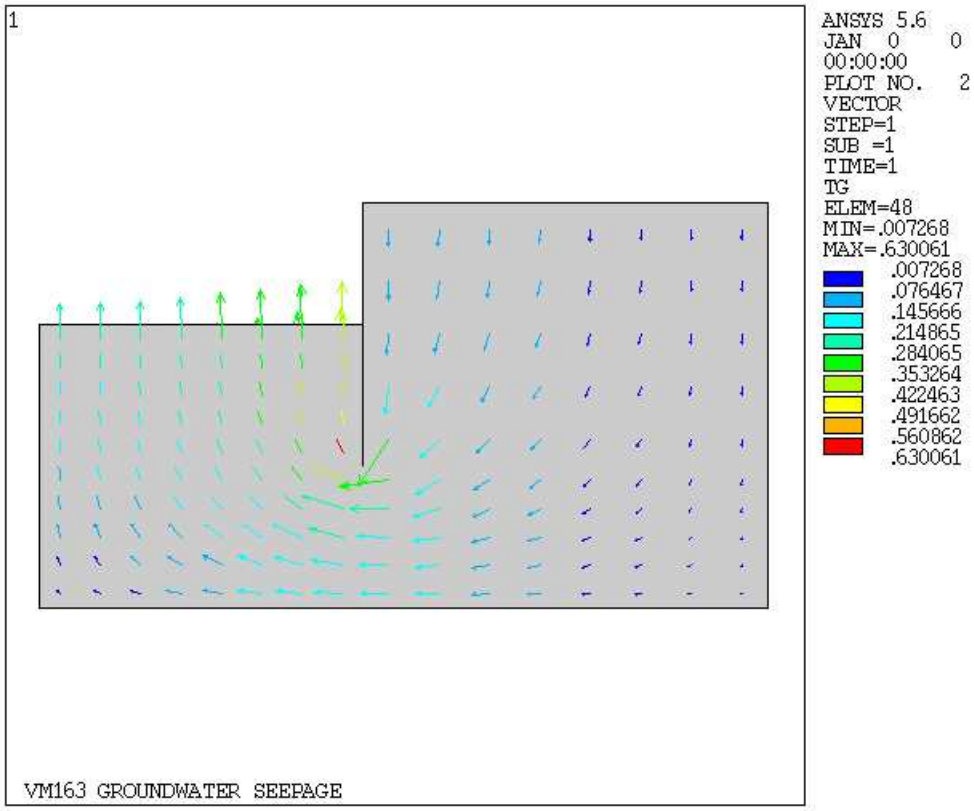

VM164: Drying of a Thick Wooden Slab (Diffusion Analogy)

Overview

Reference:	W. M. Rohsenow, H. Y. Choi, *Heat, Mass and Momentum Transfer*, 2nd Printing, Prentice-Hall, Inc., Englewood Cliffs, NJ, 1963, pg. 392, article 15.4.
Analysis Type(s):	Transient Thermal Analysis (**ANTYPE** = 4) with Analogous Diffusion Variables
Element Type(s):	2-D Conduction Bar Elements (LINK32)
Input Listing:	vm164.dat

Test Case

A slab of wood of thickness b originally has a uniform moisture concentration c_i (relative to dry wood) when a drying period begins. The ambient moisture concentration of the drying air is c_e. Determine the moisture concentration c at the centerline of the slab after 127 hours.

Figure 164.1 Wooden Slab Problem Sketch

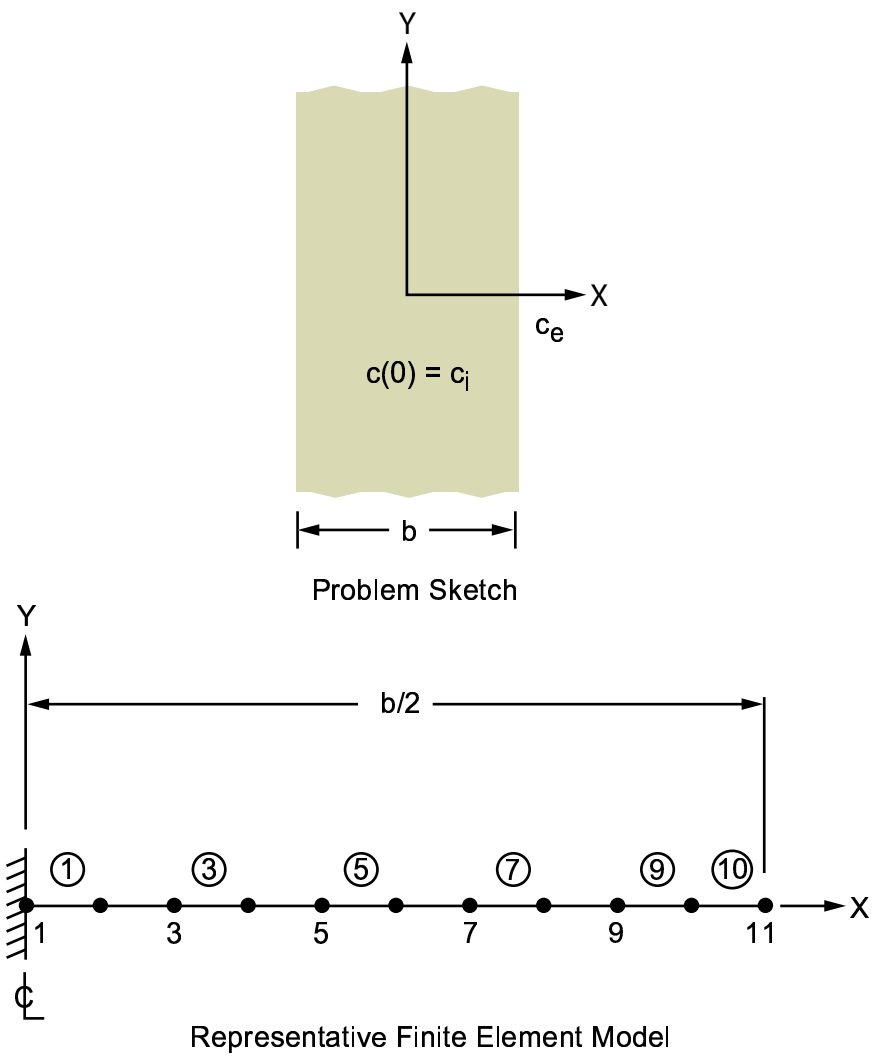

Material Properties	Geometric Properties	Loading
$D = 4 \times 10^{-5}$ ft^2/hr	b = 2 in = (2/12) ft	$c_i = 30\%$ $c_e = 5\%$

Analysis Assumptions and Modeling Notes

The thermal analysis, which solves the Laplace equation, is used to solve this problem since the diffusion problem is also governed by the Laplace equation. The following analogy (thermal : diffusion) of input and output variables is used: (temperature : moisture concentration), (thermal conductivity : diffusion coefficient). The slab is assumed to have a large surface area compared with its thickness and a negligible surface resistance. The density and specific heat properties are arbitrarily set to 1.0 and the thermal conductivity is used for the diffusion coefficient input. The solution is obtained for an arbitrary cross-sectional area of 1 ft^2.

The initial integration time step of 0.434 hr. is determined from $\delta^2/4D$, where δ is a characteristic element length (0.008333 ft) and D is the diffusion coefficient. Automatic time stepping is used to reduce the number of iterations if possible.

Results Comparison

	Target[1]	ANSYS	Ratio[1]
c, %	10.0	10.2	1.02

1. Based on graphical estimates.

VM165: Current-Carrying Ferromagnetic Conductor

Overview

Reference:	W. B. Boast, *Principles of Electric and Magnetic Fields*, Harper & Brothers, New York, NY, 1948, pg. 225.
Analysis Type(s):	Nonlinear Static Magnetics Analysis (**ANTYPE** = 0)
Element Type(s):	2-D Coupled-Field Solid Elements (PLANE13) 2-D Infinite Boundary Elements (INFIN9)
Input Listing:	vm165.dat

Test Case

A long cylindrical shell of cast steel carries a constant current I uniformly distributed within the conductor cross-section. Determine the tangential magnetic flux density B_θ at several locations within the conductor.

Figure 165.1 Current-Carrying Ferromagnetic Conductor Problem Sketch

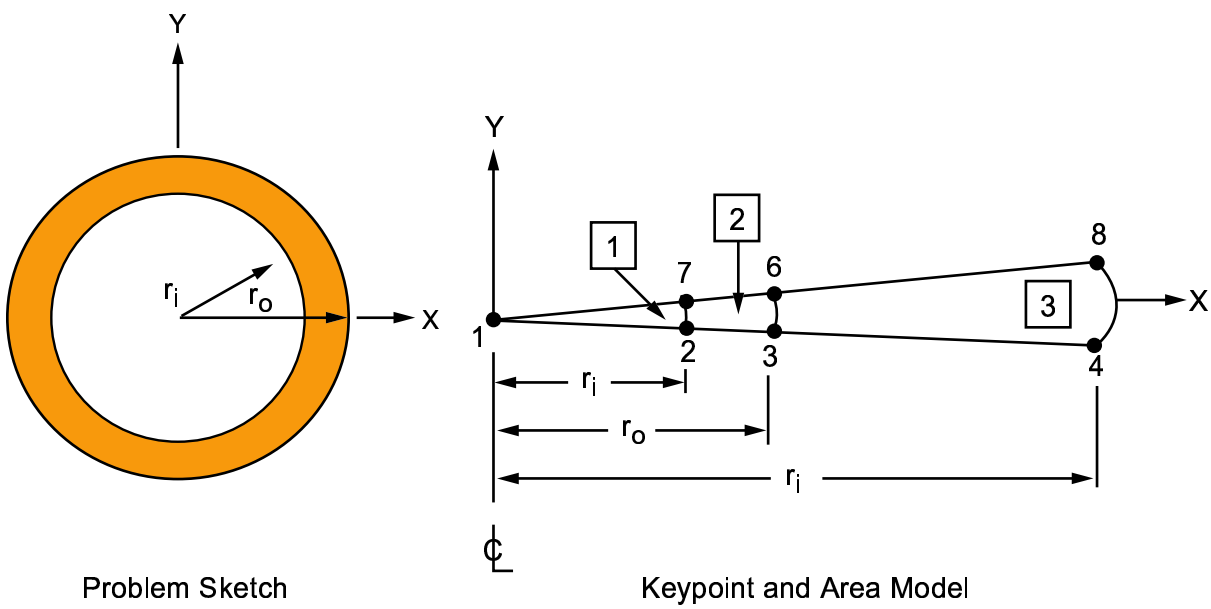

Material Properties	**Geometric Properties**	**Loading**
B-H curve as shown in Table 165.1: "B-H Data"	r_i = .3 in r_o = .45 in r_1 = .75 in	I = 100 A

Table 165.1 B-H Data

B(T)[1]	.21	.55	.80	.95	1.0	1.1	1.15	1.25	1.40
H(A/m)[1]	150	300	460	640	720	890	1020	1280	1900

1. Graphical estimate from reference.

Analysis Assumptions and Modeling Notes

The conductor is assumed to be infinitely long, thus end effects are ignored allowing for a two-dimensional planar analysis. Since the field is symmetric around the circumference, only a 5° slice is chosen for modeling. The external air is modeled to a boundary at r_1= 0.75 in, where the infinite boundary element is placed.

Six elements are arbitrarily modeled through the conductor thickness, line segment divisions and spacing ratios for the inner and outer air regions are chosen to provide compatible element sizes with the steel elements. The solution procedure consists of ramping the boundary conditions over 5 iterations in the first load step and iterating to convergence in a second load step with a convergence criterion of 1 x 10.

The MKS system of units is used for the analysis. The conversion factor used in the **KPSCALE** command, from inches to meters is 0.0254. The current density is calculated as $J = I/A = I/\pi(r_o2 - r_i2) = 2.28019 \times 10^{-4}$ A/in^2 = 438559 A/m^2.

Results Comparison

	Target	ANSYS	Ratio
B_{angle}, T @ r r=.325 in	0.48	0.45	0.94
B_{angle}, T @ r=.375 in	1.03	1.02	0.99
B_{angle}, T @ r=.425 in	1.22	1.21	1.00

Figure 165.2 B-H Curve

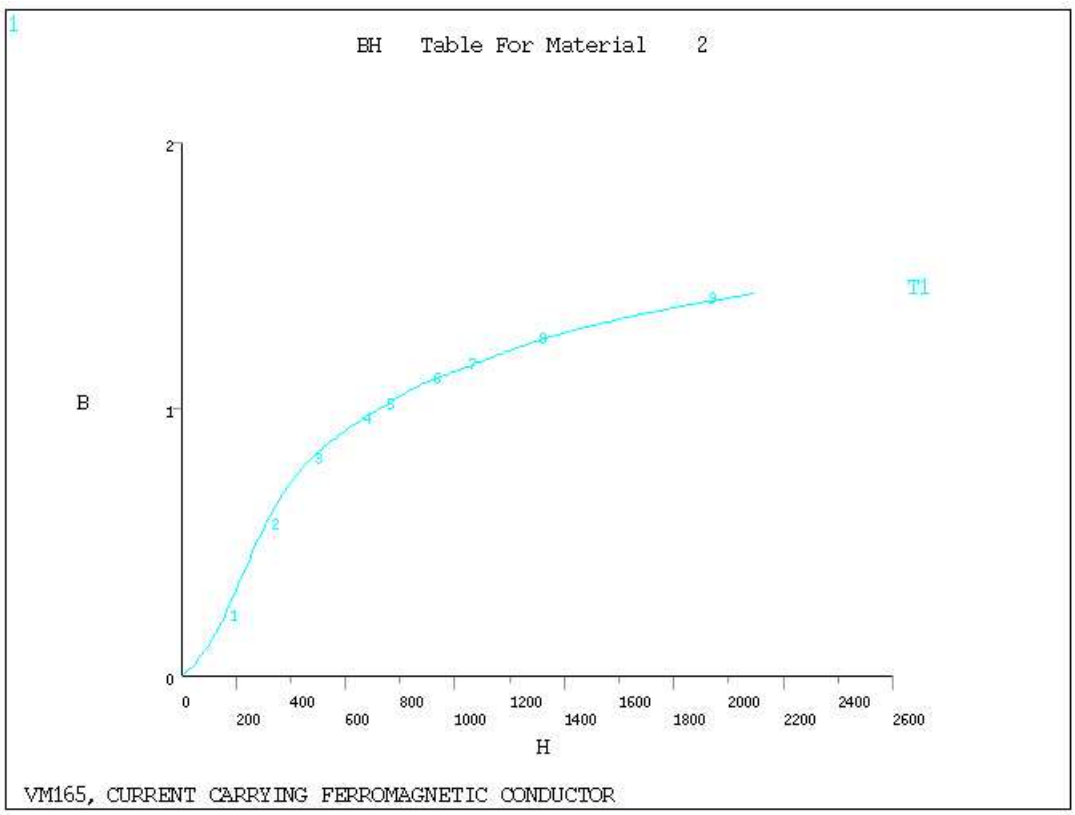

Figure 165.3 NU-B^2 Curve

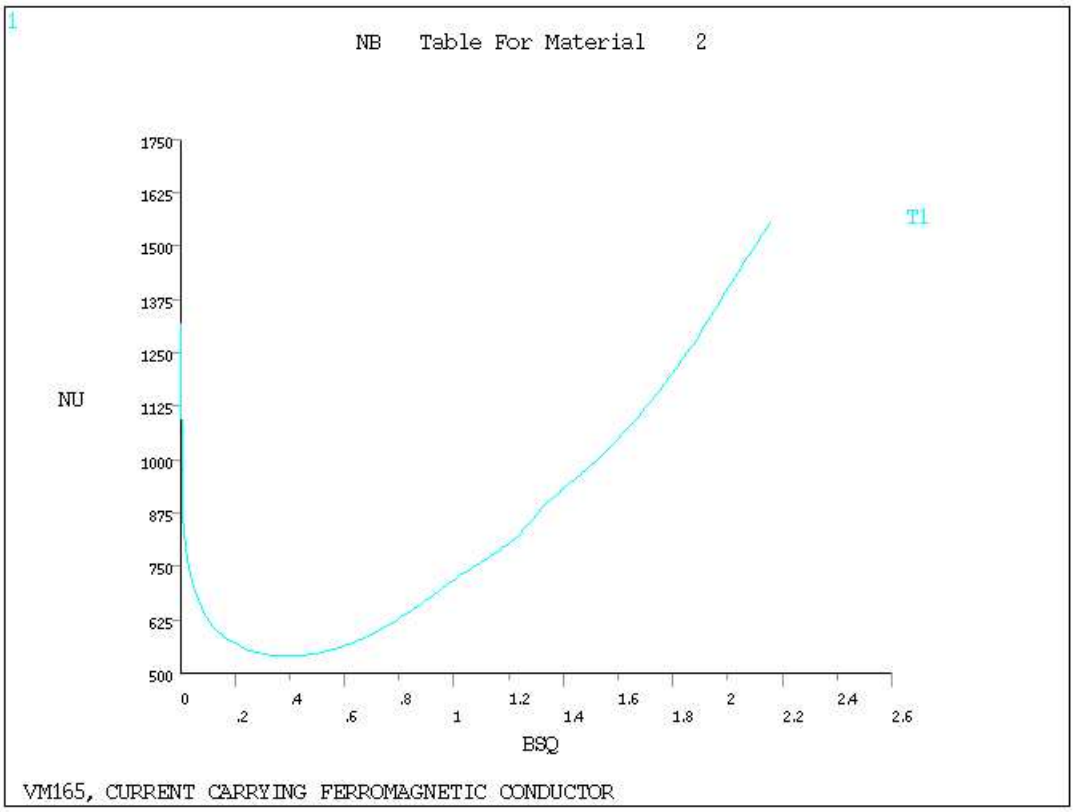

VM166: Long Cylinder in a Sinusoidal Magnetic Field

Overview

Reference:	C. R. I. Emson, "Electromagnetic Workshop", Report No. RAL-86-049, Rutherford Appleton Laboratory, Chitton, Didcot, Oxon, U.K., 1986, pg. 39.
Analysis Type(s):	Full Harmonic Analysis (**ANTYPE** = 3)
Element Type(s):	2-D Coupled-Field Solid Elements (PLANE13)
Input Listing:	vm166.dat

Test Case

A long hollow aluminum cylinder is placed in a uniform magnetic field. The magnetic field is perpendicular to the axis of the cylinder and varies sinusoidally with time. Determine the magnetic flux density at the center of the cylinder and the average power loss in the cylinder.

Figure 166.1 Long Cylinder Problem Sketch

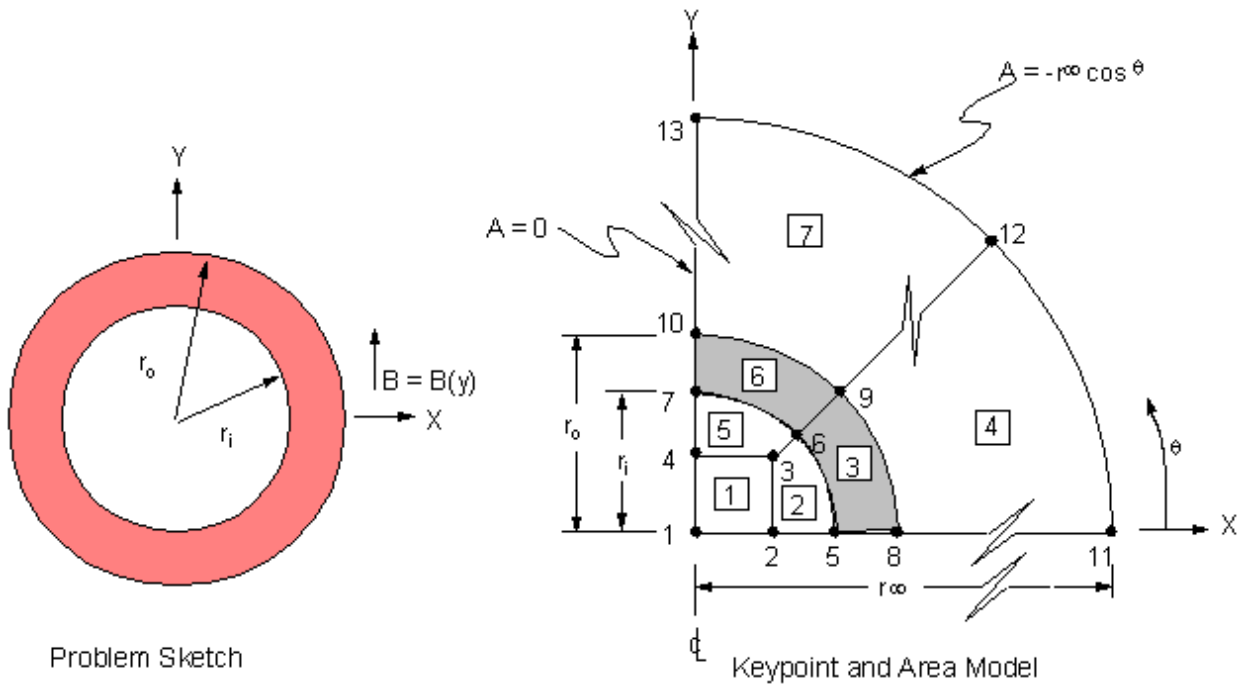

Material Properties	**Geometric Properties**	**Loading**
$\sigma = 2.5380711 \times 10^7$ S/m	$r_i = .05715$ m $r_o = .06985$ m $r_\infty = 0.84$ m	$B = B(y) = B \cos \omega t$, where $B_o = 0.1$T, $\omega = 60$ Hz

Analysis Assumptions and Modeling Notes

The external radial boundary is set at $r_\infty = 0.84$ m. The applied external field is calculated as $B(y) = -\delta A / \delta x$, so at $\theta = 0$ and $r = r_\infty$, $A = -B_o r = -.084$. The vector potential A varies along r_∞ as $A_\theta = -B_o r \cos \theta$.

The cylinder is assumed to be infinitely long, thus end effects are ignored allowing for a two-dimensional planar analysis. The problem can be modeled in quarter symmetry with the flux-parallel (A = 0) boundary condition at x = 0, and the flux-normal (natural) boundary condition at y = 0. The average power loss in the cylinder is calculated from the real and imaginary power loss density (JHEAT) terms available in the database:

$$P_{avg} = \sum_{i=1}^{n} (JHEAT_i^{Re} + JHEAT_i^{Im}) V_i$$

when n is the number of elements in the aluminum cylinder, V_i is the element volume (per-unit-depth). A fine mesh is defined in the cylinder for accurate calculation of the power loss.

Results Comparison

	Target	ANSYS	Ratio
B_x (0,0), T	$0 + {}_j0$	$0 + {}_j0$	1.0
B_y (0,0), T	$-.00184 - {}_j0.02102$	$-.00192 - {}_j0.02140$	1.043, 1.018
Power Loss, W/m	2288	2341	1.023

VM167: Transient Eddy Currents in a Semi-Infinite Solid

Overview

Reference:	J. P. Holman, *Heat Transfer*, 4th Edition, McGraw-Hill Book Co., Inc., New York, NY, 1976, pg. 104, eqn. 4-14 (analogous field solution).
Analysis Type(s):	Transient Magnetic Field Analysis (**ANTYPE** = 4)
Element Type(s):	2-D Coupled-Field Solid Elements (PLANE13)
Input Listing:	vm167.dat

Test Case

A semi-infinite solid is initially under no external magnetic field (vector potential A is zero throughout). The surface is suddenly subjected to a constant magnetic potential A_o. Determine the eddy current density, flux density and the vector potential field solution in the solid during the transient.

Figure 167.1 Semi-Infinite Solid Transient Eddy Currents Problem Sketch

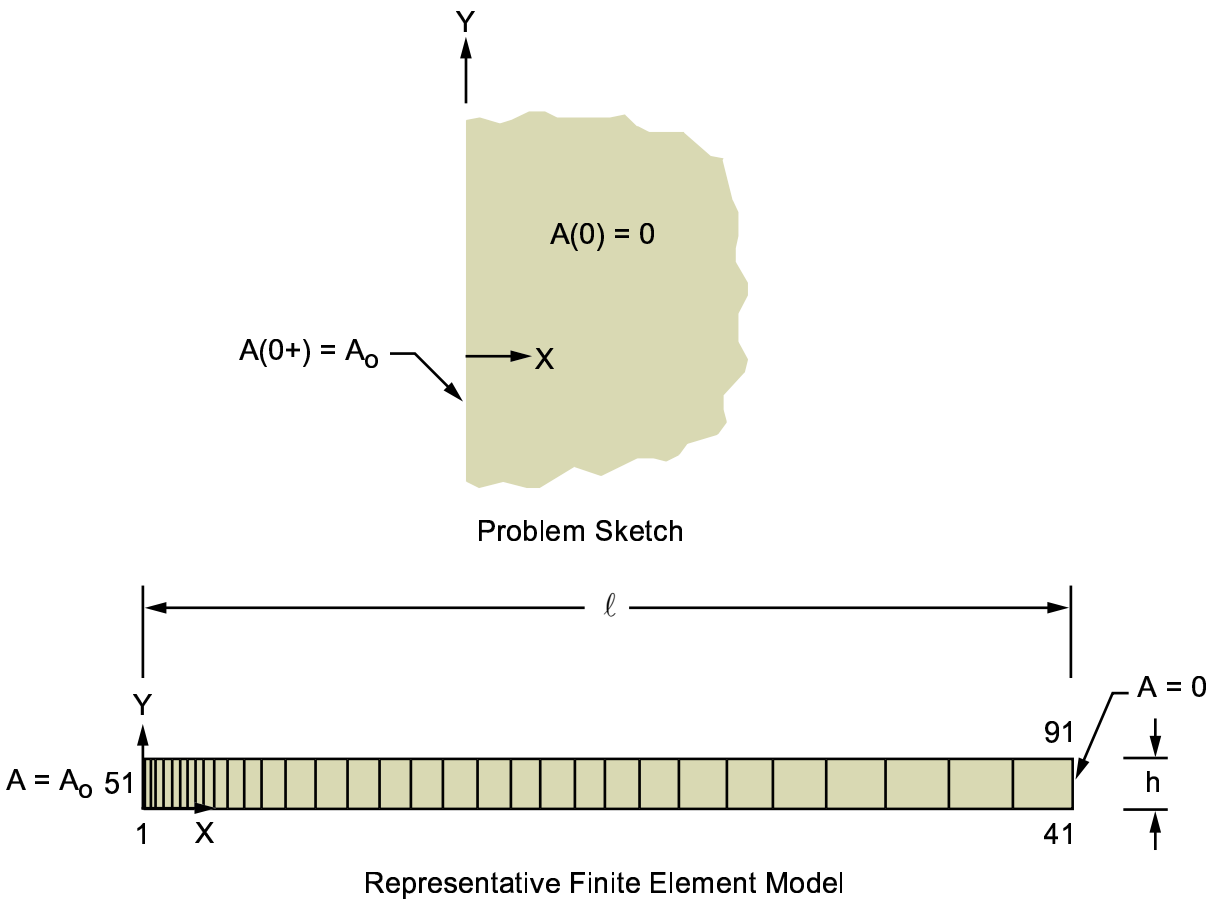

Material Properties	Geometric Properties	Loading
$\mu = 4\pi \times 10^{-7}$ H/m $\rho = 4 \times 10^{-7}$ ohm-m	$\ell = 20$ m h = 0.4 m	$A_o = 2.0$ Wb/m

Analysis Assumptions and Modeling Notes

A 0.4m^2 area is arbitrarily selected for the elements. The model length (20 m) is arbitrarily selected such that no significant potential change occurs at the end points (nodes 41, 91) for the time period of interest. The node locations are defined with a higher density near the surface to accurately model the transient behavior.

The transient analysis makes use of automatic time step optimization over a time period of 0.24 sec. A maximum time step size ((.24/48) = .005 sec.) is based on $\approx \delta^2/4\alpha$, where δ is the conduction length within the first element (δ = .0775m) and α is the magnetic diffusivity ($\alpha = \rho / \mu$ = .31822 m^2/sec.). The minimum time step (.0002 sec) is selected as 1/25 of the maximum time step. The starting time step of 0.0002 sec. is arbitrarily selected. The problem is solved with two load steps to provide solution output at the desired time points. In the first load step, the step potential load is applied while setting initial boundary conditions of zero at all other potentials.

Results Comparison

t = 0.15 sec	Target	ANSYS	Ratio
Vector Potential (Wb/m)			
@ x = .2517	.831	.831	1.000
@ x = .4547	.282	.278	0.986
@ x = .6914	.050	.044	0.880
Flux Density (T)			
@ x = .2517	3.707	3.687	.0995
@ x = .4547	1.749	1.794	1.026
@ x = .6914	.422	.454	1.076
Eddy Current Density (x107A/m2)			
@ x = .2517	-.777	-.780	1.004
@ x = .4547	-.663	-.677	1.021
@ x = .6914	-.243	-.245	1.008

ANSYS Verification Manual . ANSYS Release 10.0 . 002184 . © SAS IP, Inc.

Figure 167.2 Vector Potential vs. Time Plot

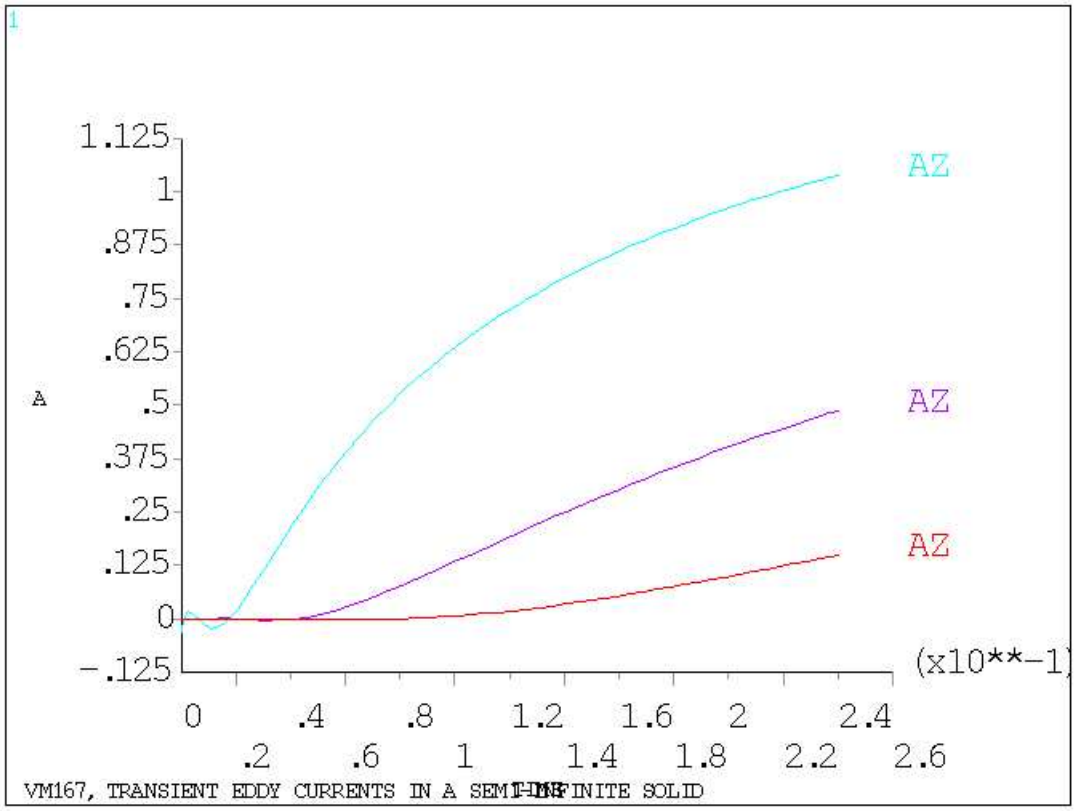

Figure 167.3 Eddy Current Density vs. Time Plot

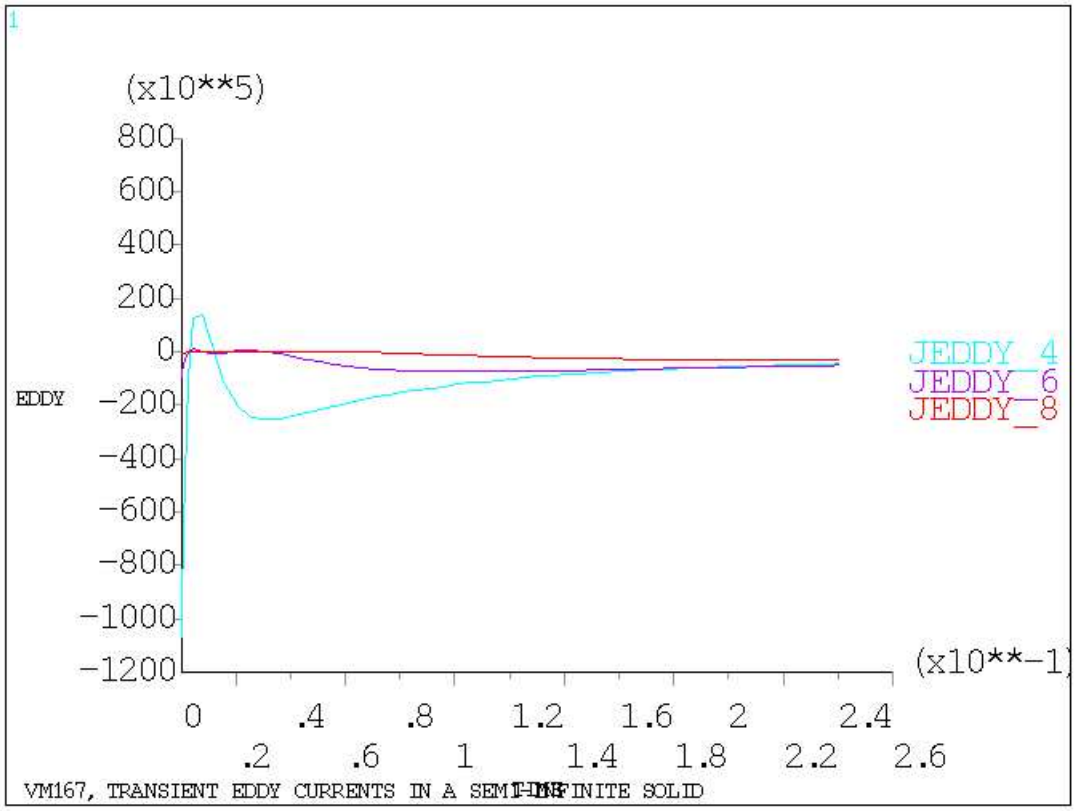

VM168: Magnetic Field in a Nonferrous Solenoid

Overview

Reference:	W. B. Boast, *Principles of Electric and Magnetic Fields*, Harper & Brothers, New York, NY, 1948, pg. 243.
Analysis Type(s):	Static Magnetic Field Analysis (**ANTYPE** = 0)
Element Type(s):	3-D Coupled-Field Solid Elements (SOLID5) Current Source Elements (SOURC36)
Input Listing:	vm168.dat

Test Case

A nonferrous solenoid is wound with one layer of No. 26 enameled wire and carries a current I. Determine the magnetic flux density on the centerline at

- the center of the coil
- the end of the coil
- at a point 5 inches from the end of the coil

Figure 168.1 Magnetic Field Problem Sketch

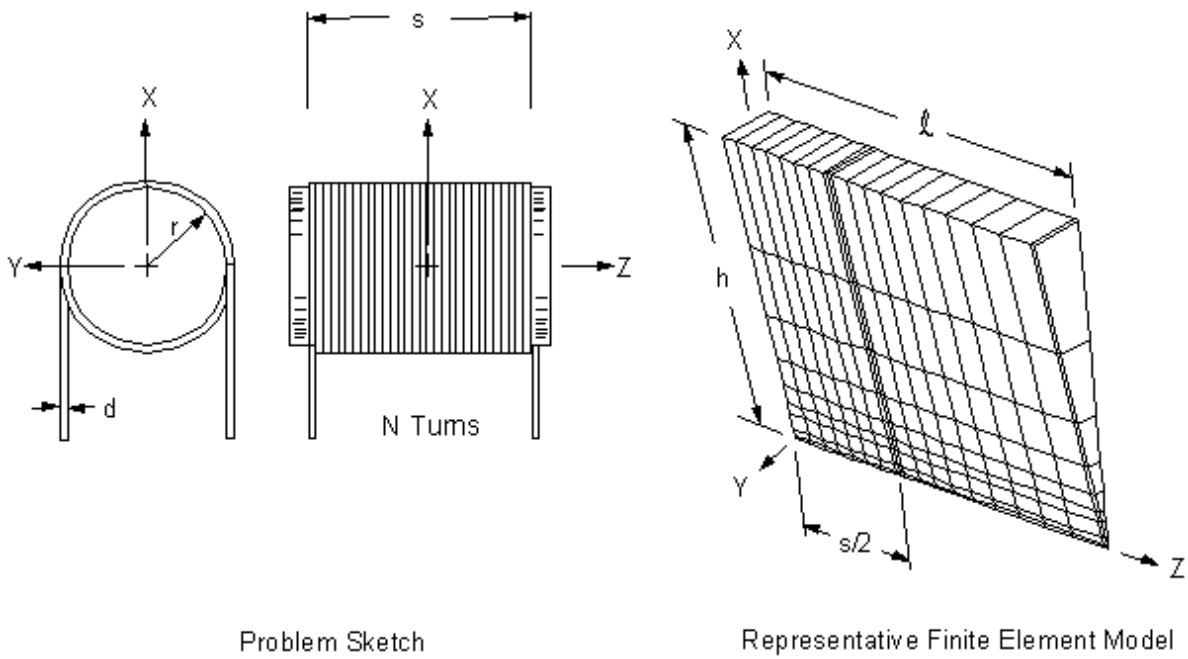

Geometric Properties	**Loading**
ℓ = 7.5 in s = 5 in r = 0.5 in h = 6 in d = 0.216	I = 0.5 A

Analysis Assumptions and Modeling Notes

The number of turns is N = s/d = 5/.0216 = 231. Therefore, N x I = 115.5 Ampere-turns. Since no ferromagnetic materials are present, the field due to induced magnetization, $H_m = 0$, and thus no scalar potential is required. The total field can be determined from the numerical integration of the coil source field upon specification of the coil with the current source element (SOURC36). Since the field is symmetric, an arbitrary arc of 10° is chosen with an additional symmetry plane taken along the coil midspan. A sufficient number of integration points (50) are chosen along the Z-axis to adequately represent the coil. Only one point is specified through the coil thickness. The Reduced Scalar Potential (RSP) is selected since only a source field is to be calculated.

Results Comparison

	Target	ANSYS	Ratio
B_z (x 10^6)T at z = 0	1120	1121	1.00
B_z (x 10^6)T at z = 7.5 in (.1905 m)	2.12	2.12	1.00

Figure 168.2 Axial Magnetic Field through Solenoid

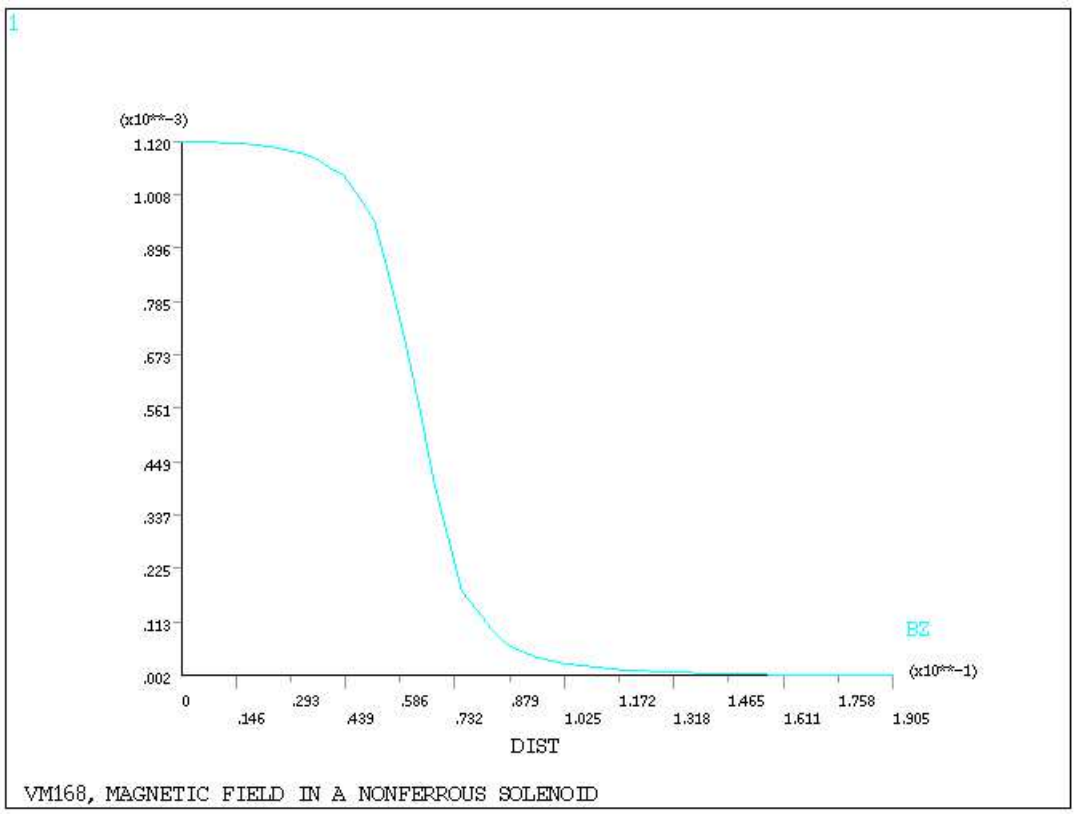

VM169: Permanent Magnet Circuit With an Air Gap

Overview

Reference:	F. C. Moon, *Magneto-Solid Mechanics*, John Wiley and Sons, Inc., New York, NY, 1984, pg. 275.
Analysis Type(s):	Magnetic Field Analysis (**ANTYPE** = 0)
Element Type(s):	Tetrahedral Coupled-Field Solid Elements (SOLID98)
Input Listing:	vm169.dat

Test Case

A permanent magnet circuit consists of a highly permeable core, a permanent magnet (the darker shading in the sketch), and an air gap. Assuming an ideal circuit with no flux leakage, determine the magnetic flux density and field intensity in the permanent magnet and the air gap.

Figure 169.1 Magnetic Circuit with Air Gap Problem Sketch

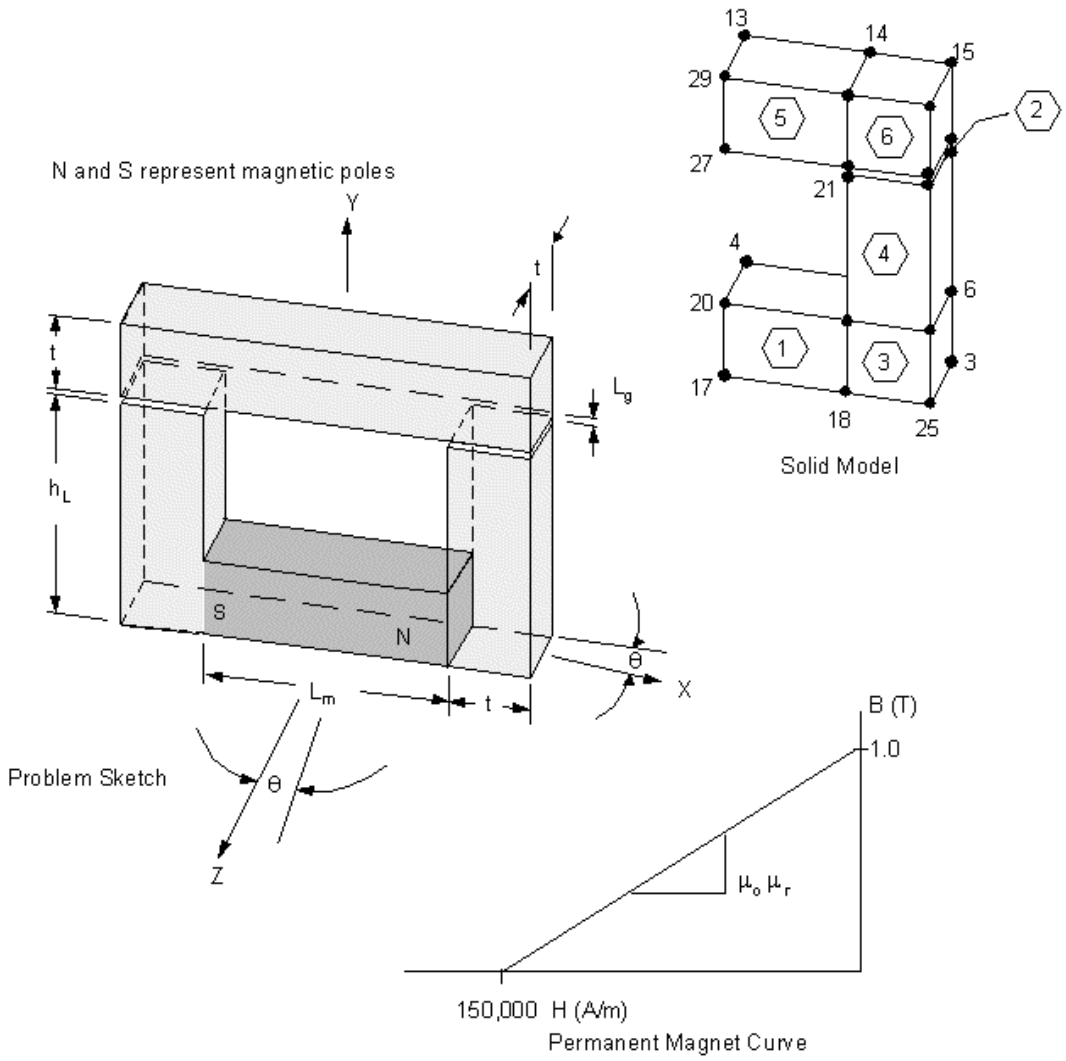

Material Properties	Geometric Properties
B_r = 1.0 T	L_m = .03 m
H_c = 150,000 A/m	L_g = .001 m
Θ = -30° (X-Z plane)	h_L = .03 m
μ_r = 1 x 10^5 (iron)	t = .01 m

Analysis Assumptions and Modeling Notes

The problem is solved using coupled-field solid elements (SOLID98). The permanent magnet is polarized along a line at Θ = -30° to the Z-axis in the X-Z plane. The coercive force components are calculated as MG169 = H_c cos Θ = 129,900, MGZZ = H_c sin Θ = -75,000. The permanent magnet relative permeability, μ_r, is calculated as:

$$\mu_r = \frac{B_r}{\mu_o H_o} = \frac{1}{(4\pi \times 10^{-7})(150{,}000)} = 5.30504$$

The iron is assumed to be highly permeable and is assigned a value μ_r = 1 x 10^5.

Since the device is symmetric only half of the circuit is required for modeling. At the symmetry plane the flux lines are orthogonal, so a flux-normal (Φ = 0) boundary condition is applied. With no leakage in the system, all the flux flows along a path circumventing the circuit. The flux-parallel boundary condition ($\delta \Phi / \delta n = 0$) holds on all other surfaces. The Reduced Scalar Potential (RSP) strategy is selected (default) since no current sources are defined. POST1 is used to extract results from the solution phase.

Results Comparison

Using SOLID98	Target	ANSYS	Ratio
|B|, T (perm. magnet)	.7387	.7387	1.000
|H|, A/m (perm. magnet)	39150	39207.5537	1.001
|B|, T (air gap)	.7387	.7386	1.000
|H|, A/m (air gap)	587860	587791.6466	1.000

Figure 169.2 Vector Display of Magnetic Flux Density

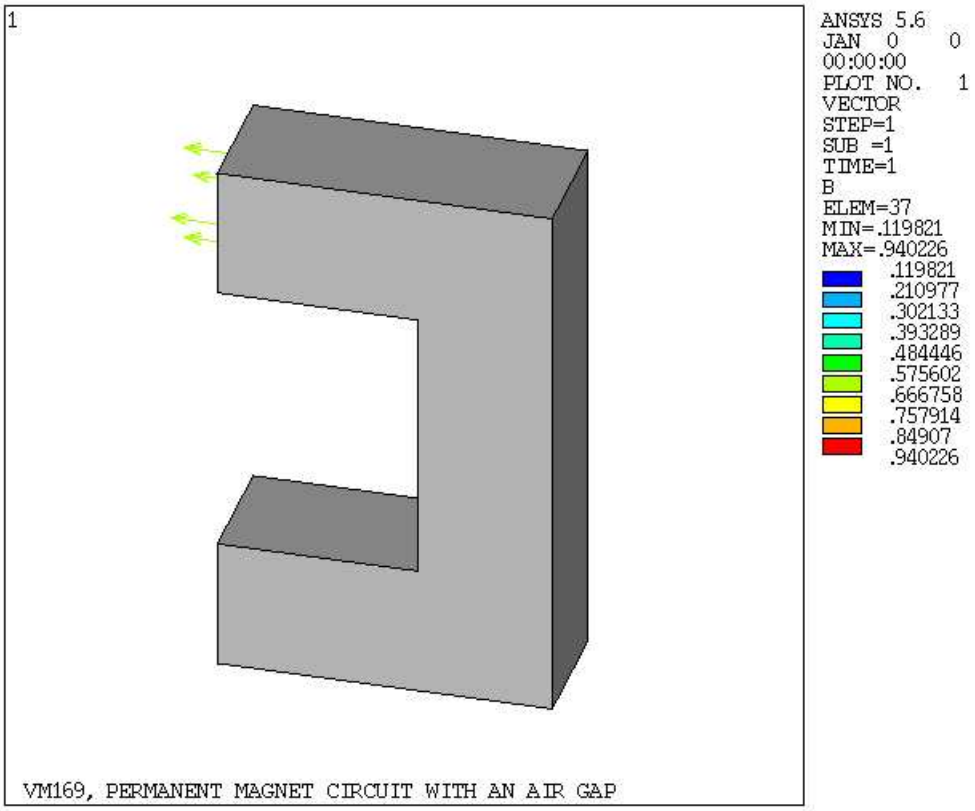

Figure 169.3 Vector Display of Magnetic Field Intensity

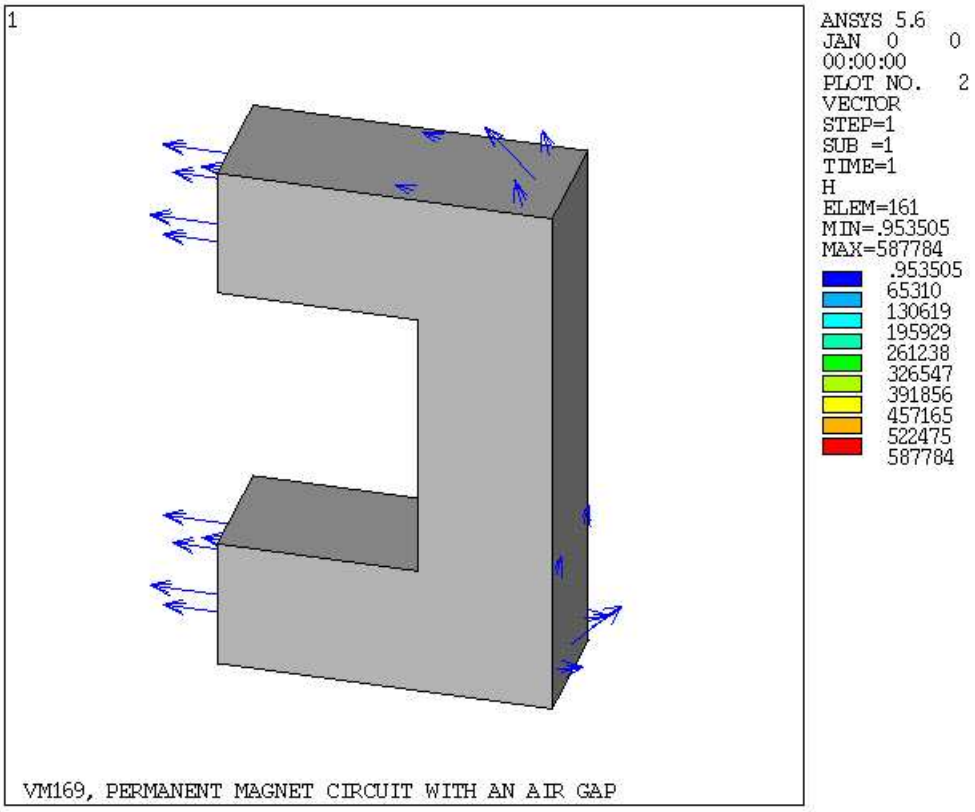

VM170: Magnetic Field From a Square Current Loop

Overview

Reference:	W. B. Boast, *Principles of Electric and Magnetic Fields*, Harper & Brothers, New York, NY, 1948, pg. 199-200.
Analysis Type(s):	Coupled-field Analysis (**ANTYPE** = 0)
Element Type(s):	Coupled Thermal-Electric Line Elements (LINK68)
Input Listing:	vm170.dat

Test Case

A current, I, is carried in a square loop of side a. The space about the current is air. Determine the magnetic flux density at point P, at a height b above the current loop.

Figure 170.1 Square Current Loop Problem Sketch

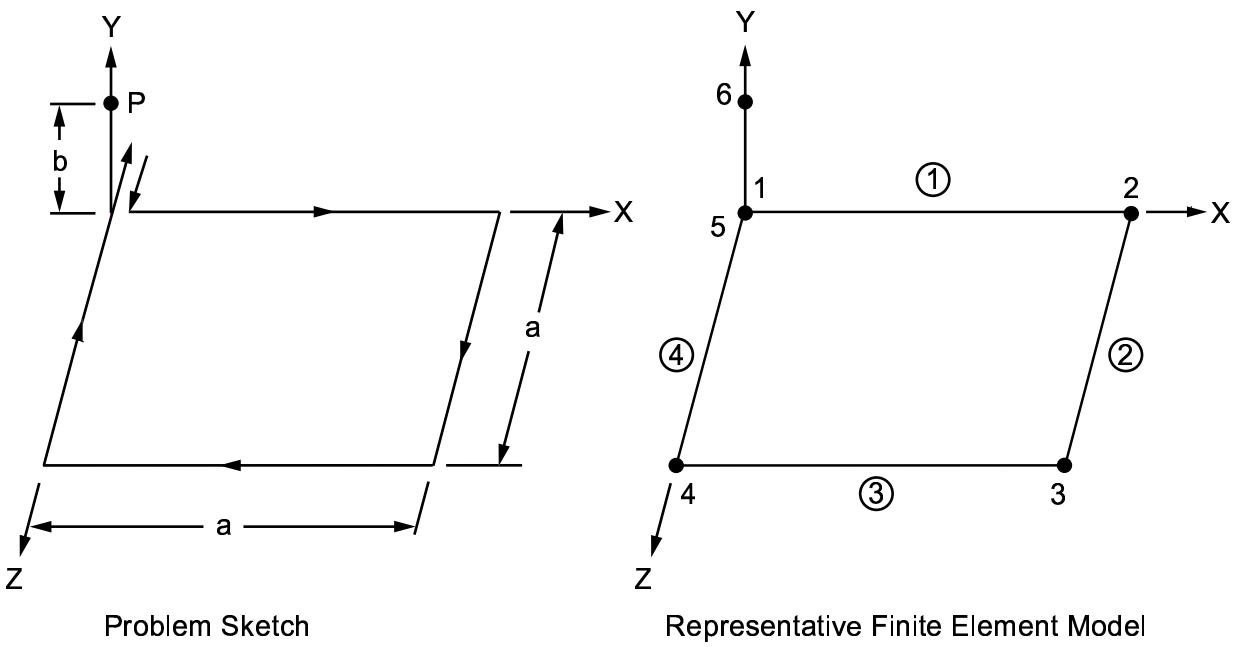

Material Properties	Geometric Properties	Loading
$\mu_o = 4\ \pi \times 10^{-7}$ H/m $\rho = 4.0 \times 10^{-8}$ ohm-m	a = 1.5 m b = 0.35 m	I = 7.5 A

Analysis Assumptions and Modeling Notes

The problem requires a coupled electromagnetic field solution. LINK68 is used to create the current field in the wire loop. The current field established by the LINK68 elements is used to calculate the magnetic field at point P.

Nodes 1 and 5 overlap to create a closed current loop. The voltage at node 5 is set to zero while the current is applied to node 1.

The first solution calculates the current distribution in the loop. The **BIOT** command is then issued to calculate the magnetic field from the current distribution.

The cross-sectional area of the wire does not enter into the solution so an arbitrary area of 1.0 is input. Only one element is required per side of the square loop since the Biot-Savart integration of the magnetic field from the line element is exact. Flux density is calculated from the field intensity as $B = \mu_o H$.

Results Comparison

Flux Density	Target	ANSYS	Ratio
BX (x 10^6 Tesla)	2.010	2.010	1.000
BY (x 10^6 Tesla)	-.0662	-0.662	1.000
BZ (x 10^6 Tesla)	2.010	2.010	1.000

VM171: Permanent Magnet Circuit With an Elastic Keeper

Overview

Reference:	F. C. Moon, *Magneto-Solid Mechanics*, John Wiley and Sons, Inc., New York, NY, 1984, pg. 275.
Analysis Type(s):	Coupled-field Analysis (**ANTYPE** = 0)
Element Type(s):	2-D Coupled-Field Solid Elements (PLANE13) Spring-Damper Elements (COMBIN14)
Input Listing:	vm171.dat

Test Case

A permanent magnet circuit consisting of a highly-permeable core and a permanent magnet is used to model a relay switch. An elastic keeper is modeled with a highly permeable iron and two springs. Assuming no flux leakage, determine the equilibrium displacements, δ, of the keeper and the operating point (flux density) in the permanent magnet.

Figure 171.1 Permanent Magnet Circuit Problem Sketch

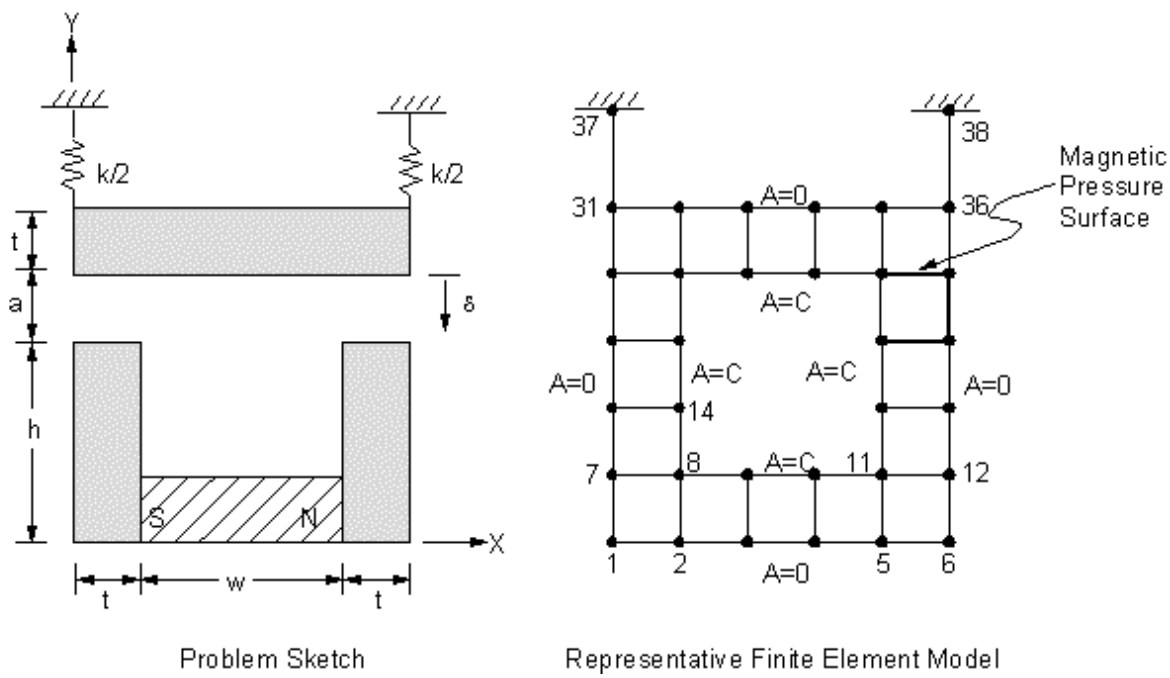

Material Properties	Geometric Properties
For permanent magnet: B_r = 1 T H_c = 150,000 A/m μ_r = 5.305 **For iron:** $\mu_r = 1 \times 10^5$ **For springs:** $k = 3.30681 \times 10^5$ N/m **For iron and permanent magnet:** $E = 10 \times 10^{10}$ N/m^2 $\nu = 0$	h = .03 m w = .03 m t = .01 m a = .01 m

Analysis Assumptions and Modeling Notes

Since no leakage is assumed, the flux path will follow a closed loop through the iron core, permanent magnet, air gap, and keeper. The flux must follow parallel to the edges of the device, thus a flux-parallel (A = 0) boundary is set at the external nodes of the model. The inner nodes are coupled to ensure a flux-parallel boundary condition at the inner edge. The iron is assumed to be infinitely permeable and is assigned $\mu_r = 10^5$. For a permanent magnet, $\mu_o\mu_r = B_r / H_c$, therefore $\mu_r = 5.305$. The modulus of elasticity for air is assigned a negligible value (100 N/m^2) compared to that of the permeable materials. The permanent magnet structure has its displacements fixed. A magnetic pressure surface is assigned to the elements adjacent to the air-keeper interface to allow for the application of magnetic forces for structural analysis. An iterative large-deflection solution is required. Convergence criteria for structural force and magnetic current-segment is defined.

Results Comparison

	Target	ANSYS	Ratio
Displacement, (m)	.00150	.00150	0.994
B, (T)	.2496	.2494	0.998

Figure 171.2 Displaced Geometry Display

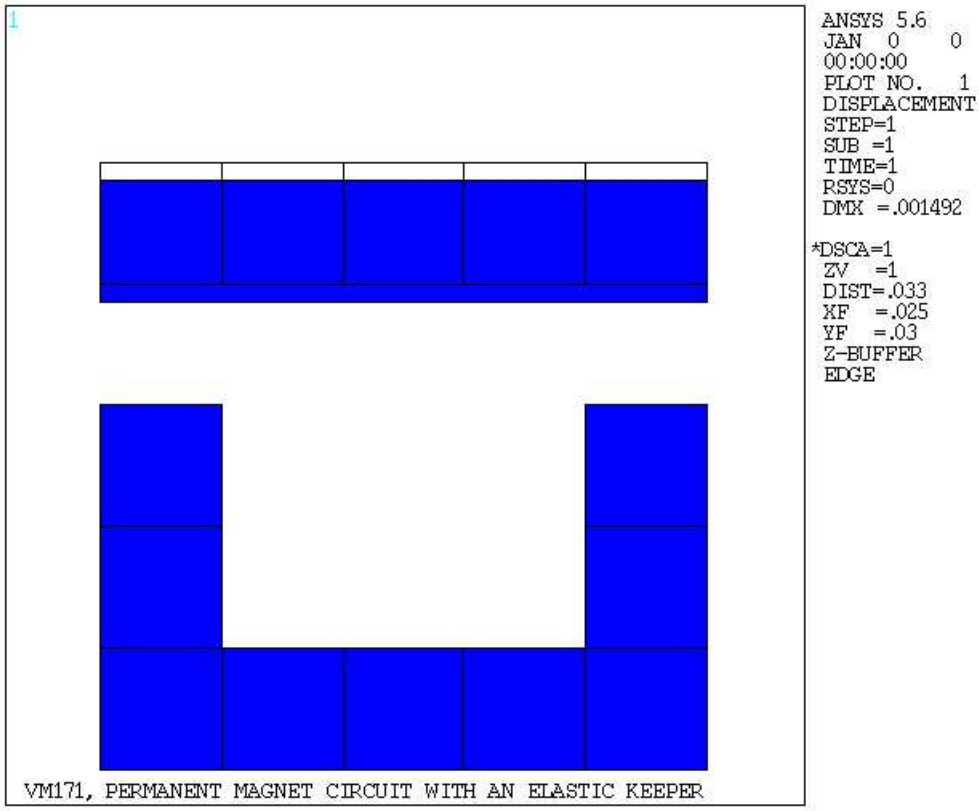

VM172: Stress Analysis of a Long, Thick, Isotropic Solenoid

Overview

Reference:	F. C. Moon, *Magneto-Solid Mechanics*, John Wiley and Sons, Inc., New York, NY, 1984, pg. 275.
Analysis Type(s):	Coupled field Analysis (**ANTYPE** = 0)
Element Type(s):	2-D Coupled-Field Solid Elements (PLANE13) 3-D Magneto-Structural Solid Elements (SOLID62) 3-D Magnetic Solid Elements (SOLID97)
Input Listing:	vm172.dat

Test Case

A long, thick solenoid carries a uniform current density distribution, J. Assuming that the turns of the solenoid can be modeled as a homogeneous isotropic material with modulus of elasticity E, and Poisson's ratio ν, determine the axial magnetic flux density distribution B_θ and the circumferential stress σ_o distribution in the solenoid.

Figure 172.1 Isotropic Solenoid Problem Sketch

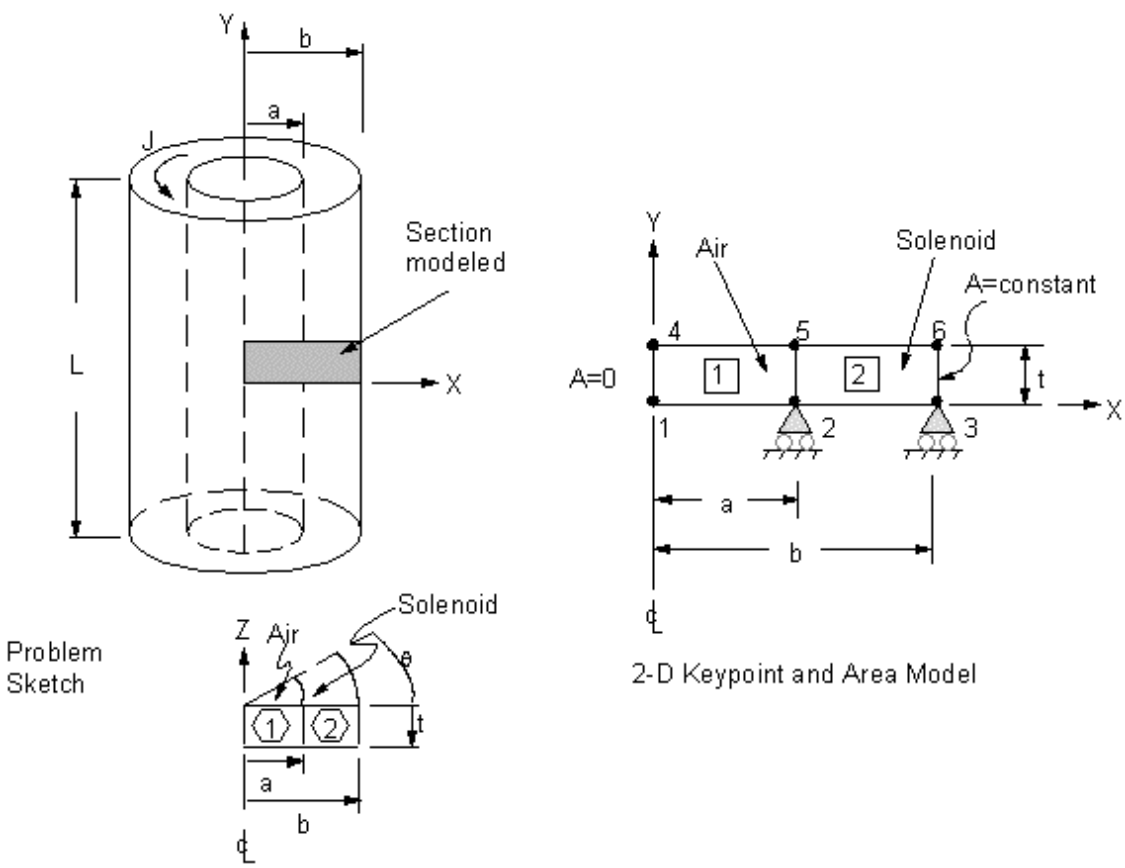

Material Properties	Geometric Properties	Loading
$E = 10.76 \times 10^{10}$ N/m^2 $\upsilon = 0.35$ $\mu = \mu_o$	a = .01 m b = .02 m t = .002 m Θ = 10 degrees	$J = 1 \times 10^6$ A/m^2

Analysis Assumptions and Modeling Notes

The problem is solved first using a 2-D axisymmetric analysis with PLANE13 elements and then a 3-D analysis using SOLID62 and SOLID97 elements. The length of the solenoid is assumed infinite ($L = \infty$), so only a section of the axisymmetric solenoid (t = .002 m, arbitrary) is required for modeling. It is assumed that the magnetic field external to the solenoid is zero, so the nodes at x = b are coupled (AZ = constant (2-D), AY = constant (3-D)) such that the proper flux-parallel boundary condition is imposed. The flux-parallel condition at x = 0 is imposed by setting A = 0. Flux-normal boundary conditions are imposed naturally (no ANSYS input necessary) at y = 0 and y = t for the 2-D analysis, while in 3-D, the normal component (AZ) is set to zero. In 3-D, the nodes are rotated into cylindrical coordinates so that all in-plane vector potentials (AX and AZ) can be set to zero since only AY is required for a true axisymmetric field solution.

Symmetric structural boundary conditions are applied to the solenoid elements at y = 0. The nodes at y = t on the solenoid are coupled in UY to ensure symmetry. The air is modeled with 5 elements in the radial direction while the solenoid is discretized with 20 elements in the radial direction to accurately model the stress distribution. The 3-D model uses SOLID97 elements to model the air and SOLID62 elements to model the coil.

Results Comparison

		Target[1]	ANSYS	Ratio
PLANE13	B_{angle}, T @ r = .01 m	.01257	.01226	0.975
	B_{angle}, T @ r = .013 m	.008796	.008797	1.000
	B_{angle}, T @ r = .01 7m	.003770	.003769	1.000
	$Stress_o$, N/m^2 @ r = .01m	146.7	144.2	0.983
	$Stress_o$, N/m^2 @ r = .013m	97.79	97.70	0.999
	$Stress_o$, N/m^2 @ r = .017m	62.44	62.61	1.003
SOLID62 / SOLID97	B_{angle}, T @ r = .01 m	.01257	.01219	0.970
	B_{angle}, T @ r = .013 m	.008796	.008747	0.994
	B_{angle}, T @ r = .01 7m	.003770	.003750	0.995
	$Stress_o$, N/m^2 @ r = .01m	146.7	144.4	0.984
	$Stress_o$, N/m^2 @ r = .013m	97.79	95.97	0.981
	$Stress_o$, N/m^2 @ r = .017m	62.44	61.34	0.982

1. Assumed to be linearly varying through solenoid

Figure 172.2 2-D Circumferential Stress through Solenoid Windings

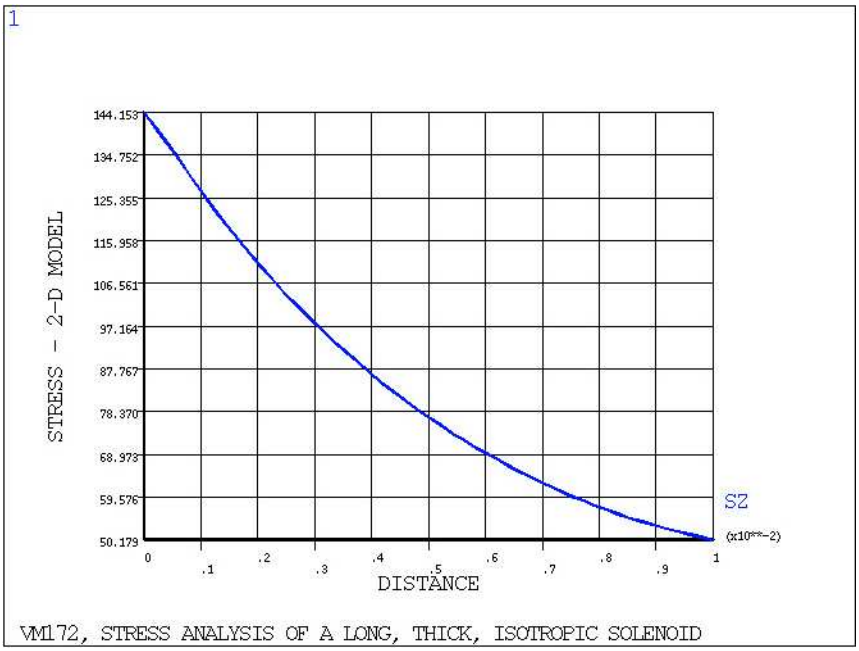

Figure 172.3 2-D Axial Flux Density through Solenoid Windings

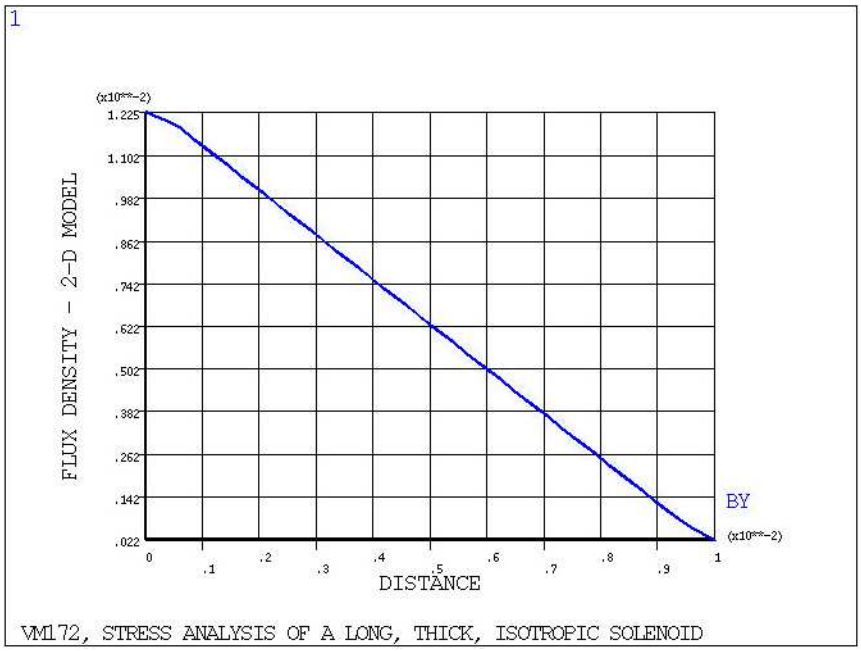

Figure 172.4 3-D Circumferential Stress through Solenoid Windings

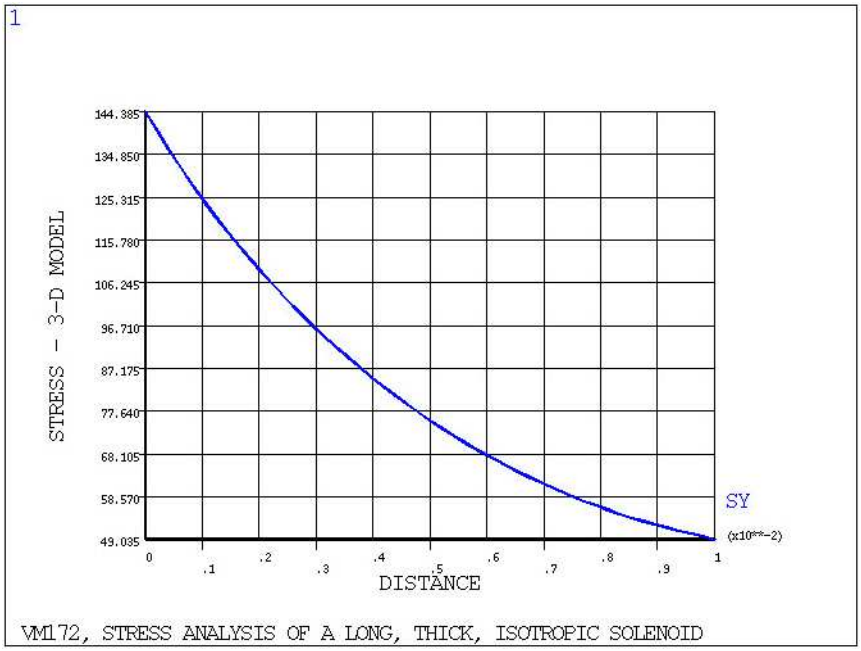

Figure 172.5 3-D Axial Flux Density through Solenoid Windings

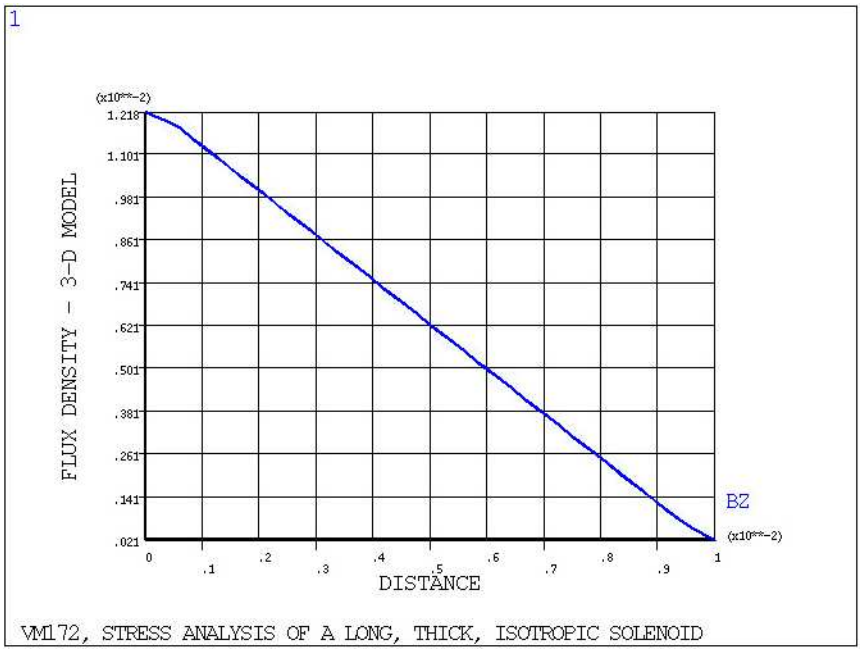

VM173: Centerline Temperature of an Electrical Wire

Overview

Reference:	W. M. Rohsenow, H. Y. Choi, *Heat, Mass and Momentum Transfer*, 2nd Printing, Prentice-Hall, Inc., Englewood Cliffs, NJ, 1963, pg. 106, ex. 6.5.
Analysis Type(s):	Static, Coupled-Field Analysis (**ANTYPE** = 0)
Element Type(s):	3-D Coupled-Field Solid Elements (SOLID5)
Input Listing:	vm173.dat

Test Case

Determine the centerline temperature $T_{\text{℄}}$ and the surface temperature T_s of a bare steel wire carrying a current I and having a resistance R/I. The surface convection coefficient between the wire and the air (at temperature T_a) is h. Also determine the heat dissipation rate q.

Figure 173.1 Electrical Wire Problem Sketch

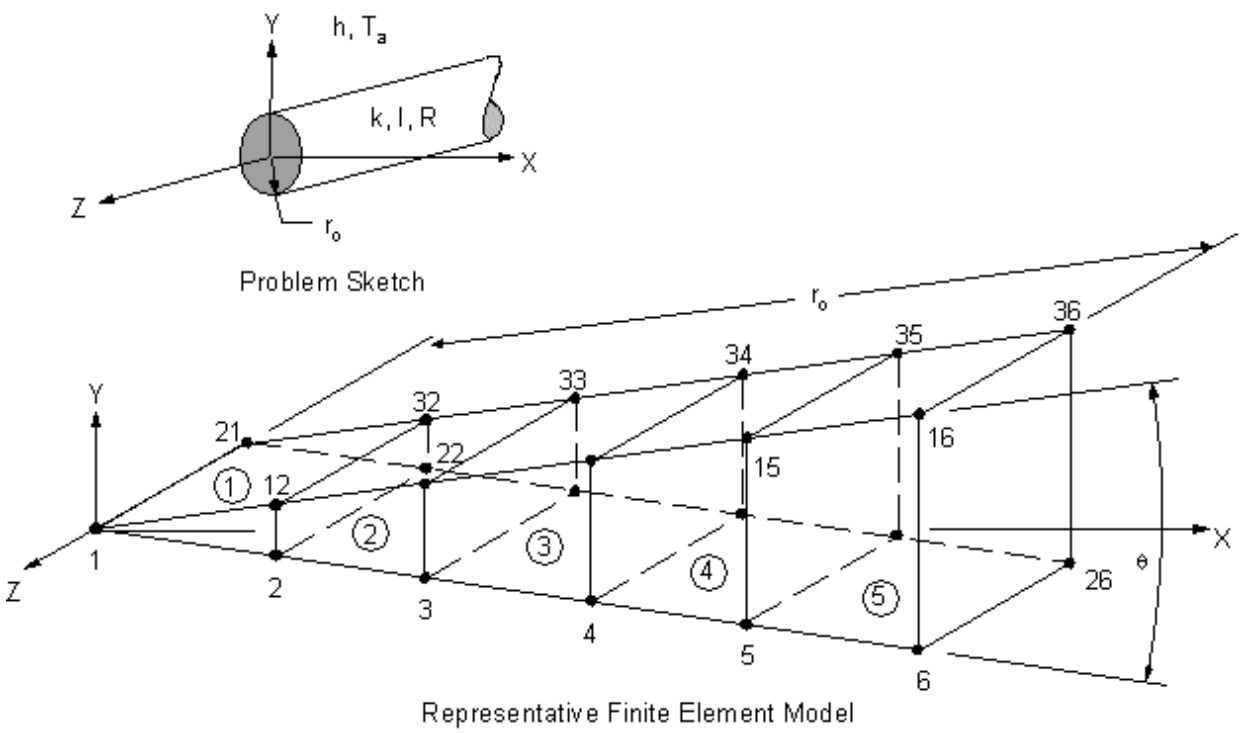

Material Properties	**Geometric Properties**	**Loading**
R = .0001 ohm/ft k = 13 Btu/hr-ft-°F h = 5 Btu/hr-ft^2-°F ρ = 8.983782 x 10^{-8} ohm-ft	ℓ = 1 in = (1/12) ft r_o = 0.375 in = 0.03125 ft Θ = 10°	I = 1000 A T_a = 70°F

Analysis Assumptions and Modeling Notes

A 1 inch axial (Z) length is chosen for convenience. Since the problem is axisymmetric, only a one-element sector is needed. A small angle Θ = 10° is used for approximating the circular boundary with a straight-sided element.

The calculated resistivity, rho = RA/l, in units of [ohms-ft] was converted to units of [(Btu/hr)/watt] using the conversion factor [3.415 (ohm-ft)] / [(Btu/hr)/watt]. With this conversion, the Joule heat units match the thermal units. The voltage drop per foot, IR/ℓ, is calculated as 0.1 volt/ft. Nodes 1 though 16 are assumed to be ground nodes for reference. The steady-state convergence procedures are used. The heat dissipation rate, q, is calculated as $q = hA(T-T_a)$ where A = exterior surface area of the wire (parameter AREA).

Results Comparison

	Target[1]	ANSYS	Ratio
Centerline Temperature, °F	419.9	418.6	0.997
T_s, °F	417.9	416.5	0.997
q, Btu/hr/ft	341.5	339.8	0.995

1. Solution recalculated

VM174: Bimetallic Beam Under Thermal Load

Overview

Reference:	B. A. Boley, J. H. Weiner, *Theory of Thermal Stress*, R. E. Krieger Publishing Co, Malabar, FL, 1985, pg. 429.
Analysis Type(s):	Coupled field Analysis (**ANTYPE** = 0)
Element Type(s):	2-D Coupled-Field Solid Elements (PLANE13)
Input Listing:	vm174.dat

Test Case

A bimetallic beam consists of two materials with different coefficients of thermal expansion, α_1 and α_2, and is initially at a reference temperature of 0°F. The beam is simply supported and a uniform temperature is applied to both surfaces. The beam is expected to undergo a large lateral deflection. Determine the midspan deflection after heating and verify the temperature T at the material interface.

Figure 174.1 Bimetallic Beam Problem Sketch

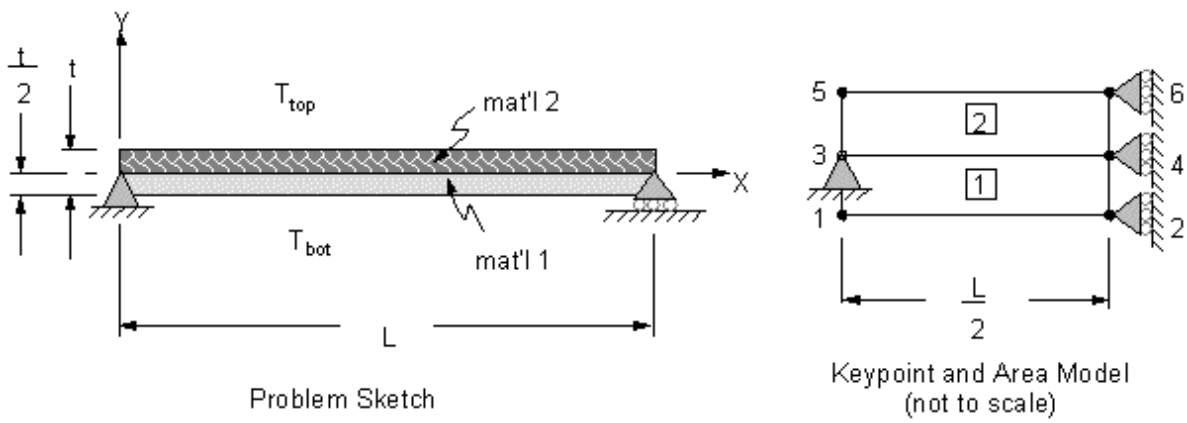

Material Properties	**Geometric Properties**
For each strip: $k_1 = k_2 = 5$ Btu/hr-in-°F **For material 1:** $E_1 = 10 \times 10^6$ psi $\alpha_1 = 14.5 \times 10^{-6}$ in/in°F **For material 2:** $E_2 = 10 \times 10^6$ psi $\alpha_2 = 2.5 \times 10^{-6}$ in/in°F	L = 5 in t = 0.1 in **Loading** $T_{top} = 400.0$°F $T_{bot} = 400.0$°F

Analysis Assumptions and Modeling Notes

The problem involves a coupled thermal-stress analysis with large deflections and thus requires an iterative solution. Since the problem is symmetric, only one-half of the beam is modeled. The AZ degree of freedom is not required in this analysis and is excluded from the matrix formulation by not specifying any magnetic material properties. A convergence criteria for force is specified with a tight tolerance to converge the large deflection behavior.

Results Comparison

	Target	ANSYS	Ratio
y, in	0.900	0.888	0.987
T, °F	400.0	400.0	1.000

Figure 174.2 Bimetallic Beam Under Thermal Load

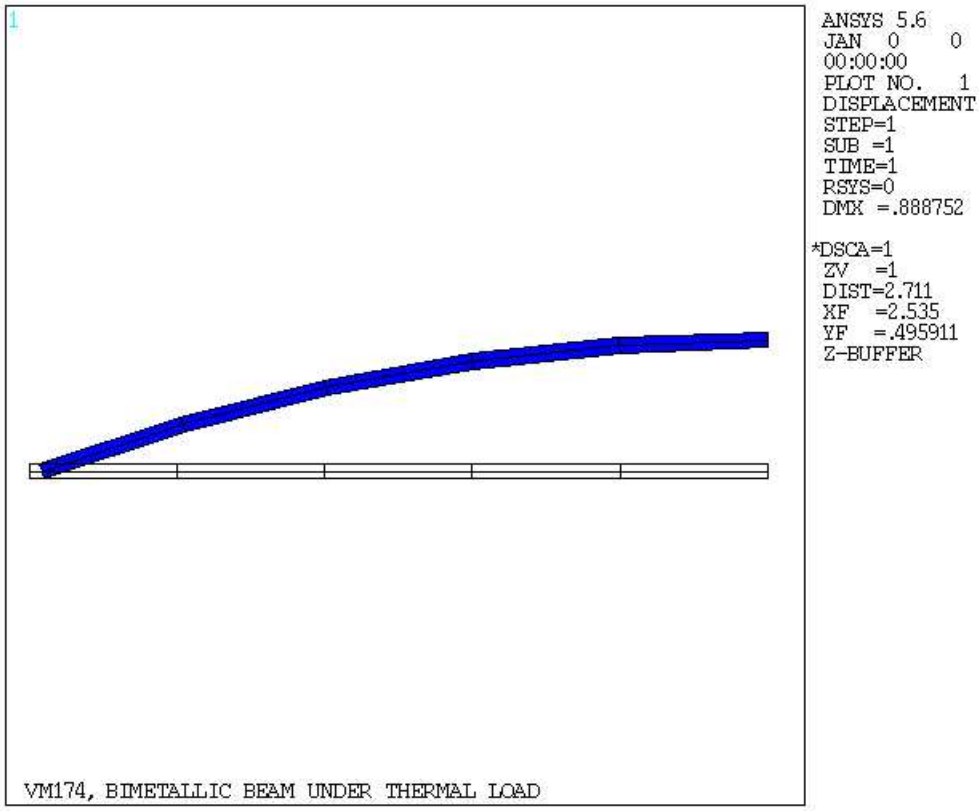

VM175: Natural Frequency of a Piezoelectric Transducer

Overview

Reference:	D. Boucher, M. Lagier, C. Maerfeld, "Computation of the Vibration Modes for Piezoelectric Array Transducers Using a Mixed Finite Element Perturbation Method", *IEEE Trans. Sonics and Ultrasonics*, Vol. SU-28 No. 5, 1981, pg. 322, table 1.
Analysis Type(s):	Mode-frequency Analysis (**ANTYPE** = 2)
Element Type(s):	3-D Coupled-Field Solid Elements (SOLID5)
Input Listing:	vm175.dat

Test Case

A piezoelectric transducer consists of a cube of PZT4 material with its polarization direction aligned along the Z axis. Electrodes are placed on the two surfaces orthogonal to the polarization axis. Determine the first two coupled-mode (breathing-type deformation) natural frequencies for the short circuit (resonance) case and the open circuit (anti-resonance) case.

Figure 175.1 Piezoelectric Transducer Problem Sketch

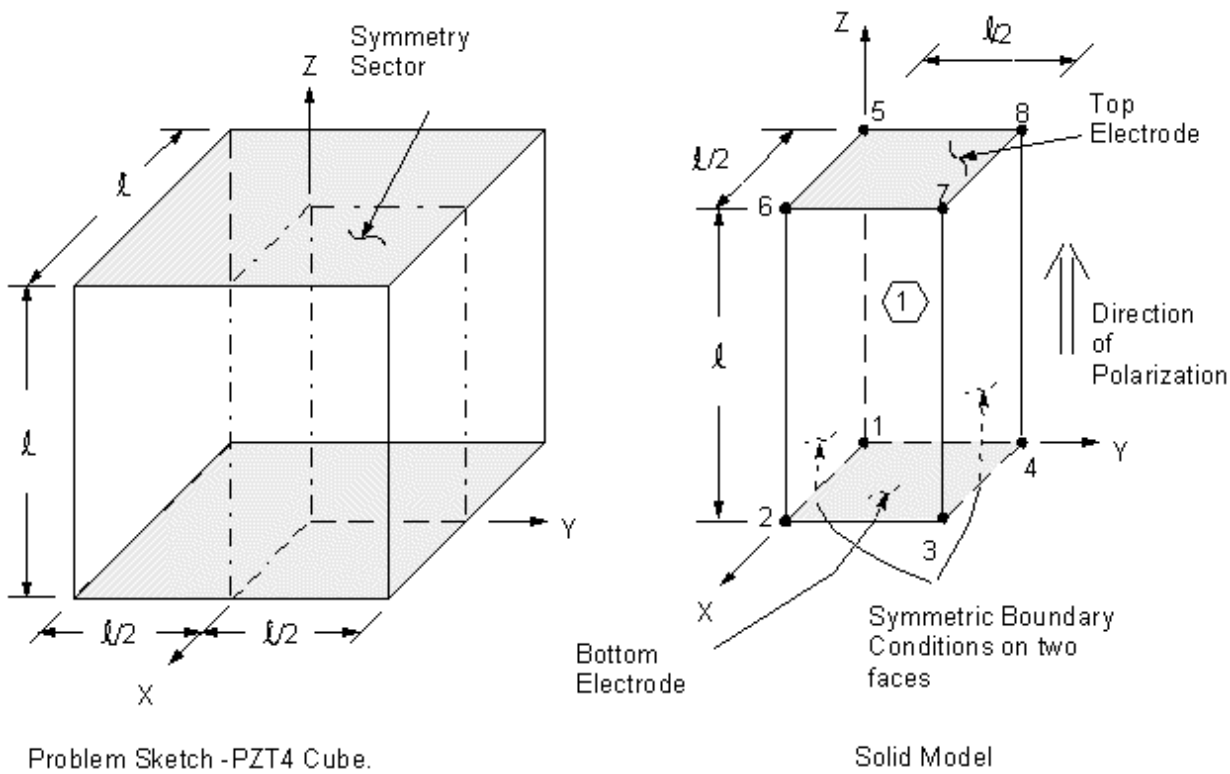

Material Properties	**Geometric Properties**
ρ = 7500 kg/m^3 See Constitutive Matrices	ℓ = .02 m

Constitutive Matrices

PZT4 Dielectric Matrix [ε_r]

$$\begin{bmatrix} 804.6 & 0 & 0 \\ 0 & 804.6 & 0 \\ 0 & 0 & 659.7 \end{bmatrix}$$

PZT4 Piezoelectric Matrix [e] C/m^2

$$\begin{bmatrix} 0 & 0 & -4.1 \\ 0 & 0 & -4.1 \\ 0 & 0 & 14.1 \\ 0 & 0 & 0 \\ 0 & 10.5 & 0 \\ 10.5 & 0 & 0 \end{bmatrix}$$

PZT4 "Stiffness" Matrix [c] x 10^{-10} N/m^2

$$\begin{bmatrix} 13.2 & 7.1 & 7.3 & 0 & 0 & 0 \\ & 13.2 & 7.3 & 0 & 0 & 0 \\ & & 11.5 & 0 & 0 & 0 \\ & & & 3.0 & 0 & 0 \\ & \text{Symmetric} & & & 2.6 & 0 \\ & & & & & 2.6 \end{bmatrix}$$

Analysis Assumptions and Modeling Notes

The electroded regions represent equipotential surfaces and are not modeled explicitly. For the short-circuit case the top and bottom electrodes are grounded (voltages are set equal to zero). For the open-circuit case only the bottom electrode is grounded. The short-circuit case represents excitation by potential while the open-circuit case represents excitation by charge.

A one-quarter symmetry sector is modeled with symmetry boundary conditions applied. The mesh density selected for analysis along the axes (X, Y, Z) are (2,2,4) elements respectively. All active displacement degrees of freedom are selected as master degrees of freedom (**TOTAL** command). All non-specified voltage degrees of freedom are condensed out during matrix reduction to allow for electro-elastic coupling.

The TEMP and MAG degrees of freedom of SOLID5 are not used in this analysis.

The modes that produce a breathing-type deformation pattern indicate the desired results. POST1 is used to display the mode shapes for determination of the desired natural frequencies.

Results Comparison

		Target[1]	ANSYS	Ratio
Short Circuit	f_1, kHz	66.56	66.45	0.998
	f_2, kHz	88.01	90.71	1.031
Open Circuit	f_1, kHz	81.59	84.26	1.033
	f_2, kHz	93.41	96.99	1.038

1. Experimentally measured values (f_1,f_2) represent breathing mode frequencies.

Figure 175.2 Short Circuit Case, Plot 3: First Breathing Mode

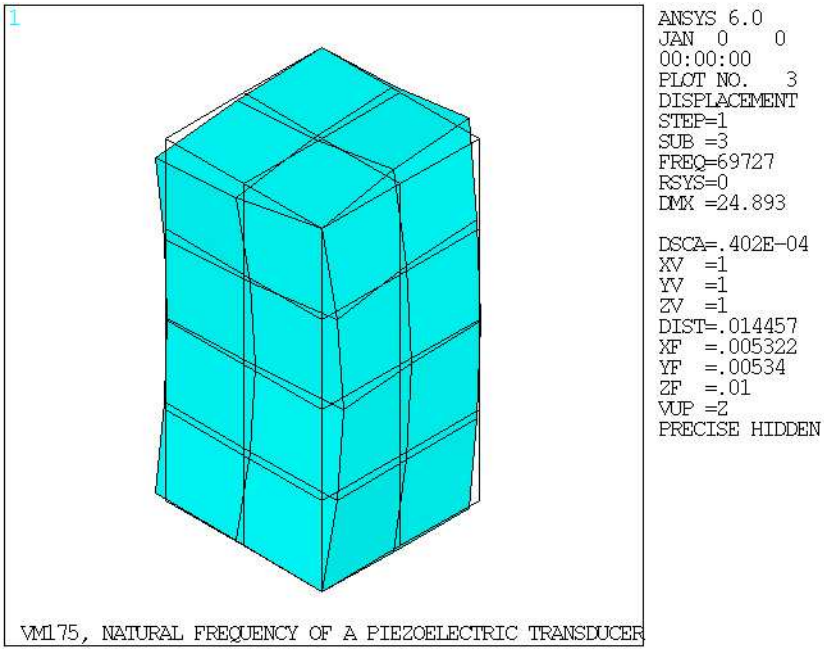

Figure 175.3 Short Circuit Case, Plot 6: Second Breathing Mode

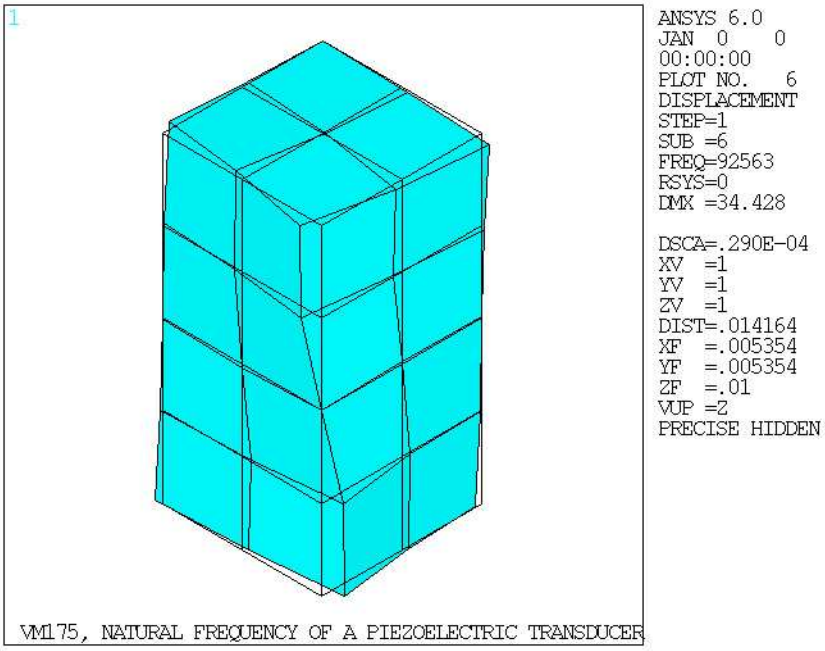

Figure 175.4 Open Circuit Case, Plot 15: First Breathing Mode

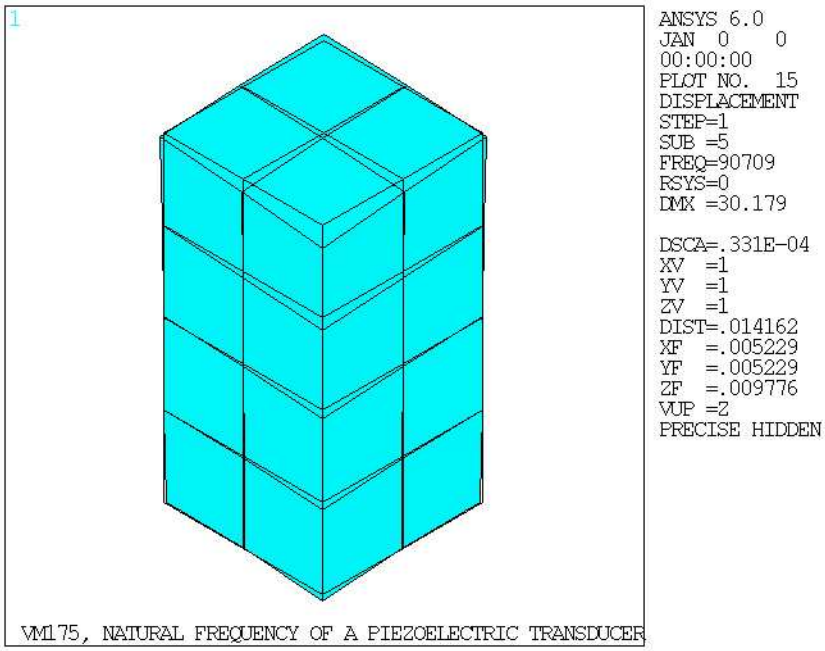

Figure 175.5 Open Circuit Case, Plot 19: Second Breathing Mode

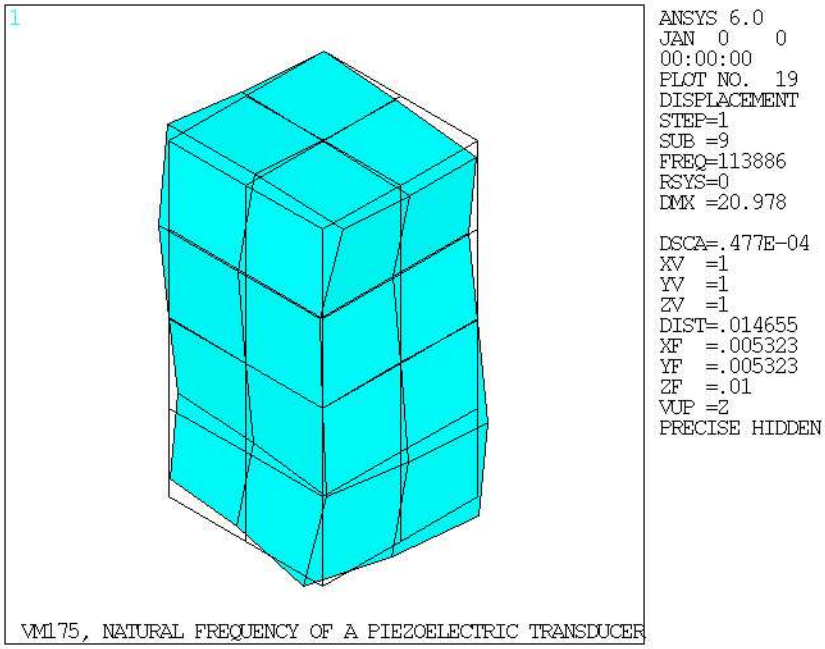

VM176: Frequency Response of Electrical Input Admittance

Overview

Reference:	Y. Kagawa, T. Yamabuchi, "Finite Element Simulation of a Composite Piezoelectric Ultrasonic Transducer", *IEEE Trans. Sonics and Ultrasonics*, Vol. SU-2 No. 2, 1979, pg. 81.
Analysis Type(s):	Full Harmonic Response Analysis (**ANTYPE** = 3)
Element Type(s):	3-D Coupled-Field Solid Elements (SOLID5)
Input Listing:	vm176.dat

Test Case

A composite piezoelectric transducer is made of a piezoceramic (NEPEC 6), aluminum, and an adhesive layer. Electrical terminals are attached to electroded surfaces of the piezoceramic where a potential V is applied. Determine the terminal input admittance Y over a frequency range spanning the first natural frequency.

Figure 176.1 Piezoelectric Transducer Problem Sketch

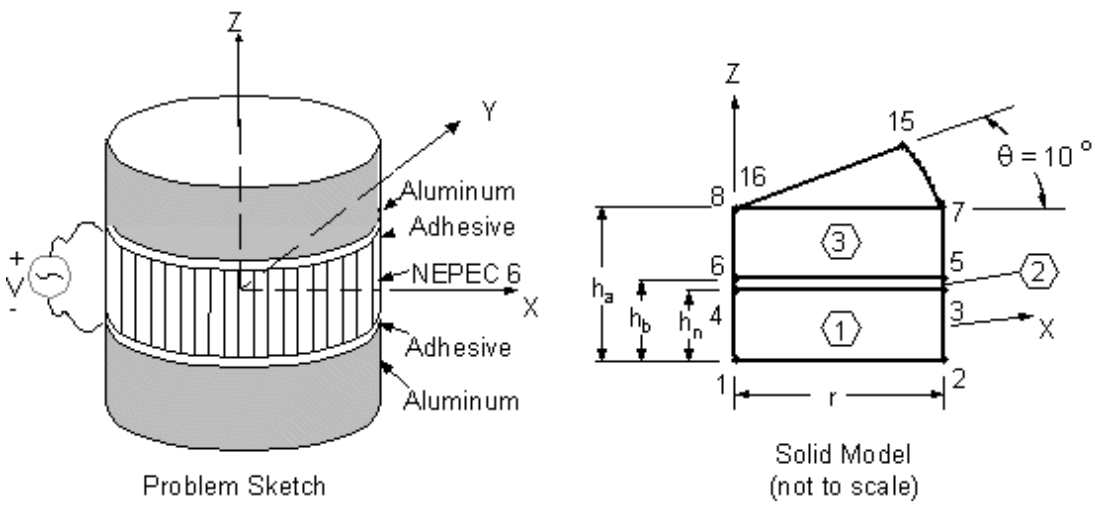

Material Properties	Geometric Properties
For aluminum: $E = 7.03 \times 10^{10}$ N/m $\rho = 2690$ kg/m^3 $\upsilon = 0.345$ **For adhesive:** $E = 10 \times 10^{9}$ N/m^2 $\rho = 1700$ kg/m^3 $\upsilon = 0.38$ **For NEPEC 6:** See Constitutive Matrices	$h_a = 15.275 \times 10^{-3}$ m $h_n = 5 \times 10^{-3}$ m $h_b = 5.275 \times 10^{-3}$ m $r = 27.5 \times 10^{-3}$ m **Loading** V = 1 volt

Constitutive Matrices

NEPEC 6 "Stiffness" Matrix [c] x 10^{-10} N/m^2

$$\begin{bmatrix} 12.8 & 6.8 & 6.6 & 0 & 0 & 0 \\ & 12.8 & 6.6 & 0 & 0 & 0 \\ & & 11.0 & 0 & 0 & 0 \\ & & & 2.1 & 0 & 0 \\ & \text{Symmetric} & & & 2.1 & 0 \\ & & & & & 2.1 \end{bmatrix}$$

NEPEC 6 Piezoelectric Matrix [e] C/m^2

$$\begin{bmatrix} 0 & 0 & -6.1 \\ 0 & 0 & -6.1 \\ 0 & 0 & 15.7 \\ 0 & 0 & 0 \\ 0 & 0 & 0 \\ 0 & 0 & 0 \end{bmatrix}$$

NEPEC 6 Dielectric Matrix [ε_r]

$$\begin{bmatrix} 993.55 & 0 & 0 \\ 0 & 993.55 & 0 \\ 0 & 0 & 993.55 \end{bmatrix}$$

Analysis Assumptions and Modeling Notes

The transducer has circumferential symmetry and is symmetric about the midplane, so the model is reduced to a single wedge of elements with an additional symmetry plane at z = 0. No internal losses (damping) are assumed. The top surface of the piezoceramic is electroded, resulting in an equipotential surface. The nodes modeling the surface have their voltage DOF coupled so that the applied potential load can be conveniently placed on a single node. The 1 volt potential load translates into a 0.5 volt potential gradient across the piezoceramic for the 1/2 symmetry model.

The TEMP and MAG degrees of freedom of SOLID5 are not used in this analysis.

Admittance Y is calculated as I/V where I is the current and V is the applied potential. The current I is related to the accumulated charge on the electrode surface as $I = j\omega\sigma Q_i$, where ω is the operating frequency, j is $\sqrt{1}$ and ΣQ_i is the summed nodal charge (nodal reaction load). Since the nodal potentials are coupled, only the reaction "load" from the single node where the voltage is applied is required for the calculation. A series of calculations are made between 20 kHz and 54 kHz in POST26, which span the first natural frequency ($\approx$ 44 kHz).

Results Comparison

	Target[1]	ANSYS[2]	Ratio
Y, mmhos @ 20kHz	.41	.43	1.047
Y, mmhos @ 35kHz	.90	.96	1.063
Y, mmhos @ 42kHz	2.0	2.8	1.400
Y, mmhos @ 45kHz	-	-1.74	-
Y, mmhos @ 50kHz	.39	.32	0.833

	Target[1]	ANSYS[2]	Ratio
Y, mmhos @ 54kHz	.65	.63	0.962

1. The experimentally measured values are presented in graphical form in the reference. The results tabulated here are obtained from interpolation of the graphical data.
2. Displayed graphically in Figure 176.2: “Electrical Input Admittance vs. Frequency”.

Figure 176.2 Electrical Input Admittance vs. Frequency

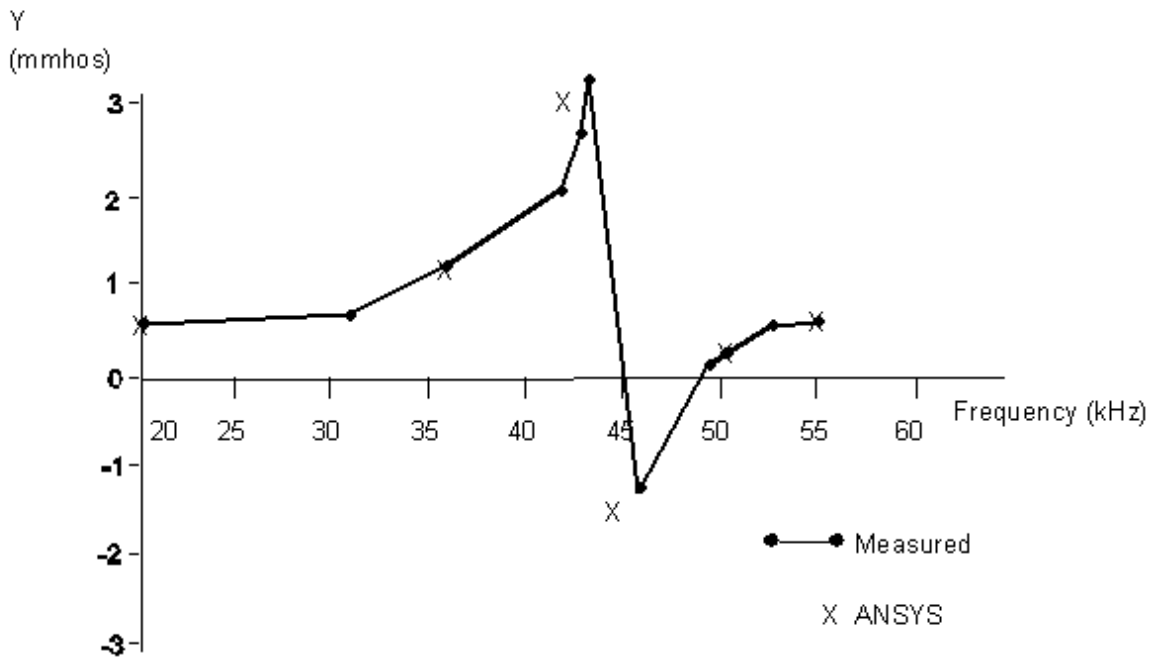

VM177: Natural Frequency of a Submerged Ring

Overview

Reference:	E. A. Schroeder, M. S. Marcus, "Finite Element Solution of Fluid Structure Interaction Problems", Shock and Vibration Symposium, San Diego, CA, 1975.
Analysis Type(s):	Full Harmonic Analysis (**ANTYPE** = 3) Unsymmetric Matrix Modal Analysis (**ANTYPE** = 2)
Element Type(s):	3-D Acoustic Fluid Elements (FLUID30) Elastic Shell Elements (SHELL63) 2-D Acoustic Fluid Elements (FLUID29) 2-D Elastic Beam Elements (BEAM3)
Input Listing:	vm177.dat

Test Case

A steel ring is submerged in a compressible fluid (water). Determine the lowest natural frequency for x-y plane bending modes of the fluid-structure system.

Figure 177.1 Submerged Ring Problem Sketch

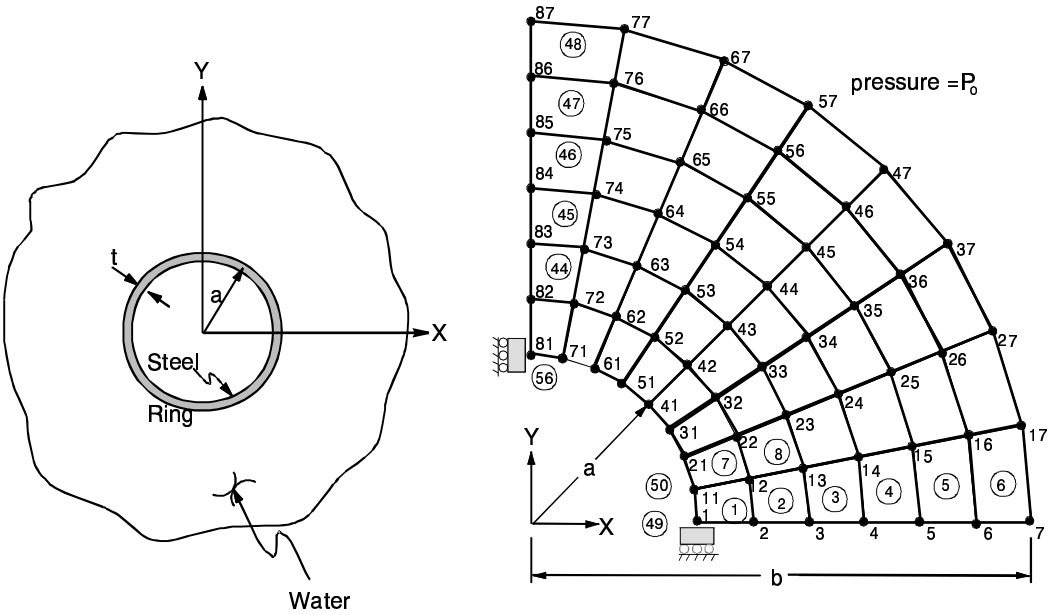

Problem Sketch

Representative Finite Element Model
(Using FLUID30 and SHELL63, with lower plane nodes shown for clarity, and using FLUID29 and BEAM3 as a 2-D model.)

Material Properties	Geometric Properties
For steel: $E = 30 \times 10^6$ psi $\upsilon = 0.3$ $\rho = 7.4167 \times 10^{-4}$ lb-sec^2/in^4 **For water:** C = 57480 in/sec (speed of sound in water) $\rho = 9.6333 \times 10^{-5}$ lb-sec^2/in^4	a = 10 in b = 30 in t = .25 in

Analysis Assumptions and Modeling Notes

For this problem, the fluid is assumed as extending only to a finite radius b where the pressure P_o is zero and b is taken to be 30 inches. From the reference, this assumption should result in an error of less than 1% compared to the frequency for an unbounded fluid ($b = \infty$). The natural boundary conditions at the coordinate axes imply that $\delta P / \delta x = 0$ at $x = 0$ and $\delta P / \delta y = 0$ at $y = 0$.

This problem is solved using two separate analyses. The first, using 3-D acoustic fluid elements (FLUID30) with quadrilateral shell elements (SHELL63), and the second, using 2-D acoustic fluid elements (FLUID29) with 2-D elastic beam elements (BEAM3).

In the first case, due to fluid-structure coupling involving unsymmetric matrices, the natural frequency is determined by performing a full harmonic (**ANTYPE** = 3) analysis with a frequency sweep. Monitoring the displacement of several key nodes (nodes 1, 41 and, 81) over the frequency range indicates the approximate desired natural frequency as the point where the nodal displacements indicate a resonant condition.

In the second case, the lowest natural frequency is obtained using an unsymmetric matrix modal analysis (**ANTYPE** = 2) corresponding to the frequency of mode one of the frequency data from the Lanczos unsymmetric eigensolver.

A preliminary finite element analysis (not shown here) was used to estimate a narrow range in which the 1st even bending mode frequency occurs. In the first case, two unit loads at nodes 1 and 81 are arbitrarily used to excite the desired bending mode of vibration.

Results Comparison

		Target[1]	ANSYS	Ratio
FLUID30 and SHELL63	f_1, Hz	35.62	$36.61 < f < 36.62$	1.028
FLUID29 and BEAM3	f_1, Hz	35.62	36.54	1.026

1. Solution from the reference under the same assumptions mentioned in the modeling notes.

ANSYS Verification Manual . ANSYS Release 10.0 . 002184 . © SAS IP, Inc.

Figure 177.2 Node 1 Displacement vs. Driving Frequency Near 1st Bending Mode Natural Frequency (Full Harmonic Analysis)

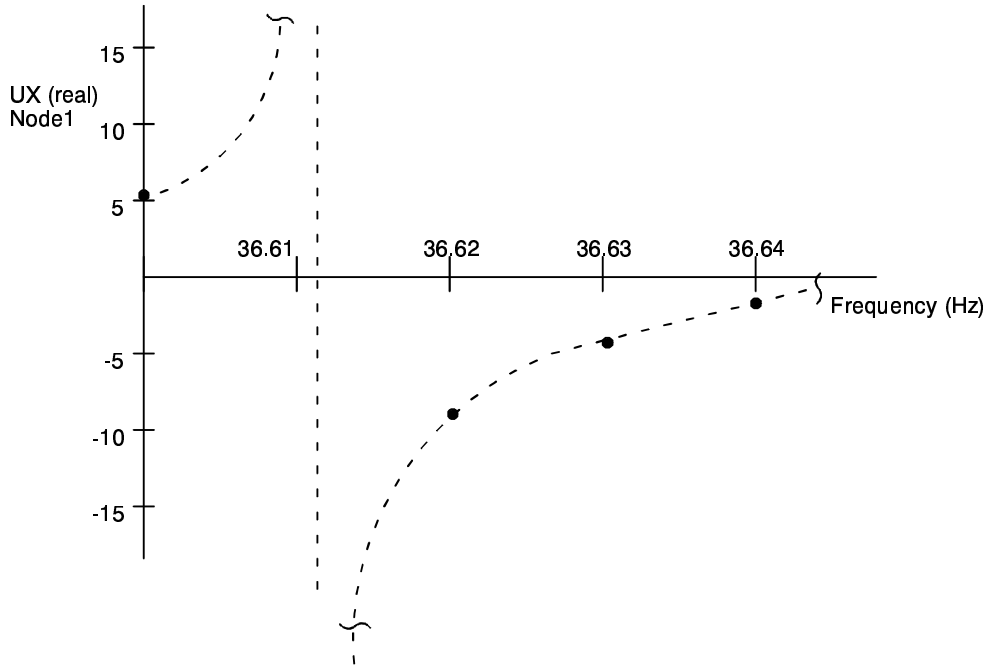

Figure 177.3 Real Displacement Component

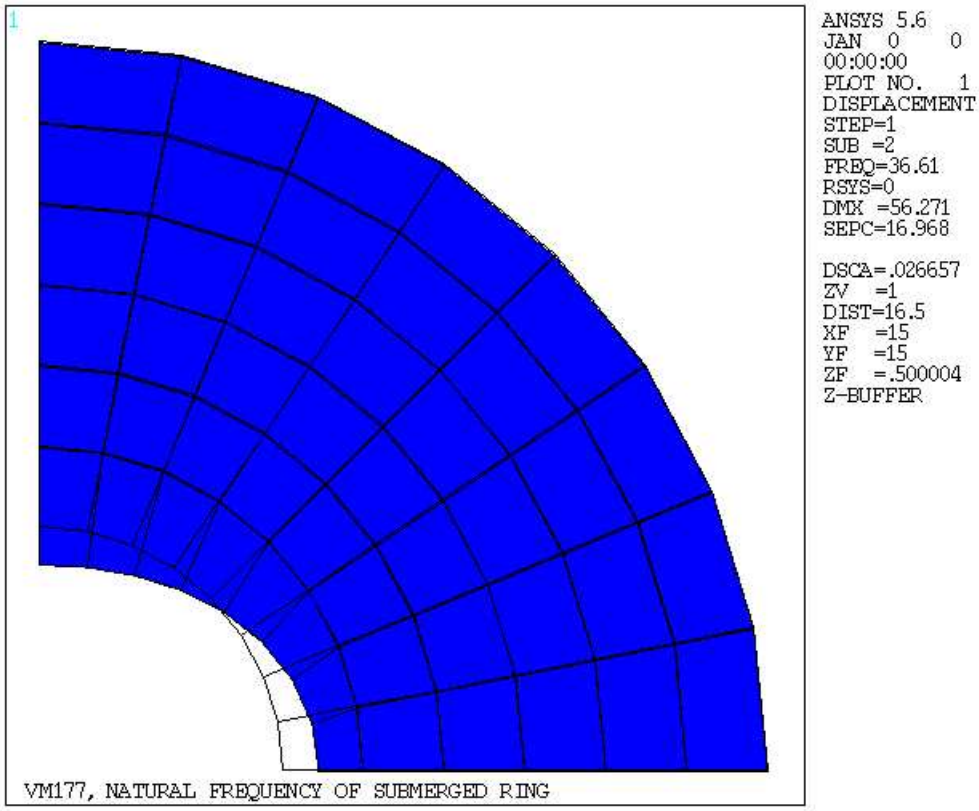

Figure 177.4 Real Displacement Component

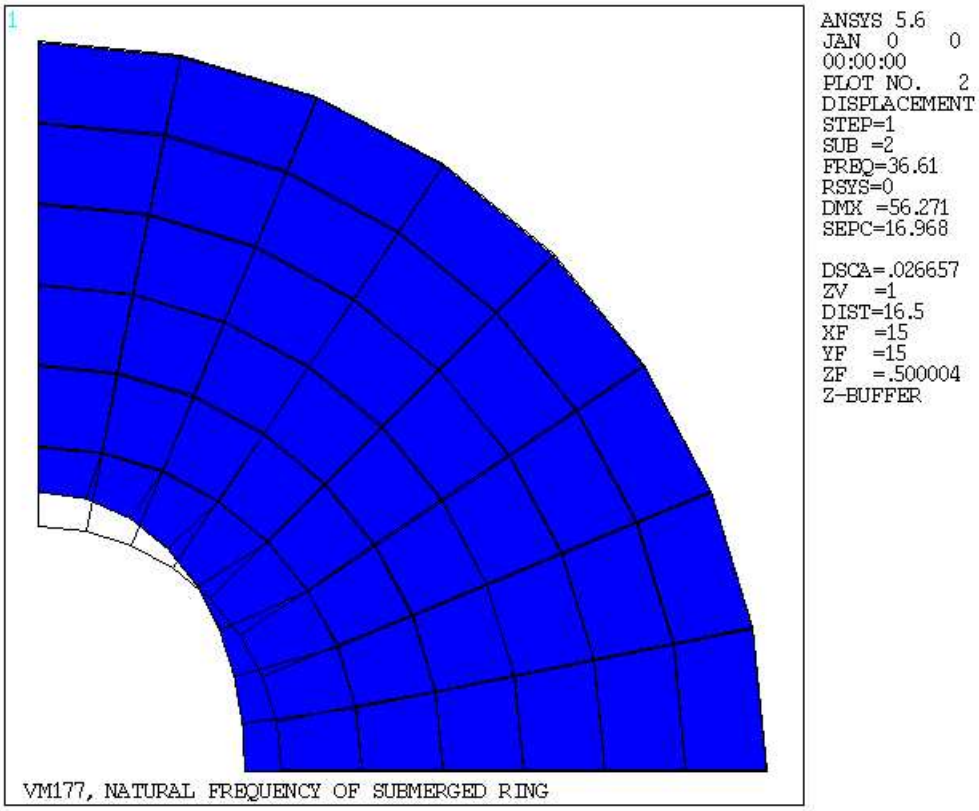

VM178: Plane Poiseuille Flow

Overview

Reference:	S. W. Yuan, *Foundations of Fluid Mechanics*, Prentice-Hall of India Private Limited, 1976, sec. 8.36.
Analysis Type(s):	Thermal, Flow Analysis (**FLOTRAN**)
Element Type(s):	2-D Fluid-Thermal Elements (FLUID141)
Input Listing:	vm178.dat

Test Case

A pressure differential is applied across a wide channel of length L and height H. The channel is filled with an incompressible fluid of density ρ, viscosity μ, thermal conductivity k, and specific heat at constant pressure C_p. Determine the steady-state velocity distribution V_x as a function of channel height.

Figure 178.1 Plane Poiseuille Flow Problem Sketch

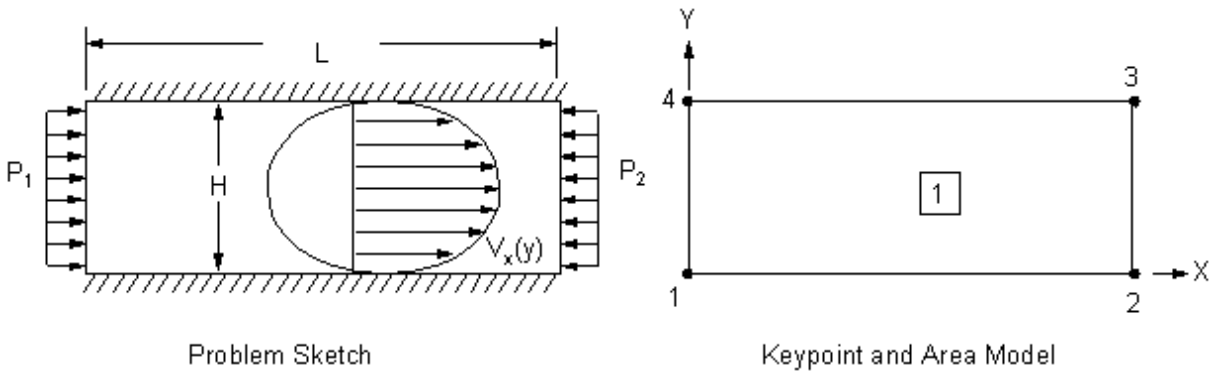

Material Properties	**Geometric Properties**	**Loading**
k = 1 Btu/in-sec-°F ρ = 1.0 lb-sec^2/in^4 C_p = 1.0 Btu in/lb-sec^2-°F α = 1.0 in/in-°F μ = 1.0 lb-sec/in^2	H = 2 in L = 10 in	P_1 = 0.1 psig P_2 = 0.0 psig

Analysis Assumptions and Modeling Notes

Zero velocity gradient in the z-direction is assumed so that a two-dimensional model is adequate. No-slip boundary conditions are applied along the channel walls (VX = VY = 0). The area is discretized with 8 elements along the length L and 6 elements across the thickness H.

Results Comparison

V_x , in/sec	Target	ANSYS	Ratio
@ y = 1.0 in	0.0050	0.0050	1.000
@ y = 1.33 in	0.0044	0.0044	1.01
@ y = 1.67 in	0.0028	0.0028	0.992

Figure 178.2 Velocity Vector Display

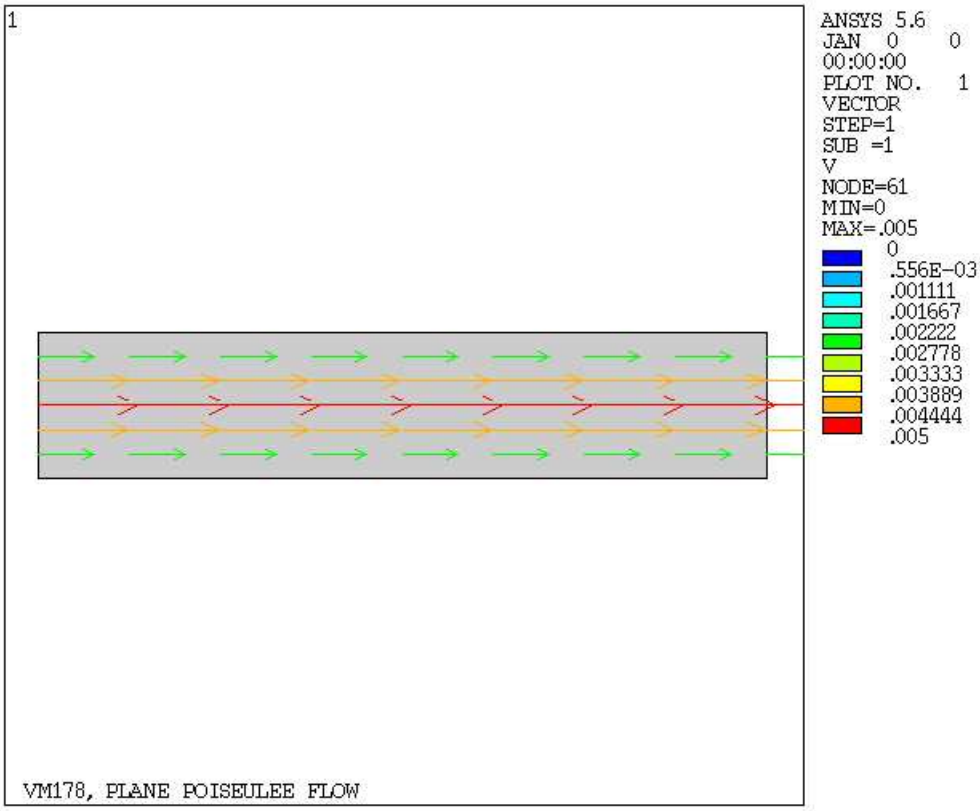

Figure 178.3 Velocity Profile Across Channel

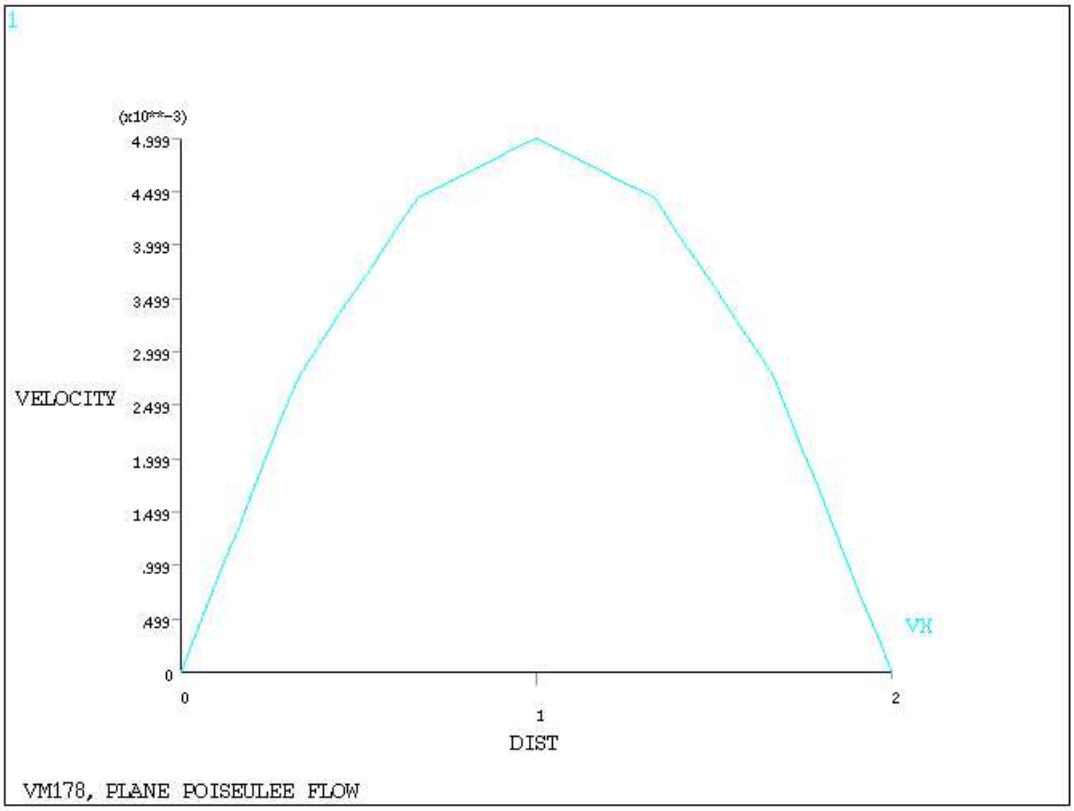

VM179: Dynamic Double Rotation of a Jointed Beam

Overview

Reference:	Any basic mechanics text
Analysis Type(s):	Full Transient Dynamic Analysis (**ANTYPE** = 4)
Element Type(s):	Revolute Joint Elements (COMBIN7) 3-D Elastic Beam Elements (BEAM4)
Input Listing:	vm179.dat

Test Case

A torque M_1 is applied at the pinned end of an aluminum beam to cause a 90° rotation. A second torque M_2 is then applied at a revolute joint in the beam to create an out-of-plane rotation. The joint has a rotational stiffness k, inertial mass J, frictional torque T_f, and locks when a 5° rotation occurs. Determine the position of the beam at the end of each rotation.

Figure 179.1 Jointed Beam Problem Sketch

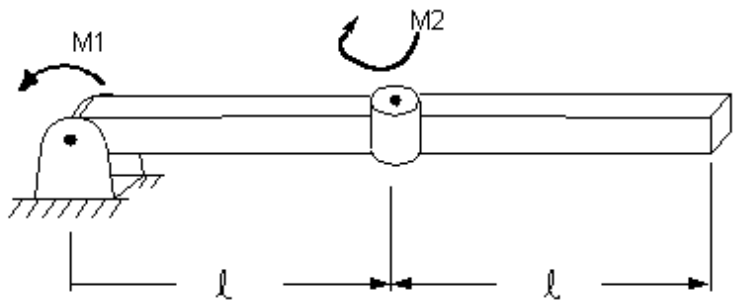

Problem Sketch

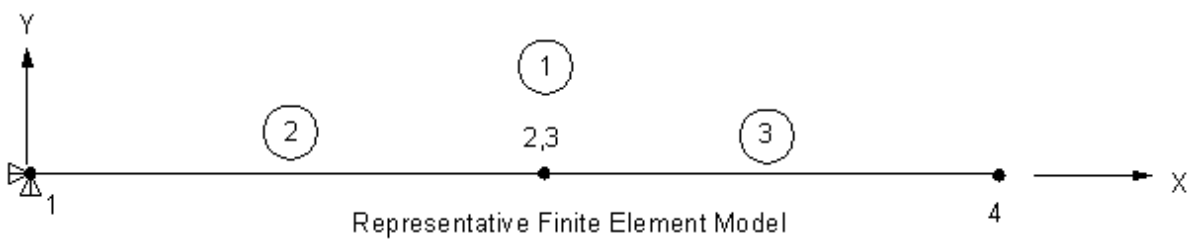

Representative Finite Element Model

Material Properties	**Geometric Properties**
$k = 10^6$ N-m/rad $J = 0.5$ N-m-sec^2/rad $T_f = 0.05$ N-m $E = 70 \times 10^9$ N-m $\rho = 1 \times 10^{-6}$ kg/m^3 $\upsilon = 0.35$	STOPU = 5° = 0.08727 rad STOPU is the COMBIN7 real constant name ℓ = 1 m **Loading** $M_1 = 0.7854$ N-m $M_2 = 0.5$ N-m

Analysis Assumptions and Modeling Notes

Since step changes in acceleration occur due to the applied step loads, load steps with small time periods are used to “ramp” the accelerations to peak values while maintaining essentially no movement in the beams. The

applied moments allow the beam to come to rest in the vertical position. A restart is included to demonstrate and test this program feature.

Results Comparison

	Target	ANSYS	Ratio
$Deflection_x$, in (t = 1.0)	-0.5858	-0.5749	0.981
$Deflection_y$, in (t = 1.0)	1.4142	1.4032	0.992
$Angle_2$, rad (t = 1.0)	0.7854	0.7777	0.990
$Deflection_x$, in (t = 2.0)	-2.000	-2.000	1.000
$Deflection_y$, in (t = 2.0)	2.000	2.000	1.000
$Angle_2$, rad (t = 2.0)	1.5708	1.5707	1.000
$Deflection_x$, in (t = 3.0)	-2.000	-2.000	1.000
$Deflection_y$, in (t = 3.0)	1.9962	1.9962	1.000
$Deflection_z$, in (t = 3.0)	0.08716	0.08712	1.000
$Angle_x$, rad (t = 3.0)	0.08727	0.08723	1.000
$Angle_2$, rad (t = 3.0)	1.5708	1.5779	1.005

VM180: Bending of a Curved Beam

Overview

Reference:	S. Timoshenko, J. N. Goodier, *Theory of Elasticity*, 3rd Edition, McGraw-Hill Book Co. Inc., New York, NY, 1970, pg. 73, article 29.
Analysis Type(s):	Static Analysis (**ANTYPE** = 0)
Element Type(s):	2-D 6-Node Triangular Structural Solid Elements (PLANE2) 2-D Elastic Beam Elements (BEAM3)
Input Listing:	vm180.dat

Test Case

A curved beam spans a 90° arc as shown. The bottom end is supported while the top end is free. For a bending moment M applied at the top end, determine the maximum tensile stress σ_t and the maximum compressive stress σ_c in the beam.

Figure 180.1 Curved Beam Problem Sketch

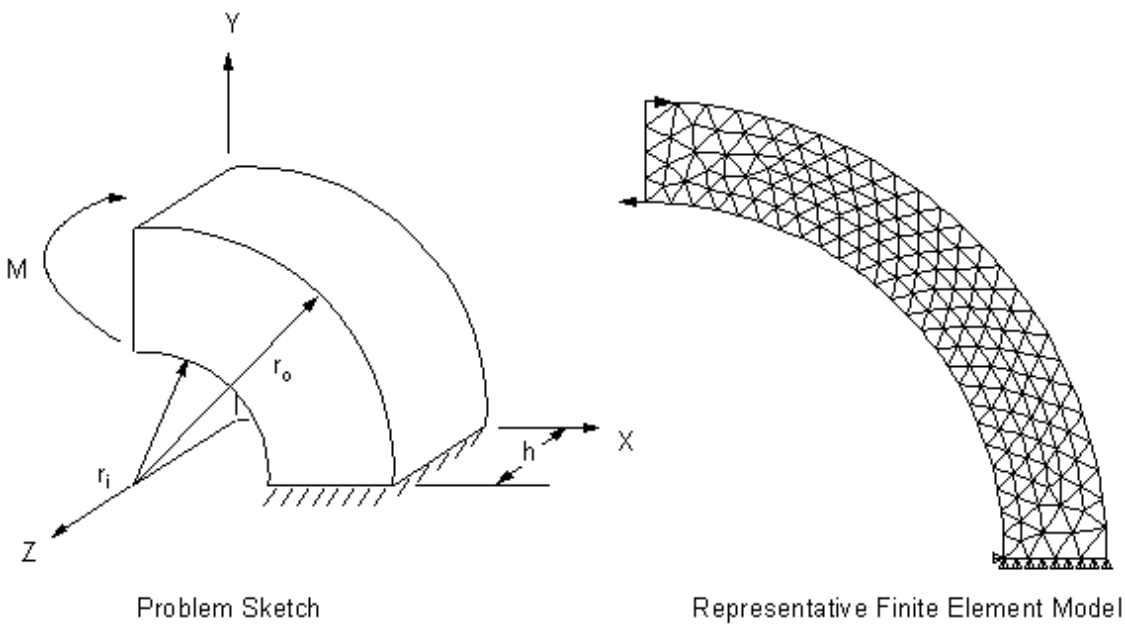

Material Properties	Geometric Properties	Loading
E = 30 x 10^6 psi υ = 0.0	r_i = 3.5 in r_o = 4.5 in h = 1.0 in	M = 100 in-lb

Analysis Assumptions and Modeling Notes

Beam elements with arbitrary properties are included at the free end of the curved beam for uniform transmission of the applied forces. This creates a pure bending situation except for the nodes at the free end at which stresses are ignored. POST1 is used to obtain the desired stress results.

Results Comparison

	Target	ANSYS	Ratio
$Stress_t$, psi	655.0	657.4	1.004
$Stress_c$, psi	-555.0	-556.6	1.003

VM181: Natural Frequency of a Flat Circular Plate

Overview

Reference:	R. D. Blevins, *Formulas for Natural Frequency and Mode Shape*, Van Nostrand Reinhold Co., New York, NY, 1979, pg. 241, no. 3.
Analysis Type(s):	Mode-frequency Analysis (**ANTYPE** = 2)
Element Type(s):	2-D 6-Node Triangular Structural Solid Elements (PLANE2)
Input Listing:	vm181.dat

Test Case

A circular plate with a clamped edge is allowed to vibrate freely. Determine the natural frequencies $f_{i,j}$ for the first three modes of vibration (j = 0, 1, 2) for the first harmonic (i = 0).

Figure 181.1 Flat Circular Plate Problem Sketch

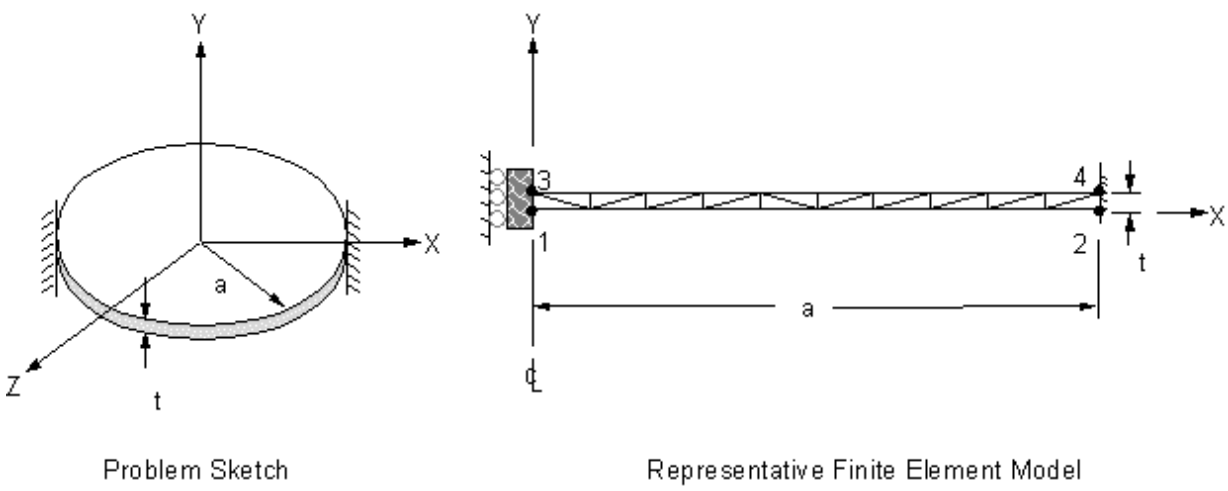

Material Properties	Geometric Properties
E = 30 x 10^6 psi υ = 0.3 ρ = .00073 lb-sec^2/in^4	t = 0.5 in a = 17 in

Analysis Assumptions and Modeling Notes

Poisson's ratio defaults to 0.3 and is not defined with the input data. Nine master degrees of freedom are requested for automatic selection with the **TOTAL** command.

Results Comparison

	Target	ANSYS	Ratio
$f_{0,0}$, Hz	172.64	172.42	.999
$f_{0,1}$, Hz	671.79	674.19	1.004
$f_{0,2}$, Hz	1505.07	1520.97	1.010

VM182: Transient Response of a Spring-mass System

Overview

Reference:	R. K. Vierck, *Vibration Analysis*, 2nd Edition, Harper & Row Publishers, New York, NY, 1979, sec. 5-8.
Analysis Type(s):	Mode-frequency Analysis (**ANTYPE** = 2) Transient Dynamic Mode Superposition Analysis (**ANTYPE** = 4)
Element Type(s):	Combination Elements (COMBIN40)
Input Listing:	vm182.dat

Test Case

A system containing two masses, m_1 and m_2, and two springs of stiffness k_1 and k_2 is subjected to a pulse load F(t) on mass 1. Determine the displacement response of the system for the load history shown.

Figure 182.1 Spring-mass System Problem Sketch

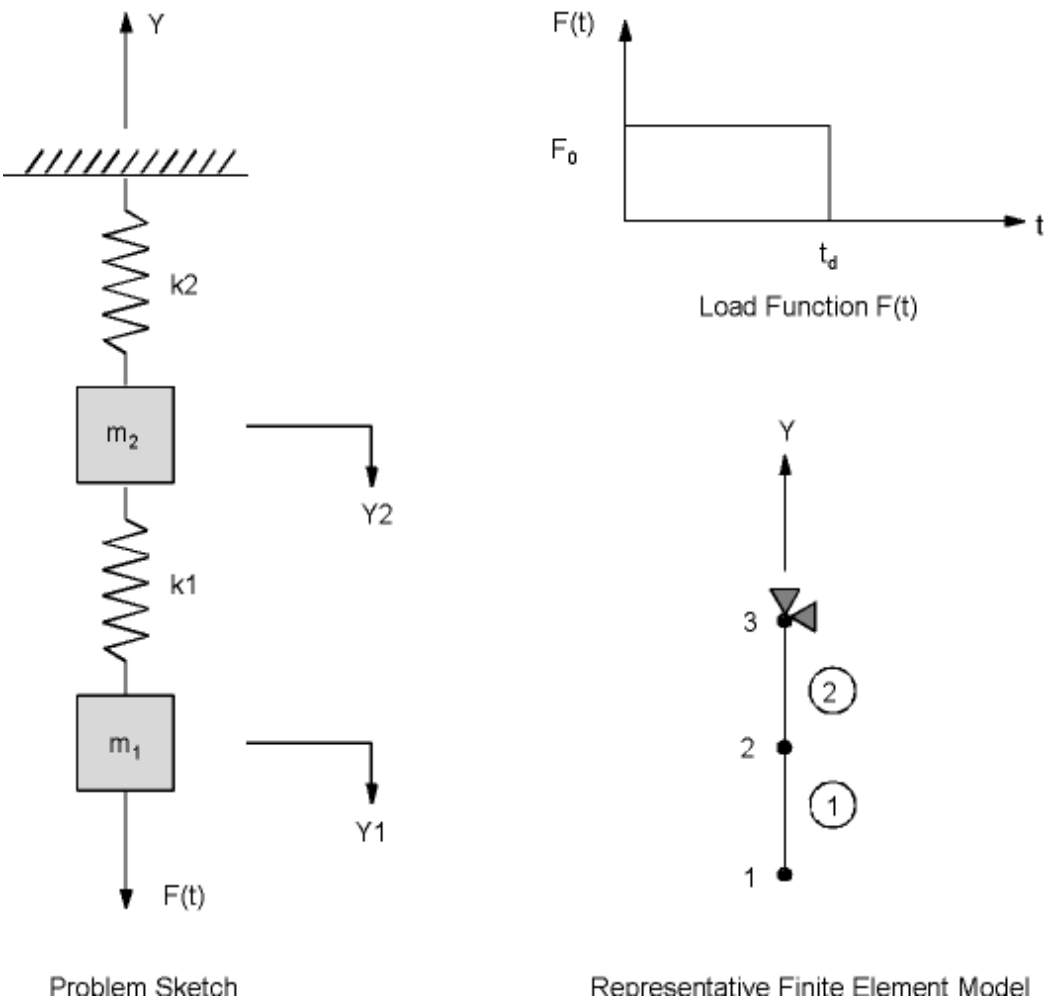

Material Properties	Loading
k_1 = 6 N/m k_2 = 16 N/m m_1 = 2 Kg m_2 = 2 Kg	F_0 = 50 N t_d = 1.8 sec

Analysis Assumptions and Modeling Notes

COMBIN40 combination elements are used to represent the springs and masses. Node locations are arbitrary. The response of the system is examined for an additional 0.6 seconds after the load is removed.

Results Comparison

	Target	ANSYS	Ratio
Y_1 , m (@ t = 1.3s)	14.48	14.40	0.995
Y_2 , m (@ t = 1.3s)	3.99	3.95	0.990
Y_1 , m (@ t = 2.4s)	18.32	18.40	1.004
Y_2 , m (@ t = 2.4s)	6.14	6.16	1.003

Figure 182.2 POST26 Displacement Display

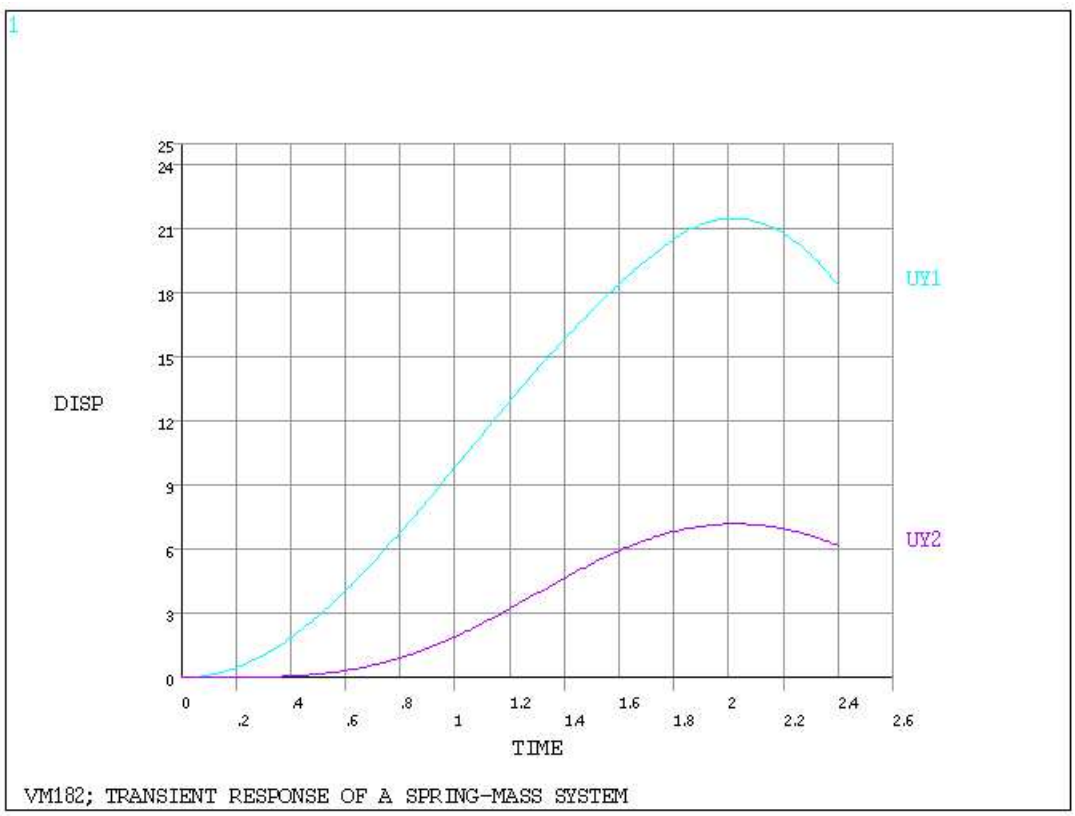

VM183: Harmonic Response of a Spring-mass System

Overview

Reference:	R. K. Vierck, *Vibration Analysis*, 2nd Edition, Harper & Row Publishers, New York, NY, 1979, sec. 4-2.
Analysis Type(s):	Mode-frequency Analysis (**ANTYPE** = 2) Harmonic Response Mode Superposition Analysis (**ANTYPE** = 3)
Element Type(s):	Combination Elements (COMBIN40)
Input Listing:	vm183.dat

Test Case

Determine the natural frequencies of the spring-mass system shown and the displacement response when excited by a harmonic load of variable frequency from 0.1 to 1.0 Hz, with an amplitude of F_o.

Figure 183.1 Spring-mass System Problem Sketch

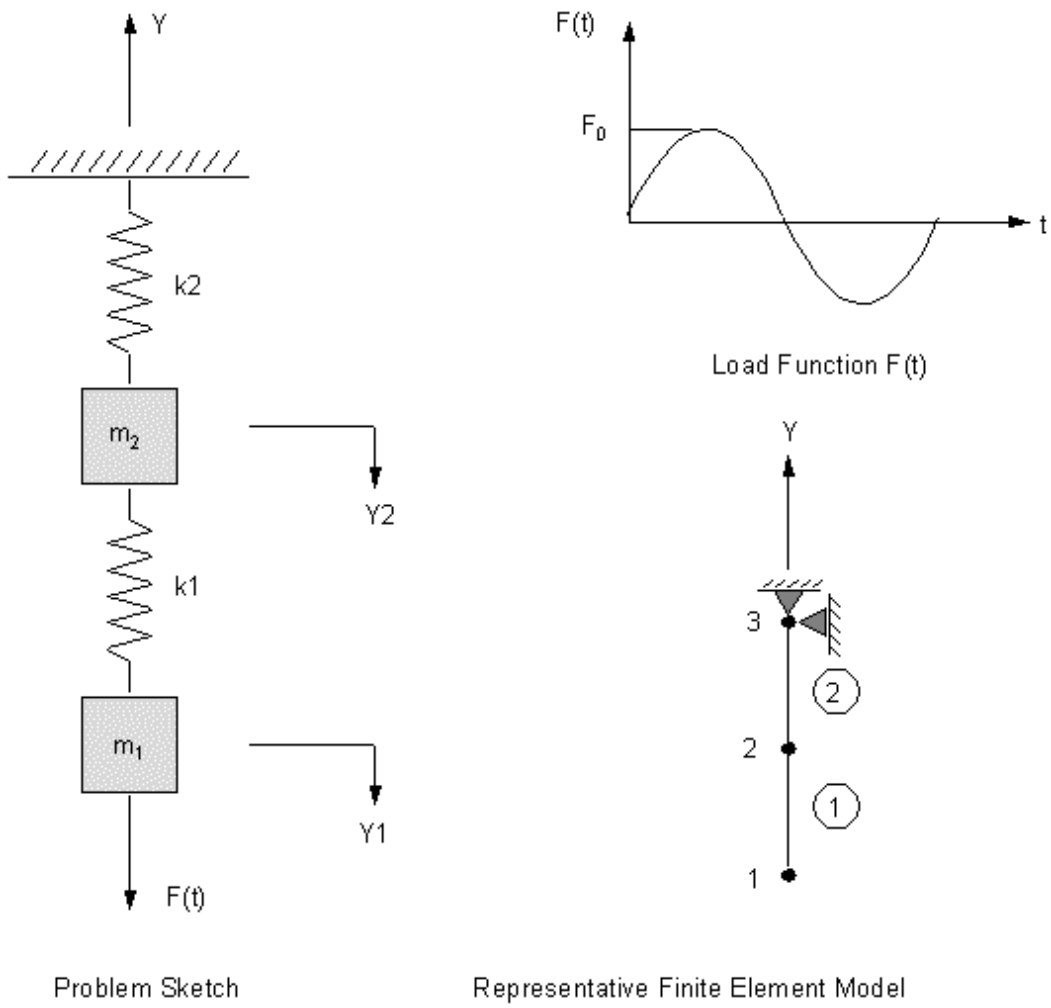

Material Properties	Loading
k_1 = 6 N/m k_2 = 16 N/m $m_1 = m_2$ = 2 kg	F_o = 50 N

Analysis Assumptions and Modeling Notes

COMBIN40 combination elements are used to represent the springs and masses. Node locations are arbitrary.

Results Comparison

	Target	ANSYS	Ratio
Y_1 , m (@ .226 Hz)	-1371.7	-1371.7	1.000
Y_2 , m (@ .226 Hz)	-458.08	-458.08	1.000
Y_1 , m (@ .910 Hz)	-0.8539	-0.8539	1.000
Y_2 , m (@ .910 Hz)	0.1181	0.1181	1.000

Figure 183.2 Displacement vs. Frequency

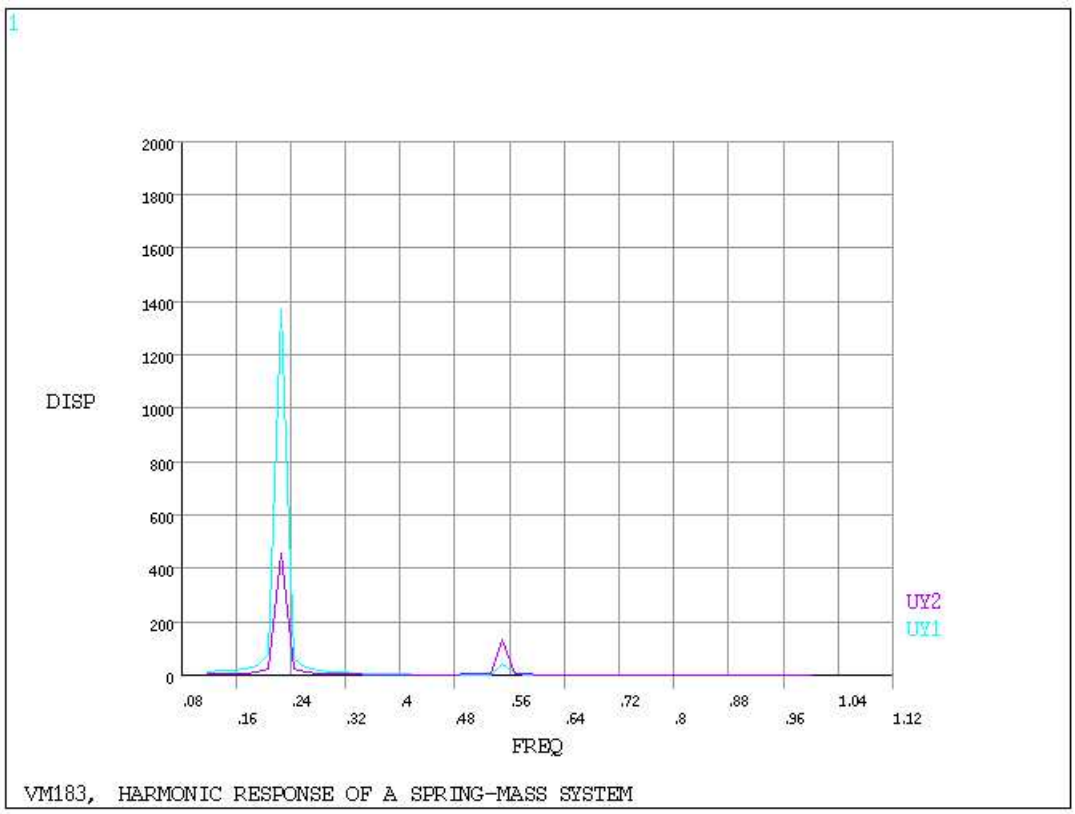

VM184: Straight Cantilever Beam

Overview

Reference:	Any Basic Mechanics of Materials Text
Analysis Type(s):	Static Analysis (**ANTYPE** = 0)
Element Type(s):	3-D Coupled-Field Solid Elements (SOLID5) 3-D 10-Node Tetrahedral Structural Solid Elements (SOLID92) Tetrahedral Coupled-Field Solid Elements (SOLID98) 3-D Brick Structural Solid p-Elements (SOLID147) 3-D 10-Node Tetrahedral Structural Solid Elements (SOLID187)
Input Listing:	vm184.dat

Test Case

A beam of length ℓ, height h, and thickness t is built-in at one end and loaded at the free end with an axial force, an in-plane shear force and an out-of-plane shear force, all of magnitude F. Determine the deflections δ_x, δ_y, and δ_z at the free end due to these loads.

Figure 184.1 Straight Cantilever Beam Problem Sketch

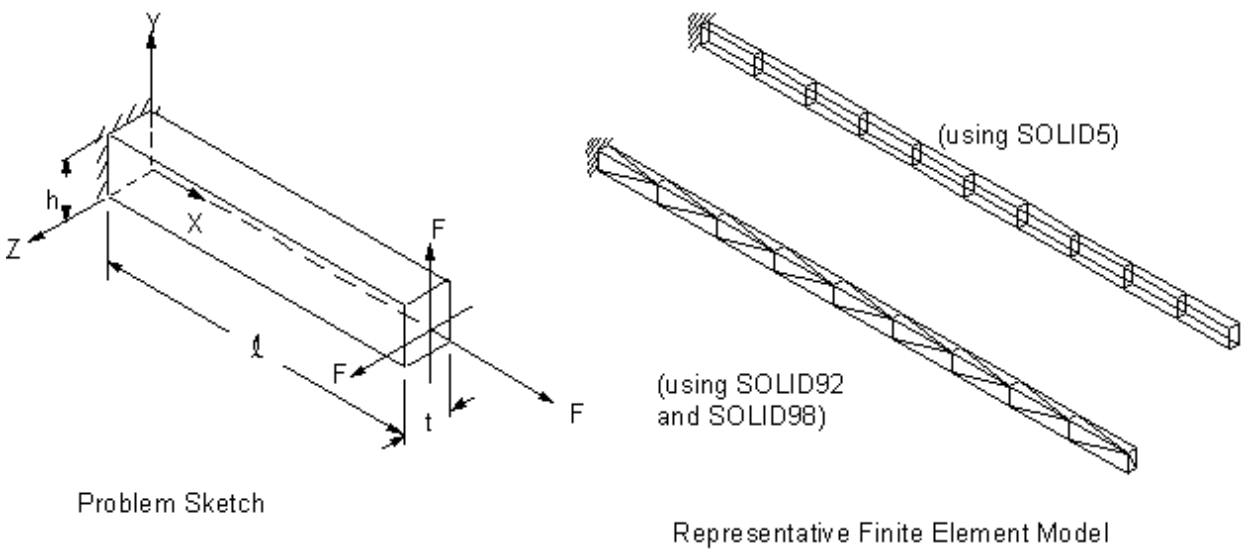

Material Properties	Geometric Properties	Loading
E = 10 x 10^6 psi υ = 0.3	ℓ = 6 in h = 0.2 in t = 0.1 in	F = 1 lb

Analysis Assumptions and Modeling Notes

The problem is solved in five different ways:

- using Coupled-Field Solid Elements (SOLID5)
- using Tetrahedral Solid Elements (SOLID92)
- using Tetrahedral coupled-Field Solid Elements (SOLID98)

- using Brick Structural Solid p-Element (SOLID147)
- using Tetrahedral Solid Elements (SOLID187)

POST1 is used to directly obtain the difference between the theoretical solution and the ANSYS results in the form of a ratio, using the maximum displacement value on the free face.

Results Comparison

		Target	ANSYS	Ratio
SOLID5	$Deflection_x$, in	3.000×10^{-5}	2.9777×10^{-5}	0.993
	$Deflection_y$, in	0.10800	0.10673	0.989
	$Deflection_z$, in	0.43200	0.42554	0.985
SOLID92	$Deflection_x$, in	3.000×10^{-5}	3.000×10^{-5}	0.995
	$Deflection_y$, in	0.108000	0.106757	0.988
	$Deflection_z$, in	0.432000	0.425708	0.985
SOLID98	$Deflection_x$, in	3.000×10^{-5}	3.000×10^{-5}	0.995
	$Deflection_y$, in	0.108000	0.106757	0.988
	$Deflection_z$, in	0.432000	0.425708	0.985
SOLID147	$Deflection_x$, in	3.000×10^{-5}	3.000×10^{-5}	1.011
	$Deflection_y$, in	0.10800	0.106989	0.991
	$Deflection_z$, in	0.43200	0.424641	0.983
SOLID187	$Deflection_x$, in	3.000×10^{-5}	3.000×10^{-5}	0.995
	$Deflection_y$, in	0.10800	0.106757	0.988
	$Deflection_z$, in	0.43200	0.425708	0.985

Figure 184.2 Element Display

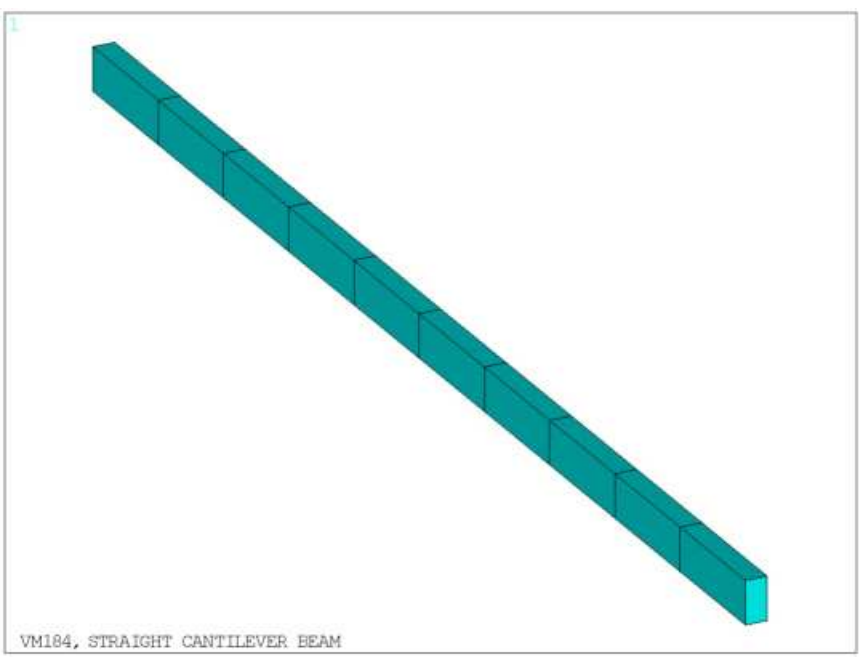

Figure 184.3 Clipped and Capped Display of Stress Contours

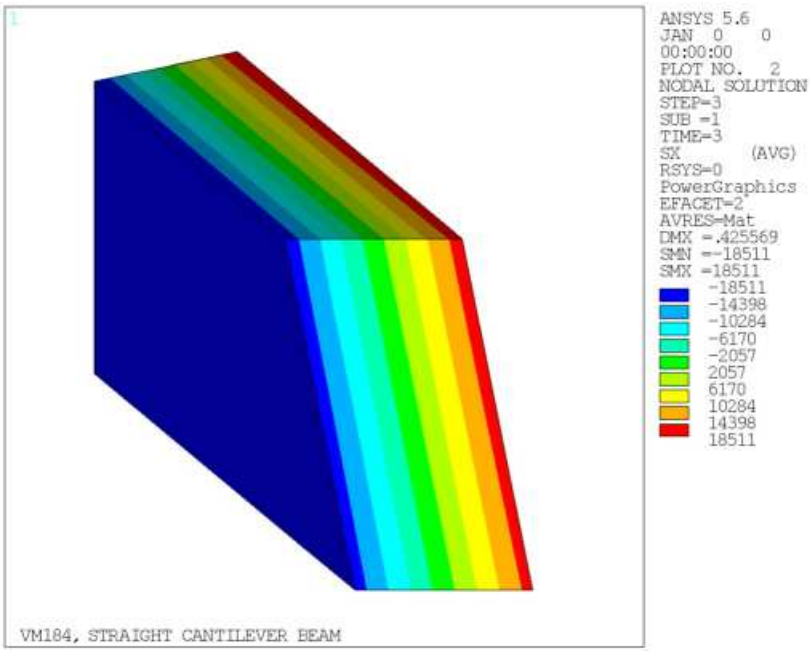

VM185: AC Analysis of a Slot Embedded Conductor

Overview

Reference:	A. Konrad, "Integrodifferential Finite Element Formulation of Two-Dimensional Steady-State Skin Effect Problems", *IEEE Trans. Magnetics*, Vol. MAG-18 No. 1, January 1982, pg. 284-292.
Analysis Type(s):	Coupled-field Analysis (**ANTYPE** = 3)
Element Type(s):	2-D Coupled-Field Solid Elements (PLANE13)
Input Listing:	vm185.dat

Test Case

A solid copper conductor embedded in the slot of an electric machine carries a current I at a frequency ω. Determine the distribution of the current within the conductor, the source current density, the complex impedance of the conductor, and the AC/DC power loss ratio.

Figure 185.1 Slot Embedded Conductor Problem Sketch

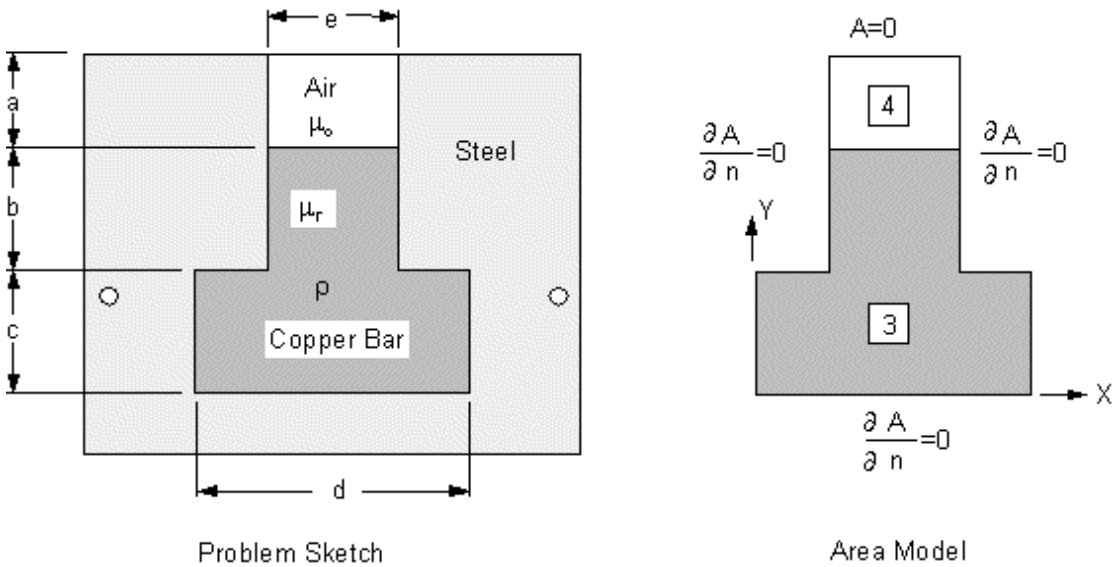

Material Properties	Geometric Properties	Loading
$\mu_o = 4\pi \times 10^{-7}$ H/m	$a = 6.45 \times 10^{-3}$ m	I = 1.0 A
$\mu_r = 1.0$	$b = 8.55 \times 10^{-3}$ m	$\omega = 45$ Hz
$\rho = 1.724 \times 10^{-8}$ ohm-m	$c = 8.45 \times 10^{-3}$ m	
	$d = 18.85 \times 10^{-3}$ m	
	$e = 8.95 \times 10^{-3}$ m	

Analysis Assumptions and Modeling Notes

The slot is assumed to be infinitely long, so end effects are ignored, allowing for a two-dimensional planar analysis. An assumption is made that the steel slot is infinitely permeable and thus is replaced with a flux-normal boundary condition. It is also assumed that the flux is contained within the slot, so a flux-parallel boundary condition is placed along the top of the slot.

The problem requires a coupled electromagnetic field analysis using the VOLT and AZ degrees of freedom. All VOLT DOFs within the copper conductor are coupled together to enforce the correct solution of the source current density component of the total current density. The eddy current component of the total current density is determined from the AZ DOF solution. The current may be applied to a single arbitrary node in the conductor, since they are all coupled together in VOLT.

The complex impedance of the slot is calculated in POST1 from the equation

$$Z = \frac{V}{I} = \frac{\rho J_s^{Re}}{I} + j\frac{\rho J_s^{Im}}{I}$$

where V = voltage drop, J_s^{Re} and J_s^{Im} are real and imaginary components of the source current density (obtained from the solution results in the database file). The real component of the impedance represents the AC resistance R_{ac} per unit length. The DC resistance per unit length R_{dc} is calculated as ρ/A. The AC/DC power loss ratio is calculated as R_{ac}/R_{dc}.

Results Comparison

	Target[1]	ANSYS	Ratio
J_s^{Re}	10183	10123.55	0.994
J_s^{Im}	27328	27337.36	1.000
Impedance (Ohm/m) x 10^6	-	174.7 + j471.3	-
Loss Ratio	2.33t[1]	2.39	1.025

1. Target solution based on graphical estimate.

Figure 185.2 Flux Lines

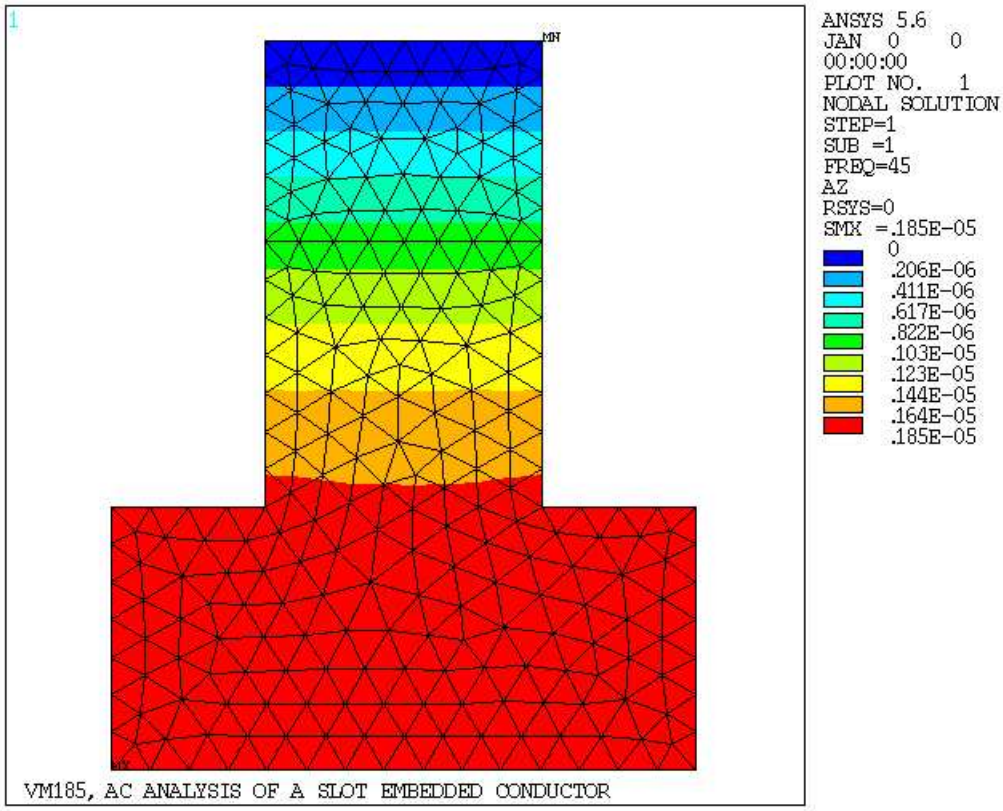

Figure 185.3 Total Current Density

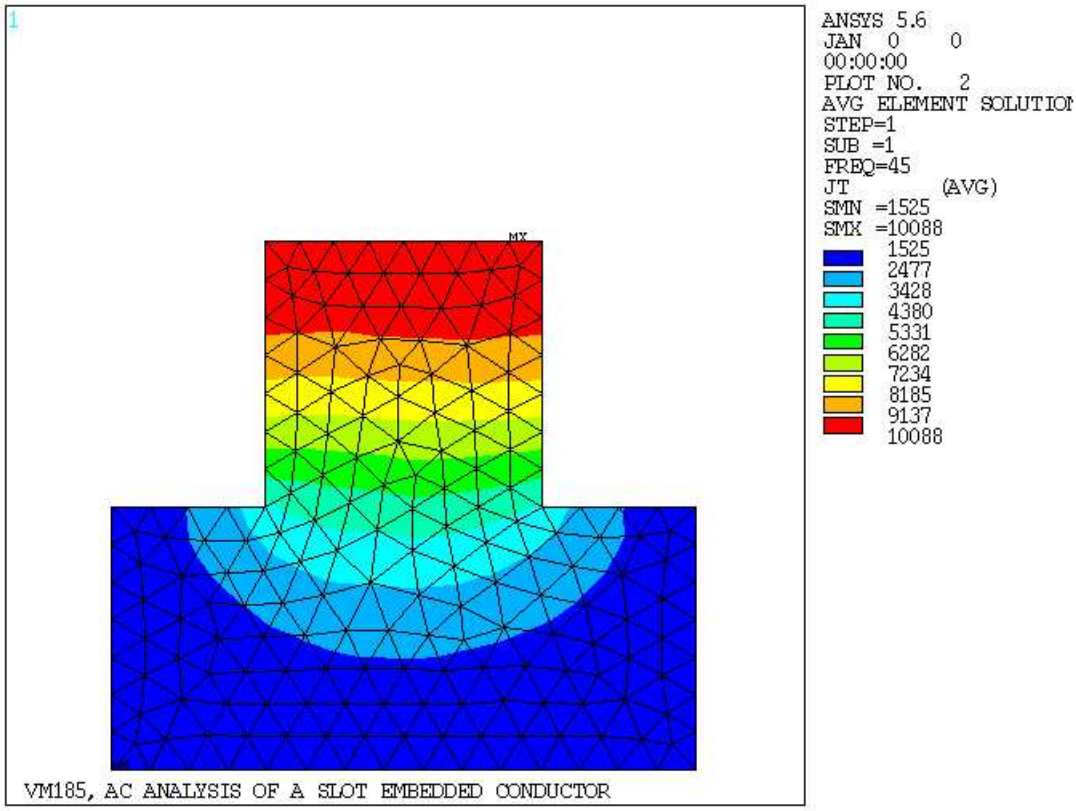

Figure 185.4 Eddy Current Density

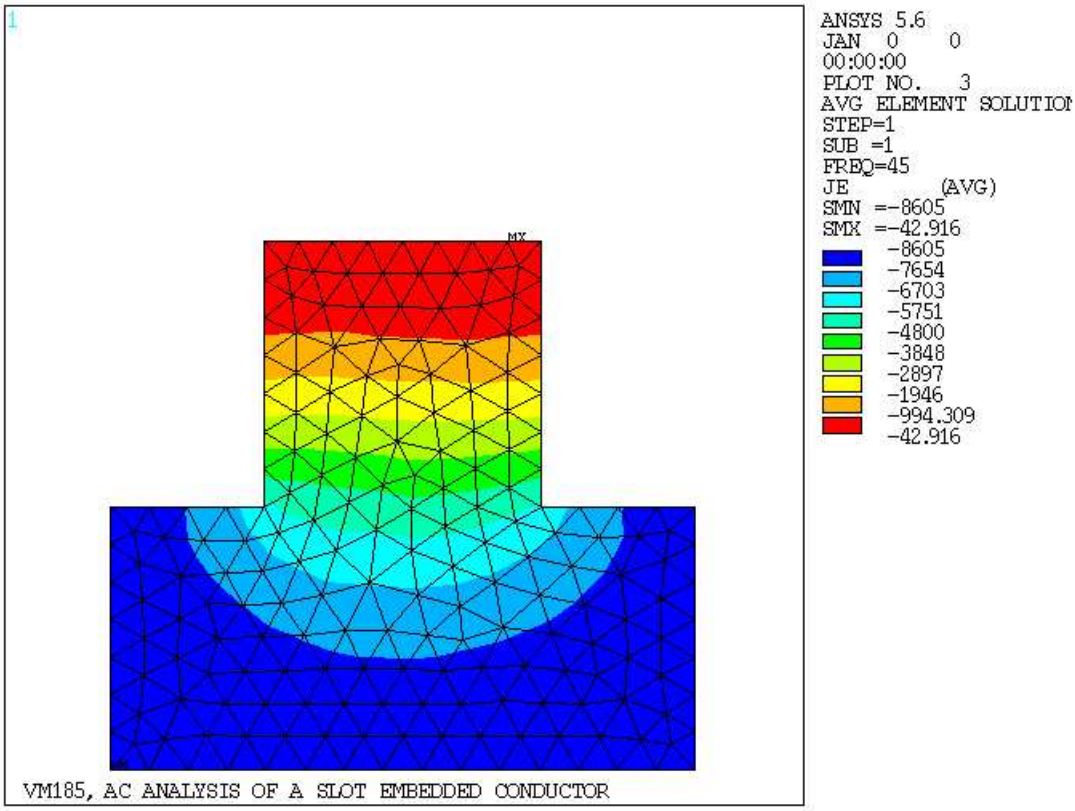

VM186: Transient Analysis of a Slot Embedded Conductor

Overview

Reference:	A. Konrad, "Integrodifferential Finite Element Formulation of Two-Dimensional Steady-State Skin Effect Problems", *IEEE Trans. Magnetics*, Vol. MAG-18 No. 1, January 1982.
Analysis Type(s):	Transient Magnetic Field Analysis (**ANTYPE** = 4)
Element Type(s):	2-D Coupled-Field Solid Elements (PLANE13)
Input Listing:	vm186.dat

Test Case

A solid conductor embedded in the slot of a steel electric machine carries a sinusoidally varying current I. Determine the vector magnetic potential solution after 3/4 and 1 period of the oscillation frequency. In addition, display the time-varying behavior of the total input current, the source current component, and the eddy current component.

Figure 186.1 Slot Embedded Conductor Problem Sketch

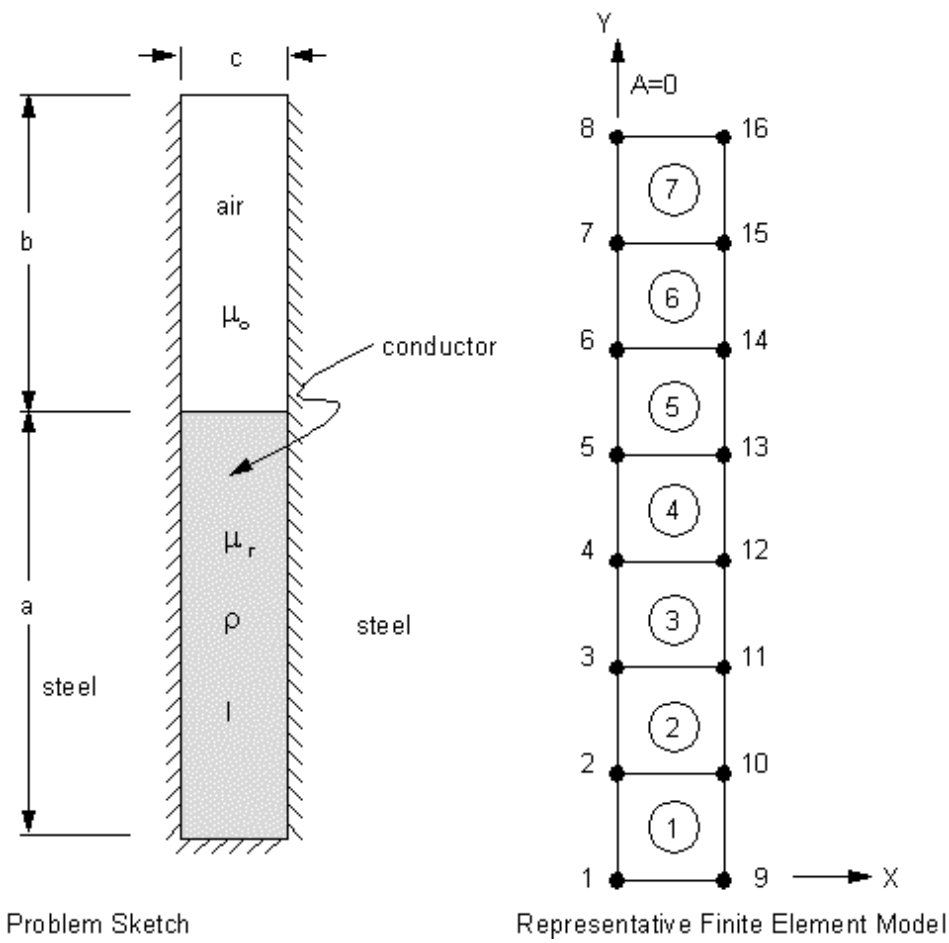

Material Properties	Geometric Properties	Loading
$\mu_o = 1.0$ $\mu_r = 1.0$ $\rho = 1.0$	a = 4 b = 3 c = 1	I = 4 A ω = 1 rad/sec

Analysis Assumptions and Modeling Notes

The slot is assumed to be infinitely long so that end effects are ignored, allowing for a two-dimensional planar analysis. An assumption is made that the steel containing the slot is infinitely permeable and so is replaced with a flux-normal boundary condition. It is also assumed that the flux is contained within the slot, so a flux-parallel boundary condition is placed along the top of the slot. The problem is stated in non-dimensional terms with properties given as unit values to match the reference.

The problem requires a coupled electromagnetic field analysis using the VOLT and AZ degrees of freedom. All VOLT DOF's within the conductor are coupled together to enforce the correct solution of the source current density component of the total current density. The eddy current component of the total current density is determined from the AZ DOF solution. The current is applied to a single arbitrary node in the conductor, since they are all coupled together in VOLT.

An initial solution is performed at a very small time step of 1×10^{-8} sec to establish a null field solution. Since no nonlinear properties are present, the **NEQIT** command is set to 1.0, suppressing equilibrium iterations at each time point. Eighty-one load steps are set up at constant time increments to accurately model the time-varying field solution. The Jacobian solver option is arbitrarily chosen.

The time-history postprocessor POST26 is used to display the time-varying current. The total, source, and eddy current density components are retrieved from the database file for each element, from which the respective current components are calculated. The currents are then summed over all the elements in the conductor for display purposes.

Results Comparison

Vector Potential	Target	ANSYS	Ratio
@ node 1 (t = 3pi/2)	-15.18	-15.03	.990
@ node 4 (t = 3pi/2)	-14.68	-14.66	.999
@ node 7 (t = 3pi/2)	-4.00	-4.00	1.00
@ node 1 (t = 2pi)	-3.26	-3.21	.985
@ node 4 (t = 2pi)	-0.92	-0.91	.989
@ node 7 (t = 2pi)	0	0	-

ANSYS Verification Manual . ANSYS Release 10.0 . 002184 . © SAS IP, Inc.

Figure 186.2 Eddy, Source and Total Current

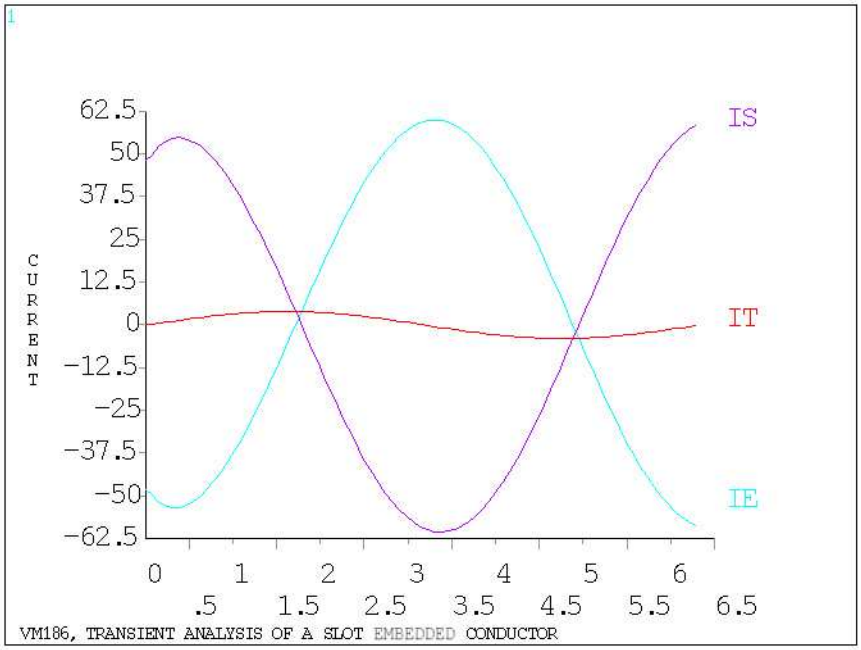

VM187: Bending of a Curved Beam

Overview

Reference:	R. J. Roark, *Formulas for Stress and Strain*, 4th Edition, McGraw-Hill Book Co., Inc., New York, NY, 1965, pg. 166, example.
Analysis Type(s):	Static Analysis (**ANTYPE** = 0)
Element Type(s):	3-D Coupled-Field Solid Elements (SOLID5) 3-D 10-Node Tetrahedral Structural Solid Elements (SOLID92) Tetrahedral Coupled-Field Solid Elements (SOLID98) 3-D Tetrahedral Structural Solid p-Elements (SOLID148) 3-D 10-Node Tetrahedral Structural Solid Elements (SOLID187)
Input Listing:	vm187.dat

Test Case

A curved beam spans a 90° arc as shown. A shear load F is applied to the top end while the bottom end is built-in. Determine the deflection d at the free end.

Figure 187.1 Bending of a Curved Beam Problem Sketch

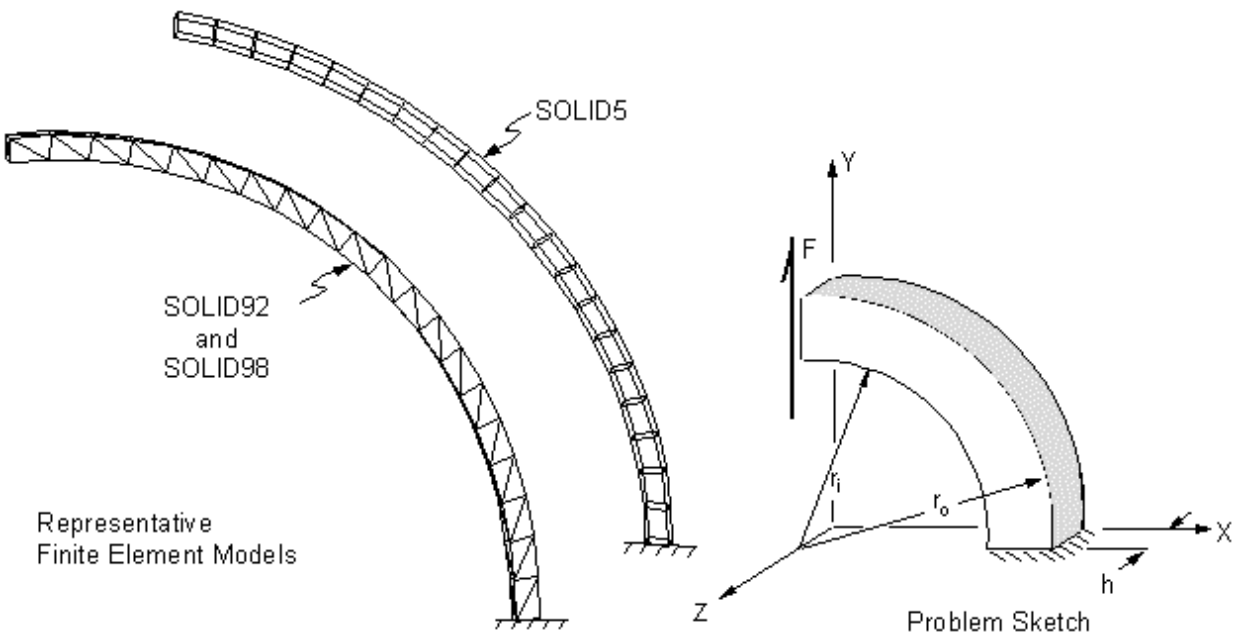

Material Properties	Geometric Properties	Loading
$E = 10 \times 10^6$ psi $\upsilon = 0.25$	$r_i = 4.12$ in $r_o = 4.32$ in $h = 0.1$ in	$F = 1$ lb

Analysis Assumptions and Modeling Notes

The problem is solved in five different ways:

- using Coupled-Field Solid Elements (SOLID5)
- using Tetrahedral Solid Elements (SOLID92)

- using Tetrahedral Coupled-Field Solid Elements (SOLID98)
- using 3-D Tetrahedral Structural Solid p-Elements (SOLID148)
- using Tetrahedral Solid Elements (SOLID187)

For the tetrahedral elements, the nodes at the free end are coupled and the shear force applied to the prime node.

Postprocessing is used to directly obtain the difference between the target solution and the ANSYS results in the form of a ratio.

Results Comparison

	Target	ANSYS	Ratio
Deflection, in (SOLID5)	0.08854	0.088136	0.995
Deflection, in (SOLID92)	0.08854	0.088333	0.998
Deflection, in (SOLID98)	0.08854	0.088333	0.998
Deflection, in (SOLID148)	0.08854	0.088460	0.999
Deflection, in (SOLID187)	0.08854	0.088333	0.998

VM188: Force Calculation on a Current Carrying Conductor

Overview

Reference:	F. C. Moon, *Magneto-Solid Mechanics*, John Wiley and Sons, Inc., New York, NY, 1984, pg. 418.
Analysis Type(s):	Static Magnetic Field Analysis (**ANTYPE** = 0)
Element Type(s):	2-D 8-Node Magnetic Solid Elements (PLANE53) 2-D Infinite Boundary Elements (INFIN9)
Input Listing:	vm188.dat

Test Case

Two rectangular conductors, separated by centerline-to-centerline distance d, are carrying equal out-of-plane currents, I. Determine the resulting force F on the conductors.

Figure 188.1 Current Carrying Conductor Problem Sketch

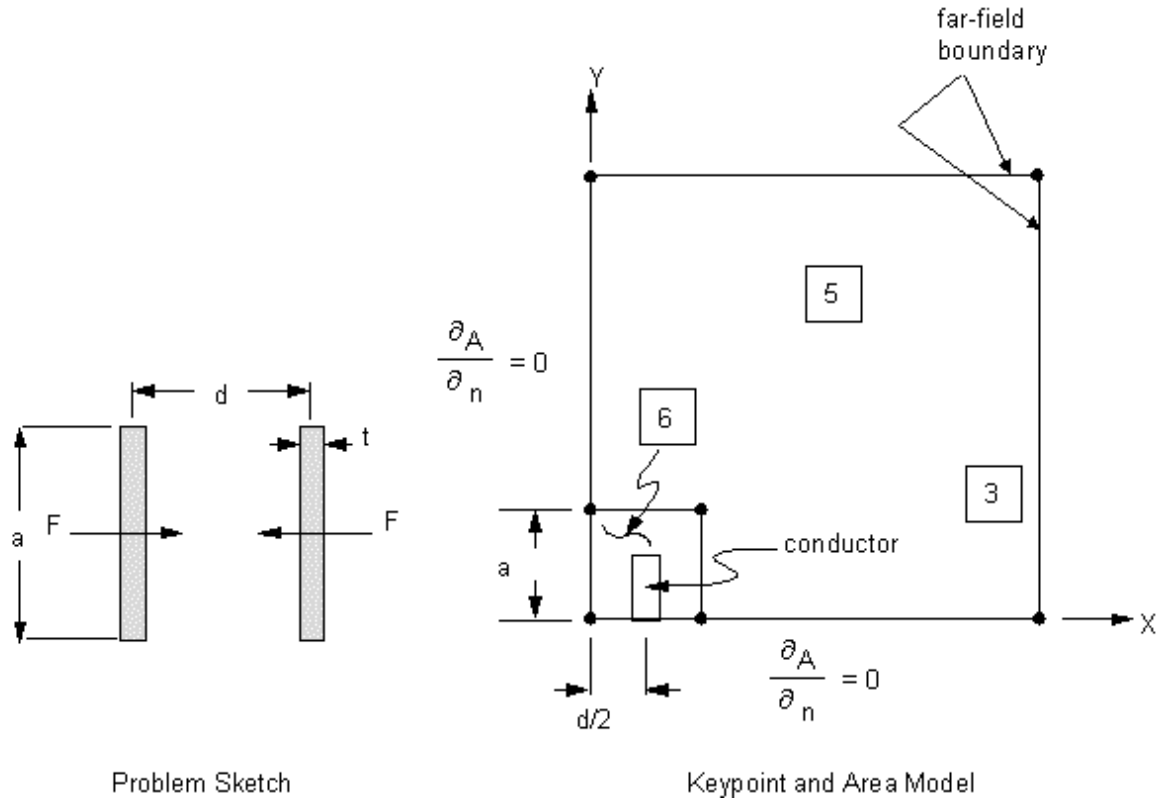

Material Properties	Geometric Properties	Loading
$\mu_r = 1$ $\mu_o = 4\pi \times 10^{-7}$ H/m	d = .010 m a = .012 m t = .002 m	I = 24 A

Analysis Assumptions and Modeling Notes

Due to the symmetric nature of the magnetic field, a 1/4 symmetry model is generated. The far-field boundaries are meshed with an infinite boundary element to model the unbounded field behavior. The lower order infinite

elements are meshed first so that the higher order plane elements will appropriately drop their midside nodes during meshing.

Lorentz forces $(\bar{J} \times \bar{B})$ in the conductor are calculated for each element and are available from the post data file. Virtual work forces are also calculated via specification of virtual displacements (MVDI). A third method of obtaining the force on a body is through the use of the Maxwell stress tensor. Forces in this manner are obtained from a surface integral (line integral in 2-D analysis) defined using the path calculation capabilities in POST1 and macro FOR2-D. Flux lines are displayed via the macro PLF2-D.

The applied source current density is calculated as I/at = 2A/(12 x 2) x 10^{-6} m^2 = 1 x 10^6 A/m^2.

To ensure that a surface integral for force calculations will yield acceptable results, a fine mesh is used for area 6 in the region of the surface integral path.

Results Comparison

	Target	ANSYS	Ratio
F, N/m (Lorentz)	-9.684 x 10^{-3}	-9.717 x 10^{-3}	1.003
F, N/m (Maxwell)	-9.684 x 10^{-3}	-9.677 x 10^{-3}	0.999
F, N/m (Virtual Work)	-9.684 x 10^{-3}	-9.717 x 10^{-3}	1.003

Figure 188.2 Magnetic Flux Lines Near Conductor

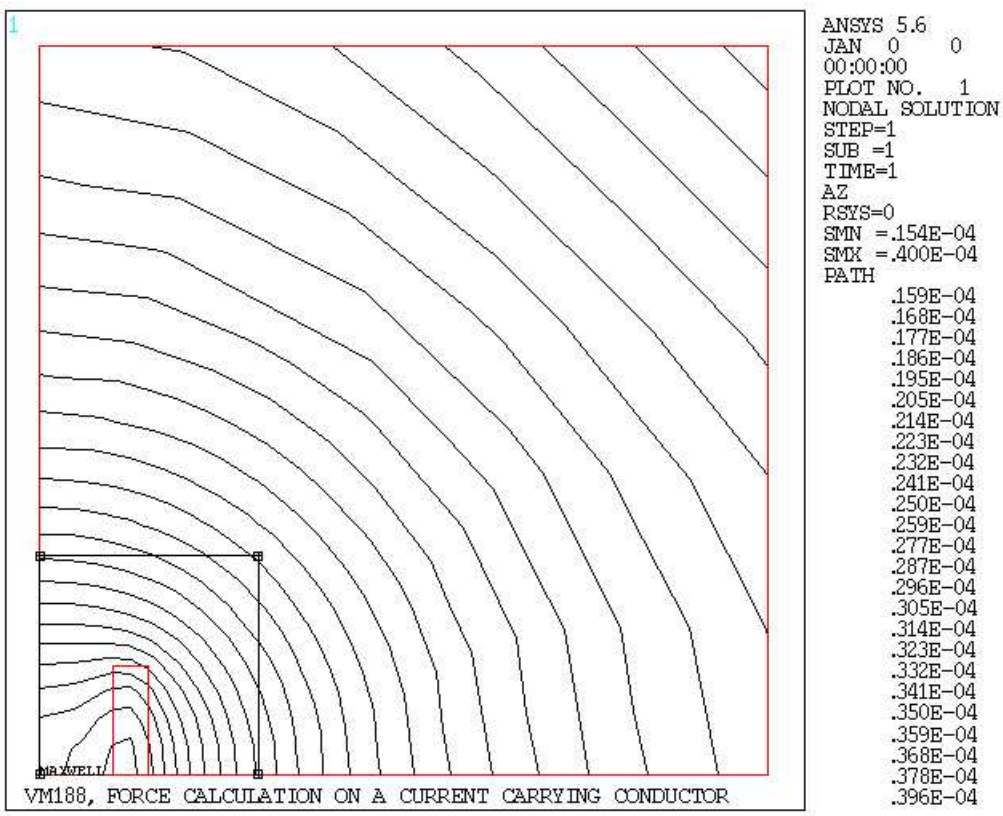

Path of the integral is highlighted.

VM189: Hollow Sphere in a Uniform Magnetic Field

Overview

Reference:	C. R. I. Emson, "Results for a Hollow Sphere in a Uniform Field (Benchmark Problem 6)", *COMPEL*, Vol. 7 Nos. 1 & 2, 1988, pp. 89-101.
Analysis Type(s):	Full Harmonic Response Analysis (**ANTYPE** = 3)
Element Type(s):	3-D Magnetic Solid Elements (SOLID97) 3-D Magnetic Scalar Solid Elements (SOLID96) 3-D Magnetic Interface Elements (INTER115)
Input Listing:	vm189.dat

Test Case

A hollow aluminum sphere is subjected to a uniform sinusoidally varying magnetic field. Determine the peak flux density at the center of the sphere and the average power loss within the sphere.

Figure 189.1 Hollow Sphere Problem Sketch

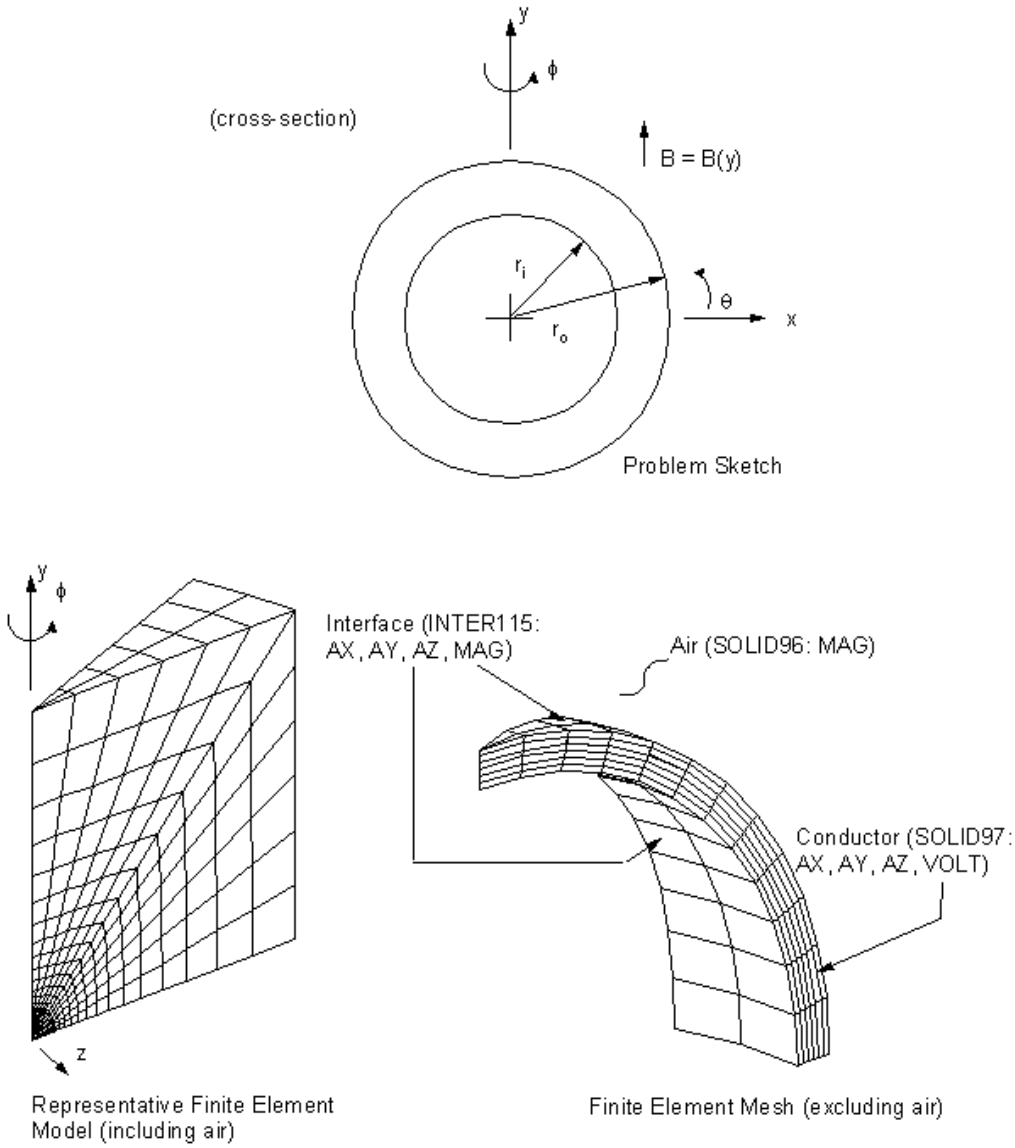

Material Properties	**Geometric Properties**	**Loading**
$\mu_r = 1$ (aluminum) $\rho = 2 \times 10^{-9}$ ohm-m	$r_i = .05$ m $r_o = .055$ m	$B = B(y) = B_o \cos \omega t$ $B_o = 1$ T $\omega = 50$ Hz

Analysis Assumptions and Modeling Notes

The problem is symmetric such that an arbitrary circumferential slice (Φ-direction) can be chosen along with a half-symmetry slice about the Y axis. A circumferential slice of $\Phi = 20$ degrees is arbitrarily selected.

A rectangular exterior boundary is located at a distance of 0.6 m where the external field load is applied. To maximize efficiency, the model is divided into two regions. Region 1 is the hollow aluminum sphere which is modeled with the vector potential formulation using the SOLID97 element. Region two is the air inside and outside of the sphere which is modeled with the Reduced Scalar Potential formulation using the SOLID96 element. The two regions are interfaced with the interface element INTER115 at the sphere-air boundary.

Flux-parallel boundary conditions are applied at the $\Phi = 0$ and $\Phi = 20$ degree planes. Flux-normal conditions are applied at the y = 0 plane. At the interface regions, the condition $\bar{A} \cdot \bar{n} = 0$ is enforced by first rotating the nodes into a spherical coordinate system and then setting the radial component of the vector potential to zero. Electric flux-normal conditions are enforced at the two circumferential symmetry planes by setting the time-integrated potential (VOLT) to zero. The external field is applied at the y = .6 m exterior plane by applying a nonzero value of the scalar potential based on the equation:

$$B_{(y)} = \mu H_{(y)} = - \mu \text{ grad } \Phi = - \mu \ \Delta \ \Phi / \ \Delta y$$

With this relationship, the scalar potential value at y = .6 m is:

$$\Phi_{y=.6} = -.6/ \mu_0$$

The command macro POWERH is used to calculate the power loss in the cylinder. Vector array displays of the eddy currents in the cylinder is produced using the PLVJ3D command macro.

The **AMAP** command is used to simplify the Mapped Meshing process. It eliminates the need for line concatenation, resulting in easier mesh extrusion into 3-D.

Results Comparison

	Target	ANSYS	Ratio
B_y (0,0), T	.0542	.0533	1.017
Power loss, W	10062	9648	1.043

Figure 189.2 Vector Display of Eddy Current Density (Real)

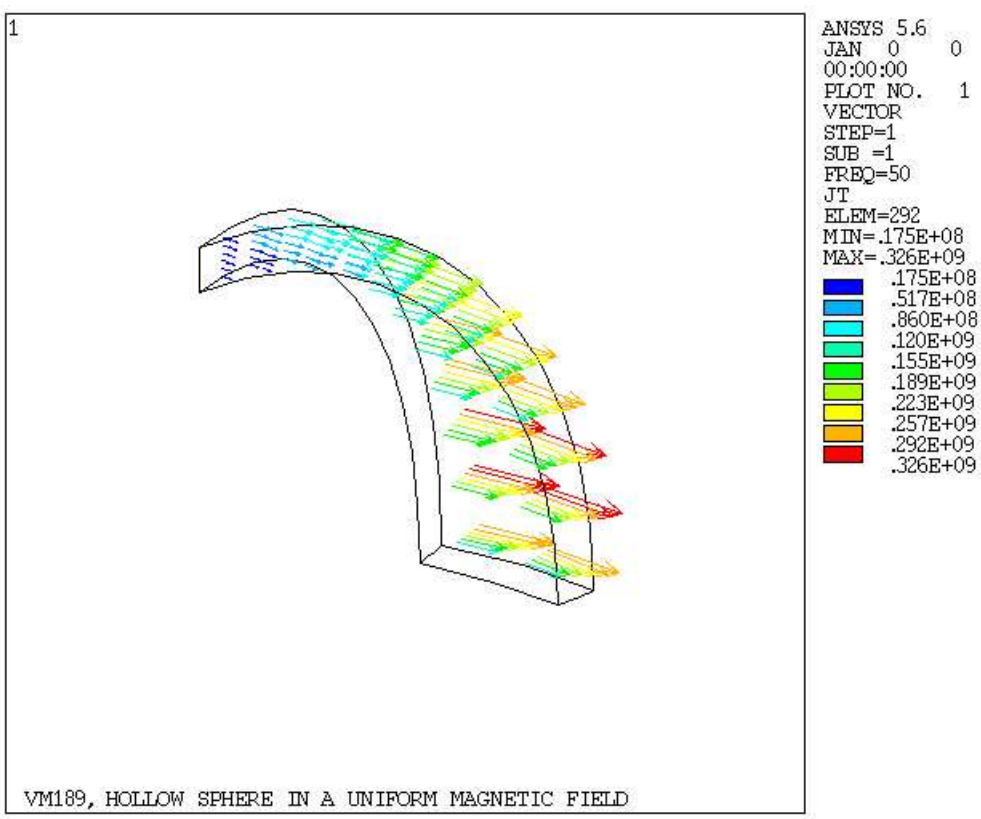

Figure 189.3 Vector Display of Eddy Current Density (Imaginary)

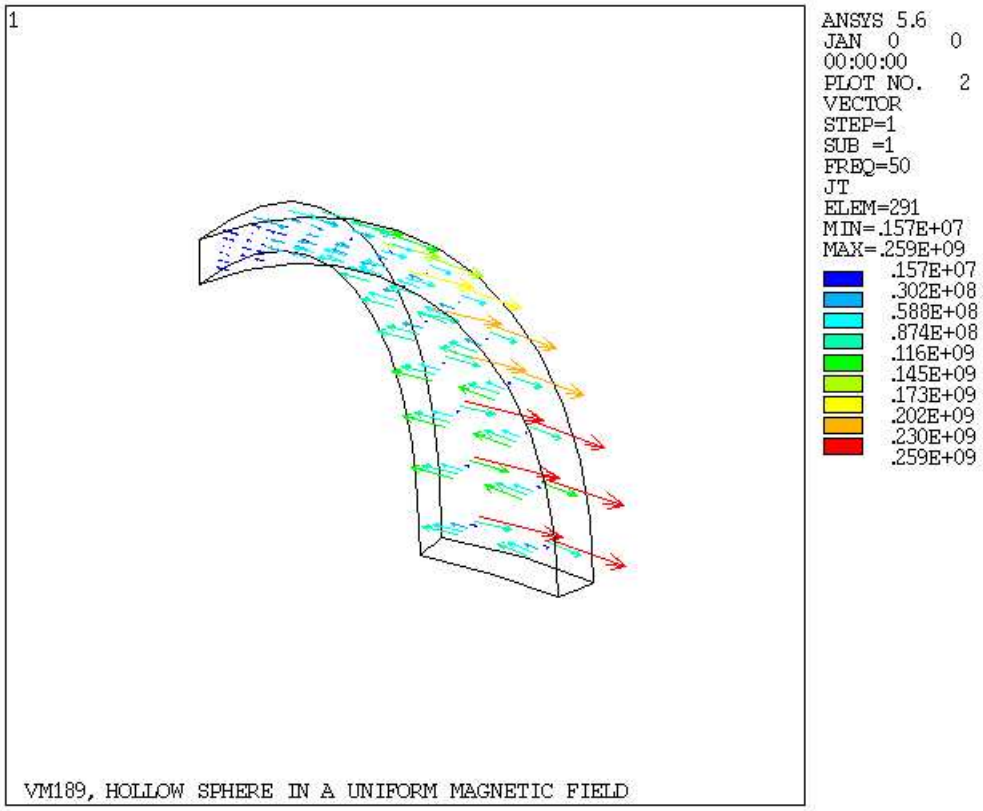

VM190: Ferromagnetic Inductor

Overview

Reference:	S. J. Chapman, *Electric Machinery Fundamentals*, McGraw-Hill Book Co., Inc., New York, NY, 1985, pg. 14, ex. 1-1.
Analysis Type(s):	Static Magnetic Field Analysis (**ANTYPE** = 0)
Element Type(s):	Tetrahedral Coupled-Field Solid Elements (SOLID98) 3-D Infinite Boundary Elements (INFIN47) Current Source Elements (SOURC36)
Input Listing:	vm190.dat

Test Case

A ferromagnetic core is wound with a 200-turn coil wrapped around one leg. Determine the mmf drop in the iron core for a coil current of 1 ampere.

Figure 190.1 Ferromagnetic Inductor Problem Sketch

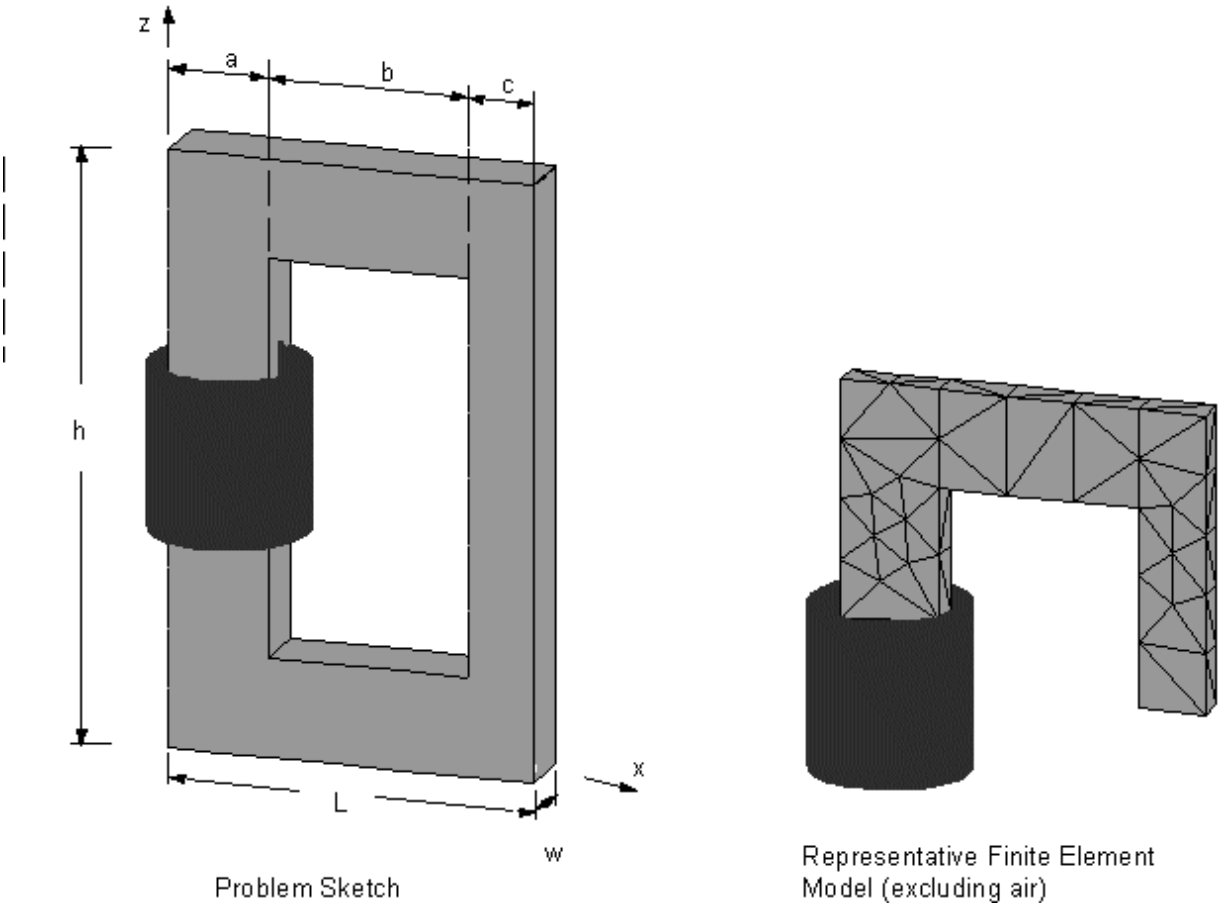

Material Properties	Geometric Properties
u_r = 2500 (iron)	h = 60 cm
Loading	L = 55 cm
I = 1.0 Ampere	w = 10 cm
	a = 15 cm
	b = 30 cm
	c = 10 cm

Analysis Assumptions and Modeling Notes

Since the core material has finite permeability air is modelled to a small distance away from the core. The open boundary is modelled with an infinite surface element at the edge of the air region. The model employs 1/4 symmetry (about the Y and Z planes). The current source is modelled by a coil primitive. Dimensions of the coil are arbitrarily chosen since they have no bearing on the mmf calculations.

The iron core, linked by a coil, has no air-gap, hence a multiply-connected domain exists requiring the use of the Generalized Scalar Potential (GSP) formulation. The GSP strategy requires three solution steps, controlled by the **MAGOPT** command.

The mmf drop in the iron is calculated by a line integral around the iron core. According to Ampere's law, $\int H \bullet d\ell = I$, where H is the field intensity, and I is the enclosed current (or mmf drop). The integral is set up and calculated using the path logic in POST1.

Results Comparison

	Target	ANSYS	Ratio
mmf drop (A-t)	200	198.61	0.993

Figure 190.2 Magnetic Flux Density

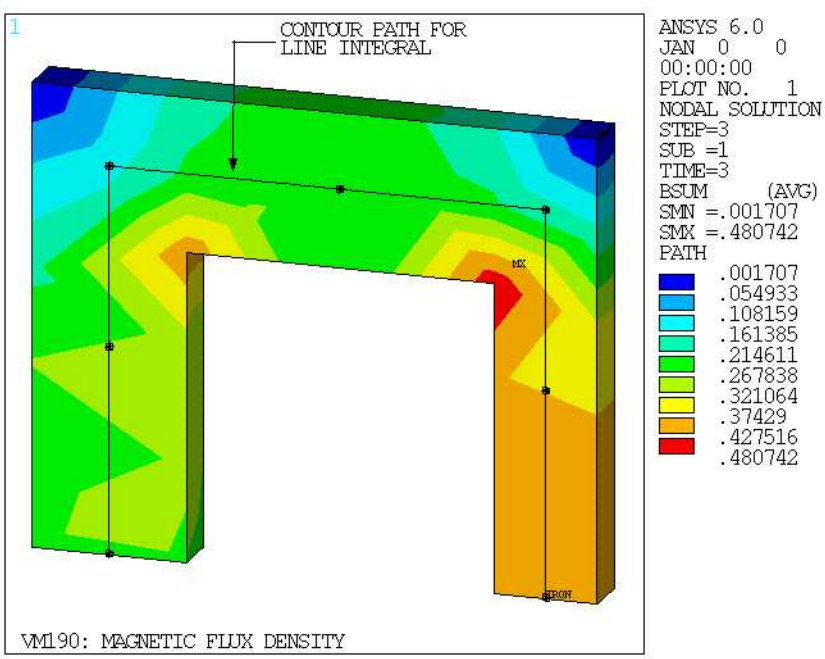

VM191: Hertz Contact Between Two Cylinders

Overview

Reference:	N. Chandrasekaran, W. E. Haisler, R. E. Goforth, "Finite Element Analysis of Hertz Contact Problem with Friction", *Finite Elements in Analysis and Design*, Vol. 3, 1987, pp. 39-56.
Analysis Type(s):	Static Analysis (**ANTYPE** = 0)
Element Type(s):	2-D Structural Solid Elements (PLANE42) 3-D Structural Solid Elements (SOLID45) 2-D/3-D Node-to-Surface Contact Elements (CONTA175) 2-D Structural Solid Elements (PLANE182) 3-D Structural Solid Elements (SOLID185)
Input Listing:	vm191.dat

Test Case

Two long cylinders of radii R_1 and R_2, in frictionless contact with their axes parallel to each other are pressed together with a force per unit length, F. Determine the semi-contact length b and the approach distance d.

Figure 191.1 Hertz Contact Between Two Cylinders Problem Sketch

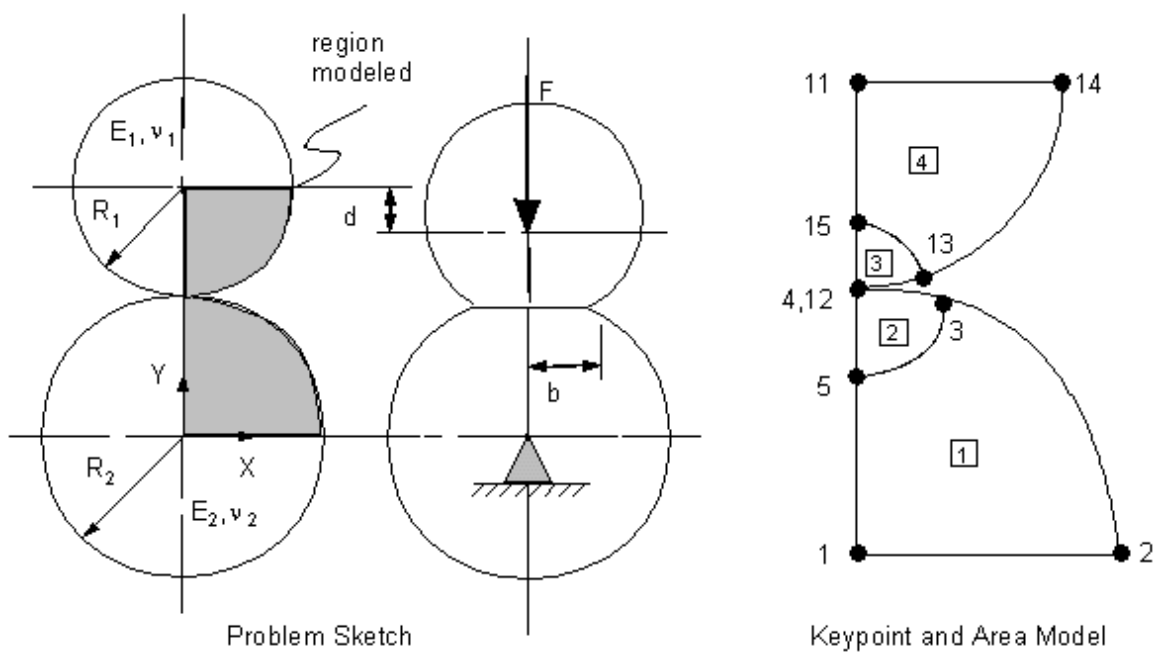

Material Properties	Geometric Properties
Cylinder 1: E_1 = 30000 N/mm^2 υ_1 = 0.25 **Cylinder 2:** E_2 = 29120 N/mm^2 υ_2 = 0.3	R_1 = 10 mm R_2 = 13 mm **Loading** F = 3200 N/mm

Analysis Assumptions and Modeling Notes

Each analysis uses two load steps; in the first load step a small imposed displacement is used on the upper cylinder to engage contact, whereas in the second load step the imposed displacement is deleted and the force load is applied.

The problem is solved in eight different ways:

Contact Algorithm: Augmented Lagrangian - KEYOPT(2) = 0

- 2-D analysis with PLANE42 and CONTA175
- 3-D analysis with SOLID45 and CONTA175
- 2-D analysis with PLANE182 and CONTA175
- 3-D analysis with SOLID185 and CONTA175

Contact Algorithm: Lagrange Multiplier - KEYOPT(2) = 3

- 2-D analysis with PLANE42 and CONTA175
- 3-D analysis with SOLID45 and CONTA175
- 2-D analysis with PLANE182 and CONTA175
- 3-D analysis with SOLID 185 and CONTA175

Plane stress condition is modeled using a unit thickness slice through the cylinders. The region modeled is shown shaded in the problem sketch. The **ESURF** command is used to automatically generate the contact and target elements between "contactor" nodes on the upper cylinder and "target" nodes on the lower cylinder. The default value of contact stiffness FKN is chosen while performing a solution using Augmented Lagrangian contact algorithm (KEYOPT(2) = 0) whereas no contact stiffness input is required to be specified while performing a solution using Lagrange Multiplier contact algorithm (KEYOPT(2) = 3).

Results Comparison

		Target	ANSYS	Ratio
CONTA175 - Algorithm: Augmented Lagrangian KEYOPT(2) = 0				
PLANE42	d,mm	-0.4181	-0.4214	1.008
	b,mm	1.20	1.1609	0.967
SOLID45	d,mm	-0.4181	-0.4207	1.006
	b,mm	1.20	1.1609	0.967
PLANE182	d,mm	-0.4181	-0.4183	1.000
	b,mm	1.20	1.1609	0.967
SOLID185	d,mm	-0.4181	-0.4191	1.002
	b,mm	1.20	1.1609	0.967
CONTA175 - Algorithm: Lagrange Multiplier KEYOPT(2) = 3				
PLANE42	d,mm	-0.4181	-0.4212	1.007
	b,mm	1.20	1.1609	0.967
SOLID45	d,mm	-0.4181	-0.4191	1.006
	b,mm	1.20	1.1609	0.967

		Target	ANSYS	Ratio
PLANE182	d,mm	-0.4181	-0.4181	1.000
	b,mm	1.20	1.1609	0.967
SOLID185	d,mm	-0.4181	-0.4190	1.002
	b,mm	1.20	1.1609	0.967

VM192: Cooling of a Billet by Radiation

Overview

Reference:	R. Siegel, J. R. Howell, *Thermal Radiation Heat Transfer*, 2nd Edition, Hemisphere Publishing Corporation, 1981, pg. 229, problem 21.
Analysis Type(s):	Transient Analysis (**ANTYPE** = 4)
Element Type(s):	3-D Thermal Solid Elements (SOLID70) 3-D Thermal Surface Effect Elements (SURF152)
Input Listing:	vm192.dat

Test Case

A carbon steel billet is initially at a temperature T_B and is supported in such a manner that it loses heat by radiation from all its surfaces to surroundings at temperature T_E. Determine the temperature T_B of the billet at the end of 3.7 hours.

Figure 192.1 Cooling of a Billet by Radiation Problem Sketch

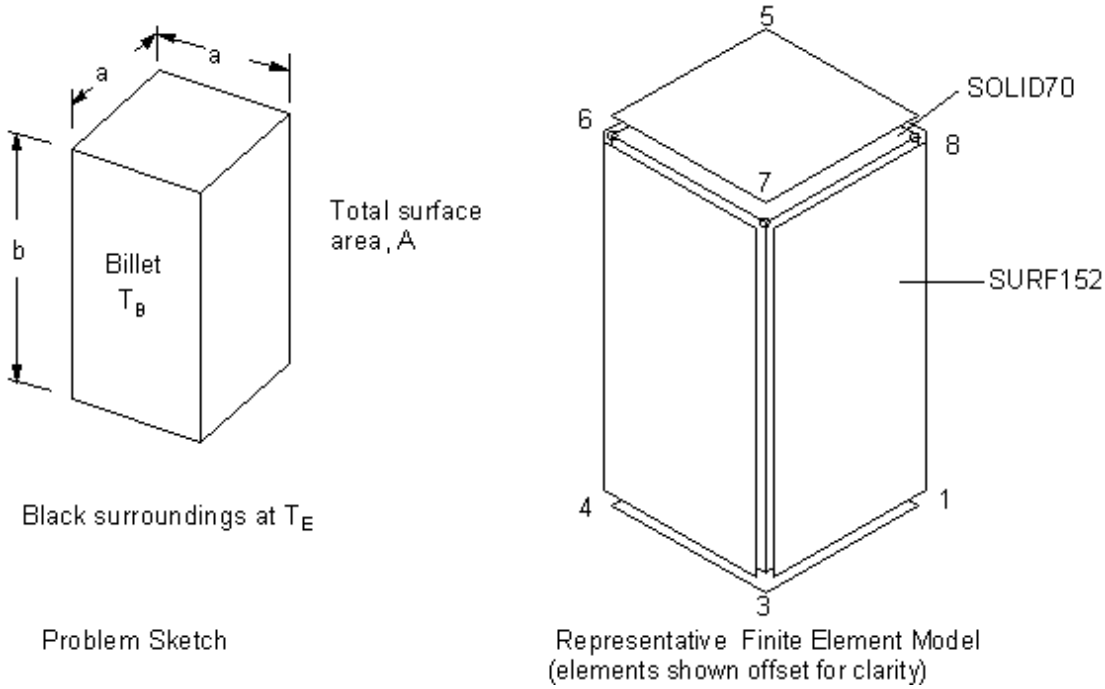

Material Properties	Geometric Properties	Loading
C = 0.11 Btu/lb-°R ρ = 487.5 lb/ft^3 ε = emissivity = 1.0 Stefan-Boltzmann constant = 0.1712x10^{-8} Btu/hr-ft^2-R^4	a = 2 ft b = 4 ft	T_E = 70°F (530°R) T_B = 2000°R (at t = 0)

Analysis of Assumptions and Modeling Notes

The billet is modeled using a single SOLID70 element overlaid with a SURF152 element on each of its faces. The surface elements have a common extra node representing the surrounding space. An arbitrary value is selected for the billet conductivity. The form factor from the billet to surrounding space is input as unity.

Results Comparison

Time = 3.7 hr	Target	ANSYS	Ratio
T_B, °R	1000.0	1002.5	1.002

ANSYS Verification Manual . ANSYS Release 10.0 . 002184 . © SAS IP, Inc.

VM193: Adaptive Analysis of 2-D Heat Transfer with Convection

Overview

Reference:	NAFEMS, "The Standard NAFEMS Benchmarks", Rev. No. TSNB, National Engineering Laboratory, E. Kilbride, Glasgow, UK, August, 1989, Test No. T4.
Analysis Type(s):	Steady-state Thermal Analysis (**ANTYPE** = 0)
Element Type(s):	2-D Thermal Solid Elements (PLANE55)
Input Listing:	vm193.dat

Test Case

Determine the temperature at point E in a long slab of rectangular cross-section subjected to the thermal loads shown below.

Figure 193.1 2–D Heat Transfer with Convection Problem Sketch

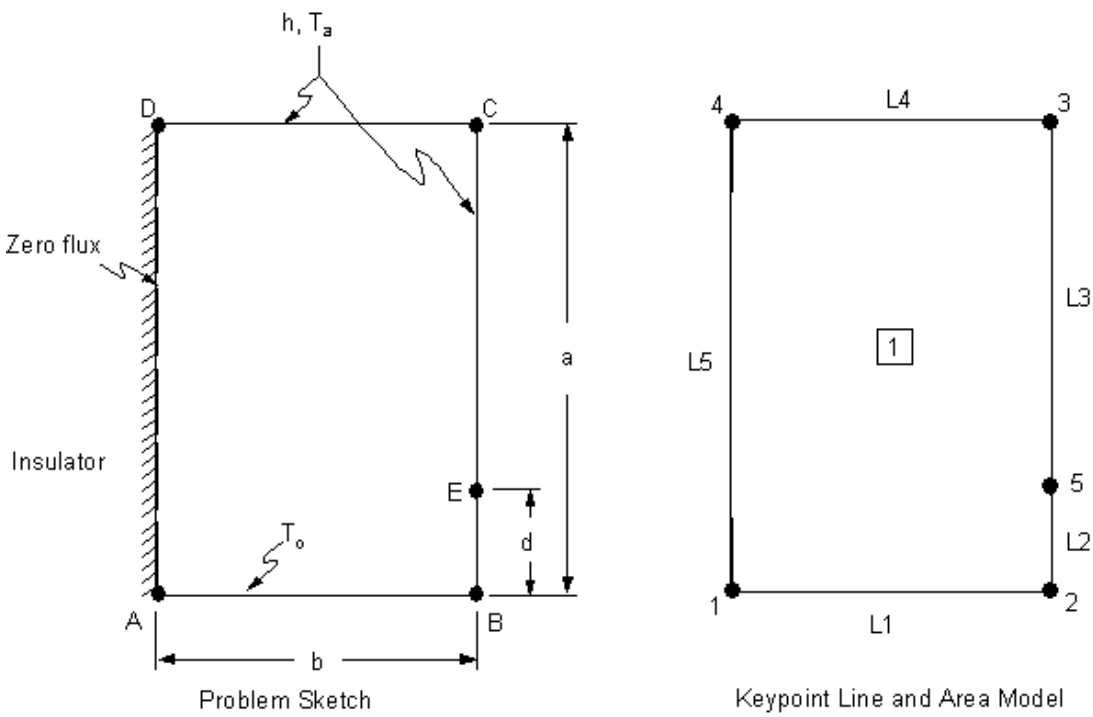

Material Properties	Geometric Properties	Loading
k = 52.0 W/m-°C h = 750.0 W/m^2-°C	a = 1.0 m b = 0.6 m d = 0.2 m	T_o = 100°C T_a = 0°C

Analysis Assumptions and Modeling Notes

Due to the conflicting boundary conditions, this problem has a singularity at point B, leading to a high gradient of temperature from point B to E. The adaptive meshing solution technique is used to obtain the solution to this problem within 10 adaptive loops such that the error in the thermal energy norm over the entire model is within 5%.

The model is created using solid model entities. A keypoint is specified at target location E to ensure that a node is created at that location. All boundary conditions are applied on the solid model. The ADAPT macro is used to invoke the automatic adaptive meshing procedure.

Results Comparison

	Target	ANSYS	Ratio
T, °C at point E	18.3	18.2	0.997

Figure 193.2 Temperature Contour Plot

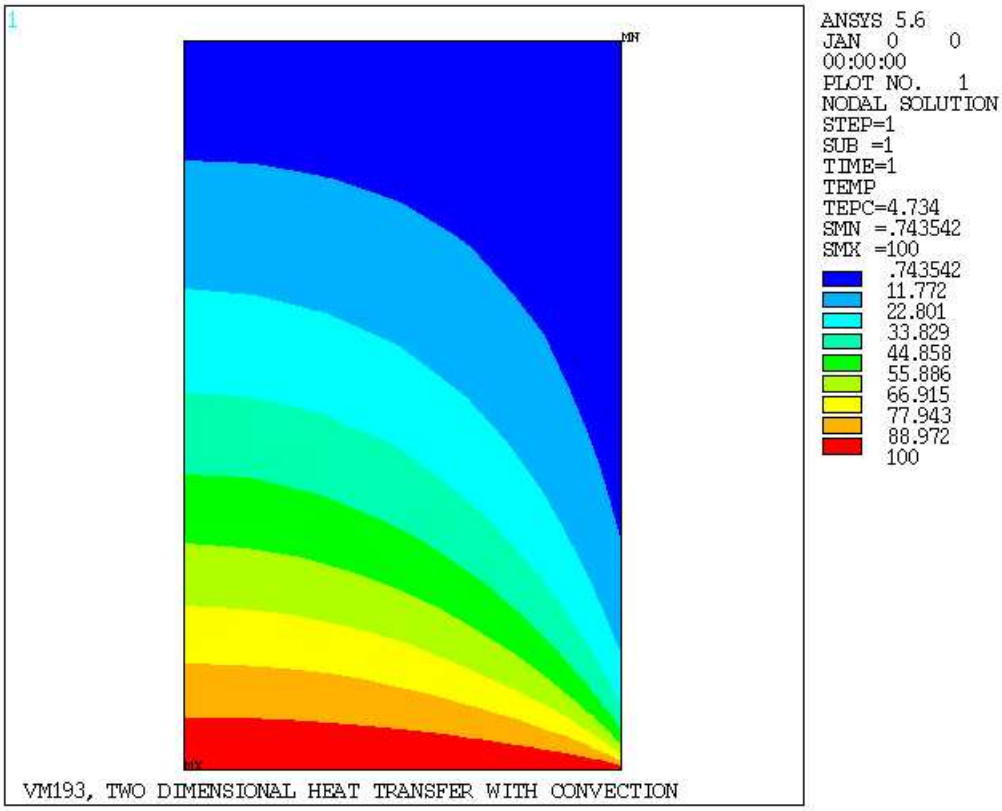

VM194: Element Birth/Death in a Fixed Bar

Overview

Reference:	Any standard mechanics of materials text
Analysis Type(s):	Static Analysis (**ANTYPE** = 0)
Element Type(s):	2-D Spar (or Truss) Elements (LINK1)
Input Listing:	vm194.dat

Test Case

A bar of uniform cross-section, fixed at both ends and subjected to a uniform thermal load (ΔT) has its center third removed. This is followed by replacing the removed part in a "strain-free" condition and then removing the uniform thermal load. Determine the axial stresses and the thermal strains in the three sections of the bar at the end of this sequence of loading operations.

Figure 194.1 Fixed Bar with Thermal Loading Problem Sketch

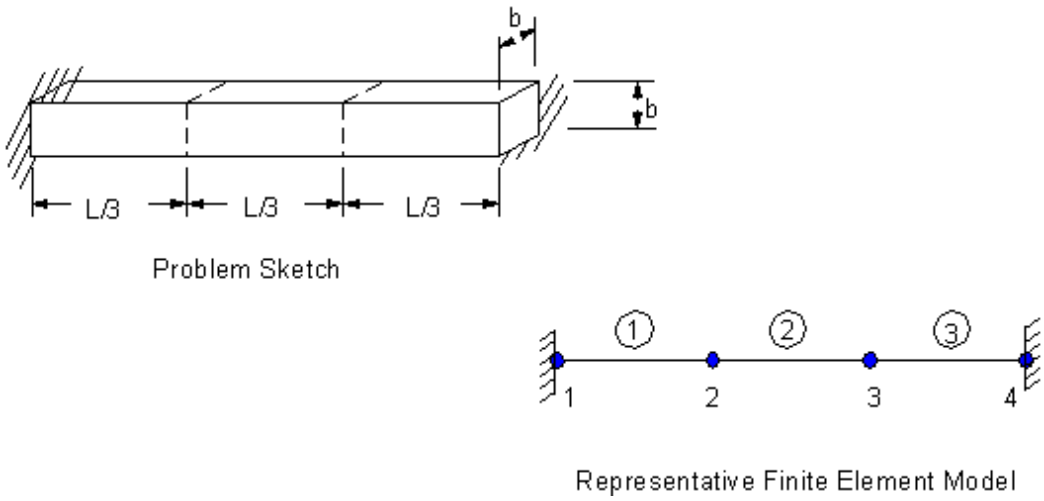

Material Properties	**Geometric Properties**	**Loading**
E = 30 x 10^6 psi α = 0.00005 in/in-°F	L = 10 in b = 1 in	Load Step 1: ΔT = 100°F Load Step 2: Elem 2 dead Load Step 3: Elem 2 alive Load Step 4: ΔT = 0°F

Analysis Assumptions and Modeling Notes

The REFT material property is used to model "rebirth" of the "dead" element such that no thermal strains exist at birth. This is achieved by specifying the value of REFT equal to the uniform temperature of the bar (100°F). Removing the thermal load in the subsequent final load step therefore results in relieving the thermal strains in elements 1 and 3. Element 2 on the other hand, experiences a thermal load of ΔT = -100°F resulting in a negative thermal strain.

Results Comparison

Load Step No. 4	Target	ANSYS[1]	Ratio
$Stress_x$, psi	150,000[1]	150,000	1.000
$Strain_{th}$, (elem1, 3)	0.0	0.0	-
$Strain_{th}$, (elem 2)	-0.005	-0.005	1.000

1. Uniform for all elements.

ANSYS Verification Manual . ANSYS Release 10.0 . 002184 . © SAS IP, Inc.

VM195: Toggle Mechanism

Overview

Reference:	G. H. Martin, *Kinematics and Dynamics of Machines*, 2nd Edition, McGraw-Hill Book Co., Inc., New York, NY, 1982, pp. 55-56, fig. 3-22.
Analysis Type(s):	Static Analysis (**ANTYPE** = 0)
Element Type(s):	Revolute Joint Elements (COMBIN7) 3-D Elastic Beam Elements (BEAM4) Spring-Damper Elements (COMBIN14) Linear Actuator Elements (LINK11)
Input Listing:	vm195.dat

Test Case

Determine the maximum force (F_{max}) of a toggle mechanism acting upon a resisting spring.

Figure 195.1 Toggle Mechanism Problem Sketch

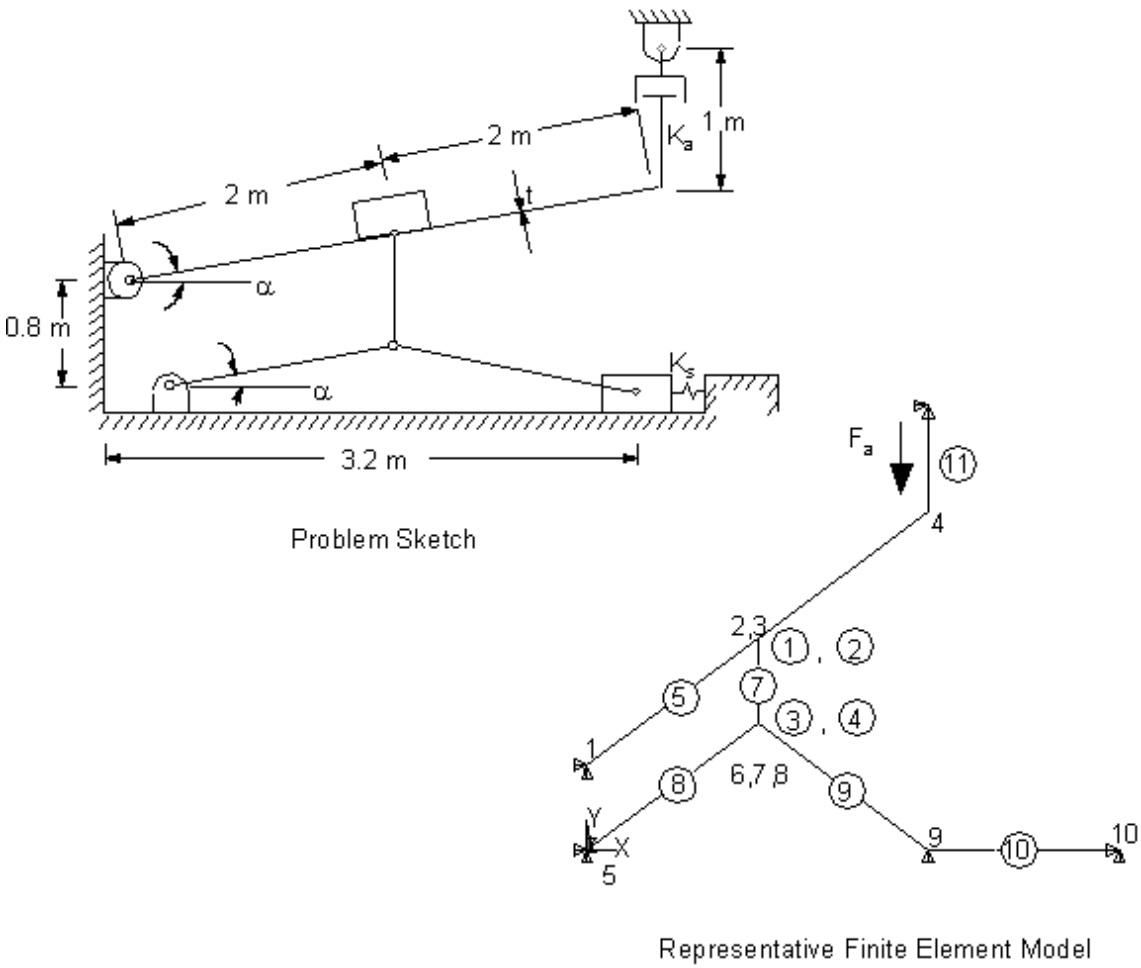

Material Properties	Geometric Properties	Loading
$E = 1 \times 10^9$ N/m^2	t = 0.1 m K_s = 166.67 N/m K_a = 100/d N/m α = 36.87°	F_a = 100 N

Analysis Assumptions and Modeling Notes

A linear actuator is used to apply a force, F_a, and move the toggle mechanism. The actuator force is increased by 2% to ensure complete mechanism motion. The actuator must expand a distance, d = 2.4928 m, to move the mechanism to the maximum force position. Either a force or a displacement could have been applied with the actuator. The **CNVTOL** commands are added to eliminate minimum reference value warnings in the output.

The maximum force exerted by the mechanism upon the spring occurs when the lower links are colinear and parallel to the input lever. The revolute joint connecting the two lower links locks up when a stop engages, after a rotation of 2 α degrees, to simulate the self-locking behavior of the mechanism.

Results Comparison

	Target	ANSYS	Ratio
F_{max}	-133.33	-133.32[1]	1.000
UY, Node 4	-2.40	-2.41	1.002
UX, Node 9	0.80	0.80	1.000

1. Spring force in element 10 (COMBIN14)

ANSYS Verification Manual . ANSYS Release 10.0 . 002184 . © SAS IP, Inc.

VM196: Counter-Balanced Loads on a Block

Overview

Reference:	Any basic mechanics text
Analysis Type(s):	Static Analysis (**ANTYPE** = 0), Inertia Relief
Element Type(s):	3-D Structural Solid Elements (SOLID45) 3-D Structural Solid Elements (SOLID185)
Input Listing:	vm196.dat

Test Case

Determine the free-body moments (MX, MY, MZ) about the origin and the rotational accelerations (ω_x, ω_y, ω_z) at the center of mass of an aluminum block due to the forces FX and FY shown.

Figure 196.1 Counter-Balanced Loads on a Block Problem Sketch

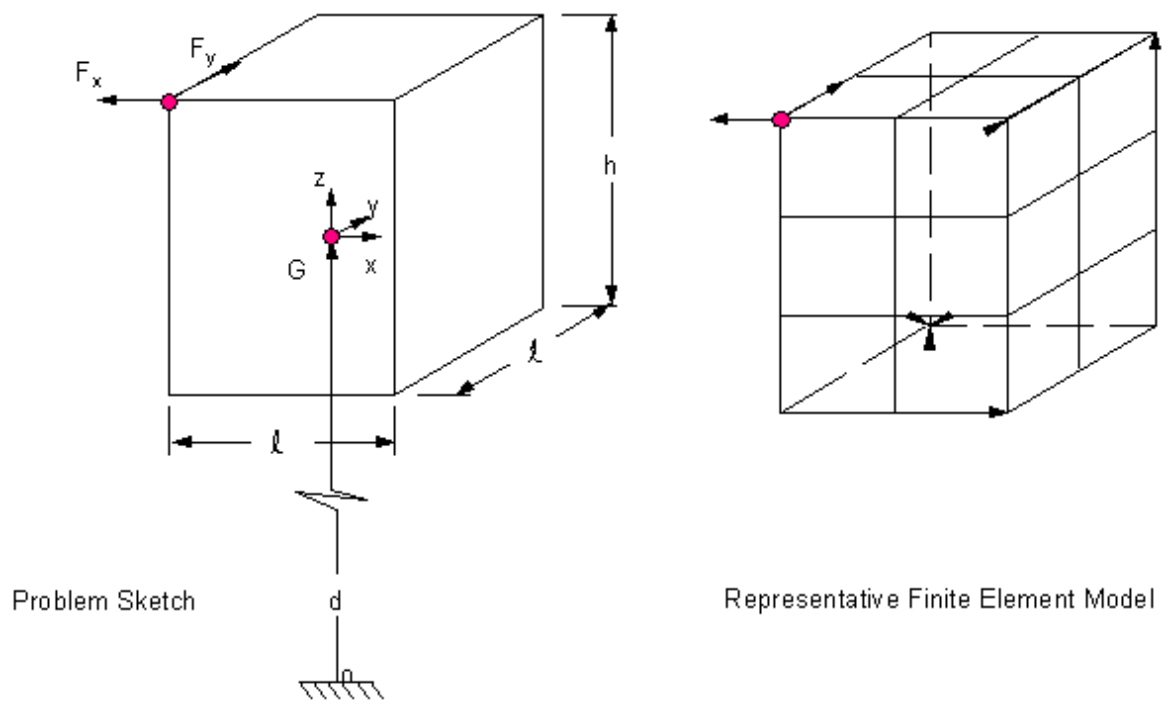

Material Properties	**Geometric Properties**	**Loading**
$E = 70 \times 10^9$ N/m^2 $\rho = 2712$ kg/m^3	h = 3 m ℓ = 2 m d = 300 m	FX = -2000 N FY = 3000 N

Analysis Assumptions and Modeling Notes

The problem is solved in two different ways:

- using 3-D solid elements (SOLID45)
- using 3-D solid elements (SOLID185)

The block must be constrained such that no rigid body motions occur. In a 3-D structure, six DOF must be constrained to prevent free-body motion by translation or rotation. The inertia relief algorithm is used to calculate accelerations to counterbalance the applied loads resulting in net zero values for the sum of the reaction forces.

Results Comparison

	Target	ANSYS	Ratio
SOLID45			
MX (N-m)	-909000	-909000	1.000
MY (N-m)	-606000	-606000	1.000
MZ (N-m)	-5000	-5000	1.000
Rotational accelerations$_x$ (rad/sec^2)	-0.12764	-0.12764	1.000
Rotational accelerations$_y$ (rad/sec^2)	-0.085092	-0.085092	1.000
Rotational accelerations$_z$ (rad/sec^2)	-0.23046	-0.23046	1.000
SOLID185			
MX (N-m)	-909000	-909000	1.000
MY (N-m)	-606000	-606000	1.000
MZ (N-m)	-5000	-5000	1.000
Rotational accelerations$_x$ (rad/sec^2)	-0.12764	-0.12764	1.000
Rotational accelerations$_y$ (rad/sec^2)	-0.085092	-0.085092	1.000
Rotational accelerations$_z$ (rad/sec^2)	-0.23046	-0.23046	1.000

VM197: IGES Write/Read for Thick-Walled Cylinder

Overview

Reference:	Any basic geometry text
Analysis Type(s):	Geometric Primitives, IGES Write/Read
Element Type(s):	None
Input Listing:	vm197.dat

Test Case

Create a thick-walled cylinder with spherical end caps using geometric primitives. Write the geometry to an IGES file. Read the geometry back in from the IGES files. Validate the correctness of the geometry by examining its volume.

Figure 197.1 Thick-Walled Cylinder Problem Sketch

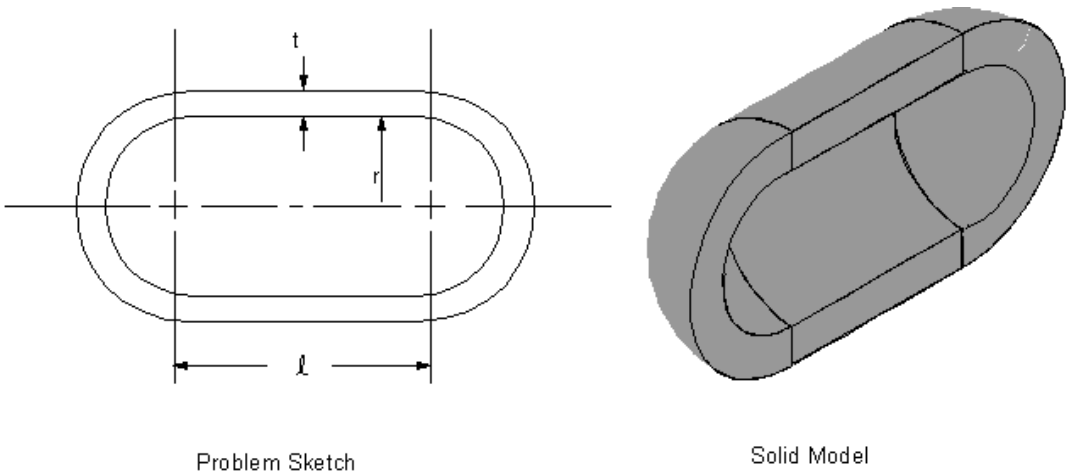

Geometric Properties
r = 20 in
t = 10 in
ℓ = 50 in

Analysis Assumptions and Modeling Notes

Only one half of the model is created. The volume is obtained with the ***GET** command and is compared to the theoretical volume which is calculated using parameters.

Results Comparison

	Target	ANSYS	Ratio
Volume	79063.	79068.	1.000

VM198: Large Strain In-plane Torsion Test

Overview

Reference:	J. C. Nagtegaal, J. E. DeJong, "Some Computational Aspects of Elastic-Plastic Strain Analysis", *Intl J. of Numerical Methods in Engineering*, Vol. 17, 1981, pp. 15–41.
Analysis Type(s):	Static Analysis (**ANTYPE** = 0)
Element Type(s):	2-D 4-Node Viscoplastic Solid Elements (VISCO106) 3-D 8-Node Viscoplastic Solid Elements (VISCO107) 2-D 8-Node Viscoplastic Solid Elements (VISCO108)
Input Listing:	vm198.dat

Test Case

A hollow, thick-walled, long cylinder made of an elastoplastic material is under an in-plane torsional loading which causes the inner surface of the cylinder to undergo a rotation of 60°. Find the maximum shear stress (τ_{max}) developed at the inner surface at the end of loading.

Figure 198.1 Large Strain In-plane Problem Sketch

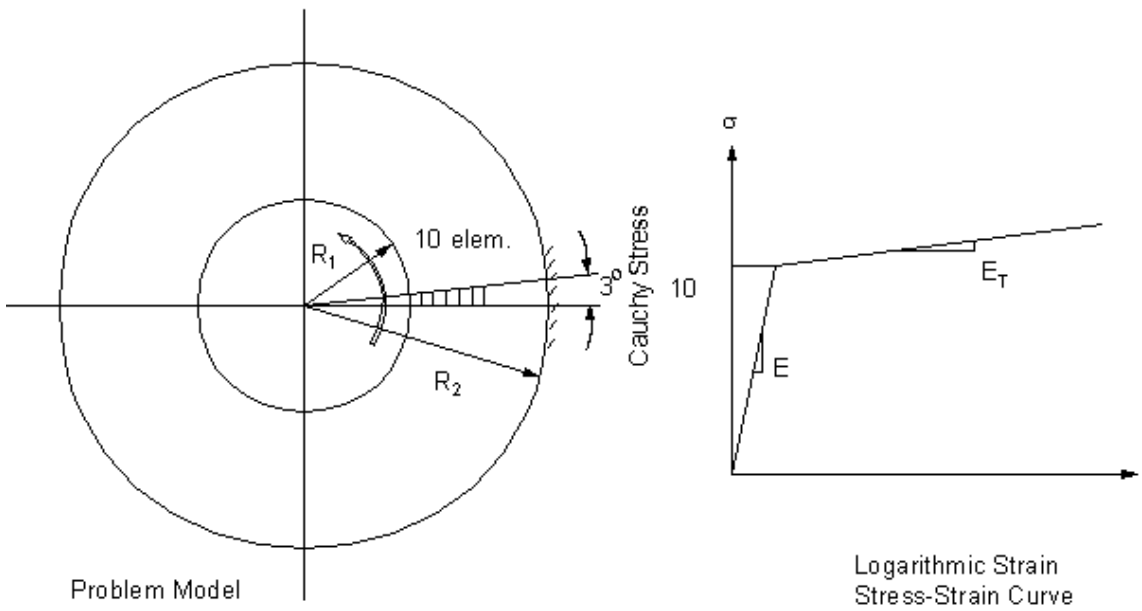

Material Properties	Geometric Properties	Loading
E = 7200 psi μ = 0.33 σ_{yp} = 10 psi E_T = 40 psi	R_1 = 10 in R_2 = 20 in	Θ = 60° At nodes on the inner surface in 10 equal load steps along the circumference

Analysis Assumptions and Modeling Notes

The problem is solved three times, each time with a different element type. The element types used are VISCO106 (2-D, 4-node viscoplastic element), VISCO108 (2-D, 8-node viscoplastic element), and VISCO107 (3-D, 8-node viscoplastic element), respectively. The plasticity is modeled using the bilinear isotropic hardening rule.

The plane strain condition is assumed along the length of the cylinder. Due to the axisymmetric loading, only a small portion (3° span) of the cross-section is modeled each time using ten elements. Nodal rotations and displacement couplings are employed to ensure the circumferential symmetry in the deformed configuration.

To illustrate the dynamic substitution of a parameter value, an alphanumeric character parameter (element type name) is used in the **/TITLE** command. In addition, a character parameter for degrees of freedom is used in the **CP** commands and in the macro SOLD.

POST1 is used to obtain the displaced configuration at the end of loading. The maximum shear stress is computed from the solution results in POST26. In order to be consistent with the reference solution, the maximum shear stress in a negative direction is observed.

Results Comparison

		Target	ANSYS	Ratio
VISCO106	Shear $Stress_{max}$, psi	-48.0	-48.6	1.012
VISCO107	Shear $Stress_{max}$, psi	-48.0	-48.6	1.012
VISCO108	Shear $Stress_{max}$, psi	-48.0	-46.1	0.960

Figure 198.2 Typical Element Deformation Display

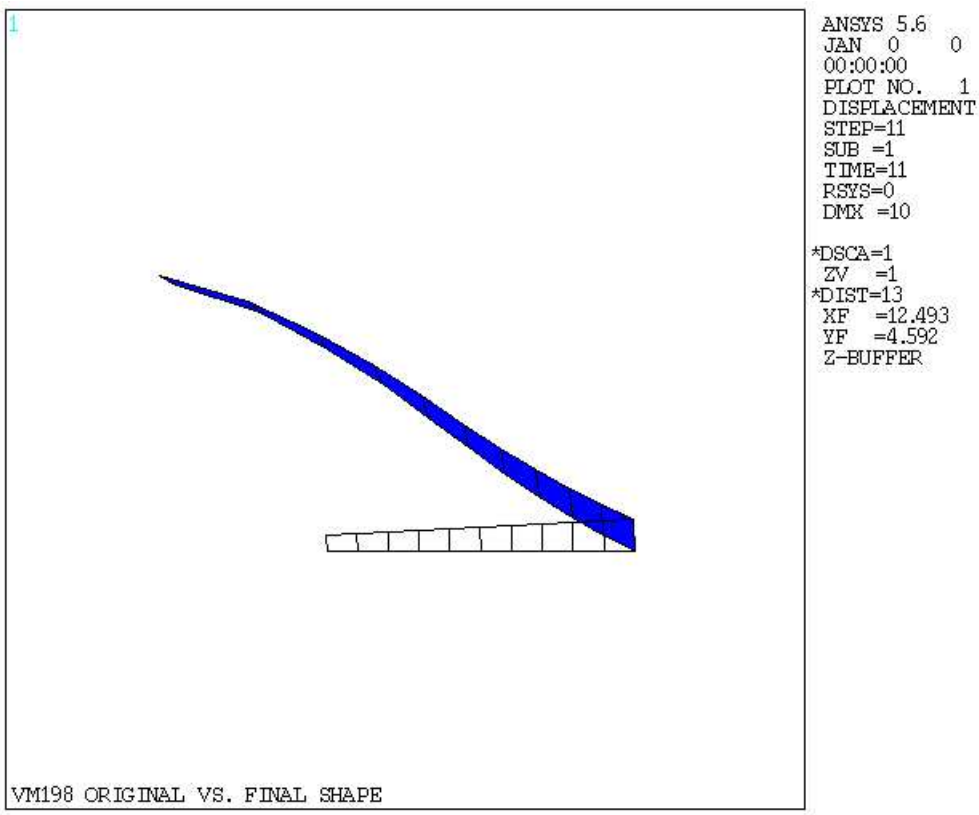

Figure 198.3 Typical Stress vs. Rotation Display

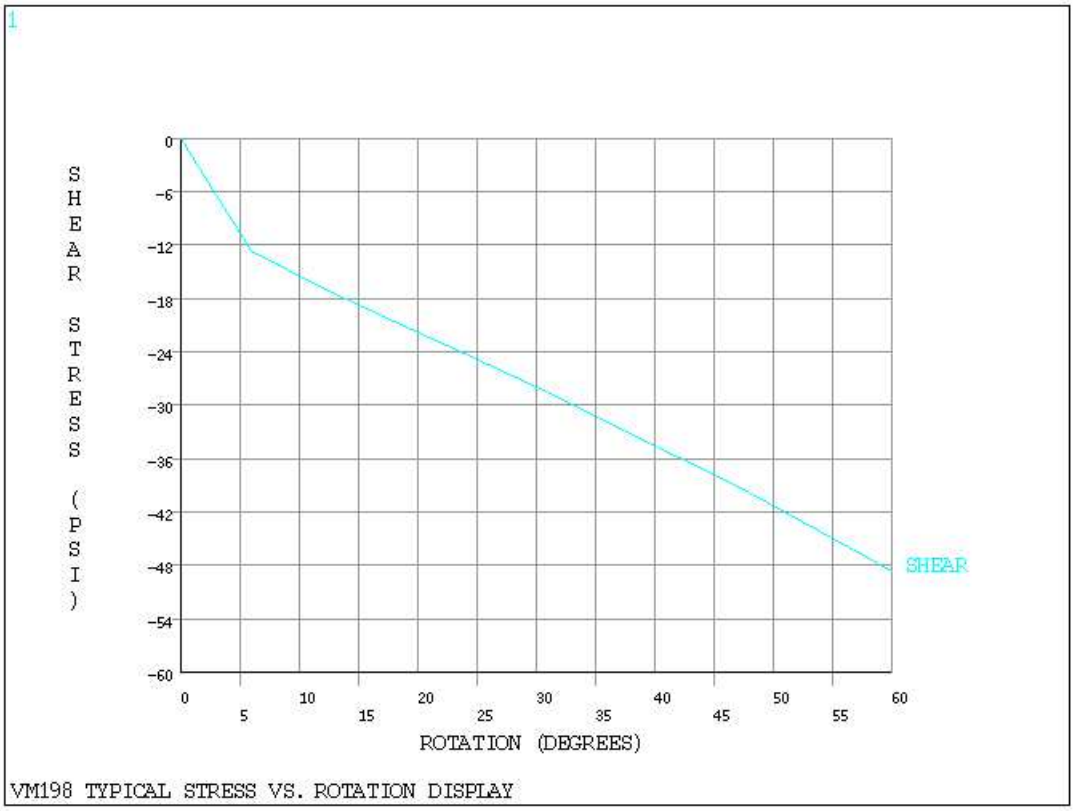

VM199: Viscoplastic Analysis of a Body (Shear Deformation)

Overview

Reference:	B. Lwo, G. M. Eggert, "An Implicit Stress Update Algorithm Using a Plastic Predictor", Submitted to Computer Methods in Applied Mechanics and Engineering, January 1991.
Analysis Type(s):	Static Analysis (**ANTYPE** = 0)
Element Type(s):	2-D 4-Node Viscoplastic Solid Elements (VISCO106) 3-D 8-Node Viscoplastic Solid Elements (VISCO107) 2-D 8-Node Viscoplastic Solid Elements (VISCO108)
Input Listing:	vm199.dat

Test Case

A cubic shaped body made up of a viscoplastic material obeying Anand's law undergoes uniaxial shear deformation at a constant rate of 0.01 cm/s. The temperature of the body is maintained at 400°C. Find the shear load (F_x) required to maintain the deformation rate of 0.01 cm/sec at time equal to 20 seconds.

Figure 199.1 Shear Deformation Problem Sketch

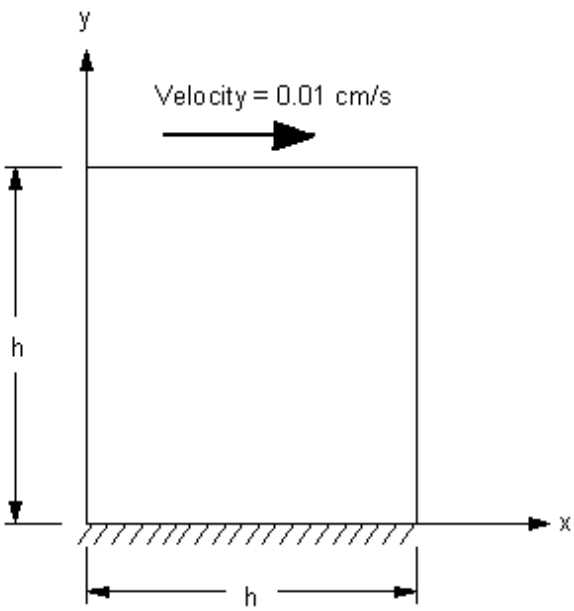

Problem Model

Material Properties	Geometric Properties
E_x (Young's Modulus) = 60.6 GPa υ (Poisson's Ratio) = 0.4999 S_o = 29.7 MPa Q/R = 21.08999E3 K A = 1.91E7 s^{-1} ξ = 7.0 m = 0.23348 h_o = 1115.6 MPa $\hat{S}$ = 18.92 MPa η = 0.07049 a = 1.3	h = 1 cm thickness = 1 cm **Loading** Temp = 400°C = 673°K Velocity (x-direction) = 0.01 cm/sec @ y = 1 cm Time = 20 sec

Analysis Assumptions and Modeling Notes

The problem is solved three times, each time with a different element type. The element types used are VISCO106 (2-D 4-node viscoplastic element), VISCO108 (2-D 8-node viscoplastic element), and VISCO107 (3-D 8-node viscoplastic element), respectively. The rate dependent viscoplastic model proposed by Anand is used in this problem.

The plane strain condition is assumed along the Z-axis. The velocity of 0.01 cm/sec in X-direction is achieved by applying x-displacement of 0.2 cm in 20 seconds. The shear load is computed from the solution results in POST26.

Results Comparison

		Target[1]	ANSYS	Ratio
VISCO106	F_x, N	845	843	0.997
VISCO108	F_x, N	845	843	0.997
VISCO107	F_x, N	845	843	0.997

1. Obtained from graphical solution

ANSYS Verification Manual . ANSYS Release 10.0 . 002184 . © SAS IP, Inc.

VM200: Viscoelastic Sandwich Seal Analysis

Overview

Reference:	T. F. Soules, R. F. Busbey, S. M. Rekhson, A. Markkovsky, M. A. Burkey, "Finite Element Calculations of Residual Stresses in Glass Parts Using MARC", General Electric Company (Nela Park), Report # 86-LRL-2022, Cleveland, OH, March 1986.
Analysis Type(s):	Static Analysis (**ANTYPE** = 0)
Element Type(s):	2-D 8-Node Viscoelastic Solid Elements (VISCO88) 3-D 20-Node Viscoelastic Solid Elements (VISCO89)
Input Listing:	vm200.dat

Test Case

A sandwich seal made of an alumina plate with G-11 glass cladding on both sides is cooled at 3° per minute from 618°C to 460°C and held isothermally for four hours. The seal is further cooled at 3° per minute to 18°C. FInd the maximum in-plane stress (σ_{max}) developed in the seal along with the corresponding temperature.

Figure 200.1 Viscoelastic Sandwich Seal Problem Sketch

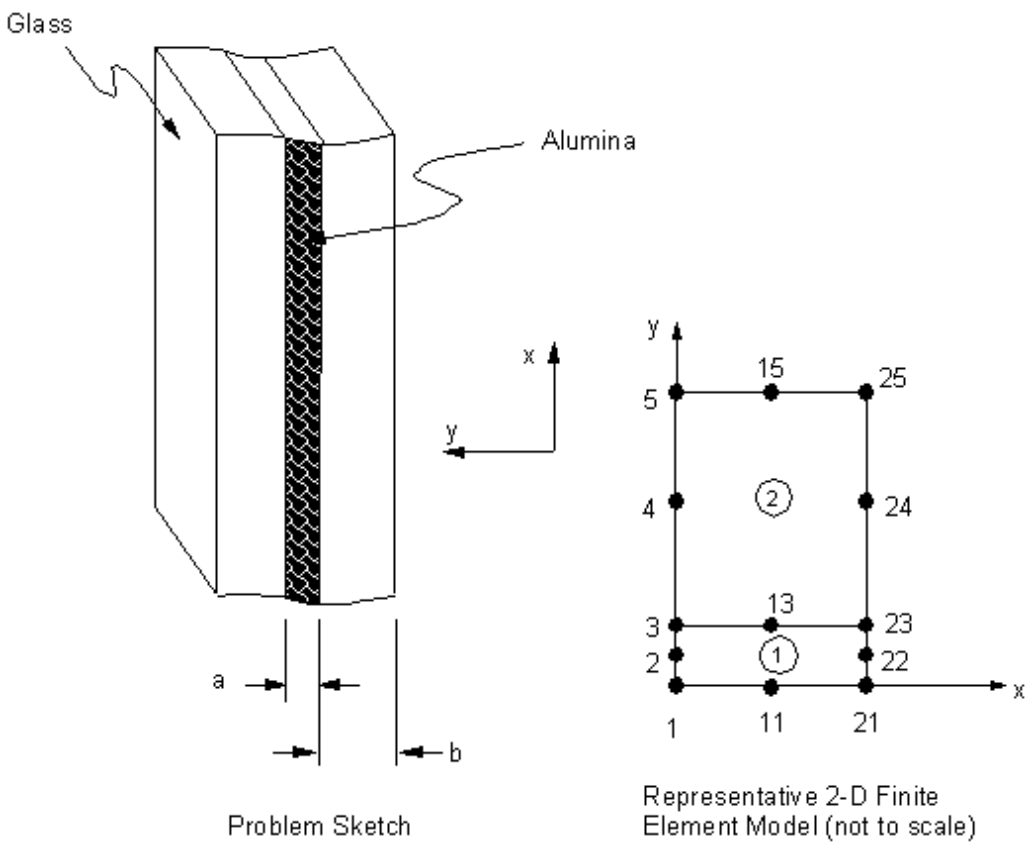

Material Properties **Material: G-11 Glass** **Material Variables** H/R (°K) = 6.45e4 X = 0.53 **No. of Maxwell Elements = 6** **For Volume Decay Function** C_{fi} = 0.108, 0.443, 0.166, 0.161, 0.046, 0.076 τ_{fi} = 3.00, 0.671, 0.247, 0.091, 0.033, 0.008 C_{li} = 3.43e-5 C_{gi} = 64.7e-7, 0.02e-7 T_{fi}(°) = 618, 618, 618, 618, 618, 618, GXY(0) = 0.0 GXY(∞) = 0.0 K(0), MPa = 6.05e4 K(∞), MPa = 6.05e4 **No. of Maxwell Elements for Shear Modulus Relaxation = 3** C_{smi} = 0.422, 0.423, 0.155 λ_{smi} = 0.0689, 0.0065, 0.0001 **No. of Maxwell Elements for Bulk Modulus Relaxation = 0** **Material: Alumina** **Material Variables** C_{gi} = 52.6e-7, 0.119e-7, -1.0e-11 GXY(0), MPa = 1.435e5 GXY(∞), MPa = 1.435e5 K(0), MPa = 3.11e5 K(∞), MPa = 3.11e5 See Viscoelastic Material Constants in the *ANSYS Elements Reference* for more explanation regarding the material parameters.	**Geometric Properties** a = 0.05 cm b = 0.325 cm **Loading** Reference Temp. = 618°C Temp. Offset = 273 **Load Step 1;** Uniform Temp. (TUNIF) = 618°C **Load Step 2:** TUNIF = 460°C TIME = 3160 sec. **Load Step 3:** TUNIF = 460°C TIME = 17560 sec. **Load Step 4:** TUNIF = 460°C TIME = 26400 sec.

Analysis Assumptions and Modeling Notes

The problem is solved first using 2-D viscoelastic elements (VISCO88) and then using 3-D viscoelastic elements (VISCO89).

In the 2-D case, due to the fact that the stresses will be the same in X and Z directions because of symmetry, an axisymmetric analysis is performed with the nodal degrees of freedom coupled in appropriate directions. The radial thickness of 0.2 cm is arbitrarily selected. Nodes 21 through 25 are coupled in the X-direction (radial coupling). Nodes with the same Y-location are coupled in Y-direction (axial coupling).

In the 3-D case, an arbitrary thickness of 0.2 cm is assumed in both Y and Z directions. Nodal degrees of freedom are coupled in appropriate directions to simulate the correct physical behavior in the finite element model.

The alumina is not a viscoelastic material, however, its material properties are input using viscoelastic format so that only one element type (VISCO88 in 2-D and VISCO89 in 3-D) can be used for both materials. Also, note that the viscoelastic material does not require the **MP** command for inputting the material properties. POST26 is used to extract the results from the solution phase.

Results Comparison

		Target	ANSYS	Ratio
VISCO88	$Stress_{max}$, MPa	12.5	12.5	1.000

	Temp, °C	460.0	460.0	1.000
		Target	**ANSYS**	**Ratio**
VISCO89	$Stress_{max}$, MPa	12.5	12.5	1.000
	Temp, °C	460.0	460.0	1.000

Figure 200.2 In-plane Stress Versus Temperature

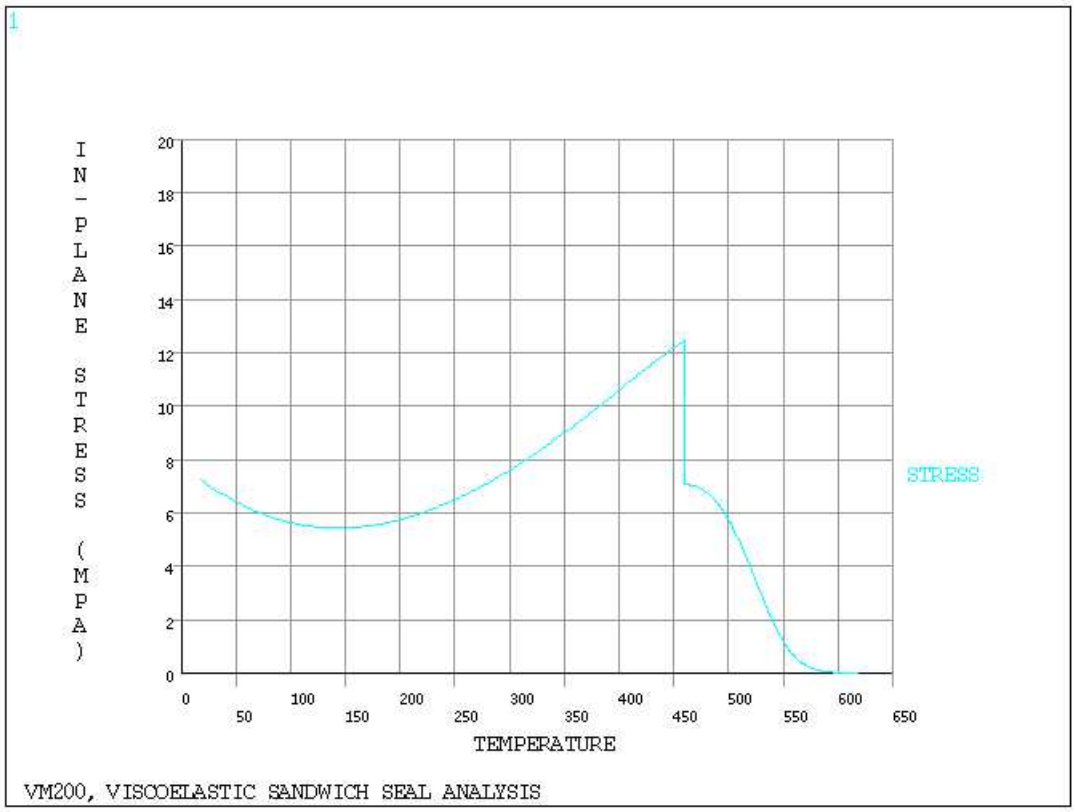

VM201: Rubber Cylinder Pressed Between Two Plates

Overview

Reference:	T. Tussman, K-J Bathe, "A Finite Element Formulation for Nonlinear Incompressible Elastic and Inelastic Analysis", *Computers and Structures*, Vol. 26 Nos 1/2, 1987, pp. 357-409.
Analysis Type(s):	Static Analysis (**ANTYPE** = 0)
Element Type(s):	2-D 4-Node Structural Solid Elements (PLANE182) 3-D 8-Node Structural Solid Elements (SOLID185) 2-D 8-Node Structural Solid Elements (PLANE183) 2-D/3-D Node-to-Surface Contact Elements (CONTA175) Meshing Facet (MESH200)
Input Listing:	vm201.dat

Test Case

A long rubber cylinder is pressed between two rigid plates using a maximum imposed displacement of δ_{max}. Determine the force-deflection response.

Figure 201.1 Rubber Cylinder Problem Sketch

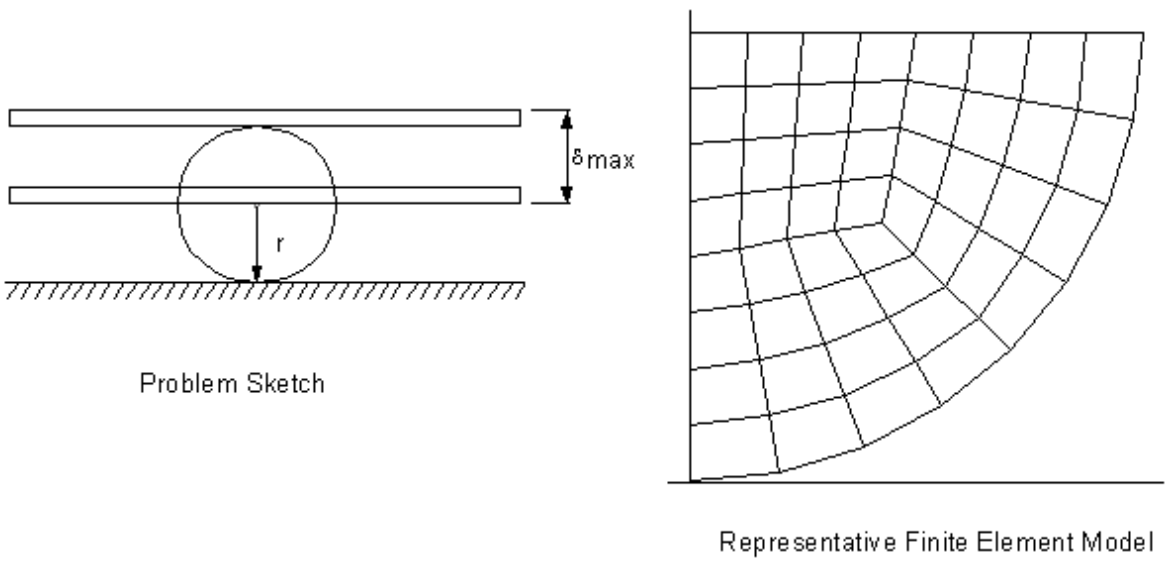

Material Properties	**Geometric Properties**
E = 2.82 MPa	r = 0.2 m
υ = 0.49967	**Loading**
Mooney-Rivlin Constants	δ_{max} = 0.2 m
C1 = 0.293 MPa	
C2 = 0.177 MPa	

Analysis Assumptions and Modeling Notes

A plane strain solution is assumed based on the geometry of the problem. Due to geometric and loading symmetry, the analysis can be performed using one quarter of the cross section. All nodes on the left edge (X = 0) are constrained, UX = 0. All nodes on the top edge (y = 0) are coupled in UY. An imposed displacement of -0.1 m acts upon the coupled nodes.

This problem was solved in several ways:

- A 2-D model using PLANE182 with CONTA175 elements
- A 3-D model using SOLID185 with CONTA175 elements
- A 2-D model using PLANE182 with CONTA175 element and solved using Lagrange Multipliers method.
- A 3-D model using SOLID185 with CONTA175 element and solved using Lagrange Multipliers method.

In the 3-D case, a MESH200 element is used as the target face for the automatic generation of contact elements. The target surface is given a high contact stiffness (KN = 2000 MPa) to model a rigid surface and no contact stiffness is required to be specified while performing the solution using Lagrange Multipliers method.

Results Comparison

	Target[1]	ANSYS	Ratio
PLANE182 with 2-D CONTA175			
Force at Displacement = 0.1	0.25	0.27	1.063
Force at Displacement = 0.2	1.40	1.40	0.996
SOLID185 with 3-D CONTA175			
Force at Displacement = 0.1	0.25	0.27	1.064
Force at Displacement = 0.2	1.40	1.40	0.998
SOLID182 with 2-D CONTA175 with KEYOPT (2) = 3			
Force at Displacement = 0.1	0.25	0.27	1.064
Force at Displacement = 0.2	1.40	1.40	0.999
SOLID185 with 3-D CONTA175 with KEYOPT (2) = 4			
Force at Displacement = 0.1	0.25	0.27	1.065
Force at Displacement = 0.2	1.40	1.40	0.999

1. Determined from graphical results. See T. Tussman, K-J Bathe, “A Finite Element Formulation for Nonlinear Incompressible Elastic and Inelastic Analysis”, pg. 385, fig. 6.14.

Figure 201.2 Displaced Shape

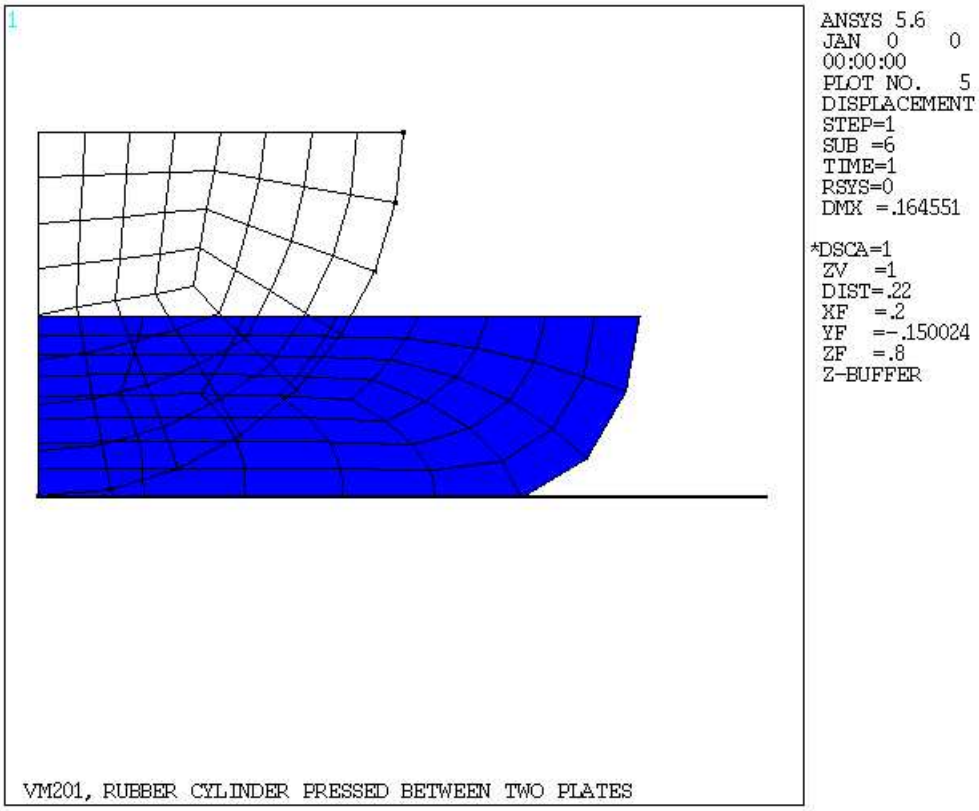

Figure 201.3 Force vs. Displacement

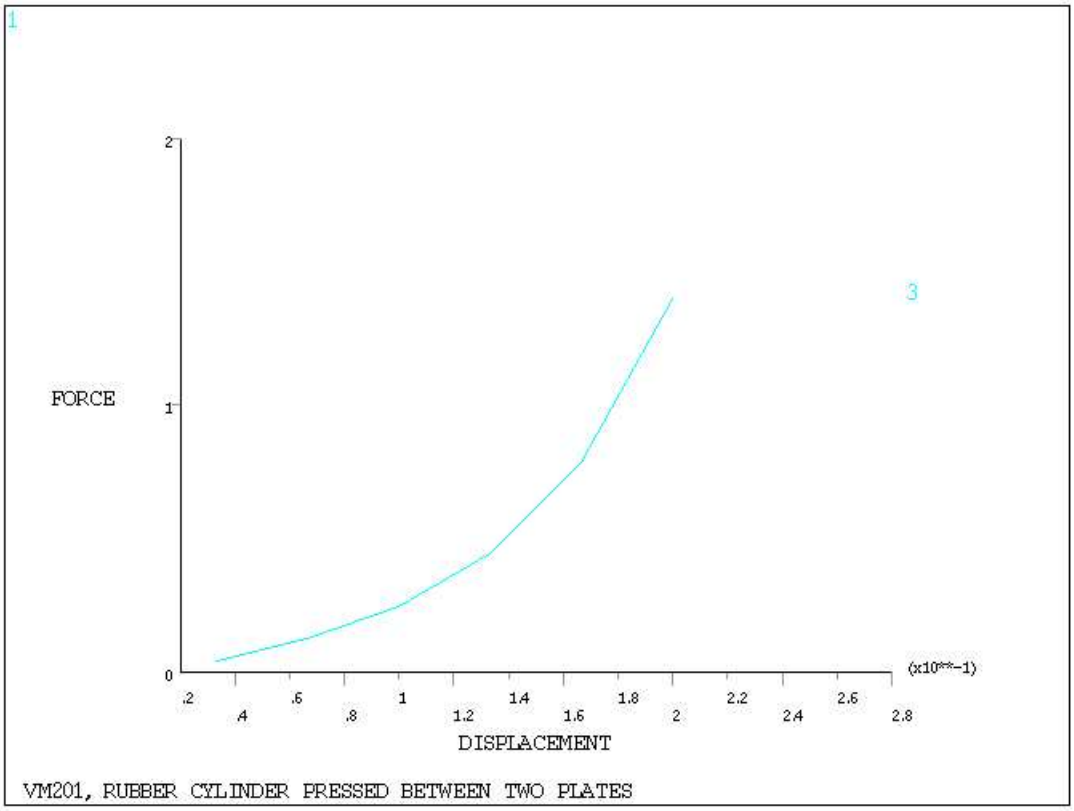

VM202: Transverse Vibrations of a Shear Beam

Overview

Reference:	R. D. Blevins, *Formulas for Natural Frequency and Mode Shape*, Van Nostrand Reinhold Co., New York, NY, 1979, pp. 171-176.
Analysis Type(s):	Mode-frequency Analysis (**ANTYPE** = 2)
Element Type(s):	Shear/Twist Panel Elements (SHELL28)
Input Listing:	vm202.dat

Test Case

A short, thin-walled uniform shear beam clamped at the base vibrates freely. Determine the first two modes of vibrations neglecting all flexural deformations.

Figure 202.1 Shear Beam Problem Sketch

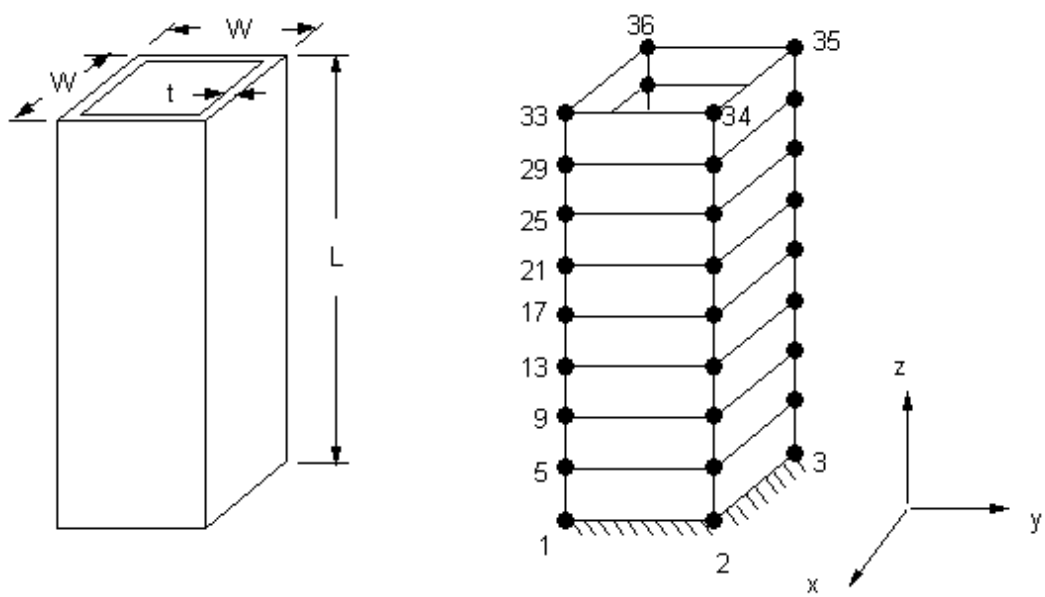

Problem Sketch Representative Finite Element Model

Material Properties	**Geometric Properties**
E = 200 GPa	L = 30 m
υ = 0.27	W = 10 m
ρ = 7860 Kg/m^3	t = 0.1 m

Analysis Assumptions and Modeling Notes

Flexural deformations were eliminated by requiring all nodes with the same Z coordinate value to be coupled in UX and UY. Since this is a square beam, the frequencies are repeated, one made in the X direction, the other in the Y direction.

Results Comparison

	Target	ANSYS	Ratio
f1, Hz	17.375	18.696	1.076
f2, Hz	52.176	57.278	1.098

Figure 202.2 Mode Shape 1 (f = 18.62 Hz)

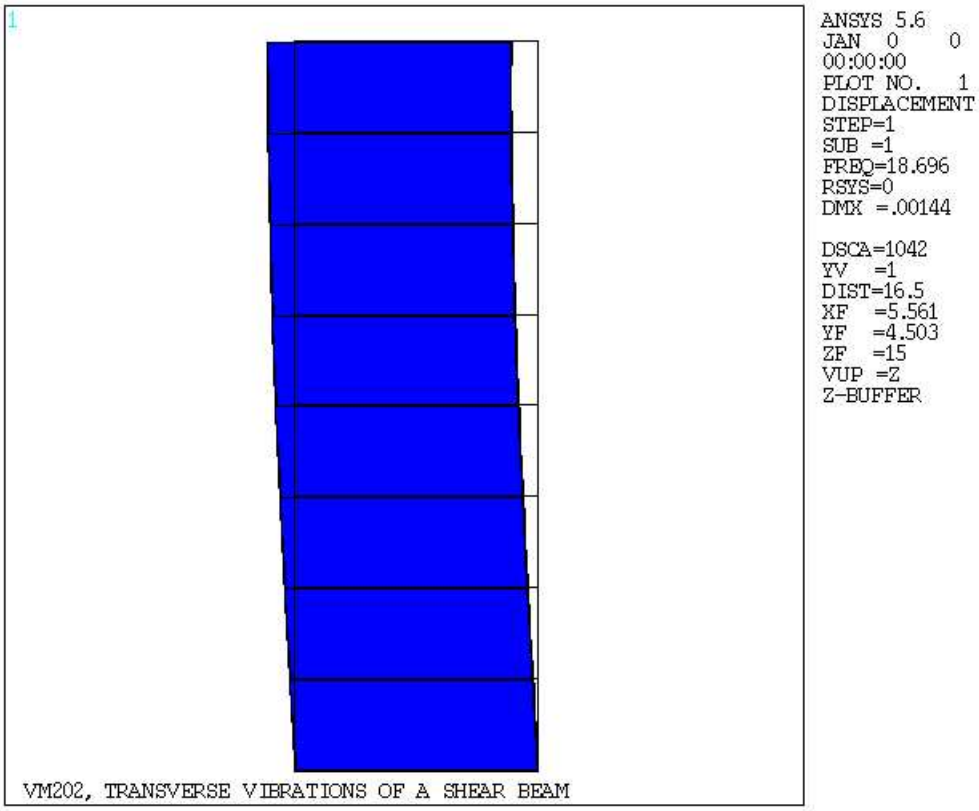

Figure 202.3 Mode Shape 2 (f = 55.15 Hz)

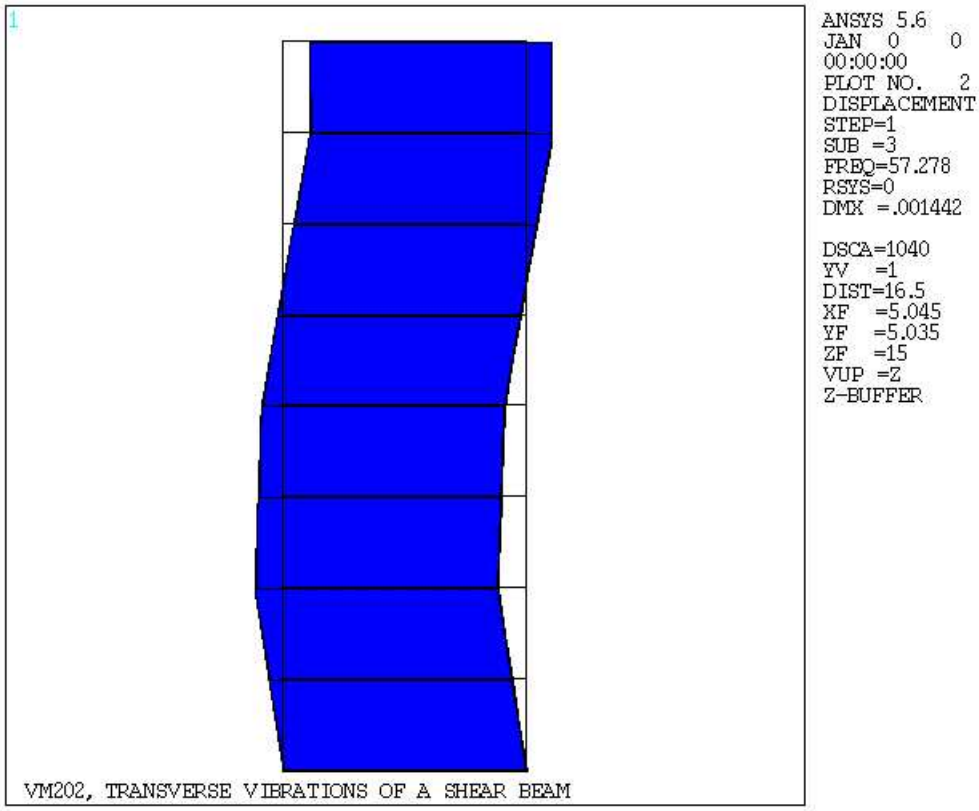

VM203: Dynamic Load Effect on Supported Thick Plate

Overview

Reference:	NAFEMS, *Selected Benchmarks for Forced Vibration*, Report prepared by W. S. Atking Engineering Sciences, April 1989, Test 21R.
Analysis Type(s):	Mode-frequency, Spectrum Analysis (**ANTYPE** = 8) Harmonic Analysis (**ANTYPE** = 3)
Element Type(s):	8-Node Structural Shell Elements (SHELL93)
Input Listing:	vm203.dat

Test Case

A simply-supported thick square plate of length ℓ, thickness t, and mass per unit area m is subject to random uniform pressure power spectral density. Determine the peak one-sigma displacement at undamped natural frequency.

Figure 203.1 Thick Square Plate Problem Sketch

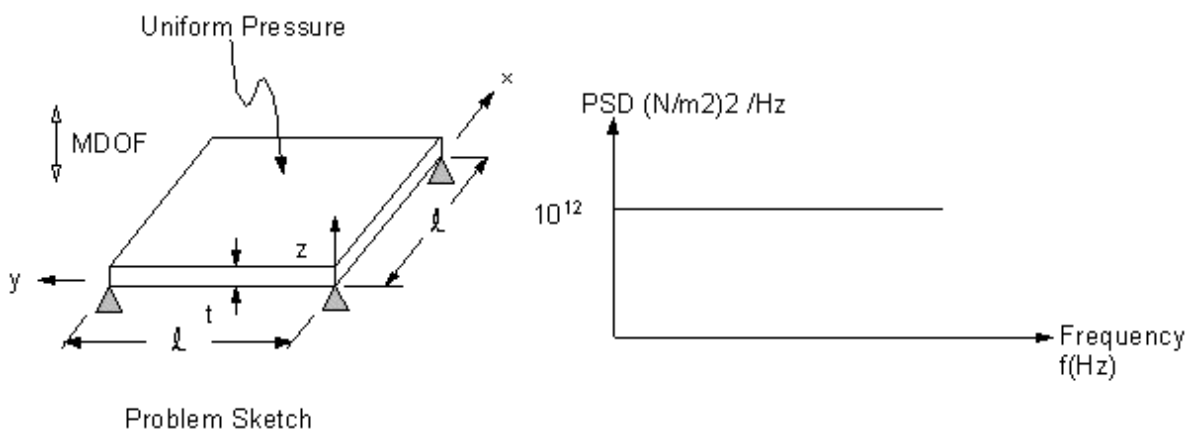

Material Properties	Geometric Properties	Loading
$E = 200 \times 10^9$ N/m^2 $\mu = 0.3$ m = 8000 kg/m^3	ℓ = 10 m t = 1.0 m	PSD = $(10^6$ N/m$^2)^2$ /Hz Damping δ = 2%

Analysis Assumptions and Modeling Notes

All degrees of freedom in the z direction are selected as master degrees of freedom (MDOF). Equivalent nodal forces are obtained from a uniform pressure load by a static run with all UZ degrees of freedom constrained.

Frequency range of 1.0 Hz to 80 Hz was used as an approximation of the white noise PSD forcing function frequency. Equivalent analyses are done with Spectrum and Harmonic (with the ANSYS POST26 random vibration calculation capabilities which used the results of a damped harmonic response analysis) analyses, to compare the peak one-sigma standard deviation.

Some of the commands in POST26 followed by harmonic analysis have been undocumented since ANSYS Revision 5.0, but they are compatible to all subsequent ANSYS revisions.

Results Comparison

	Target	ANSYS	Ratio
Frequency f (Hz)	45.9	46.30[1]	1.009
Peak Deflection PSD (mm^2/Hz)	3401.8	3595.0[2]	1.057

1. From modal analysis solution
2. Peak amplitude ($x10^6$) from Harmonic analysis results using POST26

The peak one-sigma standard deviation from spectrum analysis (102.18 mm) agrees with the value from Harmonic analysis (108.16 mm), (No closed form solution is available from the reference for this entity.)

Figure 203.2 Harmonic Response to Uniform PSD Force

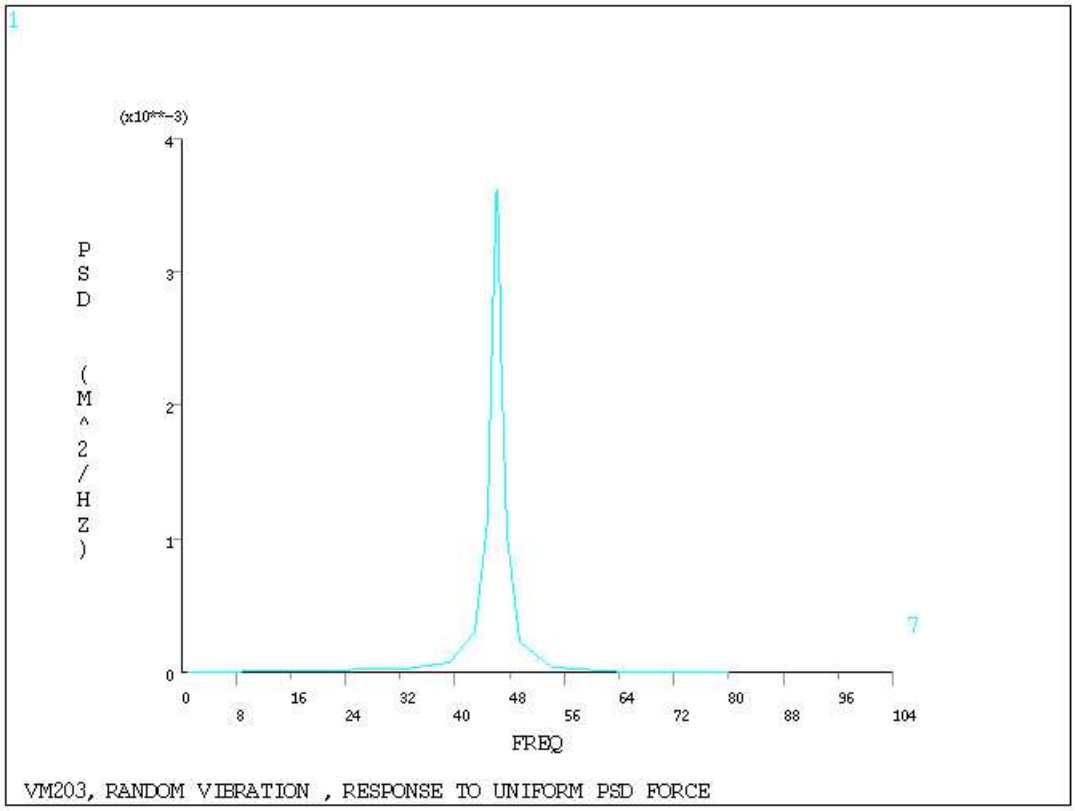

VM204: Solid Model of an Axial Bearing

Overview

Reference:	Any basic geometry text
Analysis Type(s):	Solid Modeling Boolean Operations
Element Type(s):	None
Input Listing:	vm204.dat

Test Case

Find the volume of the axial bearing shown below.

Figure 204.1 Axial Bearing Problem Sketch

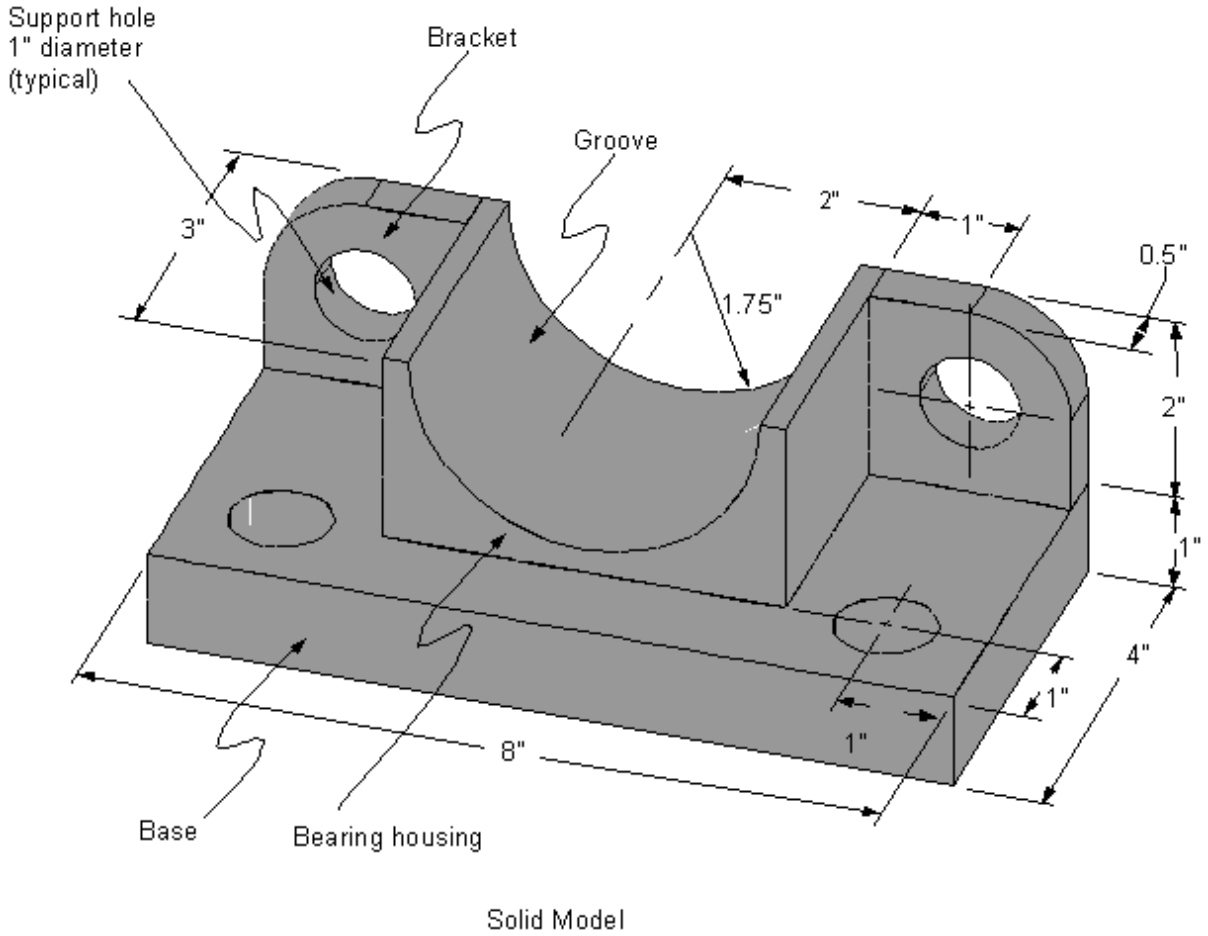

Analysis Assumptions and Modeling Notes

The model is created entirely using only geometric primitives and solid model Boolean operations. A glue operation is used to provide continuity between model entities.

Results Comparison

	Target	ANSYS	Ratio
Volume	42.997	42.995	1.000

Figure 204.2 Solid Model of an Axial Bearing

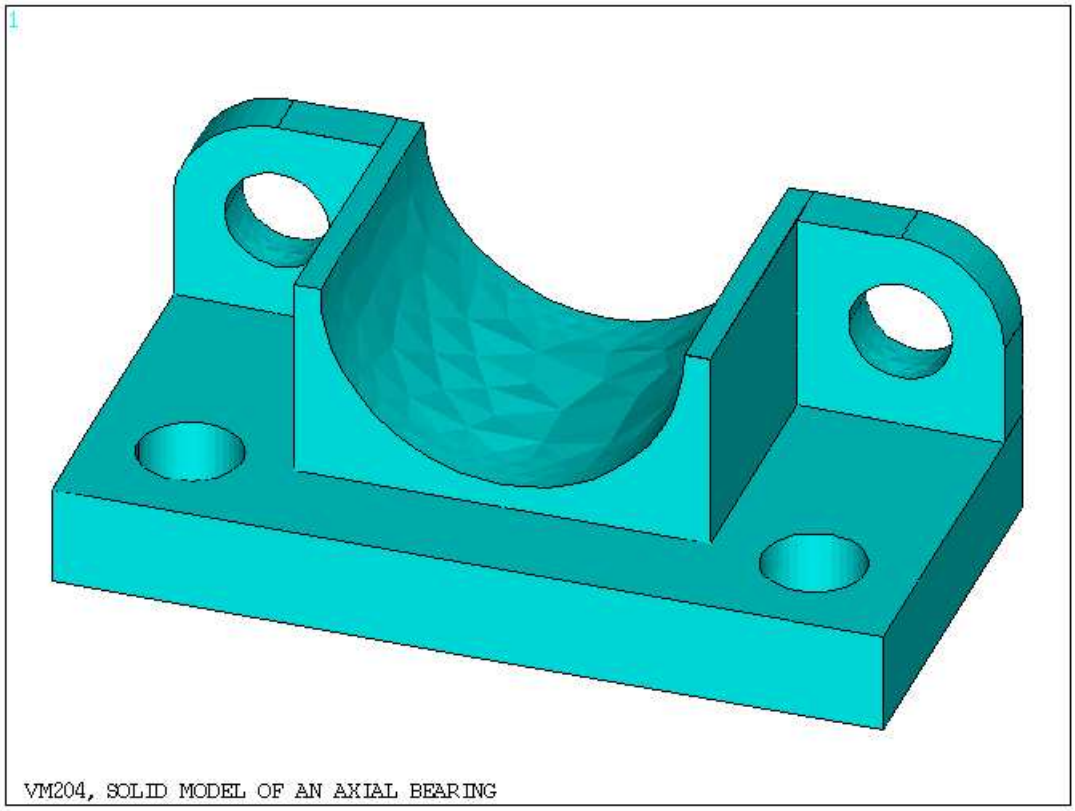

VM205: Adaptive Analysis of an Elliptic Membrane

Overview

Reference:	J. Barlow, G. A. O. Davis, "Selected FE Benchmarks in Structural and Thermal Analysis", *NAFEMS Report FEBSTA*, Rev. 1, October 1986, Test No. LE1 (modified).
Analysis Type(s):	Static Analysis (**ANTYPE** = 0)
Element Type(s):	2-D Structural Solid Elements (PLANE42) 2-D 8-Node Structural Solid Elements (PLANE82)
Input Listing:	vm205.dat

Test Case

An elliptic membrane structure of thickness t is subjected to a uniformly distributed outward pressure P. Determine the tangential edge stress σ_y at target point D.

Figure 205.1 Elliptic Membrane Problem Sketch

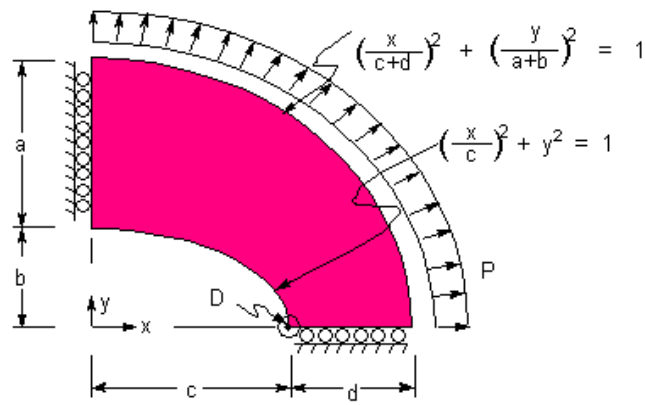

Problem Sketch

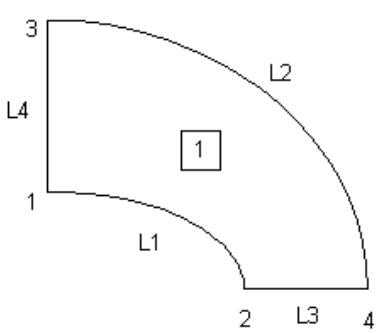

Area, Line and Keypoint Model

Material Properties	Geometric Properties	Loading
E = 210 x 10^3 MPa υ = 0.3	a = 1.75 m b = 1.0 m c = 2.0 m d = 1.25 m t = 0.1 m	At x = 0 UX = 0 At y = 0 UY = 0 Along outer edge P = -10 MPa

Analysis Assumptions and Modeling Notes

The problem is solved first using lower order 2-D structural solid elements (PLANE42) and then higher order 2-D structural solid elements (PLANE82). For both cases, the membrane is modeled with one area and the automatic adaptive meshing procedure is used to refine the mesh in the area of stress concentration (target location at point D).

In the first case, the analysis is performed by running the problem until the SEPC (structural percent error in energy norm) is close to 7.0 percent, whereas in the second case, analysis is performed until the SEPC is close to 5.0 percent. In the second case, the target value of SEPC is set less than the first case since higher order elements are generally more accurate.

POST1 is used to obtain the final value of SEPC and the ***GET** command is used to obtain the tangential stress, σ_y, at the target point D.

Results Comparison

		Target	ANSYS	Ratio
PLANE42[1]	$Stress_y$ (MPa)	92.70	92.48	0.998
PLANE82[1]	$Stress_y$ (MPa)	92.70	91.83	0.991

1. Corresponding to the final mesh with SEPC of 5.5 (for a PLANE42 model) and 0.1 (for a PLANE82 model)

Figure 205.2 Final PLANE42 Mesh (SEPC = 5.5)

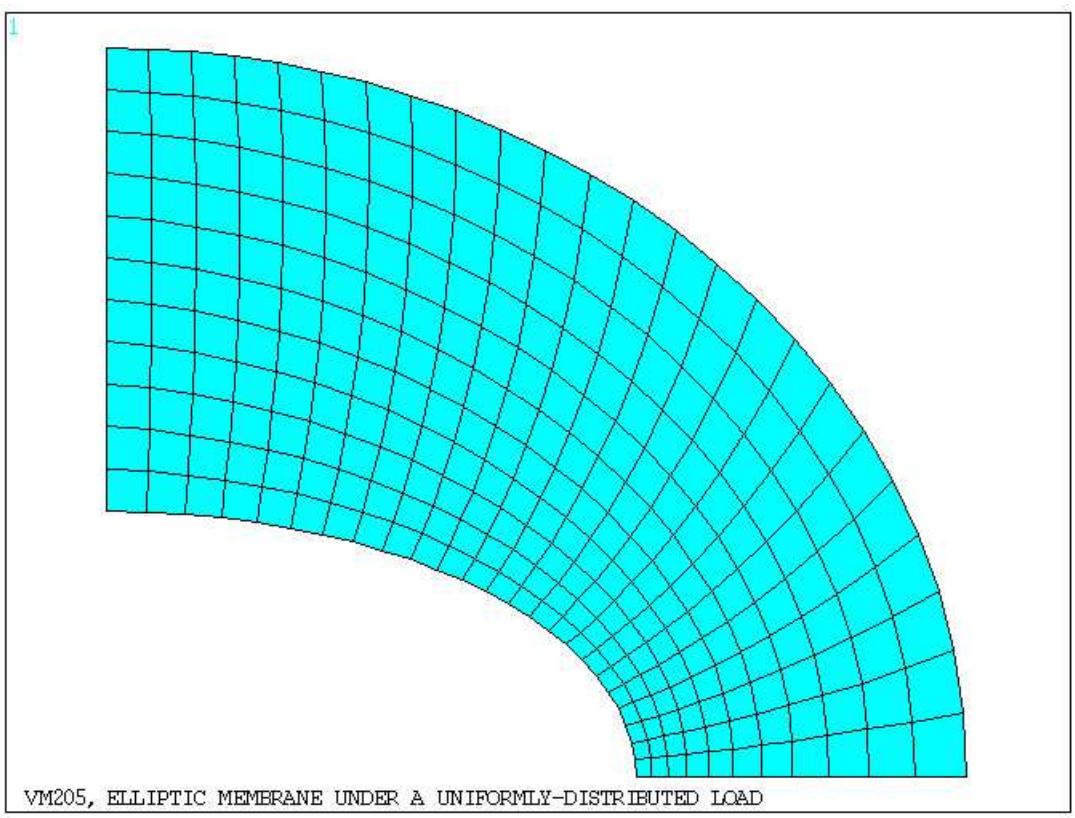

Figure 205.3 Final PLANE82 Mesh (SEPC = 0.1)

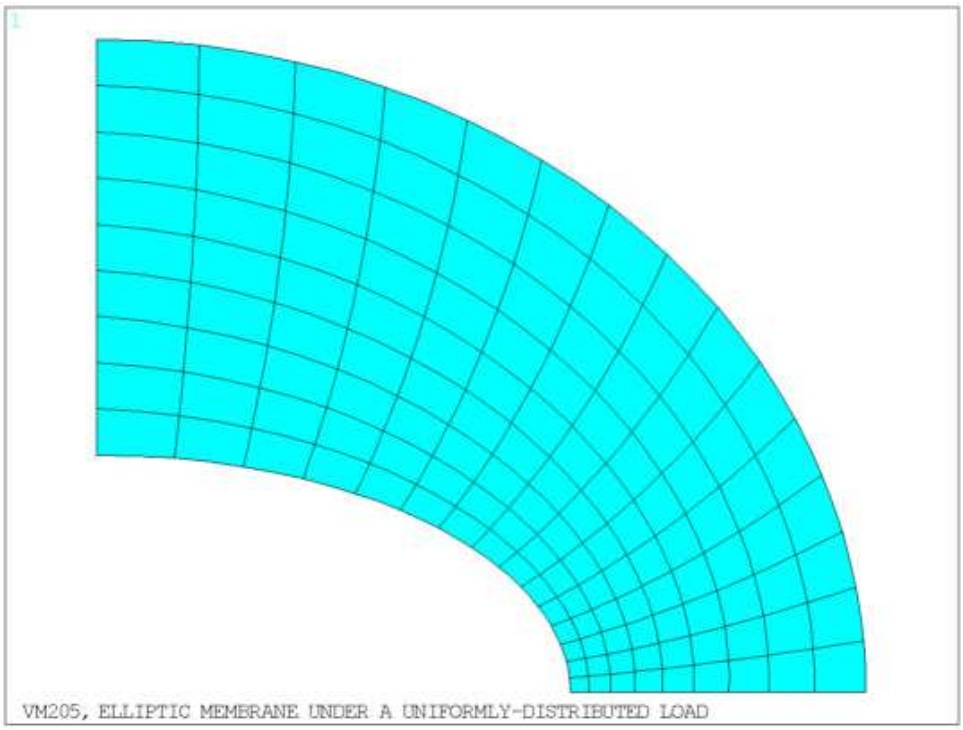

VM206: Stranded Coil with Voltage Excitation

Overview

Reference:	W. B. Boast, *Principles of Electric and Magnetic Fields*, Harper & Brothers, New York, NY, 1948, pg. 247, eq. 12.18.
Analysis Type(s):	Static, Harmonic
Element Type(s):	2-D 8-Nnode Magnetic Solid Elements (PLANE53) 2-D Infinite Solid Elements (INFIN110)
Input Listing:	vm206.dat

Test Case

A stranded coil with 500 turns is modeled in free space. A static analysis with a 12 volt DC excitation is run first to calculate the coil resistance and inductance. A 1/4 symmetry model is constructed. An AC (harmonic) analysis is run to simulate an RL circuit response with an applied excitation of 12 volts at 60 Hz. The complex coil current is calculated.

Figure 206.1 Stranded Coil Problem Sketch

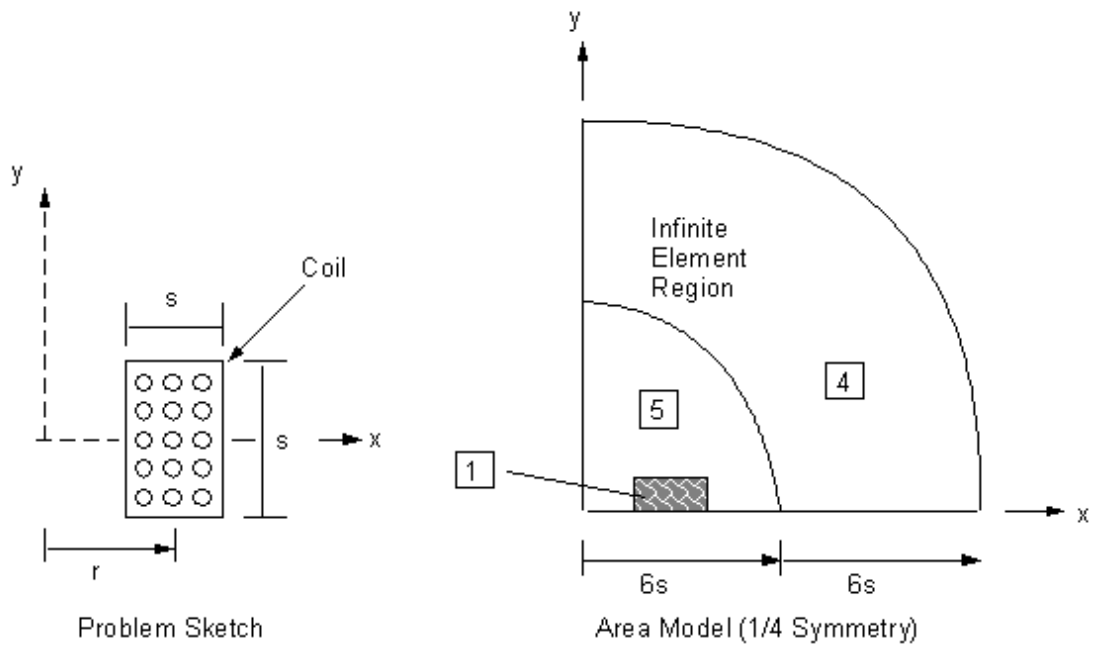

Material Properties	Geometric Properties	Loading
$\mu_r = 1.0$ (coil) $\mu_r = 1.0$ (air) $\rho = 3 \times 10^{-8}$ ohm-m (coil)	n = 500 turns s = .02 (coil winding width and depth) m r = (3 x s)/2 m	$V_o = 12$ volts (static) $V = V_o \cos \omega t$ (harmonic) where $V_o = 12$ volts $\omega = 60$ Hz

Analysis Assumptions and Modeling Notes

Due to symmetry only 1/4 of the problem domain is required. The open boundary is modeled with infinite elements to accurately represent the decaying field. The infinite element region is set to a depth (6xs) equal to the problem domain (6xs) for optimal performance.

The coil is characterized through the real constant table. A direct voltage load is applied to the coil region. Nodes in the coil region are coupled in the CURR degree of freedom to solve for a single valued coil current (per turn).

The coil resistance and inductance are calculated by summing element values in POST1. The real and imaginary current are extracted from the AC solution. From these calculated currents, and the applied voltage, the coil impedance can be calculated.

Results Comparison

		Target	ANSYS	Ratio
Static Analysis	Inductance, H	.01274	.01275	1.00
	Resistance, Ohm	3.534	3.534	1.00
	Coil current, Amps	3.395	3.395	1.00
Harmonic Analysis	Real solution, Amps	1.192	1.19209	1.00
	Imag solution, Amps	-1.621	-1.62063	1.00

VM207: Stranded Coil Excited by External Circuit

Overview

Reference:	W. B. Boast, *Principles of Electric and Magnetic Fields*, Harper & Brothers, New York, NY, 1948, pg. 247, eq. 12.18.
Analysis Type(s):	Static
Element Type(s):	2-D 8-Node Magnetic Solid Elements (PLANE53) 2-D Infinite Solid Elements (INFIN110) Electric Circuit Elements (CIRCU124)
Input Listing:	vm207.dat

Test Case

A stranded coil with 500 turns and a fill factor of 0.9 is connected to an external circuit consisting of an independent voltage source and a 2 ohm resistor. A static analysis is run with a 12 volt DC excitation to determine the coil resistance and inductance. A transient analysis is run to calculate the coil current response to a step 12 volt excitation.

Figure 207.1 Stranded Coil Problem Sketch

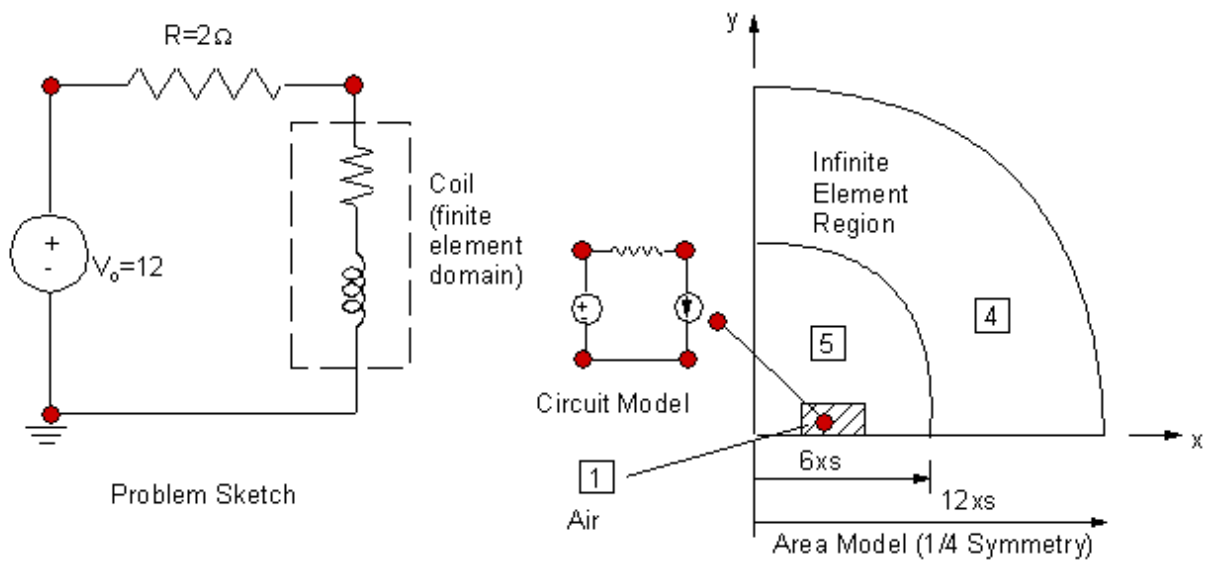

Material Properties	**Geometric** Properties	**Loading**
$R_{ext} = 2\ \Omega$ $\mu_r = 1.0$ (coil) $\mu_r = 1.0$ (air) $\rho = 3.04878 \times 10^{-8}$ ohm-m (coil)	N = 500 turns S = .02 m R = 3(s)/2 m FC = .9 Fill factor	$V_o = 12$ volts (static) $V_o\|_{t=0+} = 12$ volts (static)

Analysis Assumptions and Modeling Notes

The problem is similar to VM206 except the coil is excited by an external circuit using the general circuit element. In the circuit, the coil is modeled by a stranded coil circuit component that shares a common node with the coil in the finite element model. The finite element model provides to the circuit the necessary coil resistance and inductance to characterize the stranded coil circuit impedance. The nodes in the coil region are coupled in the EMF and CURR degrees of freedom so that a single voltage drop (EMF) and coil current (CURR) are calculated.

A static analysis is run to obtain the coil resistance and inductance so that an analytical solution of the transient response can be calculated and compared to the solution results. A transient solution to a step voltage excitation is run for .01 seconds. The calculated coil current is compared to the solution current. The coil current response is plotted versus time.

Results Comparison

		Target	ANSYS	Ratio
Static Analysis	Inductance, Henry	.01274	0.01275	1.00
	Resistance, Ohm	3.991	3.99084	1.00
Transient Analysis	Current, Amps	1.985	1.98324	.999

Figure 207.2 Current vs. Time

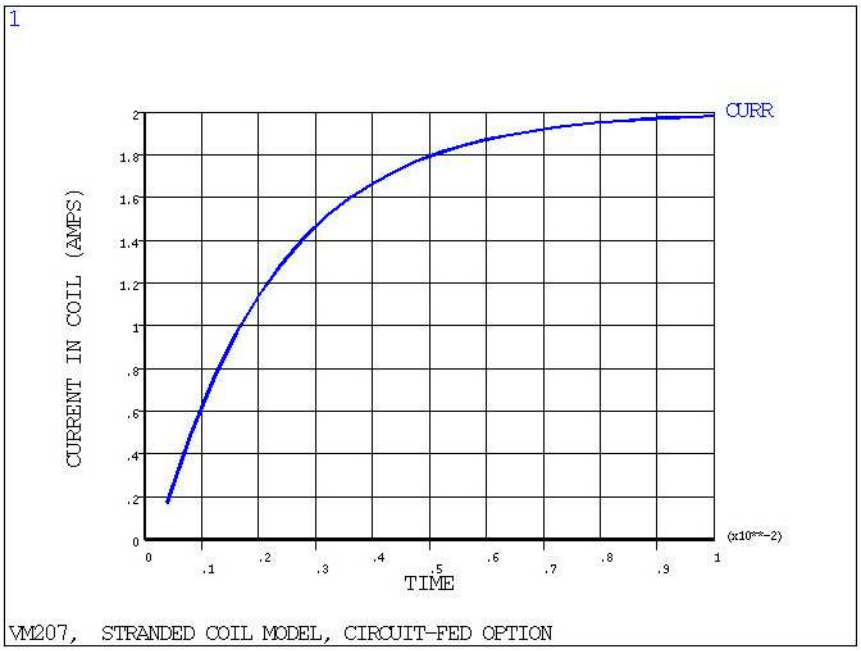

VM208: RL Circuit with Controlled Source

Overview

Reference:	J. O'Malley, *Schaum's Outline of Theory and Problems of Basic Circuit Analysis*, 2nd Edition, McGraw-Hill Book Co., Inc., New York, NY, 1992, Problem 14.23, Figure 14.25.
Analysis Type(s):	Harmonic
Element Type(s):	Electric Circuit Elements (CIRCU124)
Input Listing:	vm208.dat

Test Case

A circuit consists of 2 resistors, an inductor, an independent voltage source, an independent current source, and a current-controlled current source. Determine the voltage at node 4 in the circuit.

Figure 208.1 RL Circuit Problem Sketch

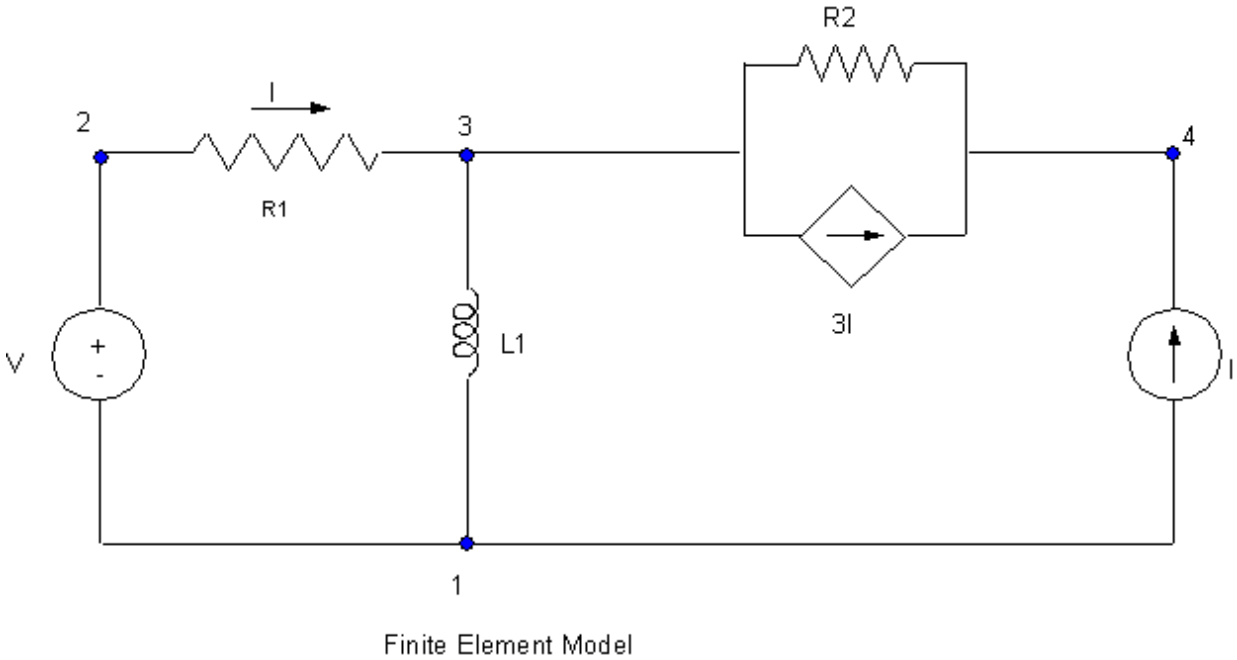

Circuit Values	**Loading**
$R_1 = 3\ \Omega$	V = 15 volts at a phaser angle of 30°
$R_2 = 2\ \Omega$	I = 5 amps at a phaser angle of -45°
$L_1 = j4\ \Omega$	
AI = -3	

Analysis Assumptions and Modeling Notes

A harmonic analysis is run at a frequency of 1/2 π Hz so that the inductor impedance value can be simply input as 4 ohms. Care must be exercised in assigning the node values to the current controlled current source (CCCS) to correctly account for the sign on the CCCS gain (AI).

Results Comparison

@ Node 4	Target	ANSYS	Ratio
Real Voltage, V	16.44	16.46	1.001
Imag Voltage, V	-1.41	-1.41	1.00

ANSYS Verification Manual . ANSYS Release 10.0 . 002184 . © SAS IP, Inc.

VM209: Multiple Species Flow Entering a Circular Pipe

Overview

Reference:	W. M. Kays, M. E. Crawford, *Convective Heat and Mass Transfer*, 3rd Edition, McGraw-Hill Book Co., Inc., New York, NY, 1993, pp. 126-134.
Analysis Type(s):	Multiple Species Analysis (**FLOTRAN**)
Element Type(s):	2-D Fluid-Thermal Elements (FLUID141)
Input Listing:	vm209.dat

Test Case

Flow of two species (A and B), entering a circular pipe is considered. The flow is hydrodynamically developed. This condition is guaranteed by specifying uniform but dissimilar pressure at the inlet and outlet of the pipe. Uniform and dissimilar mass fractions are specified at the pipe inlet and wall. Fluid properties are assumed to be the same for both species, so that computed results can be compared with analytical solution.

Figure 209.1 Multiple Species Flow Problem Sketch

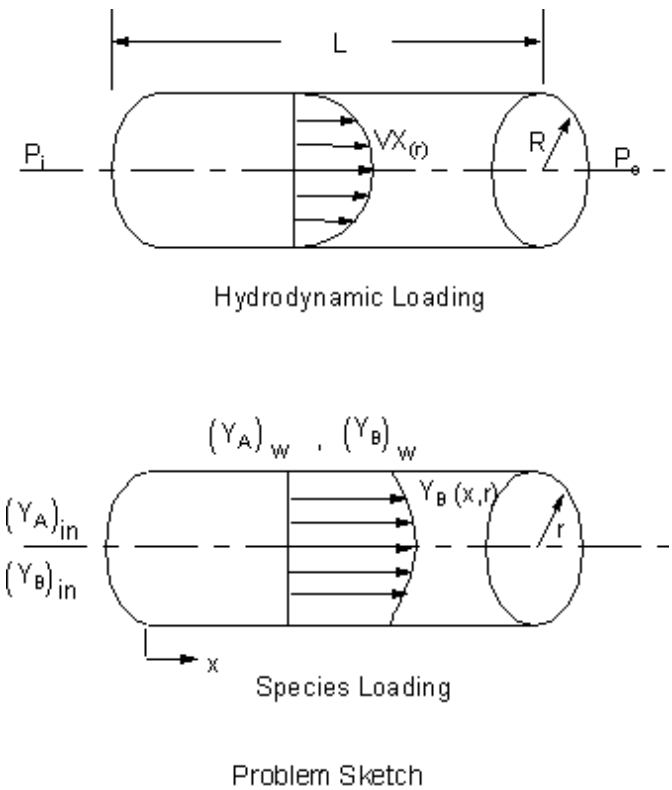

Material Properties	Geometric Properties
Species A ρ = 1 kg/m^3 μ = 1.0 x 10^{-5} Pa-s D_{BA} = 1.43 x 10^{-5} m^2/s **Species B** ρ = 1 kg/m^3 μ = 1.0 x 10^{-5} Pa-s D_{BA} = 1.43 x 10^{-5} m^2/s	Pipe length = 0.1 m Pipe radius = 0.0025 m **Loading** Pressure Differential between the pipe inlet and outlet, ΔP = 1.28 Pa Mass fraction of species A at pipe inlet, $(Y_A)_{in}$ = 0.0 Mass fraction of species B at pipe inlet, $(Y_B)_{in}$ = 1.0 Mass fraction of species A at pipe wall, $(Y_A)_w$ = 1.0 Mass fraction of species A at pipe wall, $(Y_B)_w$ = 0.0

Analysis Assumptions and Modeling Notes

- Steady-state flow
- Incompressible flow
- Fully developed velocity field
- Fluid properties are the same and constant for both species
- No source terms
- No body forces

With the above assumptions, axial momentum equation for the mixture becomes:

$$\frac{\mu}{r}\frac{d}{dr}\left(r\frac{dVX}{dr}\right)=\left(\frac{d\rho}{dx}\right)$$

Applying the boundary conditions:

$$VX = 0 \text{ at } r = R \quad \text{and} \quad \frac{dVX}{dr} = 0 \text{ at } r = 0$$

we readily obtain:

$$VX = \frac{R^2}{4\mu}\left(\frac{\Delta P}{L}\right)\left(1-\frac{r^2}{R^2}\right)$$

or

$$VX = 2(VX)_{average}\left(1-\frac{r^2}{R^2}\right)$$

where

$$(VX)_{average} = \frac{1}{R^2}\int_0^R V_X\, r\, dr$$

For this problem, species transport equation can be simplified as follows:

$$\frac{\partial^2 Y_i}{\partial r^2}+\frac{1}{r}\frac{\partial Y_i}{\partial r}=\frac{VX}{D_{AB}}\frac{\partial Y_i}{\partial x}-\frac{\partial^2 Y_i}{\partial x^2} \quad , \; i = A,B$$

Let us introduce the following dimensionless variables:

$$\theta_i = \frac{(Y_i)_w - Y_i}{(Y_i)_w - (Y_i)_{in}}$$

$$r^+ = \frac{r}{R} \quad , \qquad VX^+ = \frac{VX}{(VX)_{average}} \quad , \qquad x^+ = \frac{x/R}{Re\,Sc}$$

where, Reynold's number is

$$Re = \frac{\rho (VX)_{average} D}{\mu}$$

and, Schmidt number is

$$Sc = \frac{\mu}{\rho D_{AB}}$$

Substituting the non-dimensional variables into the species transport equation, we get:

$$\frac{\partial^2 \theta_i}{\partial r^{+2}} + \frac{1}{r^+}\frac{\partial \theta_i}{\partial r^+} = \frac{VX^+}{2}\frac{\partial \theta_i}{\partial x^+} - \frac{1}{(Re\,Sc)^2}\frac{\partial^2 \theta_i}{\partial x^{+2}}$$

For large values of the product (ReSc) second term on the right-hand side of the equation can be neglected. For our problem:

$$VX = \frac{(0.0025)^2}{(4)(1.0\times 10^{-5})}\left(\frac{1.28}{0.1}\right)(1 - 1.6\times 10^5\, r^2)$$

$$(VX)_{average} = \frac{1}{(1.6\times 10^5)^2}\int_0^{0.1} 2.0\,(1-(1.6\times 10^5) r^2)\, r\, dr = 1 m/sec$$

so

$$Re = \frac{(1.0)(1.0)(0.005)}{1\times 10^{-5}} = 500$$

$$Sc = \frac{1.0\times 10^{-5}}{1.43\times 10^{-5}} \cong 0.7$$

So, we can neglect the second term on the RHS.

Substituting the dimensionless velocity profile in the species transport equation we obtain:

$$\frac{\partial^2 \theta_i}{\partial r^{+2}} + \frac{1}{r^+}\frac{\partial \theta_i}{\partial r^+} = (1 - r^{+2})\frac{\partial \theta}{\partial x^+}$$

And boundary conditions become:

$$\theta_i = 1 \text{ at } x^+ = 0$$

$$\theta_i = 0 \text{ at } r^+ = 1$$

$$\frac{\partial \theta_i}{\partial r^+} = 0 \text{ at } r^+ = 0$$

The final solution takes the form:

$$\theta_i(x^+, r^+) = \sum_{n=0}^{\infty} C_n R_n(r^+) \exp(-\lambda_n^2 x^+)$$

where the λ_n are the eigenvalues, the R_n are the corresponding eigenfunctions, and C_n are constants.

Next, averaged mass fractions $(\Theta_i)_m$ can be evaluated as:

$$(\theta_i)_m = \frac{(Y_i)_w - (Y_i)_m}{(Y_i)_w - (Y_i)_{in}} = 8 \sum_{n=0}^{\infty} \frac{G_n}{\lambda_n^2} \exp(-\lambda_n^2 x^+)$$

or in dimensional form:

$$(Y_i)_m = (Y_i)_w - 8\{(Y_i)_w - (Y_i)_{in}\} \sum_{n=0}^{\infty} \frac{G_n}{\lambda_n^2} \exp\left(-\lambda_n^2 \frac{x D_{AB}}{2R^2 (VX)_{average}}\right)$$

The values of G_n and λ_n^2 are tabulated below.

n	λ_n^2	Gn
0	7.313	0.749
1	44.61	0.544
2	113.9	0.463
3	215.2	0.415
4	348.6	0.383

Results Comparison

Average Mass Fraction of Species B

Axial location (m)	Target	ANSYS	Ratio
0.0100	0.8225	0.7829	0.9519
0.0200	0.7308	0.7108	0.9727
0.0300	0.6593	0.6537	0.9915
0.0400	0.5992	0.6031	1.0066
0.0500	0.5469	0.5568	1.0181
0.0600	0.5006	0.5140	1.0268
0.0700	0.4589	0.4742	1.0334
0.0800	0.4212	0.4375	1.0385
0.0900	0.3869	0.4034	1.0427
01.000	0.3555	0.3720	1.0464

ANSYS Verification Manual . ANSYS Release 10.0 . 002184 . © SAS IP, Inc.

Figure 209.2 Contours of Axial Velocity

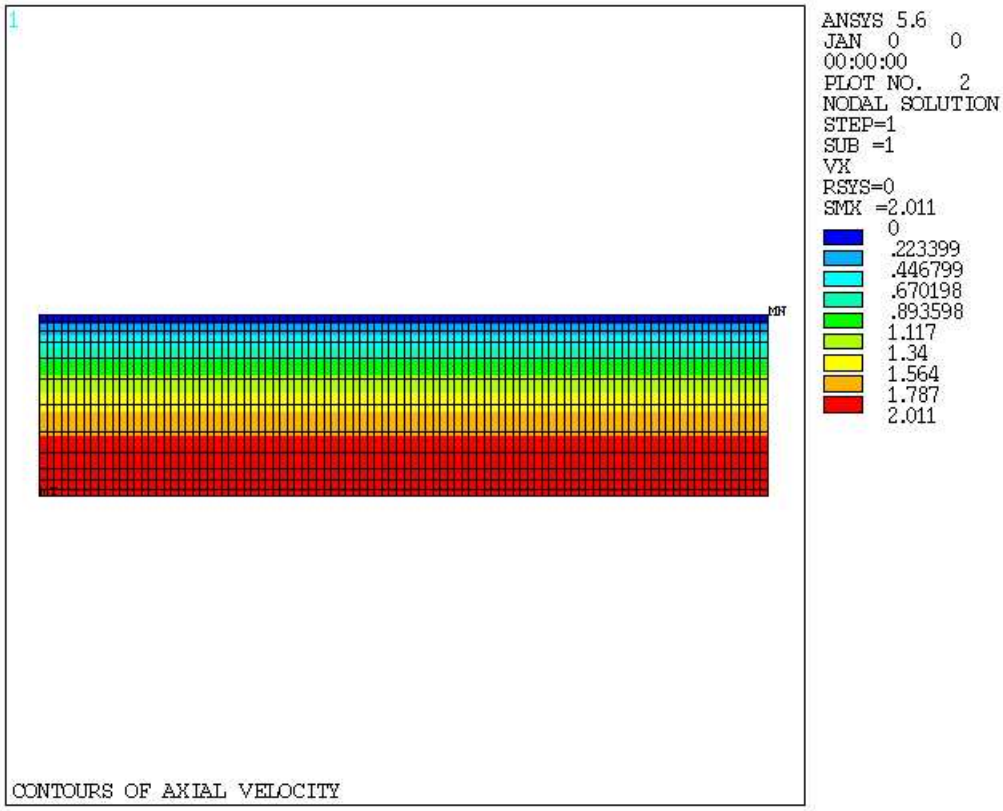

Figure 209.3 Contours of Mass Fraction of Species A

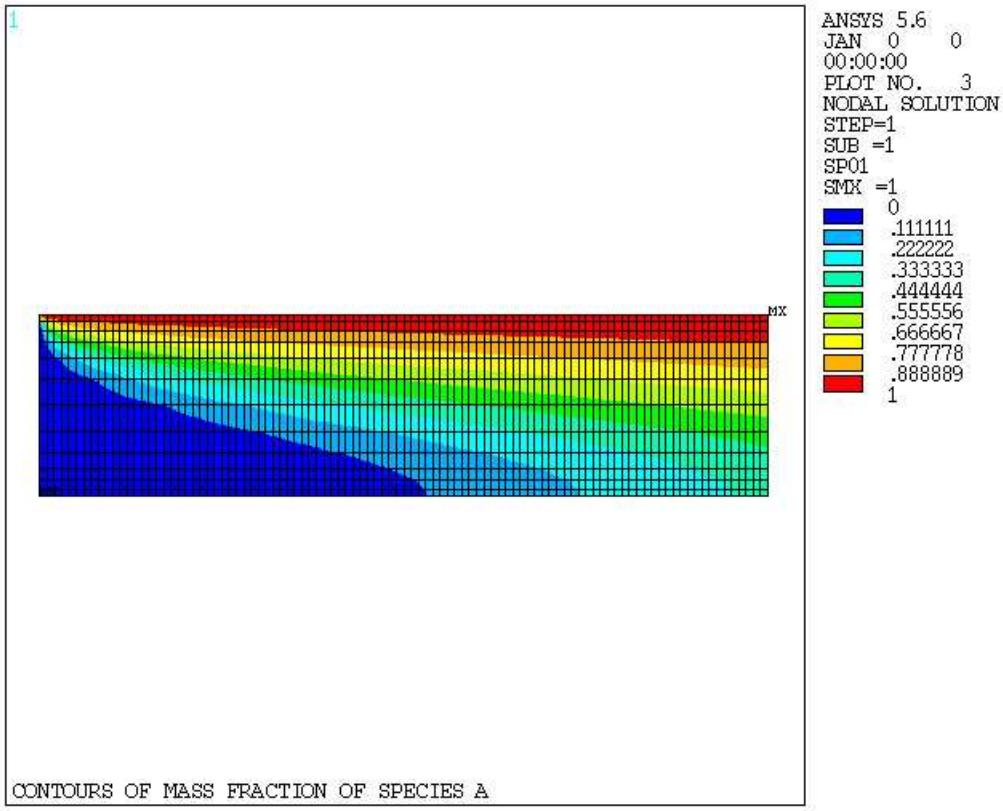

VM210: Pyramid Validation of Tetrahedron to Hexahedron

Overview

Reference:	E. P. Popov, *Introduction to Mechanics of Solids*, Prentice-Hall, Inc., Englewood Cliffs, NJ, 1998, pp. 182-185.
Analysis Type(s):	Static Analysis (**ANTYPE** = 0)
Element Type(s):	3-D 20-Node Structural Solid Elements (SOLID95) 3-D 20-Node Structural Solid Elements (SOLID186)
Input Listing:	vm210.dat

Test Case

For an elastic beam subjected to pure bending, validate the use of pyramids in a tetrahedron to hexahedron interface. Find the axial stress at the top, midplane, and bottom surfaces.

Figure 210.1 Tetrahedron to Hexahedron Interface Problem Sketch

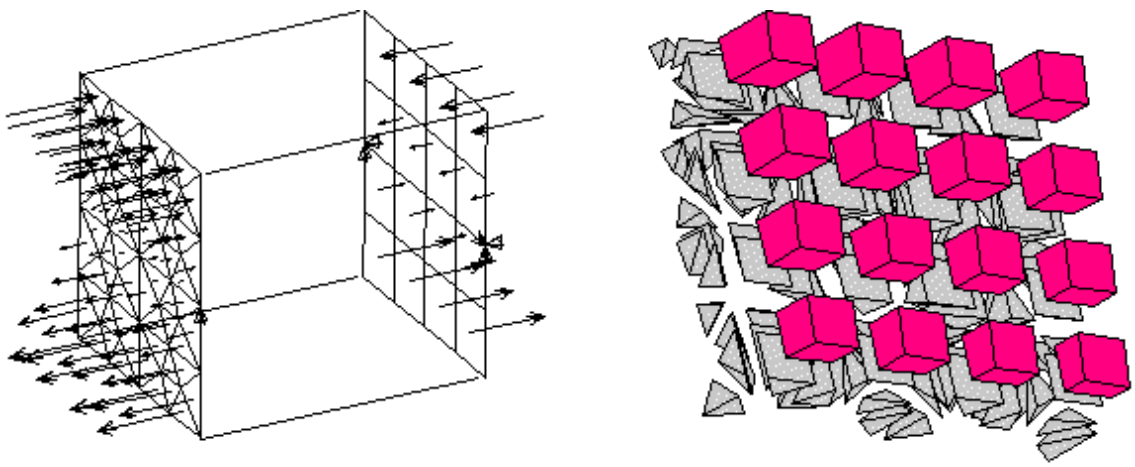

Problem Sketch Hex to Tet Transition Mesh

Material Properties	**Geometric Properties**	**Loading**
E = 30E6 υ = 0.3	W = 31.071 H = 33.917 L = 37.264	at z = 0, L area pressure load sf gradient: (-0.18979 at y = H/2) (0.18979 at y = -H/2)

Analysis Assumptions and Modeling Notes

The problem is solved in two different ways:

- using 3-D solid elements (SOLID95)
- using 3-D solid elements (SOLID186)

The model is generated using the block primitive which is divided into 8 sub-blocks. The pyramid interface is created by meshing the hexahedra first, followed by the tetrahedra. The working plane describes the hex-tet interface region.

Full displacement constraints placed upon three corners in the model midplane does not allow generation of significant reaction forces. A pure bending condition is created by the application of a pressure gradient on the faces of elements lying in the z = 0 and z = L planes. The linear gradient varies from -0.18979 on the bottom to 0.18979 on the top.

$$\sigma_z = (M_z y) / (I_c)$$

where

σ_Z = stress in z-direction
M_z = effective moment, z-direction
y = distance from neutral surface
I_c = second moment of area about the horizontal centroidal axis

$$I_c = \left(\frac{1}{12}\right)(W H^3) \text{ for the rectangular ends of the block}$$

Results Comparison

	Target	ANSYS	Ratio
SOLID95			
$Stress_Z$, Top (AVG)	-0.1898	-0.1899	1.001
$Stress_Z$, Neutral Axis (AVG)	0	-0.0002	1.000
$Stress_Z$, Bottom Axis (AVG)	0.1898	0.1898	1.000
SOLID186			
$Stress_Z$, Top (AVG)	-0.1898	-0.1899	1.001
$Stress_Z$, Neutral Axis (AVG)	0	-0.0002	1.000
$Stress_Z$, Bottom Axis (AVG)	0.1898	0.1898	1.000

Figure 210.2 Bending of Hex-to-tet Interface

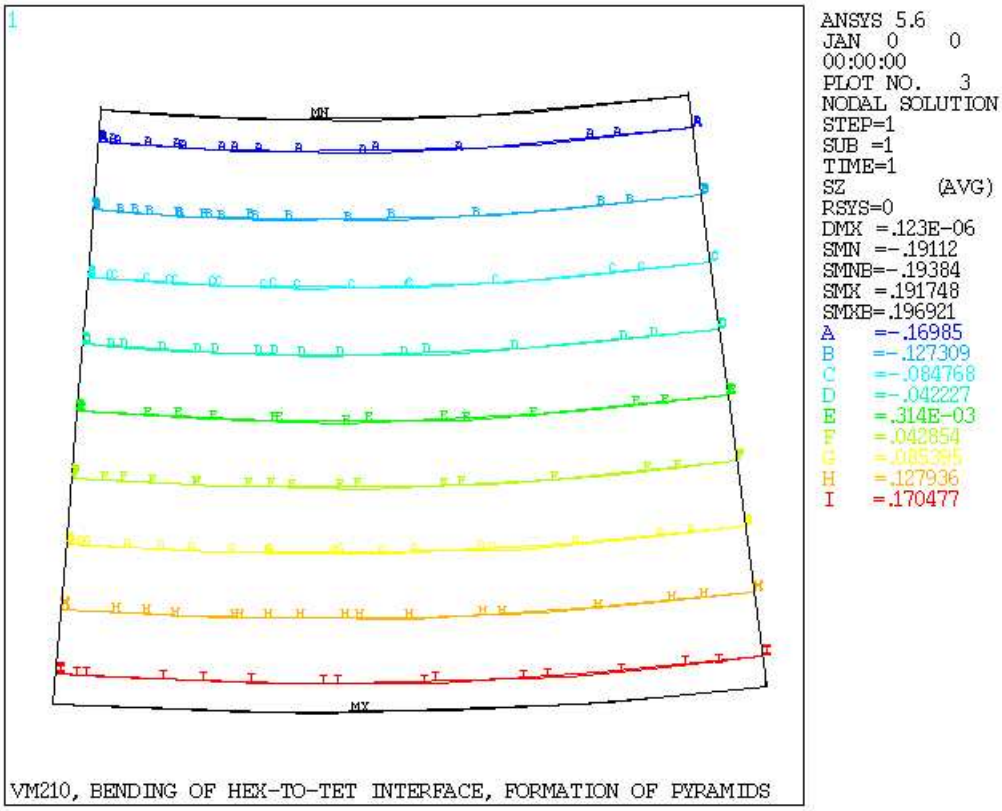

VM211: Rubber Cylinder Pressed Between Two Plates

Overview

Reference:	T. Tussman, K-J Bathe, "A Finite Element Formulation for Nonlinear Incompressible Elastic and Inelastic Analysis", *Computers and Structures*, Vol. 26 Nos 1/2, 1987, pp. 357-409.
Analysis Type(s):	Static Analysis (**ANTYPE** = 0)
Element Type(s):	2-D 4-Node Structural Solid Elements (PLANE182) 2-D 8-Node Structural Solid Elements (PLANE183) 3-D 8-Node Structural Solid Elements (SOLID185) 3-D 20-Node Structural Solid or Layered SolidElements (SOLID186) 2-D 2-Node Surface-to-Surface Contact Elements (CONTA171) 2-D 3-node Surface-to-Surface Contact Elements (CONTA172) 3-D 4-Node Surface-to-Surface Contact Elements (CONTA173) 3-D 8-Node Surface-to-Surface Contact Elements (CONTA174) 2-D Target Segment Elements (TARGE169) 3-D Target Segment Elements (TARGE170)
Input Listing:	vm211.dat

Test Case

A long rubber cylinder is pressed between two rigid plates using a maximum imposed displacement of δ_{max}. Determine the force-deflection response.

Figure 211.1 Rubber Cylinder Problem Sketch

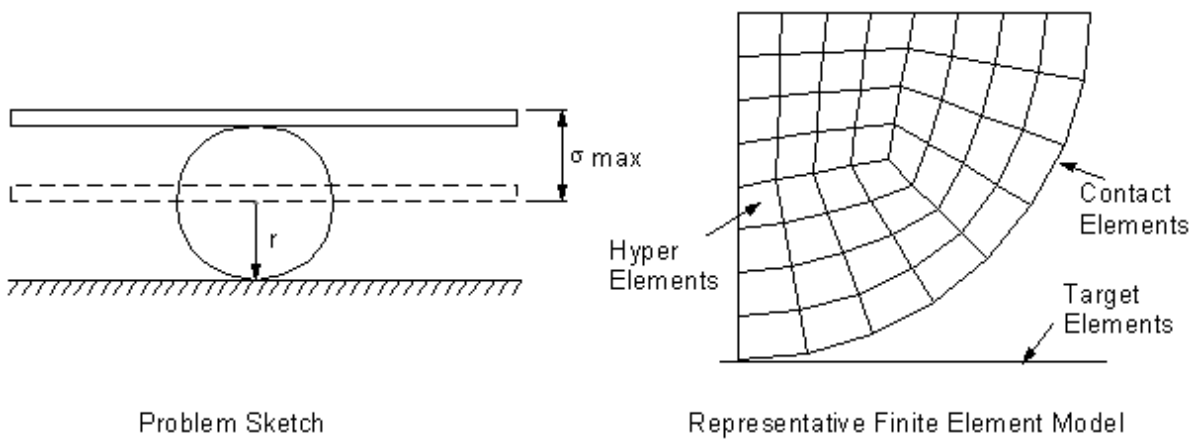

Material Properties	**Geometric Properties**
E = 2.82 MPa	r = 0.2 m
ν = 0.49967	**Loading**
Mooney-Rivlin Constants:	δ_{max} = 0.2 m
C1 = 0.293 MPa	**Real Constant**[1]
C2 = 0.177 MPa	FKN = 8

1. Applicable to CONTA171, CONTA172, CONTA173, and CONTA174.

Analysis Assumptions and Modeling Notes

This test case solves the problem of VM201 using the 2-D and 3-D rigid target and contact elements. A plane strain solution is assumed based on the geometry of the problem. Due to geometric and loading symmetry, the analysis can be performed using one quarter of the cross section. All nodes on the left edge (X = 0) are constrained, UX = 0. All nodes on the top edge (y = 0) are coupled in UY. An imposed displacement of -0.1 m acts upon the coupled nodes.

This problem is solved in eight different ways. The first four solutions are performed using default contact algorithm and the last four solution are performed using Lagrange multipliers method (KEYOPT(2) = 3) of contact elements.

- The lower order 2-D model used PLANE182 with CONTA171 and TARGE169 elements.
- A higher order 2-D model used PLANE183 with CONTA172 and TARGE169.
- The lower order 3-D model used SOLID185 with CONTA173 and TARGE170.
- The higher order 3-D model used SOLID186 with CONTA174 and TARGE170.
- The lower order 2-D model used PLANE182 with CONTA171 and TARGE169 and solved using Lagrange Multipliers method.
- A higher order 2-D model used PLANE183 with CONTA172 and TARGE169 and solved using Lagrange Multipliers method.
- The lower order 3-D model used SOLID185 with CONTA173 and TARGE170 and solved using Lagrange Multipliers method.
- The higher order 3-D model used SOLID186 with CONTA174 and TARGE170 and solved using Lagrange Multipliers method.

Results Comparison

		Target[1]	ANSYS	Ratio
PLANE182	Force at Displacement = 0.1	0.25	0.26	1.042
	Force at Displacement = 0.2	1.40	1.38	0.986
PLANE183	Force at Displacement = 0.1	0.25	0.26	1.044
	Force at Displacement = 0.2	1.40	1.38	0.995
SOLID185	Force at Displacement = 0.1	0.25	0.25	0.984
	Force at Displacement = 0.2	1.40	1.38	0.983
SOLID186	Force at Displacement = 0.1	0.25	0.26	1.028
	Force at Displacement = 0.2	1.40	1.40	1.001
With KEYOPT (2) = 3 of CONTA171				
PLANE182	Force at Displacement = 0.1	0.25	0.27	1.069
	Force at Displacement = 0.2	1.40	1.40	1.003
With KEYOPT (2) = 3 of CONTA172				
PLANE183	Force at Displacement = 0.1	0.25	0.27	1.077
	Force at Displacement = 0.2	1.40	1.41	1.010
With KEYOPT (2) = 3 of CONTA173				
SOLID185	Force at Displacement = 0.1	0.25	0.25	1.000
	Force at Displacement = 0.2	1.40	1.40	0.999
With KEYOPT (2) = 3 of CONTA174				

		Target[1]	ANSYS	Ratio
SOLID186	Force at Displacement = 0.1	0.25	0.27	1.099
	Force at Displacement = 0.2	1.40	1.43	1.023

1. Determined from graphical results. See T. Tussman, K-J Bathe, "A Finite Element Formulation for Nonlinear Incompressible Elastic and Inelastic Analysis", pg. 385, fig. 6.14.

Figure 211.2 Displaced Shape

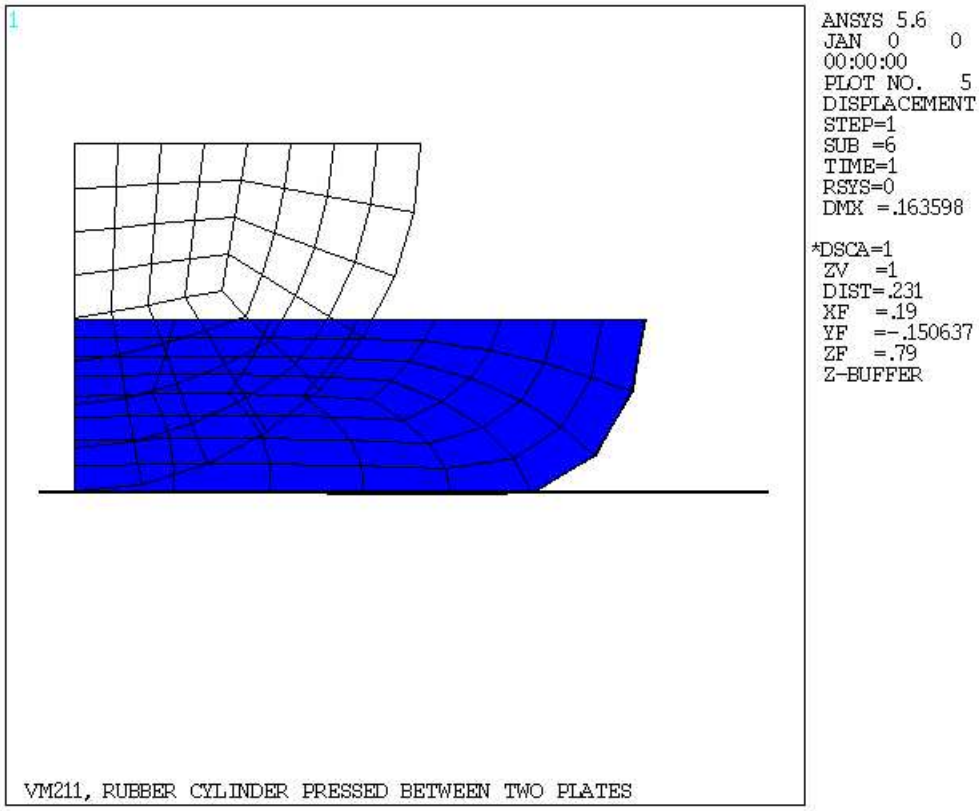

Figure 211.3 Force vs. Displacement

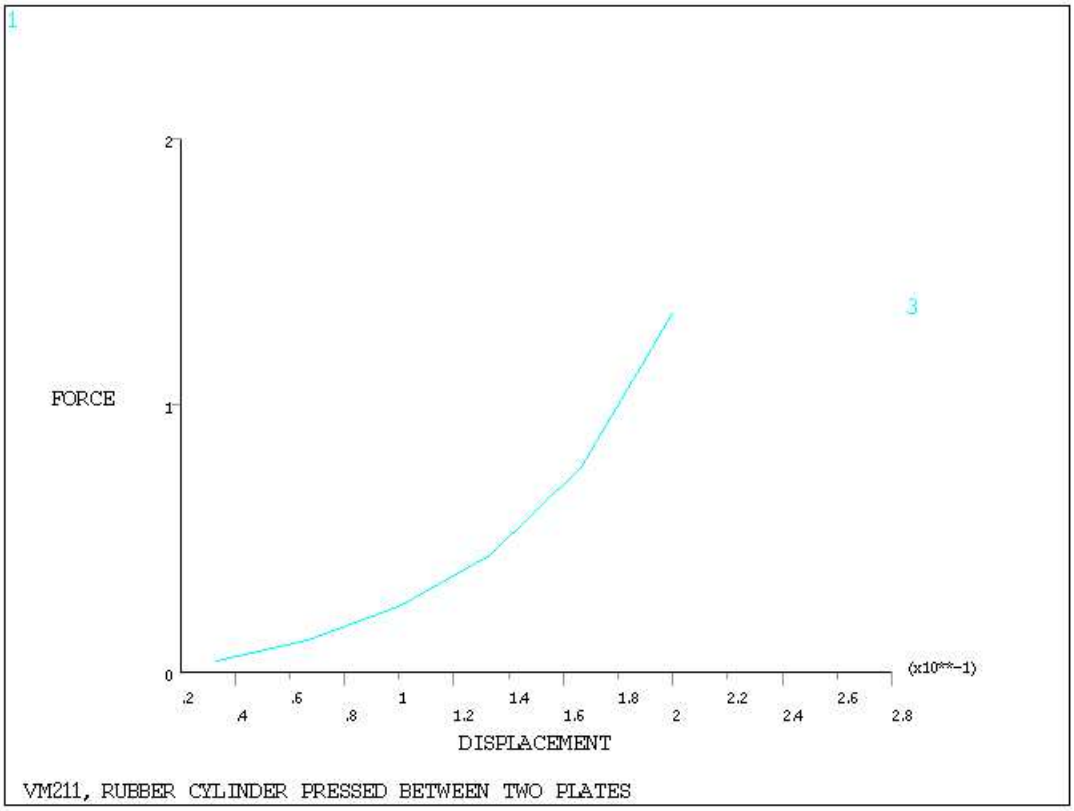

VM212: Modal Analysis of a Rectangular Cavity

Overview

Reference:	R. S. Elliot, *An Introduction to Guided Waves and Microwave Circuits*, Prentice Hall, Inc., Englewood Cliffs, NJ, 1993, pp. 266-270.
Analysis Type(s):	Mode-frequency Analysis (**ANTYPE** = 2)
Element Type(s):	3-D High-Frequency Tetrahedral Solid Elements (HF119) 3-D High-Frequency Brick Solid Elements (HF120)
Input Listing:	vm212.dat

Test Case

Determine the TE101 mode natural frequency for a rectangular lossless cavity.

Figure 212.1 Rectangular Cavity Problem Sketch

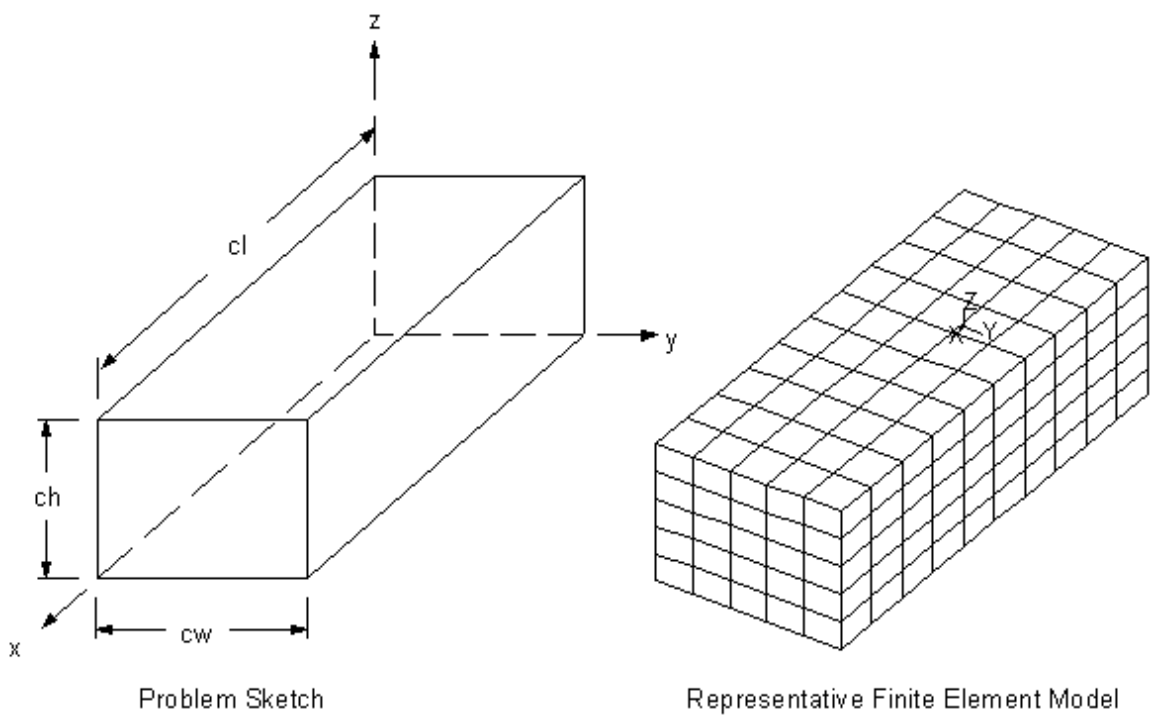

Material Properties	Geometric Properties
$\mu = \mu_0$	ch = .30 m
$\varepsilon = \varepsilon_0$	cw = .40 m
	cl = 1.0 m

Analysis Assumptions and Modeling Notes

The rectangular cavity mesh is prescribed with 5 element divisions along the cavity width and 10 divisions along the cavity length to resolve the TE101 mode. The Block Lanczos Eigensolver is selected with the frequency range limited to selecting only mode frequencies between .35 GHz and .55 GHz. The mode is expanded for purposes of displaying the field solutions.

Results Comparison

	Target	ANSYS	Ratio
f, GHz	.40389	.403660	0.999
f, 119 - No Refine	.40389	.435794	1.079
f, 119 - Refine	.40389	.403815	1.000

Figure 212.2 Modal Analysis of a Rectangular Cavity

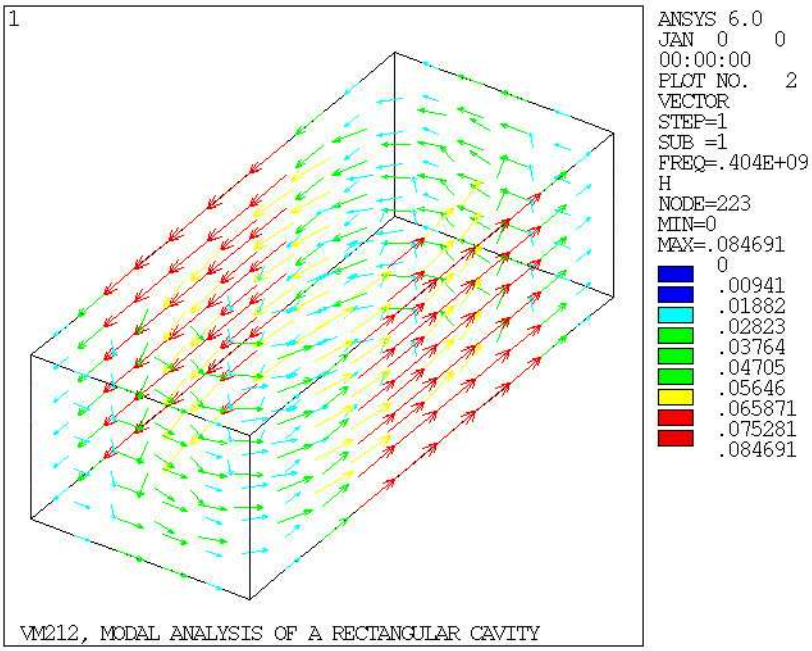

Figure 212.3 Modal Analysis of a Rectangular Cavity

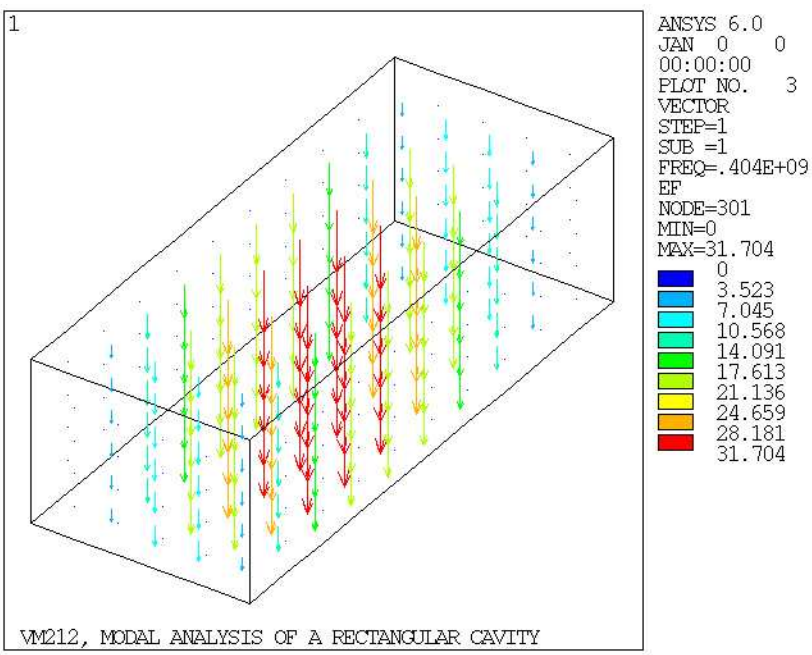

VM213: Harmonic Response Analysis of a Coaxial Cable

Overview

Reference:	R. S. Elliot, *An Introduction to Guided Waves and Microwave Circuits*, Prentice Hall, Inc., Englewood Cliffs, NJ, 1993, pp. 48-51.
Analysis Type(s):	Full Harmonic Analysis (**ANTYPE** = 3)
Element Type(s):	3-D High-Frequency Brick Solid Elements (HF120)
Input Listing:	vm213.dat

Test Case

A coaxial cable with an inner radius of 2.5 cm, an outer radius of 7.5 cm, and a length of 37.5 cm is excited by a 1 Volt excitation at one end of the cable. Calculate the S-parameters, impedance, power, and the electric and magnetic field at the other end of the cable.

Figure 213.1 Coaxial Cable

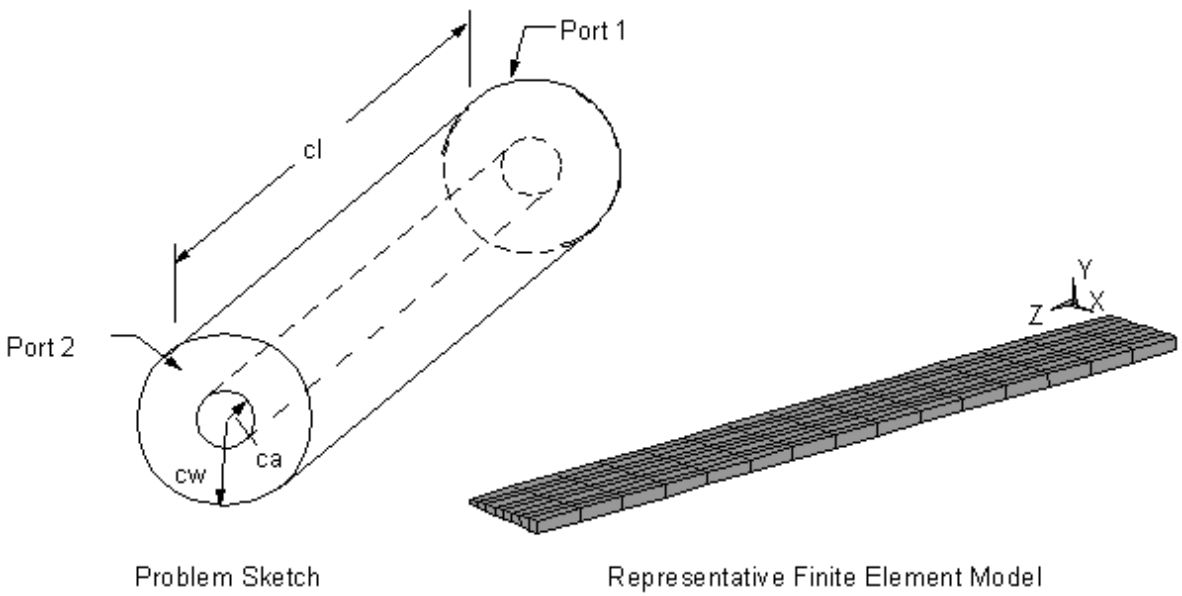

Material Properties	Geometric Properties	Loading
$\mu = \mu_0$ $\varepsilon = \varepsilon_0$	ca = 2.5 cm cw = 7.5 cm cl = 37.5 cm	V = 1.0 at input port f = 0.8 GHz

Analysis Assumptions and Modeling Notes

The excitation is applied with a port load at one end of the coax (Port 1). The other end of the coax cable is terminated as a matched impedance (Port 2). The coaxial cable is modeled with the 2nd order Key Option in the HF120 element to accurately resolve the field calculation at the output port. Since the coax cable is symmetric about it's axis, only a circumferential slice of any arbitrary angle is required. A slice of 5 degrees is selected. The cable length is 1 wavelength and 15 elements are used along the cable length to accurately resolve the field solution. The problem makes use of the commands **SPARM** and **IMPD** to calculate the S-parameters and impedance at the output port. The incident power at the output port is calculated by summing the appropriate term from the element records.

Results Comparison

	Target	ANSYS	Ratio
S11	0	0	-
S12	1.0	1.000	1.000
Power (W)	.01	.01	1.000
EF (Radial) V/m	12.14	12.12	.998
H (Circum) H/m	.03	.03	1.000
Impedance (Ohms)	65.87	66.06[1]	1.003

1. Real component of impedance

Figure 213.2 Harmonic Response Analysis of a Coaxial Cable

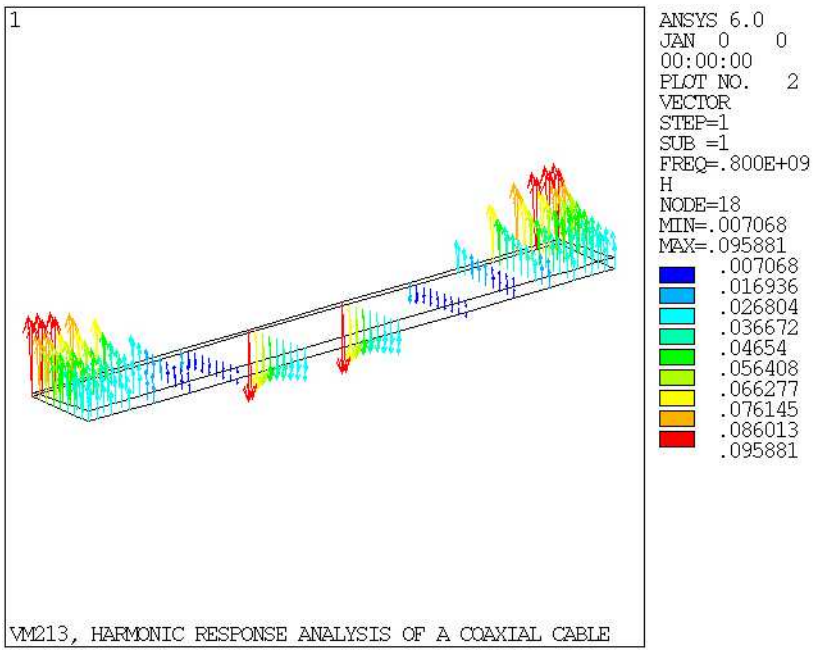

Figure 213.3 Harmonic Response Analysis of a Coaxial Cable

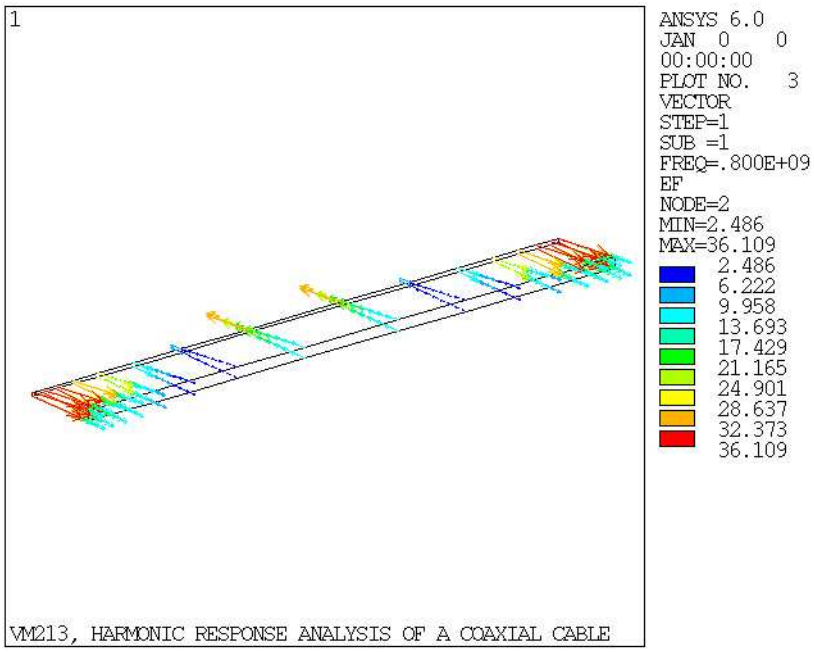

VM214: Harmonic Response of a Rectangular Waveguide

Overview

Reference:	R. S. Elliot, *An Introduction to Guided Waves and Microwave Circuits*, Prentice Hall, Inc., Englewood Cliffs, NJ, 1993, pp. 82-87.
Analysis Type(s):	Full Harmonic Analysis (**ANTYPE** = 3)
Element Type(s):	3-D High Frequency Tetrahedral Solid Elements (HF119)
Input Listing:	vm214.dat

Test Case

A rectangular waveguide is subjected to a TE10-mode loading at one port while the other port is matched. Determine the S-parameters, power input, and field solution.

Figure 214.1 Rectangular Waveguide Problem Sketch

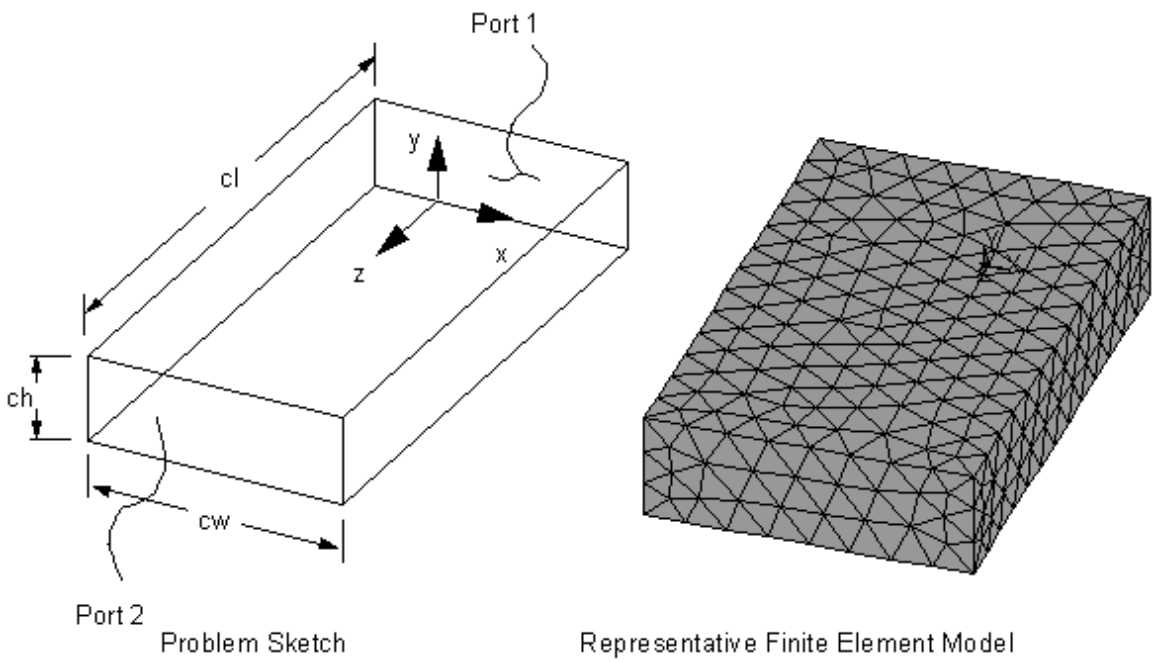

Material Properties	Geometric Properties	Loading
$\mu = \mu_0$ $\varepsilon = \varepsilon_0$	ch = 1 cm cw = 3 cm cl = 4.8 cm	E_y = 1.0 at input port f = 8 GHz

Analysis Assumptions and Modeling Notes

The excitation is applied with a TE10 port load at one end of the waveguide (Port 1). The other end of the waveguide is terminated as a matched impedance (Port 2). The length of the waveguide is 1 wavelength. The finite element mesh is defined to create 10 elements along the length of the waveguide to resolve the field solution accurately. The input power at Port 1 is calculated by summing the appropriate term from the element record. The problem makes use of the **SPARM** command to calculate the S-parameters. The magnetic field H illustrates the complete wavelength field pattern along the length of the waveguide.

Results Comparison

	Target	ANSYS	Ratio
S11	0	0.00312335	0.00
S12	1.0	0.99868294	.999
Power Input W	.1554e-6	.1553e-6	.999
EY(0,0,0) v/m	1.00	1.00084427	1.001
Hx(0,0,0) a/m	-.2072e-2	-.204229e-2	.986

VM215: Thermal-Electric Hemispherical Shell with Hole

Overview

Reference:	Any standard electrical engineering text
Analysis Type(s):	Coupled Thermal-Electric Shell
Element Type(s):	Thermal-Electric Shell Elements (SHELL157)
Input Listing:	vm215.dat

Test Case

A conducting hemisphere of radius, r, has a hole subtending an angle Θ_1. The edge of the hole is electrically and thermally grounded. A voltage, V_2, is applied at the equator. A Φ degree sector in the azimuthal plane is analyzed.

Figure 215.1 Hemispherical Shell Problem Sketch

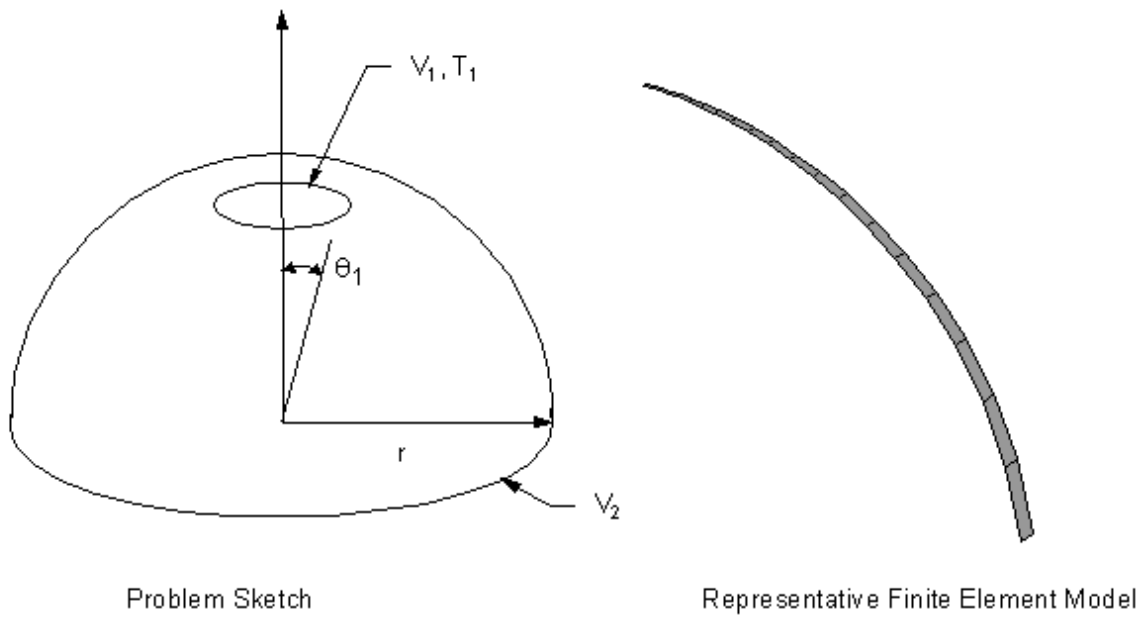

Material Properties	**Geometric Properties**	**Loading**
ρ = 7 ohm-m K = 3 W/m-K	t = 0.2 m r = 10 m Θ_1 = 10° Φ = 3°	V_1 = 0 volts V_2 = 100 volts T_1 = 0°C

Analysis Assumptions and Modeling Notes

A hemispherical shell with a hole is analyzed. The symmetry of the model is utilized and only a 3 degree sector in the azimuthal direction is analyzed.

The electric current (I) in the sphere is given by:

$$I = \frac{V}{R} = \frac{(V_2 - V_1)}{R}$$

Where resistance R is given by:

$$R = \rho \int \frac{dL}{A}$$

$$= \rho \int \frac{r d\theta}{2\pi r t \cos\theta} \left(\frac{2\pi}{\phi} \right) \text{with } \phi \text{ in radians}$$

$$= \left(\frac{pr}{2\pi r t} \right) \left(\frac{2\pi}{\phi} \right) \int_{\theta=0}^{\theta-90-\theta_1} \frac{d\theta}{\cos\theta}$$

$$= \left(\frac{pr}{2\pi r t} \right) \left(\frac{360^\circ}{3^\circ} \right) \frac{1}{2} \ln \left[\frac{1+\sin(90-\theta_1)}{1-\sin(90-\theta_1)} \right]$$

The total heat flow is due to Joule Heating and is given by $Q = I (V_2 - V_1)$

Results Comparison

SHELL157	Target	ANSYS	Ratio
I (Amps) Node 21	0.06140	0.06143	1.000
Q (Watts) Node 21	6.14058	6.14291	1.000

VM216: Lateral Buckling of a Right Angle Frame

Overview

Reference:	J. C. Simo, L. Vu-Quoc, "Three-Dimensional Finite-Strain Rod Model, Part II", *Computer Methods in Applied Mechanical Engineering*, Vol. 58, 1986, pp. 79-116.
Analysis Type(s):	Static Analysis (**ANTYPE** = 0)
Element Type(s):	3-D Linear Finite Strain Beam Elements (BEAM188) 3-D Quadratic Finite Strain Beam Elements (BEAM189)
Input Listing:	vm216.dat

Test Case

A cantilever right angle frame is subjected to an in-plane fixed end load. The frame is driven to buckling mode by a perturbation load applied at the free end, normal to the plane of the frame. This perturbation is removed close to the buckling load. Determine the critical load.

Figure 216.1 Right Angle Frame Problem Sketch

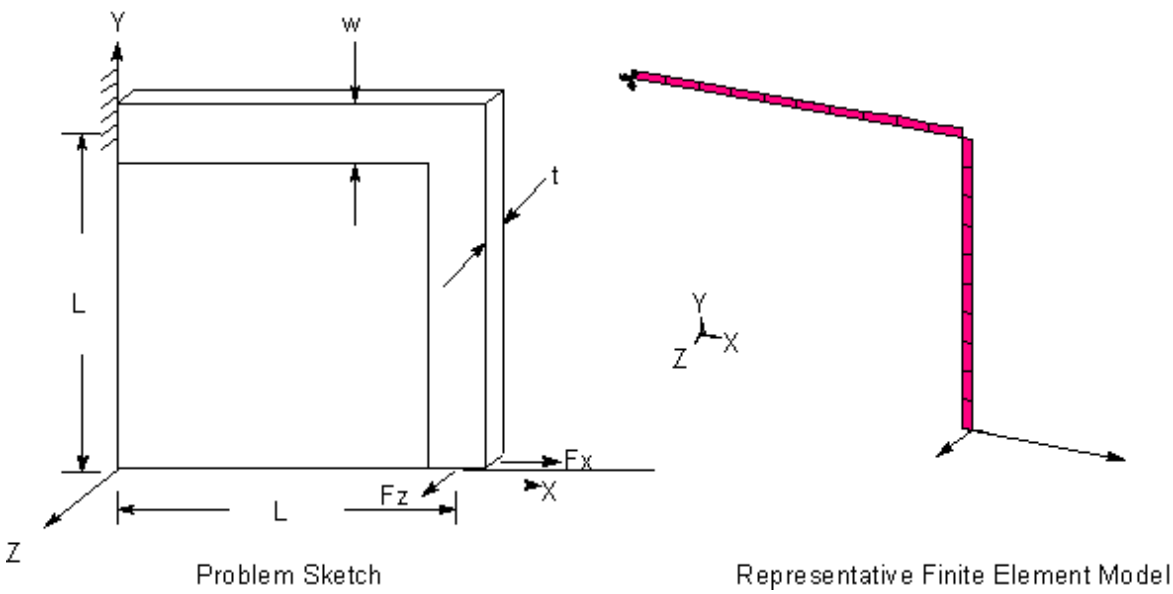

Material Properties	**Geometric Properties**
Ex = 71240 psi	Izz = 0.54 in
Nuxy = 0.31	Iyy = 1350 in^4
Loading	t = 0.6 in
Fz = 1 x 10^{-3} lb	w = 30 in
Fx = 1,485 lb	L = 240 in

Analysis Assumptions and Modeling Notes

A first analysis is performed using BEAM188 elements. A second analysis is also performed using BEAM189 elements.

Results Comparison

Critical Load	Target	ANSYS	Ratio
BEAM188	1.09	1.066	0.978
BEAM189	1.09	1.065	0.978

Figure 216.2 Displacement Tip vs. End Force

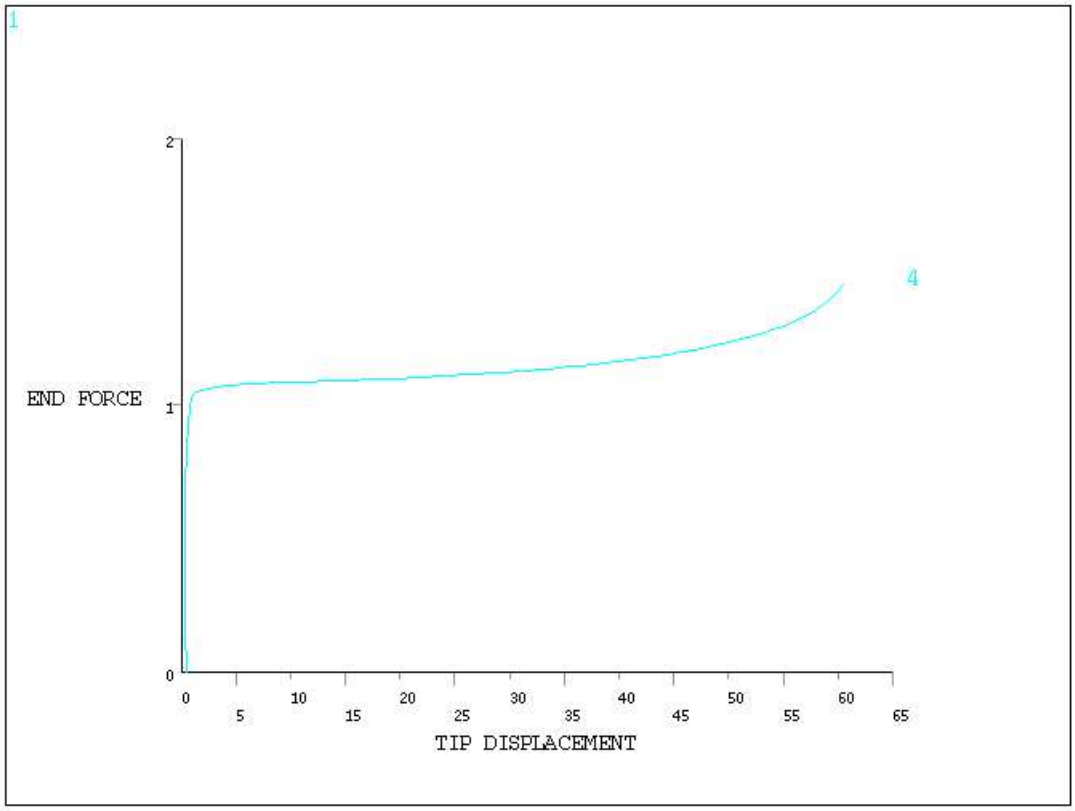

Figure 216.3 Deformed Shape, Side View

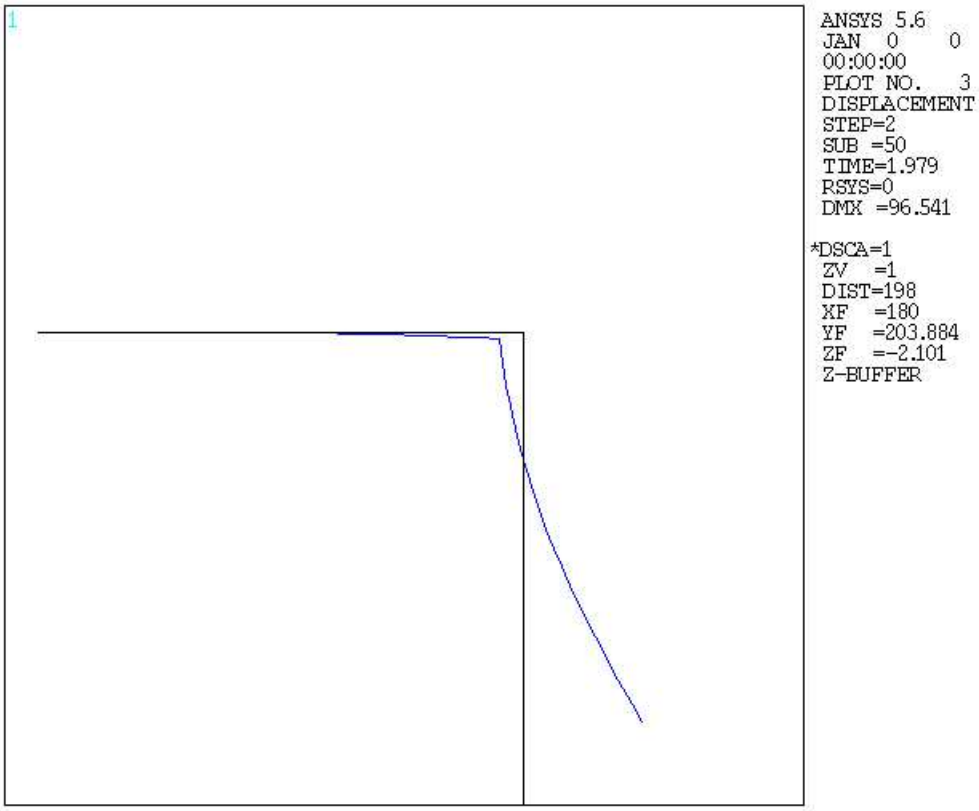

Figure 216.4 Deformed Shape, Top View

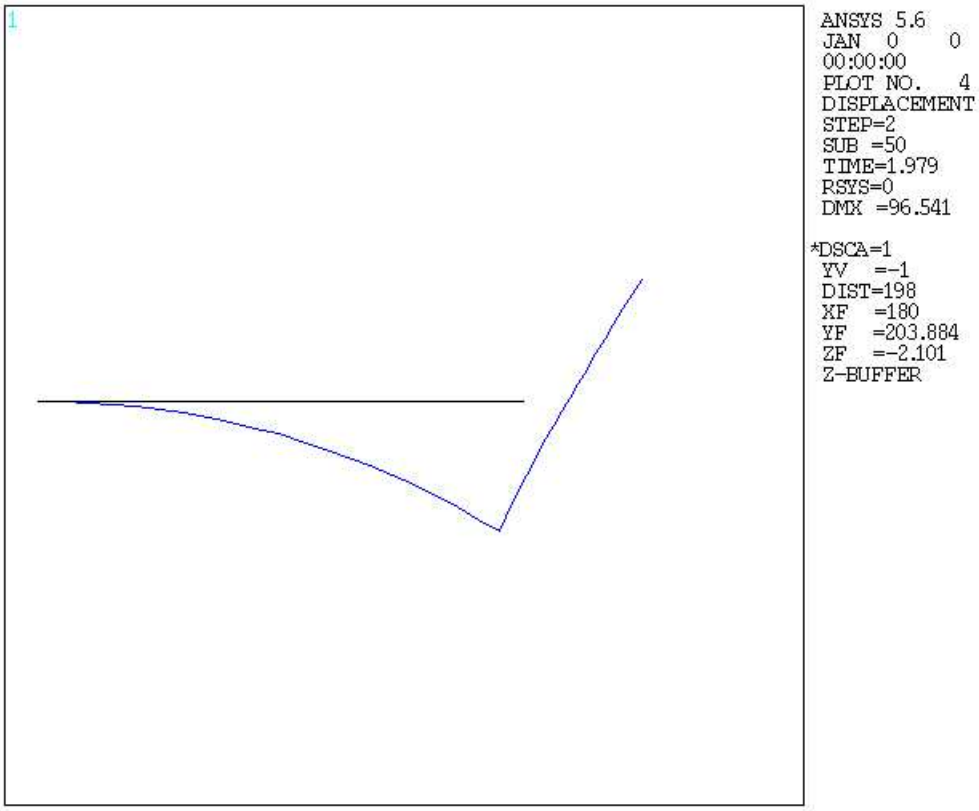

VM217: Portal Frame Under Symmetric Loading

Overview

Reference:	N. J. Hoff, *The Analysis of Structures*, John Wiley and Sons, Inc., New York, NY, 1956, pp. 115-119.
Analysis Type(s):	Static Structural (**ANTYPE** = 0)
Element Type(s):	3-D Linear Finite Strain Beam Elements (BEAM188) 3-D Quadratic Finite Strain Beam Elements (BEAM189)
Input Listing:	vm217.dat

Test Case

A rigid rectangular frame is subjected to a uniform distributed load ω across the span. Determine the maximum rotation, and maximum bending moment. The moment of inertia for the span, I_{span} is five times the moment of inertia for the columns, I_{col}.

Figure 217.1 Portal Frame Problem Sketch

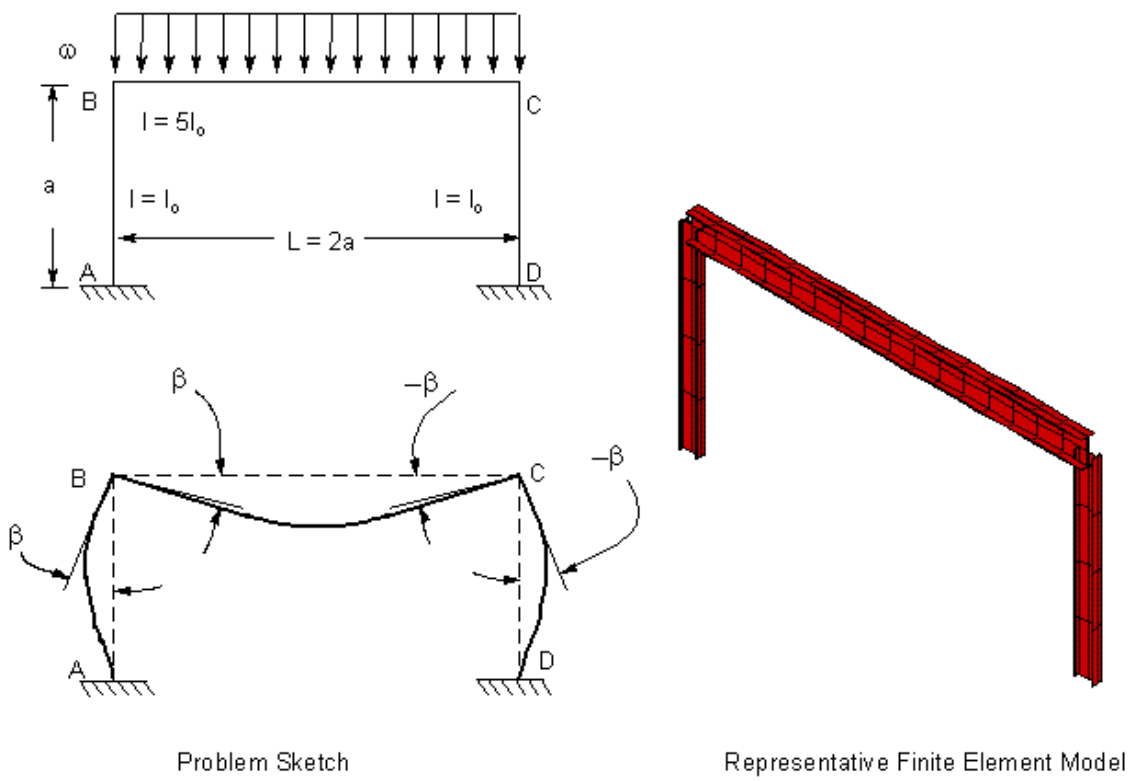

Material Properties	**Geometric** Properties	**I-Beam Section Data**
Ex = 30 x 10^6 psi Nuxy = 0.3 **Loading** ω = -500 lb/in	a = 400 in L = 800 in I_{span} = 5 I_{col} I_{col} = 20300 in^4	W1 = W2 = 16.655 in W3 = 36.74 in t1 = t2 = 1.68 in t3 = 0.945 in

Analysis Assumptions and Modeling Notes

All the members of the frame are modeled using an I-Beam cross section. The cross section for the columns is chosen to be a W36 x 300 I-Beam Section. The dimensions used in the horizontal span are scaled by a factor of 1.49535 to produce a moment of inertia that is five times the moment of inertia in the columns. The columns are modeled with BEAM188, while the span is modeled with BEAM189 elements. The theoretical maximum rotation is $\beta = (1/27)\ (w(a^3)/E(I_{col}))$, and the theoretical maximum bend moment is $M_{max} = (19/54)(w(a^2))$.

Results Comparison

	Target	ANSYS	Ratio
Max. Rotation	0.195E-2	0.213E-2	1.093
Max. Bend Moment in lb	0.281E8	0.287E8	1.019

Figure 217.2 I-Section

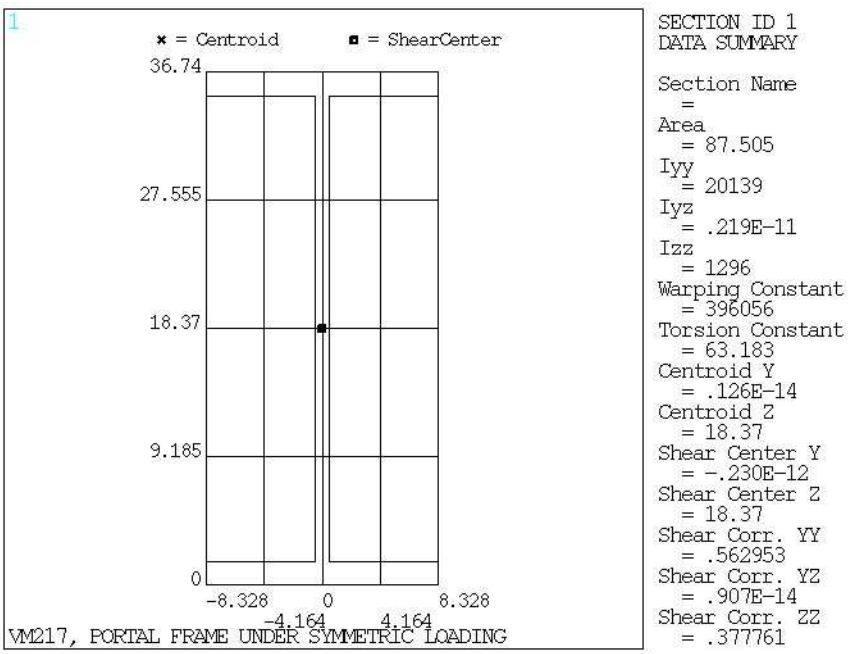

Figure 217.3 I-Section Under Symmetric Loading

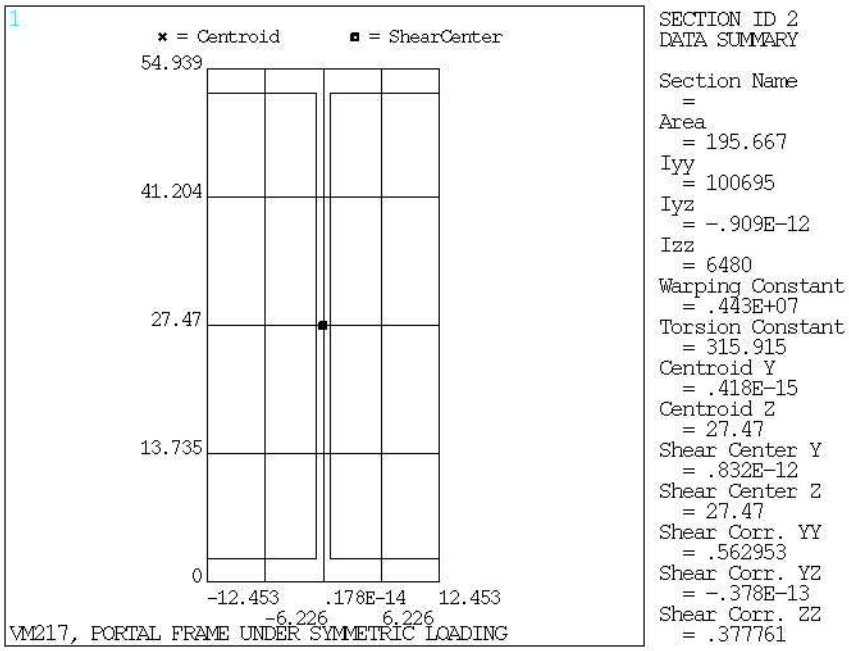

Figure 217.4 Moment Diagram

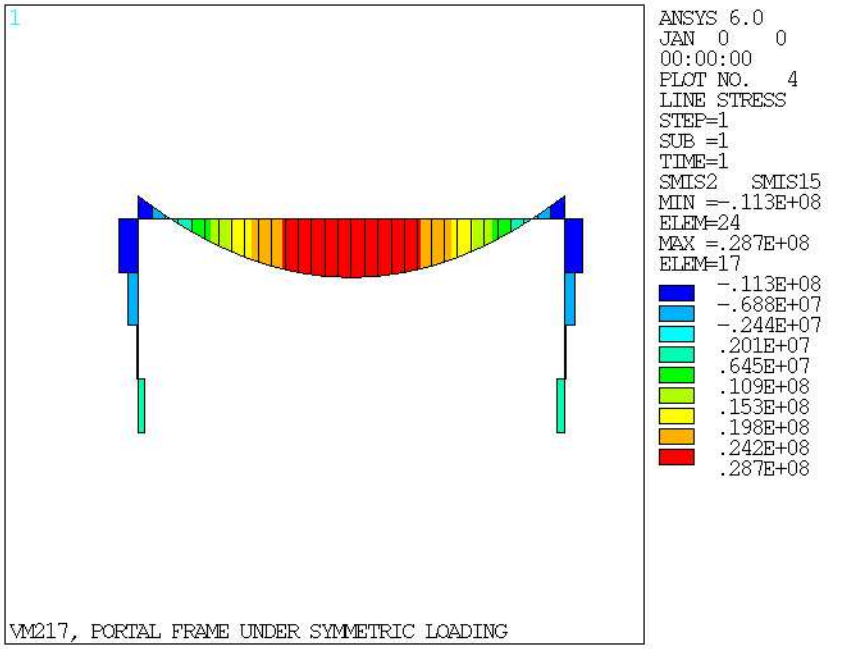

Figure 217.5 Displaced Shape (front view)

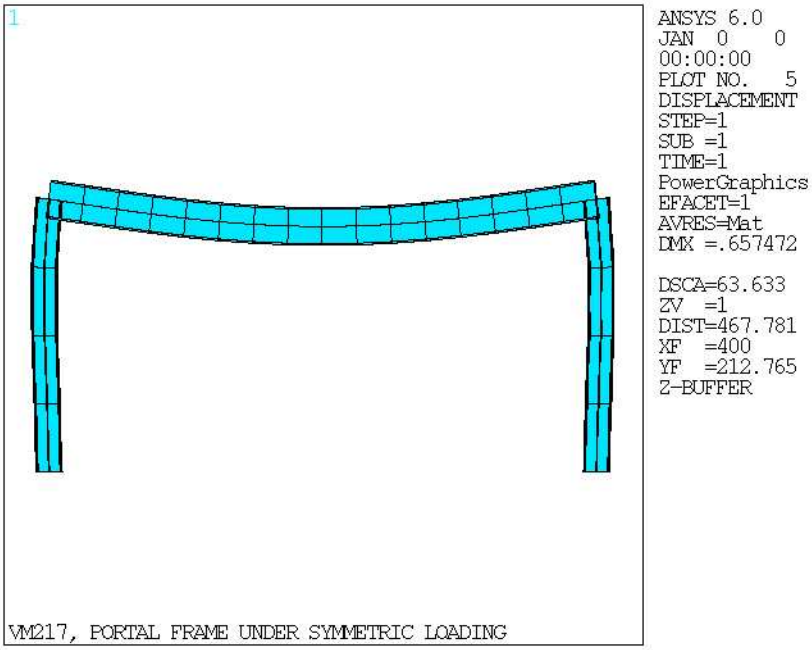

VM218: Hyperelastic Circular Plate

Overview

Reference:	J. T. Oden, *Finite Elements of Nonlinear Continua*, McGraw-Hill Book Co., Inc., New York, NY, 1972, pp. 318-321.
Analysis Type(s):	Static Analysis (**ANTYPE** = 0)
Element Type(s):	4-Node Finite Strain Shell Elements (SHELL181)
	2-Node Finite Strain Axisymmetric Shell Elements (SHELL208)
Input Listing:	vm218.dat

Test Case

A flat circular membrane made of a rubber material is subjected to uniform water pressure. The edges of the membrane are fixed. Determine the response as pressure is increased to 50 psi.

Figure 218.1 Hyperelastic Circular Plate Project Sketch

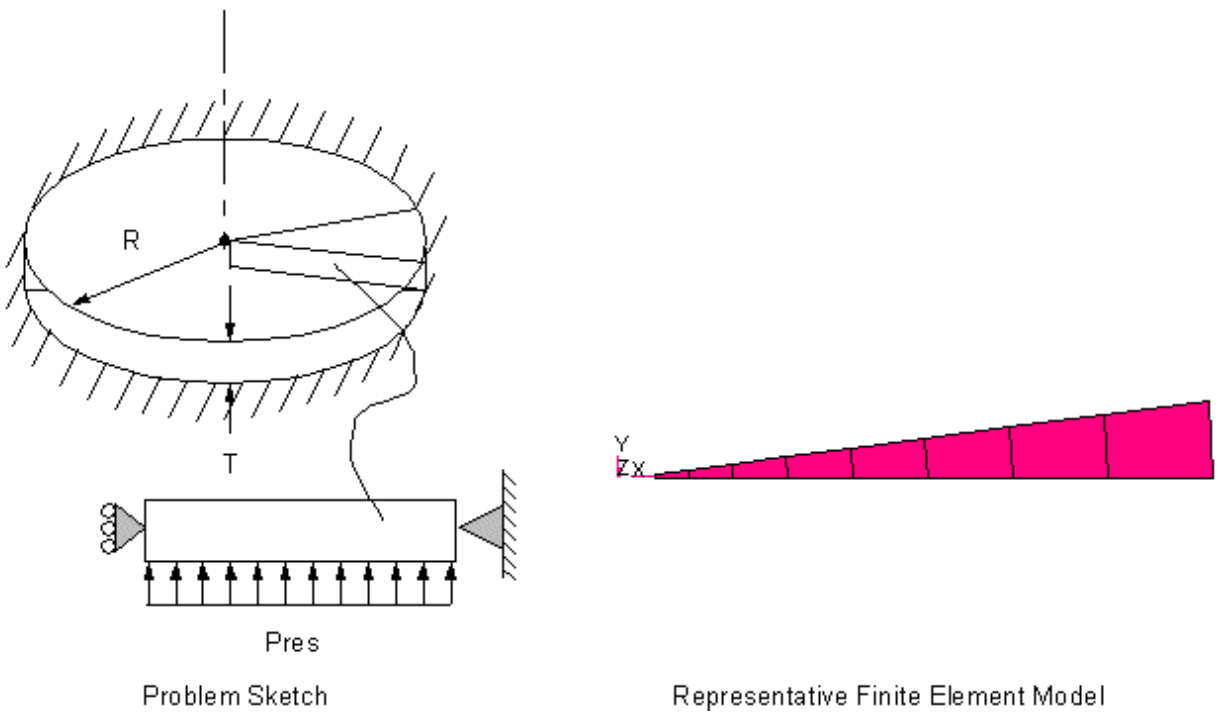

Material Properties	**Geometric Properties**	**Loading**
Ex = 1 x 10^6 psi Nuxy = 0.5 DENS = 0.1 lb/in^3 C_1 = 80 psi C_2 = 20 psi	R = 7.5 in T = 0.5 in	Pres = 50.0 psi

Analysis Assumptions and Modeling Notes

This analysis is first solved as a 3-D SHELL181 model. The full circular plate is reduced to a 7.5 degree sector for analysis. The midplane of the outer edge of the circle is considered to be fixed. A pressure of 50 psi is applied to

the bottom surface of the shell sector. The SHELL181 model is solved using standard formulation and the membrane option. In each of the SHELL181 cases, the analysis was performed using reduced integration.

The analysis is also performed using a SHELL208 axisymmetric model.

Results Comparison

Pressure	Target	ANSYS	Ratio
SHELL181			
4.0	2.250	2.295	1.020
24.0	6.200	5.707	0.921
38.0	10.900	10.017	0.919
SHELL181 Membrane Option			
4.0	2.250	2.295	1.020
24.0	6.200	5.707	0.921
38.0	10.900	10.017	0.919
SHELL208			
4.0	2.250	2.301	1.023
24.0	6.200	5.730	0.924
38.0	10.900	10.079	0.925
SHELL209			
4.0	2.250	2.288	1.017
24.0	6.200	5.704	0.920
38.0	10.900	10.118	0.928

ANSYS Verification Manual . ANSYS Release 10.0 . 002184 . © SAS IP, Inc.

Figure 218.2 Results Plot 1 - UZ vs. Thickness

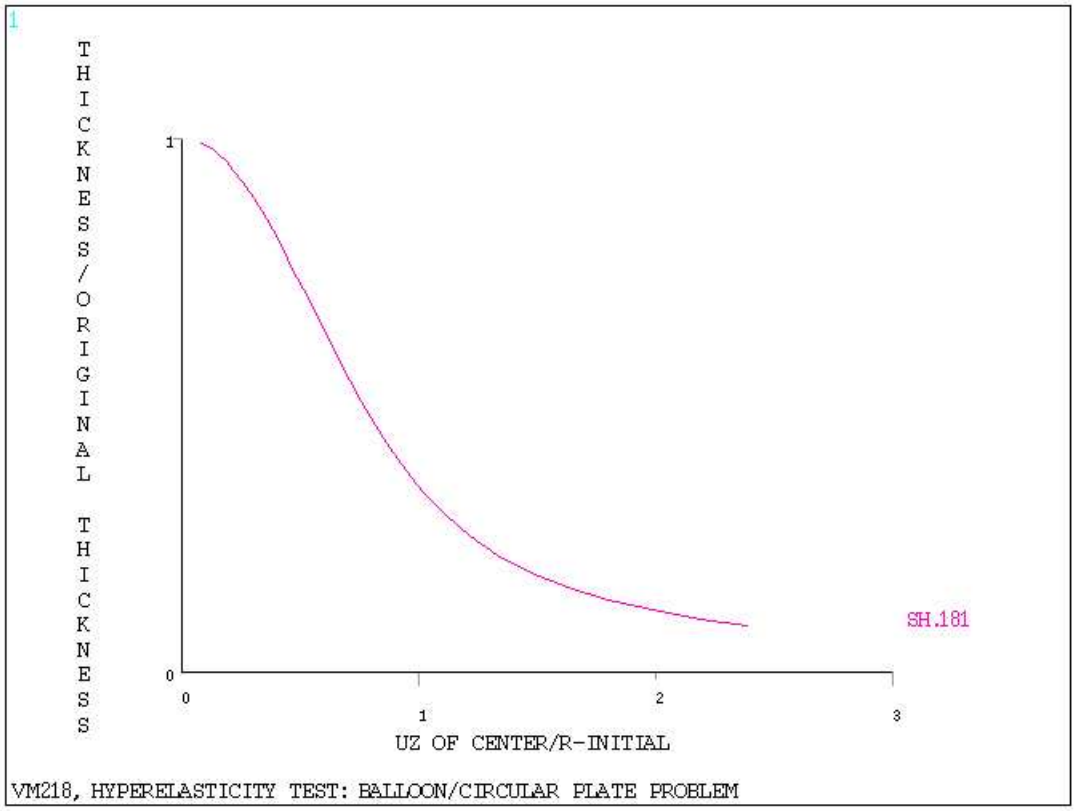

Figure 218.3 Results Plot 2 - UZ vs. Pressure

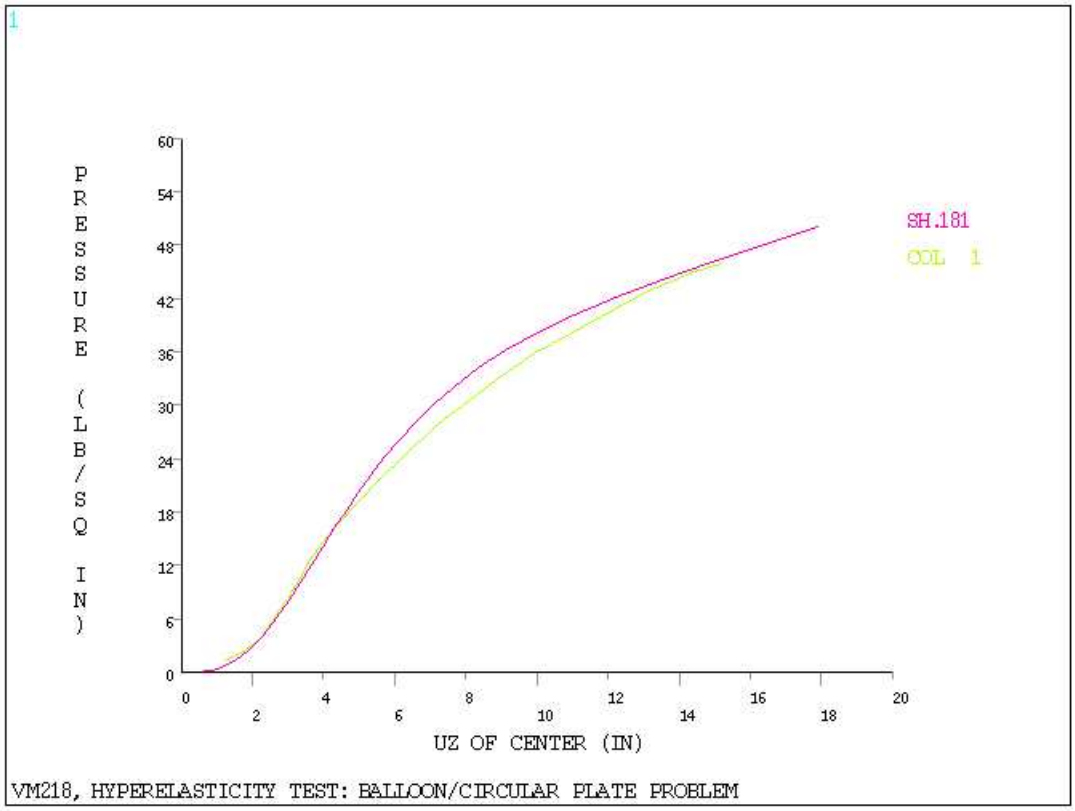

Figure 218.4 Results Plot 3 - Displaced Shape

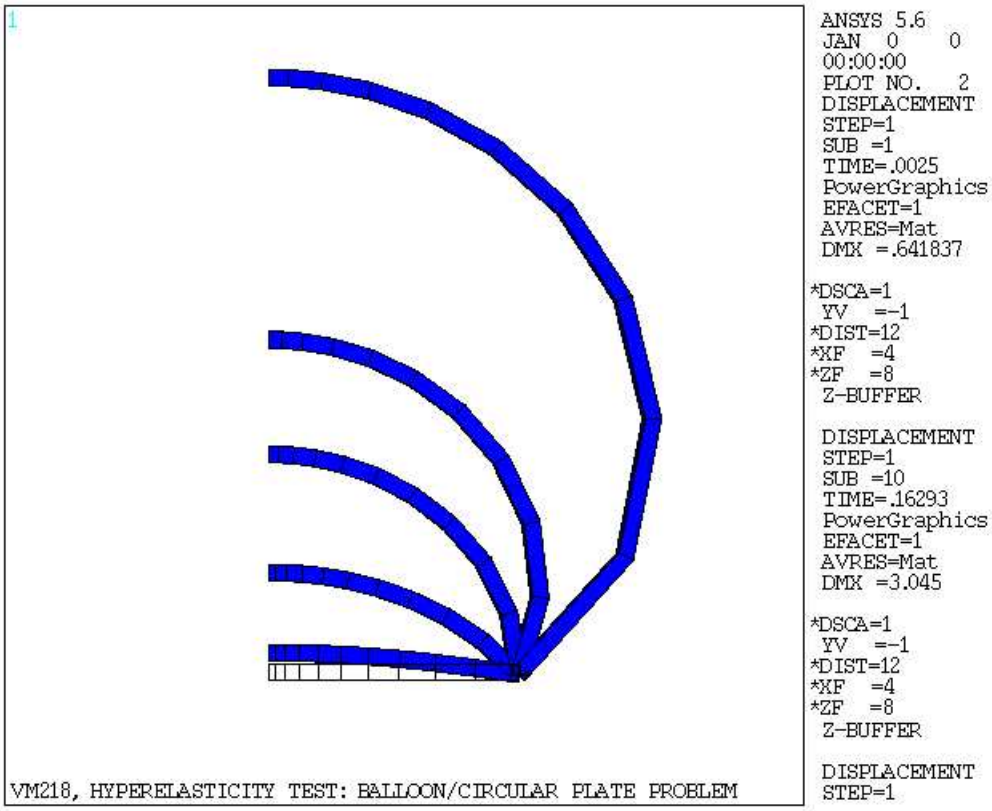

VM219: Non-Newtonian Pressure Driven Sector Flow

Overview

Reference:	W. F. Hughes, J. A. Brighton, *Schaum's Outline of Theory and Problems of Fluid Dynamics*, McGraw-Hill Book Co., Inc., New York, NY, 1991.
Analysis Type(s):	Fluid, Flow Analysis (**FLOTRAN**)
Element Type(s):	2-D Fluid-Thermal Elements (FLUID141)
Input Listing:	vm219.dat

Test Case

Fully developed pressure driven flow of a power law non-Newtonian fluid is created within a pipe. Assuming steady-state incompressible flow and that there are no body forces, solve for the velocity in the Y direction.

Figure 219.1 Sector Flow Problem Sketch

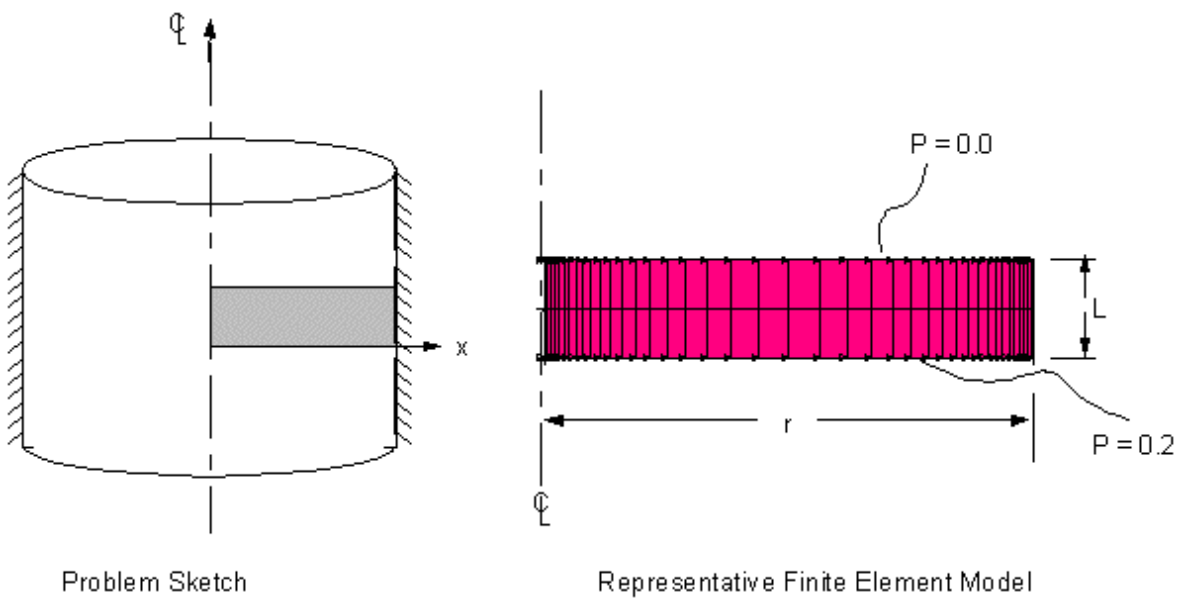

Material Properties ρ = 1.0 Kg/m^3 **Power Law Coefficient** μ_o = 1.297 k = 1.0 D0 = 1e-6 n = 0.8	**Geometric Properties** r = 1.0 m L = 0.2 m **Loading** ΔP = 0.20 Pa

Results Comparison

	Target	ANSYS	Ratio
Vy for x = 0.000	0.13503	0.13440	0.995
Vy for x = 0.006	0.13503	0.13440	0.995
Vy for x = 0.013	0.13502	0.13439	0.995
Vy for x = 0.021	0.13500	0.13438	0.995

	Target	ANSYS	Ratio
Vy for x = 0.500	0.10664	0.10628	0.997

Figure 219.2 Results Plot - VY Contours

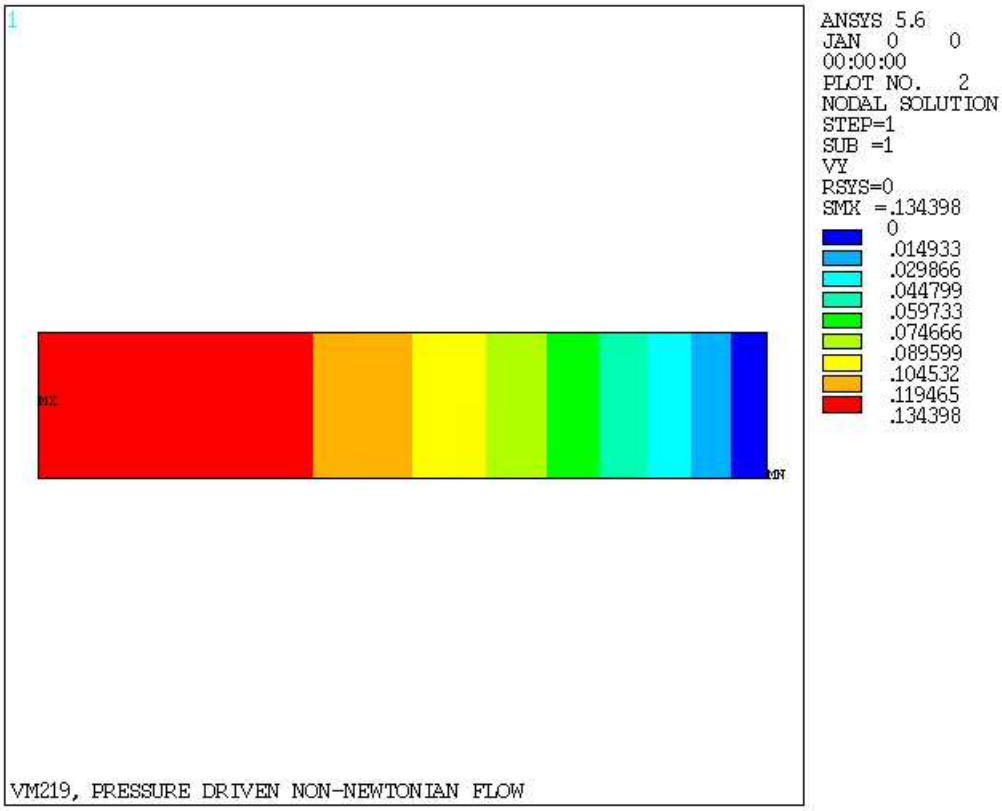

VM220: Eddy Current Loss in Thick Steel Plate

Overview

Reference:	K. K. Lim, P. Hammond, "Universal Loss Chart for the Calculation of Eddy-Current Losses in Thick Steel Plates", *Proc. IEE*, Vol. 117 No. 4, April 1970, pg. 861.
Analysis Type(s):	2-D Harmonic Response Analysis (**ANTYPE** = 3)
Element Type(s):	2-D 8-Node Magnetic Solid Elements (PLANE53)
Input Listing:	vm220.dat

Test Case

A 5 mm thick semi-infinite steel plate is subject to a tangential field created by a coil, H = 2644.1 A/m at a frequency of 50 Hz. The material conductivity, σ is 5 x 10^6 S/m. The B-H curve is defined by the equation B = H/(a+b |H|), where a = 156, b = 0.59. η, a geometry constant, is given to be 10.016. Compute the eddy current loss.

Figure 220.1 Thick Steel Plate Problem Sketch and Finite Element Model

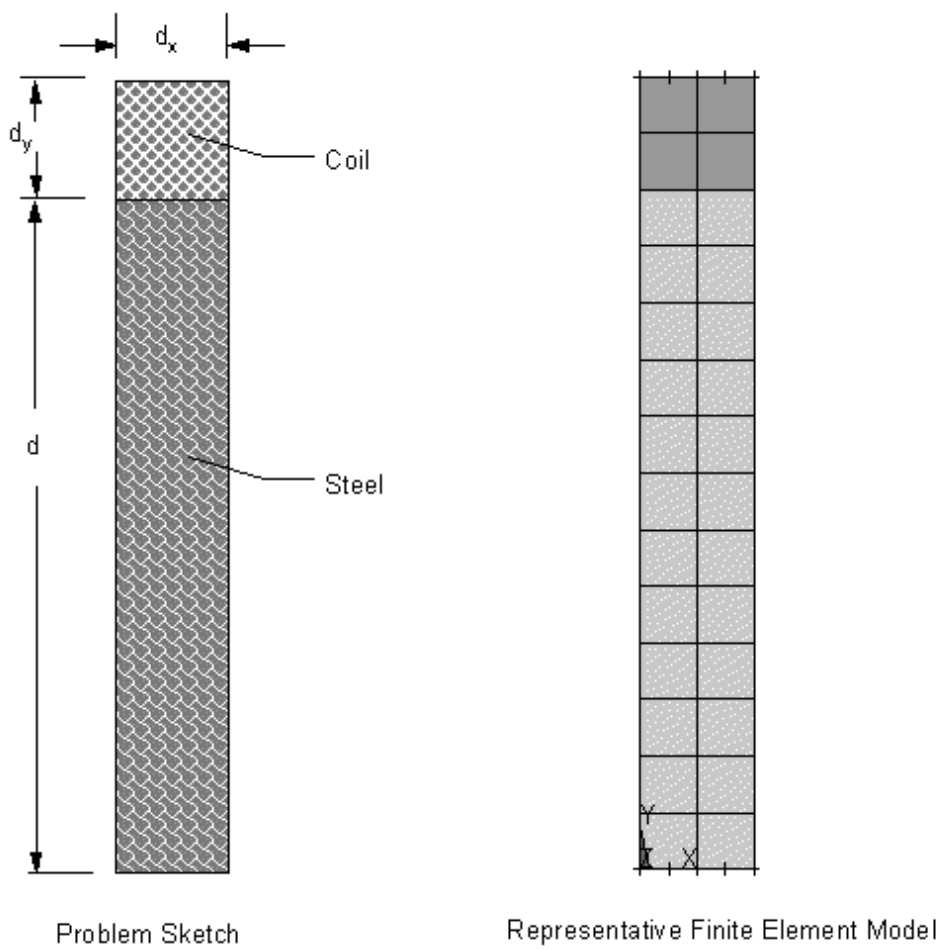

Material Properties	Geometric Properties	Loading
$\mu = 4\pi * 10^7$ H/m $\sigma = 5.0 \times 10^6$ S/m	d = 2.5 mm (half thickness of plate) d_x = d/6 (plate width) d_y = d/6 (coil height) η = 10.016	H = 2644.1 A/m (imposed H-field) f = 50 Hz

Analysis Assumptions and Modeling Notes

A nonlinear harmonic analysis is performed with PLANE53. The command macro POWERH is used to calculate the power loss in the plate.

Verification was performed by comparing the ANSYS results to those obtained through the use of the universal loss chart shown in the reference. The values of h_o and η are required to use the universal loss chart η, which is given to be 10.016 in this case.

The equation for h_o is $H / \xi = a/b$.

The universal loss chart (Lim Fig. 6), h_o vs. P_n, can now be used to extract P_n. By using the curve that is given for the value η, and h_o located at the x-axis, P_n is the corresponding value on the y-axis. The value found for P_n (1.2 W/m) is used to calculate the average losses, $P = P_n(H^2 / \sigma d)$. The loss was calculated to be 671.16 W/m^2.

Note that this result is for the half plate thickness. The full plate loss is twice the half plate, or 1342.3 W/m^2.

Results Comparison

Eddy Current Loss	Target	ANSYS	Ratio
PLANE53 (w/m^2)	1342.323[1]	1339.862	0.998

1. Results based on graphical data

Figure 220.2 B-H Curve

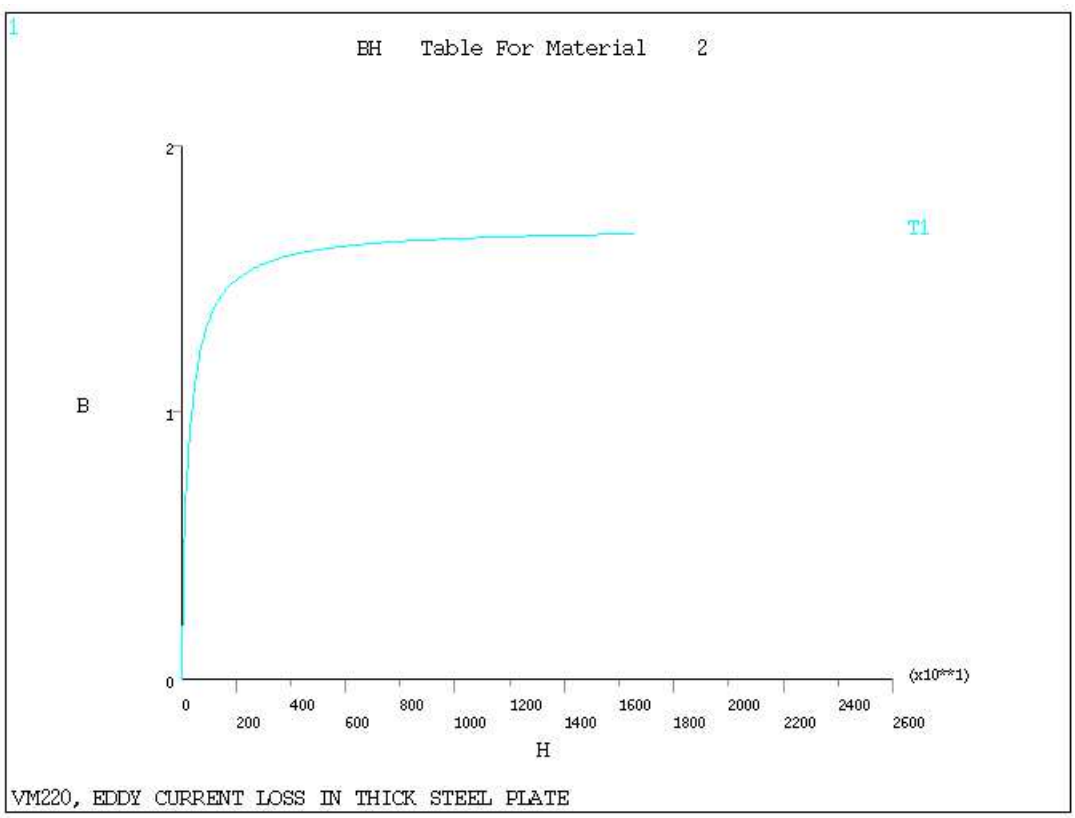

VM221: Inductance Calculation of a Transformer

Overview

Reference:	M. Gyimesi, D. Ostergaard, "Force Analysis with Edge Elements", *1998 ANSYS Conference Proceedings*, Vol. 2, ANSYS, Inc., Canonsburg, PA, 1998, pp. 299–302.
Analysis Type(s):	Nonlinear Magnetic Static Analysis (**ANTYPE** = 0)
Element Type(s):	3-D 20-Node Magnetic Solid Elements (SOLID117)
Input Listing:	vm221.dat

Figure 221.1 Representative Finite Element Model

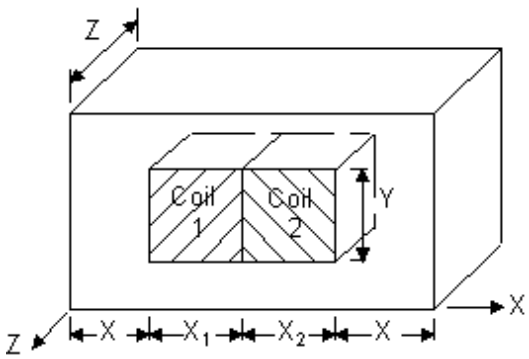

Test Case

A transformer with a nonlinear iron core is wound with two separate coils. Coil 1 is excited by a current of 0.2 A, while coil 2 is excited by a small current of 0.025 A. Calculate the self-inductance of both coil 1 and coil 2, and also the mutual inductance between the two coils.

Material Properties	**Geometric Properties**	**Loading**
$B = B_S \sqrt{\frac{H}{H_S}}$ where $B_S = 2T$ and $H_S = 100A / m$	$X = X_1 = X_2 = Y = Z = 0.015m$ $N_1 = 10$ (number of turns in coil 1) $N_2 = 20$ (number of turns in coil 2)	$I_1 = 0.2A$ (applied current in coil 1) $I_2 = 0.025A$ (applied current in coil 2)

Analysis Assumptions and Modeling Notes

In this problem the **LMATRIX** macro is used to solve the coil inductance about an operating point (I1, I2). The finite element representation is modeled by three blocks, coil 1, coil 2, and the nonlinear iron core. The blocks are meshed using magnetic-edge element SOLID117. The target results are based on the Enhanced Incremental Energy Method (EIEM - see M. Gyimesi, D. Ostergaard, "Force Analysis with Edge Elements") for finding inductance of coils when the core is nonlinear.

Results Comparison

		Target	ANSYS	Ratio
Inductance	Self Coil 1	0.40	0.399	0.999
	Self Coil 2	1.60	1.599	0.999

	Mutual	0.80	0.799	0.999
		Target	**ANSYS**	**Ratio**
Energy (J)	Energy	.0166	.0167	1.005
	Coenergy	.0333	.0333	1.000
Flux (W)	Coil1	.2	.1999	.999
	Coil2	.4	.3998	.999

Figure 221.2

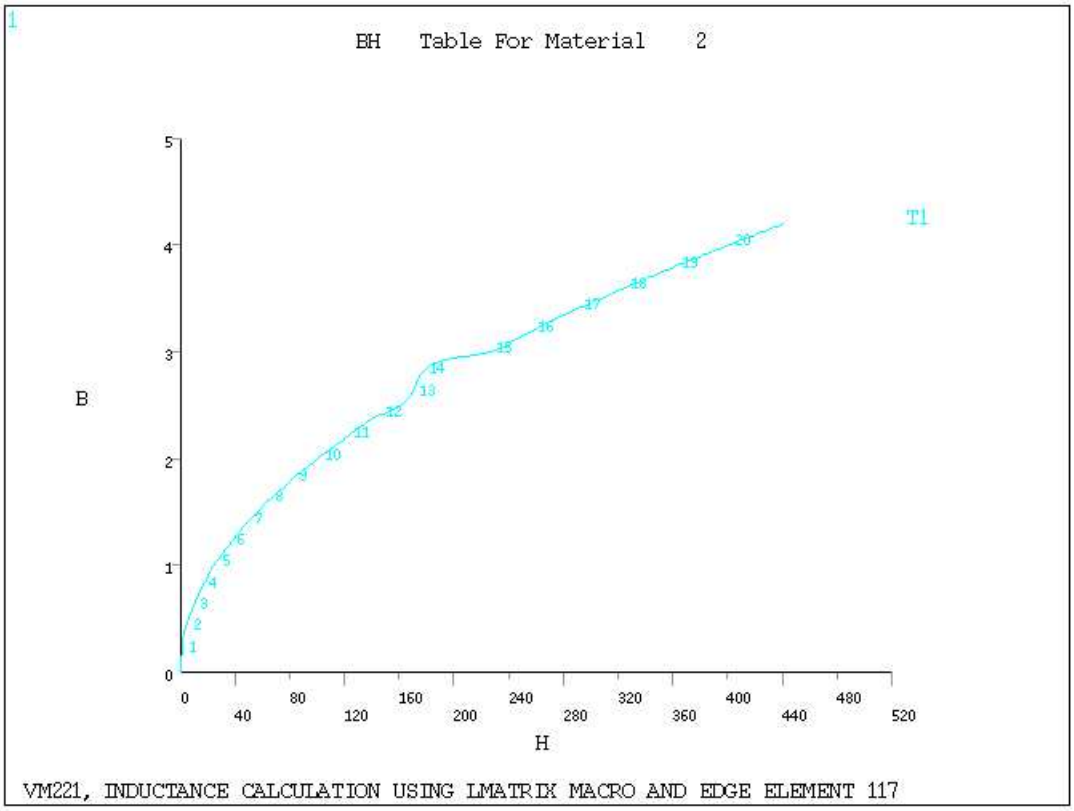

Figure 221.3

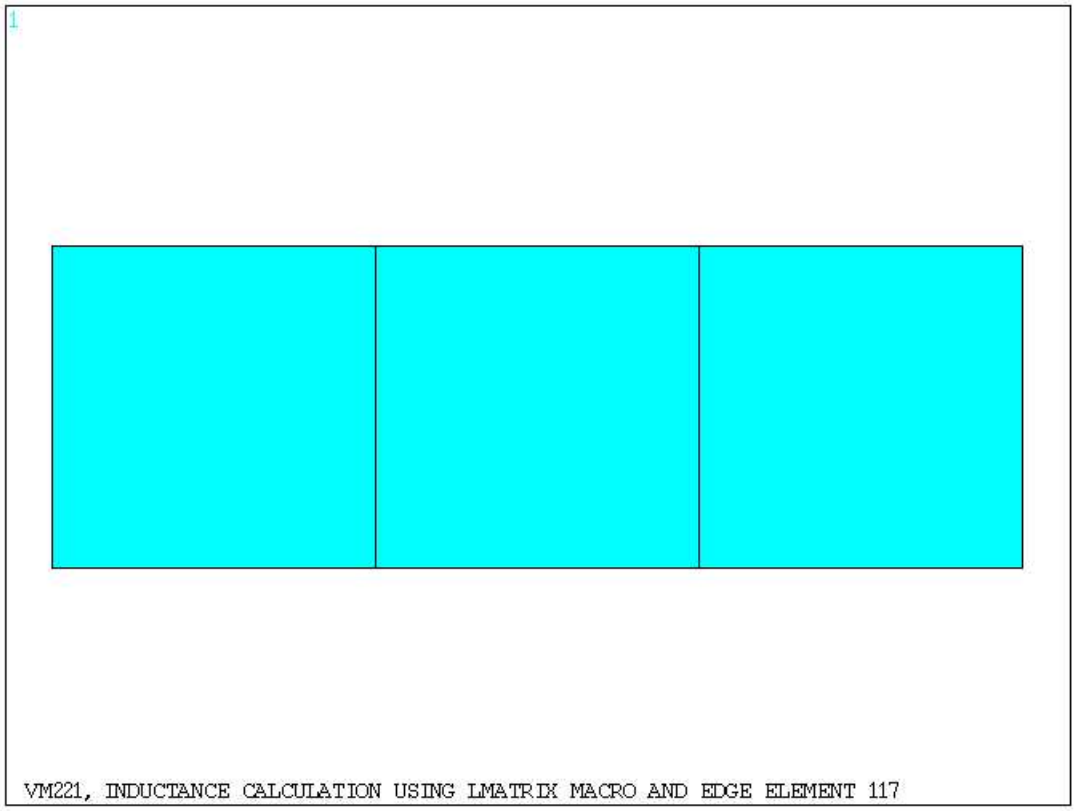
1
VM221, INDUCTANCE CALCULATION USING LMATRIX MACRO AND EDGE ELEMENT 117

VM222: Warping Torsion Bar

Overview

Reference:	C-N Chen, "The Warping Torsion Bar Model of the Differential Quadrature Method", *Computers and Structures*, Vol. 66 No. 2-3, 1998, pp. 249-257.
Analysis Type(s):	Static Structural (**ANTYPE** = 0)
Element Type(s):	3-D Linear Finite Strain Beam Elements (BEAM188) 3-D Quadratic Finite Strain Beam Elements (BEAM189)
Input Listing:	vm222.dat

Test Case

A cantilever I-beam is fixed at both ends and a uniform moment, M_x, is applied along its length.

Figure 222.1 Warping Torsion Bar Problem Sketch

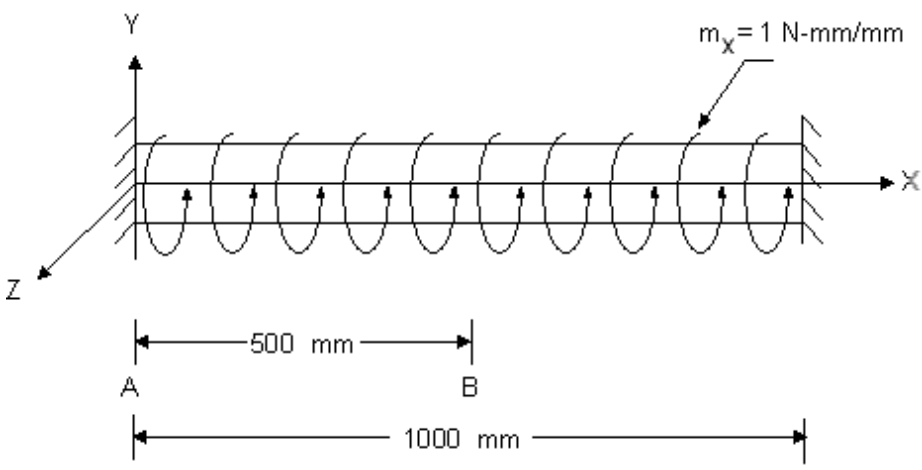

Material Properties	**Geometric Properties**
Warping rigidity (EC_W) = 7.031467e12 Nmm^4 and GJ=3.515734e7 Nmm^2 Warping constant (C_W) =0.323e8 and J=431.979 (E=217396.3331684 N/mm^2 and G=81386.6878 N/mm^2) Poisson's Ratio = (E/(2*G))-1 = 0.33557673 **Loading** Moment = 1Nmm/mm	b=40mm h=80mm t=2mm L=1000mm

Figure 222.2 I-Beam Section Plot

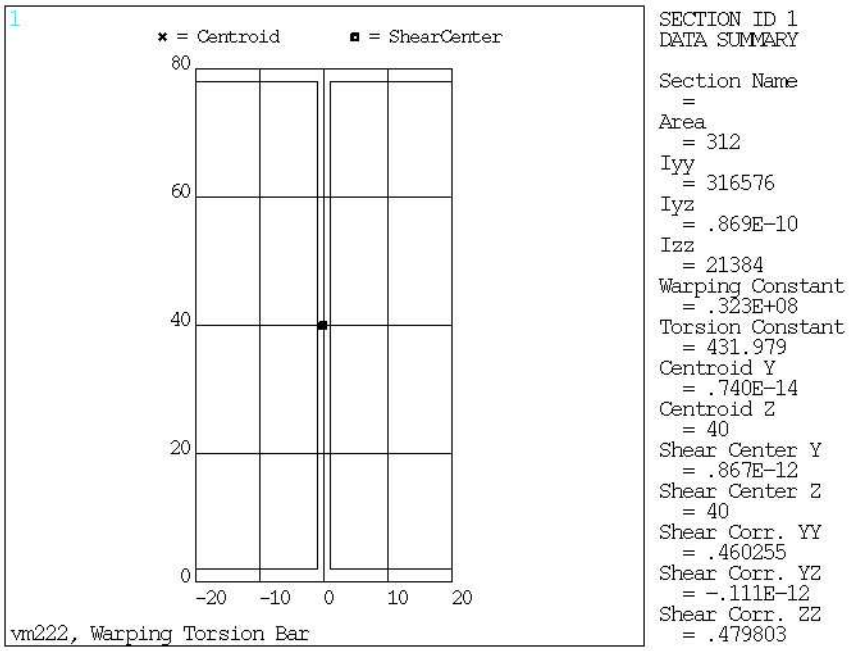

Analysis Assumptions and Modeling Notes

Given that:

EC_w = 7.031467E12 Nmm^4(warping rigidity)
Iyy = 316576 mm^4 for this beam cross section

and

GJ = 3.515734E7 Nmm^2
C_w = 0.323E8 mm^6 (warping constant)
J = 431.979 mm^4 (torsion constant)
E = 217396.333 N/mm^2 (Young's modulus)

Therefore υ = E/2G-1 = 0.33557673 (Poisson's ratio)

Uniformly distributed moments are converted to a moment load on each element.

mload1 and mload2 are the loads on the beam ends.

The warping DOF results are compared to the reference at the midspan.

Results Comparison

MX Twist in X-Direction	Target	ANSYS	Ratio
BEAM188	0.3293E-03	0.3326E-03	1.010
BEAM189	0.3293E-03	0.3330E-03	1.011

Figure 222.3 Warping Torsion Bar Plot

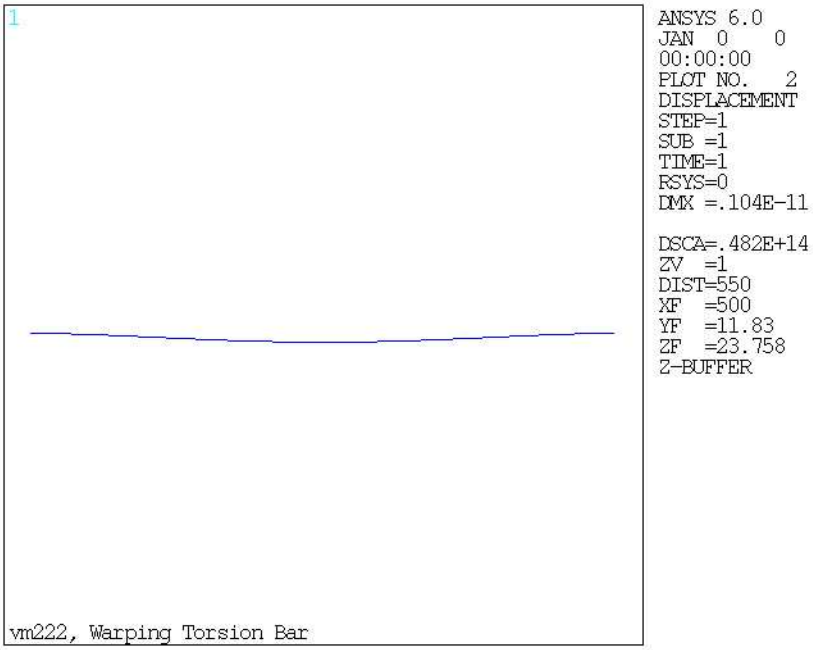

Figure 222.4 Warping Torsion Bar Plot

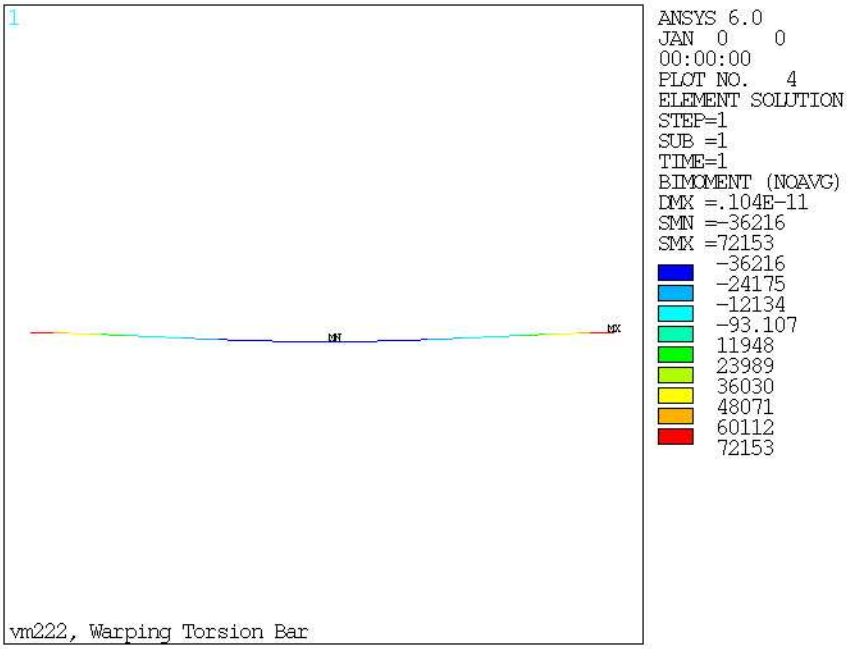

VM223: Frequency Response of a Prestressed Beam

Overview

Reference:	R. D. Blevins, *Formulas for Natural Frequency and Mode Shape*, Van Nostrand Reinhold Co., New York, NY, 1979, pg. 144, eq. 8-20.
Analysis Type(s):	Static Analysis (**ANTYPE** = 0), Modal (**ANTYPE** = 2)
Element Type(s):	2-D Elastic Beam Elements (BEAM3) Electromechanical Transducer Elements (TRANS126)
Input Listing:	vm223.dat

Test Case

A parallel-plate capacitor is attached to the end of a long slender beam. A DC voltage drop is applied across the capacitor, loading the beam in tension. Compute the natural frequency of the beam.

Material Properties	**Geometric Properties**
I = B X H^3 / 12 Beam moment of inertia E = 169 X 10^3 μN / μm^2 Modulus D = 2332 X 10^{-18} kg / μm^3 Density ε_0 = 8.85 X 10^{-6} pF / μm Free space permittivity **Loading** V = 150.162 volts Applied voltage to plate	L = 150 μm Beam length B = 4 μm Beam width H = 2 μm Beam height P_A = 100 μm^2 Capacitor plate area CAP_1 = 1 μm Initial gap C3 = 0.885 X 10^{-5} Transducer capacitance real constant

Analysis Assumptions and Modeling Notes

The beam is assumed to be pinned at both ends. Furthermore, the analysis uses an unsymmetric matrix. Calculations assume the gap stiffness is much less than the beam stiffness and will not effect the frequency solution.

Results Comparison

Pre- stress	Target	ANSYS	Ratio
Freq1	0.3517E06	0.3517E06	1.000
Freq2	0.1381E07	0.1381E07	1.000
Freq3	0.3097E07	0.3095E07	0.999

Figure 223.1 Freq1 Results Plot

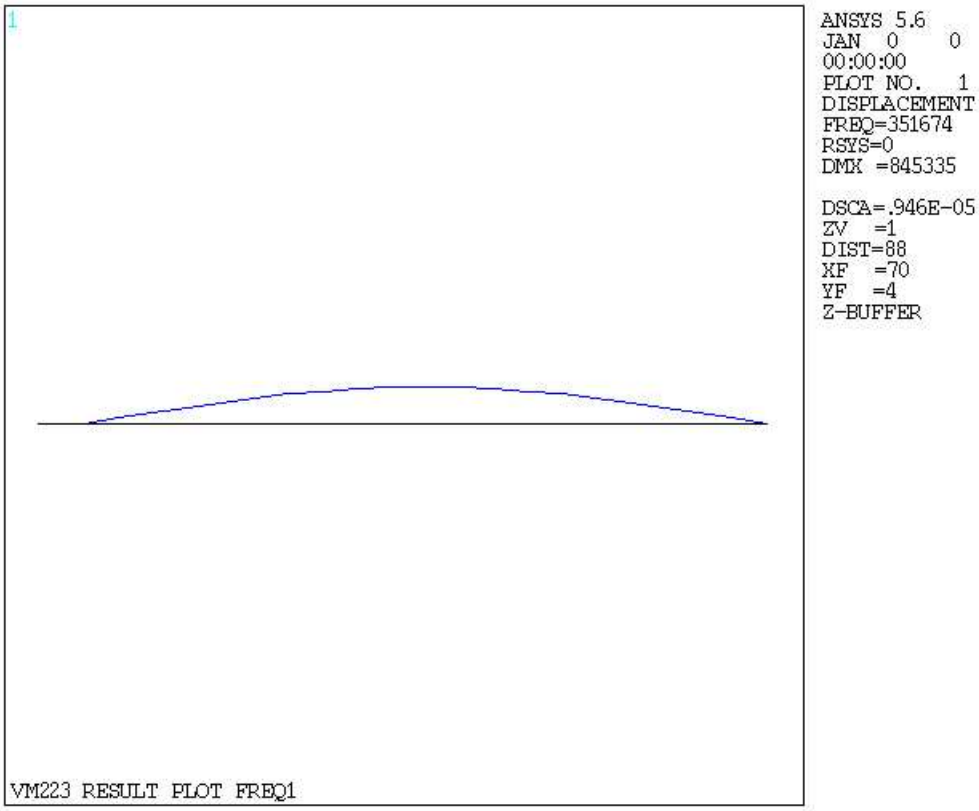

Figure 223.2 Freq2 Results Plot

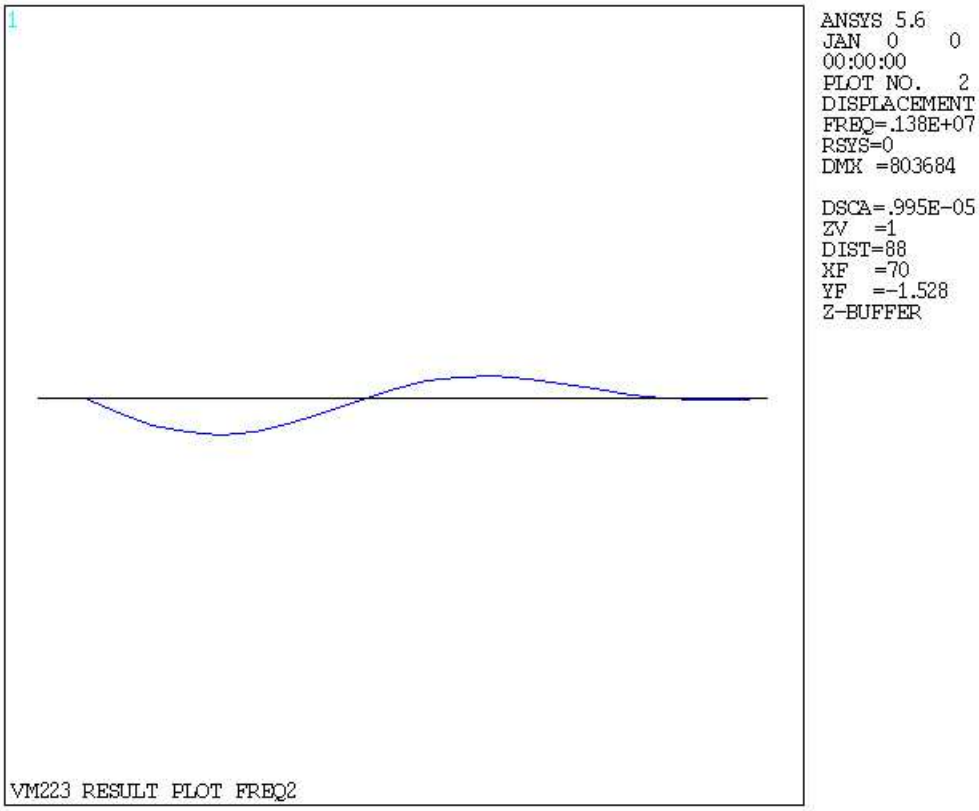

Figure 223.3 Freq3 Results Plot

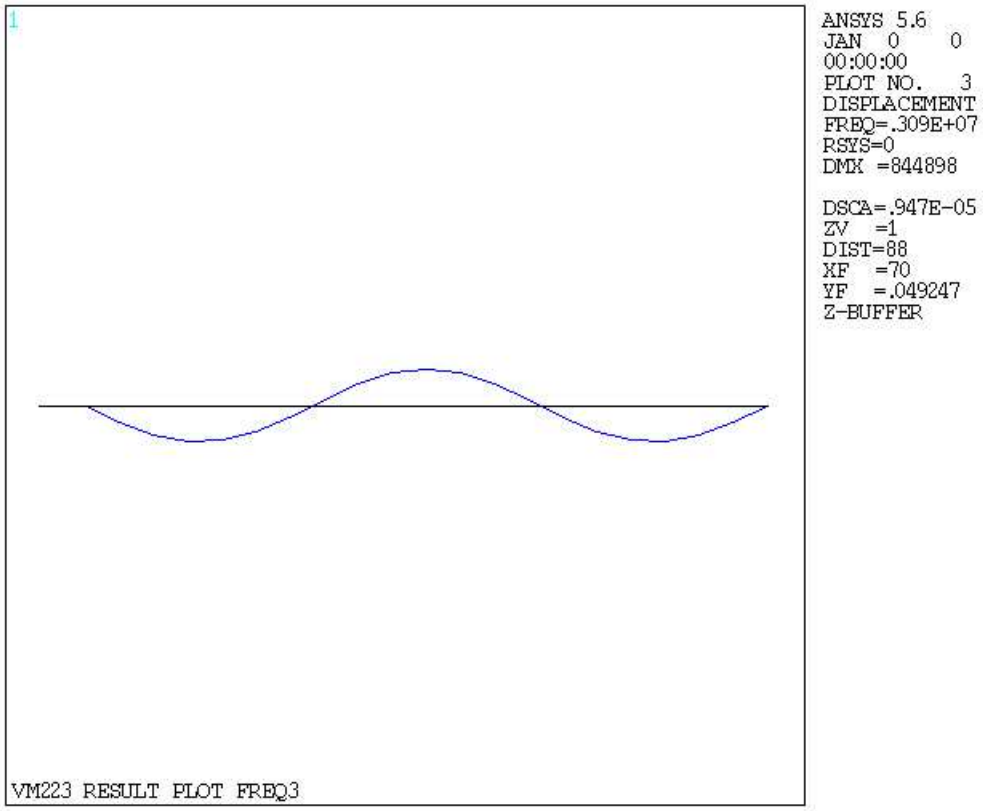

VM224: Implicit Creep under Biaxial Load

Overview

Reference:	A. A. Becker, T. H. Hyde, *Fundamental Test of Creep Behavior*, 2nd Edition, NAFEMS, Ref.: R0027, Test 10a.
Analysis Type(s):	2-D Plane Stress - Biaxial (Negative) Load
Element Type(s):	2-D 4-Node Structural Solid Elements (PLANE182) 2-D 8-Node Structural Solid Elements (PLANE183)
Input Listing:	vm224.dat

Test Case

A specimen under plane stress conditions is constrained on the left and bottom edges. It is biaxially loaded with tensile stress σ_1 on the right edge and compressive stress σ_2 on the top edge. Determine the creep strain after 1000 hours.

Figure 224.1 Implicit Creep Under Biaxial Load Problem Sketch

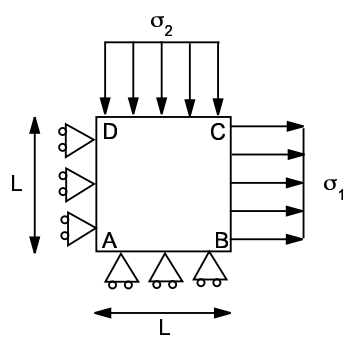

Problem Sketch

Material Properties	**Creep Law**	**Loading**
$E = 200 \times 10^3$ N/mm^2 $\nu = 0.3$ **Geometric Properties** L = 100 mm	$\varepsilon = A\,\sigma^n t^m$ $A = 3.125 \times 10^{-14}$ per hour n = 5 m = 0.5	$\sigma_1 = 200$ N/mm^2 $\sigma_2 = -200$ N/mm^2 Total creep time 1000 hours

Analysis Assumptions and Modeling Notes

For a 2-D plane stress condition a biaxial load is applied as follows:

$$\sigma_{xx} = \sigma_0$$

$$\sigma_{yy} = \alpha\sigma_0$$

In this case the effective stress is given by the following equation, where $\alpha = -1$

$$\sigma_{eff} = \sigma_0 \left(\alpha^2 - \alpha + 1\right)^{\frac{1}{2}}$$

And the creep strains may be obtained as follows:

$$\varepsilon_{xx}^{c} = A(\sigma_0)^n \left[\frac{1}{2}(2-\alpha)(\alpha^2-\alpha+1)^{\frac{(n-1)}{2}} \right] t^m$$

$$\varepsilon_{yy}^{c} = A(\sigma_0)^n \left[\frac{1}{2}(2\alpha-1)(\alpha^2-\alpha+1)^{\frac{(n-1)}{2}} \right] t^m$$

$$\varepsilon_{zz}^{c} = A(\sigma_0)^n \left[\frac{1}{2}(\alpha+1)(\alpha^2-\alpha+1)^{\frac{(n-1)}{2}} \right] t^m$$

This gives the following reference solution:

$$\varepsilon_{xx}^{c} = 0.135t^{0.5}$$

$$\varepsilon_{yy}^{c} = -0.135t^{m}$$

$$\varepsilon_{zz}^{c} = 0$$

Results Comparison

@ Time = 1000	Target	ANSYS	Ratio
PLANE182 2-D 4-Node Structural Solid			
ecrxx	4.2691	4.2691	1.000
ecryy	-4.2691	-4.2691	1.000
PLANE183 2-D 8-Node Structural Solid			
ecrxx	4.2691	4.2691	1.000
ecryy	-4.2691	-4.2691	1.000

Figure 224.2 Creep Strain

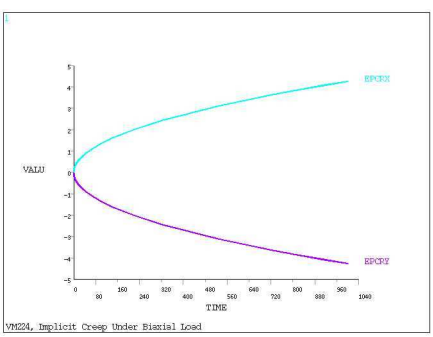

VM225: Rectangular Cross-Section Bar with Preload

Overview

Reference:	Engineering Statics Text
Analysis Type(s):	Static, Preloading Analysis
Element Type(s):	3-D Structural Solid Elements (SOLID45) Pretension Elements (PRETS179) 3-D Structural Solid Elements (SOLID185)
Input Listing:	vm225.dat

Test Case

A compressive preload is applied to a rectangular cross-section bar. Determine the resulting stress and displacement.

Figure 225.1 Finite Element Model

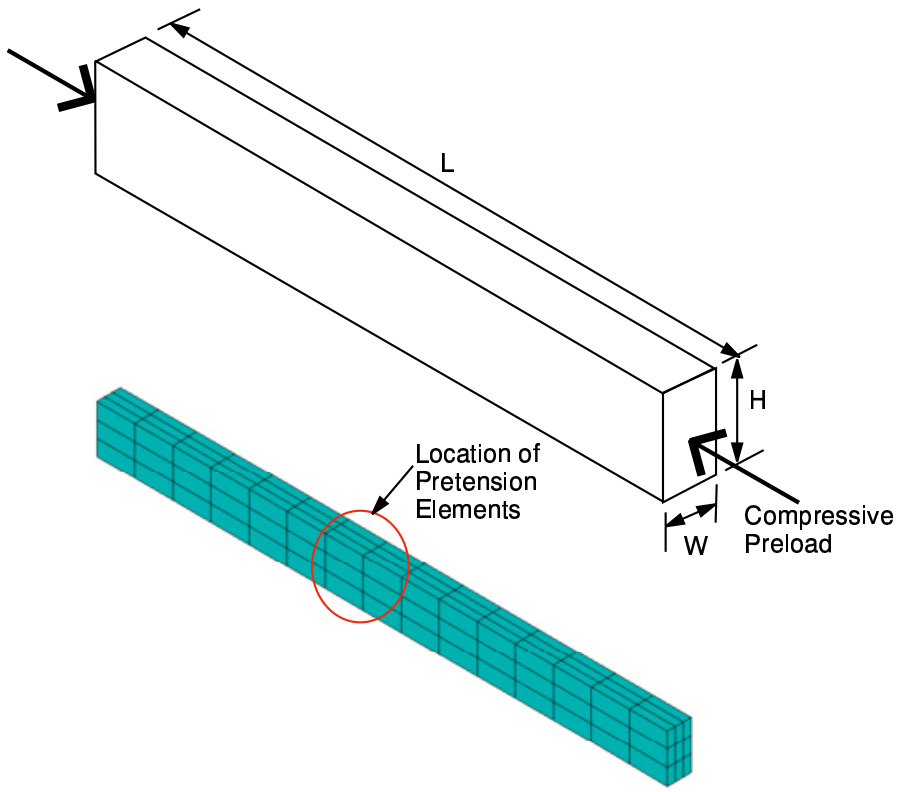

Material Properties	Geometric Properties	Loading
E = 30,000,000 psi ν = 0.3	L = 12 in W = 1 in H = 2 in	F = 500 lbf

Analysis Assumptions and Modeling Notes

The problem is solved in two different ways:

- using 3-D solid elements (SOLID95)
- using 3-D solid elements (SOLID186)

Due to symmetry, only one-quarter of the bar is modeled. The preload is applied using the PRETS179 2-D/3-D Pretension Element and the **SLOAD** command.

Results Comparison

	Target	ANSYS	Ratio
SOLID45			
Stress SigX (psi)	250.0	250.0	1.0
Displacement (UX)	0.00010	0.00010	1.0
SOLID185			
Stress SigX (psi)	250.0	250.0	1.0
Displacement (UX)	0.00010	0.00010	1.0

VM226: Fourier Series Analysis of a Diode Rectified Circuit

Overview

Reference:	A. S. Sedra, K. C. Smith, *Microelectronic Circuits*, 4th Edition, Oxford University Press, 1977.
Analysis Type(s):	Transient
Element Type(s):	Electric Circuit Elements (CIRCU124) Diode Elements (CIRCU125)
Input Listing:	vm226.dat

Test Case

Compute the Fourier series coefficients of the output voltages from the following two circuits, the first with no capacitance, second with a capacitance of 1E-6F, third with a capacitance of 10E-6F, and finally with a capacitance of 1E-3F.

Figure 226.1 Diode Rectified Circuit Problem Sketch

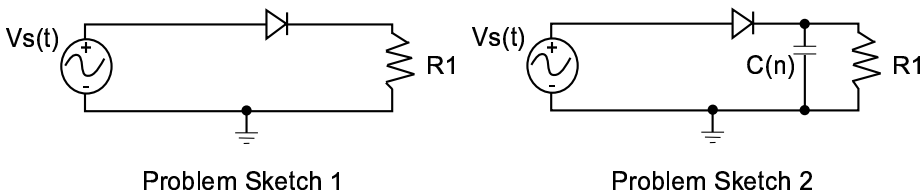

Geometric Properties	**Loading**
R1 = 2500 Ohm C1 = 1E-6 F C2 = 10E-6 F	Vs = 135 sin (60 * pi * t) V

Analysis Assumptions and Modeling Notes

These circuits make use of CIRCU125 diode elements, which have parameters that are set up to produce ideal characteristics. The circuit in Problem Sketch 1 is modeled to be a simple half-wave rectifier with three elements:

- a voltage source
- an ideal diode
- a single load resistor

In this case computing the Fourier series coefficients is a minor task. However, in Problem Sketch 2, a capacitor is introduced into the circuit which causes a combination, sinusoidal-exponential output waveform, and hence making the Fourier series calculation much more complex.

Definition:

$$V_{LOAD}(t) = \frac{a0}{2} + \sum_{n>0} \left(an\cos\left(\frac{2n\pi}{T}t\right) + bn\sin\left(\frac{2n\pi}{T}t\right) \right)$$

Problem Sketch One: Resistor, Diode and Voltage Source

We have: Vs(t) = Vsl*SIN(ωt)

where:

Vsl = 135 Volts
ω = 2πf and f = (1)/T = 60 Hz

Fourier coefficients:

$$-a_0 = \frac{2}{T}\int_0^{T/2} Vs(t)\,dt = \frac{2*Vs1}{\pi}$$

$$-a_n = \frac{2}{T}\int_0^{T/2} Vs(t)\cos(n\omega t)\,dt$$

So we have:

$$\begin{cases} n>1,\ a_n = \dfrac{Vs1}{\omega T}\left[\dfrac{1}{n+1}(1-\cos((n+1)\pi)) - \dfrac{1}{n-1}(1-\cos((n-1)\pi)\right] \\ a_1 = 0 \end{cases}$$

That is to say:

$$\begin{cases} p \geq 0,\quad a_{2p} = \dfrac{-2Vs1}{\pi((2p)^2-1)} \\ p \geq 0,\quad a_{2p+1} = 0 \end{cases}$$

$$b_n = \frac{2}{T}\int_0^{T/2} Vs(t)\sin(n\omega t)\,dt$$

So we have:

$$\begin{cases} n>1,\ b_n = \dfrac{Vs1}{\omega T}\left[\dfrac{-1}{n+1}\sin\left((n+1)\dfrac{\omega T}{2}\right) + \dfrac{1}{n-1}\sin\left((n-1)\dfrac{\omega T}{2}\right)\right] \\ b_1 = \dfrac{Vs1}{2} \end{cases}$$

That is to say:

$$\begin{cases} b_1 = \dfrac{Vs1}{2} \\ n>1,\ b_0 = 0 \end{cases}$$

Figure 226.2 Output Voltage with No Capacitance

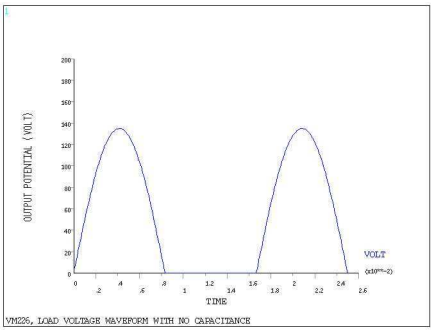

Figure 226.3 Plot of Fourier Series Without Capacitance

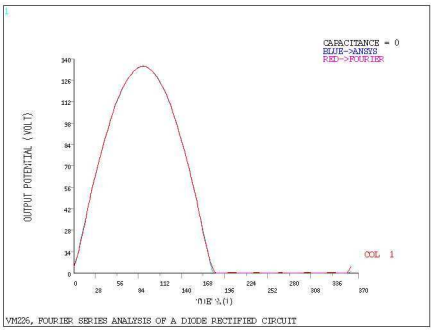

Figure 226.4 Resistor, Capacitor, Diode and Voltage Source

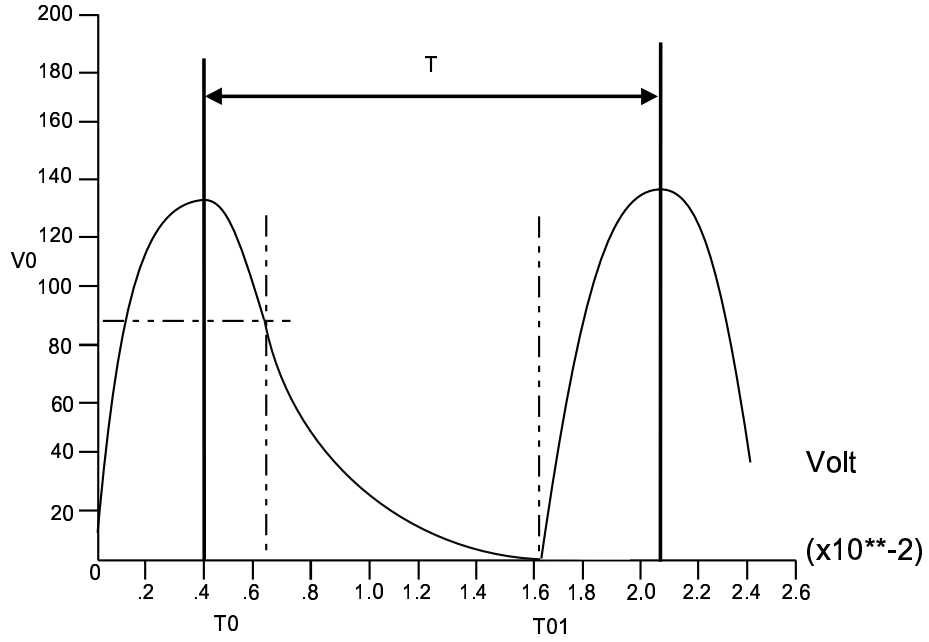

To compute the Fourier coefficients, take a periodic signal such that the first time (TO) will be the first maximum of Vs(t) and the end time (TO1) will be the second maximum of Vs(t).

We have:

Vsl = 135 Volts

$\omega = 2\pi f$ and $f = (1)/T = 60$ Hz
$\tau = RC$
$0 < t < T0$: $Vs(t) = Vsl*COS(\omega.t)$
$T0 < t < T01$: $Vs(t) = V0*EXP(-(t-T0)/\tau)$
$T01 < t < T$: $Vs(t) = Vsl*COS(\omega.t)$

How to Find T0 and T01

For T0 we have:

$$\begin{cases} \frac{dVs(t)}{dt}(t < T0) = \frac{dVs(t)}{dt}(t > T0) \\ -\omega Vs1\sin(\omega t) = -\frac{V0}{\tau}\exp(-\frac{t-T0}{\tau}) = -\frac{Vs1\cos(\omega t)}{\tau} \\ t = \frac{1}{\omega}\arctan(\frac{1}{\omega\tau}) \end{cases}$$

Due to the discontinuity of the function, T01 must be found using a Newton's Method algorithm which can be done using ANSYS. The code that performs this operation can be found in the input listing.

T01 verifies this equation:

$$Vs1\cos(\omega t) = Vo\exp(-\frac{t-T0}{\tau})$$

Compute only the first three Fourier coefficients: a_0, a_1 and b_1.

First Fourier Coefficient:

$$a_0 = \frac{2}{T}\int_0^T Vs(t)\,dt$$

$$a_0 = \frac{Vs1}{\pi}(\sin(\omega T0) - \sin(\omega T01)) + \frac{2V0\tau}{T}\left(1 - \exp\left(-\frac{T01-T0}{\tau}\right)\right)$$

Second Fourier Coefficient:

$$a_1 = \frac{2}{T}\int_0^T Vs(t)\cos(\omega t)\,dt$$

$$a_1 = \frac{2}{T}\left(\int_0^{T0} Vs1*\cos^2(\omega t)\,dt + \int_{To1}^{T} Vs1*\cos^2(\omega t)\,dt\right) + A1$$

$$a_1 = \frac{2Vs1}{T}\left(\frac{T0+T-T01}{2} + \frac{1}{4\omega}(\sin(2\omega T0) - \sin(2\omega T01))\right) + A1$$

$$A1 = \frac{2V0}{T}\int_{T0}^{T01} \exp\left(-\frac{t-T0}{\tau}\right)\cos(\omega t)\,dt$$

$$A1 = \frac{2V0\tau}{T(1+\omega^2\tau^2)}\left[\cos(\omega T0) + \omega\tau\sin(\omega T01) - (\cos(\omega T01) - \omega\tau\sin(\omega T01))\exp\left(-\frac{T01-T0}{\tau}\right)\right]$$

Third Fourier Coefficient:

$$b_1 = \frac{2}{T}\int_0^T Vs(t)\sin(\omega t)\,dt$$

$$b_1 = \frac{2}{T}\left(\int_0^{T0} Vs1\cos(\omega t)\sin(\omega t)\,dt + \int_{T0}^{T01} Vs1\cos(\omega t)\sin(\omega t)\,dt\right) + B1$$

$$b_1 = \frac{Vs1}{2\pi}(\sin^2(\omega T0) - \sin^2(\omega T01)) + B1$$

$$B1 = \frac{2V0}{T}\int_{T0}^{T01} \exp\left(-\frac{t-T0}{\tau}\right)\sin(\omega t)\,dt$$

$$B1 = \frac{2V0\tau}{T(1+\omega^2\tau^2)}\left[\sin(\omega T0) + \omega\tau\cos(\omega T0) - (\sin(\omega T01) + \omega\tau\cos(\omega T01))\exp\left(-\frac{T01-T0}{\tau}\right)\right]$$

Figure 226.5 VLOAD with Capacitance of 1E-6F

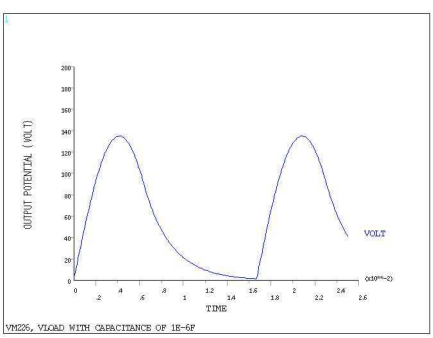

Figure 226.6 Plot of Fourier Series With Capacitance

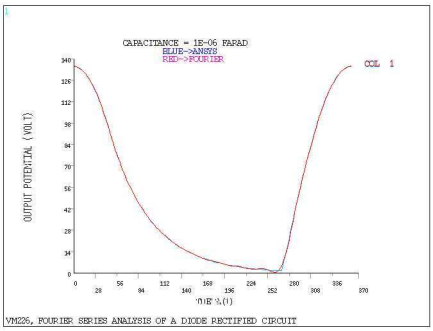

Figure 226.7 VLOAD With Capacitance of 10E-6F

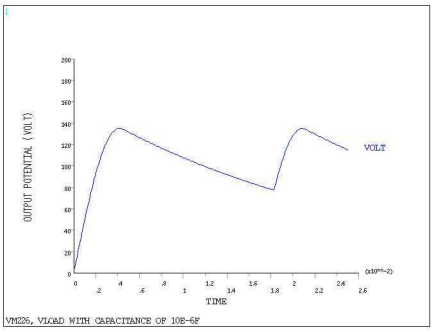

Results Comparison

		Target	ANSYS	Ratio
Tau = 0	A0/2	42.9718	42.9834	0.9997
	A1	0	0.0151	0
	B1	67.5	67.4920	1.0001
Tau = 0.0025	A0/2	50.7897	50.7893	1.0000
	A1	61.7634	61.7542	1.0001
	B1	10.3401	10.3463	0.9994
Tau = 0.025	A0/2	105.4741	105.4266	1.0005
	A1	13.8684	13.8831	0.9989
	B1	16.4932	16.4729	1.0012

VM227: Radiation Between Finite Coaxial Cylinders

Overview

Reference:	M. Modest, *Radiative Heat Transfer*, McGraw-Hill Book Co., Inc., New York, NY, 1992, p. 791, View Factor Evaluations 44, 45.
Analysis Type(s):	Steady State Radiosity
Element Type(s):	2-D 8-Node Thermal Solid Elements (PLANE77)
Input Listing:	vm227.dat

Test Case

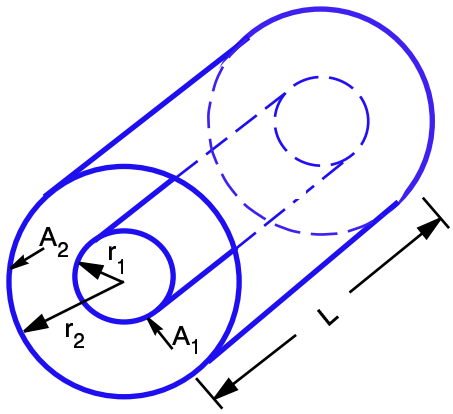

Problem Sketch

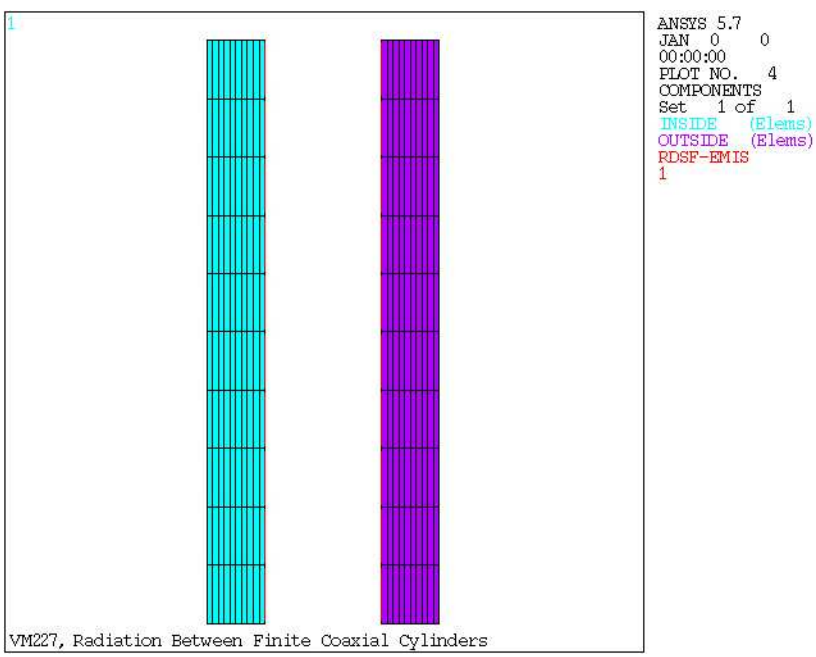

This test is designed to show a quick calculation of the end effects which are present in the radiation solution of two finite concentric cylinders. Concentric cylinders of length L, with radii r_1 and r_2, are created, and the radiosity method is used to determine radiation view factors upon the facing surfaces.

Geometric Properties	Loading
l = 10	Interior surface of external cylinder $\varepsilon = 1$
$r_1 = 1$	Axial surface of internal cylinder $\varepsilon = 1$
$r_2 = 3$	All other surfaces $\varepsilon = 0$

Analysis Assumptions and Modeling Notes

The model is reduced to a 2-D axisymmetric case. The material is assumed to be isotropic, the surface is assumed to have uniform emissivity.

A = 108

B = 92

Results

	Target	ANSYS	Ratio
VF (1-1)	0.000	0.000	0.000
VF (2-1)	0.288	0.288	1.000
VF (2-2)	0.503	0.480	0.950

VM228: Radiation Between Infinite Coaxial Cylinders

Overview

Reference:	R. Siegel, J. R. Howell, *Thermal Radiation Heat Transfer*, Hemisphere Publishing, 1992, p. 188.
Analysis Type(s):	Steady State Radiosity
Element Type(s):	2-D 6-Node Triangular Thermal Solid Elements (PLANE35)
Input Listing:	vm228.dat

Test Case

Two concentric infinite cylinders are transferring heat to each other through radiation. The problem is modeled as a 2-D pair of concentric circles. The facing surfaces are given surface emissivity values, the non facing surfaces are at fixed temperatures

Material Properties	**Geometric Properties**	**Loading**
E = 30e6	r1 = 1	Interior of exterior cylinder $\varepsilon = 1$
$K_{xx} = 1$	r2 = 4	Exterior of interior cylinder $\varepsilon = 1$
$\rho = 0.21$	$\sigma = 1.19e\text{-}11$	All other surfaces $\varepsilon = 0$
$\alpha_x = .21$		Exterior of Exterior cylinder T = 1000
$\nu_{xy} = .27$		Interior of Interior cylinder T = 100

Analysis Assumptions and Modeling Notes

The cylinders are assumed to be infinite length, with no end effects, and with uniform surface characteristics. As such, any point on one surface should have the same view factor and characteristics as any other point on the same surface.

F(11) = 0 As a circle, it cannot see itself from any part of its surface.
F(12) = 1 Consequence of no radiation to space
F(21) = (A1/A2)F(12) Basic rule of view factors
F(21) = (r1/r2)F(12)
F(21) = r1/r2
F(22) = 1 - (r1/r2) Consequence of no radiation to space

As a check on the system, the heat flux at two points are compared to that expected by $\sigma(T_1^4 - T_2^4)$

Results Comparison

	Target	**ANSYS**	**Ratio**
$F_{(11)}$	0	0	n/a
$F_{(21)}$	0.25	0.249	0.996
$F_{(22)}$	0.75	0.751	1.001
Heat flux (interior) at node 4	11.036	11.537	0.963
Heat flux (exterior) at node 13	2.742	2.884	0.95

VM229: Friction Heating of Sliding Block

Overview

Reference:	P. Wiggers, C. Miehe, "Contact Constraints Within Coupled Thermomechanical Analysis - A Finite Element Model", *Computer Methods in Applied Mechanics and Engineering*, Vol. 113, 1994, pp. 301-319.
Analysis Type(s):	Transient (**ANTYPE** = 4)
Element Type(s):	2-D Coupled-Field Solid Elements (PLANE13) 2-D Target Segment Elements (TARGE169) 2-D 2-Node Surface-to-Surface Contact Elements (CONTA171)
Input Listing:	vm229.dat

Test Case

Consider a block sliding over another fixed block. Calculate the temperature changes caused by friction between the blocks.

Material Properties	**Geometric Properties**	**Loading**
E = 70000 ρ = 2.7E-9 N s^2/mm^4 α = 23.86E-6 K^{-1} ν = 0.3 μ = 0.2 K_{xx} = 150 N/s K C = 9E8 mm^2/s^2 K	**Sliding Block:** Height = 1.25mm Width = 1.25mm **Fixed Block:** Height = 1.25mm Width = 5mm	Displacement = 3.75mm

Analysis Assumptions and Modeling Notes

In this test the two blocks are modeled using PLANE13 elements with CONTA171 elements placed on the bottom surface of the sliding block, and TARGE169 elements placed at the top surface of the fixed block. In the first load step, the sliding block moves 3.75 mm on the surface of the fixed block with an applied pressure of 10 N/mm^2. The displacement of the sliding block occurs within a time period of 3.75 ms. Heat is generated by friction and is absorbed by the two blocks. To obtain the steady-state solution, a second load step with 100 time steps was performed with no loading at a duration of 1s. The calculated steady-state results were taken from the end of the final load step.

The same analysis is repeated using Pure Lagrange Multipliers method (KEYOPT(2) = 4 -- Pure Lagrange multiplier on contact normal and tangent) of CONTA171 elements.

Results Comparison

	Target	**ANSYS**	**Ratio**
Temp 1 (K)	1.235	1.2346	1.000
Temp 2 (K)	0.309	0.3087	0.999
With KEYOPT (2) = 3 of CONTA171			
Temp 1 (K)	1.2350	1.2346	1.000
Temp 2 (K)	0.3090	0.3087	0.999

Figure 229.1 Temperature Change for Sliding Block with Friction

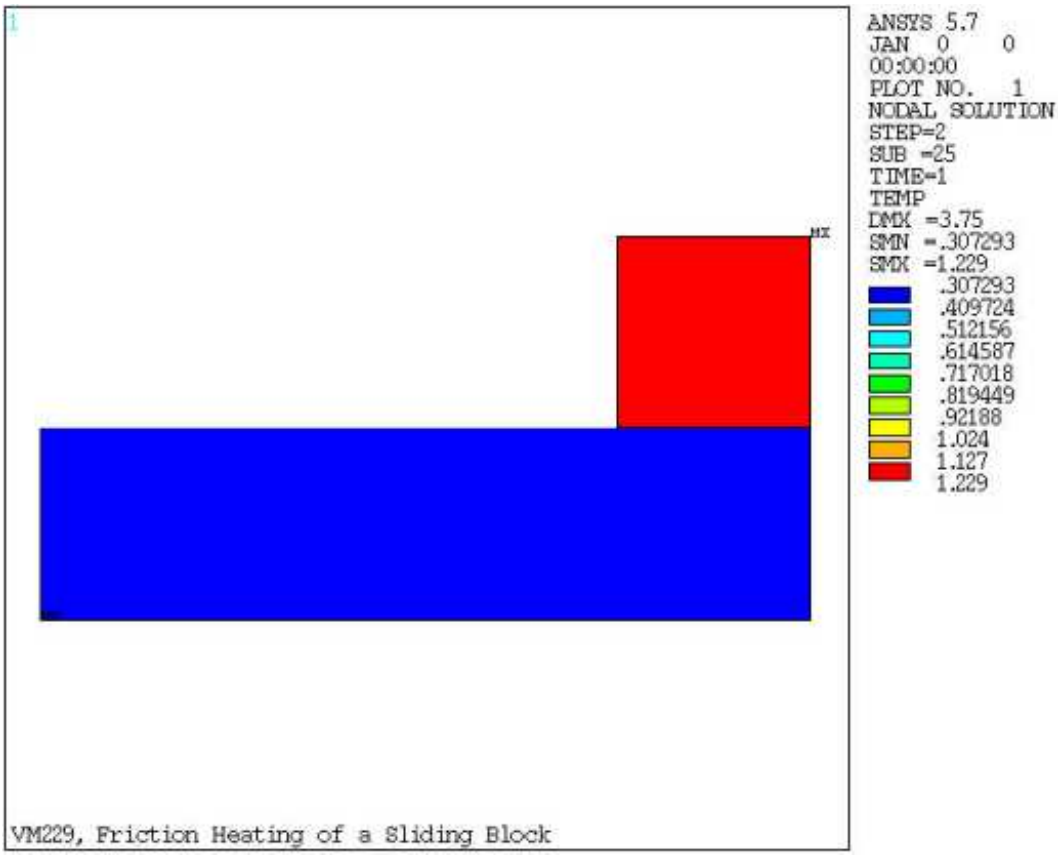

VM230: Analytical Verification of PDS Results

Overview

Reference:	A. H-S. Ang and W. H. Tang, *Probability Concepts in Engineering Planning and Design*, Vol 1 - Basic Principles, John Wiley & Sons, 1975.
Analysis Type(s):	PDS
Element Type(s):	None
Input Listing:	vm230.dat

Test Case

Five statistically independent random input variables are defined, X_1 to X_5. All random input variables follow log-normal distribution with a logarithmic mean value ξ_i and a logarithmic deviation δ_i and $i = 1,...,5$ as distribution parameters. A random output parameter Y is defined as a function of the random input variables.

$$Y = \frac{X_1 X_2 X_3}{X_4 X_5}$$

Verify the mean value and the standard deviation of the random output parameter Y.

Figure 230.1 Distribution of Input Variable

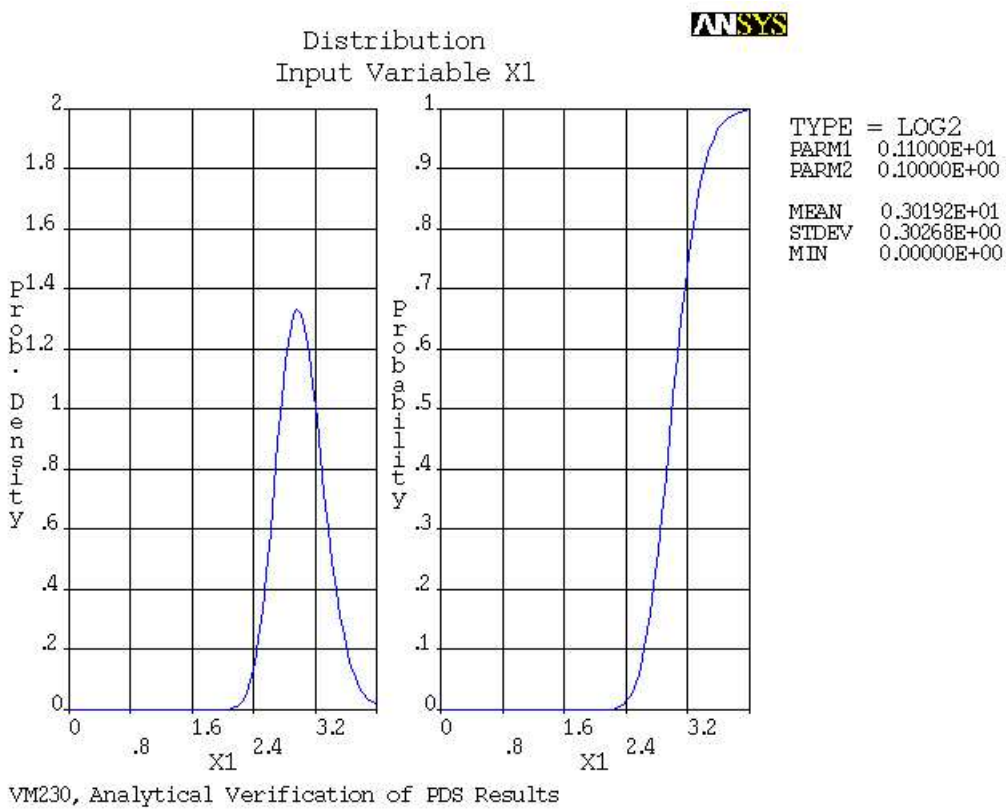

Analysis Assumptions and Modeling Notes

From the reference A. H-S. Ang and W. H. Tang, *Probability Concepts in Engineering Planning and Design*, the random output parameter Y follows a log-normal distribution with a logarithmic mean of:

$$Y = \frac{X_1 X_2 X_3}{X_4 X_5}$$

$$\xi_y = \xi_1 + \xi_2 + \xi_3 - \xi_4 - \xi_5$$

and a logarithmic deviation of

$$\delta_y = \sqrt{\delta_1^2 + \delta_2^2 + \delta_3^2 + \delta_4^2 + \delta_5^2}$$

The mean value of the random output parameter *Y* is:

$$\mu_y = \exp(\xi_y + 0.5\delta_y^2)$$

and the standard deviation is:

$$\sigma_y = \sqrt{\exp(2\xi_y + \delta_y^2)(\exp(\delta_y^2) - 1)} = \mu_y \sqrt{(\exp(\delta_y^2) - 1)}$$

Using the following values:

$\xi_1 = 1.1$	$\delta_1 = 0.1$
$\xi_2 = 1.2$	$\delta_2 = 0.2$
$\xi_3 = 1.3$	$\delta_3 = 0.3$
$\xi_4 = 1.4$	$\delta_4 = 0.4$
$\xi_5 = 1.5$	$\delta_5 = 0.5$

the following analytical results are obtained:

$\xi_y = 0.7$

$\delta_y = 0.74162$

$\mu_y = 2.651167$

$\sigma_y = 2.2701994$

For the ANSYS PDS analysis, a loop file is created which contains the random input variables and the random output variable. In the /PDS module, X_1 through X_5 are defined as probabilistic design variables and *Y* is defined as a response parameter. The PDS mean parameter values and deviations are defined with the values used in the analytical solution above.

The 2000 Latin Hypercube samples were post-processed to determine the logarithmic mean and logarithmic deviation of Y. A cumulative distribution function was plotted for Y showing the 95% confidence limit. This confirms that the distribution type of Y is log-normal, because the CDF is very close to a straight line.

Figure 230.2 Cumulative Distribution Function (Probability vs. Log Y)

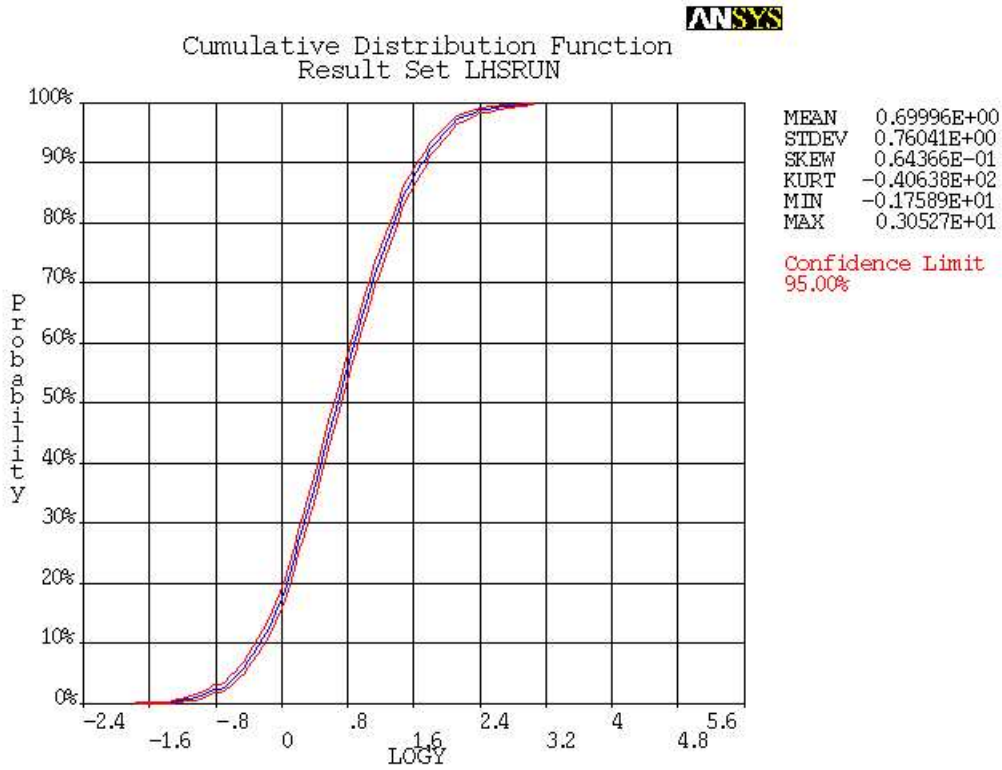

Results Comparison

	Target	ANSYS	Ratio
Mean Value of Y	2.6957898	2.6957898	1.000
Standard Deviation of Y	2.3744199	2.3744198	1.000

VM231: Piezoelectric Rectangular Strip Under Pure Bending Load

Overview

Reference:	V. Z. Parton, B. A. Kudryavtsev, N. A, Senik, *Applied Mechanics: Soviet Review*, Vol. 2: Electromagnetoelasticity, pg. 28.
Analysis Type(s):	Static
Element Type(s):	2-D Coupled-Field Solid Elements (PLANE13)
Input Listing:	vm231.dat

Test Case

A piezoceramic (PZT-4) rectangular strip occupies the region $|x| \leq l$, $|y| \leq h$. The material is oriented such that its polarization direction is aligned with the Y axis. The strip is subjected to the pure bending load $\sigma_x = \sigma_1 y$ at $x = \pm l$. Determine the electro-elastic field distribution in the strip.

Figure 231.1 Piezoelectric Strip Problem Sketch

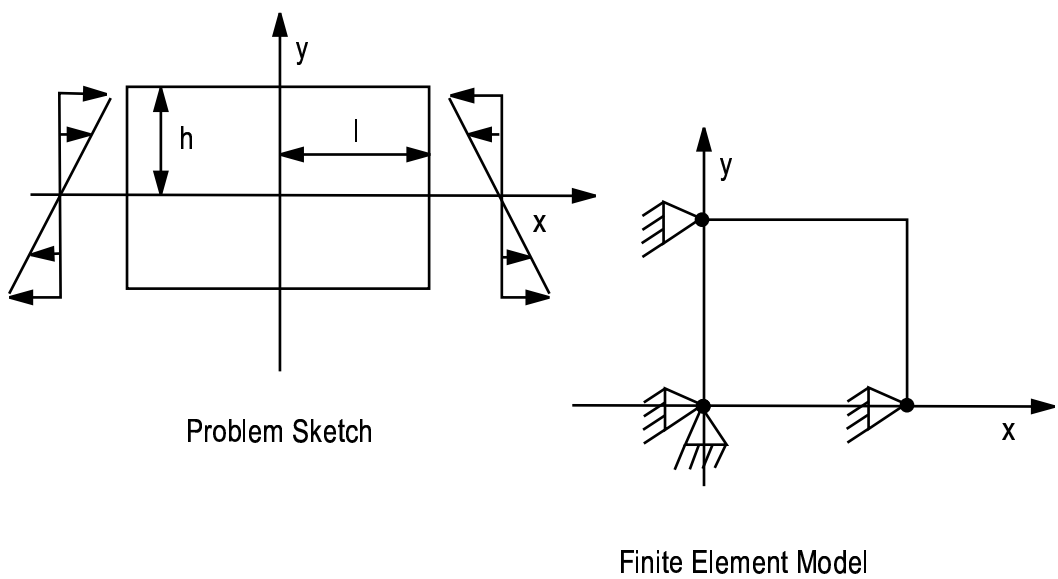

Material Properties	**Geometric Properties**	**Loading**
See Constitutive Matrices for PZT4 Polarized Along the Y Axis	l = 1mm h = 0.5 mm	Pressure slope σ_1 = -20 N/mm^3

Constitutive Matrices for PZT4 Polarized Along the Y Axis

PZT4 Dielectric Matrix $[\varepsilon_r]$

$$\begin{bmatrix} 728.5 & 0 & 0 \\ 0 & 634.7 & 0 \\ 0 & 0 & 728.5 \end{bmatrix}$$

PZT4 Piezoelectric Matrix [e] C/m^2

$$\begin{bmatrix} 0 & -5.2 & 0 \\ 0 & 15.1 & 0 \\ 0 & -5.2 & 0 \\ 12.7 & 0 & 0 \\ 0 & 0 & 12.7 \\ 0 & 0 & 0 \end{bmatrix}$$

PZT4 Stiffness matrix [c] x 10^{-10} N/m^2

$$\begin{bmatrix} 13.9 & 7.43 & 7.78 & 0 & 0 & 0 \\ & 11.5 & 7.43 & 0 & 0 & 0 \\ & & 13.9 & 0 & 0 & 0 \\ & & & 2.56 & 0 & 0 \\ & & & & 2.56 & 0 \\ & & & & & 3.06 \end{bmatrix}$$

Analysis Assumptions and Modeling Notes

Only a one-quarter symmetry sector of the rectangular strip is modeled. Symmetric and antisymmetric boundary conditions are applied. The finite element model uses a single 4-node 2-D quadrilateral element with extra displacement and potential modes to produce a correct response to the pure bending load.

Results Comparison

Node 3	Target	ANSYS	Ratio
UX, µm	-0.110	-0.110	1.000
UY, µm	0.115	0.115	1.000
VOLT, V	27.378	27.378	1.000
Stress x, N/mm^2	-10.000	-10.000	1.000
Electric Field y, V/mm	-109.511	-109.511	1.000

VM232: PDS Response Surface Study

Overview

Reference:	A. H-S. Ang and W. H. Tang, *Probability Concepts in Engineering Planning and Design*, Vol 1 - Basic Principles, John Wiley & Sons, 1975.
Analysis Type(s):	PDS
Element Type(s):	None
Input Listing:	vm232.dat

Test Case

Assume that there are two random input variables, defined as X_W and X_E. The random input variable X_W follows a Weibull distribution with a Weibull exponent of $m = 2.0$, a Weibull characteristic value of $x_{chr} = 1.0$ and a lower limit of $x_{W,min} = 0.0$. The random input variable X_E follows an exponential distribution with a decay parameter generally expressed as λ and lower limit of $x_{E,min} = 0.0$.

Figure 232.1 Distribution of Input Variable X_W

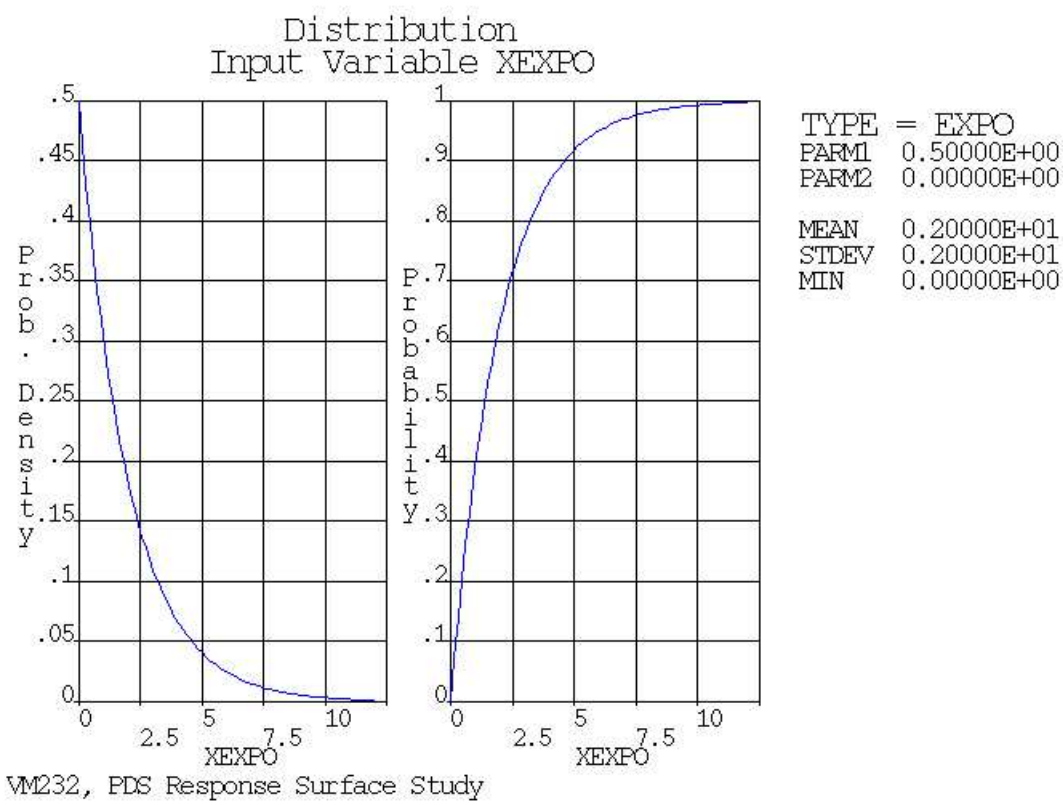

Figure 232.2 Distribution of Input Variable X_E

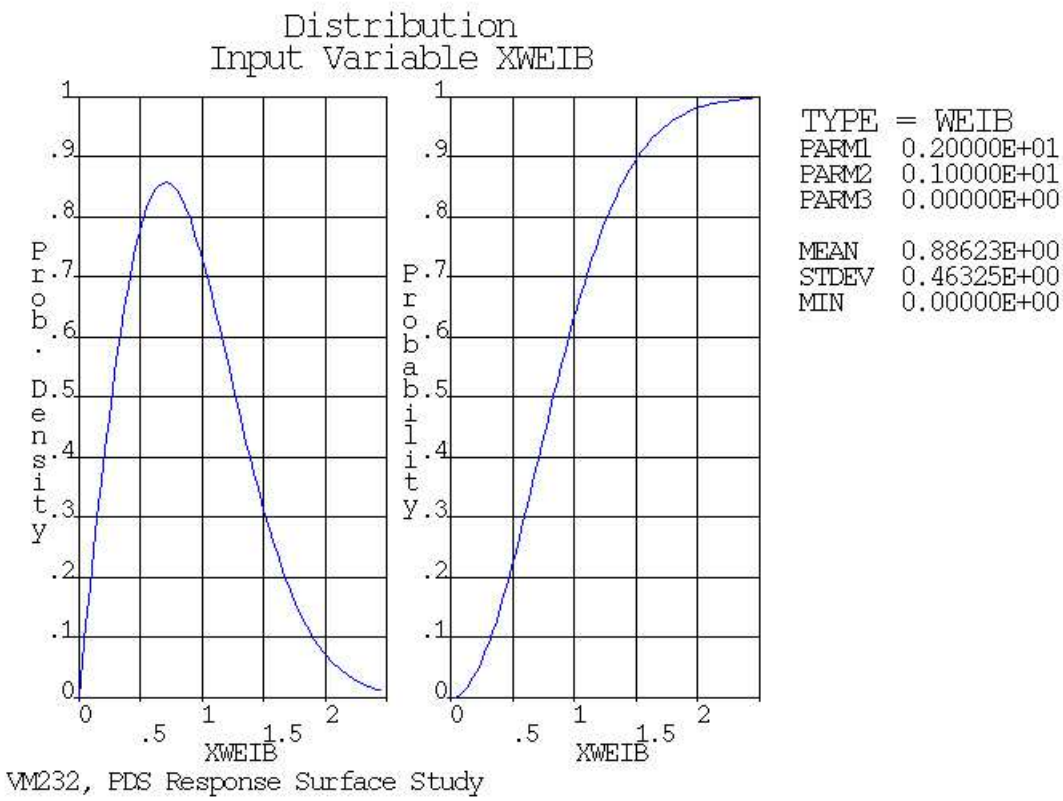

Analysis Assumptions and Modeling Notes

The probability density function of X_W is:

$$f_W(x_W) = \frac{m(x_W - x_{W,min})^{m-1}}{(x_{chr} - x_{W,min})^m} \exp\left(-\left(\frac{x_W - x_{W,min}}{x_{chr} - x_{W,min}}\right)^m\right)$$

Using the values of $m = 2.0$, $x_{chr} = 1.0$ and $x_{min} = 0.0$, the probability density function of X_W reduces to:

$$f_W(x_W) = 2x_W \exp(-x_W^2)$$

The probability density function of X_E is:

$$f_E(x_E) = \lambda \exp(-\lambda(x - x_{E,min}))$$

Using the value x_{min}, the probability density function of X_E reduces to:

$$f_E(x_E) = \lambda \exp(-\lambda x_E)$$

The random output parameter Y as a function of the random input variables is defined as:

$$y = c_1 x_W^2 - c_2 x_E$$

Next, the probability that Y is negative, i.e. $P(Y < 0)$ is evaluated. For this case the probability is:

$$P(Y<0)=\iint_{Y<0} f_W(x_W)f_E(x_E)dx_W dx_E$$

The integration domain *Y < 0* can be expressed as:

$$c_1x_W^2 - c_2x_E < 0$$

or

$$c_2x_E > c_1x_W^2$$

or

$$x_E > \frac{c_1}{c_2}x_W^2$$

Therefore, the integration domain of the integral can be written as:

$$P(Y<0)=\int_0^\infty \int_{\frac{c_1}{c_2}x_W^2}^\infty f_W(x_W)f_E(x_E)dx_E dx_W$$

Separating the product in the integrator leads to:

$$P(Y<0)=\int_0^\infty f_W(x_W)\left(\int_{\frac{c_1}{c_2}x_W^2}^\infty f_E(x_E)dx_E\right)dx_W$$

Using eqs. 2 and 4 leads to:

$$P(Y<0)=\int_0^\infty 2x_W \exp(-x_W^2)\left(\int_{\frac{c_1}{c_2}x_W^2}^\infty \lambda\exp(-\lambda x_E)dx_E\right)dx_W$$

Solving the inner integral is:

$$P(Y<0)=\int_0^\infty 2x_W \exp(-x_W^2)\left[\exp(-\lambda x_E)\big|_{x_E=\frac{c_1}{c_2}x_W^2} - \exp(-\lambda x_E)\big|_{x_E=\infty}\right]dx_W$$

or

$$P(Y<0)=\int_0^\infty 2x_W \exp(-x_W^2)\exp\left(-\lambda\frac{c_1}{c_2}x_W^2\right)dx_W$$

or

$$P(Y<0)=\int_0^\infty 2x_W \exp\left(-\left(1+\lambda\frac{c_1}{c_2}\right)x_W^2\right)dx_W$$

The solution of this integral is:

$$P(Y<0)=\frac{1}{1+\lambda\frac{c_1}{c_2}}\left[\exp\left(-\left(1+\lambda\frac{c_1}{c_2}\right)x_W^2\right)\Bigg|_{x_W=0}-\exp\left(-\left(1+\lambda\frac{c_1}{c_2}\right)x_W^2\right)\Bigg|_{x_W=\infty}\right]$$

or

$$P(Y<0)=\frac{1}{1+\lambda\frac{c_1}{c_2}}$$

For $\lambda = 0.5$, $c_1 = 1.0$ and $c_2 = 0.1$ the probability *P(Y < 0)* becomes:

$$P(Y<0)=\frac{1}{6}\cong 0.1666667$$

In this test case, numerical results are first obtained from a Monte Carlo Simulation method using Latin Hypercube Sampling.

P(Y < 0) = 0.165096

A response surface method using a central composite design is evaluated to show that it delivers an acceptable analysis.

P(Y < 0) = 0.166829

Figure 232.3 Response Surface plot

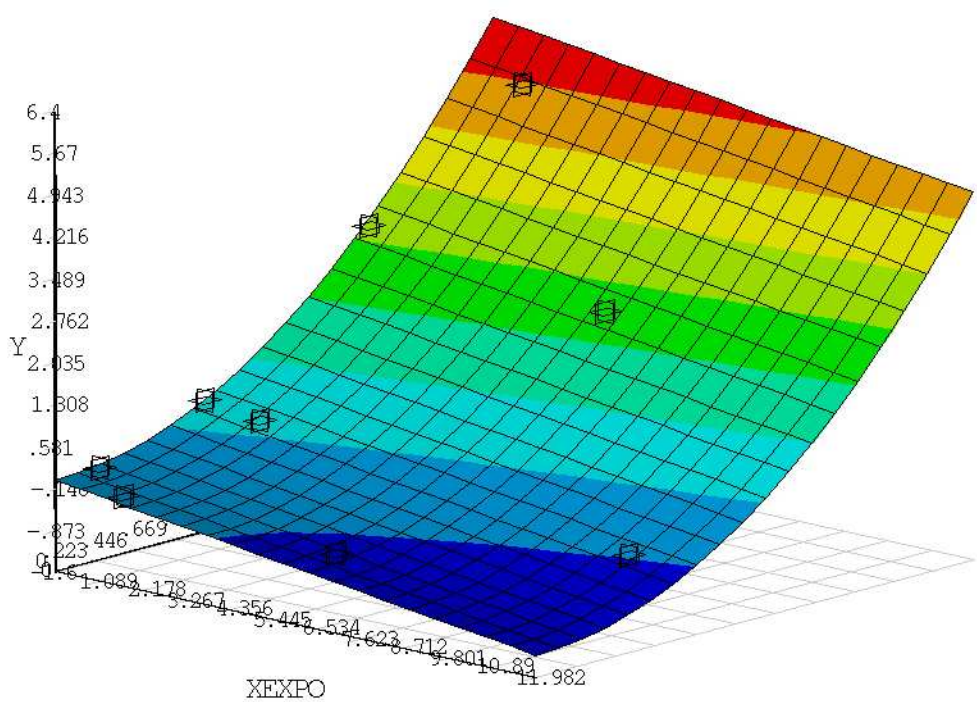

Results Comparison

	Target	ANSYS	Ratio
P (Y < 0) from Monte Carlo	0.16666667	0.165096	0.9906
P (Y < 0) from Response Surface	0.16666667	0.166829	1.001

VM233: Static Force Computation of a 3-D Solenoid Actuator

Overview

Reference:	M. Gyimesi, D. F. Ostergaard, "Analysis of Benchmark Problem TEAM20 with Various Formulations", *Proceedings of TEAM Workshop, COMPUMAG, Rio*, 1997. M. Gyimesi, D. F. Ostergaard, "Mixed Shape Non-Conforming Edge Elements", *IEEE Transactions on Magnetics*, Vol. 35 No. 3, 1999, pp. 1407-1409. M. Gyimesi, D. F. Ostergaard, "Non-Conforming Hexahedral Edge Elements for Magnetic Analysis", *IEEE Transactions on Magnetics*, Vol 34 No. 5, 1998, pp. 2481-2484.
Analysis Type(s):	Static (**ANTYPE** = 0)
Element Type(s):	Tetrahedral Coupled-Field Solid Elements (SOLID98)
Input Listing:	vm233.dat

Test Case

For the given solenoid actuator with an applied total coil current of 1000 A-turns, find the magnetic flux density (BZ) of the Pole, the magnetic flux density (BZ) of the Arm, and the Virtual Work Force in the Z-direction (See Problem Description for location of parts).

Material Properties	**Geometric Properties**	**Loading**
Murx =1	X1 = 63.5mm X2 = 12.5mm Y1 = 12.5mm Y2 = 5mm Y3 = 18mm Z1 = 25 mm Z2 = 100mm Z3 = 98.5mm Z4 = 96.6mm	Total Current = 5000 A-turns

Figure 233.1 B-H Curve

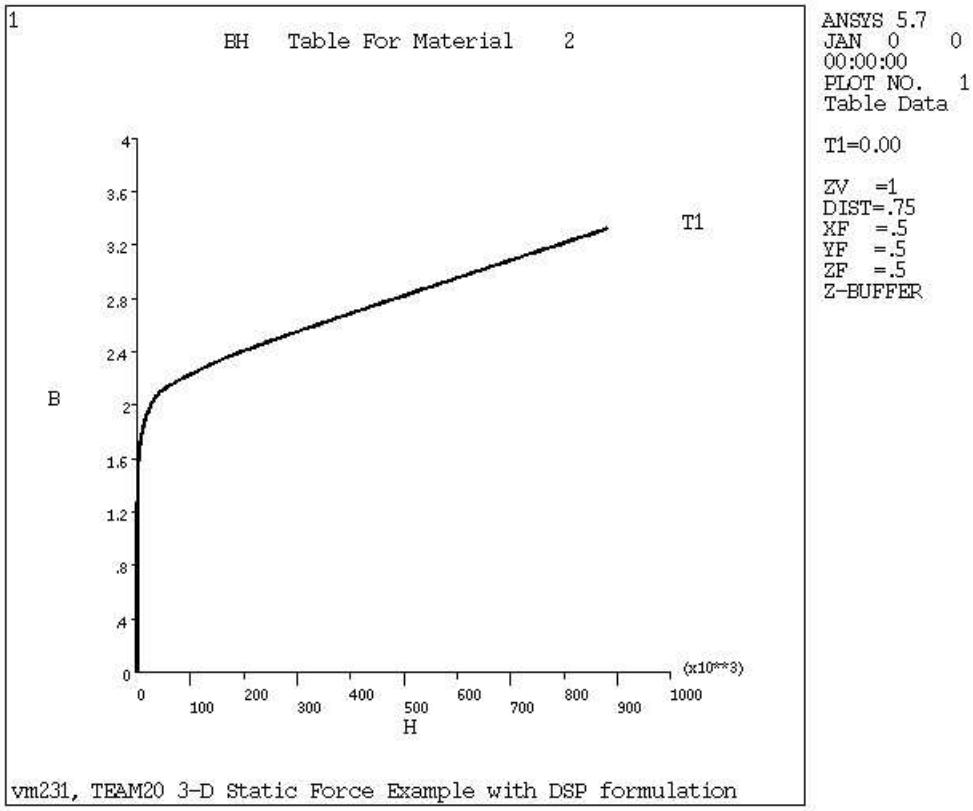

Analysis Assumptions and Modeling Notes

This analysis is based on the TEAM workshop problem 20. It utilizes the Difference Scalar Potential (DSP) element formulation with tetrahedral shaped SOLID98 elements. DSP formulation was used because it has much better accuracy than the Magnetic Vector Potential (MVP) method. Additionally, it is more efficient than the EDGE formulation method. To simplify meshing, the **SMRTSIZE** meshing option was used to automatically determine line divisions and spacing ratios while taking into account the line proximity effects. Mesh density can be adjusted using the SmartSize parameter, for this case, a SmartSizing level of 10 was applied. The analysis is performed using a quarter symmetry model of the solenoid actuator. The magnetic coil was created using the **RACE** command. Magnetic force and boundary conditions were placed on the armature component by using the **FMAGBC** command.

Figure 233.2 Finite Element Model

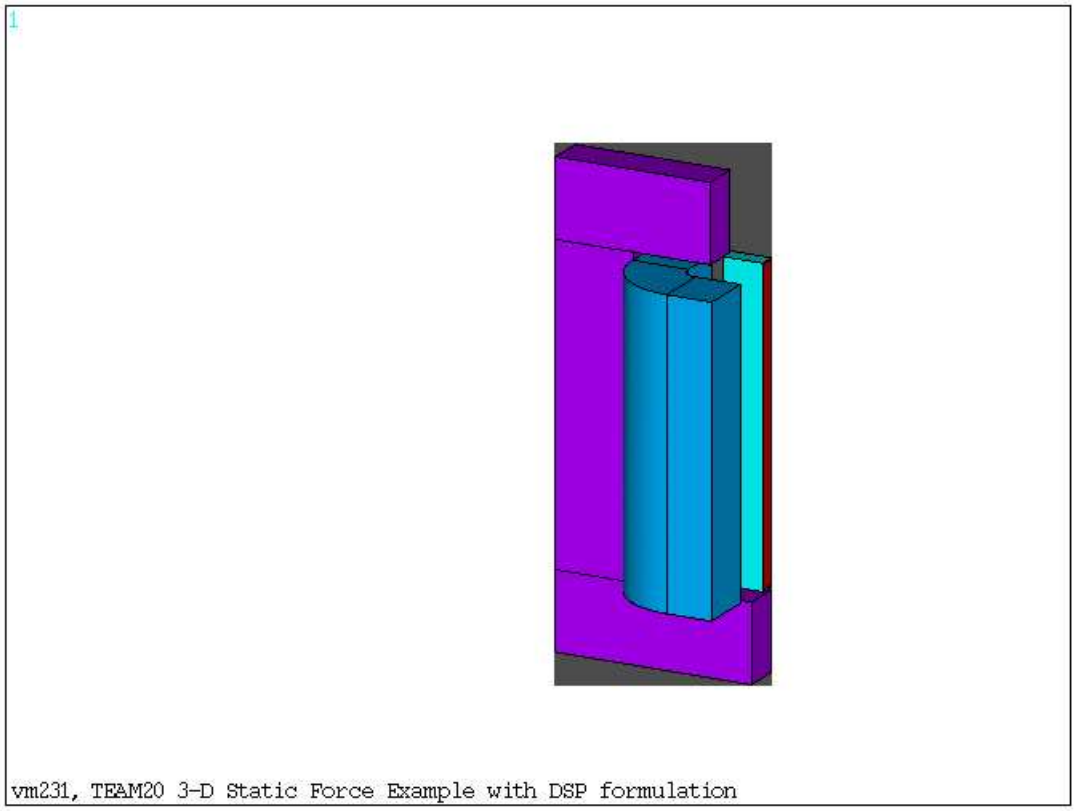

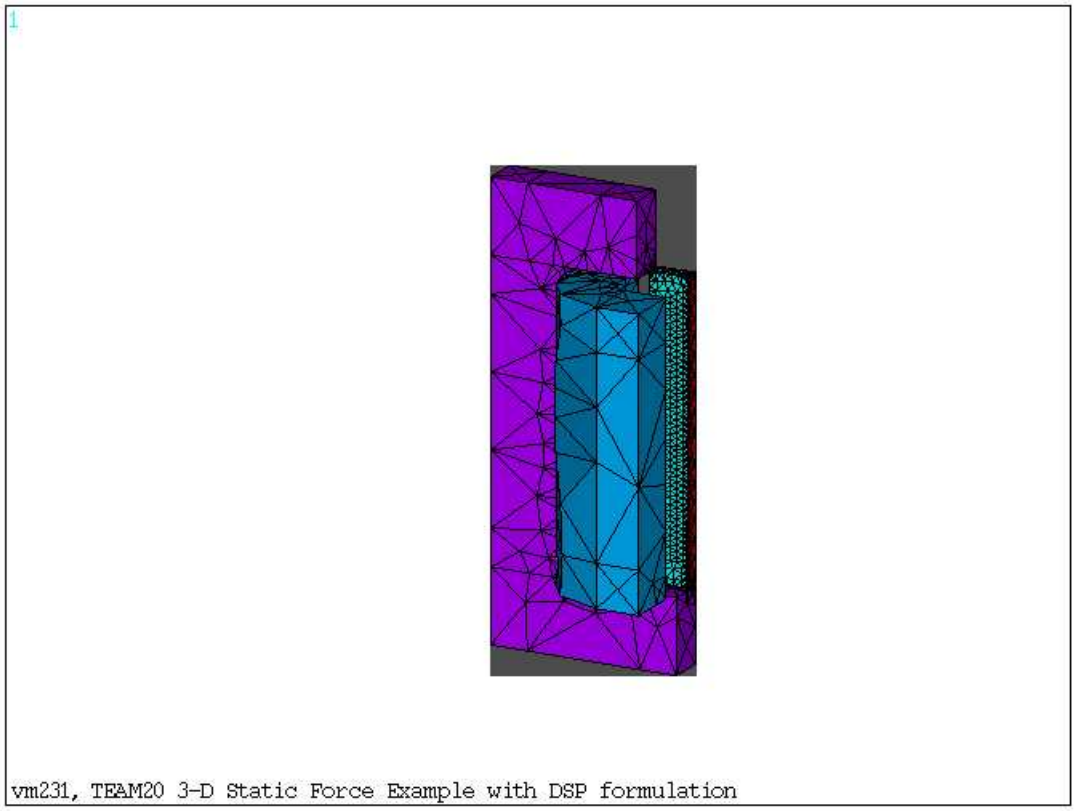

Results Comparison

Total Current = 5000 A-turns	Target	ANSYS	Ratio
Virtual Work Force (N)	80.1	80.917	1.010
Pole Flux Density (BZ, Tesla)	0.46	0.474	1.030
Arm Flux Density (BZ, Tesla)	2.05	2.048	0.999

VM234: Cyclic Loading of a Rubber Block

Overview

Reference:	G. A. Holzapfel, "On Large Strain Viscoelasticity: Continuum Formulation and Finite Element Applications to Elastomeric Structures", *International Journal for Numerical Methods in Engineering*, Vol. 39, 1996, pp. 3903-3926.
Analysis Type(s):	Transient Structural Analysis (**ANTYPE** = 4)
Element Type(s):	3-D 8-Node Structural Solid Elements (SOLID185)
Input Listing:	vm234.dat

Test Case

A cube of rubber is subjected to a sinusoidal displacement controlled load with a mean value of zero (completely reversed). The load amplitude is constant within a full cycle (4 seconds) and increases with each successive cycle. For the first period A = 0.01 and it increases by 0.01 each cycle until the fourth when A = 0.04. At t = 16 seconds the load is removed and the residual stresses are permitted to relax.

Figure 234.1 Rubber Block Model

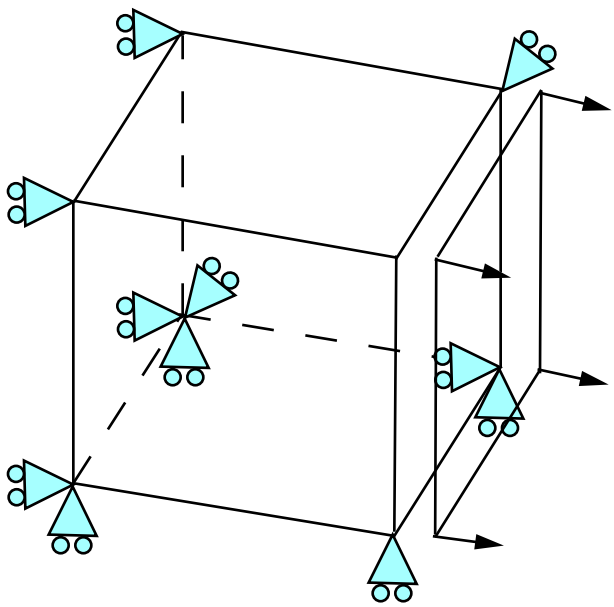

Material Properties	Geometric Properties	Loading
τ_1 = 0.40 sec τ_2 = 0.40 sec $\beta_1 = \beta_2 = 1$	L = 0.1 m	A = 0.01

Analysis Assumptions and Modeling Notes

The analysis was performed using a single SOLID185 element. The rubber was simulated with an Ogden material model. The load was applied using a looping application of the displacement boundary condition. The plot displays the Cauchy stress evolution over the specified time periods. The accumulated stress relaxes after the load is removed at t = 16 seconds. The accumulated stress at t = 16 seconds and the relaxed stress state at t = 20 seconds are the verified results for this test.

Figure 234.2 Stress Evolution Over Time

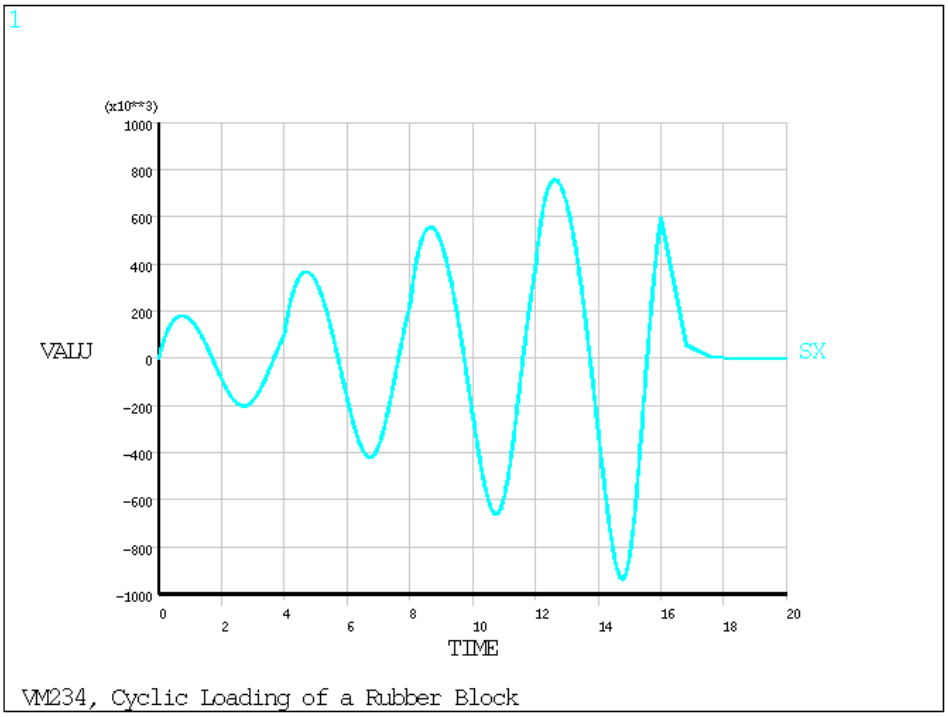

Results Comparison

	Target	ANSYS	Ratio
Cauchy Stress *(N/m^2)* t = 16 sec	6.013E5	5.993889E5	0.997
Cauchy Stress *(N/m^2)* t = 20 sec	0.0	17.7	0.000

VM235: Frequency Response of a Prestressed Beam

Overview

Reference:	R. D. Blevins, *Formulas for Natural Frequency and Mode Shape*, Van Nostrand Reinhold Co., pg. 144, equation 8-20.
Analysis Type(s):	Modal (**ANTYPE**=2)
Element Type(s):	2-D Elastic Beam Elements (BEAM3) Electromechanical Transducer Elements (TRANS126)
Input Listing:	vm235.dat

Test Case

A beam is in series with an electromechanical transducer. With a voltage applied to the beam, determine the prestressed natural frequencies of the beam.

Figure 235.1 Element Plot

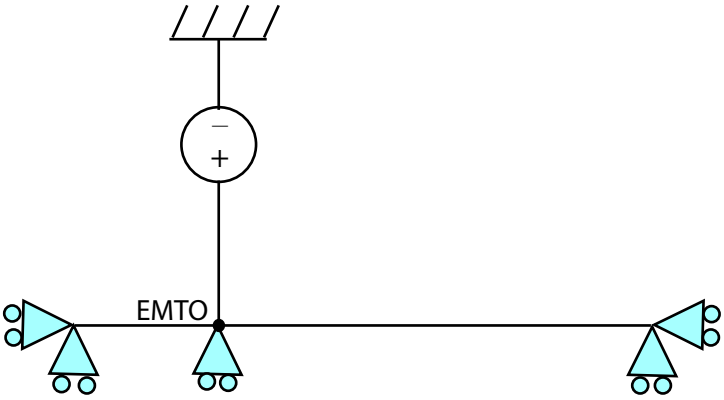

Material Properties	Geometric Properties	Loading
Ex = 169E3 DENS = 2332E-18 Beam Stiff = 112666.667 Gap Stiff = 20.022	L = 150μm W = 4 μm H = 2 μm Initial Gap = 1 μm Gap = 0.999 μm	Volt = 150.162V

Analysis Assumptions and Modeling Notes

The beam is created using BEAM3 elements which are used in series with one TRANS126 element. The node that connects the transducer and beam is free to move in the X-direction, while the end node of the beam and the ground node of the transducer are constrained in both the X and Y directions. It should also be noted that the transducer gap stiffness is much less than the beam stiffness and will not have any effect on the frequency solution.

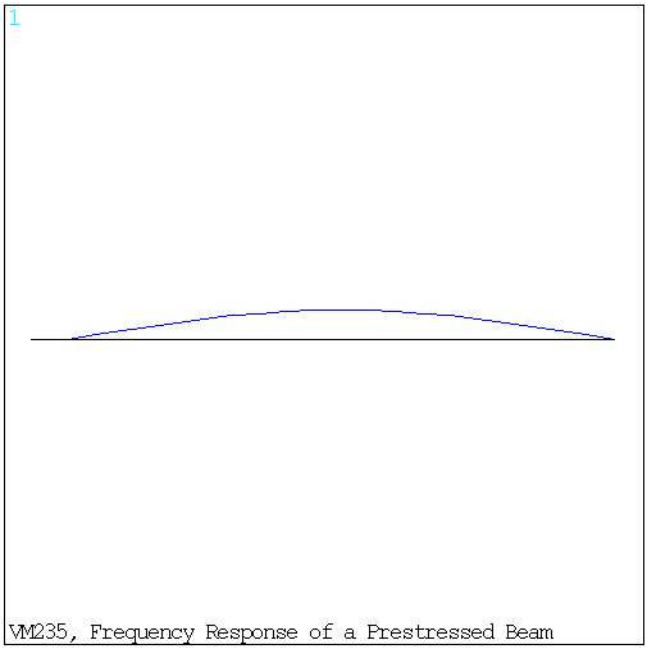
1
VM235, Frequency Response of a Prestressed Beam

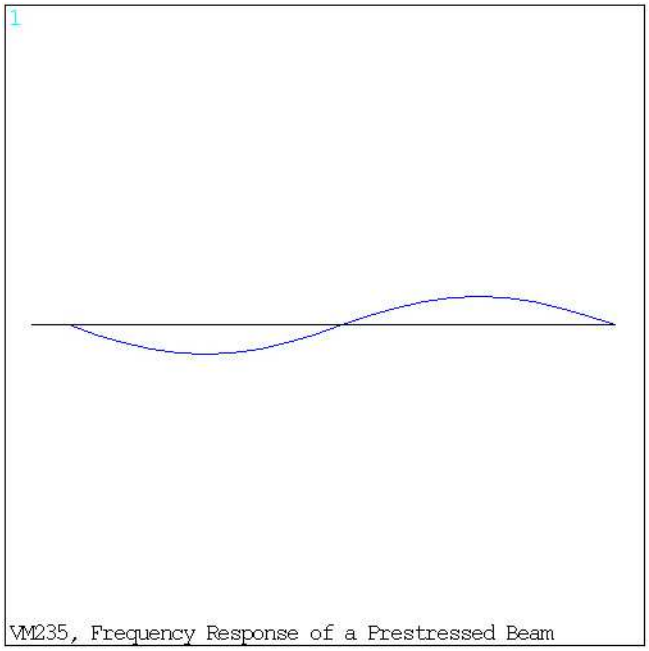
1
VM235, Frequency Response of a Prestressed Beam

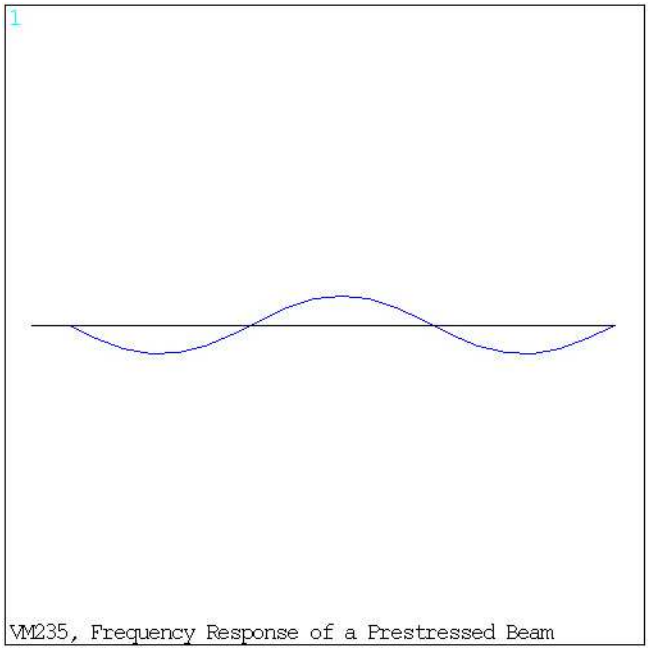

Results Comparison

	Target	ANSYS	Ratio
Frequency (mode 1)	351699.332	351673.733	1.000
Frequency (mode 2)	1381162.303	1380767.749	1.000
Frequency (mode 3)	3096816.034	3094885.115	1.001

VM236: Hysteresis Calculation of a Beam Under Electrostatic Load

Overview

Reference:	J. R. Gilbert, G. K. Ananthasuresh, S. D. Senturia, "3D Modeling of Contact Problems and Hysteresis in Coupled Electro-Mechanics", MEMS, 1996, pp. 127-132.
Analysis Type(s):	TRANS (**ANTYPE** = 4)
Element Type(s):	2-D Electromechanical Transducer Elements (TRANS109) 2-D Structural Solid Elements (PLANE42) 2-D Point-to-Point Contact Elements (CONTAC12)
Input Listing:	vm236.dat

Test Case

A beam of length L = 80 μm at a height T = 0.5 μm is suspended 0.7 μm above a ground plane and is clamped at either end. Using this beam, model the hysteresis (pull-in and release behaviors) when it is placed under electrostatic load.

Figure 236.1 Beam Under Electrostatic Load

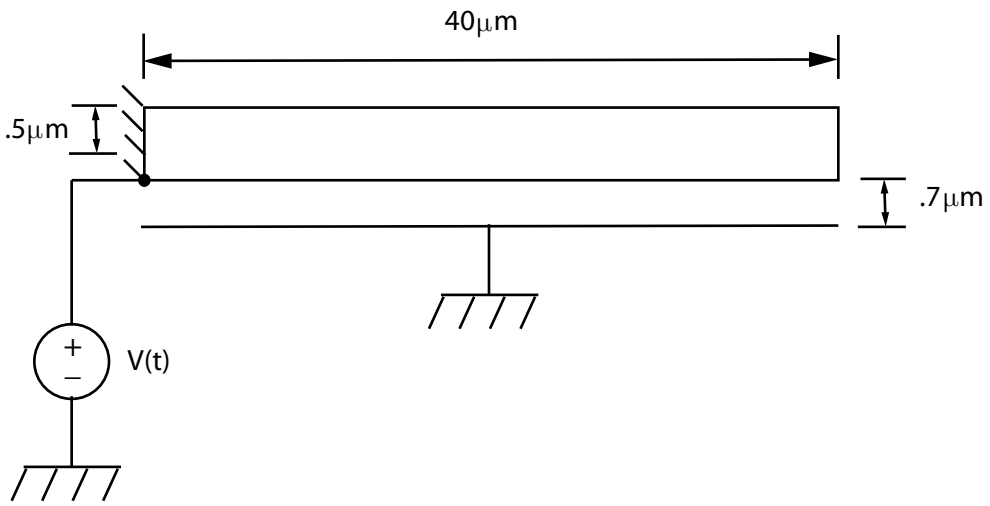

Beam at beginning and unloading.

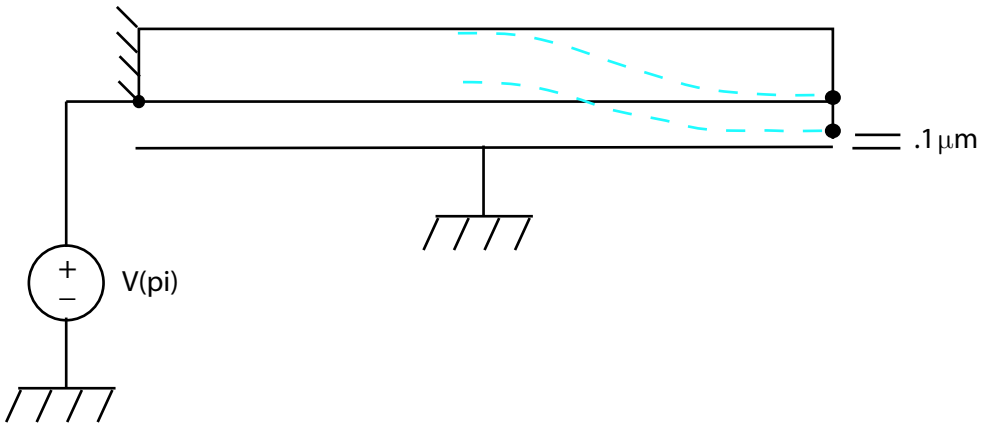

Beam at pull-in voltage.

Model the hysteresis (pull-in and release behaviors) of a structural beam under electrostatic load.

Material Properties	**Geometric Properties**	**Loading**
EX = 169E3	Beam Length = 80 microns	V(1) = 11.0V
NUXY = 0.25	Beam Height = 0.5 microns	V(2) = 14.5V
PERX = 1	Gap = 0.7 microns	V(3) = 18.0V
MU = 0		

Analysis Assumptions and Modeling Notes

Using symmetry at a length L=40 µm, the solid beam is modeled with quad shaped PLANE42 elements. The air gap is modeled with 2-D tri-shaped TRANS109 elements with KEYOPT(1) = 1 for area weighted morphing. Node-Node contact is modeled in the air gap using CONTAC12 elements. The beam is constrained in the X and Y directions on the left side and is free only in the Y-direction along the span. The beam is suspended 0.7 µm over the ground plane with a contact stop at 0.1µm.

Results Comparison

	Target	**ANSYS**	**Ratio**
UY @ 11.0V	-0.0722	-0.0722	1.000
UY @ 14.5V	-0.1451	-0.1451	1.000
UY @ 18.0V	-0.6004	-0.6002	1.000
UY @ 14.5V	-0.6002	-0.6002	1.000
UY @ 11.0V	-0.0723	-0.0726	1.004

VM237: RLC Circuit with Piezoelectric Transducer

Overview

Reference:	*IEEE Standard on Piezoelectricity*, Piezoelectric part of the problem: 176-1987. J. Vlach, *Basic Network Theory with Computer Applications*, Circuit part of the problem: Ch. 9, Van Nostrand Reinhold, 1992.
Analysis Type(s):	Static (**ANTYPE** = 1)
	Transient (**ANTYPE** = 4)
Element Type(s):	2-D 8-Node Coupled-Field Solid (PLANE223)
	Piezoelectric Circuit (CIRCU94)
Input Listing:	vm237.dat

Test Case

A piezoelectric transducer consists of a simply supported circular plate of radius a and thickness t (figure a below) made of PZT-5A ceramic polarized along the Z axis. The circular surfaces of the plate are fully covered by electrode and connected in series with a resistor (R), inductor (L), and a source of constant voltage (V) (figure b below). Determine the voltage across the piezoelectric transducer over the time interval of 2 ms.

Figure 237.1 Problem Sketch

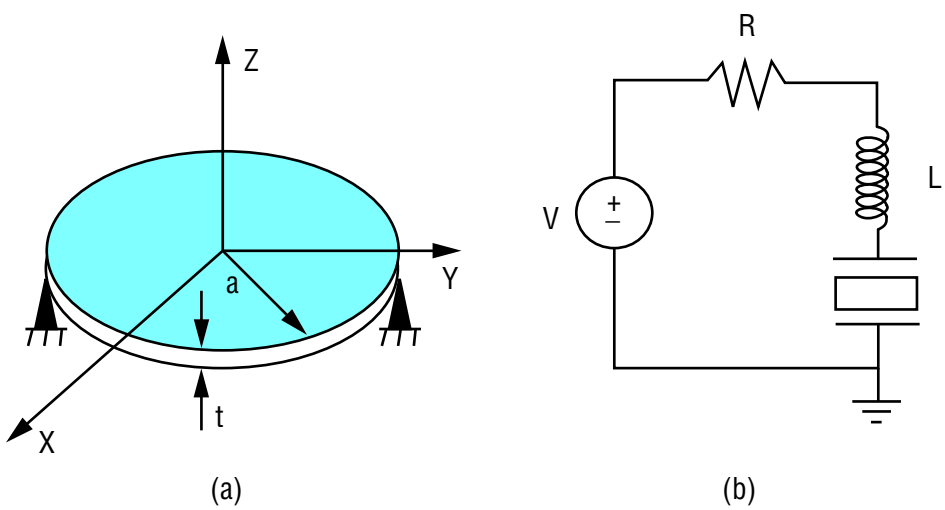

Material Properties	Geometric Properties	Loading
ρ = 7750 kg/m^3 See "Constitutive Matrices" **Circuit Parameters** R = 3kΩ L = 15 H	a = 1 mm t = 0.1 mm	Stepped voltage V = 1 V

Constitutive Matrices (polar axis aligned along the Y axis)

PZT-5A Dielectric Permittivity Matrix at Constant Stress $[\varepsilon^T_r]$

$$\begin{bmatrix} 1730 & 0 & 0 \\ & 1700 & 0 \\ \text{Symmetric} & & 1730 \end{bmatrix}$$

PZT-5A Piezoelectric Strain Matrix [d], 10^{10} C/N

$$\begin{bmatrix} 0 & -1.71 & 0 \\ 0 & 3.74 & 0 \\ 0 & -1.71 & 0 \\ 5.84 & 0 & 0 \\ 0 & 0 & 5.84 \\ 0 & 0 & 0 \end{bmatrix}$$

PZT-5A Elastic Compliance Matrix [s], 10^{12} m^2/N

$$\begin{bmatrix} 16.4 & -7.22 & -5.74 & 0 & 0 & 0 \\ & 18.8 & -7.22 & 0 & 0 & 0 \\ & & 16.4 & 0 & 0 & 0 \\ & & & 47.5 & 0 & 0 \\ \text{Symmetric} & & & & 47.5 & 0 \\ & & & & & 44.3 \end{bmatrix}$$

Analysis Assumptions and Modeling Notes

The piezoelectric circular plate is modeled with 10 axisymmetric PLANE223 elements (Figure 237.2: "Finite Element Model of a Transducer"). The constitutive matrices used by the 2-D model are adjusted to orient the PZT-5A polarization direction along the Y axis. The electrodes are modeled by coupling the VOLT dof on the top and bottom surfaces of the plate. The resistor, inductance, and voltage source are modeled using the respective options of the CIRCU94 element. A transient analysis is performed to determine the time response of the circuit to the unit (1V) step voltage load. Numerical results are compared with an analytical solution, obtained using the Laplace transformation technique applied to an equivalent RLC-circuit, where C is the static capacitance of the piezoelectric transducer.

Figure 237.2 Finite Element Model of a Transducer

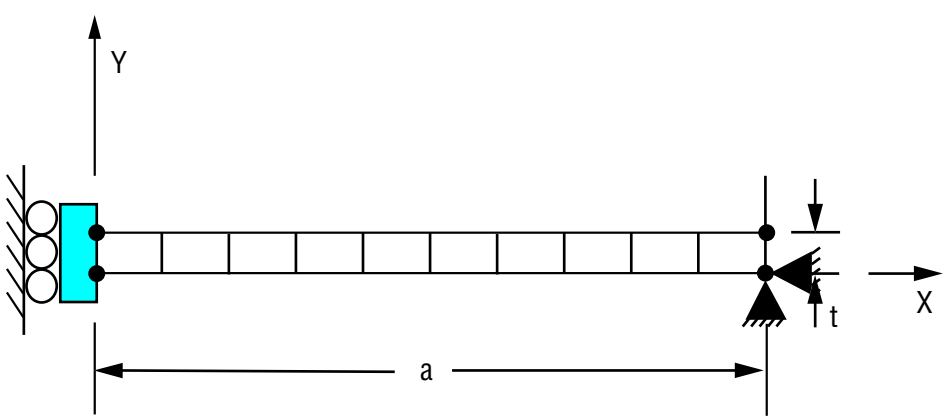

Results Comparison

VC for t @	Target	ANSYS	Ratio
1.8E-2s	1.5201	1.4951	0.984
4.0E-2s	0.9726	0.9974	1.026
8.8E-2s	1.4829	1.5094	1.018
1.3E-2s	1.8437	1.8022	0.978
1.86E-1s	1.8273	1.8099	0.990

VM238: Wheatstone Bridge Connection of Piezoresistors

Overview

Reference:	M.-H. Bao, "Micro Mechanical Transducers: Pressure Sensors, Accelerometers and Gyroscopes", *Handbook of Sensors and Actuators*, v.8, ch.5.
Analysis Type(s):	Static (**ANTYPE** = 1)
Element Type(s):	2-D 8-Node Coupled-Field Solid (PLANE223) 2-D 8-Node Structural Solid (PLANE82)
Input Listing:	vm238.dat

Test Case

Four p-type silicon piezoresistors R_1-R_4 of length *a* and width *b* are placed on a silicon beam (Figure 238.1: "Piezoresistors on a Beam Problem Sketch"). The beam of length *l* and width *w* is oriented such that its length is in the <110> direction of silicon crystal. The resistors are connected to form a Wheatstone bridge (Figure 238.2: "Wheatstone Bridge Arrangement of Piezoresistors") with a supply voltage V_s. The beam is subjected to a uniform pressure *p* in the X-direction. Determine the output voltage V_o of the Wheatstone bridge.

Figure 238.1 Piezoresistors on a Beam Problem Sketch

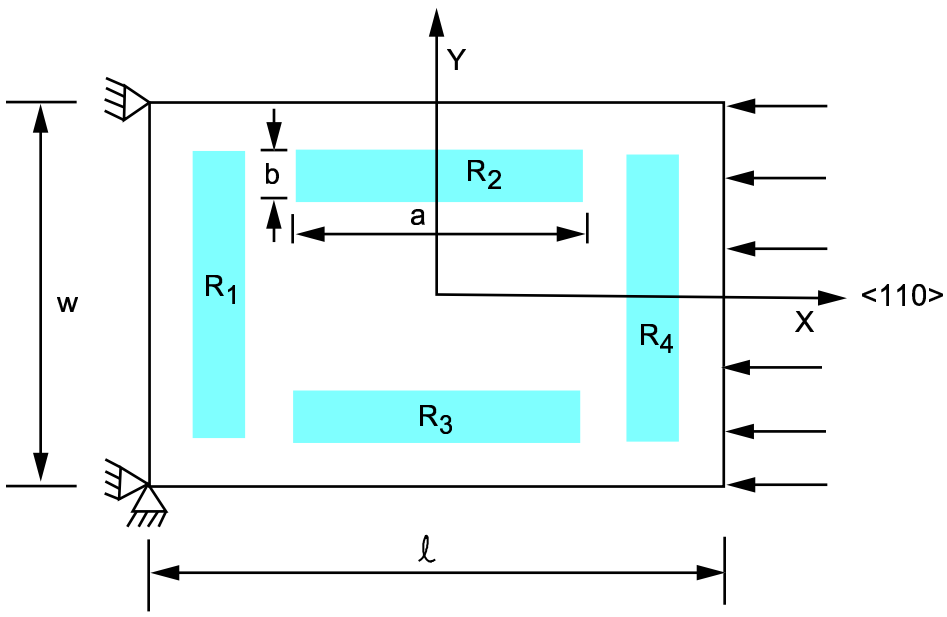

Figure 238.2 Wheatstone Bridge Arrangement of Piezoresistors

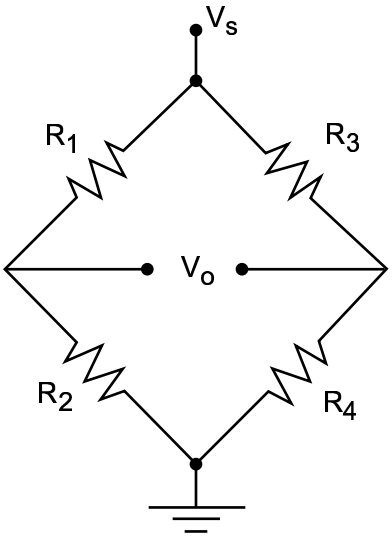

Material Properties	Geometric Properties	Loading
Elastic properties: E = 165e3 MPa ν = 0.25 Resistivity: ρ = 7.8e-8 TΩµm Piezoresistive stress coefficients: π_{11} = 6.5e-5 (MPa)$^{-1}$ π_{12} = -1.1e-5 (MPa)$^{-1}$ π_{44} = 138.1e-5 (MPa)$^{-1}$	*l* = 180 µm *w* = 120 µm *a*= 100 µm *b*= 20 µm	Supply voltage V_s=5 V Pressure *p* = 1MPa

Analysis Assumptions and Modeling Notes

The resistors areas are modeled using the piezoresistive option of the coupled-field solid PLANE223. The structural part of the beam is modeled using PLANE82. The resistors are connected into a Wheatstone bridge arrangement by coupling the VOLT degrees of freedom on width sides of the resistors. The supply voltage is applied to the master node of the driving electrode.

The applied pressure results in a uniform stress S_x distribution. Two of the resistors (R_2 and R_3) are parallel to the direction of stress, and change their resistance due to the longitudinal piezoresistive effect. Two other resistors (R_1 and R_4) are perpendicular to the applied stress, and change their resistance due to the transverse piezoresistive effect. A static analysis is performed to determine the output voltage V_o. Results are compared to the analytical solution given by

$$V_o = \frac{\pi_{44} S_x}{2\left(1 + \frac{\pi_{11} + \pi_{12}}{2}\right)} V_s$$

Results Comparison

	Target	ANSYS	Ratio
Output voltage V_o, mV	3.4524	3.4524	1.000

VM239: Mechanics of the Revolute and Universal Joints

Overview

Reference:	J. E. Shigley, J. J. Uicker, Jr., *Theory of Machines and Mechanisms*, 2nd Edition, McGraw-Hill, Inc., 1995, p.115.
Analysis Type(s):	Static Analysis (**ANTYPE** = 0)
Element Type(s):	Linear (2-Node) Beam Elements (BEAM188)
	Multipoint Constraint Elements - Universal Joint, Revolute Joint, Slider Element (MPC184)
Input Listing:	vm239.dat

Test Case

A double universal joint drive shaft drives a simple slider-crank mechanism. Compare the rotations at different points in the drive shaft with the applied rotation. Also, show the linear motion caused by the slider-crank satisfied the appropriate equation.

Figure 239.1 Shaft-driven Slider-Crank Mechanism

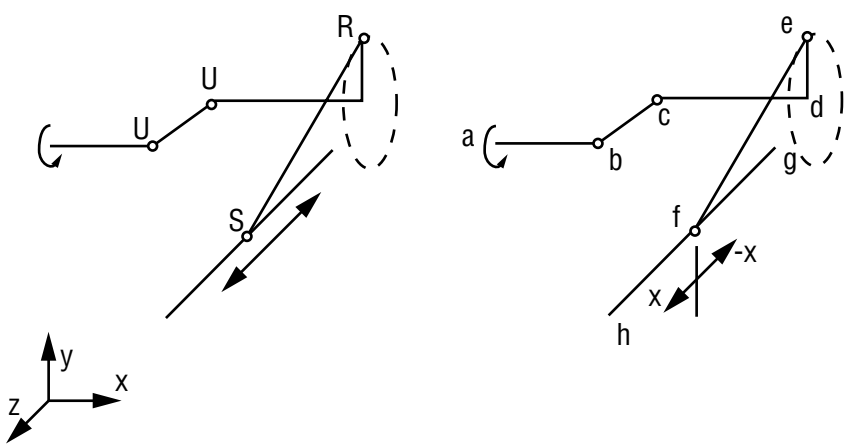

Material Properties	Geometric Properties	Loading
E = 30 x 10^6 psi υ = 0.33	ab = 1.0 in. cd = 1.0 in. de = 0.5 in. ef = 1.5 in. gh = 1.5 in.	At "a": ROTX = 2π rad. (= 360°)

Analysis Assumptions and Modeling Notes

The rotation of 2π rad., which is applied at node "a", is first transmitted through the three shafts, existing in the x-y plane, that are joined together by the MPC184 universal joints. The rotation is compared with the resulting rotation at node "c". This graph should result in an expression determined by the following function:

α_2 = arc tan (tanα_1/cosβ)

where:
$\alpha 1$ = the angle of twist of the drive shaft

α_2 = the angle of twist of the driven shaft
β = relative angle between axis of rotation of the shafts

The input rotation is next compared to the resulting rotation at node "d". The plot shows a linear relationship in which the rotations at "a" should be equal to the rotations at "d".

Warning: The revolute joint at junction "e" is tested by comparing the results of the input rotation at "a" (which is transferred perfectly to "d") with the linear, sliding motion generated by the slider-crank mechanism lying in the y-z plane. This relationship is defined in the supplied reference, and reflected below in the results.

Results Comparison

Input Rotation vs. Linear Motion of Slider-Crank Mechanism

Applied Rotation	Target	ANSYS	Ratio
Linear Motion (x) for $\pi/4$ (45°)	0.39708	0.39708	1:1
Linear Motion (x) for $\pi/2$ (90°)	0.58579	0.58579	1:1
Linear Motion (x) for $3\pi/4$ (135°)	0.39708	0.39708	1:1
Linear Motion (x) for π (180°)	0.00000	0.00000	1:1

Figure 239.2 Relationship of Rotations at "a" and "c"

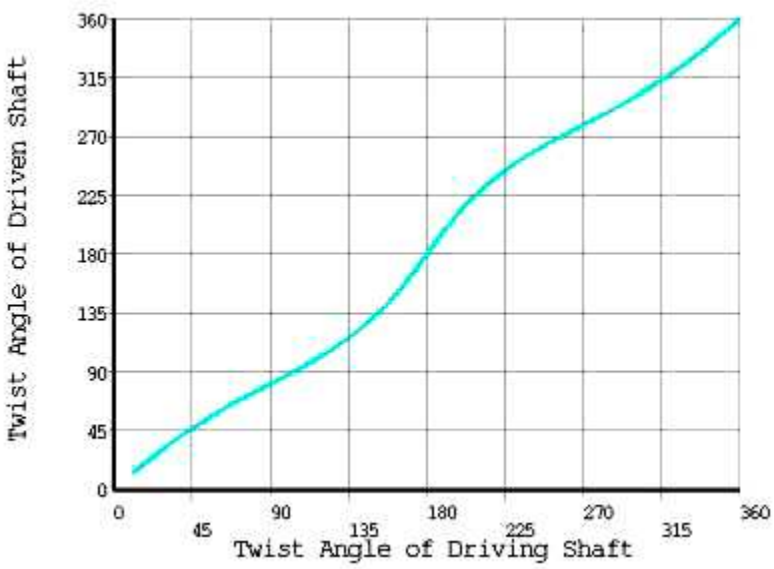

Figure 239.3 Relationship of Rotations at "a" and "d"

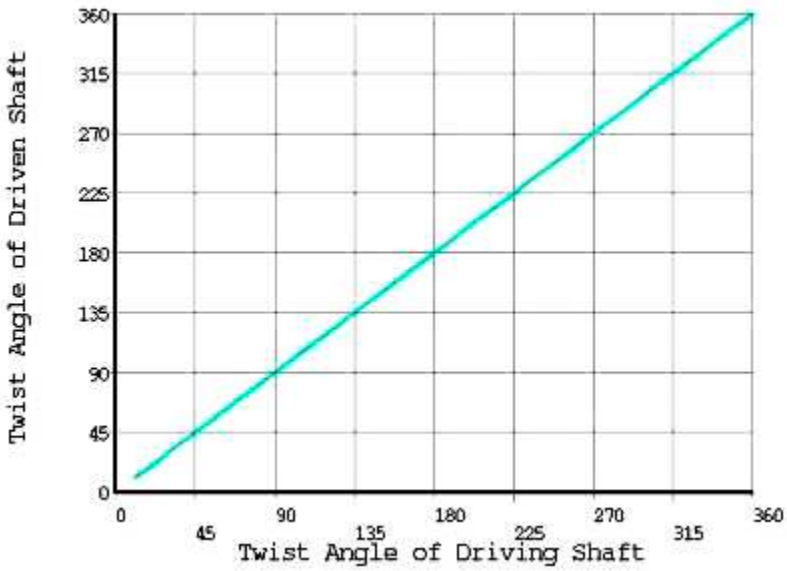

VM240: Thermal Expansion of Rigid Beams in a Composite Bar

Overview

Reference:	J.M. Gere, S.P. Timoshenko, *Mechanics of Materials*, 2nd Edition, PWS Publishers, 1984, p. 20-21,71
Analysis Type(s):	Static Analysis (**ANTYPE** = 0)
Element Type(s):	Nonlinear (8-Node) Solid Elements (SOLID185) Multipoint Constraint Elements - Rigid Beams (MPC184)
Input Listing:	vm240.dat

Test Case

A composite bar consists of two base materials with 25 rigid beams embedded along its length. A coefficient of thermal expansion is defined for only the rigid beams. Compare the stresses resulting in both solid composite materials when a temperature is applied.

Figure 240.1 Thermal Expansion of Composite Bar

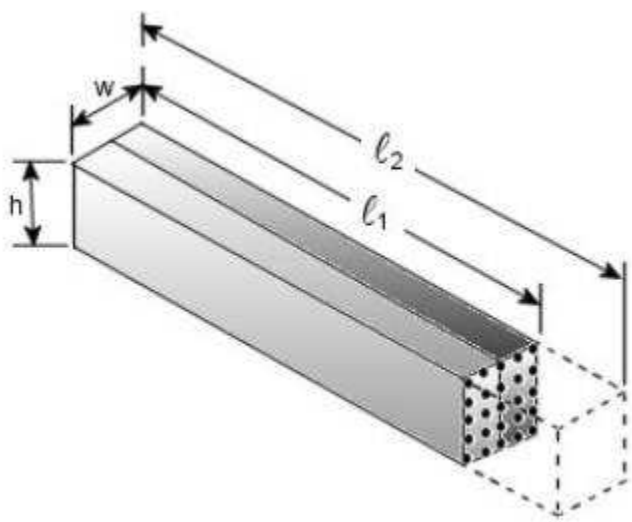

Material Properties	Geometric Properties	Loading
E_1 = 10 x 10e^6 psi υ_1 = 0.3 E_2 = 5 x 10e^6 psi υ_2 = 0.3 /in./°F (at 100 °F)	ℓ_1 = 40 in. w = 4 in. h = 4 in.	T_1 = 0 °F T_2 = 100 °F

Analysis Assumptions and Modeling Notes

A composite bar with a 4" x 4" cross-section is modeled using SOLID185 elements. The bar consists of two different materials with the material properties E_1, E_2, υ_1, and υ_2 as shown above. Twenty five MPC184 rigid beam elements are then modeled running along the length of the bar. The rigid beam elements are given a coefficient of thermal expansion, α_3. The bar is fixed in all DOF's at one end. As a temperature is applied to the model, the rigid beam elements expand, in turn deforming the rest of the composite bar. As a result, two distinctly different stress levels

can be seen through the bar's cross-section. These stresses reflect the material property differences of the two materials making up the composite

The equations below are used to calculate theoretical stress values for comparison:

$$\ell 2 = \ell_1 [1 + \alpha(T_2 - T_1)]$$

$$\sigma = \frac{E(\ell_2 - \ell_1)}{\ell_1}$$

Results Comparison

	Target	ANSYS	Ratio
1 - Equivalent Stress (von Mises)	300,000	302,106	1.007
2 - Equivalent Stress (von Mises)	150,000	151,083	1.007

Figure 240.2 Stress Results in Composite Material

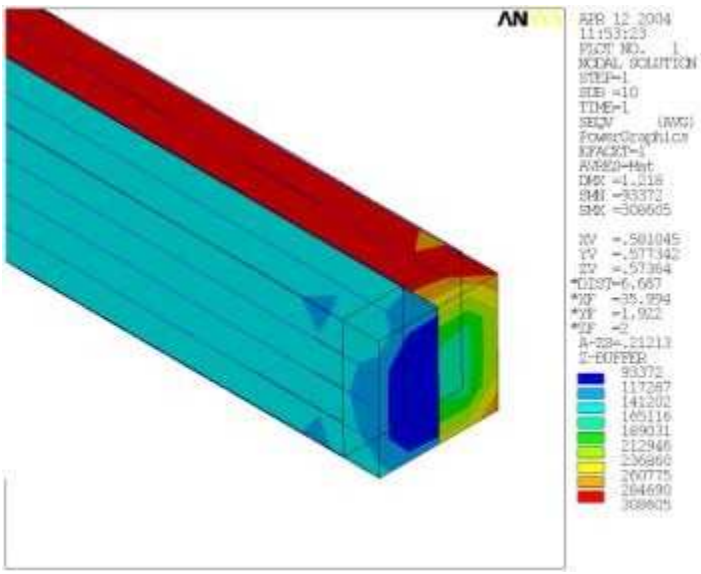

VM241: Static Force Computation of a 3-D Solenoid Actuator

Overview

Reference:	M. Gyimesi, D. F. Ostergaard, "Analysis of Benchmark Problem TEAM20 with Various Formulations", *Proceedings of TEAM Workshop, COMPUMAG, Rio*, 1997. M. Gyimesi, D. F. Ostergaard, "Mixed Shape Non-Conforming Edge Elements", *IEEE Transactions on Magnetics*, Vol. 35 No. 3, 1999, pp. 1407-1409. M. Gyimesi, D. F. Ostergaard, "Non-Conforming Hexahedral Edge Elements for Magnetic Analysis", *IEEE Transactions on Magnetics*, Vol 34 No. 5, 1998, pp. 2481-2484.
Analysis Type(s):	Static (**ANTYPE** = 0)
Element Type(s):	Tetrahedral Coupled-Field Solid Elements (SOLID117)
Input Listing:	vm241.dat

Test Case

For the given solenoid actuator with an applied total coil current of 1000 A-turns, find the magnetic flux density (BZ) of the Pole, the magnetic flux density (BZ) of the Arm, and the Virtual Work Force in the Z-direction (See Problem Description for location of parts).

Material Properties	**Geometric Properties**	**Loading**
Murx =1	X1 = 63.5mm X2 = 12.5mm Y1 = 12.5mm Y2 = 5mm Y3 = 18mm Z1 = 25 mm Z2 = 100mm Z3 = 98.5mm Z4 = 96.6mm	Total Current = 5000 A-turns

Figure 241.1 B-H Curve

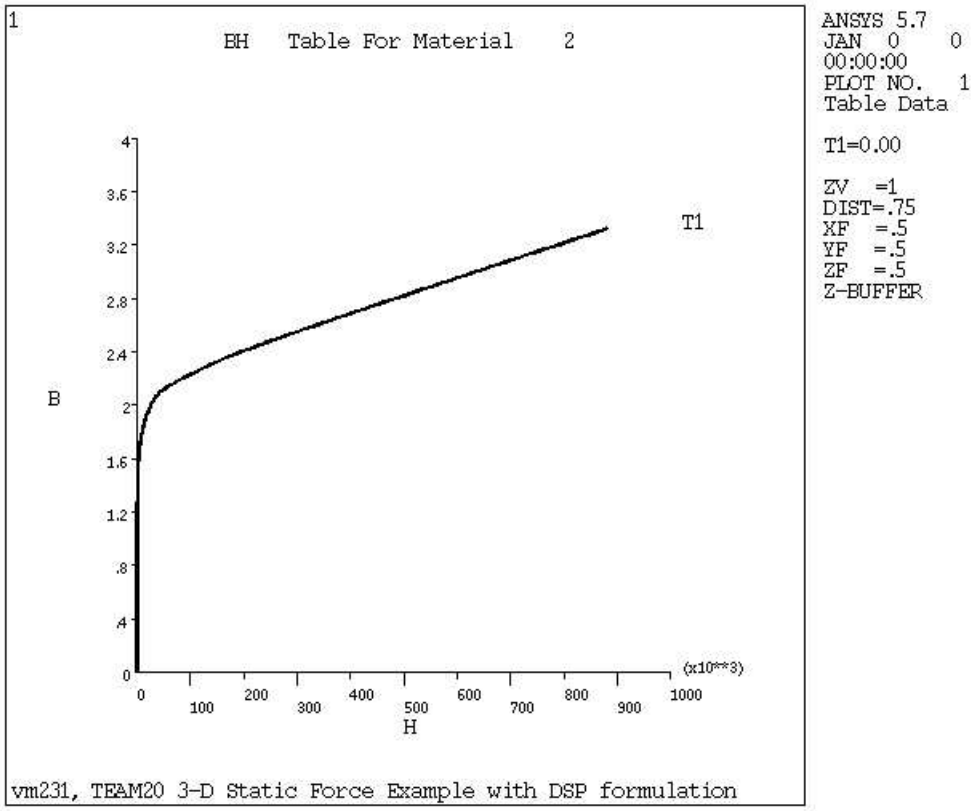

Analysis Assumptions and Modeling Notes

This analysis is based on the TEAM workshop problem 20. It utilizes the edge-flux element formulation with tetrahedral shaped SOLID117 elements. To simplify meshing, the **SMRTSIZE** meshing option was used to automatically determine line divisions and spacing ratios while taking into account the line proximity effects. Mesh density can be adjusted using the SmartSize parameter, for this case, a SmartSizing level of 10 was applied. The analysis is performed using a quarter symmetry model of the solenoid actuator. The magnetic coil was created using the **RACE** command. Magnetic force and boundary conditions were placed on the armature component by using the **FMAGBC** command.

Figure 241.2 Finite Element Model

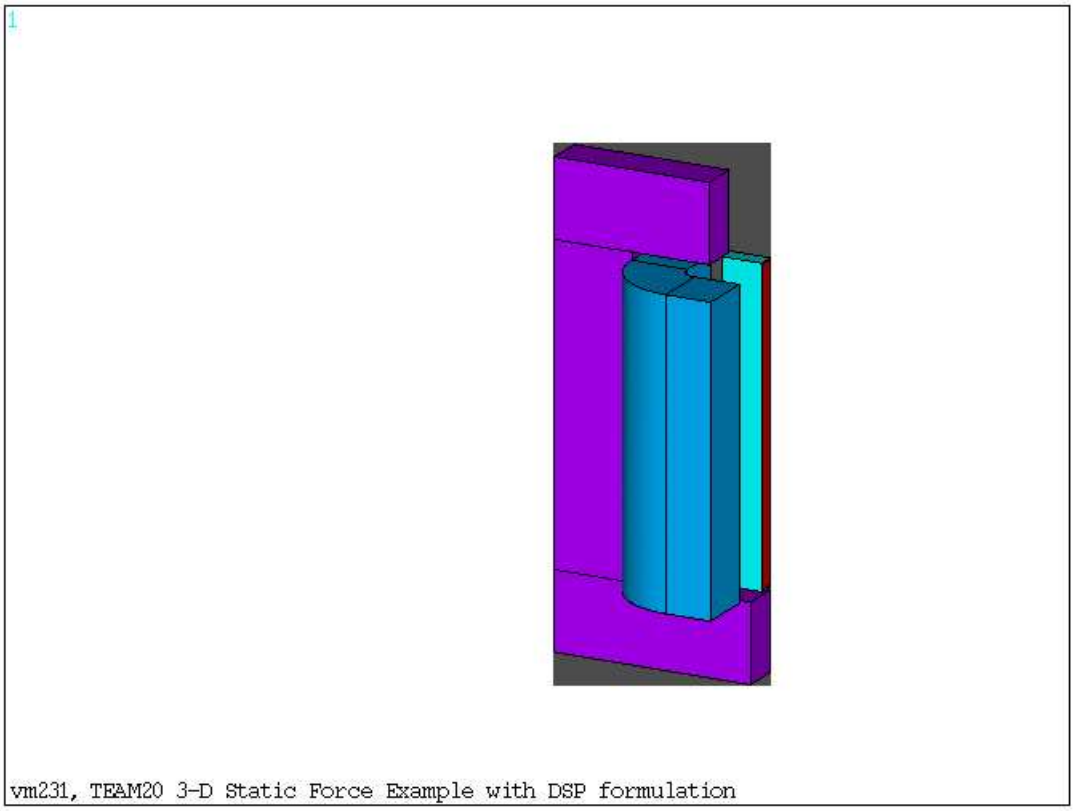

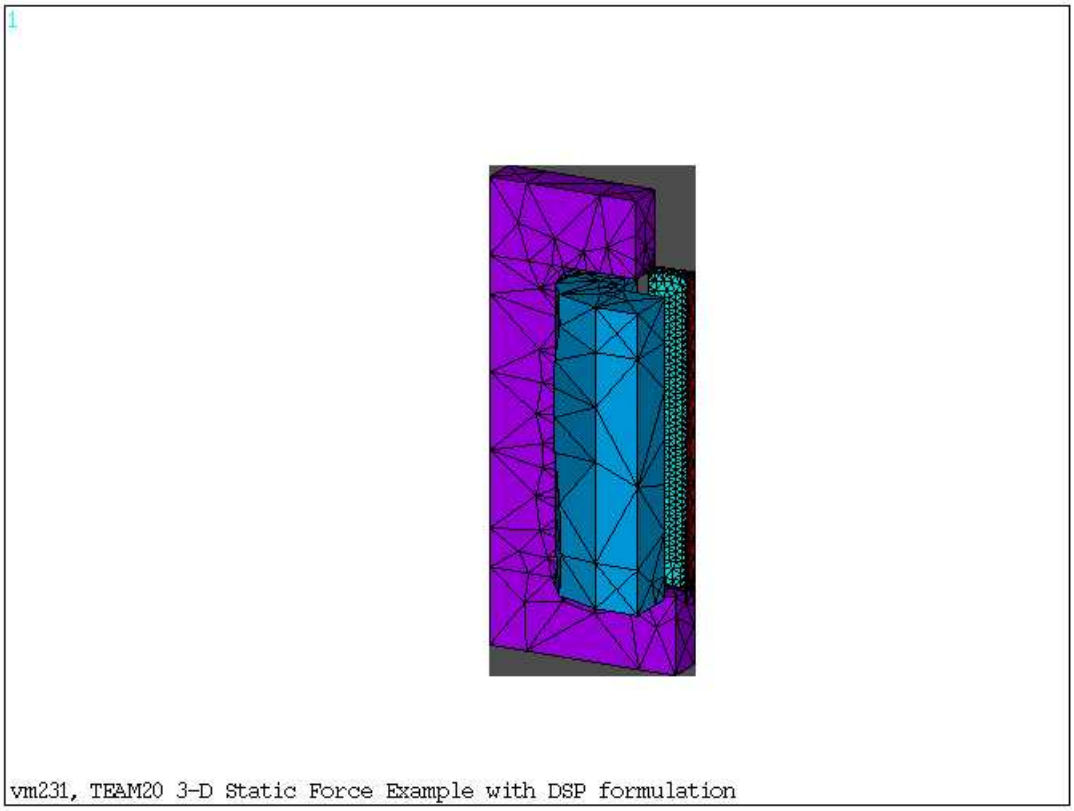

Results Comparison

Total Current = 5000 A-turns	Target	ANSYS	Ratio
Virtual Work Force (N)	80.100	78.691	0.982
Pole Flux Density (BZ, Tesla)	0.460	0.456	0.992
Arm Flux Density (BZ, Tesla)	2.050	2.028	0.990

VM242: Series Expansion Study of an Annular Plate

Overview

Reference:	R.J. Roark and W.C. Young, *Formulas for Stress and Strain*, 5th Edition. McGraw-Hill Book Co. Inc., New York, NY., 1975, Pg 406, Table 24 - Case 2e
Analysis Type(s):	Static Analysis (**ANTYPE** = 0)
Element Type(s):	4-Node Finite Strain Shell Elements (SHELL181)
Input Listing:	vm242.dat

Test Case

Figure 242.1 Annular Plate

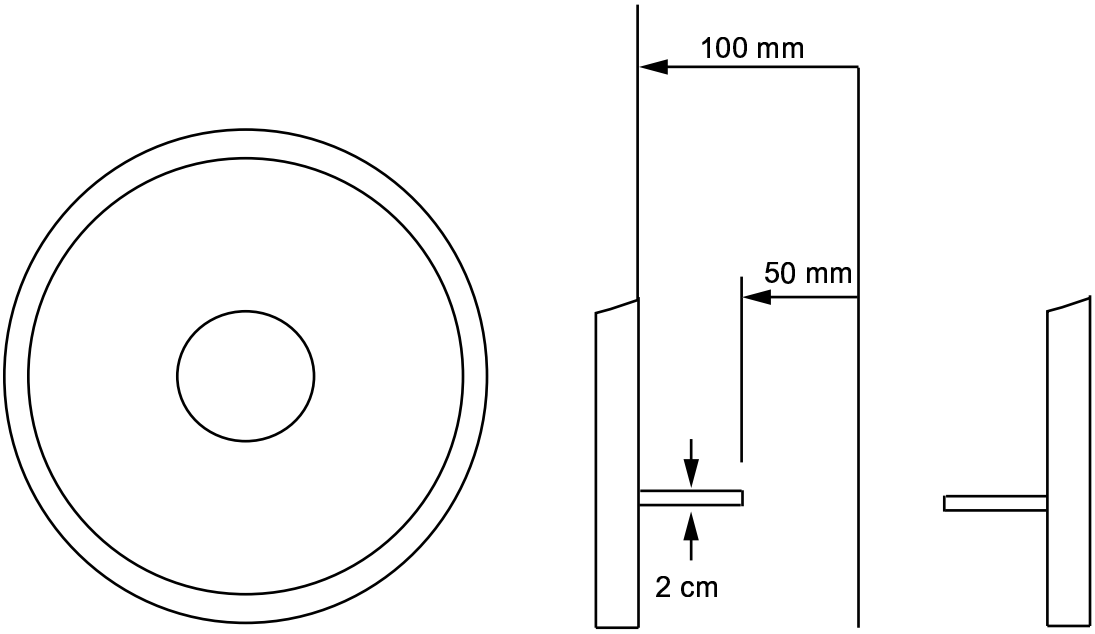

An annular plate subjected to uniform pressure is studied using a series expansion analysis. The elastic modulus and the shell thickness are simultaneously varied by ± 10%. The outer radius is fixed and the inner radius is free. The maximum deformations for the extreme parameter values are compared to the theoretical results.

Material Properties	**Geometric Properties**	**Loading**
E(min) = 180 x $10e^9$ Pa E(max) = 220 x $10e^9$ Pa ν = 0.3	Thick (min) = 1.8 mm Thick (max) = 2.2 mm Inner Radius = 50 mm Outer Radius = 100 mm	Uniform Pressure = -2000 Pa

Analysis Assumptions and Modeling Notes

This analysis uses the variational technology series expansion method to obtain results for all of the specified parameter ranges in a single solution pass. Since more than one parameter is varied in each element the Taylor method must be used (**SXMETH**,FULL,TAYLOR). The results are stored in an rsx file and must be extracted for each set of parameter values with the **SXVMOD** and **SXEVAL** commands.

Results Comparison

	Target	ANSYS	Ratio
Case 1 (Max E, Max Thick)	-0.4941E-05	-0.5076E-05	1.027
Case 2 (Max E, Min Thick)	-0.9022E-05	-0.9110E-05	1.010
Case 3 (Min E, Max Thick)	-0.6039E-05	-0.6060E-05	1.003
Case 4 (Min E, Min Thick)	-0.1103E-04	-0.1105E-04	1.002

VM243: Cantilever Beam with Triangular Loading Defined by Function

Overview

Reference:	F. P. Beer and E. J. Johnston, Jr., *Mechanics of Materials*, Mc-Graw-Hill, New York, NY, 1981, pp. 356, 366, 397, 613
Analysis Type(s):	Static
Element Type(s):	PLANE183
Input Listing:	vm243.dat

Test Case

Figure 243.1 Cantilever Beam with Triangular Loading

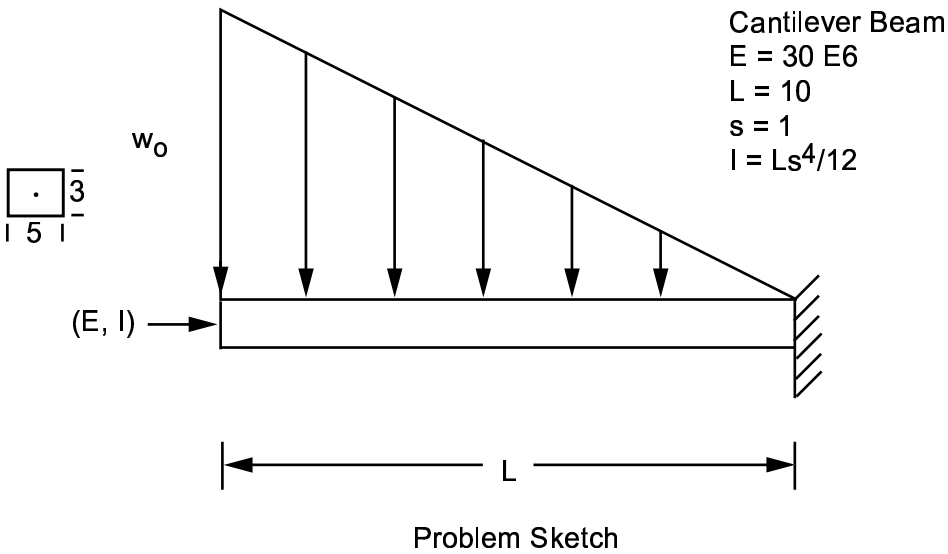

Problem Sketch

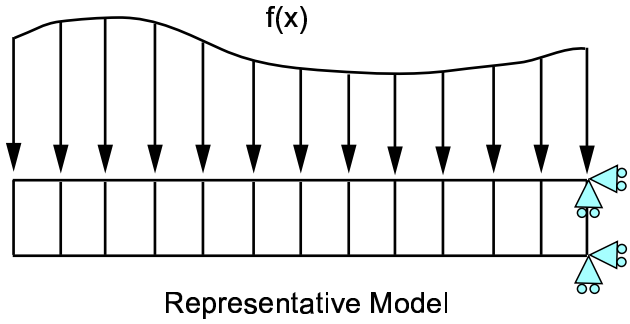

Representative Model

Material Properties	Geometric Properties	Loading
E = 30E6 $I = \frac{s^4}{12}$	s = 1 L = 1	w(x = 0) = 1 w(x = L) = 0 linear variation between them

Analysis Assumptions and Modeling Notes

Two models are used to test the method of creating a functional load. In the first case, the loading function P(x) is applied using the functional loading to create a load corresponding to P(x) = (x/L) In the second case, the loading is applied using the established two value linear loading. According to beam theory, the equation for maximum displacement of this loading is:

$$U_{max} = \frac{11L^4 w(0)}{120EI}$$

This result is then compared against the results

Results Comparison

	Target	**ANSYS**	**Ratio**
Displacement (max), tabular loading	0.367E-3	0.370E-3	1.01
Displacement (max), two value linear loading	0.367E-3	0.370E-3	1.01

VM244: Modal Analysis of a Cyclic Symmetric Annular Plate

Overview

Reference:	R. D. Blevins, *Formulas for Natural Frequency and Mode Shape*, New York, NY, VanNostrand Reinhold Publishing Inc., 1979, PP. 246-247, 286-287.
Analysis Type(s):	Mode-frequency analysis (**ANTYPE** = 2)
Element Type(s):	3-D 8-Node Structural Solid (SOLID185) 3-D 20-Node Structural Solid (SOLID186) 3-D 10-Node Tetrahedral Structural Solid (SOLID187) 4-Node Finite Strain Shell (SHELL181)
Input Listing:	vm244.dat

Test Case

Figure 244.1 An Annular Plate

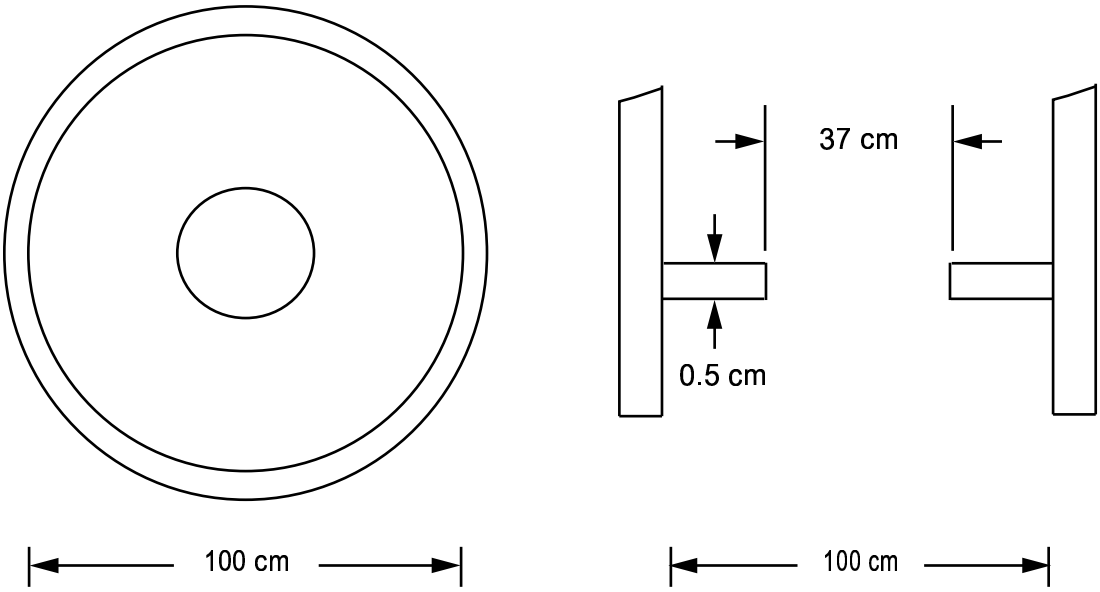

The fundamental natural frequency of an annular plate is determined using a mode-frequency analysis. The lower bound is calculated from the natural frequency of the annular plates, which are free on the inner radius and fixed on the outer. The bounds for the plate frequency is compared to the theoretical results.

Material Properties	**Geometric Properties**	**Loading**
$E = 7.03 \times 10^5$ kg/cm^2 $\nu = 0.3$ $\rho = 2.79 \times 10^{-9}$ kg/cm^2 $\gamma = 1.415 \times 10^{-6}$ kg-sec^2/cm^3	Outside Radius (a) = 50 cm Inside Radius (b) = 18.5 cm Thickness (h) = 0.5 cm	Free modal analysis

Analysis Assumptions and Modeling Notes

According to Blevins, the lower bound for the fundamental natural frequency of the annular plate is found using the formula presented in Table 11-2:

$$f = \frac{\lambda^2}{2\pi a^2}\left[\frac{Eh^3}{12\gamma(1-\upsilon^2)}\right]^{\frac{1}{2}}$$

Where,

$$\lambda^2 = 4.80$$

In ANSYS, a 30° symmetric sector of the annular plate is created via CYCLIC expansion with **CYCOPT**, NODDIA. The outer edge of the model is constrained in all directions and no dampening or loading is applied. The element types SOLID185, SOLID186, SOLID187, and SHELL181 are used to solve for the lower bound of the fundamental natural frequency (Hz).

Results Comparison

	Target	**ANSYS**	**Ratio**
Frequency (SOLID185)	23.38	23.14	0.99
Frequency (SOLID186)	23.38	23.12	0.99
Frequency (SOLID187)	23.38	23.15	0.99
Frequency (SHELL181)	23.38	22.96	0.98

VM245: Squeeze Film Damping: Rectangular Plate

Overview

Reference:	J. J. Blech, *On Isothermal Squeeze Films*, Journal of Lubrication Technology, Vol. 105, pp. 615-620, 1983
Analysis Type(s):	harmonic
Element Type(s):	FLUID136
Input Listing:	vm245.dat

Test Case

Figure VM245.1 Rectangular Plate

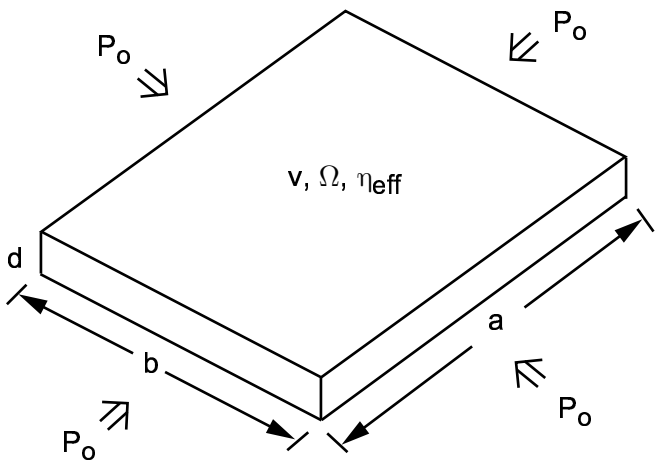

Material Properties	Geometric Properties	Loading
Fluid Viscosity = 1.83e - 12N/(μm)^2	a = 2000μm b = 1000 μm d = 5 μm	Operating frequency, Ω = 100000 Hz Velocity, v = 2000(μm)/s Pressure at edges = 1e5 Pa

Analysis Assumptions and Modeling Notes

The problem is modeling the fluid gap region between two rigid, non-deforming surfaces. The pressure of the fluid entering and exiting the gap creates a damped elastic response which can modeled by a spring-damper system. The calculations of the stiffness and damping constants are done by summing the pressure distribution over the area, then taking these force calculations and feeding them into the equations

$$C = \frac{F^{Re}}{v_z}$$

$$K = \frac{F^{Im}\omega}{v_z}$$

where F(im) and F(re) are the “imaginary” and “real” parts of the force calculated from the harmonic analysis.

According to Blech an analytical solution for the damping and squeeze coefficient for a rigid plate moving with a transverse motion is given by:

$$C(\Omega) = \frac{64\sigma(\Omega)p_o A}{\pi^6 d\Omega} \sum_{m=odd} \sum_{n=odd} \frac{m^2 + n^2 c^2}{(mn)^2 \left[(m^2 + n^2 c^2)^2 + \frac{\sigma(\Omega)^2}{\pi^4} \right]}$$

$$K_S(\Omega) = \frac{64\sigma(\Omega)p_o A}{\pi^8 d} \sum_{m=odd} \sum_{n=odd} \frac{1}{(mn)^2 \left[(m^2 + n^2 c^2)^2 + \frac{\sigma(\Omega)^2}{\pi^4} \right]}$$

where:

$C(\Omega)$ = frequency-dependent damping coefficient
$K_S(\Omega)$ = squeeze stiffness coefficient,
p_o = ambient pressure
A = surface area
c = ratio of plate length a divided by plate width b
d = film thickness
Ω = response frequency
σ = squeeze number of the system

The squeeze number is given by:

$$\sigma(\Omega) = \frac{12\eta_{eff} a^2}{p_o d^2}$$

for rectangular plates where η_{eff} is the effective viscosity.

Results Comparison

	Target	**ANSYS**	**Ratio**
Stiffness, K (Ns/m)	28650.00	28549.65	0.996
Damping constant, C (N/m)	0.0153	0.0151	0.988

VM246: Cyclic Analysis of an End-Loaded Hollow Cylindrical Cantilever Beam

Overview

Reference:	F. P. Beer, E. R. Johnston, Jr., *Mechanics of Materials*, McGraw-Hill, Inc., New York, NY, 1981, pg 598.
Analysis Type(s):	Static-structural analysis
Element Type(s):	3-D 8-Node Structural Solid (SOLID185)
	3-D 20-Node Structural Solid (SOLID186)
	3-D 10-Node Tetrahedral Structural Solid (SOLID187)
Input Listing:	vm246.dat

Test Case

Figure 246.1 Hollow Cylindrical Cantilever Beam and Loading

Figure 246.2 Beam Cross-Section

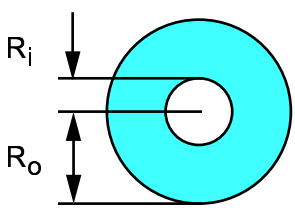

Determine the maximum deflection of an end-loaded hollow cylindrical beam. The beam is fixed at one end and free on the other. The load consists of a downward force of 5 pounds at the free end.

Material Properties	**Geometric Properties**	**Loading**
$E = 70 \times 10^3$ psi	Outside Radius (R_o) = 0.5 in	P = 5 lb
$\nu = 0.3$	Inside Radius (R_i) = 0.25 in	
	Length (L) = 10 in	

Analysis Assumptions and Modeling Notes

From the reference, the maximum deflection (δ) in a cantilever beam with end loading can be found using:

$$\delta = -\frac{PL_3}{3EI} = 0.519\,\text{in}$$

Where,

$$I = \frac{\pi}{4}(R_o^4 - R_i^4) = 0.046\,in^4$$

The analysis is accomplished with SOLID185, SOLID186, and SOLID187 element types. For each run, a 30° portion of the beam is modeled, meshed and then expanded using the **CYCLIC** and **/CYCEXPAND** commands.

To obtain accurate results, KEYOPT settings were issued for each element type. Enhanced strain formulation (KEYOPT,1,2,2) was used for SOLID185. Full integration (KEYOPT,1,2,1) was used for SOLID186. Pure displacement formulation (KEYOPT,1,6,0) was necessary for SOLID187.

Results Comparison

	Target	**ANSYS**	**Ratio**
Deflection (SOLID185)	0.5187	0.5213	1.005
Deflection (SOLID186)	0.5187	0.5212	1.005
Deflection (SOLID187)	0.5187	0.5221	1.007

Part II. Benchmark Study Descriptions

Chapter 2: Overview

This manual also provides information on the applicability, selection and performance of ANSYS finite elements, meshing algorithms, and solution algorithms by a series of benchmark test cases. The benchmark studies are designed to illustrate both proper, and in some cases, improper application of finite element techniques in various modeling situations. Improper use may take the form of inappropriate element selection, mesh discretization, or master degree of freedom selection. The results presented here for some test cases may appear in error, but are in fact the "expected" solutions for the chosen element, discretization, and loading condition. By providing the results for such test cases, we hope to provide guidance in the selection of appropriate analysis options.

While ANSYS cannot provide an exhaustive set of benchmark studies, we have included the most commonly-used elements and analysis types. Using these benchmark studies as a guideline, you can extend the applicability to other element types or solution methods. In many instances, existing benchmark standards were used as the basis of the test case construction.

The following benchmark topics are available:

2.1. Description of the Benchmark Studies
2.2. Benchmark Test Case Content and Nomenclature
2.3. Running the Benchmark Test Cases
2.4. Energy Norm
2.5. Benchmark Test Case Coverage Index

2.1. Description of the Benchmark Studies

The benchmark test cases are designed to test element performance, meshing algorithm's effect on solution performance, alternative solution algorithms (for modal analysis), and element energy error norm performance.

Element performance (accuracy) is checked for a subset of some of the more frequently used ANSYS solid and shell elements including PLANE2, PLANE35, PLANE42, SHELL43, SOLID45, PLANE55, SHELL63, SOLID70, PLANE77, PLANE82, SOLID92, SHELL93, SOLID95, VISCO106, and VISCO107. The tests are designed to check the element performance under various load conditions and element shapes. Solution accuracy and convergence rates are also presented for the elements.

The effect of alternative meshing schemes on solution accuracy is studied for several test cases. The meshing schemes include quadrilateral and triangle meshing for areas, and brick and tetrahedral meshing for volumes. Solution accuracy is based on the energy error norm and/or localized stress and displacement evaluation.

For mode-frequency analysis, comparison is made between solutions using alternative eigenvalue extraction techniques (subspace and Householder). Also tested is the influence and accuracy of automatic master degree of freedom selection in Householder analyses.

For benchmark test cases using 2-D and 3-D solid elements in a static analysis, results are in part expressed in terms of an energy error norm. Energy error norms can be used as a guide in evaluating the mesh discretization used in a finite element analysis. See Section 2.4: Energy Norm for more information.

The benchmarks are categorized into VMD*XX* test cases and VMC*XX* test cases (where *XX is the problem number). The VMD series is specifically designed to test individual finite element performance under distorted, or irregular shapes. The VMC series is designed to test solution accuracy and convergence for a series of test cases that undergo increasing mesh refinement or use alternate element types. The benchmark studies follow the documentation of the VM test cases in this manual.*

Three types of analyses are included in the benchmark tests:

- Static analysis (ANTYPE = 0)
- Mode frequency analysis (ANTYPE = 2)
- Transient analysis (ANTYPE = 4)

The benchmark test cases are drawn from a variety of resources, such as NAFEMS (National Agency for Finite Element Methods and Standards) based in the United Kingdom, proposed benchmarks in the literature, and textbook problems. Where applicable, test cases that conform to published benchmark specifications are identified.

2.2. Benchmark Test Case Content and Nomenclature

Format and content for the benchmark test cases are as follows:

- **Overview**--a list of the major reference for the problem, the analysis type, the element type(s), and the name of the test case file (in the printed manual) or a link to the test case file (in the online version).
- **Test Case**--a brief description of the problem and desired solution output. Also included are necessary material properties, geometric properties, loadings, boundary conditions, and parameter definitions. The parameters listed in the parameter definition area are used to define model variables that distinguish each test case run. Each test case is uniquely defined by these parameters and noted in the Results Comparison section.
- **Representative Mesh Options**--a graphics display of a sampling of the finite element meshes created by the test. Parameters defined in the Test Case section are used to specify the finite element mesh patterns shown.
- **Target Solution**--solution used for comparison purposes. The target solution is obtained from the problem reference unless specifically mentioned otherwise in the Assumptions, Modeling Notes, and Solution Comments section.
- **Results Comparison**--results from the ANSYS solution compared with the target solution. Where applicable, the ANSYS results are normalized with respect to the target solution and presented as the ratio of the ANSYS results divided by the target results.
- **Graphical Results** (optional)--results displayed in graphical form.
- **Assumptions, Modeling Notes, and Solution Comments**--general comments on the test case modeling, assumptions, and results interpretation.

In addition to the abbreviations, symbols, and units defined in Section 1.14: Abbreviation, Element, and Product Lists, one additional symbol is used throughout the benchmark studies to identify the location of a target point where a solution comparison is made. The target point symbol is a bull's-eye: ◉

Several target points may be used in a test case, so each is identified separately as Target Point*xx* (or TP-*XX*). The example below shows two target points on a simple 2-D finite element mesh.

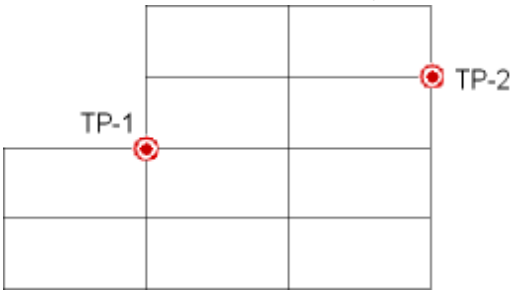

Solution comparisons between the target solution and the ANSYS solution at target points are listed in the Results Comparison section.

2.3. Running the Benchmark Test Cases

The benchmark test cases are contained on the installation media. Each test case input file is designed to be executed in one of two ways:

- Execute the single documented test case input (as shown in the Data Input Listing section for the problem in this manual; see Appendix B:, Benchmark Input Listings)
- Execute all test cases for the problem. The single test case executions are designed to run quickly, with run times comparable to the larger tests in Chapter 2, “Overview”. Executing all test cases is, in many instances, very time consuming and may require extremely large amounts of disk space and memory.

2.4. Energy Norm

The finite element solution is an approximation to the true solution of a mathematical problem. From an analyst's standpoint, it is important to know the magnitude of error involved in the solution. The ANSYS program offers a method for a posteriori estimation of the solution error due to mesh discretization. The method involves calculating the energy error within each finite element and expressing this error in terms of a global error energy norm.

The error energy within each finite element is calculated as

$$e_i = 1/2 \int_v \{\Delta\sigma\}^T [D]^{-1} \{\Delta\sigma\} \, dV$$

where:

e_i = error energy in element i
$\{\Delta\sigma\}$ = nodal stress error vector
[D] = stress-strain matrix

The nodal stress error vector $\{\Delta\sigma\}$ is the averaged nodal stresses minus the unaveraged nodal stresses.

By summing all element error energies e, the global energy error in the model, e, can be determined. This can be normalized against the total energy (u + e), where u is the strain energy, and expressed as a percent error in energy norm, E:

The percent error in energy norm E is a good overall global estimate of the discretization or mesh accuracy. Several VMD and VMC tests use this error norm to illustrate its behavior as a function of known displacement or stress error. It should be recognized that the correlation of the error energy norm to displacements or stress error is problem-dependent, and therefore this norm should only be viewed as a relative measure of accuracy.

2.5. Benchmark Test Case Coverage Index

Table 2.1 Structural Solid Elements

Test Case No.	Element Number							
	2	42	45	82	92	95	106	107
C1			X		X	X		
C2	X	X		X				

Test Case No.	Element Number							
	2	42	45	82	92	95	106	107
C5			X		X			
C8	X	X	X	X		X	X	X
D1	X	X	X	X	X	X		
D3	X	X	X	X	X	X		

Table 2.2 Structural Shell Elements

Test Case No.	Element Number		
	43	63	93
C3	X	X	X
C4	X	X	X
D2	X	X	X

Table 2.3 Thermal Solid Elements

Test Case No.	Element Number		
	35	55	77
C6	X	X	X
C7	X	X	X

Table 2.4 Analysis Type Coverage

Test Case No.	ANTYPE Analysis Type		
	0	2	4
C1	X		
C2	X		
C3	X		
C4		X	
C5		X	
C6	X		
C7	X		
C8			X
D1	X		
D2	X		
D3		X	

ANSYS Verification Manual . ANSYS Release 10.0 . 002184 . © SAS IP, Inc.

VMC1: Built-In Plate Under Uniformly Distributed Load

Overview

Reference:	S. Timoshenko, S, Woinowsky-Knieger, *Theory of Plates and Shells*, McGraw-Hill Book Co., Inc., New York, NY, 1959, pg. 202, Approximate Solution
Analysis Type(s):	Static Analysis (**ANTYPE** = 0)
Element Type(s):	3-D Structural Solid Elements (SOLID45) 3-D 8-Node Structural Solid Elements (SOLID185) 3-D 10-Node Tetrahedral Structural Solid Elements (SOLID92, SOLID187) 3-D 20-Node Structural Solid Elements (SOLID95, SOLID186)
Input Listing:	vmc1.dat

Test Case

A rectangular plate with built-in edges is subjected to a uniform pressure load on the top and bottom surface. Monitor displacement and stress results at three target points for a series of mesh refinements for different elements. Compare the effect of increased mesh refinement on the percent energy error norm.

Figure C1.1 Built-in Plate Problem Sketch

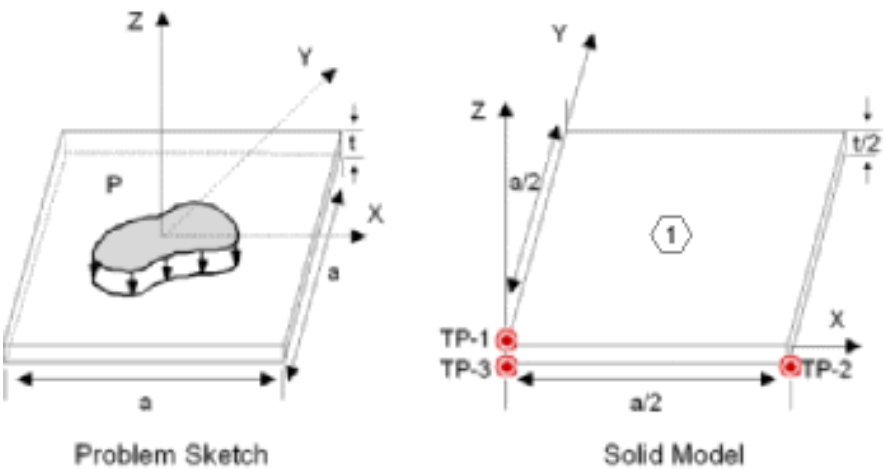

Material Properties	**Loading and Boundary Conditions**
E = 1 x 10^7 psi	At X = a/2, UX = 0
υ = 0.3	At x = a/2 and Z = 0, UZ = 0
Geometric Properties	At Y = a/2, UY = 0
a = 10 in	At Y = a/2 and Z = 0, UZ = 0
t = 1 in	At X = 0, UX = 0
Parameter Definitions	At Y = 0, UY = 0
N1 = no. elements along each horizontal edge	At Z = 0, UX = UY = 0
N2 = no. elements through thickness	At Z = -t/2, P = -500

Figure C1.2 Representative Mesh Options

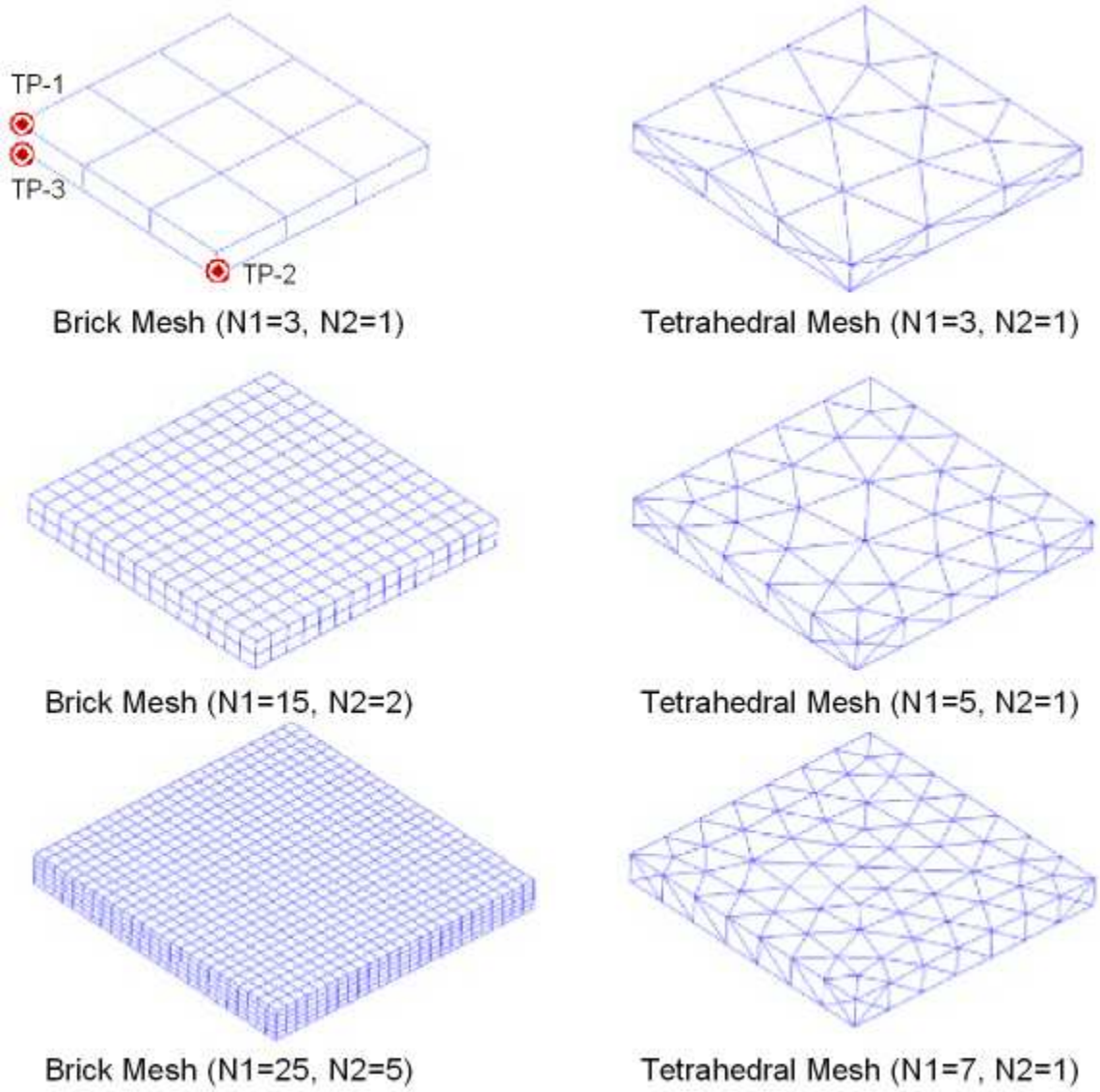

Solution Information

Table C1.1 Target Solution

ETYP	N1	N2	DOF	% Error Norm	UZ(1), in	SX(2), ksi	SX(3), ksi
95	25	10	45708	10	-.0172	-32.124	14.465

Table C1.2 Results Comparison

					Ratio		
ETYP	N1	N2	DOF	% Error Norm	UZ(1)	SX(2)	SX(3)
45	3	1	96	57	.925	.461	.983
45	6	1	294	33	.961	.663	.985

ETYP	N1	N2	DOF	% Error Norm	UZ(1)	Ratio SX(2)	SX(3)
45	15	2	2304	19	.980	.851	.992
45	20	4	6615	15	.987	.913	.996
45	25	5	12168	13	.990	.936	.997
95	3	1	288	8.4	.958	.829	1.037
95	6	1	945	7.7	.978	.955	1.006
95	15	2	8160	10	.991	.961	.999
95	20	4	24507	10	.997	1.000	1.000
92	3	1	687	39	.948	.680	1.003
92	5	1	1377	28	.974	.933	1.001
92	7	1	2493	24	.980	.961	1.000
92	10	2	4575	21	.984	.958	0.997
185	3	1	96	56.946	0.928	0.434	0.935
185	6	1	294	34.017	0.962	0.653	0.973
185	15	2	2304	19.154	0.980	0.850	0.991
185	20	4	6615	14.591	0.987	0.913	0.996
185	25	5	12168	13.202	0.990	0.936	0.997
186	3	1	288	8.365	0.958	0.829	1.037
186	6	1	945	8.365	0.958	0.955	1.006
186	15	2	8160	10.250	0.991	0.961	0.999
186	20	4	24507	10.160	0.997	1.001	1.000
187	3	1	687	39.985	0.948	0.677	1.005
187	5	1	1377	27.360	0.974	0.934	1.001
187	7	1	2493	23.585	0.980	0.959	1.000
187	10	2	4575	21.035	0.983	0.960	0.997

Table C1.3 Results Comparison - Shell Element and Analytical Solution

ETYP	N1	N2	DOF	% Error Norm	UZ(1), in	SX(2), ksi	SX(3), ksi
35	5	1	576	NA	-.0165	-29.580	14.303
Approximate Analytical Solution (neglecting shear deflection)					-.0138	-30.780	13.860

Assumptions, Modeling Notes, and Solution Comments

1. The problem exhibits symmetry about the midplane of the plate, and about the X and Y axes. This symmetry allows for a 1/8 symmetry sector to be modeled.
2. The approximate analytical solution neglects shear deflection. Shear deflection is accounted for in the finite element solutions.
3. The target solution is obtained from a fine mesh solution using SOLID95.

4. The 8-node isoparametric shell (SHELL93), subjected to the same loading, has results in line with the target solution. The SHELL93 element takes into account shear deflection effects.
5. Deflection and bending stresses converge quickly to the target solution at the center of the plate (target points 1 and 3) for the solid element test cases.
6. Bending-stresses are maximum at the built-in edges, peaking at the midspan of the plate (target point 2). It can be seen that a significant number of elements through the plate thickness are required to accurately predict the bending stresses at the built-in edge for the solid elements.
7. The percent error in energy norm remains relatively high as the mesh is refined, with most of the error energy located at the built-in edges. This behavior is expected at built-in edges where point-wise inaccuracies in the solution occur. The displacement and stress results for which the refinement was targeted are quite good, despite the high energy error.

VMC2: Elliptic Membrane Under a Uniformly Load

Overview

Reference:	J. Barlow, G. A. O. Davis, "Selected FE Benchmarks in Structural and Thermal Analysis", *NAFEMS Rept. FEBSTA*, Rev. 1, October 1986, Test No. LE1 (modified)
Analysis Type(s):	Static Analysis (**ANTYPE** = 0)
Element Type(s):	2-D 6-Node Triangular Structural Solid Elements (PLANE2) 2-D Structural Solid Elements (PLANE42) 2-D 4-Node Structural Solid Elements (PLANE182) 2-D 8-Node Structural Solid Elements (PLANE82, PLANE183)
Input Listing:	vmc2.dat

Test Case

An elliptic membrane structure of thickness t is subjected to a uniformly distributed outward pressure P. Monitor the tangential edge stress σ_y at target point 1 for a series of uniform mesh refinements using quadrilateral and triangular elements. Compare the effect of increased mesh refinement with the percent energy error norm.

Figure C2.1 Elliptic Membrane Problem Sketch

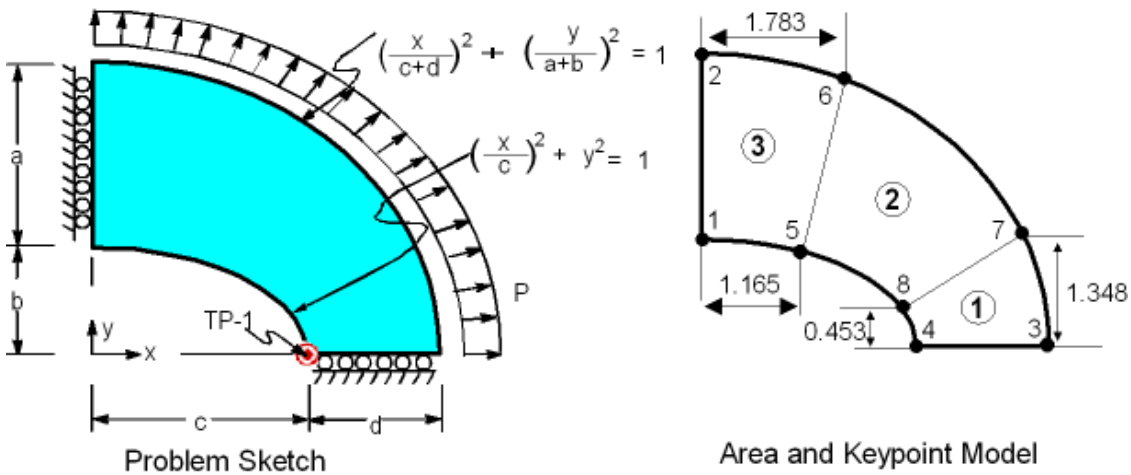

Material Properties E = 210 x 10^3 MPa υ = 0.3 **Parameter Definitions** N1 = no. elements in circumferential direction, per area N2 = no. elements in radial direction per area	**Loading and Boundary Conditions** At x = 0 UX = 0 At y = 0 UY = 0 Along outer edge P = -10 MPa **Geometric Properties** a = 1.75 m b = 1.0 m c = 2.0 m d = 1.25 m t = 0.1 m

Figure C2.2 Representative Mesh Options

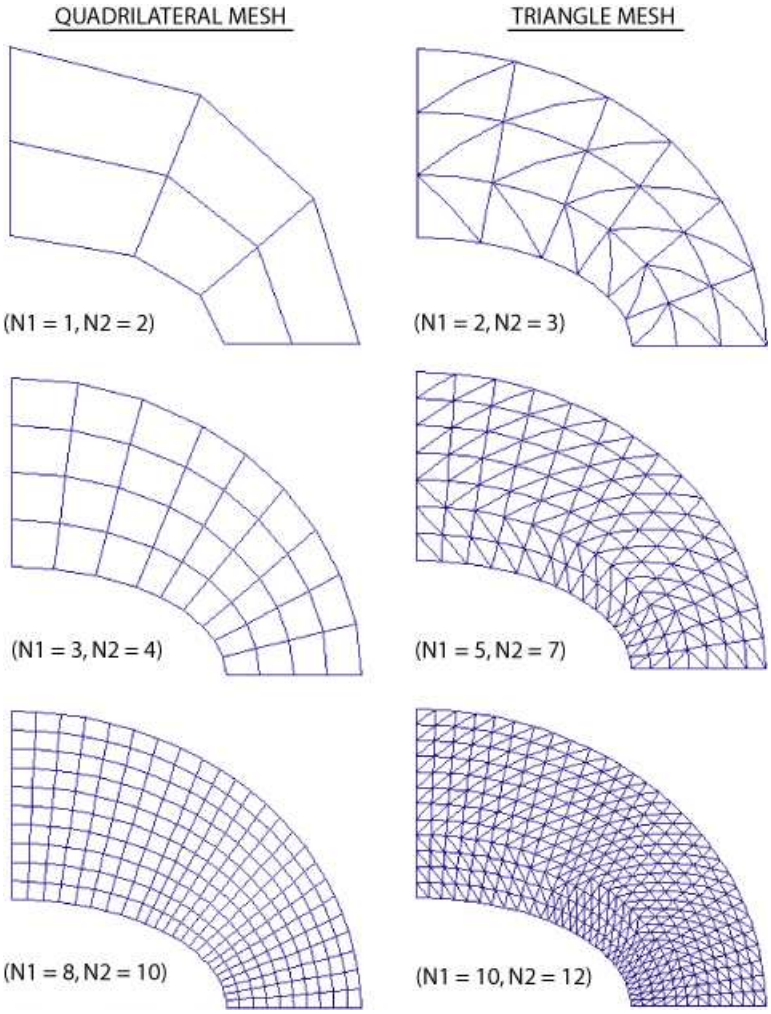

Results Tables

Target Solution: SY = 92.7 MPa Results Comparison - Quadrilateral Meshing

ETYP	N1	N2	DOF	% Error Norm	SY Ratio
42	1	2	24	36.452	0.634
42	2	3	56	22.545	0.809
42	3	4	100	16.549	0.885
42	5	7	256	10.781	.960
42	8	10	550	7.513	0.987
42	10	12	806	6.306	0.994
82	1	2	58	15.914	0.844
82	2	3	146	5.764	0.899
82	3	4	270	3.157	0.924
82	5	7	720	0.981	0.963
82	8	10	1578	0.422	0.977
82	10	12	2330	0.270	0.982

ETYP	N1	N2	DOF	% Error Norm	SY Ratio
182	1	2	24	33.020	0.720
182	2	3	56	26.575	0.861
182	3	4	100	20.817	0.923
182	5	7	256	14.197	0.987
182	8	10	550	9.906	1.007
182	10	12	806	8.290	1.012
183	1	2	58	15.914	0.844
183	2	3	146	5.764	0.899
183	3	4	270	3.157	0.924
183	5	7	720	0.981	0.963
183	8	10	1578	0.422	0.977
183	10	12	2330.	0.270	0.982

Results Comparison - Triangular Meshing

ETYP	N1	N2	DOF	% Error Norm	Normalized SY
2	1	2	70	22.484	0.737
2	2	3	182	10.657	0.837
2	3	4	342	6.612	0.882
2	5	7	930	2.665	0.942
2	8	10	2058	1.480	0.965
2	10	12	3050	1.159	0.973

Assumptions, Modeling Notes, and Solution Comments

1. From an element performance standpoint, the problem is designed to test membrane elements for accurate modeling of the strain variation, nodal stress extrapolation, and curved boundary modeling (of higher order elements).
2. From a modeling standpoint, the problem is designed to test quadrilateral and triangular meshes for solution accuracy with various element types. For the areas modeled, all exterior line segment specifications for mesh density are made equal for the various mesh options.
3. For quadrilateral and triangle element meshes under uniform mesh refinement (parameters N1 and N2 varied), the calculated percent error in energy norm follows a log-log linear relationship to the number of degrees of freedom in the model. The higher order elements (PLANE2 and PLANE82) exhibit nearly identical log-log slopes while the lower order element (PLANE42) exhibits a more gradual slope. These results illustrate that the PLANE2 and PLANE82 solutions converge at nearly the same rate under uniform refinement while PLANE42 converges at a slower rate. The percent error in energy norm results indicate that global accuracy is best obtained by PLANE82 for any given DOF set. However, the σ_y stress at target point 1 shows that for uniform refinement, PLANE42 gives better results (at that point) under moderate mesh refinement. A fine mesh using PLANE42 in place of a coarse mesh of PLANE2 or PLANE82 may produce better localized stress values.

VMC3: Barrel Vault Roof Under Self Weight

Overview

Reference:	R. D. Cook, *Concepts and Applications of Finite Element Analysis*, 2nd Edition, John Wiley and Sons, Inc., 1981, pp. 284-287.
Analysis Type(s):	Static Analysis (**ANTYPE** = 0)
Element Type(s):	4-Node Plastic Large Strain Shell Elements (SHELL43) Elastic Shell Elements (SHELL63) 8-Node Structural Shell Elements (SHELL93) 4-Node Finite Strain Shell Elements (SHELL181)
Input Listing:	vmc3.dat

Test Case

A cylindrical shell roof is subjected to gravity loading. The roof is supported by walls at each end and is free along the sides. Monitor the y displacement and bottom axial stress (σ_z) at target point 1, along with the bottom circumferential stress (σ_θ) at target point 2 for a series of test cases with increasing mesh refinement using quadrilateral and triangular element shapes. A companion problem that studies irregular element shapes is VMD2.

Figure C3.1 Barrel Vault Roof Problem Sketch

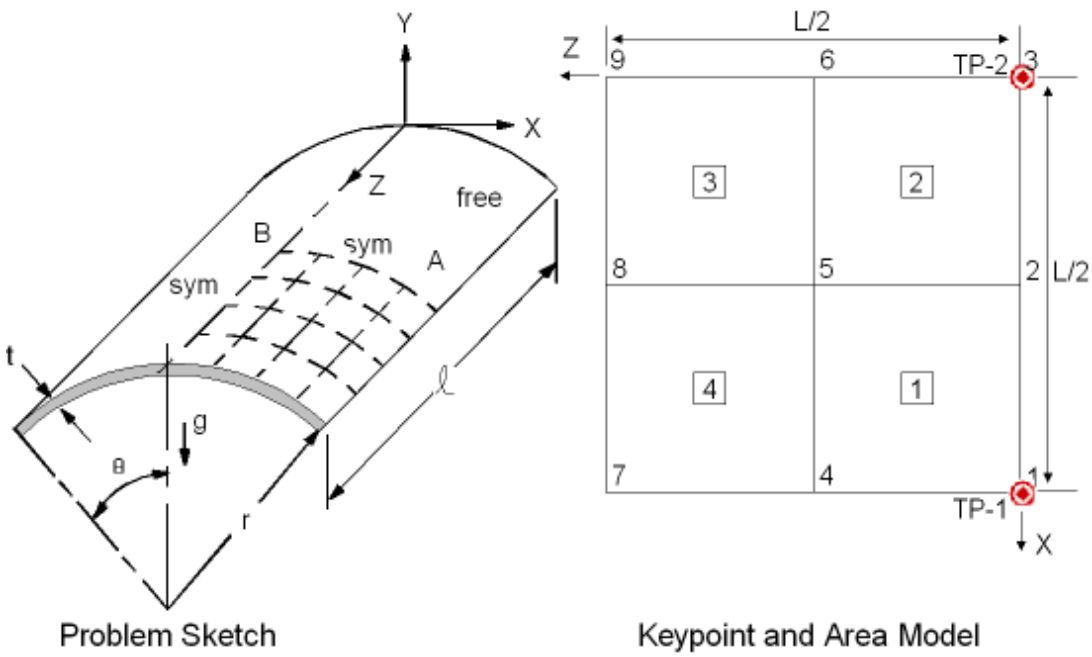

Material Properties	**Geometric Properties**
$E = 4.32 \times 10^8$ N/m^2 $\upsilon = 0.3$ $\rho = 36.7347$ kg/m^3 **Loading and Boundary Conditions** At x = 0 Symmetric At z = 0 Symmetric At x = L/2 UX = UY = ROTZ = 0	L = 50 m R = 25 m t = 0.25 m $\Theta = 40°$ g = 9.8 m/sec^2 **Parameter Definitions** N = No. elements along each edge

Figure C3.2 Representative Mesh Options

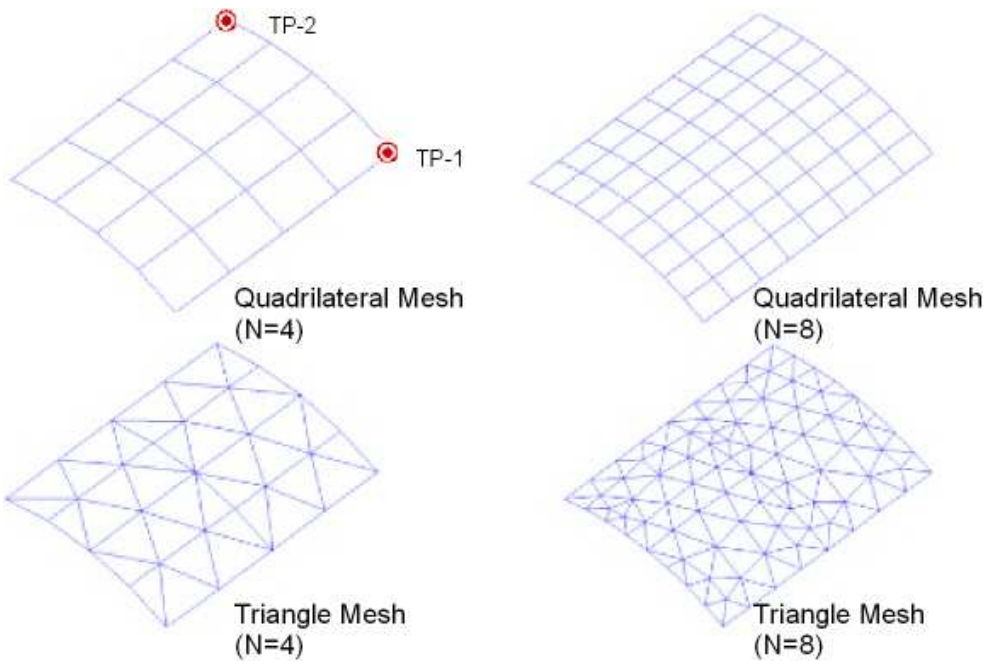

Target Solution

Target solution is obtained from an 8-node quadrilateral shell element solution with *N*=8, (see R. D. Cook, *Concepts and Applications of Finite Element Analysis*).

ETYP	N	DOF	UY(1), m	σ_z (1), Bottom	σ_θ (2), Bottom
--	8	2310	3016	358,420	-213,400

ETYP	N	DOF	Ratio		
			UY(1)	σ_z (1), Bottom	σ_θ (2), Bottom
Results Comparison - Quadrilateral Elements					
43	4	150	1.049	.940	.983
43	8	486	1.008	.998	.985
63	4	150	1.008	.928	1.017
63	8	486	.997	.994	.994
93	4	390	1.012	.956	1.028
93	8	1350	1.002	1.001	1.002
181	4	150	1.048	0.940	0.983
181	8	486	1.008	0.999	0.985
Results Comparison - Triangular Elements					
43[1]	4	222	.763	.507	.721
43[1]	8	546	.905	.731	.887
63	4	222	.791	.525	.771
63	8	546	.916	.737	.900
93	4	774	.971	.954	.985
93	8	1974	.991	.990	.995

ETYP	N	DOF	Ratio		
			UY(1)	σ_z (1), Bottom	σ_θ (2), Bottom
181	4	222	.780	.512	.742
181	8	546	.899	.723	.893

1. SHELL43 in triangular form is not recommended.

Assumptions, Modeling Notes, and Solution Comments

1. The problem is designed to test singly-curved shell elements under membrane and bending deformation. The quadrilateral mesh patterns produce uniform rectangular shapes while the triangle mesh patterns are as generated by the meshing algorithm in the solid modeler.
2. Results for SHELL43 in triangular form are presented, though they are not recommended for use. SHELL43 is based on a hybrid formulation for a quadrilateral element shape. Hence, degeneration of the element to a triangular shape will show some slight node-ordering dependence on the element solution.
3. The target solution is obtained in the prescribed reference for the author's 8-node shell element.
4. Results for the linear SHELL43 and SHELL63 singly-curved quadrilateral elements are comparable, with SHELL63 showing better accuracy in displacement for a given mesh discretization. As expected, the quadratic SHELL93 performs better than the linear elements for comparable meshes.
5. Results for the linear triangular-shaped elements is poor due to the constant-strain membrane behavior within the element. The effect of constant-strain membrane behavior is to overly stiffen the element under this type of loading, hence underpredicting both displacement and stresses. For triangular elements, only a fine mesh using the quadratic SHELL93 elements produces acceptable results.

VMC4: Simply-Supported Thin Annular Plate

Overview

Reference:	J. Barlow, G. A. O. Davis, "Selected FE Benchmarks in Structural and Thermal Analysis", *NAFEMS Rept. FEBSTA*, Rev. 1, October 1986, Test No. 14 (modified).
Analysis Type(s):	Mode-frequency Analysis (**ANTYPE** = 2)
Element Type(s):	4-Node Plastic Large Strain Shell Elements (SHELL43) Elastic Shell Elements (SHELL63] 8-Node Structural Shell Elements (SHELL93]
Input Listing:	vmc4.dat

Test Case

A simply-supported thin annular plate of thickness t is to be analyzed to determine the first nine natural frequencies. Determine the natural frequencies for two mesh densities using both quadrilateral and triangular element shapes with subspace eigenvalue extraction. Next, determine the natural frequencies considering a single mesh density of quadrilateral elements using Householder eigenvalue extraction for three sets of master degrees of freedom.

Figure C4.1 Thin Annular Plate Problem Sketch

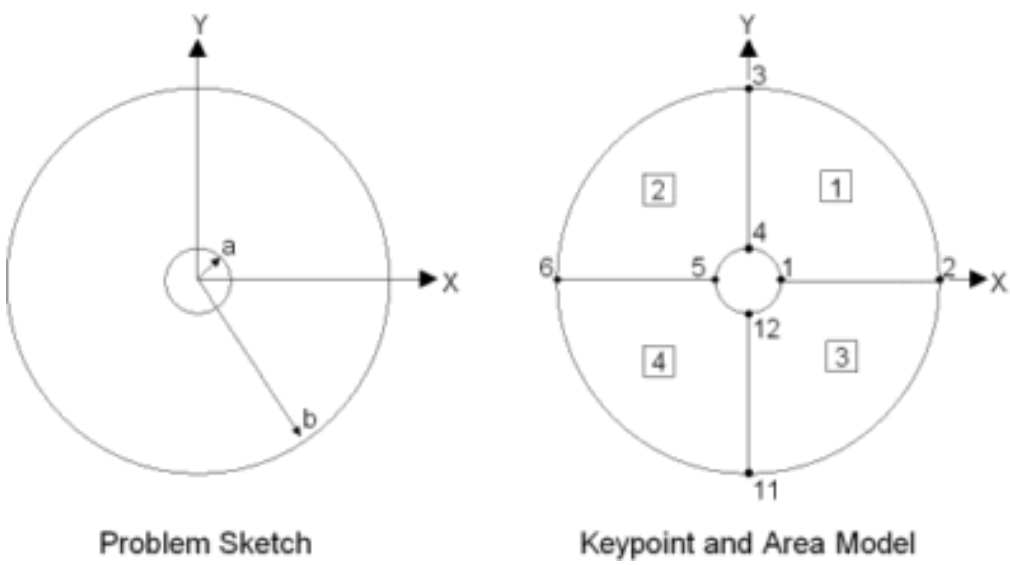

Material Properties $E = 200 \times 10^9$ N/m^2 $\upsilon = 0.3$ $\rho = 8000$ kg/m^3 **Geometric Properties** a = 1.8 m b = 6.0 m t = 0.06 m	**Loading and Boundary Conditions** All nodes UX = UY = ROTZ = 0 in cylindrical coordinate system; At x = b UZ = 0 At x = b ROTX = 0 **Parameter Definitions** N1 = No. elements along radial direction N2 = No. elements along circumferential direction

Figure C4.2 Representative Mesh Options

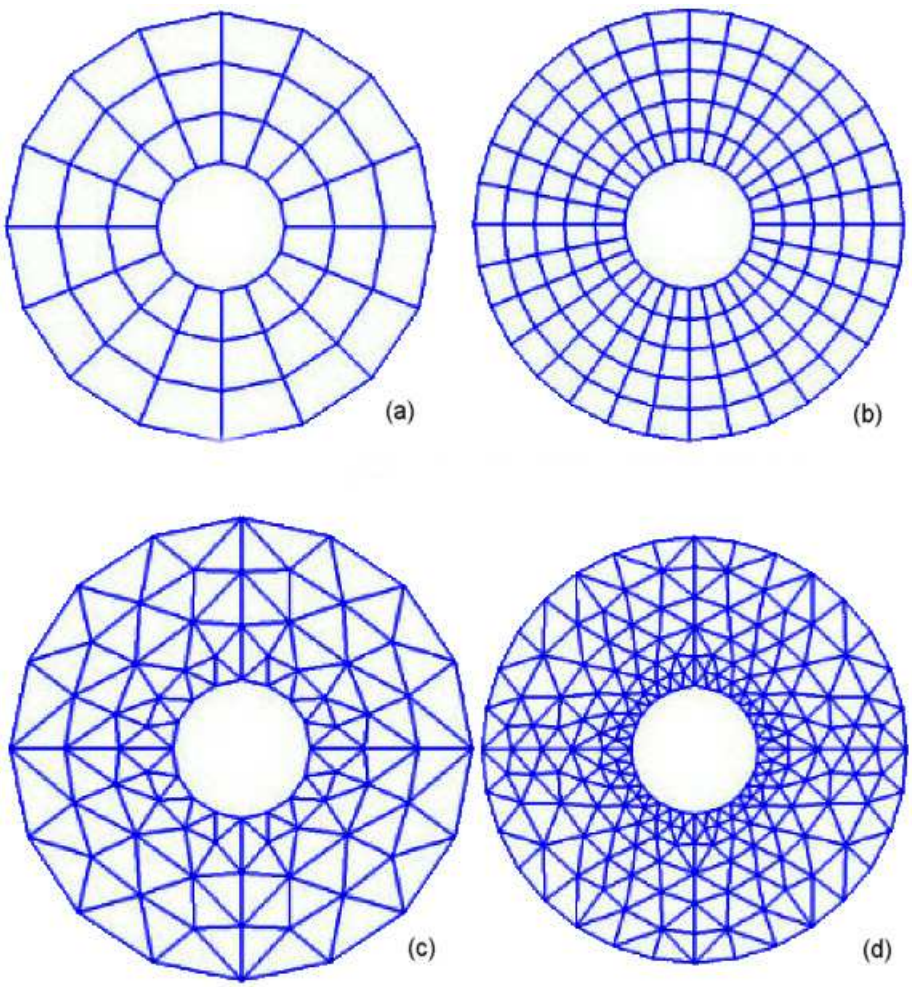

(a) Quadrilateral Mesh (N1 = 3, N2 = 16)
(b) Quadrilateral Mesh (N1 = 5, N2 = 32)
(c) Triangle Mesh (N1 = 3, N2 = 16)
(d) Triangle Mesh (N1 = 5, N2 = 32)

Target Solution

Mode	1	2	3	4	5	6	7	8	9
Frequency (Hz)	1.870	5.137	5.137	9.673	9.673	14.850	15.573	15.573	18.382

Results Comparison - First Study on Subspace Extraction Method Frequency Ratio

ETYP	N1	N2	DOF	1	2	3	4	5	6	7	8	9
Quadrilateral Mesh												
43	3	16	480	0.972	1.103	1.103	1.132	1.132	0.901	1.098	1.098	0.947
43[1]	5	32	1296	0.991	1.024	1.020	1.022	1.022	0.961	1.015	1.015	0.974
63	3	16	480	1.009	1.024	1.024	0.983	0.983	0.994	0.958	0.958	1.026
63[1]	5	32	1296	1.007	1.013	1.013	0.998	0.998	1.001	0.986	0.986	1.013

ETYP	N1	N2	DOF	1	2	3	4	5	6	7	8	9
93[2]	3	16	1224	1.001	0.994	0.994	1.000	1.000	1.005	1.015	1.015	0.994
93	5	32	3528	1.001	0.994	0.994	1.000	1.000	1.001	0.998	0.998	0.995
Triangular Mesh												
43[2]	3	16	600	1.055	1.851	1.336	1.348	1.583	1.140	1.518	1.598	1.358
43[2]	5	32	1416	1.010	1.066	1.068	1.058	1.069	1.047	1.094	1.097	1.133
63	3	16	600	1.001	1.004	1.007	0.981	0.983	0.985	0.968	0.969	0.999
63	5	32	1416	1.002	1.003	1.003	0.995	0.996	0.998	0.987	0.989	1.000
93	3	16	1992	1.016	1.030	1.031	1.027	1.029	1.040	1.045	1.052	1.068
93	5	32	4968	1.004	1.008	1.008	1.010	1.010	1.012	1.014	1.017	1.017

1. Test case corresponds to NAFEMS test specification for mesh discretization.
2. SHELL43 in triangular form is not recommended.

Results Comparison - Second Study on Reduced Householder Extraction Method

Model Information	
N1 = 5	DOF = 1296
N2 = 32	Quadrilateral Elements
Element = SHELL63	No. Elements = 160

Householder Extraction										
	Frequency Ratio									
MDOF[1]	**1**	**2**	**3**	**4**	**5**	**6**	**7**	**8**	**9**	**CPU Ratio[2]**
2P	1.026	1.072	1.195	1.158	1.347	1.165	1.321	1.452	1.498	.55
4P	1.011	1.027	1.066	1.064	1.082	1.072	1.079	1.099	1.117	.596
8P	1.007	1.015	1.015	1.001	1.005	1.017	0.995	0.998	1.041	.677

1. Master degrees of freedoms based on multiples of P = 9 eigenvectors.
2. Computing time CPU is normalized to a solution using the Subspace Extraction

Assumptions, Modeling Notes, and Solution Comments

1. The problem is designed to test a solution involving repeated eigenvalues and the use of various eigenvalue extraction techniques.
2. The representative input data listing is for a subspace extraction analysis. Modifications to the input data are required to execute a Householder extraction analysis.
3. For the linear elements, SHELL63 shows better solution results than SHELL43. These results are consistent with other similar observations: that for thin, flat elastic structures and regular-shaped elements, SHELL43 does not perform as well as SHELL63.
4. Results for SHELL43 in triangular form are presented, though they are not recommended for use. SHELL43 is based on a hybrid formulation for a quadrilateral element shape. Hence, degeneration of the element to a triangular shape will show some slight node-ordering dependence on the element solution.

5. For the reduced analysis, the **TOTAL** option is used to automatically select master degrees of freedom. Masters are chosen in multiples of two, four, and eight times the number of desired frequencies (abbreviated as P).
6. For the reduced analysis using quadrilateral elements, engineering accuracy (2%) is obtained for the first natural frequency with a total of 18 MDOF ($\approx$ 2P) specified. Engineering accuracy for the first eight natural frequencies requires a specification of 72 MDOF ($\approx$ 8P).
7. The Householder method can provide considerable computational time savings over full eigenvalue extraction. In this example, roughly 25-50% time savings is achieved.

ANSYS Verification Manual . ANSYS Release 10.0 . 002184 . © SAS IP, Inc.

VMC5: Simply-Supported Solid Square Plate

Overview

Reference:	NAFEMS, "The Standard NAFEMS Benchmarks", Rev. No. TSNB, National Engineering Laboratory, E. Kilbride, Glasgow, UK, August, 1989, Test No. FV52 (modified).
Analysis Type(s):	Mode-frequency Analysis (**ANTYPE** = 2)
Element Type(s):	3-D Structural Solid Elements (SOLID45) 3-D 10-Node Tetrahedral Structural Solid Elements (SOLID92)
Input Listing:	vmc5.dat

Test Case

A simply-supported rectangular solid of thickness t is analyzed to determine the first P = 10 natural frequencies (the first three of which are rigid body modes). Determine the natural frequencies and mode shapes using Householder eigenvalue extraction for six sets of master degree of freedom selections for both element types.

Figure C5.1 Solid Square Plate Problem Sketch

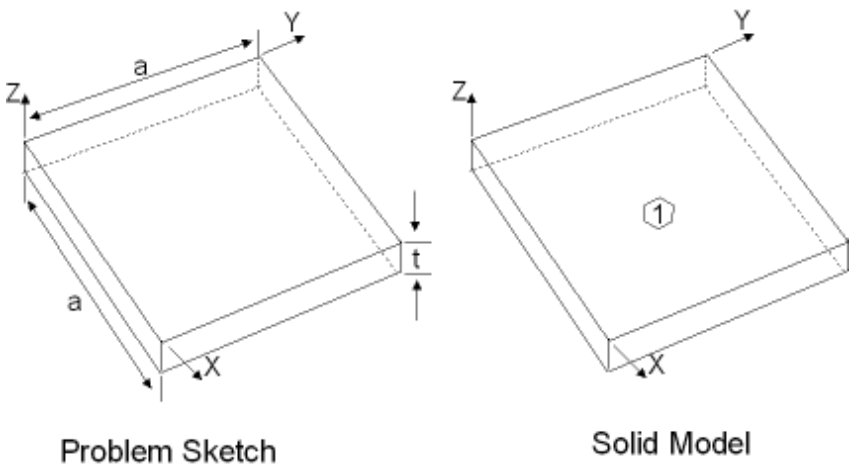

Material Properties	Geometric Properties	Parameter Definitions
E = 200 x 10^9 N/m^2 υ = 0.3 ρ = 8000 kg/m^3	a = 10.0 m t = 1.0 m Loading At Z = 0 UZ = 0 along 4 edges	N1 = No. elements along edges N2 = No. elements through thickness

Target Solution

Modes 1-3 are rigid body modes (zero frequency).

Mode	4	5	6	7	8	9	10
Frequency (Hz)	45.897	109.44	109.44	167.89	193.59	206.19	206.19

Results Comparison

					Frequency Ratio						
ETYP	**N1**	**N2**	**MDOF**	**% of DOF**	**4**	**5**	**6**	**7**	**8**	**9**	**10**
45	8	3	20	2.128	1.145	1.568	1.850	1.706	1.514	1.641	2.089
45	8	3	40	4.255	1.050	1.159	1.464	1.434	1.251	1.212	1.321
45	8	3	80	8.511	1.043	1.200	1.281	1.296	1.197	1.143	1.172
45	8	3	120	12.770	1.004	1.157	1.178	1.265	1.105	1.104	1.155
45	8	3	160	17.020	1.009	1.099	1.112	1.118	1.066	1.049	1.096
45[1]	8	3	940	100.000	0.987	1.041	1.041	1.032	1.016	1.016	1.016
92	6	1	20	1.265	0.986	1.090	1108	1.273	1.298	1.328	1.363
92	6	1	40	2.530	0.979	1.034	1.066	1.146	1.257	1.209	1.267
92	6	1	80	5.060	0.975	1.011	1.030	1.042	1.130	1.083	1.102
92	6	1	120	7.590	0.973	1.014	1.018	1.047	1.079	1.067	1.077
92	6	1	160	10.120	0.973	1.010	1.017	1.046	1.057	1.057	1.065
92	6	1	500	31.626	0.970	0.995	0.995	0.997	1.011	1.011	1.018

1. Test case corresponds to NAFEMS test specification

Figure C5.2 Representative Mesh Options

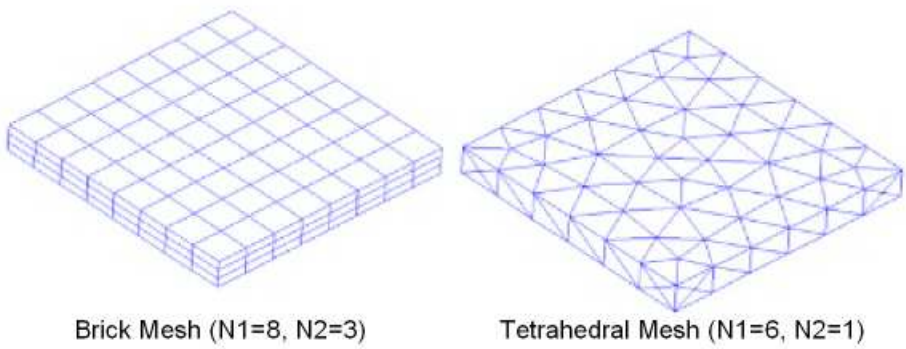

Figure C5.3 Graphical Results - Mode Shapes

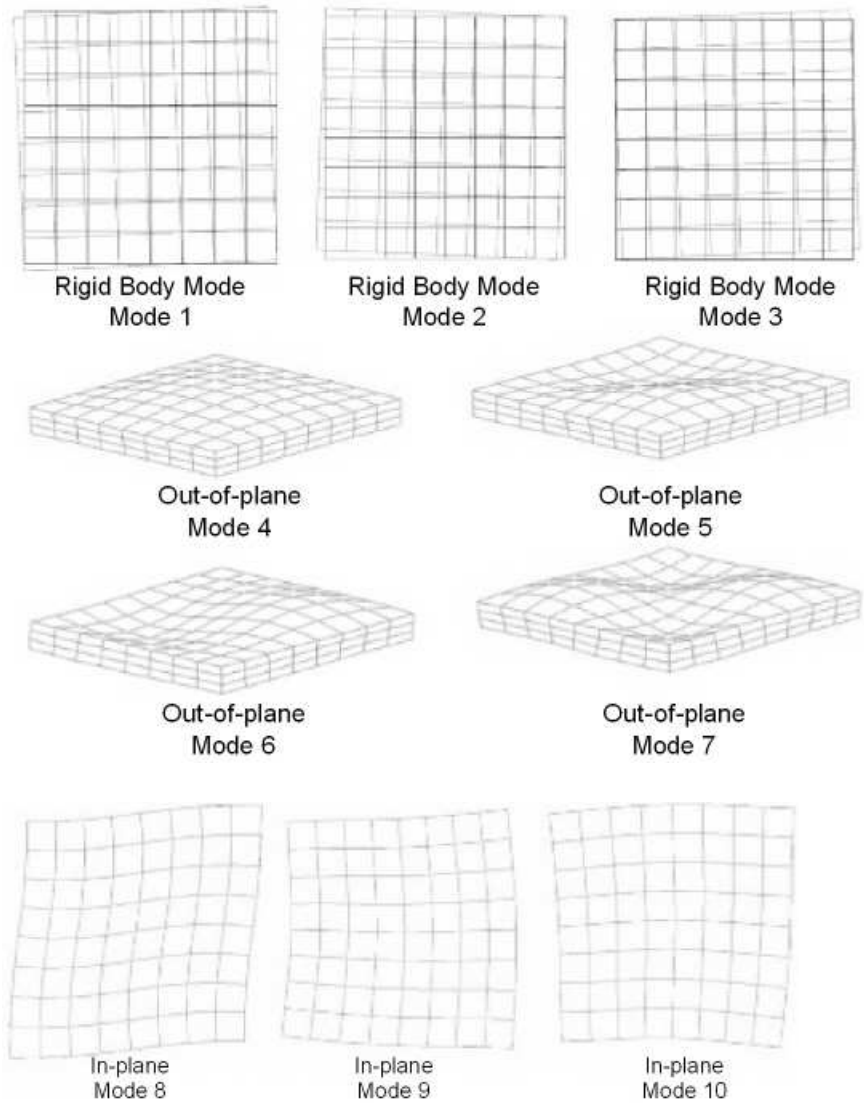

Assumptions, Modeling Notes, and Solution Comments

1. The problem is designed to test the calculation of rigid body modes, coincident frequencies, and associated mode shapes.
2. Master degree of freedom selection for the tests is based on an even multiple of the desired number of modes (P = 10). Masters are chosen using the TOTAL command.
3. The plate is simply supported on the bottom plate edges only (not at the midplane).
4. Three rigid body modes are correctly predicted in every test case analyzed.
5. The level of error introduced by mesh discretization is small compared to the level of error introduced by an insufficient number of master degrees of freedom.
6. For the primary bending mode (mode 4), both SOLID45 and SOLID92 accurately predict the eigenvalue with only two percent of the degrees of freedom selected as MDOFs. However, for higher modes (modes 5-10), accurate eigenvalue prediction requires considerably more MDOFs.
7. The mode shape for mode 10 is not captured unless sufficient numbers of MDOFs are chosen. This is due to the fact that the TOTAL option in this test case does not choose a uniformly distributed set of in-

plane MDOFs, hence allowing for possible inaccurate in-plane mode representation at higher modes. For SOLID45, 8P (or 80 MDOFs) are required to capture the tenth mode shape while 16P (or 160 MDOFs) are required for SOLID92. In both cases roughly 7 to 8 percent of the degrees of freedom are required as MDOF in order to capture the tenth mode.

8. Coincident frequencies (modes 5-6, modes 9-10) are predicted only for the following test cases

   - SOLID45 with all DOFs chosen as MDOF
   - SOLID92 with 50P DOFs chosen as MDOF. For cases with significantly reduced MDOF sets, the correct coincident mode shapes are predicted but the frequencies are slightly different.

VMC6: 2-D Heat Transfer With Convection

Overview

Reference:	J. Barlow, G. A. O. Davis, "Selected FE Benchmarks in Structural and Thermal Analysis", *NAFEMS Rept. FEBSTA*, Rev. 1, October 1986, Test No. T4 (modified).
Analysis Type(s):	Thermal Analysis (**ANTYPE** = 0)
Element Type(s):	2-D 6-Node Triangular Thermal Solid Elements (PLANE35) 2-D Thermal Solid Elements (PLANE55) 2-D 8-Node Thermal Solid Elements (PLANE77)
Input Listing:	vmc6.dat

Test Case

A two-dimensional rectangular body is insulated at the left edge and has the bottom edge held at a prescribed temperature T_1. Two other edges are subjected to a convection environment with a convection coefficient h and an ambient temperature T_0. Determine the steady-state temperature on the right edge, at a location 0.2 m above the bottom (Target Point-1) for a series of test cases with increasing mesh refinements for each element type.

Figure C6.1 2-D Rectangular Body Problem Sketch

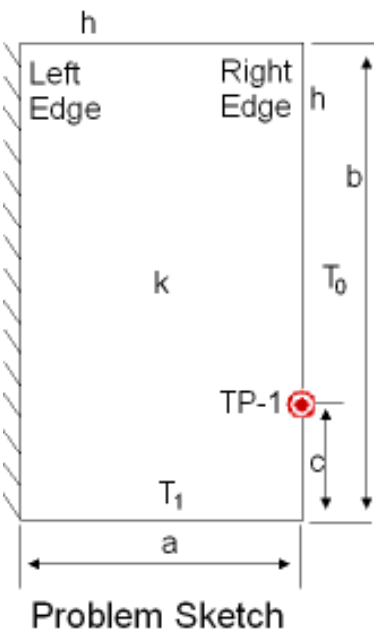

Material Properties	Geometric Properties	Loading
k = 52 W/m°C **Parameter Definition** N1 = Element edge length	a = 0.6 m b = 1.0 m c = 0.2 m	h = 750 W/m^2°C T_0 = 0°C T_1 = 100°C

Figure C6.2 Representative Mesh Options

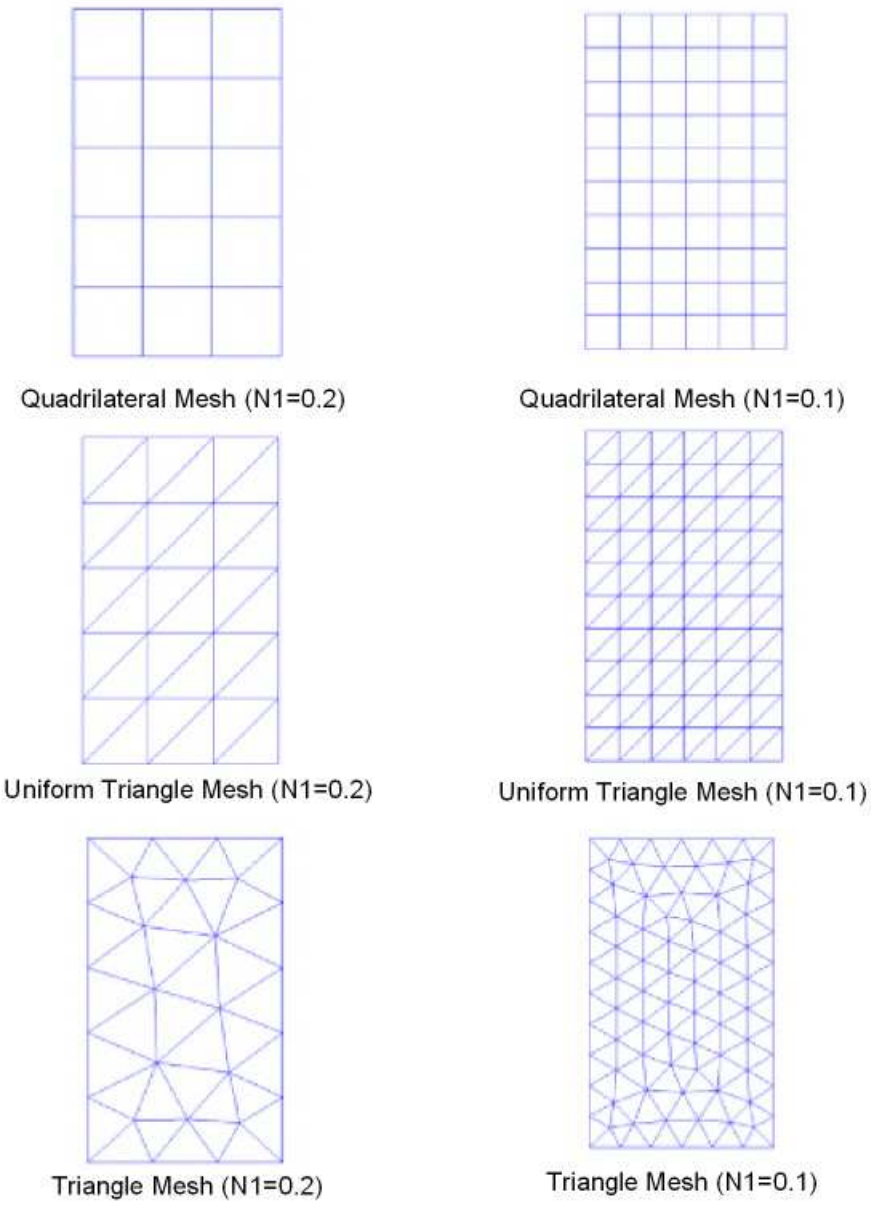

Results Comparison - Triangle Mesh

ETYP	N1	DOF	Temp(°C)	Temperature Ratio
Quadrilateral Mesh				
55[1]	.2	24	19.3	1.06
55	.1	77	18.9	1.03
77[1]	.2	62	16.4	0.90
77	.1	213	18.7	1.02
Triangle Mesh				
35	.2	93	17.9	0.98
35	.1	317	18.3	1.00
55	.2	28	20.9	1.14

ETYP	N1	DOF	Temp(°C)	Temperature Ratio
55	.1	88	19.0	1.04
77	.2	93	17.9	0.98
77	.1	317	18.3	1.00
Uniform Triangle Mesh				
35[1]	2	77	16.5	0.90
35	.1	273	18.3	1.00
55	.2	24	22.4	1.22
55	.1	77	18.9	1.04
77[1]	2	77	16.5	0.90
77	.1	273	18.3	1.00

1. Test case corresponds to NAFEMS test specification

Assumptions, Modeling Notes, and Solution Comments

1. The lower order PLANE55 element converges toward the solution from above the target temperature while, in general, the higher order PLANE35 and PLANE77 elements converge from below the target temperature.
2. For the coarse meshes, the lower order PLANE55 element, in triangular form, does not predict accurate results. However, further mesh refinement produces more accurate results.
3. The higher order PLANE35 triangular element and the higher order PLANE77 element in triangular form, produce identical results.

VMC7: One-Dimensional Transient Heat Transfer

Overview

Reference:	J. P. Holman, *Heat Transfer*, 4th Edition, McGraw-Hill Book Co., Inc., New York, NY, 1976, pg. 106.
Analysis Type(s):	Thermal Analysis (**ANTYPE** = 4)
Element Type(s):	2-D 6-Node Triangular Thermal Solid Elements (PLANE35) 2-D Thermal Solid Elements (PLANE55) 2-D 8-Node Thermal Solid Elements (PLANE77)
Input Listing:	vmc7.dat

Test Case

A semi-infinite solid, initially of temperature T_o, is suddenly subjected to a convection environment with convection coefficient h and ambient temperature T_1. Determine the surface temperature after 2 seconds for a series of test cases with increasing mesh refinement for each element type.

Figure C7.1 Semi-Infinite Solid Problem Sketch

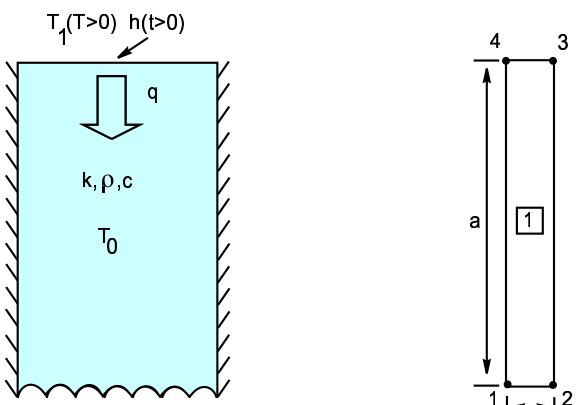

Problem Sketch Keypoint and Area Model

Material Properties	**Loading**
k = 54 W/m-°C ρ = 7833 kg/m^3 c = 0.465 J/kg-°C **Geometric Properties** a = 1.0 m See Comments below b = a/2 Nm	h = 50 W/m^2-°C T_o = 0°C T_1 = 1000°C **Parameter Definitions** N = No. of elements in longitudinal direction N3 = Initial Δt increment

Representative Mesh Options

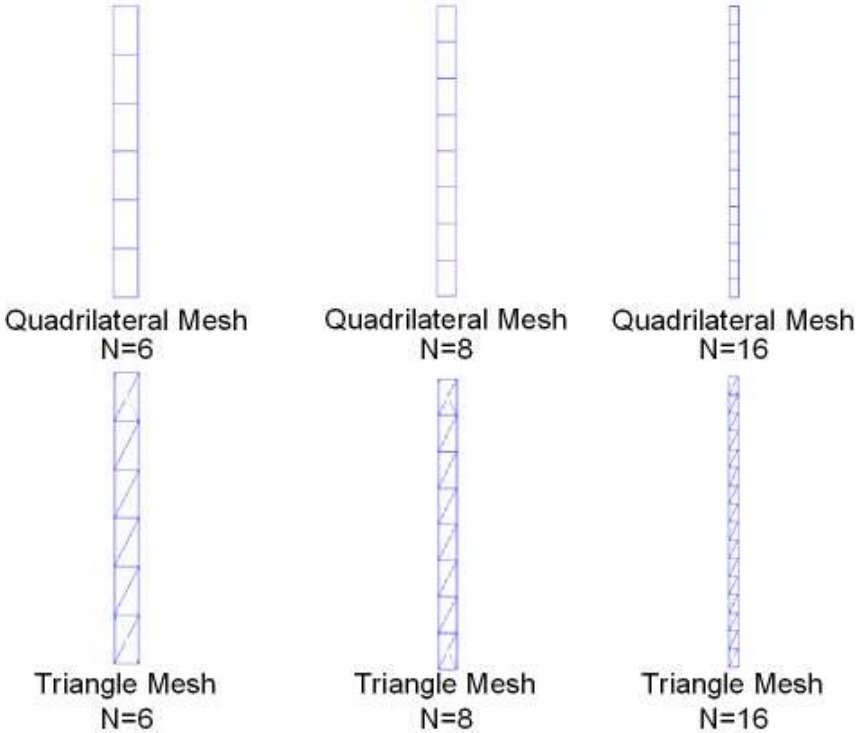

Results Comparison

Target Solution: T = 157.25

ETYP	N	Deflection Δt_{min}	Cumulative Iterations	Surface Temperature	Temperature Ratio
55	6	.5	4	142.953	.909
55	8	.25	8	150.472	.957
55	16	.0667	30	155.655	.990
77	6	.5	4	151.993	.967
77	8	.25	8	154.573	.983
77	16	.0667	30	156.523	.995
35	6	.5	4	151.934	.966
35	8	.25	8	154.560	.983
35	16	.0667	30	156.524	.995

Assumptions, Modeling Notes, and Solution Comments

1. One-dimensional heat transfer is assumed along the model length, a, which is chosen such that no significant change in temperature occurs at the end region. This is done to ensure an infinite length approximation. The model width, b, is chosen such that the element aspect ratio remain constant for all test cases.
2. Time step optimization was activated to automatically increment the time step during the solution. The minimum Δt increments chosen were arbitrary.

3. Results tabulation includes the cumulative number of iterations per run. From these results it is shown that the time step opened up from the initial value, for the $\Delta t = 0.5$ and 0.0667 cases.
4. All three elements are shown to converge to the correct solution. The quadratic elements (PLANE35, PLANE77) provide a more accurate solution than the linear PLANE55 element for a similar mesh configuration.

VMC8: Aluminum Bar Impacting a Rigid Boundary

Overview

Reference:	M. L. Wilkins, M. W. Guinan, "Impact of Cylinders on a Rigid Boundary", *Journal of Applied Physics*, Vol. 44 No. 3, 1973, pp. 1200.
Analysis Type(s):	Nonlinear Transient Dynamic Analysis (**ANTYPE** = 4)
Element Type(s):	2-D 6-Node Triangular Structural Solid Elements (PLANE2) 2-D Structural Solid Elements (PLANE42) 2-D 8-Node Structural Solid Elements (PLANE82) 2-D 4-Node Structural Solid Elements (PLANE182) 2-D 9-Node Structural Solid Elements (PLANE183) 2-D 4-Node Viscoplastic Solid Elements (VISCO106)
Input Listing:	vmc8.dat

Test Case

A cylindrical aluminum bar impacts a rigid wall at a velocity V_o. Determine the deformed length of the bar and perform axisymmetric analyses with the element types noted above.

Figure C8.1 Aluminum Bar Problem Sketch

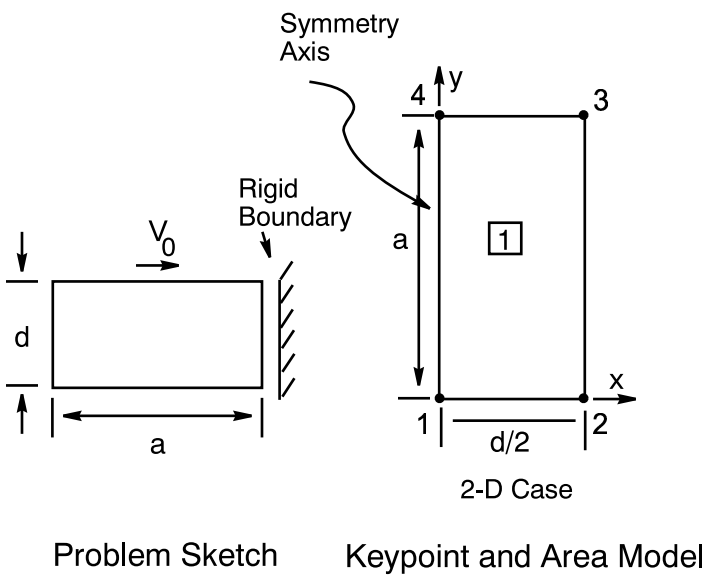

Material Properties	**Geometric Properties**
$E = 70 \times 10^9$ N/M^2	ℓ = 2.347 cm
$ET = 100 \times 10^6$ N/M^2	d = 0.762 cm
$\sigma_{yp} = 420 \times 10^6$ N/M^2	**Loading**
$\upsilon = 0.3$	V_o = 478 m/sec
$\rho = 2700$ Kq/m^3	

Representative Finite Element Models

2-D Axisymmetric Model (PLANE2 Only)

2-D Axisymmetric Model

Assumptions, Modeling Notes, and Solution Comments

1. The test case is modelled as a 2-D axisymmetric analysis with elements PLANE2, PLANE42, PLANE82, VISCO106, PLANE182 ,and PLANE183. Each analysis consists of two load steps. The first load step is static and serves to define the initial velocity. The second load step resolves the nonlinear transient effects.
2. The material behavior is assumed to be elastic perfectly plastic and obey a bilinear isotropic hardening law. The elastic wave propagation speed is defined as $\sqrt{E/\ell}$. The time required for the elastic wave to travel across a typical element in the radial direction is used to define the minimum number of substeps. A time span of 4.5×10^{-5} seconds allows the bar to impact and realize its maximum deflection. Auto time stepping (**AUTOTS**) is used to control the time step increments. The large deflection effects are included using **NLGEOM**. Solution efficiency is improved by relaxing the convergence criteria (**CNVTOL**).
3. The 2-D axisymmetric analysis with PLANE42 elements fails to converge due to excessive element distortion or collapse (Figure C8.2: "Deformed Shape"). The element distortion can be attributed to an increased stiffness in element edges along the axis of symmetry resulting from dropped extra shape functions. The axisymmetric formulation removes extra shape functions along the axis of symmetry, hence incompressibility associated with large-strain plasticity is not maintained.
4. In comparison, the plane and solid elements perform equally well as the viscoplastic elements for the strain levels encountered in this problem. Introducing a rate-dependent material property to the problem would illustrate advantage to viscoplastic elements.
5. Using POST26, plots of the displacement vs. time (Figure C8.2: "Deformed Shape") and equivalent plastic strain (Figure C8.3: "VISCO106 Graphs" - for the center node on the impact face) vs. time are produced.

Results Comparison

Target Solution: L_f = .01319 m (Obtained experimentally)

ETYP	L_f,m	Ratio
2	.014	1.068
42	.017 [1]	1.298
82	.014	1.065
106	.014	1.065
182	.014	1.078
183	.014	1.068

1. Solution did not converge

Figure C8.2 Deformed Shape

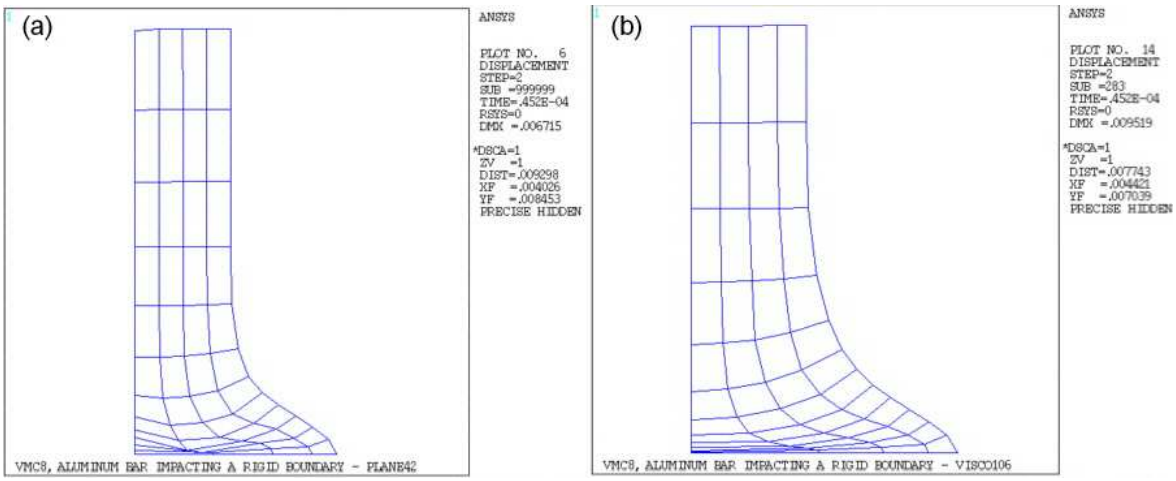

(a) PLANE42 Elements and (b) VISCO106 Elements

Figure C8.3 VISCO106 Graphs

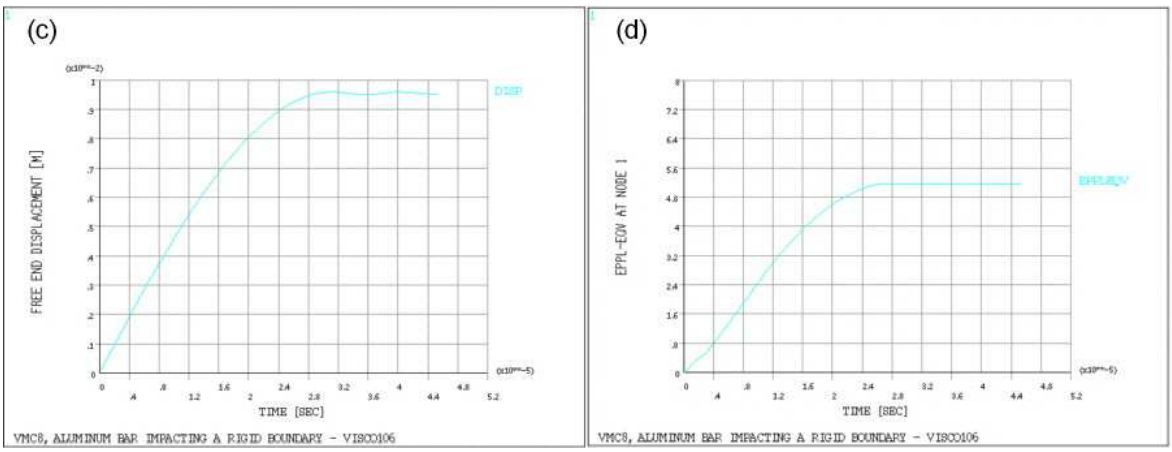

(c) Free End Displacement vs. Time and (d) Impact Face - Equivalent Plastic Strain vs. Time

VMD1: Straight Cantilever Beam Under Unit Load

Overview

Reference:	R. H. MacNeal, R. L. Harder, "A Proposed Standard Set of Problems to Test Finite Element Accuracy", *Proceedings, 25th SDM Finite Element Validation Forum*, 1984.
Analysis Type(s):	Static Analysis (**ANTYPE** = 0)
Element Type(s):	2-D 6-Node Triangular Structural Solid Elements (PLANE2) 2-D Structural Solid Elements (PLANE42) 2-D 8-Node Structural Solid Elements (PLANE82) 3-D Structural Solid Elements (SOLID45) 3-D 10-Node Tetrahedral Structural Solid Elements (SOLID92) 3-D 20-Node Structural Solid Elements (SOLID95)
Input Listing:	vmd1.dat

Test Case

A straight cantilever beam, fixed at one end, is subjected to a unit load. Determine the displacement at the end of the beam for unit loads including extension, in-plane shear, out-of-plane shear, and twist (where applicable). Examine the influence of rectangular, trapezoidal, and parallelogram element shape models on tip displacement and the percent energy error norm.

Figure D1.1 Straight Cantilever Beam Problem Sketch

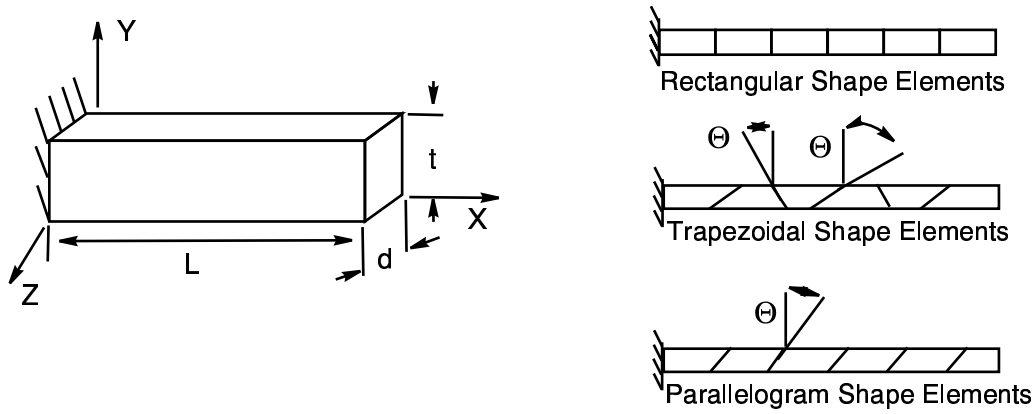

Problem Sketch

Representative Finite Element Model

Material Properties	**Loading**
E = 10 x 10^6 psi υ = 0.3 **Geometric Properties** L = 6 in d = 0.1 in t = 0.2 in **Parameter Definitions** Θ = Element Distortion Angle	At X = 0 UX = UY = UZ = 0 At X = L Unit Load a. Extension (FX = 1) b. In-plane (FY = 1) c. Out-plane (FZ = 1) d. Twist (Equivalent FX, FY forces applied)

Representative Mesh Options

2-D Quad - Trapezoidal (θ = 15°)

2-D Triangle - Parallelogram (θ = 30°)

3-D Brick - Trapezoidal (θ = 45°)

3-D Brick - Parallelogram (θ = 15°)

3-D Tetrahedron - Trapezoidal (θ = 30°)

3-D Tetrahedron - Parallelogram (θ = 45°)

Results Comparison

Tip Loading Shape/Direction	Tip Displacement Ratio / % Error In Energy Norm											
	PLANE2		PLANE42		PLANE82		SOLID45		SOLID92		SOLID95	
Rectangular												
Extension	.997	6	.996	0	.999	5	.988	0	.993	11	.994	3
In-Plane Shear	.983	22	.993	24	.987	0	.978	25	.960	30	.971	17
Out-Of-Plane Shear							.973	27	.959	33	.861	22
Twist							.892	10	.910	24	.903	8
Trapezoidal (θ = 15°)												
Extension	.997	6	.997	4	.999	5	.991	5	.993	11	.994	3
In-Plane Shear	.982	23	.293	66	.986	7	.272	66	.959	31	.969	18
Out-Of-Plane Shear							.215	67	.958	33	.960	23
Twist							.854	16	.910	24	.903	8
Trapezoidal (θ = 30°)												
Extension	.997	6	.999	4	1.000	4	.993	6	.993	11	.994	3
In-Plane Shear	.976	26	.109	64	.982	17	.100	64	.954	32	.957	23
Out-Of-Plane Shear							.072	64	.954	34	.954	25

Tip Loading Shape/Direction	Tip Displacement Ratio / % Error In Energy Norm											
	PLANE2		PLANE42		PLANE82		SOLID45		SOLID92		SOLID95	
Twist							.742	27	.910	25	.903	8
Trapezoidal ($\theta = 45°$)												
Extension	.997	6	.999	3	1.000	4	.994	4	.993	11	.994	3
In-Plane Shear	.961	32	.052	59	.967	36	.047	59	.939	37	.891	34
Out-Of-Plane Shear							.030	60	.941	38	.921	36
Twist							.563	40	.910	25	.903	8
Parallelogram ($\theta = 15°$)												
Extension	.998	6	.997	4	.999	5	.991	5	.993	11	.994	3
In-Plane Shear	.983	22	.812	38	.988	1	.798	40	.959	31	.971	18
Out-Of-Plane Shear							.749	49	.958	33	.960	23
Twist							.886	19	.910	24	.903	8
Parallelogram ($\theta = 30°$)												
Extension	.998	6	.999	4	.999	5	.993	5	.993	11	.994	3
In-Plane Shear	.980	24	.680	51	.991	4	.669	53	.954	33	.972	21
Out-Of-Plane Shear							.608	65	.953	35	.955	26
Twist							.866	34	.910	25	.903	8
Parallelogram ($\theta = 45°$)												
Extension	.998	6	.999	3	1.000	4	.994	4	.992	11	.994	3
In-Plane Shear	.970	29	.632	55	.997	8	.624	57	.940	38	.968	27
Out-Of-Plane Shear							.528	74	.935	40	.942	32
Twist							.820	51	.909	26	.903	8

Assumptions, Modeling Notes, and Solution Comments

1. The straight cantilever beam is a frequently used test problem applicable to beam, plate, and solid elements. The problem tests elements under constant and linearly varying strain conditions. Although the problem appears rather simplistic in nature, it is a severe test for linear elements, especially when distorted element geometries are present.
2. The fixed boundary conditions at the left edge of the beam are not representative of a "patch test." Thus, under extensional loading, the finite element solution will not agree with the beam theory solution.
3. Element solution accuracy degrades as elements are distorted. The degradation is more pronounced for linear elements (PLANE42, SOLID45) than it is for quadratic elements (PLANE2, PLANE82, SOLID92, SOLID95). The degradation in performance for linear elements is most pronounced for bending loads coupled with irregular element shapes. The linear elements experience a locking phenomena due to their inability to properly account for shear energy in bending resulting in excessive stiffness in the element. The inclusion of extra shape functions in the element formulation helps in correcting the shear energy prediction, but this is only applicable to rectangular element shapes. Hence results for PLANE42 and SOLID45 in rectangular form show very acceptable results.
4. Distorted linear elements show more pronounced locking (excessive stiffness) for trapezoidal element shapes than for parallelogram shapes. Results clearly show underpredicted displacements for trapezoidal element shapes for PLANE42 and SOLID45.

5. The quadratic elements show very good performance under all loadings and geometries. The good performance is attributed to the ability of the elements to properly handle bending and shear energy, in contrast to the linear elements.
6. The percent error in energy norm for each test case is displayed against the tip displacement ratio to illustrate the general correlation between the two for this particular problem. The linear elements show a patterned correlation between solution accuracy and the percent error in energy norm. For the quadratic elements the correlation pattern is similar. In both cases, the results illustrate that a considerable bandwidth on norm values may exist at any desired solution accuracy level for problems under a variety of load conditions with irregular element shapes.

VMD2: Barrel Vault Roof Under Self Weight

Overview

Reference:	R. D. Cook, *Concepts and Applications of Finite Element Analysis*, 2nd Edition, John Wiley and Sons, Inc., 1981, pp. 284-287.
Analysis Type(s):	Static Analysis (**ANTYPE** = 0)
Element Type(s):	4-Node Plastic Large Strain Shell Elements (SHELL43) Elastic Shell Elements (SHELL63) 8-Node Structural Shell Elements (SHELL93)
Input Listing:	vmd2.dat

Test Case

A cylindrical shell roof is subjected to gravity loading. The roof is supported by walls at each end and is free along the sides. Monitor the y-displacement and bottom axial stress (σ_z) at target point 1 along with the bottom circumference stress (σ_θ) at target point 2 for a series of test cases with varying skew angle β for each element type. A companion problem that studies uniform element mesh refinement is VMC3.

Figure D2.1 Cylindrical Shell Roof Problem Sketch

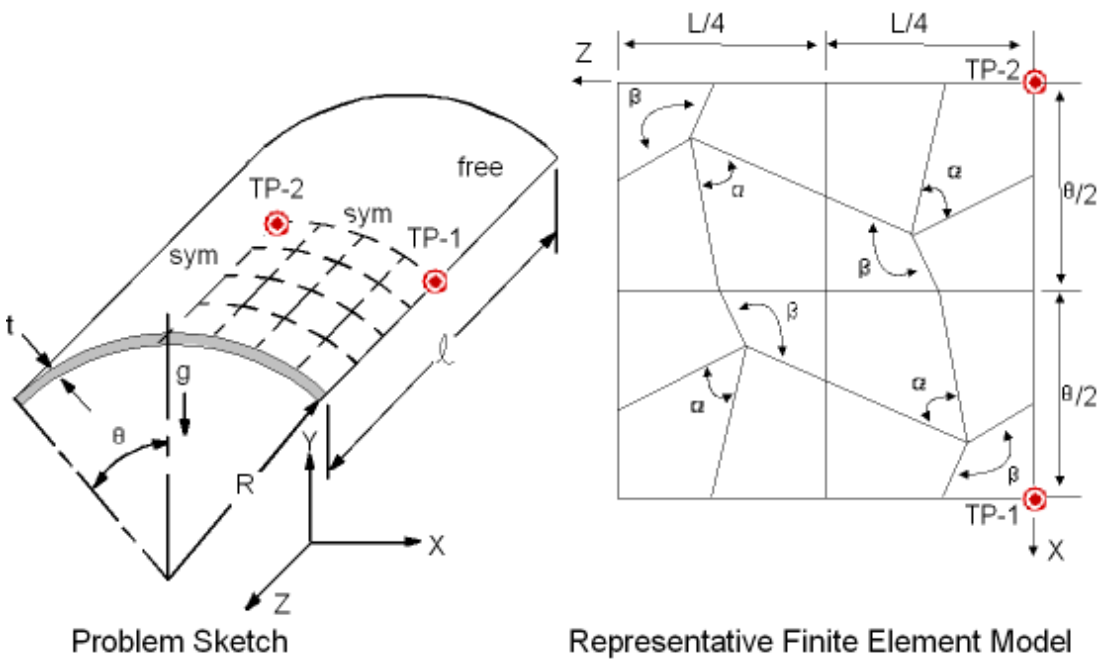

Material Properties	Geometric Properties	Loading and Boundary Conditions
$E = 4.32 \times 10^8$ N/m^2 $\upsilon = 0.0$ $\rho = 36.7347$ kg/m^3	L = 50 m R = 25 m t = 0.25 m $\Theta = 40°$ g = 9.8 m/sec^2	At x = 0 Symmetric At z = 0 Symmetric At x = L UX = UY = ROTZ = 0 **Parameter Definitions** β = Skew Angle

Representative Mesh Options

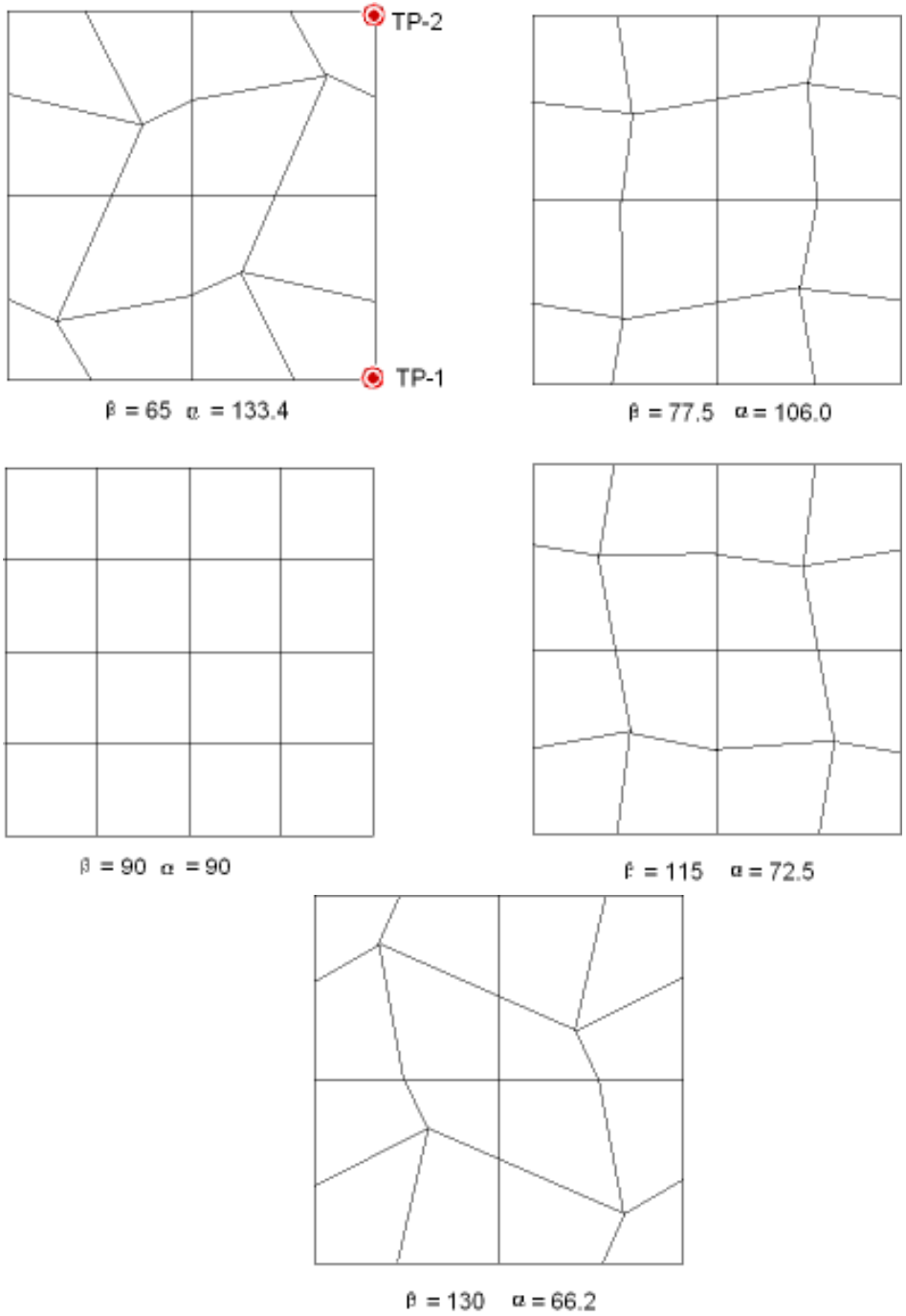

Target Solution

Target solution is obtained using a uniform 8 x 8 quadrilateral mesh of an 8-node quadrilateral shell element, (see R. D. Cook, *Concepts and Applications of Finite Element Analysis*).

ETYP	Beta (Deg.)	Alpha (Deg.)	UY (1), in	Axial Stress (1) Bottom,kPa	Hoop Stress (2) Bottom,kPa
--	90	90	-.3016	358.42	-213.40

Results Comparison - Quadrilateral Elements

			Ratio		
ETYP	Beta	Alpha	UY (1)	Axial Stress (1) Bottom	Hoop Stress (2) Bottom
43	65.0	133.4	1.005	0.948	0.844
43	77.5	106.0	1.036	0.951	0.941
43	90.0	90.0	1.049	0.940	0.983
43	110.0	75.1	1.052	0.913	0.986
43	130.0	66.2	1.045	0.876	0.950
63[1]	65.0	133.4	1.003	1.136	0.958
63[2]	77.5	106.0	1.006	1.025	1.002
63	90.0	90.0	1.008	0.928	1.017
63[3]	110.0	75.1	1.009	0.796	1.022
63[4]	130.0	66.2	1.008	0.674	1.018
93	65.0	133.4	0.982	0.985	1.085
93	77.5	106.0	1.001	0.968	1.045
93	90.0	90.0	1.004	0.953	1.029
93	110.0	75.1	0.996	0.934	1.024
93	130.0	66.2	0.978	0.923	1.013

1. Test case results in ANSYS warning message on element warping:

   .155 < Warping Factor < .278

2. Test case results in ANSYS warning message on element warping:

   .105 < Warping Factor < .105

3. Test case results in ANSYS warning message on element warping:

   .114 < Warping Factor < .131

4. Test case results in ANSYS warning message on element warping:

   .179 < Warping Factor < .257

Assumptions, Modeling Notes, and Solution Comments

1. The problem is designed to test singly-curved shell elements under combined membrane and bending deformation. The solid model is set up to produce irregular element shapes for quadrilateral elements. The angle β is prescribed, while the angle α is calculated from the resulting geometry. The range of β is set such that all element interior angles fall within 90° ± 45°.
2. The target solution is obtained from the author's 8-node shell element, (see R. D. Cook, *Concepts and Applications of Finite Element Analysis*), under a uniform rectangular element geometry using an 8 x 8 mesh pattern.
3. Results for uniform quadrilateral element shapes are noted in the tabular and graphical output for β = 90° and should be used as a basis for comparison of distorted element performance.

4. SHELL63 is permitted for use in a curved shell environment for slightly warped shapes. Excessive warping produces warning messages. These are noted in the tabular output.
5. Displacement results over the range of element distortion vary the greatest for SHELL43 and the least for SHELL63. In this problem, SHELL63 and SHELL93 predict the displacement more accurately for mild element geometry distortion.
6. Axial (σ_z) stress results, over the range of element distortion, show wide variation for SHELL63, but considerably less variation for SHELL43 and SHELL93. The wide variation in results for SHELL63 is due to nodal stress extrapolation inaccuracies for distorted, warped element configurations. Hoop (σ_θ) stress results are less affected by irregular element shapes except at the extreme β angle range.

VMD3: Free-Free Vibration of a Solid Beam

Overview

Reference:	R. D. Blevins, *Formulas for Natural Frequency and Mode Shape*, Van Nostrand Reinhold Co., New York, NY, 1979, Tables 8-1 and 8-16.
Analysis Type(s):	Mode-frequency analysis (**ANTYPE** = 2)
Element Type(s):	2-D 6-Nnode Triangular Structural Solid Elements (PLANE2) 2-D Structural Solid Elements (PLANE42) 2-D 8-Node Structural Solid Elements (PLANE82) 3-D Structural Solid Elements (SOLID45) 3-D 10-Node Tetrahedral Structural Solid Elements (SOLID92) 3-D 20-Node Structural Solid Elements (SOLID95)
Input Listing:	vmd3.dat

Test Case

A free-free solid beam is analyzed to determine the first axial and bending mode natural frequencies. For the axial mode case use Householder eigenvalue extraction and for the bending mode case use subspace eigenvalue extraction to extract the required eigenvalues. Examine the influence of rectangular, trapezoidal, and parallelogram element shape models on the eigenvalue calculations.

Figure D3.1 Free-Free Solid Beam Problem Sketch

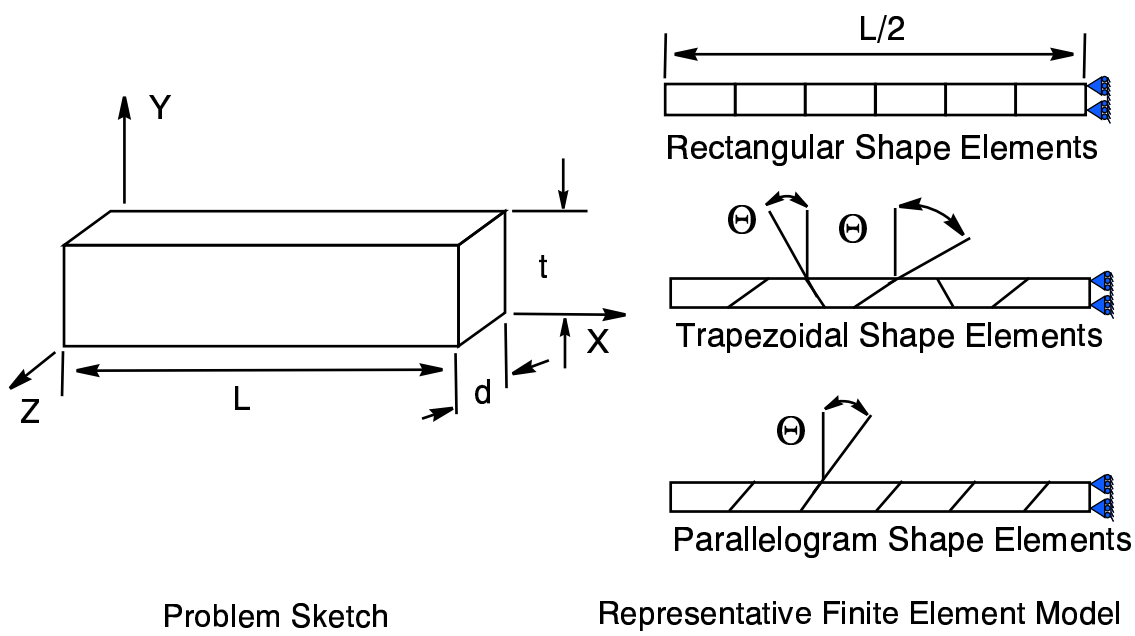

Material Properties E = 200 x 10^9 N/m^2 υ = 0.3 ρ = 8000 kg/m^3 **Parameter Definitions** Θ = Element Distortion Angle	**Loading and Boundary Conditions** At X = L/2 UX = 0 At Z = 0 UZ = 0 At Y = 0 UY = 0 (Axial mode) **Geometric Properties** L = 12 m d = 0.1 m t = 0.2 m

Representative Mesh Options

2-D Quad - Trapezoidal (θ = 15°)

2-D Triangle - Parallelogram (θ = 30°)

3-D Brick - Trapezoidal (θ = 45°)

3-D Brick - Parallelogram (θ = 15°)

3-D Tetrahedron - Trapezoidal (θ = 30°)

3-D Tetrahedron - Parallelogram (θ = 45°)

Target Solution and Results Comparison

Target Solution:

Freq = 208.333 Hz (Axial Mode)

Freq = 7.138 Hz (Bending Mode)

Results Comparison:

		1st Natural Frequency Ratio					
Axial Mode							
Shape	Angle	PLANE2	PLANE42	PLANE82	SOLID45	SOLID92	SOLID95
Rectangular	0	1.000	1.004	1.001	1.005	1.000	1.001
Trapezoidal	15	1.000	1.004	1.001	1.005	1.000	1.001
Trapezoidal	30	1.000	1.004	1.001	1.005	1.000	1.001
Trapezoidal	45	1.000	1.005	1.001	1.006	1.000	1.001
Parallelogram	15	1.000	1.004	1.001	1.005	1.000	1.001
Parallelogram	30	1.000	1.004	1.001	1.005	1.000	1.001
Parallelogram	45	1.000	1.004	1.001	1.005	1.000	1.001
Bending Mode							

		1st Natural Frequency Ratio					
Rectangular	0	1.003	1.010	0.999	1.010	1.004	1.002
Trapezoidal	15	1.003	1.567	1.000	1.598	1.005	1.003
Trapezoidal	30	1.006	1.973	1.003	2.015	1.008	1.010
Trapezoidal	45	1.016	2.207	1.012	2.254	1.020	1.051
Parallelogram	15	1.003	1.040	0.999	1.043	1.005	1.002
Parallelogram	30	1.005	1.091	0.999	1.097	1.009	1.004
Parallelogram	45	1.011	1.119	0.999	1.127	1.020	1.010

Assumptions, Modeling Notes, and Solution Comments

1. The problem tests the influence of irregular element shapes on eigenvalue calculations. Although the problem appears rather simplistic in nature, it is a severe test for linear irregular shaped elements where accurate bending mode frequencies are required.
2. Since the beam is free of any constraints, only one-half of the beam is required for modeling. Symmetry constraints are applied at the mid-length of the models. To obtain the desired bending mode (in the XY plane) all nodes at Z = 0 are constrained in the Z direction. Additionally, for the axial mode only, all nodes at Y = 0 are constrained in the Y direction.
3. For the axial mode case, Householder extraction is used with all UX degrees of freedom chosen as MDOFs. For the bending mode case, subspace extraction is used with shifted subspace to circumvent zero energy modes.
4. All load cases show good agreement in the prediction of the first axial natural frequency. This mode is simply linearly-varying longitudinal motion which is easily handled by both linear and quadratic elements. Irregular element shapes have only a minor effect on solution accuracy since axial motion is predominant.
5. For the linear elements (PLANE42, SOLID45), prediction of the first bending mode is significantly affected by irregularly shaped elements. Linear elements have an inherent inability to properly account for shear energy in bending modes resulting in excessive stiffness within the element. The inclusion of extra shape functions in the element formulation help in correcting the shear energy prediction, but are only suitable to rectangular element shapes. Hence, rectangular element results for PLANE42 and SOLID45 are in good agreement. However, as the elements are distorted, the stiffness of the element increases hence over-predicting the bending mode natural frequency.
6. For the quadratic elements (PLANE2, PLANE82, SOLID92, SOLID95), prediction of the first bending mode is very good. Irregular element shapes for quadratic elements have little effect on the solution accuracy.

Part III. ANSYS LS-DYNA Study Descriptions

Chapter 3: ANSYS LS-DYNA Study Overview

This section of the manual contains ANSYS LS-DYNA studies. The related input listings appear in Appendix C:, ANSYS LS-DYNA Input Listings.

The ANSYS LS-DYNA Studies are presented to demonstrate the use of the LS-DYNA Solver with the ANSYS pre-processor and postprocessor.

The LS-DYNA Solver that is packaged with ANSYS LS-DYNA is not an ANSYS product. It is a Livermore Software Technology Corporation (LSTC) product which ANSYS resells. Test cases including the LS-DYNA Solver exist in the ANSYS test set. ANSYS, Inc. reports any errors in the LS-DYNA Solver to LSTC.

The results presented in these studies are representative of the platform and version on which the studies were completed. It is normal that these results will be slightly different in different platforms and other versions of LS-DYNA. The difference is due to different numerical accuracy in different platforms and/or due to the improvements made by LSTC.

VME1: Response of Spring-Mass System to Step Input

Overview

Reference:	W. T. Thomson, *Vibration Theory and Applications*, 2nd Printing, Prentice-Hall, Inc., Englewood Cliffs, NJ, 1965, pp. 98-99.
Analysis Type(s):	Explicit Dynamics with ANSYS LS-DYNA
Element Type(s):	Explicit 3-D Structural Mass Elements (MASS166) Explicit Spring-Damper Elements (COMBI165)
Input Listing:	vme1.dat

Test Case

The one-DOF system consists of a spring, K, and mass, M. The load is a step function with a rise time, as shown. The peak displacement of M from the finite element solution is compared to an analytical result.

Figure E1.1 Response of Spring-Mass System Problem Sketch

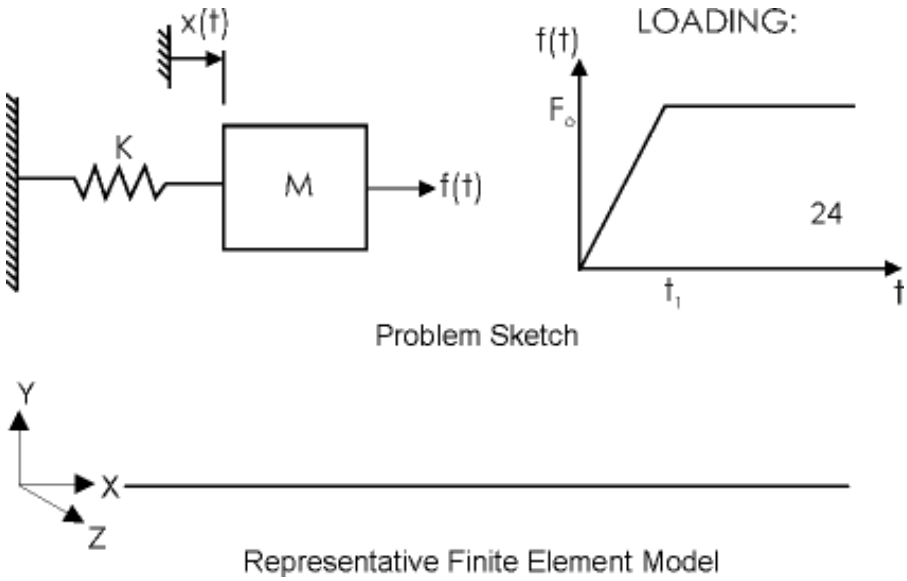

Material Properties	**Geometric Properties**	**Loading**
M = 1kg K = 100 N/m	Spring L.C. = 1m	Applied force, f(t), to the mass in the form shown in Figure E1.1: "Response of Spring-Mass System Problem Sketch", with t_1=1 second, and F_o = 3 N.

Analysis Assumptions and Modeling Notes

The magnitude and rise time of the force input were chosen arbitrarily. As outlined in W. T. Thomson, *Vibration Theory and Applications*, for the system in Figure E1.1: "Response of Spring-Mass System Problem Sketch", with the force input shown, the peak response is given by:

$$x_{peak} = (F_o/K)\left[1 + \frac{1}{\omega_n t_1}\sqrt{2(1-\cos(\omega_n t_1))}\right]$$

where ω_n is the system undamped natural frequency in units of radians per second.

Results Comparison

	Target	ANSYS	Ratio
Peak Ux of Mass	3.575E-2	3.575E-2	1.000

VME2: Drop Analysis of a Block Onto a Spring Scale

Overview

Reference:	F. P. Beer, E. R. Johnston, Jr., *Vector Mechanics for Engineers, Statics and Dynamics*, 5th Edition, McGraw-Hill Book Co., Inc., New York, NY, 1962, pg. 635.
Analysis Type(s):	Explicit Dynamics with ANSYS LS-DYNA
Element Type(s):	Explicit 3-D Structural Solid Elements (SOLID164) Explicit Spring-Damper Elements (COMBI165)
Input Listing:	vme2.dat

Test Case

A 30 kg block is dropped from a height of 2 m onto a 10 kg pan of a spring scale. The maximum deflection of the pan will be determined for a spring with a stiffness of 20 kN/m.

Figure E2.1 Drop Analysis Of A Block Onto A Spring Scale Problem Sketch and Finite Element Model

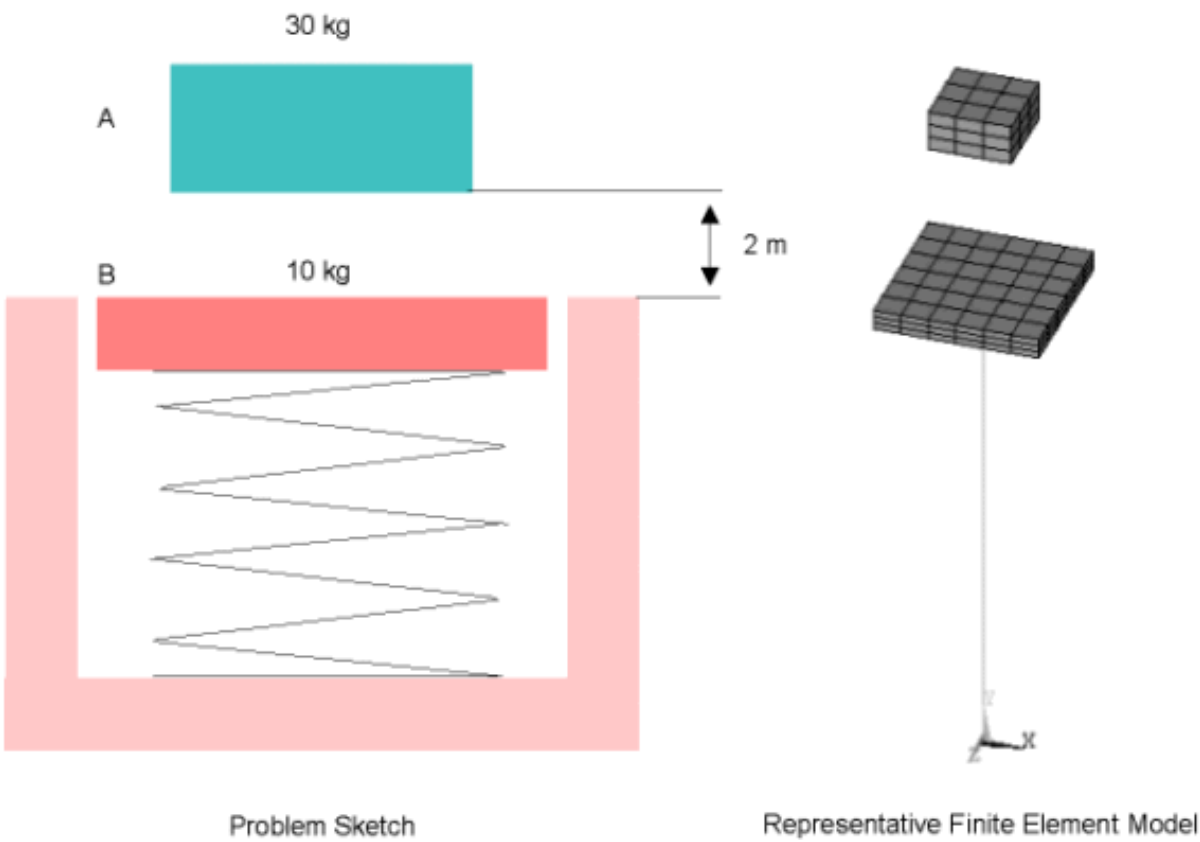

Material Properties	Geometric Properties	Loading
Block E = 207 GPa ρ = 60 kg/m^3 υ = .29 **Pan** E = 207 GPa ρ = 10 kg/m^3 υ = .29 **Spring** k = 20 kN/m	**Block** base = 1 m width = 1 m height = .5m **Pan** base = 2 m width = 2 m height = .25 m **Spring** length = 6m	The block is dropped from rest at a height of 2 m. g = 9.81 m/sec^2

Analysis Assumptions and Modeling Notes

The sizes of the block, pan, and spring have been arbitrarily selected. The densities of the block and pan, however, are based on the respective volumes of each component. A relatively course mesh was chosen for both the block and pan.

Results Comparison

	Target	ANSYS	Ratio
Maximum Uy of Pan	.225	.226	1.003

VME3: Response of Spring-Mass-Damper System

Overview

Reference:	C. M. Close, D. R. Frederick, *Modeling and Analysis of Dynamic Systems*, 2nd Edition, John Wiley and Sons, Inc., New York, NY, 1994, pp. 314-315, G. F. Franklin, J. D. Powell, A. Emami-Naeini, *Feedback Control of Dynamic Systems*, 3rd Edition, Addison-Wesley Publishing Co., Inc., Reading, MA, 1994, pp. 126-127.
Analysis Type(s):	Explicit Dynamics with ANSYS LS-DYNA
Element Type(s):	Explicit 3-D Structural Mass Elements (MASS166) Explicit Spring-Damper Elements (COMBI165)
Input Listing:	vme3.dat

Test Case

The one-DOF system consists of a spring, K, and mass, M, with viscous damping, C. There are two loading cases:

- Case 1: f(t) = A = constant (step input)
- Case 2: f(t) = At (ramp input)

For this underdamped system, the displacement of M for Case 1 overshoots the steady-state static displacement. The overshoot and the peak time, t_p are compared to theory outlined in C. M. Close, D. R. Frederick, *Modeling and Analysis of Dynamic Systems*. Based on the discussion in G. F. Franklin, J. D. Powell, A. Emami-Naeini, *Feedback Control of Dynamic Systems*, the mass velocity in response to the ramp input, in theory, is equal to the mass displacement due to the step input.

Figure E3.1 Response of Spring-Mass-Damper System

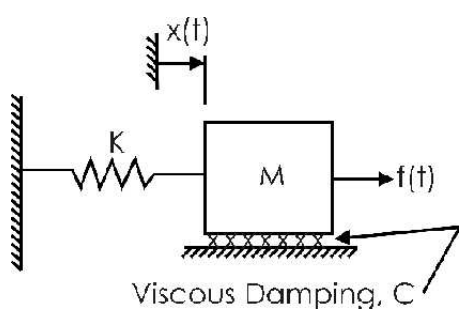

Problem Sketch

Material Properties	**Geometric Properties**
Mass M = 1.0 kg **Spring** K = $4\pi^2$ N/m **Damper** C = 0.21545376	**Spring** Length = 1 m
Loading Case 1: A step force input, f(t) = $4\pi^2$ on the mass M in the +x direction. Case 2: A ramp force input, f(t) = ($4\pi^2$)t, on the mass M in the +x direction.	

Analysis Assumptions and Modeling Notes

The magnitude of the step force input for Case 1 was chosen to equal the spring stiffness constant to produce a steady-state static deflection of unity. The ramp input for Case 2 was defined such that the input for Case 1 is the time derivative of the input for Case 2. The value of the stiffness constant was chosen so that the system undamped natural frequency equals 2 Hz. The damping constant was chosen to produce a damping ratio that results in a theoretical 50% overshoot of the steady-state deflection for the step input.

As outlined in G. F. Franklin, J. D. Powell, A. Emami-Naeini, *Feedback Control of Dynamic Systems*, for a single DOF system subjected to a step input, the relationship between overshoot, M_p, and damping ratio, ζ, is given by:

$$M_p = \exp\left(-\pi\zeta / \sqrt{1 - \zeta^2}\right)$$

For the system in Figure 3.1: "Support Structure Problem Sketch":

$$M_p = (X_{max} - X_{steady\text{-}state})/X_{steady\text{-}state}$$

The expression for peak time, t_p which is the time to reach x_{max} is given by:

$$t_p = \pi / \left(\omega_n \sqrt{1 - \zeta^2}\right)$$

where $\omega_n$is the system undamped natural frequency in units of radians per second.

Results Comparison

Table E3.1 Case 1: Step Input

	Target	ANSYS	Ratio
Maximum Ux of Mass	1.5000	1.5001	1.000
Peak Time for Mass Ux	0.2560	0.2559	1.000

Table E3.2 Case 2: Ramp Input

	Target	ANSYS	Ratio
Maximum Vx of Mass	1.5000	1.5001	1.000
Peak Time for Mass Vx	0.2560	0.2559	1.000

VME4: Undamped Vibration Absorber

Overview

Reference:	L. Meirovitch, *Elements of Vibration Analysis*, 2nd Edition, McGraw-Hill Book College Division, 1986, pp. 131-134.
Analysis Type(s):	Explicit Dynamics with ANSYS LS-DYNA
Element Type(s):	Explicit Spring-Damper Elements (COMBI165) Explicit 3-D Structural Mass Elements (MASS166)
Input Listing:	vme4.dat

Test Case

A sinusoidal force is applied to the main mass, M_1 of the undamped system with a dynamic vibration absorber. The response of the main mass is zero for the case of a tuned main system / absorber system at steady-state. The absorber system consists of a spring, K_2 and an absorber mass, M_2.

Material Properties **Main Mass** M_1 = 5 kg **Main Spring** K_1 = 10 N/m **Absorber Mass** M_2 = 1 kg **Absorber Spring** K_2 = 10 N/m	**Geometric Properties** **Spring** Length of Springs = 1 m **Loading** Force of Main Mass = 1.0 sin(10t) (Entered as discrete values in an array.) Initial Absorber Mass Velocity = -0.1 m/s

Analysis Assumptions and Modeling Notes

As outlined in L. Meirovitch, *Elements of Vibration Analysis*, if a sinusoidal force, of the form $f(t)=F_o \sin(\omega t)$, acts on the main mass of a system with a vibration absorber, and if the forcing frequency equals the natural frequency of the absorber system alone:

$$(\omega = \omega_a = \sqrt{K_2 / M_2})$$

then at steady-state, the main mass motion, $x_1(t)$, is zero, and the absorber mass motion, $x_2(t)$ is given by:

$$x_2(t) = -\frac{F_o}{K_2} \sin(\omega t)$$

In the analysis, a sinusoidal force, of unit amplitude, is approximated by entering discrete values in an array and specifying the array in a dynamic load definition. An initial velocity is provided to the absorber mass, corresponding to the steady-state condition. The resulting motion agrees with the theory of the vibration absorber. The system parameters were selected arbitrarily, resulting in a natural frequency for the absorber system alone of 10 radians per second. This is the required absorber natural frequency for eliminating main mass motion if the input frequency is also 10 radians per second. Also, the chosen parameters result in a steady-state absorber mass response amplitude of 0.01 m.

Results Comparison

	Target	ANSYS	Ratio
Amplitude of Absorber Deflection	0.01	0.01	1.000
Maximum Main Mass Deflection	0.00	5.96E-7	

VME5: Pinned Bar Under Gravity Loading

Overview

Reference:	W. G. McLean, E. W. Nelson, C. L. Best, *Schaum's Outline of Theory and Problems of Engineering Mechanics, Statics and Dynamics*, McGraw-Hill Book Co., Inc., New York, NY, 1978, p. 336.
Analysis Type(s):	Explicit Dynamics with ANSYS LS-DYNA
Element Type(s):	Explicit 3-D Beam Elements (BEAM161)
Input Listing:	vme5.dat

Test Case

A homogeneous bar, pinned at a distance **a** from one end, with total length, L, is subjected to gravity loading and released from rest at an angle $\theta = 30°$ from the vertical. The rotational speed when it passes through $\theta = 0°$ is calculated and compared to an analytical expression.

Figure E5.1 Pinned Bar Under Gravity Loading Problem Sketch

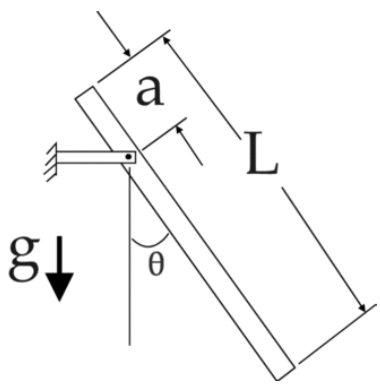

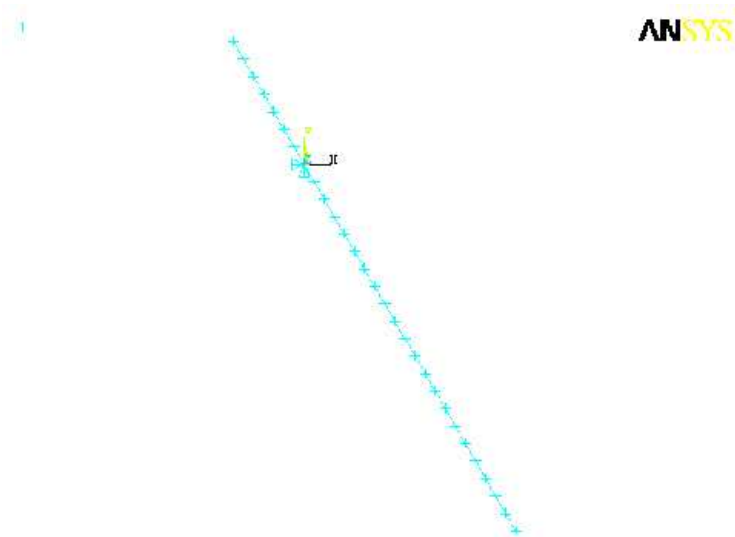

Material Properties	Geometric Properties	Loading
Density = 1.0 kg/m^3 Modulus of Elasticity = 10E6 N/m^2 Poisson's Ratio = 0.30	Constant square cross-section of 0.1 x 0.1 m^2 Total Length, L = 1.0 m; a = 0.25m	The acceleration due to gravity is 9.8 m/s^2 in the y-direction. One node is constrained in UX, UY, and UZ. All other nodes constrained only in UZ. At y = 0 UY = 0

Analysis Assumptions and Modeling Notes

The material properties were selected arbitrarily. As noted in W. G. McLean, E. W. Nelson, C. L. Best, *Schaum's Outline of Theory and Problems of Engineering Mechanics, Statics and Dynamics*, the magnitude of the bar's angular velocity when $\theta = 0°$, can be written as,

$$|\omega| = \sqrt{\frac{0.402g(L-2a)}{L^2 - 3La + 3a^2}}$$

assuming the bar is released at $\theta = 30°$. Based on the geometry chosen for this analysis, it can be seen that, at the time the bar passes through $\theta = 0°$, $\omega = v_x / 0.75$, where v_x is the translational velocity in the global Cartesian x-direction of the end of the bar. Twenty-eight BEAM161 elements were used to model the bar.

Results Comparison

	Target	ANSYS	Ratio
| Angular Velocity | when $\theta = 0°$ (rad/sec)	2.121	2.07	0.976

VME6: Projectile with Air Resistance

Overview

Reference:	J. B. Marion, S. T. Thornton, *Classical Dynamics of Particles & Systems*, 3rd Edition, Saunders College Publishing, 1988, pp. 60-63.
Analysis Type(s):	Explicit Dynamics with ANSYS LS-DYNA
Element Type(s):	Explicit 3-D Structural Solid Elements (SOLID164)
Input Listing:	vme6.dat

Test Case

A projectile is subjected to gravity and air resistance loading. The total travel time and travel distance are calculated for an assumed initial velocity and air resistance proportionality constant, k.

Figure E6.1 Projectile with Air Resistance Problem Sketch

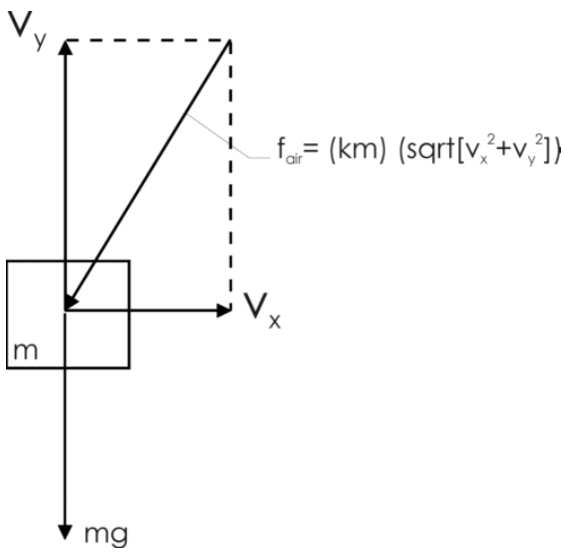

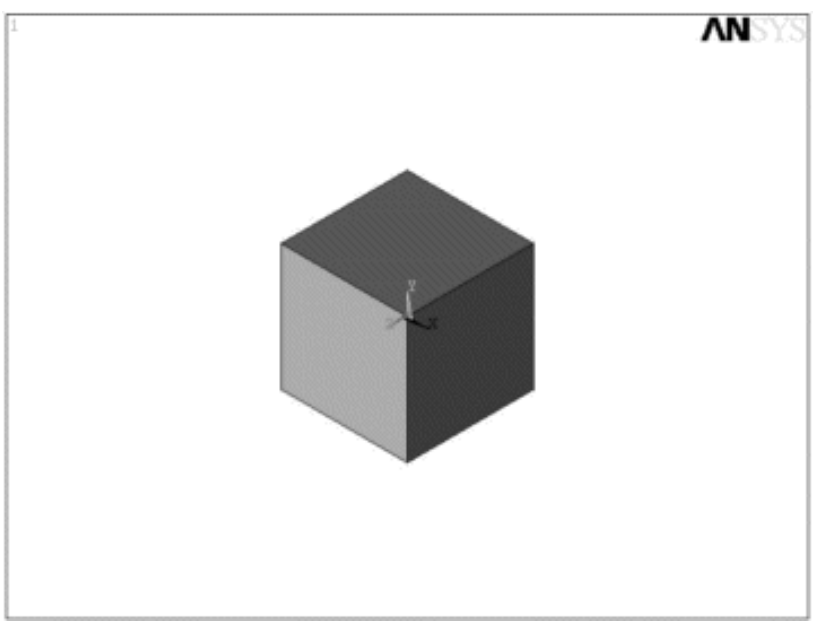

Material Properties	Geometric Properties	Loading
Projectile Density = 1.0 lb-s^2/in Modulus of Elasticity = 1.0 lb/in^2 Poisson's Ratio = 0.30 **Air Resistance (Viscous Damping)** Alpha Damping Used, Alpha = 1.0	**Projectile** Volume = 1 in^3 (1 in x 1 in x 1 in)	The acceleration due to gravity is a_y = 386.4 in/s^2 in the y-direction. The initial velocity in the x-direction is V_{xi} = 100 in/s^2, and the initial velocity in the y-direction is V_{yi} = 500 in/s^2.

Analysis Assumptions and Modeling Notes

The acceleration due to gravity is a_y = 386.4 in/s^2 in the y-direction. The initial velocity in the x-direction is V_{xi} = 100 in/s^2, and the initial velocity in the y-direction is V_{yi} = 500 in/s^2.

The material properties have no effect on the results of interest, so they are selected arbitrarily. As outlined in J. B. Marion, S. T. Thornton, *Classical Dynamics of Particles & Systems*, the force due to the air resistance is assumed to be proportional to the mass, m, and the velocity, v, according to:

$$f_{air} = -kmv$$

where k is a constant of proportionality. If the initial projectile velocity in the x-direction is U, the initial projectile velocity in the y-direction (vertical) is V, and the acceleration due to gravity is g, then the x and y-direction projectile displacements are given by:

$$x = \frac{U}{k}(1-\exp(-kt)) \; ; \; y = -\frac{gt}{k} + \frac{kV+g}{k^2}(1-\exp(-kt))$$

For a projectile fired from the ground, the total travel time, T, before returning to the ground, is given by the transcendental equation:

$$T = \frac{kV+g}{gk}(1-\exp(-kT))$$

In this analysis, for simplicity, k was taken to equal 1. This produces a theoretical total travel time of T = 1.976 seconds, and a total x-direction travel distance of 86.138. In the analysis, the total travel time and the total x-direction travel distance are estimated by linearly interpolating between two time points. This is because there is not a time point in the solution, after the initial condition, at which the projectile y-location is exactly zero, but a close estimate is obtained by interpolation between two time points in the solution.

Results Comparison

	Target	ANSYS	Ratio
Travel Time for Projectile (sec)	1.9760	1.9756	1.000
X-direction Travel Distance (in)	86.138	86.112	1.000

Figure E6.2 Displacement of Projectile Over Time

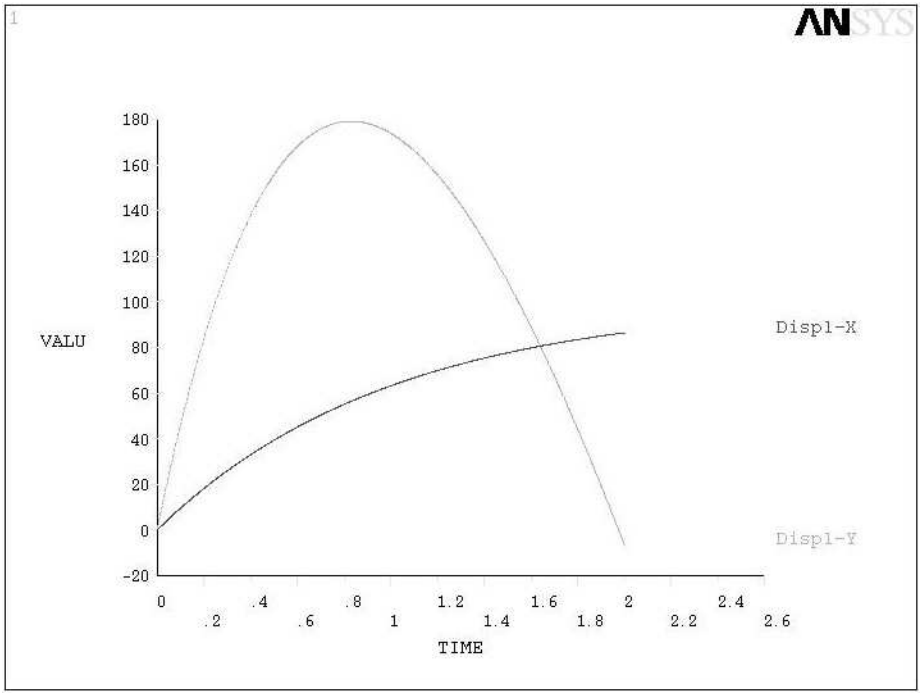

Part IV. NAFEMS Benchmarks

Chapter 4: NAFEMS Benchmarks Overview

The following section contains ANSYS solutions of several NAFEMS benchmark publications. NAFEMS (National Agency for Finite Element Methods and Standards) has published many excellent technical reports on engineering analysis subjects which have become industry standard benchmarks. Some of those benchmarks have been reproduced here as ANSYS Verification Manual test cases.

In this chapter benchmarks from the following publications are presented:

R0027 Fundamental Tests of Creep Behavior, A. A. Becker and T. H. Hyde
R0049 Background to Material Non-Linear Benchmarks, A. A. Becker

Each different load condition is presented as a problem to be solved by appropriate ANSYS element types. The test case includes a text description of the geometry, material properties, boundary conditions and loads. A results table of the verified solution is included at the end of the description of each test case. Test case inputs for each element type are also included.

If you are interested in the benchmark technical reports, you can contact NAFEMS using the following information;

NAFEMS Ltd
Whitworth Building
Scottish Enterprise Technology Park
East Kilbride
Glasgow G75 0QD
United Kingdom
Tel: +44 13 55 22 56 88
Fax: +44 13 55 24 91 42
USA Freephone +1 888 601 4207
www.nafems.org

VMR027-3A: 2-D Plane Stress - Biaxial (negative) Load Secondary Creep

Test Description

A square of length L and height L is constrained in the Y-direction on the bottom edge and constrained in the X-direction on the left edge. A tensile distributed load, σ_1, is applied on the right edge and a compressive distributed load, σ_2, is applied to the top edge.

Geometic Properties L = 100 mm	**Material Properties** E = 200 x 10^3 N/mm^2 ν = 0.3 **Creep Law:** $\varepsilon = A\sigma^n t^m$ A = 3.125 x 10^{-14} per hour (σ in N/mm^2) n = 5
Boundary Conditions Bottom Edge: $u_y = 0$ Left Edge: $u_x = 0$	**Loading** Right Edge: σ_1 = 200 N/mm^2 Top Edge: σ_2 = -200 N/mm^2

Results

Results are tabulated and displayed as NAFEMS manual.

```
              |   ANSYS   |   RATIO  |         INPUT         |

  SHELL181
  ECR6X         133.952       0.9922     vmr027-cr3a-181
  ECR6Y        -133.952       0.9922     vmr027-cr3a-181
  PLANE182
  ECR6X         135.000       1.0000     vmr027-cr3a-182
  ECR6Y        -135.000       1.0000     vmr027-cr3a-182
  PLANE183
  ECR6X         135.000       1.0000     vmr027-cr3a-183
  ECR6Y        -135.000       1.0000     vmr027-cr3a-183

 ----------------------------------------------------------------
```

vmr027-cr3a-181.dat
vmr027-cr3a-182.dat
vmr027-cr3a-183.dat

VMR027-3B: 2-D Plane Stress - Biaxial (negative) Displacement Secondary Creep

Test Description

A square of length L and height L is constrained in the Y-direction on the bottom edge and constrained in the X-direction on the left edge. The model is displaced in the X-direction by u_1 and in the Y-direction by u_2

Geometic Properties	**Material Properties**
L = 100 mm	E = 200 x 10^3 N/mm^2 ν = 0.3 **Creep:** $\varepsilon = A\sigma^n t^m$ n = 5 m = 0.5
Boundary Conditions Top Edge: u_y = -0.1, Bottom Edge: u_y = 0 Right Edge: u_x = 0.1, Left Edge: u_x = 0	**Loading** No applied forces

Results

Results are tabulated and displayed as NAFEMS manual.

```
              |   ANSYS   |   RATIO  |         INPUT         |

   SHELL181
   ECR6X           7.976       1.0318     vmr027-cr3b-181
   PLANE182
   ECR6X           7.976       1.0318     vmr027-cr3b-182
   PLANE183
   ECR6X           7.976       1.0318     vmr027-cr3b-183

  ----------------------------------------------------------------
```

vmr027-cr3b-181.dat
vmr027-cr3b-182.dat
vmr027-cr3b-183.dat

VMR027-4C: 2-D Plane Stress - Shear Loading Secondary Creep

Test Description

A square of length L and height L is constrained in the Y-direction at the corners on the bottom edge and constrained in the X-direction on the bottom edge, left corner. The same shear stress, τ, is applied on all four faces as shown in the figure.

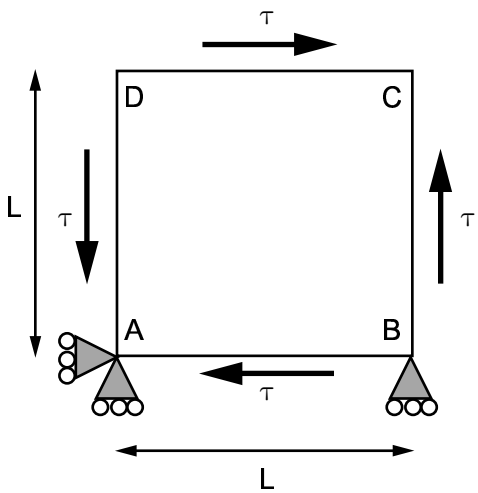

Geometic Properties L = 100 mm	**Material Properties** E = 200 x 10^3 N/mm^2 ν = 0.3 **Creep Law:** $\varepsilon = A\sigma^n t^m$ n = 5
Boundary Conditions Bottom Edge: u_y = 0.0 at Points (0,0) and (L,0) Bottom Edge: u_x = 0 at Point (0,0)	**Loading** τ = 100 N/mm^2 Shear Force on all Edges: $\tau/6$, $2\tau/3$, $\tau/6$

Results

Results are tabulated and displayed as NAFEMS manual.

```
              |   ANSYS   |   RATIO  |         INPUT         |

   SHELL181
   ECR2X           8.359       0.9907     vmr027-cr4c-181
   PLANE182
   ECR2X           8.437       1.0000     vmr027-cr4c-182
   PLANE183
   ECR2X           8.437       1.0000     vmr027-cr4c-183

  ---------------------------------------------------------------
```

vmr027-cr4c-181.dat
vmr027-cr4c-182.dat
vmr027-cr4c-183.dat

VMR027-5B: 2-D Plane Strain - Biaxial Displacement Secondary Creep

Test Description

A square of length L and height L is constrained in the X-direction on the left edge and constrained in the Y-direction on the bottom edge. A displacement, u_1, is applied in the X-direction on the right edge and another displacement, u_2, is applied in the Y-direction on the top edge.

Geometic Properties L = 100 mm	**Material Properties** $E = 200 \times 10^3$ N/mm^2 $\nu = 0.3$ **Creep Law:** $\varepsilon = A\sigma^n t$ $A = 3.125 \times 10^{-14}$ per hour (σ in N/mm^2) n = 5
Boundary Conditions Bottom Edge: $u_y = 0$, Top Edge: $u_y = 0.05$ Right Edge: $u_x = 0.1$, Left Edge: $u_x = 0$	**Loading** No applied forces

Results

Results are tabulated and displayed as NAFEMS manual.

```
              |   ANSYS   |   RATIO  |         INPUT         |

  PLANE182
  ECR6X         257.947       1.0008     vmr027-cr5b-182
  PLANE183
  ECR6X         257.947       1.0008     vmr027-cr5b-183

 ----------------------------------------------------------------
```

vmr027-cr5b-182.dat
vmr027-cr5b-183.dat

VMR027-6B: 3-D - Triaxial Displacement Secondary Creep

Test Description

A block of length, height, and width L is constrained on the left face in the X-direction and constrained on the bottom face in the Y-direction. The model is displaced in all three directions by a given quantity.

Geometic Properties L = 100 mm	**Material Properties** $E = 200 \times 10^3$ N/mm^2 $\nu = 0.3$ **Creep Law:** $\varepsilon = A\sigma^n t$ $A = 3.125 \times 10^{-14}$ per hour (σ in N/mm^2) n = 5
Boundary Conditions Left Face: $u_x = 0$, Right Face: $u_x = 0.3$ Bottom Face: $u_y = 0$, Top Face: $u_y = 0.2$ Front Face: $u_z = 0$, Back Face: $u_z = 0.1$	**Loading** No applied forces

Results

Results are tabulated and displayed as NAFEMS manual.

```
              |   ANSYS   |   RATIO  |         INPUT         |

  SOLID185
  ISOCRX       1007.950       1.0002     vmr027-cr6b-185
  ANICRX       1007.950       1.0002     vmr027-cr6b-185
  SOLID186
  ISOCRX       1007.950       1.0002     vmr027-cr6b-186
  ANICRX       1007.950       1.0002     vmr027-cr6b-186
  SOLID187
  ISOCRX       1007.950       1.0002     vmr027-cr6b-187
  ANICRX       1007.950       1.0002     vmr027-cr6b-187

 ----------------------------------------------------------------
```

vmr027-cr6b-185.dat
vmr027-cr6b-186.dat
vmr027-cr6b-187.dat

VMR027-10A: 2-D Plane Stress - Biaxial (negative) Load Primary Creep

Test Description

A square of length L and height L is constrained in the Y-direction on the bottom edge and constrained in the X-direction on the left edge. A tensile distributed load, σ_1, is applied on the right edge and a compressive distributed load, σ_2, is applied to the top edge.

Geometic Properties L = 100 mm	**Material Properties** E = 200 x 10^3 N/mm^2 ν = 0.3 **Creep Law:** $\varepsilon = A\sigma^n t^m$ n = 5 m = 0.5
Boundary Conditions Bottom Edge: $u_y = 0$ Left Edge: $u_x = 0$	**Loading** Right Edge: σ_1 = 200 N/mm^2 Top Edge: σ_2 = -200 N/mm^2

Results

Results are tabulated and displayed as NAFEMS manual.

```
              |   ANSYS   |   RATIO  |         INPUT         |

   SHELL181
   ECR6X           4.242       0.9937     vmr027-cr10a-181
   EFFCR           4.899       0.9936     vmr027-cr10a-181
   PLANE182
   ECR6X           4.267       0.9996     vmr027-cr10a-182
   EFFCR           4.928       0.9995     vmr027-cr10a-182
   PLANE183
   ECR6X           4.267       0.9996     vmr027-cr10a-183
   EFFCR           4.928       0.9995     vmr027-cr10a-183

  ----------------------------------------------------------------
```

vmr027-cr10a-181.dat
vmr027-cr10a-182.dat
vmr027-cr10a-183.dat

VMR027-10B: 2-D Plane Stress - Biaxial (negative) Displacement Primary Creep

Test Description

A square of length L and height L is constrained in the Y-direction on the bottom edge and constrained in the X-direction on the left edge. The model is displaced in the X-direction by u_1 and in the Y-direction by u_2.

Geometic Properties	**Material Properties**
L = 100 mm	E = 200 x 10^3 N/mm^2 ν = 0.3 **Creep Law:** $\varepsilon = A\sigma^n t^m$ n = 5 m = 0.5
Boundary Conditions Top Edge: u_y = -0.1, Bottom Edge: u_y = 0 Right Edge: u_x = 0.1, Left Edge: u_x = 0	**Loading** No applied forces

Results

Results are tabulated and displayed as NAFEMS manual.

	ANSYS	RATIO	INPUT
SHELL181			
S6	19.061	1.0393	vmr027-cr10b-181
S7	26.636	1.0206	vmr027-cr10b-181
PLANE182			
S6	19.061	1.0393	vmr027-cr10b-182
S7	26.636	1.0206	vmr027-cr10b-182
PLANE183			
S6	19.061	1.0393	vmr027-cr10b-183
S7	26.636	1.0206	vmr027-cr10b-183

vmr027-cr10b-181.dat
vmr027-cr10b-182.dat
vmr027-cr10b-183.dat

VMR027-10C: 2-D Plane Stress - Biaxial (negative) Stepped Load - Primary Creep

Test Description

A square of length L and height L is constrained in the Y-direction on the bottom edge and constrained in the X-direction on the left edge. A tensile distributed load, σ_1, is applied on the right edge and a compressive distributed load, σ_2, is applied to the top edge.

Geometic Properties	**Material Properties**
Plane Stress L = 100 mm	E = 200 x 10^3 N/mm^2 ν = 0.3 **Creep Law:** $\varepsilon = A\sigma^n t^m$ n = 5 m = 0.5
Boundary Conditions Bottom Edge: $u_y = 0$ Left Edge: $u_x = 0$	**Loading** Right Edge: σ = 200 N/mm^2 (t = 100 hrs) σ = 250N/mm^2 (t > 100 hrs) Top Edge: σ = -200 N/mm^2 (t = 100 hrs) σ = -250N/mm^2 (t > 100 hrs)

Results

Results are tabulated and displayed as NAFEMS manual.

```
            |   ANSYS   |   RATIO  |         INPUT         |

  SHELL181
  S2              2.900       0.9488     vmr027-cr10c-181
  S7              4.188       0.9660     vmr027-cr10c-181
  PLANE182
  S2              2.934       0.9598     vmr027-cr10c-182
  S7              4.211       0.9714     vmr027-cr10c-182
  PLANE183
  S2              2.934       0.9598     vmr027-cr10c-183
  S7              4.211       0.9714     vmr027-cr10c-183

 ----------------------------------------------------------------
```

vmr027-cr10c-181.dat
vmr027-cr10c-182.dat
vmr027-cr10c-183.dat

VMR027-12B: 2-D Plane Stress - Uniaxial Displacement Primary-Secondary Creep

Test Description

A square of length L and height L is constrained in the X-direction on the left edge and constrained in the Y-direction at the midpoint of the left edge. A displacement, u_1, is applied in the X-direction.

Geometic Properties	**Material Properties**
L = 100 mm	$E = 200 \times 10^3$ N/mm^2 $\nu = 0.3$ **Creep Law:** $\varepsilon = A_1\sigma^{n_1}t + A_2\sigma^{n_2}t^m$ $n_1 = n_2 = 5$ $m = 0.5$
Boundary Conditions Bottom Edge: $u_y = 0$ Left Edge: $u_x = 0$ Left Edge (midpoint): $u_y = 0$ Right Edge: $u_x = 0.1$	**Loading** No applied forces

Results

Results are tabulated and displayed as NAFEMS manual.

```
              |   ANSYS   |   RATIO  |         INPUT         |

  SHELL181
  ECR11X         42.218       1.0146     vmr027-cr12b-181
  PLANE182
  ECR11X         42.218       1.0146     vmr027-cr12b-182
  PLANE183
  ECR11X         42.218       1.0146     vmr027-cr12b-183

 ----------------------------------------------------------------
```

vmr027-cr12b-181.dat
vmr027-cr12b-182.dat
vmr027-cr12b-183.dat

VMR027-12C: 2-D Plane Stress - Stepped Load Primary - Secondary Creep

Test Description

A square of length L and height L is constrained in the X-direction on the left edge and constrained in the Y-direction at the midpoint of the left edge. A distributed load, σ_1, is applied in the X-direction on the right edge.

Geometic Properties L = 100 mm	**Material Properties** $E = 200 \times 10^3$ N/mm^2 $\nu = 0.3$ **Creep Law:** $\varepsilon = A_1\sigma^{n_1}t + A_2\sigma^{n_2}t^m$ $n_1 = n_2 = 5$ $m = 0.5$
Boundary Conditions Left Edge: $u_x = 0$ Left Edge (midpoint): $u_y = 0$	**Loading** Right Edge: $\sigma = 100$ N/mm^2 (t = 10000 hrs) $\sigma = 110$ N/mm^2 (t > 10000 hrs)

Results

Results are tabulated and displayed as NAFEMS manual.

```
              |   ANSYS   |   RATIO  |         INPUT         |

   SHELL181
   ECR11X          0.043       0.9952     vmr027-cr12c-181
   PLANE182
   ECR11X          0.043       0.9988     vmr027-cr12c-182
   PLANE183
   ECR11X          0.043       0.9988     vmr027-cr12c-183

  ----------------------------------------------------------------
```

vmr027-cr12c-181.dat
vmr027-cr12c-182.dat
vmr027-cr12c-183.dat

VMR049-CR1: Constant-Load Creep Benchmark

Test Description

A 2-D box of length L and height L is constrained at left edge in Y-direction and in both X and Y directions at midpoint. A distributed load, σ, is applied on the right edge.

Geometric Properties	**Material Properties**
L = 100 mm	$E = 200 \times 10^3$ N/mm ^{2} $\nu = 0.3$ **Secondary Creep:** $\varepsilon = A\sigma^n t^m$ $A = 3.125 \times 10^{-14}$ (t in hours, σ in N/mm^2) m = 1, n = 5 **Primary Creep:** As Secondary Creep, except m = 0.5 **Combined Primary-Secondary Creep:** $\varepsilon\ A_1\sigma_{n1}t + A_2\sigma_{n2}t^m$ $A_1 = 10^{-16}$ $A_2 = 10^{-14}$ (t in hour,σ in N/mm^2) $n_1 = n_2 = 5$
Boundary Conditions Left End: $u_x = 0$ Left End Midpoint: $u_y = 0$	**Loading** $\sigma = 200$ N/mm^2 (Secondary Creep and Primary Creep) $\sigma = 100$ N/mm ^{2} (Combined Primary-Secondary Creep)

Results

Reference: Creep strain results are displayed at intervals of 200 ending at 1000.

	ANSYS	RATIO	INPUT
SHELL181			
ECR2X	9.9118	0.9912	vmr049-cr1a-181
ECR2Y	-4.9415	0.9883	vmr049-cr1a-181
PLANE182			
ECR2X	10.0000	1.0000	vmr049-cr1a-182
ECR2Y	-5.0000	1.0000	vmr049-cr1a-182
PLANE183			
ECR2X	10.0000	1.0000	vmr049-cr1a-183
ECR2Y	-5.0000	1.0000	vmr049-cr1a-183

	ANSYS	RATIO	INPUT
PLANE181			
ECR2X	0.2502	0.9969	vmr049-cr1b-181
ECR2Y	-0.1250	0.9999	vmr049-cr1b-181
PLANE182			
ECR2X	0.2509	0.9997	vmr049-cr1b-182
ECR2Y	-0.1255	1.0037	vmr049-cr1b-182
PLANE183			
ECR2X	0.2509	0.9997	vmr049-cr1b-183
ECR2Y	-0.1255	1.0037	vmr049-cr1b-183

```
 ----------------------------------------------------------------


            |   ANSYS   |   RATIO  |         INPUT         |

 PLANE181
 ECR11X        0.0041       0.9999     vmr049-cr1c-181
 ECR11Y       -0.0021       0.9993     vmr049-cr1c-181
 PLANE182
 ECR11X        0.0042       1.0032     vmr049-cr1c-182
 ECR11Y       -0.0021       1.0031     vmr049-cr1c-182
 PLANE183
 ECR11X        0.0042       1.0032     vmr049-cr1c-183
 ECR11Y       -0.0021       1.0031     vmr049-cr1c-183

 ----------------------------------------------------------------
```

vmr049-cr1c-181.dat
vmr049-cr1c-182.dat
vmr049-cr1c-183.dat

VMR049-CR2: Constant-Displacement Creep Benchmark

Test Description

A box of length L and height L (and thickness L if 3D) is constrained in the Y-direction along the bottom edge and in the X-direction along the left edge. The box is displaced in all directions by a set amount.

Geometric Properties L = 100 mm	**Material Properties** $E = 200 \times 10^3$ N/mm^2 $\nu = 0.3$ **Creep Law:** $\varepsilon = A\sigma^n t^m$ $A = 3.125\times10^{-14}$ (t in hours, σ in N/mm^2) n = 5 2D Plane Stress: m = 0.5 3D: m = 1
Boundary Conditions **2D Plane Stress** Left Edge: $u_x = 0$, Right Edge: $u_x = 0.1$ Top Edge: $u_y = 0.1$, Bottom Edge: $u_y = 0$ **3D** Left Face: $u_x = 0$, Right Face: $u_x = 0.3$ Top Face: $u_y = 0.2$, Bottom Face: $u_y = 0$ Front Face: $u_z = 0$, Back Face: $u_z = 0.1$	**Loading** No applied forces

Results

Reference: Stress results are displayed at incremented time intervals of 200 hours ending at 1000 hours

```
            |   ANSYS   |   RATIO  |         INPUT         |

SHELL181
S6           37.2112       1.0000     vmr049-cr2-181
S7           51.6610       1.0000     vmr049-cr2-181
PLANE182
S6           37.2112       1.0000     vmr049-cr2-182
S7           51.6610       1.0000     vmr049-cr2-182
PLANE183
S6             37.211       1.0000     vmr049-cr2-183
S7             51.661       1.0000     vmr049-cr2-183
SOLID185
S6X          1009.911       1.0009     vmr049-cr2-185
S6Y          1000.000       1.0000     vmr049-cr2-185
S6Z           990.089       0.9991     vmr049-cr2-185
SOLID187
S6X          1008.189        0.9991     vmr049-cr2-187
S6Y          1000.000        1.0000     vmr049-cr2-187
S6Z           991.811        1.0009     vmr049-cr2-187

-----------------------------------------------------------------
```

vmr049-cr2-181.dat
vmr049-cr2-182.dat
vmr049-cr2-183.dat
vmr049-cr2-182.dat
vmr049-cr2-183.dat

VMR049-CR3: Variable-Load Uniaxial Creep Benchmark

Test Description

A 2-D box of length L and height L is constrained at left edge in Y-direction and in both X and Y directions at midpoint. A distributed load, σ, is applied on the right edge

Geometric Properties L = 100 mm	**Material Properties** E = 200 x 10^3 N/mm^2 ν = 0.3 **Creep Law:** $\varepsilon = A\sigma^n t^m$ n = 5 m = 0.5
Boundary Conditions Left End: $u_x = 0$ Midpoint of Left End: $u_y = 0$	**Loading** Tensile Stress,σ_1, on right edge **Uniaxial Load** σ_1 = 200 N/mm^2 (t = 0-100hrs) σ_1 = 250 N/mm^2 (t > 100hrs)

Results

Reference: Creep strain results in X-direction are displayed by incrementing the time every 50 hours ending at 200 hours.

```
              |   ANSYS   |   RATIO  |         INPUT         |

   SHELL181
   S2            0.2183       0.9878     vmr049-cr3-181
   S7            0.3139       0.9966     vmr049-cr3-181
   PLANE182
   S2            0.2213       1.0015     vmr049-cr3-182
   S7            0.3148       0.9994     vmr049-cr3-182
   PLANE183
   S2            0.2213       1.0015     vmr049-cr3-183
   S7            0.3149       0.9997     vmr049-cr3-183

  ----------------------------------------------------------------
```

vmr049-cr3-181.dat
vmr049-cr3-182.dat
vmr049-cr3-183.dat

VMR049-CR4: Pressurised Cylinder Creep Benchmark

Test Description

A box of length R_2-R_1 and height H is offset from the origin by a distance R_1. The bottom and top edge is constrained in the Y-direction and a distributed load, P, is applied to the left edge.

Geometric Properties	**Material Properties**
R_1 = 100 mm R_2 = 200 mm H = 25 mm P = 100 N/mm^2	E = 200 x 10^3 N/mm^2 ν = 0.3 **Creep Law:** $\varepsilon = A\sigma^n t^m$ A = 3.125 x 10^{-14} (t in hours, σ in N/mm^2) n = 5 m = 1
Boundary Conditions Bottom and Top Edge: $u_z = 0$	**Loading** Pressure, P, applied to left edge.

Results

Reference: Stress results are displayed at incremented intervals of 25 starting at 0 and ending at 100.

```
            |   ANSYS   |   RATIO  |         INPUT         |

 PLANE182
 RESULTS TAKEN AT RADIUS=175
 ELS6X        -20.8547       1.0702     vmr049-cr4-182
 ELS6Z        154.1880       1.0089     vmr049-cr4-182
 SSS6X        -34.4550       0.9983     vmr049-cr4-182
 SSS6Z        229.4624       0.9991     vmr049-cr4-182
 PLANE183
 RESULTS TAKEN AT RADIUS=175
 ELS6X        -19.4872       1.0000     vmr049-cr4-183
 ELS6Z        152.8205       1.0000     vmr049-cr4-183
 SSS6X        -34.5117       1.0000     vmr049-cr4-183
 SSS6Z        229.6722       1.0000     vmr049-cr4-183

-----------------------------------------------------------------
```

vmr049-cr4-182.dat
vmr049-cr4-183.dat

VMR049-CR5: Torsional Creep of Square Shaft

Test Description

A block of length L_1, height L_2, and thickness $L_3$is rotated about the Z axis by β.

Geometric Properties	**Material Properties**
L_1 = 1 mm L_2 = 2 mm L_3 = 0.2 mm Angle of Rotation: β = 0.01 radians per unit length	E = 10.0 N/mm^2 ν = 0.3 **Creep Law:** $d\varepsilon/dt = A\sigma^n t^m$ A = 10^4 (t in hours, σ in N/mm^2) n = 5 m = -0.5
Boundary Conditions	**Loading**
Back Face: $u_x = 0$, $u_y = 0$ Bottom Face and Left Face: u_z = unknown (multi-point constraints) $u_z = 0$ at location (0,0,0), (L_1,0,0), and (0,L_2,0)	No applied forces

Note — Front face and mid-plane, located at half the thickness, are rotated by an angle β. All nodes on the front face and mid-plane have $u_x = -r\beta L\sin\theta$ and $u_y = r\beta L\sin\theta$, where L = 0.2 mm for the front face and L = 0.1 mm for the mid-plane. θ = angle measured anticlockwise from the X axis.

Results

Reference: Shear stress values in YZ-direction are displayed at each decade starting at 0.001 and ending at 100.

```
              |   ANSYS   |   RATIO  |         INPUT         |

  SOLID185
  SYZ2          0.0143       1.0004     vmr049-cr5-185
  SOLID186
  SYZ2          0.0143       1.0000     vmr049-cr5-186
  SOLID187
  SYZ2          0.0142       0.9966     vmr049-cr5-187

 ----------------------------------------------------------------
```

vmr049-cr5-185.dat
vmr049-cr5-186.dat
vmr049-cr5-187.dat

VMR049-CR6: Thermally Induced Creep Benchmark

Test Description

A 10° slice of an axisymmetric sphere having an inner radius of R_1 and outer radius of R_2 is constrained at the top and bottom edges in the Y-direction. A distributed load, P, is applied to the left edge.

Geometric Properties	**Material Properties**
R_1 = 200 mm R_2 = 500 mm β = 10° P = 30 N/mm^2	E = 10x10^3 N/mm^2 ν = 0.25 **Creep Law:** $d\varepsilon/dt = A\sigma^n f(T)$ A = 3.0x10^{-6} (t in hours, σ, in N/mm^2) n = 5.5 $f(T) = e^{-12500/T}$ where T is temperature in °K
Boundary Conditions Bottom Edge: $u_z = 0$ Top Edge: Perpendicular Displacement = 0 (symmetry condition) Temperature prescibed at all nodes as follows: T = 333(1+100/r) where r is radius measured from the center of the sphere.	**Loading** Pressure, P, on left edge.

Results

Reference: Effective stress results are displayed for each hour starting from 0 and ending at 10 (log scale).

	ANSYS	RATIO	INPUT
PLANE182			
SR205	11.2551	1.0005	vmr049-cr6-182
SR350	17.5837	1.0002	vmr049-cr6-182
SR495	21.1643	1.0002	vmr049-cr6-182
PLANE183			
SR205	11.5369	1.0255	vmr049-cr6-183
SR350	17.6113	1.0018	vmr049-cr6-183
SR495	21.0756	0.9960	vmr049-cr6-183

VMR049-PL1: 2D Plane Strain Plasticity Benchmark

Test Description

A square of length L and height L is constrained in the Y-direction along the bottom edge and in the X-direction along the left edge. The model is displaced in the X and Y directions.

Geometric Properties L = 1.0 mm	**Material Properties** E = 250.0 x 10^3 N/mm^2 ν = 0.25 **Plasticity Model** Perfect Plasticity: σ_{ys} = 5.0 N/mm^2 Isotropic Hardening: E_T = 50.0 x 10^3 N/mm^2
Boundary Conditions Left Edge: $u_x = 0$ Bottom Edge: $u_y = 0$ Right Edge: $u_x = \delta_x$ Top Edge: $u_y = \delta_y$	
Loading No applied forces Displacements prescribed in 8 increments (R = 2.5x10^{-5}), as follows:	
Step: Disp. Change	**Step: Stress State**
Step 1: Δu_x= +R	**Step 1:** First Yield
Step 2: Δu_x = +R	**Step 2:** Plastic Flow
Step 3: Δu_y = +R	**Step 3:** Elastic Unloading
Step 4: Δu_y = +R	**Step 4:** Plastic Reloading
Step 5: Δu_x = -R	**Step 5:** Plastic Flow
Step 6: Δu_x = -R	**Step 6:** Plastic Flow
Step 7: Δu_y = -R	**Step 7:** Elastic Unloading
Step 8: Δu_y = -R	**Step 8:** Plastic Flow

Results

Reference: Stress results are displayed as the step is incremented by 1 starting with 0 and ending at 8.

```
            |   ANSYS   |   RATIO  |         INPUT         |

PLANE182
RESULTS LISTED USING LOAD STEP 6
SX            5.1140       0.9961     vmr049-pl1a-182
SY           10.6919       0.9951     vmr049-pl1a-182
SZ            9.1935       1.0081     vmr049-pl1a-182
PLANE183
RESULTS LISTED USING LOAD STEP 6
SX            5.1140       0.9961     vmr049-pl1a-183
SY           10.6919       0.9951     vmr049-pl1a-183
SZ            9.1935       1.0081     vmr049-pl1a-183

-----------------------------------------------------------------
```

```
            |   ANSYS   |   RATIO  |         INPUT         |

  PLANE182
  RESULTS REPORTED USING LOAD STEP 7
  SX            1.5057       0.9701     vmr049-pl1b-182
  SY            4.9217       0.9937     vmr049-pl1b-182
  SZ            6.0725       1.0129     vmr049-pl1b-182
  PLANE183
  RESULTS REPORTED USING LOAD STEP 7
  SX            1.5057       0.9701     vmr049-pl1b-183
  SY            4.9217       0.9937     vmr049-pl1b-183
  SZ            6.0725       1.0129     vmr049-pl1b-183

 ----------------------------------------------------------------
```

vmr049-pl1a-182.dat (a)
vmr049-pl1a-183.dat (a)
vmr049-pl1b-183.dat (b)

VMR049-PL2: 2D Plane Stress Plasticity Benchmark

Test Description

A square of length L and height L is constrained in the Y-direction along the bottom edge and in the X-direction along the left edge. The model is displaced in the X and Y directions.

Geometry L = 1.0 mm	**Material Properties** E = 250.0 x 10^3 N/mm^2 ν = 0.25 **Plasticity Model** Perfect Plasticity: σ_{ys} = 5.0 N/mm^2 Isotropic Hardening: E_T = 50.0 x 10^3 N/mm^2
Boundary Conditions Left Edge: $u_x = 0$ Bottom Edge: $u_y = 0$ Right Edge: $u_x = \delta_x$ Top Edge: $u_y = \delta_y$	
Loading No applied forces Displacements prescribed in 8 increments (R = 2.5 x 10^{-5}), as follows:	
Step: Disp. change	**Step: Stress state**
Step 1: $\Delta u_x = +R$	**Step 1:** First Yield
Step 2: $\Delta u_x = +R$	**Step 2:** Plastic Flow
Step 3: $\Delta u_y = +R$	**Step 3:** Elastic Unloading
Step 4: $\Delta u_y = +R$	**Step 4:** Plastic Reloading
Step 5: $\Delta u_x = -R$	**Step 5:** Plastic Flow
Step 6: $\Delta u_x = -R$	**Step 6:** Plastic Flow
Step 7: $\Delta u_y = -R$	**Step 7:** Elastic Unloading
Step 8: $\Delta u_y = -R$	**Step 8:** Plastic Flow

Results

Reference: Stress results are displayed as the step is incremented by 1 starting with 0 and ending at 8.

```
             |   ANSYS   |   RATIO  |         INPUT         |

SHELL181
SX           -3.3494       1.0001     vmr049-pl2a-181
SY           -5.7473       1.0001     vmr049-pl2a-181
SEFF          5.0000       1.0000     vmr049-pl2a-181
PLANE182
SX           -3.3494       1.0001     vmr049-pl2a-182
SY           -5.7473       1.0001     vmr049-pl2a-182
SEFF          5.0000       1.0000     vmr049-pl2a-182
PLANE183
SX           -3.3494       1.0001     vmr049-pl2a-183
SY           -5.7473       1.0001     vmr049-pl2a-183
SEFF          5.0000       1.0000     vmr049-pl2a-183
```

```
-----------------------------------------------------------------


            |   ANSYS   |   RATIO  |         INPUT         |

 SHELL181
 SX           -9.1555       1.0001     vmr049-pl2b-181
 SY           -8.4910       1.0000     vmr049-pl2b-181
 SEFF          8.8420       1.0000     vmr049-pl2b-181
 PLANE182
 SX           -9.1555       1.0001     vmr049-pl2b-182
 SY           -8.4910       1.0000     vmr049-pl2b-182
 SEFF          8.8420       1.0000     vmr049-pl2b-182

-----------------------------------------------------------------
```

vmr049-pl2a-181.dat (a)
vmr049-pl2a-182.dat (a)
vmr049-pl2a-183.dat (a)
vmr049-pl2b-181.dat (b)
vmr049-pl2b-182.dat (b)

VMR049-PL3: 3D Plasticity Benchmark

Test Description

A block with length, height, and length L is constrained at Z = L in the Y-direction and constrained in the X-direction when Z = L and Y ranges from 0 to L. The block is displaced according to the given boundary conditions.

Geometry L = 1.0 mm	**Material Properties** $E = 250 \times 10^3$ N/mm^2 $\nu = 0.25$ **Plasticity Model** Perfect Plasticity: $\sigma_{ys} = 5.0$ N/mm^2 Isotropic Hardening: $E_T = 50 \times 10^3$ N/mm^2
Boundary Conditions Left Face: $u_x = 0$ Bottom Face: $u_y = 0$ Front Face: $u_z = 0$ Right Face: $u_x = \delta_x$ Top Face: $u_y = \delta_y$ Back Face: $u_z = \delta_z$	
Loading No applied forces Displacements prescribed in 12 steps ($R = 2.5 \times 10^{-5}$) as follows:	
Step:	**Disp. change**
Step 1:	$\Delta u_x = +R$
Step 2:	$\Delta u_x = +R$
Step 3:	$\Delta u_y = +R$
Step 4:	$\Delta u_y = +R$
Step 5:	$\Delta u_z = +R$
Step 6:	$\Delta u_z = +R$
Step 7:	$\Delta u_x = -R$
Step 8:	$\Delta u_x = -R$
Step 9:	$\Delta u_y = -R$
Step 10:	$\Delta u_y = -R$
Step 11:	$\Delta u_z = -R$
Step 12:	$\Delta u_z = -R$

Results

Reference: Stress results are displayed for each step as the step is incremented by 1 starting from 0 and ending at 12.

```
                |   ANSYS    |   RATIO   |         INPUT         |

SOLID185
SX            2.7470       1.0000     vmr049-pl3a-185
```

```
 SY            0.2618       0.9991     vmr049-pl3a-185
 SZ           -3.0087       0.9999     vmr049-pl3a-185
 SEFF          5.0000       1.0000     vmr049-pl3a-185
 SOLID186
 SX            2.7470       1.0000     vmr049-pl3a-186
 SY            0.2618       0.9991     vmr049-pl3a-186
 SZ           -3.0087       0.9999     vmr049-pl3a-186
 SEFF          5.0000       1.0000     vmr049-pl3a-186
 SOLID187
 SX            2.7470       1.0000     vmr049-pl3a-187
 SY            0.2618       0.9991     vmr049-pl3a-187
 SZ           -3.0087       0.9999     vmr049-pl3a-187
 SEFF          5.0000       1.0000     vmr049-pl3a-187

-----------------------------------------------------------------


            |   ANSYS   |   RATIO  |         INPUT         |

 SOLID185
 SX            1.9340       1.0000     vmr049-pl3b-185
 SY           -0.5406       0.9993     vmr049-pl3b-185
 SZ           -1.3934       1.0003     vmr049-pl3b-185
 SEFF          2.9936       0.9999     vmr049-pl3b-185
 SOLID186
 SX            1.9340       1.0000     vmr049-pl3b-186
 SY           -0.5406       0.9993     vmr049-pl3b-186
 SZ           -1.3934       1.0003     vmr049-pl3b-186
 SEFF          2.9936       0.9999     vmr049-pl3b-186
 SOLID187
 SX            1.9340       1.0000     vmr049-pl3b-187
 SY           -0.5406       0.9993     vmr049-pl3b-187
 SZ           -1.3934       1.0003     vmr049-pl3b-187
 SEFF          2.9936       0.9999     vmr049-pl3b-187
 SOLSH190
 SX            1.9340       1.0000     vmr049-pl3b-190
 SY           -0.5406       0.9993     vmr049-pl3b-190
 SZ           -1.3934       1.0003     vmr049-pl3b-190
 SEFF          2.9936       0.9999     vmr049-pl3b-190

-----------------------------------------------------------------
```

vmr049-pl3a-185.dat (a)
vmr049-pl3a-186.dat (a)
vmr049-pl3a-187.dat (a)
vmr049-pl3b-185.dat (b)
vmr049-pl3b-186.dat (b)
vmr049-pl3b-187.dat (b)
vmr049-pl3b190.dat (b)

VMR049-PL5: Pressurised Cylinder Plasticity Benchmark

Test Description

A square of length R_2-R_1 and height H is constrained in the Z-direction on the top and bottom edges and offset a distance R_1 from the origin. A distributed pressure load is applied to the left edge.

Geometric Properties (Axisymmetric) R_1 = 100 mm R_2 = 200 mm H = 100 mm	**Material Properties** E = 21.0 x 10^3 N/mm^2 ν = 0.3 **Plasticity Model** Perfect Plasticity: σ_{ys} = 24.0 N/mm^2 Isotropic Hardening: E_T = 4.2 x 10^3 N/mm^2
Boundary Conditions Top and Bottom Edges: u_z = 0	
Loading Internal pressure, P, at the bore (left edge) applied in 4 steps.	
Step: Perfect Plasticity	**Step: Iso. Hardening**
1: P = 10.0 N/mm^2	**1:** P = 10.0 N/mm^2
2: P = 14.0 N/mm^2	**2:** P = 14.0 N/mm^2
3: P = 16.6 N/mm^2	**3:** P = 24.0 N/mm^2
4: P = 19.2 N/mm^2	**4:** P = 34.0 N/mm^2

Results

Reference: Stress results are displayed for each step as the step is incremented by 1 starting at 0 and ending at 4.

```
            |   ANSYS   |   RATIO  |         INPUT         |

PLANE182
SRAD         -15.3322       0.9720     vmr049-pl5a-182
SAXI          -1.9040       1.0133     vmr049-pl5a-182
SHOOP         12.3762       1.0371     vmr049-pl5a-182
SEFF          24.0000       1.0000     vmr049-pl5a-182
PLANE183
SRAD         -16.2156       1.0280     vmr049-pl5a-183
SAXI          -1.8541       0.9868     vmr049-pl5a-183
SHOOP         11.4910       0.9629     vmr049-pl5a-183
SEFF          24.0000       1.0000     vmr049-pl5a-183

-----------------------------------------------------------------
```

```
            |   ANSYS   |   RATIO  |         INPUT         |

PLANE182
SRAD         -26.7817       0.9910     vmr049-pl5b-182
SAXI           3.1492       0.8671     vmr049-pl5b-182
SHOOP         38.6501       1.0231     vmr049-pl5b-182
PLANE183
SRAD         -27.2679       1.0090     vmr049-pl5b-183
SAXI           4.1140       1.1327     vmr049-pl5b-183
```

```
  SHOOP         36.9054       0.9769     vmr049-pl5b-183

 ----------------------------------------------------------------
```

vmr049-pl5a-182.dat (a)
vmr049-pl5a-183.dat (a)
vmr049-pl5b-182.dat (b)
vmr049-pl5b-183.dat (b)

Index

Symbols

*VWRITE command, 1–119
/OPT command, 1–352

A

A command, 2–5
abbreviations, 1–33
ACEL command, 2–36
ACLEAR command, 2–29
acoustic analysis
  harmonic, 1–403
adaptive descent, 1–30, 1–37, 1–63, 1–97, 1–438
adaptive meshing, 1–443, 1–470, 3–10, 3–12
ADD command, 2–29
AMAP command, 1–432
AMESH command, 2–9, 2–15, 2–23, 2–26, 2–29, 2–36
analogous field applications
  diffusion, 1–368
  electrostatics, 1–119, 1–123, 1–272
  seepage through porous media, 1–365
analysis type
  acoustic, 1–403, 1–487
  buckling, 1–49, 1–291, 1–293
  coupled-field, 1–61, 1–84, 1–269, 1–289, 1–383, 1–385, 1–388, 1–392, 1–394, 1–396, 1–400, 1–403, 1–421, 1–425, 1–475, 1–498
  current conduction, 1–265
  fluid flow, 1–112, 1–281, 1–283, 1–285, 1–334, 1–336, 1–407, 1–479, 1–511
  harmonic magnetic, 1–373, 1–432, 1–513
  harmonic response, 1–53, 1–176, 1–199, 1–201, 1–203, 1–207, 1–400, 1–403, 1–416, 1–466, 1–473, 1–477
  high frequency electromagnetic harmonic, 1–493, 1–496
  high frequency electromagnetic modal, 1–491
  modal, 1–111, 1–115, 1–117, 1–121, 1–127, 1–129, 1–131, 1–133, 1–137, 1–141, 1–143, 1–145, 1–147, 1–155, 1–157, 1–159, 1–161, 1–163, 1–176, 1–205, 1–338, 1–340, 1–342, 1–344, 1–396, 1–413, 1–414, 1–416, 1–463, 1–466, 2–15, 2–19, 2–40
  restart, 1–69, 1–409
  spectrum, 1–53, 1–159, 1–161, 1–163, 1–466
  static magnetic, 1–370, 1–378, 1–380, 1–430, 1–436, 1–473, 1–475
  static structural, 1–19, 1–21, 1–23, 1–24, 1–26, 1–28, 1–30, 1–36, 1–37, 1–39, 1–41, 1–43, 1–45, 1–47, 1–51, 1–55, 1–57, 1–59, 1–63, 1–65, 1–69, 1–71, 1–75, 1–80, 1–82, 1–87, 1–90, 1–92, 1–94, 1–97, 1–99, 1–103, 1–105, 1–107, 1–109, 1–129, 1–131, 1–133, 1–135, 1–141, 1–150, 1–152, 1–176, 1–180, 1–188, 1–291, 1–293, 1–299, 1–301, 1–303, 1–305, 1–307, 1–308, 1–311, 1–313, 1–314, 1–316, 1–318, 1–320, 1–322, 1–324, 1–326, 1–328, 1–332, 1–340, 1–342, 1–347, 1–352, 1–411, 1–418, 1–428, 1–438, 1–445, 1–447, 1–449, 1–452, 1–455, 1–457, 1–460, 1–466, 1–470, 1–484, 1–500, 1–503, 1–507, 2–5, 2–9, 2–12, 2–23, 2–32, 2–36, 3–10, 3–12
  steady-state thermal, 1–82, 1–139, 1–212, 1–214, 1–217, 1–219, 1–221, 1–223, 1–226, 1–228, 1–231, 1–233, 1–235, 1–241, 1–243, 1–244, 1–246, 1–267, 1–287, 1–330, 1–359, 1–361, 1–363, 1–443
  substructuring, 1–287, 1–318
  transient dynamic, 1–34, 1–101, 1–153, 1–165, 1–167, 1–169, 1–172, 1–174, 1–178, 1–182, 1–184, 1–186, 1–190, 1–193, 1–196, 1–209, 1–350, 1–354, 1–409, 1–414
  transient magnetic, 1–375, 1–475
  transient thermal, 1–73, 1–215, 1–237, 1–248, 1–250, 1–252, 1–254, 1–255, 1–258, 1–260, 1–262, 1–356, 1–441, 2–26
ANG command, 2–36
ANTYPE command, 1–69, 2–5
APDL
  array parameters, 1–119, 1–295, 1–297, 1–438, 1–477, 2–32, 2–40
  branching, 1–33, 1–150, 1–322, 1–425, 1–430, 2–36, 2–40
  character parameters, 1–452
  dynamic parameter substitution, 1–452
  looping, 1–150, 1–221, 1–223, 1–322, 1–332, 1–342, 1–373, 1–396, 1–396, 1–425, 1–432, 1–452, 1–460, 2–32
  macros, 1–30, 1–33, 1–63, 1–87, 1–150, 1–322, 1–342, 1–418, 1–425, 1–428, 1–430, 1–432, 1–436, 1–452, 1–460, 2–32, 2–40
  repeating, 1–109, 1–150, 1–188, 1–255, 1–285, 1–305, 1–313, 1–322, 1–334, 1–336, 1–347, 1–365, 1–373, 1–385, 1–394, 1–400, 1–418, 1–425, 1–428, 2–5, 2–19, 2–32
  scalar parameters, 1–24, 1–26, 1–30, 1–33, 1–37, 1–69, 1–84, 1–87, 1–139, 1–150, 1–161, 1–163, 1–221, 1–223, 1–226, 1–228, 1–265, 1–267, 1–269, 1–308, 1–318, 1–322, 1–334, 1–336, 1–342, 1–347, 1–352, 1–370, 1–373, 1–378, 1–383, 1–392, 1–396, 1–400, 1–421, 1–425, 1–430, 1–432, 1–436, 1–451, 1–452, 1–468, 1–470, 1–473, 1–475, 1–477, 2–5, 2–9, 2–12, 2–15, 2–19, 2–23, 2–26, 2–32, 2–36, 2–40, 3–10, 3–12
ARSYM command, 2–15
ATYP command, 2–29
automatic time stepping
  contact, 1–71, 1–190
  hyperelasticity, 1–507
  large-deflection, 1–69
  magnetics, 1–375
  plasticity, 1–37
  stress-stiffening, 1–57
  thermal, 1–73, 1–84, 1–237, 1–248, 1–250, 1–252, 1–254, 1–255, 1–258, 1–260, 1–262, 1–356, 1–441, 2–26
AUTOTS command, 1–37, 1–71, 1–73, 2–29
axisymmetric analysis

arc-length method, 1–49
electric, 1–269
fluid, 1–334, 1–344, 1–479
magnetic, 1–388
nonaxisymmetric load, 1–340
radiation, 1–330
structural, 1–65, 1–82, 1–97, 1–107, 1–150, 1–157, 1–316, 1–338, 1–340, 1–388, 1–413, 1–457
thermal, 1–82, 1–233, 1–246, 1–252, 1–254, 1–269, 1–330, 1–359, 1–365
w/nonaxisymmetric load, 1–246, 1–316, 1–338, 1–359
/AXLAB command, 2–29

B

B-H curve, 1–370
Beam offset, 1–43
BEAM188 element, 1–500, 1–503, 1–518
BEAM189 element, 1–500, 1–503, 1–518
BEAM23 element, 1–63, 1–303
BEAM24 element, 1–305
BEAM3 element, 1–21, 1–101, 1–103, 1–121, 1–127, 1–145, 1–163, 1–178, 1–291, 1–308, 1–352, 1–403, 1–411, 1–521
BEAM4 element, 1–53, 1–57, 1–92, 1–137, 1–141, 1–409, 1–447
BEAM44 element, 1–87
BEAM54 element, 1–36, 1–43, 1–307
BETA command, 2–36
biaxial loads, 1–524
BIOT command, 1–383
Biot-Savart option, 1–378, 1–383, 1–436
birth and death, 1–445
body loads
coupled-field, 1–82
current density, 1–370, 1–430
fluence, 1–303
heat generation, 1–139, 1–215, 1–235, 1–241, 1–260, 1–267
temperature, 1–23, 1–71, 1–84, 1–135, 1–152, 1–237, 1–248, 1–250, 1–254, 1–255, 1–260, 1–301, 1–303, 1–311, 1–324, 1–340, 1–342, 1–356, 1–445, 1–457, 2–26
uniform, 1–23, 1–71, 1–73, 1–84, 1–90, 1–135, 1–152, 1–237, 1–248, 1–250, 1–254, 1–260, 1–301, 1–311, 1–324, 1–340, 1–342, 1–356, 1–445, 2–26
voltage, 1–473
Boolean operations
add, 1–77, 1–484
fillet, 1–77
glue, 1–421, 1–436, 1–468, 1–484
overlap, 1–123, 1–430, 1–432, 1–436, 1–473, 1–475
subtract, 1–468
buckling analysis
reduced, 1–291
subspace, 1–293

C

calculations
electromagnetic high frequency S-parameters, 1–493, 1–496
CBDOF command, 1–320
CHECK command, 2–36
CIRCU124 element, 1–265, 1–475, 1–477, 1–528
CIRCU125 element, 1–528
CIRCU94, 1–560
circuit analysis
transient, 1–528
CNVTOL command, 2–29
COMBI165 element, 3–2, 3–4, 3–6, 3–8
COMBIN14 element, 1–34, 1–111, 1–115, 1–127, 1–205, 1–207, 1–344, 1–385, 1–447
COMBIN37 element, 1–356
COMBIN39 element, 1–350
COMBIN40 element, 1–34, 1–92, 1–159, 1–161, 1–165, 1–167, 1–169, 1–172, 1–174, 1–182, 1–186, 1–190, 1–199, 1–201, 1–203, 1–414, 1–416
COMBIN7 element, 1–409, 1–447
components, 1–322, 1–342, 1–438, 1–460
composite elements
shell elements, 1–90, 1–143, 1–180, 1–188, 1–324
solid elements, 1–188, 1–324
concentrated loads
current, 1–119, 1–383, 1–421
current segment, 1–432
flow, 1–281, 1–283
force, 1–19, 1–23, 1–24, 1–26, 1–34, 1–36, 1–37, 1–39, 1–41, 1–43, 1–47, 1–49, 1–51, 1–57, 1–59, 1–69, 1–75, 1–80, 1–87, 1–92, 1–99, 1–103, 1–133, 1–141, 1–165, 1–167, 1–172, 1–174, 1–176, 1–178, 1–180, 1–182, 1–184, 1–188, 1–193, 1–196, 1–199, 1–201, 1–203, 1–207, 1–291, 1–293, 1–303, 1–307, 1–308, 1–316, 1–318, 1–324, 1–326, 1–328, 1–332, 1–352, 1–403, 1–409, 1–414, 1–416, 1–428, 1–438, 1–449, 1–500, 2–32
heat flow rate, 1–356
voltage, 1–477
concrete elements, 1–328
constraint equations
direct, 1–103, 1–109, 1–328
CONTA171, 1–537
CONTA171 element, 1–487
CONTA172 element, 1–487
CONTA173 element, 1–487
CONTA174 element, 1–487
CONTA175 element, 1–153, 1–438, 1–460, 1–460, 1–460
CONTAC12 element, 1–71, 1–75
CONTAC178 element, 1–150
CONTAC52 element, 1–71
contact
contact surface, 1–61, 1–150, 1–152, 1–153, 1–438, 1–460

ANSYS Verification Manual . ANSYS Release 10.0 . 002184 . © SAS IP, Inc.

node-to-node, 1–71
rigid target, 1–487
surface-to-surface, 1–487
convection
evaluated at bulk temp., 1–139
film coefficient, 1–139, 1–212, 1–215, 1–217, 1–221, 1–223, 1–228, 1–235, 1–244, 1–250, 1–255, 1–267, 1–269, 1–356, 1–361, 1–363, 1–392, 1–443, 2–23, 2–26
convergence criteria
fluid, 1–285
magnetic, 1–370, 1–385
structural, 1–43, 1–63, 1–84, 1–92, 1–101, 1–153, 1–169, 1–186, 1–303, 1–311, 1–350, 1–354, 1–385, 1–394, 1–409, 1–447
thermal, 1–84
coordinate systems
Cartesian, 1–28, 1–33, 1–34, 1–71, 1–105, 1–157, 1–217, 1–219, 1–318, 1–322, 1–373, 1–436, 1–452, 1–460, 1–473, 1–475, 1–477, 1–493, 1–496, 2–15, 2–32, 2–36
cylindrical, 1–28, 1–30, 1–33, 1–49, 1–55, 1–84, 1–97, 1–99, 1–105, 1–119, 1–135, 1–139, 1–150, 1–219, 1–231, 1–235, 1–241, 1–252, 1–254, 1–267, 1–269, 1–318, 1–320, 1–322, 1–342, 1–361, 1–370, 1–373, 1–378, 1–392, 1–400, 1–403, 1–411, 1–428, 1–432, 1–452, 1–460, 1–470, 1–493, 2–12, 2–15, 2–36, 3–10, 3–12
rotating, 1–112
spherical, 1–123, 1–143, 1–432, 1–438
working plane, 1–94, 1–436, 1–449, 1–484
Coriolis effect, 1–299
coupled nodes, 1–23, 1–41, 1–55, 1–65, 1–69, 1–82, 1–87, 1–92, 1–97, 1–139, 1–157, 1–180, 1–217, 1–235, 1–252, 1–254, 1–267, 1–269, 1–324, 1–344, 1–385, 1–388, 1–392, 1–400, 1–425, 1–438, 1–460, 1–463, 1–473, 1–475
Coupled nodes, 1–30, 1–84
coupled-field analysis
acoustic-structural, 1–403
circuit-magnetic, 1–475
DC electromagnetic, 1–383, 1–421, 1–425
magnetic-structural, 1–385, 1–388
piezoelectric, 1–396, 1–400
thermal stress, 1–84, 1–394
thermal-electric, 1–61, 1–269, 1–498
thermal-flow, 1–289
crack-tip, 1–322
*CREATE command, 1–33, 2–32
creep, 1–301, 1–303
implicit, 1–524
CSYS command, 2–9
current conduction analysis, 1–265, 1–383, 1–392

D

D command, 2–5
damping
alpha, 1–354
beta, 1–201
harmonic response analysis, 1–199, 1–203
nonlinear structural analysis, 1–34
PSD, 1–53, 1–466
spectrum analysis, 1–466
transient dynamic analysis, 1–167, 1–169, 1–172, 1–174, 1–190
Damping
ratio, 1–159
DEGR command, 2–36
degree-of-freedom constraints
CURR, 1–473, 1–475, 1–477, 1–513
electric potential, 1–123, 1–265, 1–269, 1–383, 1–392, 1–396, 1–400, 1–403, 1–425, 1–477, 1–493, 1–496, 1–498
EMF, 1–475
fluid pressure, 1–281, 1–283, 1–285, 1–479, 1–511
fluid velocity, 1–407
magnetic potential, 1–375, 1–378, 1–380, 1–385, 1–388, 1–421, 1–432, 1–436, 1–473, 1–475
species concentration, 1–479
structural, 1–19, 1–21, 1–23, 1–24, 1–26, 1–28, 1–30, 1–34, 1–36, 1–37, 1–39, 1–41, 1–43, 1–47, 1–51, 1–55, 1–57, 1–59, 1–61, 1–63, 1–65, 1–69, 1–71, 1–75, 1–80, 1–82, 1–84, 1–87, 1–90, 1–92, 1–94, 1–97, 1–99, 1–101, 1–103, 1–105, 1–107, 1–109, 1–111, 1–115, 1–117, 1–127, 1–133, 1–135, 1–137, 1–141, 1–143, 1–145, 1–147, 1–150, 1–152, 1–155, 1–157, 1–159, 1–161, 1–163, 1–165, 1–167, 1–169, 1–172, 1–174, 1–176, 1–178, 1–180, 1–182, 1–184, 1–186, 1–190, 1–199, 1–201, 1–203, 1–205, 1–207, 1–209, 1–291, 1–293, 1–299, 1–301, 1–305, 1–308, 1–311, 1–313, 1–314, 1–316, 1–318, 1–322, 1–324, 1–326, 1–328, 1–332, 1–334, 1–336, 1–340, 1–342, 1–344, 1–347, 1–350, 1–352, 1–354, 1–385, 1–388, 1–394, 1–396, 1–400, 1–403, 1–409, 1–413, 1–414, 1–416, 1–418, 1–428, 1–430, 1–438, 1–445, 1–447, 1–449, 1–452, 1–455, 1–457, 1–460, 1–466, 1–470, 1–484, 1–487, 1–500, 1–503, 1–507, 2–5, 2–9, 2–12, 2–15, 2–19, 2–32, 2–36, 2–40, 3–10, 3–12
temperature, 1–61, 1–82, 1–84, 1–212, 1–214, 1–217, 1–219, 1–221, 1–226, 1–231, 1–233, 1–241, 1–243, 1–246, 1–248, 1–250, 1–260, 1–262, 1–287, 1–289, 1–330, 1–356, 1–359, 1–363, 1–365, 1–385, 1–394, 1–441, 1–443, 2–23
turbulent kinetic energy, 1–498
DELTIM command, 2–26, 2–29
DELX command, 2–32
*DIM command, 2–32
diodes, 1–528
distribution
Weibull, 1–544
*DO command, 2–32
/DSCALE command, 2–29
DSYM command, 2–5, 2–9, 2–29, 2–36

E

elastic foundation, 1–307
element attributes
element type, 1–30, 1–34, 1–71, 1–82, 1–92, 1–103, 1–111, 1–115, 1–117, 1–127, 1–127, 1–135, 1–137, 1–139, 1–150, 1–152, 1–153, 1–178, 1–184, 1–190, 1–205, 1–207, 1–209, 1–212, 1–217, 1–221, 1–244, 1–248, 1–250, 1–262, 1–287, 1–318, 1–328, 1–344, 1–350, 1–356, 1–370, 1–385, 1–403, 1–409, 1–411, 1–425, 1–438, 1–441, 1–443, 1–447, 1–460, 1–470, 1–477, 3–10, 3–12
material, 1–23, 1–30, 1–49, 1–92, 1–111, 1–212, 1–287, 1–326, 1–328, 1–361, 1–385, 1–403, 1–425, 1–438, 1–443, 1–445, 1–447, 1–457, 1–470, 3–10, 3–12
real constant, 1–30, 1–34, 1–49, 1–71, 1–103, 1–115, 1–117, 1–127, 1–137, 1–150, 1–152, 1–153, 1–172, 1–174, 1–178, 1–182, 1–184, 1–190, 1–205, 1–207, 1–209, 1–217, 1–221, 1–244, 1–248, 1–265, 1–328, 1–344, 1–350, 1–352, 1–356, 1–403, 1–409, 1–411, 1–414, 1–416, 1–438, 1–441, 1–447, 1–470, 1–477, 3–10, 3–12
solid model, 1–237
element reordering, 1–380
*ELSE command, 2–29, 2–36
*END command, 2–32
*ENDDO command, 2–32
*ENDIF command, 2–29, 2–36
error analysis
energy error, 1–443, 2–32
energy norm, 1–470, 2–5, 2–9, 2–32, 3–10, 3–12
/ESHAPE command, 2–9, 2–15, 2–23, 2–36
ESIZE command, 2–5, 2–9, 2–19, 2–23, 2–26, 2–29, 2–36
ESLN command, 2–29
ET command, 2–5
ETABLE command, 1–336
ETYPE command, 2–9, 2–15, 2–19, 2–23, 2–26, 2–29, 2–36
/EXIT command, 2–29
expansion pass
harmonic response analysis, 1–53, 1–53
modal analysis, 1–53, 1–127, 1–129, 1–133, 1–141, 1–147, 1–155, 1–157, 1–159, 1–161, 1–163, 1–338, 1–342, 1–396, 1–491, 2–19, 2–40
substructuring, 1–318
transient dynamic analysis, 1–178, 1–196

F

failure criteria
Tsai-Wu, 1–180
far-field elements, 1–119, 1–123, 1–370
FDEL command, 2–32
files
external, 1–196, 1–318, 1–320, 1–342, 1–409, 1–414, 1–416
FILL command, 2–32
fluid
non-flowing, 1–334
nonflowing, 1–336, 1–344
FLUID 141 element, 1–479
fluid flow analysis
multiple species, 1–479
steady-state, 1–112, 1–281, 1–283, 1–285, 1–289, 1–407, 1–479, 1–511
FLUID116 element, 1–281, 1–283, 1–285, 1–289
FLUID136 element, 1–580
FLUID141 element, 1–274, 1–407, 1–511
FLUID142 element, 1–112
FLUID29 element, 1–403
FLUID30 element, 1–403
FLUID38 element, 1–344
FLUID79 element, 1–334
FLUID80 element, 1–336
FLUID81 element, 1–344
Fourier analysis, 1–297
Fourier series analysis, 1–528
fracture, 1–322
friction
dynamic coefficient, 1–92
static coefficient, 1–75

G

GAM command, 2–36
gap condition, 1–182, 1–186, 1–196
GEOM command, 1–330
*GET command, 1–470, 2–5, 2–15
/GOPR command, 2–36
graphics
array parameter graphs, 1–297
beam section display, 1–500, 1–503
contours, 1–94, 1–99, 1–112, 1–228, 1–231, 1–262, 1–272, 1–320, 1–342, 1–365, 1–373, 1–421, 1–430, 1–436, 1–443, 1–484
displaced shapes, 1–21, 1–26, 1–45, 1–99, 1–107, 1–109, 1–338, 1–340, 1–385, 1–394, 1–396, 1–403, 1–452, 1–463, 1–487, 1–500, 1–503, 1–507
edge displays, 1–365, 1–380, 1–385, 1–407, 1–421, 1–430
element displays, 1–320, 1–430, 1–470, 1–484, 3–10, 3–12
ETABLE displays, 1–421
hidden-line options, 1–468
material properties, 1–370
path graphs, 1–65, 1–112, 1–237, 1–241, 1–342, 1–378, 1–388, 1–407, 1–436
scaling displacements, 1–308, 1–320, 1–385, 1–394
scaling vector load symbols, 1–365, 1–380
shrunken displays, 1–484
superimposing displays, 1–45, 1–99, 1–107, 1–109, 1–308, 1–320, 1–338, 1–340

time-history graphs, 1–53, 1–84, 1–101, 1–153, 1–165, 1–167, 1–169, 1–174, 1–176, 1–184, 1–190, 1–193, 1–196, 1–207, 1–209, 1–237, 1–248, 1–258, 1–262, 1–354, 1–354, 1–414, 1–416, 1–425, 1–452, 1–457, 1–460, 1–475, 1–487
vector results, 1–272, 1–365, 1–380, 1–407, 1–432
viewing angle, 1–468
viewing direction, 1–94, 1–99, 1–107, 1–109, 1–380, 1–396, 1–463
Graphics
annotation, 1–219
isosurfaces, 1–219
superimposing displays, 1–430
/GRID command, 2–29

H

harmonic response analysis
full method, 1–400, 1–403, 1–432, 1–473, 1–477, 1–493, 1–496
mode superposition method, 1–53, 1–176, 1–416
reduced method, 1–53, 1–176, 1–199, 1–201, 1–203, 1–207, 1–463
Heat generation
body load, 1–139
heat generation
body load, 1–215, 1–235, 1–241, 1–260, 1–267, 1–498
HF119 element, 1–491, 1–496
HF120 element, 1–491, 1–493
hyperelasticity
Mooney-Rivlin, 1–135, 1–460, 1–487, 1–507

I

IC command, 1–350
*IF command, 2–29, 2–36
IGES, 1–101, 1–451
IMPD command, 1–493
implicit creep, 1–524
inertia loading
acceleration, 1–105, 1–107, 1–109, 1–131, 1–153, 1–186, 1–190, 1–209, 1–334, 1–336, 1–354, 2–12, 2–36
angular acceleration, 1–285
angular velocity, 1–65, 1–131, 1–299, 1–334
inertia relief, 1–449
INFIN110 element, 1–119, 1–473, 1–475
INFIN111 element, 1–123
INFIN47 element, 1–436
INFIN9 element, 1–370, 1–430
initial conditions
transient dynamic analysis, 1–101, 1–153, 1–190, 1–350
transient magnetic analysis, 1–99, 1–161, 1–359, 1–375, 1–394
transient thermal analysis, 1–356, 1–378, 1–441
initial strain, 1–80, 1–301
INTER115 element, 1–432

K

K command, 2–5
KBC command, 2–26
KCALC command, 1–323
KEYOPT command, 2–29
KGEN command, 2–5
kinematic analysis, 1–409, 1–447
KMOVE command, 2–9
KPSCALE command, 1–370
KSCON command, 1–323

L

L command, 2–5
large deflection/rotation, 1–34, 1–43, 1–69, 1–101, 1–209, 1–308, 1–311, 1–313, 1–314, 1–354, 1–385, 1–394, 1–409, 1–44
1–500, 1–507
large strain
hyperelasticity, 1–135, 1–460, 1–487, 1–507
plasticity, 1–452
viscoplasticity, 1–455
latent heat, 1–237
Latin Hypercube Sampling, 1–544
LCDEF command, 2–32
LESIZE command, 2–5, 2–9, 2–15, 2–19, 2–26, 2–29
line search, 1–69
linearized stresses, 1–65
LINK1 element, 1–19, 1–23, 1–24, 1–37, 1–71, 1–176, 1–184, 1–193, 1–196, 1–301, 1–350, 1–445
LINK10 element, 1–80, 1–129
LINK11 element, 1–447
LINK131 element, 1–250
LINK132 element, 1–250
LINK31 element, 1–243, 1–244
LINK32 element, 1–212, 1–214, 1–215, 1–250, 1–260, 1–262, 1–287, 1–330, 1–368
LINK33 element, 1–217, 1–258
LINK34 element, 1–212, 1–215, 1–217, 1–221, 1–244, 1–248, 1–250, 1–262, 1–356
LINK68 element, 1–265, 1–383
LINK8 element, 1–71, 1–209, 1–328
listings
element data, 1–34, 1–63, 1–84, 1–87, 1–99, 1–101, 1–109, 1–150, 1–153, 1–163, 1–169, 1–169, 1–180, 1–250, 1–262, 1–265, 1–289, 1–301, 1–303, 1–336, 1–356, 1–409, 1–425
nodal data, 1–21, 1–28, 1–30, 1–34, 1–57, 1–59, 1–63, 1–65, 1–69, 1–73, 1–84, 1–87, 1–90, 1–94, 1–101, 1–105, 1–107, 1–109, 1–135, 1–150, 1–153, 1–159, 1–163, 1–165, 1–167, 1–169, 1–174, 1–176, 1–186, 1–188, 1–190, 1–193, 1–196, 1–207, 1–209, 1–212, 1–215, 1–217, 1–219, 1–221, 1–223, 1–226, 1–228, 1–231, 1–233, 1–237, 1–241, 1–248, 1–252, 1–254, 1–255, 1–262, 1–267, 1–269, 1–289, 1–314, 1–316, 1–318, 1–320, 1–324, 1–336, 1–347, 1–350, 1–354, 1–356, 1–370, 1–373, 1–375, 1–380, 1–385,

1–388, 1–392, 1–403, 1–409, 1–411, 1–414, 1–414, 1–416, 1–418, 1–428, 2–32
path data, 1–65, 1–237, 1–318, 1–378
reaction load data, 1–57, 1–135, 1–163, 1–221, 1–287, 1–365, 1–400, 1–498
sorting, 1–87, 1–219, 1–258, 1–320, 1–347
time-history data, 1–63, 1–73, 1–84, 1–101, 1–153, 1–165, 1–169, 1–174, 1–176, 1–184, 1–186, 1–190, 1–193, 1–196, 1–207, 1–209, 1–262, 1–303, 1–350, 1–354, 1–356, 1–375, 1–400, 1–403, 1–452, 1–455, 1–457, 1–475
vector data, 2–15, 2–32
Listings
nodal data, 1–258
time-history data, 1–167
loads
biaxial, 1–524
LOCAL command, 2–9, 2–29
LSEL command, 2–5, 2–9, 2–15

M

magnetic field analysis
2-D, 1–370, 1–373, 1–375, 1–388, 1–425, 1–430, 1–473, 1–475
3-D, 1–378, 1–380, 1–388, 1–432, 1–432, 1–436
CMVP method, 1–432
GSP method, 1–436
RSP - MVP method, 1–388
RSP method, 1–378, 1–380
RSP-MVP method, 1–432
harmonic, 1–373, 1–421, 1–473, 1–513
static, 1–370, 1–378, 1–380, 1–388, 1–430, 1–436, 1–473
transient, 1–375, 1–425, 1–475
MAGOPTcommand, 1–436
MASS166 element, 3–2, 3–6, 3–8
MASS21 element, 1–111, 1–115, 1–117, 1–127, 1–137, 1–153, 1–178, 1–184, 1–186, 1–205, 1–207, 1–209, 1–299, 1–350
MASS71 element, 1–248, 1–356
master degrees of freedom, 1–111, 1–115, 1–117, 1–176, 1–178, 1–203, 1–291, 1–338, 1–344
master degrees-of-freedom, 1–121, 1–127, 1–133, 1–137, 1–141, 1–143, 1–145, 1–147, 1–155, 1–157, 1–163, 1–165, 1–167, 1–172, 1–174, 1–182, 1–186, 1–193, 1–196, 1–199, 1–201, 1–205, 1–207, 1–340, 1–396, 1–413, 1–414, 1–416, 1–466, 2–40, 2–40
material properties
anisotropic, 1–326, 1–396
fatigue, 1–28
linear, 1–19, 1–21, 1–23, 1–24, 1–26, 1–34, 1–36, 1–39, 1–41, 1–43, 1–45, 1–47, 1–51, 1–55, 1–57, 1–59, 1–65, 1–69, 1–71, 1–73, 1–75, 1–82, 1–84, 1–87, 1–90, 1–92, 1–94, 1–101, 1–103, 1–105, 1–107, 1–109, 1–111, 1–115, 1–117, 1–121, 1–127, 1–129, 1–133, 1–137, 1–139, 1–141, 1–143, 1–145, 1–147, 1–150, 1–152, 1–153, 1–155, 1–157, 1–159, 1–161, 1–163, 1–165, 1–167, 1–169, 1–172, 1–174, 1–176, 1–178, 1–186, 1–188, 1–190, 1–193, 1–196, 1–199, 1–201, 1–205, 1–207, 1–209, 1–212, 1–214, 1–215, 1–217, 1–219, 1–223, 1–226, 1–228, 1–231, 1–233, 1–233, 1–235, 1–241, 1–243, 1–244, 1–246, 1–248, 1–250, 1–252, 1–254, 1–255, 1–258, 1–260, 1–262, 1–262, 1–265, 1–267, 1–269, 1–281, 1–283, 1–287, 1–289, 1–291, 1–293, 1–299, 1–307, 1–308, 1–311, 1–313, 1–314, 1–316, 1–318, 1–320, 1–322, 1–332, 1–334, 1–336, 1–338, 1–340, 1–342, 1–344, 1–347, 1–352, 1–354, 1–356, 1–359, 1–361, 1–363, 1–363, 1–368, 1–373, 1–375, 1–378, 1–380, 1–383, 1–385, 1–388, 1–392, 1–394, 1–400, 1–403, 1–407, 1–407, 1–411, 1–416, 1–418, 1–421, 1–425, 1–428, 1–430, 1–432, 1–436, 1–438, 1–443, 1–445, 1–447, 1–449, 1–463, 1–466, 1–470, 1–473, 1–498, 1–500, 1–503, 1–511, 2–5, 2–9, 2–12, 2–19, 2–23, 2–26, 2–32, 2–36, 3–10, 3–12
constant, 1–19, 1–21, 1–23, 1–24, 1–26, 1–34, 1–36, 1–39, 1–41, 1–43, 1–45, 1–47, 1–51, 1–55, 1–57, 1–59, 1–65, 1–69, 1–71, 1–73, 1–75, 1–82, 1–84, 1–87, 1–90, 1–92, 1–94, 1–101, 1–103, 1–105, 1–107, 1–109, 1–111, 1–115, 1–117, 1–121, 1–127, 1–129, 1–133, 1–137, 1–139, 1–141, 1–143, 1–145, 1–147, 1–150, 1–152, 1–153, 1–155, 1–157, 1–159, 1–161, 1–163, 1–165, 1–167, 1–169, 1–172, 1–174, 1–176, 1–178, 1–186, 1–188, 1–190, 1–193, 1–196, 1–199, 1–201, 1–205, 1–207, 1–209, 1–212, 1–215, 1–217, 1–219, 1–223, 1–226, 1–228, 1–231, 1–233, 1–235, 1–243, 1–244, 1–246, 1–248, 1–250, 1–252, 1–254, 1–255, 1–258, 1–260, 1–262, 1–265, 1–267, 1–269, 1–281, 1–283, 1–287, 1–289, 1–291, 1–293, 1–299, 1–307, 1–308, 1–311, 1–313, 1–314, 1–316, 1–318, 1–320, 1–322, 1–332, 1–334, 1–336, 1–338, 1–340, 1–342, 1–344, 1–347, 1–352, 1–354, 1–356, 1–359, 1–361, 1–363, 1–363, 1–368, 1–373, 1–375, 1–378, 1–380, 1–383, 1–385, 1–388, 1–392, 1–394, 1–400, 1–403, 1–407, 1–407, 1–411, 1–416, 1–418, 1–421, 1–425, 1–428, 1–430, 1–432, 1–436, 1–438, 1–443, 1–445, 1–447, 1–449, 1–463, 1–466, 1–470, 1–473, 1–498, 1–500, 1–503, 1–511, 2–5, 2–9, 2–12, 2–19, 2–23, 2–26, 2–32, 2–36, 3–10, 3–12
temperature dependent, 1–214, 1–233, 1–241, 1–262
nonlinear, 1–30, 1–37, 1–63, 1–97, 1–135, 1–180, 1–184, 1–237, 1–285, 1–289, 1–301, 1–303, 1–305, 1–328, 1–370, 1–452, 1–455, 1–457, 1–507, 1–513, 1–515
orthotropic, 1–324, 1–326
Material properties
linear, 1–80, 1–414
constant, 1–80, 1–414
MATRIX27 element, 1–103
MATRIX50 element, 1–287, 1–318, 1–330
merging, 1–147, 1–150, 1–231, 1–322, 1–365, 1–370, 1–378, 1–392, 1–400, 1–432
meshing
contact surfaces, 1–438
free, 1–28, 1–45, 1–90, 1–105, 1–135, 1–139, 1–145, 1–147, 1–150, 1–155, 1–188, 1–237, 1–260, 1–272, 1–287, 1–318, 1–320,

1–334, 1–336, 1–347, 1–365, 1–380, 1–411, 1–413, 1–418, 1–421, 1–428, 1–436, 1–473, 1–475, 1–484, 2–19, 2–26
mapped, 1–65, 1–65, 1–69, 1–94, 1–107, 1–121, 1–121, 1–123, 1–135, 1–143, 1–219, 1–255, 1–318, 1–320, 1–373, 1–400, 1–430, 1–432, 1–438, 1–484, 1–487, 2–5, 2–9, 2–12, 2–15, 2–23, 2–36
surface elements, 1–123, 1–139
tetrahedron to hexahedron interface, 1–484
MLAB command, 2–32
modal analysis, 1–491
householder reduced, 1–53, 1–111, 1–115, 1–117, 1–121, 1–127, 1–133, 1–137, 1–141, 1–145, 1–147, 1–155, 1–157, 1–161, 1–163, 1–205, 1–338, 1–340, 1–344, 1–396, 1–413, 1–414, 1–416, 1–466, 2–19, 2–19
prestressed, 1–129, 1–131, 1–133, 1–141, 1–176, 1–340, 1–342
subspace, 1–129, 1–131, 1–137, 1–143, 1–159, 1–176, 1–342, 2–15, 2–15
unsymmetric matrix, 1–403
modal cyclic symmetry, 1–342
MODOPT command, 2–15, 2–19
MP command, 1–233, 1–350, 1–457, 2–5
MPC184 element, 1–568
MXPAND command, 2–19

N

NARAY command, 2–15
NBOT command, 2–29
NCNV command, 2–29
NDELE command, 2–32
NDOF, 2–5, 2–9, 2–23
NEQIT command, 2–29
Newton-Raphson
arc-length, 1–49
full, 1–84, 1–97, 1–101, 1–135, 1–190, 1–209, 1–237, 1–241, 1–248, 1–250, 1–252, 1–254, 1–255, 1–258, 1–260, 1–262, 1–305, 1–308, 1–311, 1–313, 1–314, 1–350, 1–356, 1–385, 1–409, 1–438, 1–441, 1–445, 1–460, 1–487, 1–507
initial stiffness, 1–186, 1–301, 1–303, 1–328, 1–432, 1–436
modified, 1–350
NLGEOM command, 1–69, 2–29
NMODIF command, 2–32
node offset option, 1–324
NROPT command, 2–29
NROTAT command, 2–15
NSLE command, 2–32
NSORT command, 2–9
NSUBST command, 2–29
NUMMRG command, 2–15

O

optimization, 1–347, 1–352
/OUT command, 2–32
OUTRES command, 2–9, 2–29

P

partial solution method, 1–121
path operations, 1–318, 1–378, 1–388, 1–407
permanent magnet, 1–380
phase change, 1–237
piezoelectric, 1–396, 1–400
PIPE16 element, 1–39, 1–117, 1–137, 1–328
PIPE18 element, 1–51
PIPE20 element, 1–30
PIPE59 element, 1–354
plane strain, 1–322, 1–452, 1–460
plane stress, 1–320, 1–347, 1–385, 1–394, 1–411, 1–438
thickness input, 1–26, 1–293, 1–318, 1–470, 2–9, 2–40, 3–10, 3–12
PLANE121 element, 1–119, 1–272
PLANE13, 1–537, 1–542
PLANE13 element, 1–61, 1–370, 1–373, 1–375, 1–385, 1–388, 1–394, 1–421, 1–425
PLANE145 element, 1–318
PLANE146 element, 1–320
PLANE182 element, 1–135, 1–460, 1–487, 1–524
PLANE183 element, 1–135, 1–460, 1–487, 1–524, 1–576
PLANE2 element, 1–150, 1–318, 1–320, 1–411, 1–413, 2–9, 2–29, 2–32, 2–40
PLANE223, 1–560
PLANE223 element, 1–563
PLANE25 element, 1–107, 1–157
PLANE35, 1–536
PLANE35 element, 1–139, 2–23, 2–26
PLANE42 element, 1–26, 1–47, 1–82, 1–97, 1–152, 1–293, 1–320, 1–347, 1–438, 1–470, 2–9, 2–29, 2–32, 2–40, 3–10
PLANE53 element, 1–430, 1–473, 1–475, 1–513
PLANE55 element, 1–82, 1–223, 1–226, 1–228, 1–233, 1–237, 1–241, 1–252, 1–255, 1–267, 1–365, 1–443, 2–23, 2–26
PLANE67 element, 1–269
PLANE75 element, 1–246
PLANE77, 1–534
PLANE77 element, 1–73, 1–254, 2–23, 2–26
PLANE78 element, 1–359
PLANE82 element, 1–26, 1–65, 1–150, 1–318, 1–322, 1–470, 1–563, 2–9, 2–29, 2–32, 2–40
PLANE83 element, 1–316
plasticity
bilinear isotropic hardening, 1–452
bilinear kinematic hardening, 1–30, 1–37, 1–63, 1–97, 1–184, 1–305
nonlinear elastic, 1–350
PLDISP command, 2–29
PLVAR command, 2–29
PRERR command, 2–32

PRETS179, 1–526
primitives
areas, 1–77, 1–94, 1–421, 1–430, 1–432, 1–473, 1–475
volumes, 1–94, 1–436, 1–449, 1–451, 1–468, 1–491

R

radiation using AUX12
hidden method, 1–287
using link element, 1–243, 1–244
using surface effect element, 1–330
random vibration, 1–53, 1–159
RAT command, 2–36
reference temperature, 1–23, 1–61, 1–71, 1–84, 1–90, 1–97, 1–152, 1–340, 1–342
*REPEAT command, 2–5
rotary inertia, 1–115, 1–117
RSYS command, 2–36

S

SAVE command, 2–29
selecting subsets
component, 1–438
element, 1–94, 1–99, 1–105, 1–139, 1–221, 1–228, 1–235, 1–287, 1–316, 1–318, 1–322, 1–370, 1–373, 1–375, 1–380, 1–385, 1–388, 1–403, 1–409, 1–421, 1–425, 1–430, 1–432, 1–436, 1–438, 1–460, 1–473, 1–475, 2–32, 2–40
node, 1–26, 1–28, 1–30, 1–34, 1–57, 1–59, 1–65, 1–69, 1–73, 1–84, 1–90, 1–94, 1–97, 1–99, 1–105, 1–107, 1–135, 1–135, 1–139, 1–143, 1–147, 1–150, 1–155, 1–163, 1–180, 1–188, 1–217, 1–219, 1–221, 1–223, 1–226, 1–228, 1–231, 1–233, 1–237, 1–241, 1–252, 1–254, 1–255, 1–267, 1–269, 1–287, 1–289, 1–311, 1–313, 1–314, 1–316, 1–318, 1–322, 1–324, 1–328, 1–332, 1–334, 1–336, 1–338, 1–344, 1–347, 1–352, 1–359, 1–361, 1–363, 1–365, 1–365, 1–370, 1–373, 1–375, 1–380, 1–385, 1–388, 1–392, 1–394, 1–396, 1–400, 1–403, 1–407, 1–411, 1–413, 1–418, 1–421, 1–425, 1–428, 1–430, 1–432, 1–436, 1–438, 1–452, 1–460, 1–463, 1–473, 1–475, 1–498, 2–5, 2–9, 2–12, 2–15, 2–19, 2–23, 2–26, 2–32, 2–36, 2–40
solid model entity, 1–94, 1–287, 1–370, 1–373, 1–380, 1–421, 1–430, 1–432, 1–443, 1–460, 1–491, 2–5, 2–5, 2–9, 2–9
SET command, 2–32
SF command, 2–9, 2–23, 2–26
SHELL command, 2–36
SHELL131 element, 1–221, 1–235
SHELL150 element, 1–28
SHELL157 element, 1–498
SHELL181 element, 1–69, 1–507, 1–574, 1–578, 2–12
SHELL208 element, 1–507
SHELL28 element, 1–463
SHELL41 element, 1–55, 1–342
SHELL43 element, 1–30, 1–69, 2–12, 2–15, 2–36
SHELL51 element, 1–41, 1–45, 1–59, 1–133, 1–311, 1–313
SHELL61 element, 1–109, 1–338, 1–340
SHELL63 element, 1–49, 1–87, 1–99, 1–131, 1–147, 1–155, 1–314, 1–403, 2–12, 2–15, 2–36
SHELL91 element, 1–90
SHELL93 element, 1–28, 1–105, 1–318, 1–466, 2–12, 2–15, 2–36
SHELL99 element, 1–143, 1–180, 1–188, 1–324
solid modeling, 1–347
attributes, 1–370, 1–380, 1–388, 1–394, 1–400, 1–411, 1–421, 1–473, 1–475
concatenation, 1–77
copying, 1–147, 1–150
dragging, 1–123, 1–380
loads, 1–45, 1–121, 1–150, 1–258, 1–260, 1–318, 1–320, 1–322, 1–411, 1–413, 1–418, 1–428, 1–443, 1–449, 1–470, 3–10, 3–12
meshing control, 1–45, 1–65, 1–69, 1–84, 1–94, 1–107, 1–121, 1–135, 1–139, 1–143, 1–147, 1–150, 1–155, 1–188, 1–219, 1–237, 1–255, 1–258, 1–260, 1–287, 1–318, 1–320, 1–334, 1–336, 1–338, 1–340, 1–347, 1–365, 1–370, 1–373, 1–388, 1–394, 1–396, 1–400, 1–407, 1–411, 1–413, 1–418, 1–428, 1–438, 1–460
rotating, 1–123, 1–432
scaling, 1–119, 1–370
splines, 1–347
Solid modeling
attributes, 1–430
SOLID117, 1–570
SOLID117 element, 1–515
SOLID122 element, 1–123
SOLID147 element, 1–418
SOLID148 element, 1–428
SOLID164 element, 3–4
SOLID185, 1–553
SOLID185 element, 1–135, 1–460, 1–487, 1–568, 1–578, 1–582, 2–5
SOLID186 element, 1–135, 1–487, 1–578, 1–582, 2–5
SOLID187 element, 1–578, 1–582, 2–5
SOLID45, 1–526
SOLID45 element, 1–30, 1–94, 1–97, 1–322, 1–438, 1–449, 2–5, 2–19, 2–32, 2–40
SOLID46 element, 1–188, 1–324
SOLID5 element, 1–84, 1–378, 1–392, 1–396, 1–400, 1–418, 1–428
SOLID62 element, 1–388
SOLID64 element, 1–326
SOLID65 element, 1–328
SOLID69 element, 1–269
SOLID70 element, 1–217, 1–231, 1–267, 1–441
SOLID87 element, 1–219
SOLID90 element, 1–361, 1–363
SOLID92 element, 1–418, 1–428, 2–5, 2–19, 2–32, 2–40
SOLID95 element, 1–322, 1–332, 1–484, 2–5, 2–32, 2–40

SOLID96 element, 1–432
SOLID97 element, 1–388, 1–432
SOLID98, 1–549
SOLID98 element, 1–380, 1–418, 1–428, 1–436
solvers
block Lanczos, 1–141, 1–145, 1–161
Block Lanczos, 1–491
conjugate gradient, 1–255, 1–425
frontal, 1–19, 1–21, 1–23, 1–24, 1–26, 1–28, 1–30, 1–34, 1–36, 1–37, 1–39, 1–41, 1–43, 1–45, 1–47, 1–51, 1–55, 1–57, 1–59, 1–63, 1–65, 1–69, 1–71, 1–73, 1–75, 1–80, 1–82, 1–84, 1–87, 1–90, 1–92, 1–97, 1–99, 1–101, 1–103, 1–105, 1–107, 1–109, 1–111, 1–115, 1–117, 1–127, 1–129, 1–131, 1–133, 1–135, 1–137, 1–139, 1–141, 1–143, 1–145, 1–147, 1–150, 1–152, 1–153, 1–155, 1–157, 1–159, 1–161, 1–163, 1–165, 1–167, 1–169, 1–172, 1–174, 1–176, 1–178, 1–180, 1–184, 1–186, 1–188, 1–190, 1–190, 1–193, 1–196, 1–199, 1–201, 1–203, 1–205, 1–207, 1–209, 1–212, 1–214, 1–215, 1–217, 1–219, 1–221, 1–223, 1–226, 1–228, 1–231, 1–233, 1–235, 1–237, 1–241, 1–243, 1–244, 1–246, 1–248, 1–250, 1–252, 1–254, 1–258, 1–260, 1–262, 1–265, 1–267, 1–269, 1–281, 1–283, 1–285, 1–287, 1–289, 1–291, 1–293, 1–299, 1–301, 1–303, 1–305, 1–307, 1–308, 1–311, 1–313, 1–314, 1–316, 1–318, 1–320, 1–322, 1–324, 1–326, 1–328, 1–332, 1–334, 1–336, 1–338, 1–340, 1–342, 1–344, 1–350, 1–350, 1–352, 1–354, 1–356, 1–359, 1–361, 1–363, 1–365, 1–368, 1–370, 1–373, 1–375, 1–378, 1–380, 1–383, 1–385, 1–388, 1–392, 1–394, 1–396, 1–400, 1–403, 1–407, 1–409, 1–411, 1–413, 1–414, 1–416, 1–418, 1–421, 1–428, 1–430, 1–432, 1–436, 1–457, 1–473, 1–475, 2–12, 2–15, 2–19, 2–23, 2–26, 2–32, 2–36, 2–40
Lanczos, 1–403
preconditioning conjugate gradient, 2–5
Solvers
frontal, 1–430
SOURC36 element, 1–378, 1–436
SPARM command, 1–493, 1–496
spectrum analysis
PSD, 1–53, 1–159, 1–466
single-point, 1–161, 1–163
spin softening, 1–131
*STATUS command, 2–5, 2–36
stress stiffening, 1–57, 1–80, 1–311, 1–313, 1–314
submodeling
solid-to-solid, 1–320
substructuring, 1–318
SURF151 element, 1–139, 1–330
SURF152 element, 1–441
SURF153 element, 1–97
SURF154 element, 1–97
surface effect elements, 1–139, 1–436, 1–436, 1–441
surface loads
beams, 1–21, 1–57, 1–305, 1–503
convection, 1–73, 1–139, 1–217, 1–221, 1–223, 1–226, 1–228, 1–235, 1–252, 1–254, 1–255, 1–361, 1–363, 1–392, 1–443, 2–23, 2–26
fluid-structure flag, 1–403
heat flux, 1–330
infinite flag, 1–119, 1–123, 1–473, 1–475
Maxwell flag, 1–385
pressure, 1–41, 1–45, 1–55, 1–65, 1–94, 1–97, 1–135, 1–188, 1–311, 1–313, 1–314, 1–320, 1–322, 1–407, 1–447, 1–466, 1–470, 1–507, 2–5, 2–9, 3–10, 3–12
swelling, 1–303
SYM command, 2–9

T

T command, 2–5
TARG command, 2–9
TARGE169, 1–537
TARGE169 element, 1–487
TARGE170 element, 1–487
TB command, 2–29
TBDAT command, 2–29
TBDATA command, 1–326
TGAM command, 2–36
thermal analysis
steady-state, 1–139, 1–212, 1–214, 1–215, 1–217, 1–219, 1–221, 1–223, 1–226, 1–231, 1–233, 1–235, 1–241, 1–243, 1–244, 1–246, 1–258, 1–267, 1–287, 1–289, 1–359, 1–361, 1–363, 1–392, 1–394, 1–443, 1–498, 2–23
transient, 1–248, 1–250, 1–252, 1–254, 1–255, 1–260, 1–262, 1–441, 2–26
TIME command, 2–26, 2–29
time step, 1–34, 1–73, 1–84, 1–101, 1–153, 1–165, 1–167, 1–169, 1–172, 1–174, 1–178, 1–184, 1–186, 1–193, 1–196, 1–20 1–237, 1–248, 1–250, 1–252, 1–254, 1–255, 1–258, 1–262, 1–30 1–303, 1–350, 1–354, 1–368, 1–375, 1–409, 1–414, 1–425, 1–44 1–475
Time step, 1–182, 1–190, 1–356
TIMINT command, 2–29
TOTAL command, 1–4, 1–396, 1–413, 2–19
TRANS126, 1–555
TRANS126 element, 1–521
transient circuit analysis, 1–528
transient dynamic analysis
full method, 1–34, 1–153, 1–169, 1–184, 1–186, 1–190, 1–209, 1–350, 1–354, 1–356, 1–409, 1–475
mode superposition method, 1–53, 1–414
reduced method, 1–53, 1–165, 1–167, 1–172, 1–174, 1–178, 1–182, 1–186, 1–193, 1–196
TUNIF command, 2–26

U

*USE command, 2–32

V

V command, 2–5
VISCO106 element, 1–452, 1–455, 2–29
VISCO107 element, 1–452, 1–455, 2–29
VISCO108 element, 1–452, 1–455
VISCO88 element, 1–457
VISCO89 element, 1–457
viscoelasticity, 1–457
viscoplasticity
  rate dependent, 1–455
  rate independent, 1–452
VMESH command, 2–5, 2–19
*VOPER command, 1–295
VROTAT command, 2–29
VTYPE command, 1–330
*VWRITE command, 2–32

W

WAVES command, 2–19
Weibull distribution, 1–544
working plane, 1–77, 1–436, 1–449, 1–451, 1–468
WSORT command, 2–36

X

XVAR command, 2–29

ANSYS Verification Manual . ANSYS Release 10.0 . 002184 . © SAS IP, Inc.